

Solida Long

**Synthesis and biological evaluation of indole alkaloid  
derivatives based on natural products**



Porto, 2019



# **Synthesis and biological evaluation of indole alkaloid derivatives based on natural products**

## **Síntese e avaliação biológica de derivados de alcalóides indólicos inspirados em produtos naturais**

**Solida Long**

Thesis presented to the Faculty of Pharmacy, University of Porto, to obtain the degree of Doctoral of Philosophy in Pharmaceutical Sciences in the specialty of Pharmaceutical and Medicinal Chemistry.

**Supervisor:**

Professor Maria Emília da Silva Pereira de Sousa

(Assistant Professor, Faculty of Pharmacy, University of Porto)

**Co-supervisor:**

Professor Madalena Maria de Magalhães Pinto

(Full Professor, Faculty of Pharmacy, University of Porto)

# Synthesis and biological evaluation of indole alkaloid derivatives based on natural products

This work was developed in the Laboratory of Organic and Pharmaceutical Chemistry, Department of Chemistry, Faculty of Pharmacy, University of Porto

This research was partially supported by the Strategic Funding UID/Multi/04423/2019 through national funds provided by FCT-Foundation for Science and Technology and European Regional Development Fund (ERDF), in the framework of the program PT2020. This research was developed under Project No. POCI-01-0145-FEDER-028736; PTDC/MAR-BIO/4694/2014 (POCI-01-0145-FEDER-016790; 3599-PPCDT); PTDC/DPT-FTO/1981/2014 (POCI-01-0145-FEDER-016581), co-financed by COMPETE 2020, Portugal 2020 and the European Union through the ERDF, and by FCT through national funds, and Erasmus-Lotus+ program (LOTUS+, LP15DF0205).

Cofinanciado por:



According to current legislation, any copying, publication, or use of this thesis or parts thereof shall not be allowed without written permission.

**Author:**

Solida Long

up201502099@ff.up.pt, solidachhann@gmail.com

**PhD Thesis in Pharmaceutical and Medicinal Chemistry**

**Title:** Synthesis and biological evaluation of indole alkaloid derivatives based on natural products

Publication date: 25<sup>th</sup> June 2019

**Supervisor:**

Professor Maria Emília da Silva Pereira de Sousa

(Assistant Professor, Faculty of Pharmacy, University of Porto)

**Co-supervisor:**

Professor Madalena Maria de Magalhães Pinto

(Full Professor, Faculty of Pharmacy, University of Porto)

Faculty of Pharmacy, University of Porto, 25<sup>th</sup> June 2019

## Author's Declaration

Under the terms of “Decreto-Lei nº 216/92, de 13 Outubro”, is hereby declared that the author afforded a major contribution to the conceptual design and technical execution of the work, interpretation of the results and manuscript preparation of the original articles included in this thesis.

Under the term of the “Decreto-Lei nº 216/92, de 13 Outubro”, is hereby declared that the following original articles/communication were prepared in the scope this thesis.

## Publications

### Articles in international peer-reviewed journals

#### Review

1. **Long, S.**; Sousa, E.; Kijjoa, A.; and Pinto, M.M. M., Marine Natural Products as Models to Circumvent Multidrug Resistance. *Molecules* **2016**, *21* (7), 892.

#### Original research

1. **Long, S.**; Resende, D. I. S. P.; Kijjoa, A.; Silva, A. M. S.; Pina, A.; Fernández-Marcelo, T.; Vasconcelos, M. H.; Sousa, E.; Pinto, M. M. M., Antitumor Activity of Quinazolinone Alkaloids Inspired by Marine Natural Products. *Marine Drugs* **2018**, *16* (8), 261.
2. **Long, S.**; Resende, D. I. S. P.; Kijjoa, A.; Silva, A. M. S.; Fernandes, R.; Xavier, C. P. R.; Vasconcelos, M. H.; Sousa, E.; Pinto, M. M. M., Synthesis of New Proteomimetic Quinazolinone Alkaloids and Evaluation of Their Neuroprotective and Antitumor Effects. *Molecules* **2019**, *24* (3), 534.
3. **Long, S.**; Pereira-Terra, P.; Freitas-Silva, J.; Resende, D. I. S. P.; Kijjoa, A.; Silva, A. M. S.; Tiritan, E.; Pinto, E.; Costa, P. M.; Sousa, E.; Pinto, M. M. M. Synthesis and Characterization of the Antimicrobial Activities of Marine-derived Indolymethyl Pyrazinoquinazoline Alkaloids. (Article in preparation).

4. **Long, S.**; Camões, V. C. F.; Resende, D. I. S. P.; Palmeira A.; Kijjoa, A.; Silva, A. M. S.; Nogueira, F.; Sousa, E.; Pinto, M. M. M. Exploring the indole-containing pyrazino[2,1-*b*]quinazoline-3,6-dione scaffold as promising antimalarial agents. (Article in preparation).
5. **Long, S.**; Loureiro, J. B.; Soares, J.; Puthongking, P.; Gales, L.; Saraiva, L.; Sousa, E.; Pinto, M. M. M. Synthesis of small molecules of amino carbazoles and their restoration of mutant p53 activity. (Article in preparation).

### **Abstract in international peer-reviewed journals- *Original research***

**Long, S.**; Thongdee, N.; Loureiro, J. B.; Pinto, M. M. M.; Puthongking, P.; Saraiva, L.; Sousa, E. Amino carbazole alkaloid derivatives as potential modulators of p53mutants. Proceedings of 18th International Conference on Medicinal Chemistry & Targeted Drug Delivery, Medicinal Chemistry, December 2017, 7(11), MED 05.

### **Oral Communications**

Sousa, E.; **Long, S.**; Boonpothong, P.; Resende, D. I. S. P.; Durães, F.; Palmeira, A.; Silva, A. M. S.; Kijjoa, A.; Pinto, M. M. M. Models from the sea: synthesis of potential new antibacterial agents. 2<sup>nd</sup> International Christmas Caparica Congress in Translational Chemistry - IC3TC-2017, Lisbon, Portugal, 4-7 December 2017.

Sousa, E.; **Long, S.**; Boonpothong, P.; Resende, D. I. S. P.; Silva, A. M. S.; Kijjoa, A.; Pinto, M. M. M. Marine-fungi natural products as models for new antibacterial agents. IL5. Transmediterranean Colloquium on Heterocyclic Chemistry (TRAMECH IX 2017), Fez, Morocco, 22-25 November 2017.

### **Poster Communications**

Sousa, E.; **Long, S.**; Resende, D. I. S. P.; Silva, A. M. S.; Kijjoa, A.; Pinto, M. M. M. Quinazoline alkaloid derivatives with promising biological activities. Italian-Spanish-Portuguese Joint Meeting in Medicinal Chemistry (MedChemSicily2018), Palermo, Italy, 17-20 July 2018.

Peerasiri S.; **Long, S.**; Nanthicha T.; Pinto M. M. M.; Puthongking P.; Sousa E. Semi synthesis of Amino carbazole Alkaloid Derivatives. 5<sup>th</sup> National Organic Meeting & 12<sup>th</sup> National Medicinal chemistry Meeting, Coimbra, Portugal, 17-19 January 2018. (P009)

**Long, S.**; Inácio A.; Resende D. I. S. P.; Kijjoa A.; Silva A. M. S.; Costa P.; Pinto E.; Sousa, E.; Pinto M. M. M. Antibacterial activity of quinazolinone alkaloids with pyrazino[1,2-b]quinazoline-3,6-dione containing indole. 5<sup>th</sup> National Organic Meeting & 12<sup>th</sup> National Medicinal chemistry Meeting, Coimbra, Portugal, 17-19 January 2018. (P022)

**Long, S.**; Thongdee, N.; Loureiro, J. B.; Pinto, M. M. M.; Puthongking, P.; Saraiva, L.; Sousa, E. Amino carbazole alkaloid derivatives as potential modulators of p53 mutants. 18<sup>th</sup> International Conference on Medicinal Chemistry & Targeted Drug Delivery, Dallas, United States of America, 6-8 December 2017.

Lopes, N.; **Long S.**; Resende D. I. S. P.; Kijjoa A.; Silva A. M. S.; Pina, A.; Fernández M. T.; Vasconcelos, M. H., Pinto M. M. M.; Sousa E. Synthesis and tumor cell growth inhibitory effects of the marine product analogues of fiscalin B, 12<sup>th</sup> Young European Scientist Meeting (YES), Porto, Portugal, 14-17 September 2017.

**Long S.**; Resende D. I. S. P.; Kijjoa A.; Silva A. M. S.; Pina, A.; Fernández M. T.; Vasconcelos, M. H.; Sousa E.; Pinto M. M. M. Antitumor Activity of Quinazolinone Alkaloids-Inspired in Marine Products. 25<sup>th</sup> National Meeting Portuguese Chemical Society, Lisbon, Portugal, 16-19 July 2017. (P21)

Resende, D. I. S. P.; **Long, S.**; Boonpothong, P.; Silva, A. M. S.; Kijjoa, A.; Sousa, E.; Pinto, M. M. M. Synthetic strategies for the synthesis of quinazoline alkaloid derivatives with promising biological activities. 20<sup>th</sup> European Symposium on Organic Chemistry (ESOC 2017), Cologne, Germany, 2-6 July 2017. (LM002)

Lopes, N.; **Long, S.**; Resende, D. I. S. P.; Kijjoa, A.; Silva, A. M. S.; Pinto, M. M. M.; Sousa, E. Synthetic Strategies for Fiscalin B and Analogues. Yong Research Meeting of the University of Porto, Porto, Portugal, 8-10 February 2017.

**Long, S.**; Resende, D. I. S. P.; Boonpothong, P.; Kijjoa, A.; Sousa, E.; Pinto, M. M. M. Towards the total synthesis of neofiscalin A, a potent antibacterial agent. BraMedChem Rio, Brazil, 27-30 November 2016.



Lopes, A.; **Long, S.**; Fernandes, C.; Pinto, M. M. M.; Sousa, E. Synthesis of new thioxanthone derivatives. Yong Research Meeting of the University of Porto, Porto, Portugal, 17-19 February 2016.

### **Electronical communication**

**Long, S.**, Resender, D.I.S.P., Pereira-Terra, P., Inácio, Costa, P.M., Pinto, E., Kijjoa, A., Pinto, M., Sousa, E. Small molecules from the sea: models for innovative antimicrobial agents. 4<sup>th</sup> international electronic conference on medicinal chemistry. 1-30 November 2018.

### **Award**

Best Poster presentation “Amino carbazole alkaloid derivatives as potential modulators of p53mutants” 18<sup>th</sup> International Conference on Medicinal Chemistry & Targeted Drug Delivery, Dallas, United States of America, 6-8 December 2017.

## Table of Contents

Table of Contents .....	x
Acknowledgments.....	xii
Abstract.....	xiv
Resumo .....	xvi
List of Figures.....	xviii
List of Tables .....	xix
List of Schemes .....	xx
Abbreviations .....	xxi
Outline of the Thesis .....	xxii
Chapter 1: Introduction .....	1
1.1 Natural products in drug development.....	3
1.2 Heterocyclic compounds-indole alkaloids in drug chemistry.....	5
1.3 Quinazolinone alkaloids.....	8
1.3.1 Chemistry of quinazolinones.....	8
1.3.2 Isolation and biological activities of pyrazinoquinazoline alkaloids containing indole.....	9
1.3.2.1 Gyantrypines and derivatives.....	11
1.3.2.2 Fumiquinolines.....	11
1.3.2.3 Fiscalins .....	14
1.3.3 Biosynthesis of quinazolinones.....	15
1.3.4 Synthesis of quinazolinones .....	18
1.3.4.1 Eguchi-aza Wittig approach.....	19
1.3.4.2 Mazurkiewicz-Ganesan approach .....	23
1.3.4.3 Microwave assisted method .....	24
1.4 Carbazole alkaloids .....	25
1.4.1 Isolation and biological activities of carbazole alkaloids .....	26
1.4.2 Biosynthesis of carbazole alkaloids .....	30

1.4.2.1 Biosynthesis of carbazole alkaloids based on the anthranilic acid pathway .....	31
1.4.3 Synthesis of carbazole alkaloids .....	34
1.4.3.1 Synthesis of oxygenated carbazole alkaloids .....	35
1.4.4 Semi-synthesis of carbazole alkaloids .....	37
Aims of the thesis and work plan .....	39
<b>Chapter 2:</b> Marine natural products as models to circumvent multidrug resistance .....	43
<b>Chapter 3:</b> Antitumor activity of quinazolinone alkaloids inspired by marine natural products .....	121
<b>Chapter 4:</b> Synthesis of new proteomimetic quinazolinone alkaloids and evaluation of their neuroprotective and antitumor effects.....	153
<b>Chapter 5:</b> Synthesis and characterization of the antimicrobial activities of marine-derived indolymethyl pyrazinoquinazoline alkaloids .....	185
<b>Chapter 6:</b> Exploring the pyrazino[2,1-b]quinazoline-3,6-dione scaffold as a promising antimalarial agent.....	221
<b>Chapter 7:</b> Gram-scale synthesis of fiscalin B and chloro derivative.....	259
<b>Chapter 8:</b> Synthesis of small molecules of amino carbazoles and their effect on restoration of p53 activity.....	285
<b>Chapter 9:</b> Overall discussion and conclusions.....	319
<b>Chapter 10:</b> References.....	331
<b>Annexes</b> .....	353

## Acknowledgments

Mere words cannot possibly do justice to my deep sense of gratitude toward my supervisors. During these years of PhD, I was given the opportunity being part of an amazing working group, meeting brilliant people, and learning about two complete different areas: chemistry and biology. It was worth every moment and I would not change it for nothing.

I would like to express my enormous gratitude to my supervisor Professor Emília Sousa for helping me started in Organic Synthesis. I also thank for her patience, guidance and continuous encouragement during my four years of PhD. My sincere thanks are due to her constant support and help during the most complicated times. Professor Emília Sousa was always present, tirelessly, supporting me and giving me guidance when I felt more lost. Her teachings on scientific thinking and her help during the entire laboratorial work and manuscript writing are invaluable I would say “without her this thesis would not have been possible to be complete”.

I am deeply grateful to Professor Madalena Pinto for the invitation to work in Laboratory of Organic and Pharmaceutical Chemistry of FFUP and to Professor Anake Kijjoa for the opportunity for their detailed and constructive comments and for their important supports through this work. They provide encouragement, advices, good teaching, and lot of good ideas. They not only provide me the opportunity doing a PhD but also the opportunity of joining some scientific and social events.

I would like to give my appreciation to Professor Artur Silva from Organic Chemistry and Natural Products Unit (QOPNA), Department of Chemistry, University of Aveiro, for the opportunity to perform microwave synthesis bringing my research successful. I am very thankful to the group of Professor Helena Vasconcelos helping to perform the antitumor activity, to the group of Professor Paulo Costa for the assistance in the evaluation of antibacterial and Professor Eugénia Pinto for antifungal activities, to the group of Professor Fátima Nogueira from Institute of Hygiene and Tropical Medicine for accepting me in her laboratory to attend the antimalarial assays, and to the group of Professor Lucília Saraiva for performing p53 biological tests, to Professor Ploenthip Puthongking for performing the isolation of carbazole alkaloids, and to Professor Luis Gales for carrying out the X-crystallography.

I am indebted to all the professors at the Laboratory of Organic and Pharmaceutical Chemistry of FFUP and to many students and colleagues as well as to Dr. Sara Cravo for technical support, Gisela Adriano and Liliana Raimundo for assistance with the reagents, Dr. Diana I. S. P. Resende for

laboratory assistance. I also thank to Erasmus Mundus Action 2 (LOTUS+, LP15DF0205) for full scholarship 36 months at University of Porto.

I also must mention my dear Saveouth Chhann who present all the time, giving me hope, strength, emotional support, and understanding. My siblings Long Touch, Long Chancharya, and Long Sokharasy and their families for being around and courage. Lastly and the most important, I wish to express my heartfelt thanks to my parents Long Lay and Sin Ny. They raised, supported, taught, and loved me with endlessness.

To them I dedicate this thesis.

## Abstract

Drug discovery from natural products (NPs) is an important approach for drug development because secondary metabolites present unique chemical structures, exclusive stereochemistry, and interesting biological activity profiles. Among NPs, alkaloids, especially containing an indole group, are of crucial importance in the area of drug discovery. In this work, we aimed to synthesize derivatives and analogues of two classes of indole containing alkaloids - quinazolinone and carbazole alkaloids. Furthermore, several diverse biological assays were performed in order to extend the chemical/biological space for these families of compounds.

Inspired by the marine-derived fiscalin B (**26**), quinazolinone alkaloid derivatives were synthesized using two different methodologies: a highly efficient and straightforward three-component one-pot microwave-assisted approach and a multi-step Mazurkiewicz-Ganesan approach. While the former proved to be efficient and practical for rapidly obtaining libraries of the compounds, the latter, although with a more intricate methodology, proved to be a good approach for the synthesis of *syn* enantiomers. Moreover, we noticed that partial epimerization under the first reaction conditions could occur. *In vitro* growth inhibitory activity against tumor cell lines revealed that among the first two series of synthesized compounds, eighteen new analogues **76-93** were found to exhibit weak to moderate tumor cell growth inhibitory activity ( $20\ \mu\text{M} < \text{GI}_{50} < 100\ \mu\text{M}$ ) with small changes in the structure of the pyrazinoquinazoline being critical for activity. Interestingly, the synthetic fumiquinazoline G (**84**) presented the best antitumor activity in all the tumor cell lines tested, with  $\text{GI}_{50}$  values lower than  $20\ \mu\text{M}$ .

It is worth noticing that among the compounds tested in a second series, only **78**, **84**, **87**, and **89** showed potential for neuroprotection in a Parkinson disease *in vitro* model. This finding highlights the neuroprotective activity of synthetic fumiquinazoline G (**84**) but also the importance of the side chain for this activity. Noteworthy, synthetic fiscalin B (**78**), which was previously reported as a substance P antagonist, was among the neuroprotective compounds.

Among the halogenated indolomethyl pyrazino[1,2-*b*]quinazoline-3,6-diones developed in a third series, chlorinated compounds **99** and **100** exhibited a potent antibacterial activity against *S. aureus* ATCC strain with MIC values of  $4\ \mu\text{g/mL}$ , and against clinical isolates resistant to methicillin (MRSA) with MIC values of  $8\ \mu\text{g/mL}$ . Isolation of the enantiomers of **99** revealed that only **99a** with the configuration (*1S*, *4R*) was active, indicating that stereochemistry is vital for activity. Comparing with the marine natural product neofiscalin A (**28**), a two-fold reduction in the MIC was observed. These excellent and inspiring results obtained in the present study show that simpler molecules than **28** can retain the antimicrobial activity for this class of compounds.

Among the 29 compounds of the studied quinazolinone alkaloid subclass, **78**, **82**, and **99** demonstrated good antimalarial activity *in vitro* in the *P. falciparum* sensitive strain (3D7). These compounds showed low cytotoxicity *in vitro* against non-tumor mammalian cells V79 (LD<sub>50</sub> <14 μM) with favorable selectivity index values (SI ≥ 19). Also, these compounds did not show significant hemolytic activity in healthy human erythrocytes. The quinazolinones **78**, **82**, and **99** have characteristics with potential for the development of new antimalarial drugs.

Twelve amino carbazoles were synthesized from natural isolated compounds, heptaphylline (**57**) and derivatives **62** and **63** using a reductive amination reaction. The syntheses were found to have shorter reaction times when dichloroethane was used as solvent. This series of natural and semisynthetic derivatives was investigated for their growth effect on p53 wild-type tumor, null-type, and p53-mutant tumor cell lines. The preliminary results showed that the natural products **57**, **62**, and **63** were active in all the investigated cell lines (GI<sub>50</sub> < 10 μM) while the semisynthetic derivatives 3-(((4-fluorobenzyl)amino)methyl)-1-(3-methylbut-2-en-1-yl)-9H-carbazol-2-ol (**117**) and 3-(((4-bromobenzyl)amino)methyl)-7-methoxy-1-(3-methylbut-2-en-1-yl)-9H-carbazole-2-ol (**123**) showed potent inhibitory effects only in some p53-mutant as MDA-MB-468 and SW837 cells, respectively; while compound 7-methoxy-1-(3-methylbut-2-en-1-yl)-3-(piperidin-1-ylmethyl)-9H-carbazol-2-ol (**120**) showed potent inhibitory effect in melanoma A375 cell line.

Throughout this work, structure-activity relationships were established and three hit compounds from the quinazolinone scaffold, **84** for antitumor activity, and **99** and **78** for antibacterial and antimalarial activity, respectively, were disclosed. These findings will help to direct the research in the future considering this scaffold for drug discovery. From the other scaffold of alkaloids, the semisynthetic carbazoles **117** and **120** were more selective than the natural isolated compounds **57** and **62-63** in reactivating p53 mutants.

## Resumo

A descoberta de fármacos a partir de produtos naturais é uma abordagem importante para o desenvolvimento de medicamentos na medida em que os metabolitos secundários apresentam estruturas químicas únicas, estereoquímica muito particular e perfis de atividade biológica interessantes. Entre os produtos naturais, os alcalóides, especialmente contendo um grupo indol, são de importância crucial para a descoberta de novos fármacos. Neste trabalho, pretendemos sintetizar derivados de duas classes de alcalóides contendo indol - os alcalóides da quinazolinona e os de carbazol. Para além disso, uma série diversificada de ensaios biológicos foi aplicada, de modo a alargar o espaço químico/biológico para estas famílias de compostos.

Tendo como inspiração a molécula da fiscalina B (**26**), um composto de origem marinha, foram sintetizados derivados de alcalóides de quinazolinona usando duas metodologias diferentes: uma abordagem num único passo com três componentes assistida por micro-ondas, simples e eficiente, e também a abordagem Mazurkiewicz-Ganesan, envolvendo múltiplos passos. Enquanto a primeira provou ser eficiente e prática na obtenção rápida de bibliotecas destes compostos, a segunda, embora com uma metodologia mais complexa, provou ser uma abordagem útil para a síntese de enantiómeros *sin*. É de notar que foi observada epimerização parcial sob as primeiras condições de reação. A atividade inibidora do crescimento de linhas celulares tumorais *in vitro* revelou que, entre as primeiras séries de compostos sintetizados, dezoito novos análogos **76-93** exibiram actividade inibidora do crescimento de células tumorais moderada a fraca ( $20 \mu\text{M} < \text{GI}_{50} < 100 \mu\text{M}$ ) com pequenas mudanças na estrutura da pirazinoquinazolina sendo críticas para a atividade antitumoral. Curiosamente, a fumiquinazolina sintética G (**84**) apresentou a melhor atividade antitumoral em todas as linhas tumorais testadas, com valores de  $\text{GI}_{50} < 20 \mu\text{M}$ .

Da segunda série de compostos testados, apenas os **78**, **84**, **87** e **89** mostraram potencial para neuroproteção num modelo *in vitro* de doença de Parkinson. Este resultado destaca a atividade neuroprotetora da fumiquinazolina sintética G (**84**), mas também a importância da cadeia lateral para essa atividade. De notar que a fiscalina B sintética (**78**), que previamente foi relatada como um antagonista da substância P, estava entre os compostos com efeito neuroprotetor.

Entre as indolometil pirazino [1,2-*b*] quinazolinona-3,6-dionas halogenadas desenvolvidas numa terceira série, os compostos clorados **99** e **100** exibiram uma potente atividade antibacteriana contra *S. aureus* ATCC com valores de MIC de  $4 \mu\text{g/mL}$  e contra isolados clínicos resistentes à metilicina (MRSA) com valores de MIC de  $8 \mu\text{g/mL}$ . O isolamento dos enantiómeros de **99** revelou que apenas o **99a** com a configuração (1*S*, 4*R*) se mostrou ativo, indicando que a estereoquímica é crucial



para esta atividade. Comparando com o produto natural neofiscalin A (**28**), observou-se uma redução de duas vezes na MIC. Estes resultados excelentes e inspiradores obtidos no presente estudo mostram que compostos mais simples do que o **28** podem reter a atividade antimicrobiana.

Entre os 29 compostos da subclasse de alcalóides quinazolinonas estudados, os **78**, **82** e **99** demonstraram boa atividade antimalárica *in vitro* em *P. falciparum* (3D7). Estes compostos mostraram baixa citotoxicidade *in vitro* contra células de mamíferos não tumorais V79 ( $LD_{50} < 14 \mu M$ ) com índices de seletividade favoráveis ( $SI \geq 19$ ). Além disso, estes compostos não mostraram atividade hemolítica significativa em eritrócitos humanos saudáveis. As quinazolinonas **78**, **82** e **99** possuem características com potencial para o desenvolvimento de novos fármacos antimaláricos.

Doze aminocarbazóis foram sintetizados a partir de produtos naturais isolados, heptaflina (**57**) e seus derivados **62** e **63**, utilizando a reação de aminação redutora. Verificou-se que o tempo de reação para estas sínteses foi menor quando foi usado o dicloroetano como solvente. Esta série de derivados naturais e semi-sintéticos foi investigada quanto ao seu efeito no crescimento de células tumorais contendo p53 do tipo selvagem, células tumorais sem p53 e células com mutantes de p53. Os resultados preliminares mostraram que os produtos naturais **57**, **62** e **63** foram ativos em todas as linhas celulares investigadas ( $GI_{50} < 10 \mu M$ ) enquanto que os derivados semisintéticos 3 - (((4-fluorobenzil) amino) metil) -1- (3-metilbut-2-en-1-il)-9H-carbazol-2-ol (**117**) e 7-metoxi-1-(3-metilbut-2-en-1-il) -3- (piperidina- 1-ilmetil) -9H-carbazol-2-ol (**120**) mostraram um potente efeito inibidor apenas em linhas celulares com mutantes de p53 como a MDA-MB-468 e a A375, respectivamente.

Ao longo deste trabalho, foi estabelecida a relação estrutura-atividade e três compostos *hit* foram identificados: o **84** na atividade antitumoral, e o composto **99** e **78** na atividade antibacteriana e antimalárica, respectivamente. Essas descobertas ajudam a direcionar a investigação no futuro, considerando este *scaffold* valioso para a descoberta de novos fármacos. Do outro *scaffold* de alcalóides, os carbazoles semi-sintéticos **117** e **123** foram mais seletivos do que os produtos naturais isolados **57** e **62-63** na reativação de mutantes de p53.

## List of Figures

<b>Figure 1:</b> Natural products in drug development.....	5
<b>Figure 2:</b> Naturally isolated indole compounds <b>1-7</b> , indole containing approved drugs <b>5-12</b> and <b>14-15</b> , and indole drug candidates under clinical trials <b>13</b> and <b>16</b> . ....	7
<b>Figure 3:</b> The most prevalent major classes of quinazolinones and the structure of naturally-occurring febrifugine ( <b>17</b> ). ....	8
<b>Figure 4:</b> Some examples of naturally-occurring pyrazinoquinazolines <b>18-37</b> . ....	10
<b>Figure 5:</b> The components for model biosynthesis and synthesis of pyrazinoquinazoline alkaloids. ....	16
<b>Figure 6:</b> Carbazole alkaloid core ( <b>38</b> ) and murrayanine ( <b>39</b> ). ....	26
<b>Figure 7:</b> Structure of PhiKan083 ( <b>76</b> ), p53 restoring agent.....	40
<b>Figure 8:</b> Schematic representation of research work in this thesis. ....	42
<b>Figure 9:</b> (A) Overall SAR of quinazolinone alkaloids for antitumor, neuroprotection, antimicrobial, and antimalarial activities. (B) Synthetic challenges in the synthesis of this library of compounds.....	326
<b>Figure 10:</b> SAR of carbazole alkaloids for restoring p53 activity.....	328

## List of Tables

<b>Table 1:</b> Summary of sources and biological activities of naturally-occurring gyantrypine ( <b>18</b> ) and derivatives. ....	11
<b>Table 2 :</b> Summary of sources and biological activities of naturally-occurring fumiquinazolines. ....	12
<b>Table 3 :</b> Summary of the sources and biological activities of naturally-occurring fiscalins. ....	14
<b>Table 4:</b> Summary of sources and biological activities of tricyclic carbazole alkaloids. ....	27

## List of Schemes

<b>Scheme 1</b> : Natural product in drug development.....	17
<b>Scheme 2</b> : Approaches to the syntheses of the pyrazinoquinazoline alkaloids. ....	19
<b>Scheme 3</b> : Total synthesis of (+)-fumiquinazoline G ( <b>20</b> ). ....	20
<b>Scheme 4</b> : Total synthesis of (+)-fumiquinazoline G ( <b>20</b> ).. ....	21
<b>Scheme 5</b> : Total synthesis of fiscalin B ( <b>26</b> ), and epi-fiscalin B.....	22
<b>Scheme 6</b> : Total synthesis of gyantrypine ( <b>18</b> ), fumiquinazoline F ( <b>19</b> ), G ( <b>20</b> ), and fiscalin B ( <b>26</b> ) in the solution phase.. ....	24
<b>Scheme 7</b> : Microwave-assisted reaction synthesis of pyrazino[1,2-b]quinazoline-3,6-diones. ....	24
<b>Scheme 8</b> : Microwave synthesis of gyantrypine ( <b>18</b> ), fumiquinazoline F ( <b>19</b> ) and fiscalin B ( <b>26</b> )... ..	25
<b>Scheme 9</b> : Biosynthesis of 3-methylcarbazole ( <b>37</b> ) via anthranilic acid pathway.....	32
<b>Scheme 10</b> : Biosynthetic oxygenation and oxidation of 3-methylcarbazole ( <b>40</b> ).....	33
<b>Scheme 11</b> : Prenylation and cyclization of 2-hydroxy-3-methylcarbazole ( <b>54</b> ) and mukonal ( <b>55</b> )....	34
<b>Scheme 12</b> : Total synthesis of heptaphylline ( <b>57</b> ).. ....	35
<b>Scheme 13</b> : Total synthesis of heptaphylline ( <b>57</b> ) .....	35
<b>Scheme 14</b> : Total synthesis of heptaphylline ( <b>57</b> ) and 7-methoxyheptaphylline ( <b>62</b> ).....	36
<b>Scheme 15</b> : The total synthesis of 7-methoxymukonal ( <b>63</b> ). ....	37
<b>Scheme 16</b> : Semi-synthesis of heptaphylline ( <b>57</b> ) and 7-methoxyheptaphylline ( <b>62</b> ).. ....	38

## Abbreviations

Ant	Anthranilic acid/ $\beta$ -amino acid anthranilate
CAN	Cerium ammonium nitrate
ED <sub>50</sub>	Effective dose causing 50% of maximum effect
Fmoc	Fluorenylmethyloxycarbonyl
GI <sub>50</sub>	Concentration causing 50% of growth inhibitory effect
IC <sub>50</sub>	Concentration causing 50% of inhibitory effect
IUPAC	International union of pure and applied chemistry
K <sub>i</sub>	Inhibitory constant
LD <sub>50</sub>	Median lethal dose
MIC	Minimum inhibitory concentration
MNPs	Marine Natural Products
MRSA	Methicillin-resistant <i>Staphylococcus aureus</i>
NBS	<i>N</i> -Bromosuccinimide
NK-1	Neurokinase-1
NP	Natural Product
NRPS	Trimodular non-ribosomal peptide synthetases
P-gp	P-Glycoprotein
Py	Pyridine
R.t	Room temperature
SAR	Structure-activity relationship
SI	Selectivity index
THF	Tetrahydrofuran
Trp	Tryptophan

## **Outline of the Thesis**

The present thesis is structured in seven main parts:

### **Chapter 1: Introduction (theoretical background)**

In the first chapter, in section 1.1, a briefing about some key concepts concerning natural products (NPs) is presented; in section 1.2, heterocyclic indole alkaloid chemistry is presented and in section 1.3, quinazolinone alkaloids including their isolation, biosynthesis, and synthetic approaches are presented; some examples of simple quinazolinones such as glyantrypins, fumiquinazolines, and fiscalins are also detailed in this section. Section 1.4 concerns carbazole alkaloids and approaches to the molecular modifications performed in these NPs. Finally, the objectives of this thesis are also included in this chapter.

### **Chapter 2: Marine natural products as models to circumvent multidrug resistance (review article)**

In this chapter, a review of the marine natural products (MNPs) with antitumor and multidrug resistant reversing activity is presented. Structure-activity relationship (SAR) and synthetic approaches were highlighted, and the most potent natural products with important roles in circumventing multidrug resistance were emphasized.

### **Chapter 3: Antitumor activity of quinazolinone alkaloids inspired by marine natural products (original research article)**

This chapter brings up the original research concerning the synthesis and biological activities of quinazolinone alkaloid derivatives with different configurations at C-1 and C-4. Two different synthetic approaches were taken, and biological activities were investigated on the inhibition of growth of tumor cell lines and on modulatory activity of P-glycoprotein (P-gp).

#### **Chapter 4: Synthesis of new proteomimetic quinazolinone alkaloids and evaluation of their neuroprotective and antitumor effects (original research article)**

This chapter includes an original article on the synthesis of quinazolinone alkaloids with modifications at C-1 side chain and stereochemistry. The biological tests consisted on the growth of tumor cell lines evaluation and neuroprotective assays were also performed.

#### **Chapter 5: Synthesis and characterization of the antimicrobial activities of marine-derived indolymethyl pyrazinoquinazoline alkaloids (article in preparation)**

This chapter reports the synthesis of new quinazolinones, halogenated in the anthranilic acid moiety. The biological activities investigated were related to the antibacterial and antifungal activities, both in sensitive and resistant strains.

#### **Chapter 6: Exploring the pyrazino[2,1-b]quinazoline-3,6-dione scaffold as a promising antimalarial agent (article in preparation)**

This chapter contains the results of the original research describing the synthesis of quinazolinone containing indole alkaloids in which the moiety of the anthranilic acid was further modified in order to evaluate the antimalarial activity of this series of fiscalins.

#### **Chapter 7: Gram-scale synthesis of fiscalin B and chloro derivative (unpublished results)**

This chapter presents the gram-scale up synthesis of synthetic fiscalin B (**78**). The chapter highlights the chemical mechanisms of the developed reactions. Also, the gram-scale up synthesis of the most potent antimicrobial quinazoline compound **99** was achieved.

## **Chapter 8: Synthesis of small molecules of amino carbazoles and their effect on restoration of p53 activity (article in preparation)**

This chapter includes an article in preparation which describes the synthesis of amino carbazole alkaloids from natural isolated carbazoles and the investigation of their antitumor and p53 restoring activity.

## **Chapter 9: Overall discussion and conclusions**

This chapter presents the overall findings of the syntheses and biological activities developed in this thesis. The overall SAR is also proposed, and the main findings highlighted.

## **Chapter 10: References**

The references are presented at the end of this thesis. The references follow the American Chemical Society style guide.

## **Annexes**

This chapter includes a table with the chemical structures and IUPAC names of the quinazolinone and carbazole alkaloid derivatives presented throughout this thesis, as well as the numbering according to the thesis, chapters/research articles.



# Chapter 1

## Introduction



## 1.1 Natural products in drug development

Medicinal chemistry in the twenty-first century has undergone innovative changes because of the biotechnology and informatic revolutions <sup>1</sup>. These advances are mainly in the lead optimization process, but a very significant portion of these leads will continue to be molecules originated from natural products (NPs) <sup>2</sup>. This concept linking the origin of drugs and NPs are an important source for drug discovery and development providing new bioactive compounds <sup>2-4</sup>. The diversity of species of terrestrial plants, animals, microorganisms as well as marine organisms results in a multitude of secondary metabolites with diverse chemical structures which play a vital role in drug discovery and development processes, so that the number of small molecules and approved drugs from natural origin has been increasing (Figure 1, A and C) <sup>5</sup>.

To date, the relative ease access to plants has resulted in the discovery of a majority of plant-derived materials as NP-derived drugs, while microbial sources were especially important in the antibiotic area. Regarding marine natural products (MNPs), these constitute a major source of biologically active compounds that may serve themselves as significantly commercial entities or as lead structures for the development of modified derivatives with enhanced activity and/or reduced toxicity <sup>6</sup> and are expected to play an important role in drug discovery, especially given the impressive advances in organic synthesis <sup>4, 7-8</sup>. The latest research on MNPs has gradually increased over the years (Figure 1B). In 2017/2018, an increase of 23% could be noted from 2014, with approximately 28,500 new compounds from the sea being isolated and/or identified <sup>3, 9</sup>. These studies clearly demonstrate that the marine environment is a rich source of bioactive compounds mostly belonging to novel chemical classes not found in terrestrial sources <sup>2</sup>, raising the possibility of superior efficacy and specificity for the treatment of many health problems. MNPs are currently one of the richest sources of antioxidants, antitumors, antivirals, antiparasitics, antifungals, and antibacterials, in addition to other activities <sup>10-11</sup>. Compounds found in the marine ecosystem are mainly isolated from sponges, algae, fungi, invertebrate, gorgonians, bryophytes, cyanobacterial, bacteria, and related microorganisms <sup>9, 12</sup>. Until 2016, eight marine drugs have been accepted by the United States Food Drug Administration (US FDA) and European Medicines Agency (EMA) <sup>12-14</sup>. Recent examples of approved drugs originated from marine sources are ziconotide known as Prialt®, a non-narcotic analgesic drug, halichondrin B known as Halaven®, a breast anticancer agent, and brentuximab vedotin (SGN-35), an agent for the treatment of Hodgkin's lymphoma and anaplastic large cell lymphoma <sup>4</sup>. Despite these examples, difficulties have to be overcome, such as related with discovery processes, problems for culturing marine organisms and identifying novel compounds. As the new technologies are being

brought forward, including nanomole structure determination, sampling techniques, target identification, structure-activity relationship (SAR) and drug optimization efforts, the contribution of MNPs to the future pharmacopeia seems to be presently much more promising and product-oriented. Lead compounds from the sea show interesting qualitative biological activities, but there are limitations in producing suitable quantities to develop all the necessary assays. In order to obtain large scale supply required, microbial fermentation, biotechnology based on genome sequencing, and total chemical synthesis play significant roles <sup>13, 15</sup>. On the other hand, terrestrial environment has kept providing enormous new and known bioactive compounds in healthcare because of different geographies and diversities <sup>16</sup>.

Although, NPs are normally valuable lead compounds, the raise in clinical application has been hampered due to (i) structural diversity and complexity <sup>17</sup>, (ii) more sp<sup>3</sup> carbon and less hetero elements, and (iii) existence of stereogenic centers and stereochemistry. Fortunately, NPs are being chemically-tailored and modified through synthetic and semi-synthetic methods based on their structural and biological properties. The semi-synthetic approach is considered as fast and effective due to the usage of suitable precursors. The strategies for structural modification include removal of redundant atoms/groups (*i.e.* from halichondrin B to eribulin <sup>18</sup> and from schizandrin C to diphenyl bicarboxylate and bicyclol <sup>19</sup>) and eliminate chirality (*i.e.* from lovastatin to other statins such as simvastatin, fluvastatin, atorvastatin, and rosuvastatin <sup>20</sup>; from trichostatin A to vorinostat <sup>21</sup>), while retaining activity and the ability of generating patentable compounds. These strategies aim to increase potency and selectivity (*i.e.* from vancomycin to telavancin and dalbavancin <sup>22</sup>), improve physiochemical properties (*i.e.* from artemisinin to dihydroartemisinin, artemether, artesunate, and artether <sup>23</sup>), increase metabolic stability (*i.e.* from phlorizin to canagliflozin <sup>24</sup>), increase pharmacokinetic properties (*i.e.* from patupilone to ixabepilone <sup>25</sup>), and eliminate or reduce adverse effects by simplifying the structural complexity. In order to accomplish these multidimensional processes, sophisticated syntheses and skillful preparations of complicated molecules are essential.

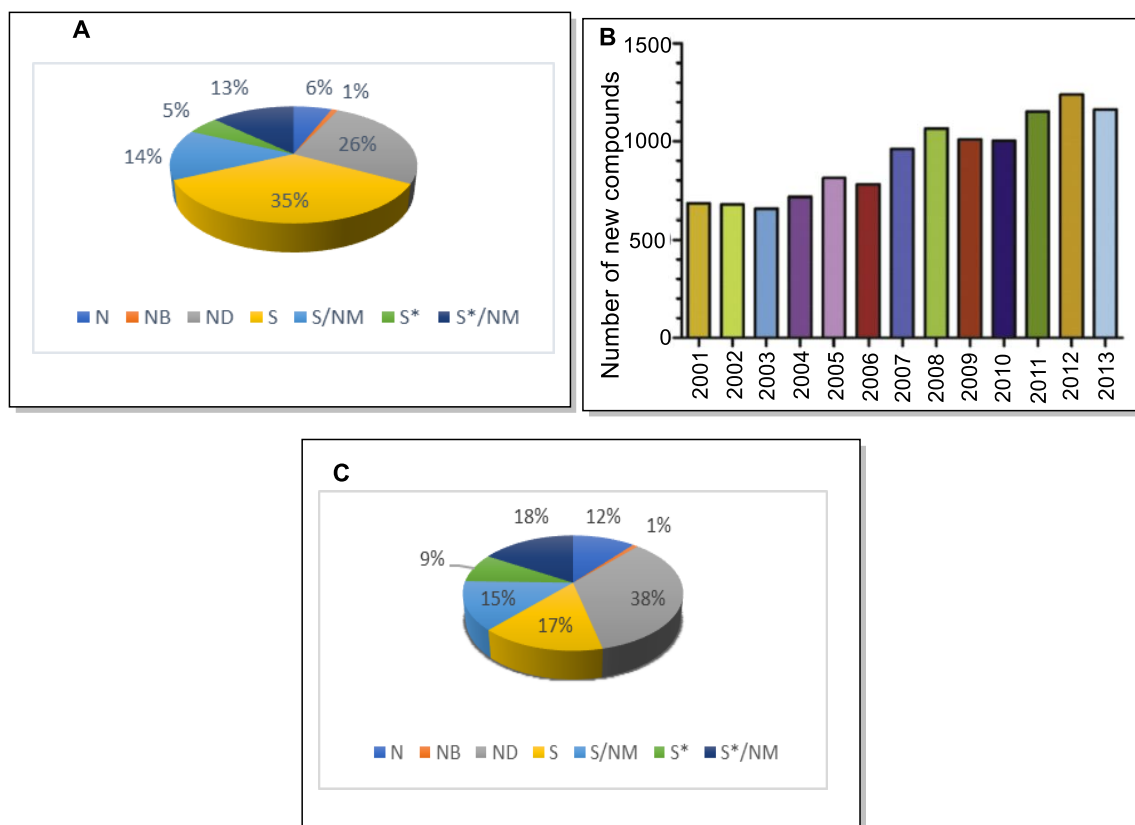


**Figure 1:** Natural products in drug development. (A) Approved small molecules from 1981 to 2014; (B) Number of new compounds isolated from marine organisms from 2001 to 2013, (C) Approved small molecule anticancer drugs from 1940-2014. N= Unaltered natural product, NB = Botanical drug, ND = Natural product derivative, S = Synthetic drug, S\*= Synthetic drug NP pharmacophore, /NM = Natural mimetic (adapted from <sup>4-5</sup>).

## 1.2 Heterocyclic compounds-indole alkaloids in drug chemistry

As a major class of NP discovered and used as 4000 year ago <sup>26</sup>, alkaloids and the species they are derived from, have been used worldwide as a source of remedies to treat a wide variety of diseases. With NPs as a whole, many have proposed differing classificatory schemes for alkaloids which divides this class into three categories: (1) true alkaloids: compounds which derived from amino acids and with an heterocyclic ring with nitrogen, (2) protoalkaloids: compounds in which the nitrogen atom is derived from an amino acid and is not a part of an heterocycle, and (3) pseudoalkaloids: compounds in which the basic carbon is not derived from amino acids.

Indole alkaloids, one of the largest classes of nitrogen-containing secondary metabolites, contain one or more indole/indoline moieties. They are widely found in plants, bacteria, fungi, and animals <sup>27</sup>. Most of indole precursors are related to L-tryptophan (Trp) (1, Figure 2), the most abundant indole-containing species of the cells <sup>26</sup>. Indole is a planar bicyclic molecule in which the phenyl ring

is fused through positions 2 and 3 of N-containing pyrrole ring. Indole (**2**, Figure 2), having 10  $\pi$ -electrons (8 from double bonds and 2 from the lone pair of electrons on nitrogen) is said to be aromatic in nature according to Huckel's rule. Due to the delocalization of excessive  $\pi$ -electrons, indole readily undergoes electrophilic substitution reactions, similar to a benzene ring. Indoles are very reactive with strong acids due to their weak basicity. Based on the molecular orbital calculations, the 3-position of indole has the highest electron density and it is the most reactive position for electrophilic substitution reaction. Since the N-H bond in indole is slightly acidic, it undergoes N-substitution reactions under basic conditions <sup>28-29</sup>.

Indole is a privileged structure known to bind to multiple receptors with a high affinity, resulting on its presence in a broad range of pharmacologically active molecules (Figure 2). As such, the exploration of these molecules in drug discovery is a rapidly emerging subject in medicinal chemistry, allowing medicinal chemists to discover biological active compounds, across a broad range of therapeutic areas, on a reasonable time scale <sup>30</sup>. Starting in the late 19<sup>th</sup> century, with the Fischer indole synthesis, to more recent times, hundreds of the synthetic pathways have been reported for the synthesis of biologically active indole derivatives. In addition to a large and diverse set of synthetic methods available to access indoles and their derivatives, this scaffold can also be commonly found and isolated from natural resources. For example, indole itself is one of the main constituents of coal tar, and the indole nucleus is also found in various NPs such as in *Cathaaranthus* alkaloids, which are well-established mitotic anticancer drugs (*i.e.* vincristine, **3**), and the marine alkaloid eudistomin K which has been proposed as a cytotoxic lead compound. Similarly, the antitumor alkylating agent antibiotic mitomycin C (**4**) contains an oxidized indole nucleus. Nowadays, there have been many more indoles added to the list of naturally-occurring alkaloids and many of these have important pharmacological activities. Indole alkaloids include such pharmacologically and structurally diverse compounds such as tryptophan (Trp, **1**); the recognition of the importance of Trp in animal and human nutrition plant hormones served to bring the renaissance in indole chemistry and therefore, indole derivatives have been synthesized and isolated from nature in abundance. Other remarkable examples are serotonin (**5**), one of the key neurotransmitters in animals, reserpine (**6**), that is used to lower blood pressure and reduce the heart rate and used as tranquilizer and sedative, and indol-3-acetic acid (**7**), a naturally plant growth hormone, known as heteroauxin. Thus, the privileged natural indole-class of compounds indicates that varying the substituents at different positions in the indole nucleus generates compounds with diverse biological actions. In addition, indole-containing compounds have been approved to be marketed (Figure 2) <sup>28</sup>. For example, indomethacin (**8**), a non-steroidal anti-inflammatory drug; pravadoline (**9**), used as analgesic and anti-inflammatory <sup>30</sup>; delavirdine (**10**), an human immunodeficiency virus-1 (HIV-1) antiretroviral agent <sup>31</sup>; yohimbine (**11**), for sexual dysfunction and

used to reduce risks of type-2 diabetes <sup>32</sup>; pinodolol (**12**), a  $\beta$ -blocker <sup>33</sup>; glufanide (**13**) or thymogen which is presently under clinical trials in patients suffering from ovarian cancer and hepatitis C virus <sup>34</sup>; apaziquone (**14**), an anticancer agent against non-muscle invasive bladder cancer <sup>35</sup>; arbidol (**15**), used for the treatment of influenza viral infections <sup>36</sup>; and panobinostat (**16**), an anti-leukemia drug tested against various cancer cell lines under various clinical trials <sup>37</sup>.

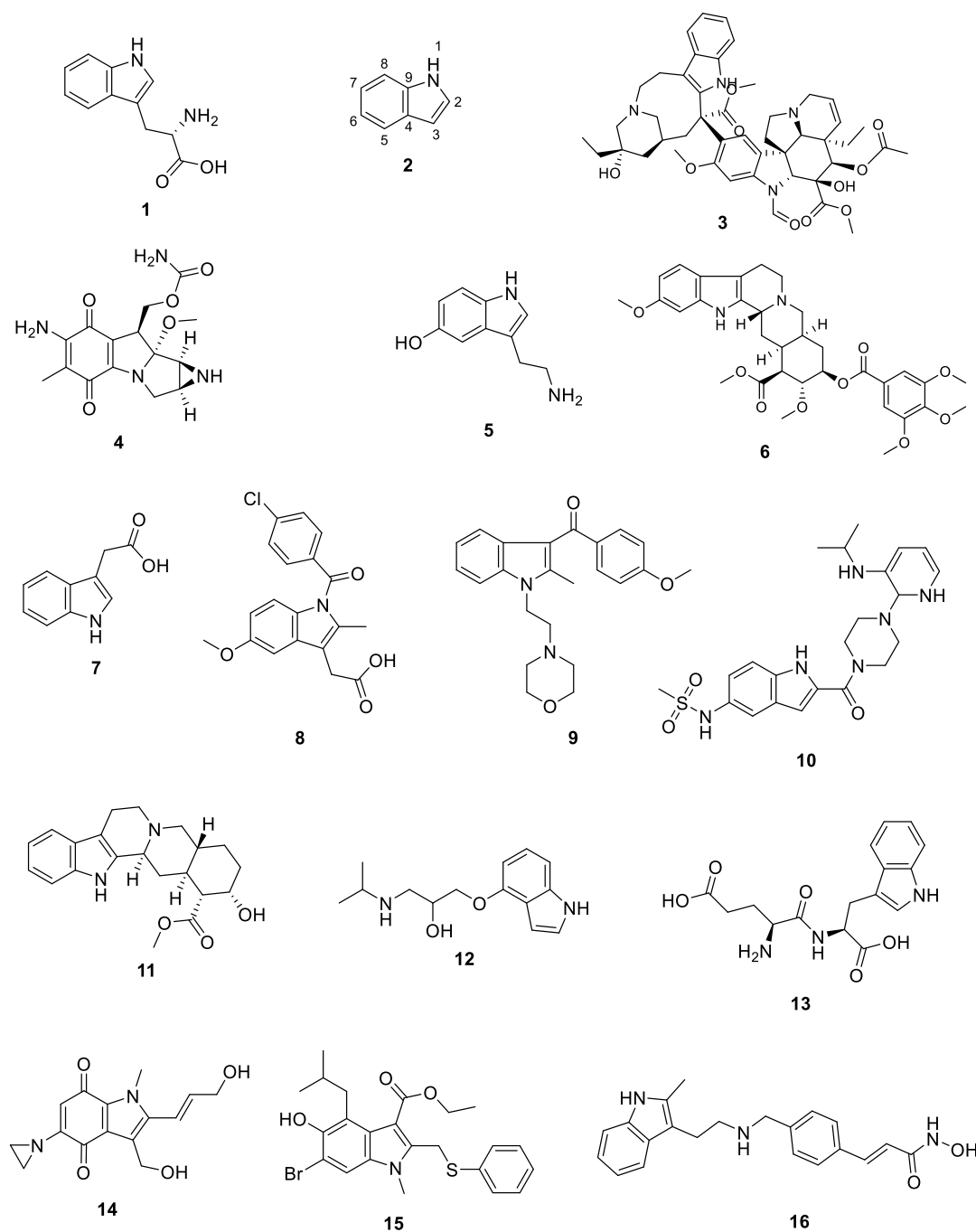


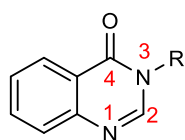
**Figure 2:** Naturally isolated indole compounds **1-7**, indole containing approved drugs **5-12** and **14-15**, and indole drug candidates under clinical trials **13** and **16**.

Considering the referred classes of alkaloids, two classes – protoalkaloids with quinazolinone containing indoles and pseudoalkaloids with carbazole alkaloids, are presented in this thesis.

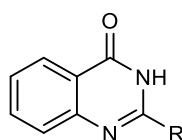
### 1.3 Quinazolinone alkaloids

#### 1.3.1 Chemistry of quinazolinones

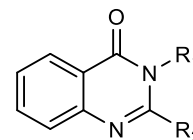
Quinazolinones are heterocyclic compounds that are of considerable interest because of their diverse range of biological activities. The quinazolin-4(3*H*)-one and its derivatives constitute an important class of fused heterocycles that are found in more than 200 naturally-occurring alkaloids. This fused bicyclic compound was earlier known as benzo-1,3-diazine. This is considered a privileged structure integrating important pharmacophores<sup>38</sup>. Quinazolinones are mainly subdivided in four major classes: 4-(3*H*)quinazolinones (2-substituted, 3-substituted, and 2,3-disubstituted), and 2-(1*H*)quinazolinones (Figure 3). One subclass of 2,3-disubstituted quinazolinones is the pyrazinoquinazoline scaffold, which comprises quinazolinones with a fused piperazine system linked to an indole moiety. So far, approximately 80 secondary metabolites of this subclass, covering structurally diverse compounds, have been isolated from fungi mainly of the genera *Penicillium*, *Aspergillus*, and *Neosartorya*<sup>39</sup>.



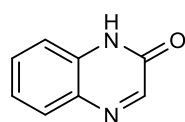
3-substituted-4(3*H*)-quinazolinone



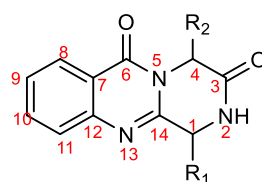
2-substituted-4(3*H*)-quinazolinone



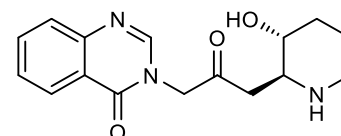
2,3-disubstituted-4(3*H*)-quinazolinone



2(1*H*)-quinazolinone



pyrazinoquinazoline scaffold



17, Febrifugine

**Figure 3:** The most prevalent major classes of quinazolinones and the structure of febrifugine (17).



### 1.3.2 Isolation and biological activities of pyrazinoquinazoline alkaloids containing indole

Quinazolinone is considered a building block of naturally-occurring alkaloids isolated from a number of plants, animals, and microorganisms <sup>40</sup>. Their derivatives gain interest in medicinal chemistry since the disclosure of the structure of quinazolinone alkaloid, 3- $[\beta$ -keto- $\gamma$ -(3-hydroxy-2-piperidyl)-propyl]-4-quinazolone, or febrifugine (**17**), an ingredient of a traditional Chinese herbal remedy, showed to be effective against malaria in 1950 <sup>41</sup>. In search of additional potential quinazolinone-based drugs, various substituted quinazolinones have been synthesized. A well-known example of a synthetic derivative is methaqualone, a sedative-hypnotic therapeutic drug <sup>42</sup>, triggering the research activities toward isolation, synthesis, and studies on the pharmacological properties of quinazolinones and related compounds.

The structural diversity of quinazolinones has been broadened with the discovery of pyrazinoquinazoline alkaloids <sup>43</sup> which can be divided into several groups, as depicted in Figure 4, based on the different types of amino acids at C-1 (glycine, alanine, valine, serine, dehydroalanine) and constituents of Trp moiety at position C-4, both linked to the nonproteinogenic anthranilic acid (Ant): i) glyantrypine (**18**) and analogues, ii) fumiquinazolines **19-25**, iii) fiscalins **26-29**, iv) ardeemins ((-)-5-*N*-acetyl-15 $\beta$ -didehydroardeemin (**30**)), v) aniquinazolines and neosartoryadins (anaquinaziline D (**31**)), neosartoryadin A (**32**) and derivatives, vi) cottoquinazolines (cottoquinazoline E (**33**)), vii) versiquinazoline (**34**) and derivatives, viii) fumigatosides (fumigatoside A, **35**), ix) spiroquinazoline (**36**) and derivatives, and scedapin (scedapin C, **37**). Following, a summary of the first three classes of quinazolinone alkaloids related to this thesis are presented, since these and the other classes have been recently reviewed <sup>39</sup>.

From a medicinal chemistry perspective, glyantrypines, fumiquinazolines, and fiscalins structures have attractive features as prototypes to pursue the discovery of potential drug candidates due to their chemical complexity and described biological activities. Nevertheless, few reports on molecular modifications to these classes of natural products have been described until now.

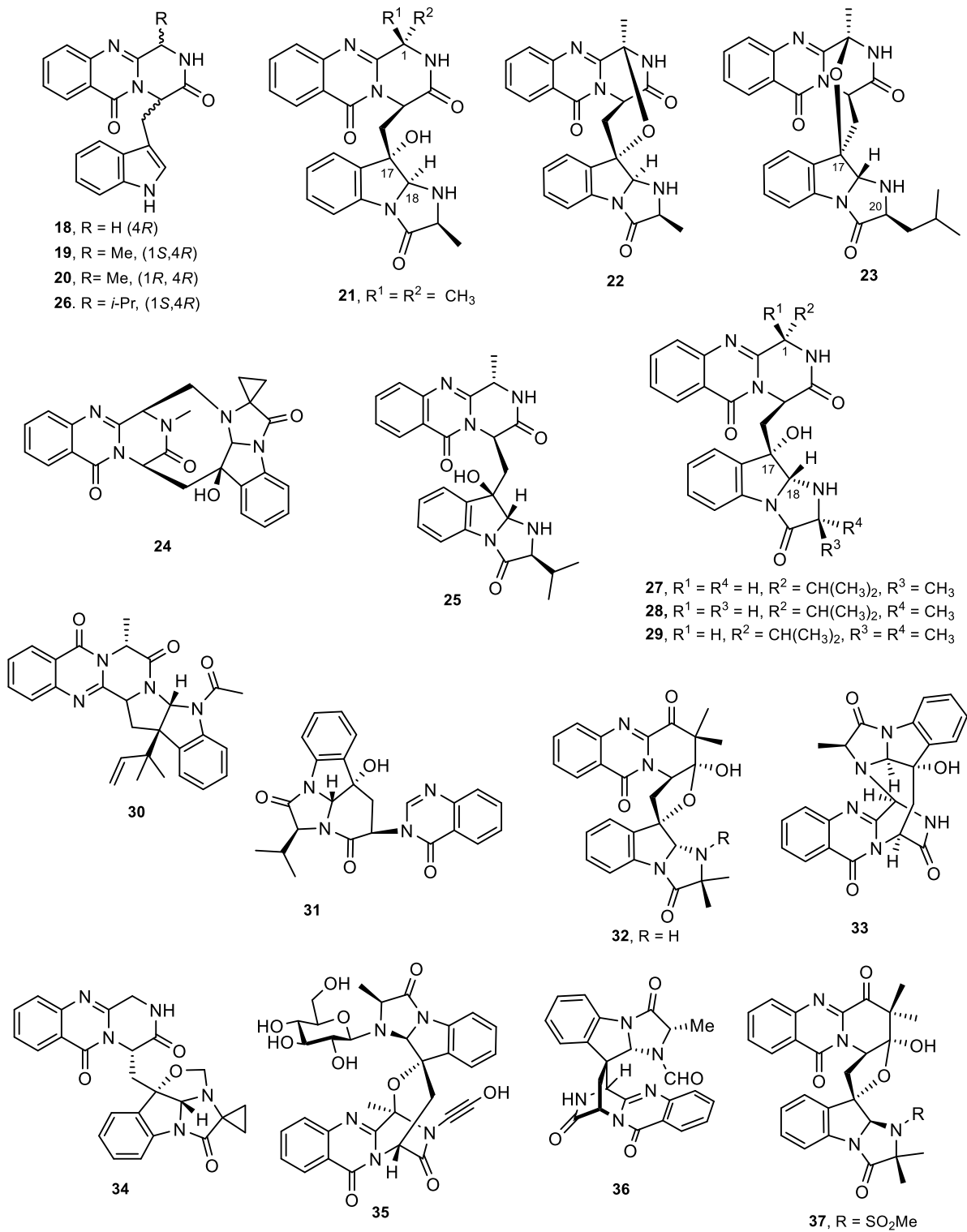


**Figure 4:** Some examples of naturally-occurring pyrazinoquinazolines 18-37.

### 1.3.2.1 Gyantrypines and derivatives

The simplest derivative containing an hydrogen atom at position C-1 is gyantrypine (**18**) being isolated from *Aspergillus clavatus* <sup>44</sup>, *Penicillium expansum* Y32 <sup>45</sup>, *P. amametzoides* AS53 <sup>46</sup>, *Cladosporium* sp. PJX-41 <sup>47</sup>, and *A. versicolor* LCJ-5-4 <sup>48</sup>, and described to display moderate activity against aqua-pathogenic bacterial *Vibrio harveyi* <sup>45</sup>. The derivatives such as 3-hydroxygyantrypine and oxogyantrypine have also been isolated <sup>47</sup> (differing from gyantrypine (**18**) by an additional carbonyl group at C-1) and described as active against influenza A virus (H1N1) <sup>44,47</sup>. The SAR studies of this series of compounds reveal that the presence of a hydroxyl group at position C-1 does not affect the anti-H1N1 activity, and the presence of the carbonyl group has a crucial role in anti-H1N1 activity. The configuration of C-4 also showed to be important with the *S* enantiomers of oxogyantrypine exhibiting stronger anti-H1N1 effect compared to the compounds with *R* configuration (Table 1).

**Table 1:** Summary of sources and biological activities of naturally-occurring gyantrypine (**18**) and derivatives.

Compounds	Sources	Biological Activities	Ref.
Gyantrypine ( <b>18</b> )	<i>Aspergillus clavatus</i>	Weakly active against Influenza A virus	44-47
	<i>Cladosporium</i> sp. PJX-41	(H1N1) (IC <sub>50</sub> = 100-150 μM)	
	<i>Penicillium adametzoides</i> AS-53	Moderate inhibitory activity against bacterial <i>V. harveyi</i> (MIC = 32 μg/mL)	
	<i>P. expansum</i> Y32	No vasculogenetic effect in a live zebrafish model	
3-Hydroxygyantrypine	<i>Cladosporium</i> sp. PJX-41	Weakly active against Influenza A virus (H1N1) (IC <sub>50</sub> = 100-150 μM)	47
(-)-Oxogyantrypine	<i>Cladosporium</i> sp. PJX-41	Strong anti-H1N1 activity (IC <sub>50</sub> = 85 μM)	47
(+)-Oxogyantrypine	<i>Cladosporium</i> sp. PJX-41	Weakly active against Influenza A virus (H1N1) (IC <sub>50</sub> = 100-150 μM)	47

IC<sub>50</sub> = Concentration causing 50% inhibitory effect, MIC= Minimum inhibitory concentration.

### 1.3.2.2 Fumiquinazolines

Fumiquinazolines have more complex structures compared to gyantrypine derivatives. Their structures include a methyl group at position C-1, and it can be presented as gyantrypine-like structure (fumiquinazoline F (**19**), and G (**20**)) <sup>49</sup>, or fused with a simple pyrrolidinone ring system

(fumiquinazoline A (**21**))<sup>49</sup>, or with more complex spiro moieties (fumiquinazoline C (**22**) and H (**23**))<sup>50</sup>. The first report on isolation of the metabolites fumiquinazoline A-G was from the fungal strain *A. fumigatus* from *Pseudolabrus japonicas*<sup>51-52</sup>. After disclosing the structures of these compounds, many fumiquinazolines derivatives have been isolated from a variety of fungi as described in Table 2. One of the members of fumiquinazolines, fumiquinazoline K (**24**), presented a rare 1-aminocyclopropane-1-carboxylic amino acid residue. The names of some fumiquinazolines were revised due to the source of isolation, *i.e.*, fumiquinazoline Q was named as fumiquinazoline K (**24**) after isolation from the soft coral (*Sinularia* sp.)-associated fungus *A. fumigatus* KMM 4631, and fumiquinazoline R was named as fumiquinazoline L after isolation from gorgonian-derived fungus<sup>53</sup>. In fact, fumiquinazoline Q and R are the same compound. Until now, there are approximately 20 fumiquinazolines, being fumiquinazoline S (**25**) the latest described fumiquinazoline, isolated from a solid-substrate culture of *Aspergillus* sp. collected from marine-submerged wood<sup>54</sup>. These derivatives showed antibacterial, antitumor, antifungal, and antiinsectan activities. The summary of fumiquinazoline members is presented in Table 2.

**Table 2** : Summary of sources and biological activities of naturally-occurring fumiquinazolines.

Compounds	Sources	Biological Activities	Ref.
Fumiquinazoline A ( <b>21</b> )	<i>Aspegillus fumigatus</i>	Moderate cytotoxicity against P-388 cells	
	<i>A. fumigatus</i> (H1-04)	(ED <sub>50</sub> = 6.1 µg/mL)	51-52,
	<i>A. sydowii</i> (SCSIO 00305)	Inhibitor of tsFT210 cell proliferation	55-57
3-Hydroxyfumiquinazoline A	<i>Penicillium lanosum</i> (MYC-1813)	Not known	58
Fumiquinazoline B	<i>A. fumigatus</i>	Moderate cytotoxicity against P-388 cells	51-52,
	<i>A. sydowii</i> (SCSIO 00305)	(ED <sub>50</sub> = 16.0 µg/mL)	55-56
Fumiquinazoline C ( <b>22</b> )	<i>A. fumigatus</i>	Moderate cytotoxicity against P-388 cells	51-52,
	<i>A. fumigatus</i> (H1-04)	(ED <sub>50</sub> = 52.0 µg/mL)	56-57,
	<i>A. sydowii</i> (SCSIO 00305)	Inhibitor of P388, HL60, A-549, and BEL-7402 and tsFT210 cell proliferation	59
2'- <i>epi</i> -Fumiquinazoline C	<i>P. lanosum</i> (MYC-1813)	Antiinsectan activity against the fall armyworm <i>Spodoptera frugiperda</i> (57% reduction in growth rate)	58
Fumiquinazoline D	<i>A. fumigatus</i>	Moderate cytotoxicity against P-388 cells	52, 55-
	<i>A. sydowii</i> (SCSIO 00305)	(ED <sub>50</sub> = 13.5 µg/mL)	56, 60
2'- <i>epi</i> -Fumiquinazoline D	<i>A. fumigatus</i> (LN-4)	Good antifungal activity (MIC = 12.5–50 µg/mL)	61

Compounds	Sources	Biological Activities	Ref.
Fumiquinazoline E	<i>A. fumigatus</i>	Moderate cytotoxicity against P-388 cells (ED <sub>50</sub> = 13.8 µg/mL)	52
2'- <i>epi</i> -Fumiquinazoline C	<i>P. corylophilum</i> Dierckx <i>A. fumigatus</i> <i>A. fumigatus</i> (H1-04) <i>Aspergillus</i> . spp (F452) <i>Neosartorya pseudofischeri</i> <i>P. thymicola</i> <i>A. sydowii</i> (SCSIO 00305)	Antimicrobial activity against <i>Micrococcus luteus</i> (MIC = 99 µg/mL) and <i>Staphylococcus aureus</i> (MIC = 137 µg/mL) Moderate cytotoxicity against P-388 cells (ED <sub>50</sub> = 14.6 µg/mL) Inhibitor of tsFT210 cell proliferation Weak inhibition against <i>Bacillus subtilis</i> (MIC = 50 µM) Weak inhibition against Na <sup>+</sup> /K <sup>+</sup> -ATPase (IC <sub>50</sub> = 17 µM)	52, 54, 56-57, 62-65
Fumiquinazoline F (19)	<i>A. fumigatus</i> <i>A. sydowii</i> (SCSIO 00305) <i>A. fumigatus</i> (H1-04)	Moderate cytotoxicity against P-388 cells (ED <sub>50</sub> = 17.7 µg/mL) Inhibitor of tsFT210 cell proliferation	52, 56
2'- <i>epi</i> -Fumiquinazoline D	<i>Acremonium</i> sp.	Weak activity toward <i>Candida albicans</i>	50
Fumiquinazoline E	<i>Acremonium</i> sp.	Weak activity toward <i>C. albicans</i>	50
Fumiquinazoline F (19)	<i>A. fumigatus</i> (H1-04)	Inhibitor of P388, HL60, A-549, and BEL-7402 and tsFT210 cell proliferation	57
Fumiquinazoline G (20)	<i>Aspergillus</i> sp. <i>A. fumigatus</i>	No cytotoxicity against L5178Y Moderate cytotoxicity against P-388 cell line	49
Fumiquinazoline H (23)	<i>Aspergillus</i> . sp. <i>Aspergillus</i> . sp. (F452)	No cytotoxicity against L5178Y Weak inhibition against Na <sup>+</sup> /K <sup>+</sup> -ATPase (IC <sub>50</sub> = 20 µM)	66
Fumiquinazoline I	<i>Aspergillus</i> . sp.	No cytotoxicity against L5178Y	49
Fumiquinazoline J	<i>Aspergillus</i> . sp.	No cytotoxicity against L5178Y	49
Fumiquinazoline K (24)	<i>Aspergillus</i> . sp.	No cytotoxicity against L5178Y	49
Fumiquinazoline L	<i>Aspergillus</i> . sp.	No cytotoxicity against L5178Y	49
Fumiquinazoline M	<i>A. fumigatus</i> (KMM 4631)	No activity against <i>S. aureus</i> , <i>B. cereus</i> , <i>Escherichia coli</i> , <i>Pseudomonas aeruginosa</i> and <i>C. albicans</i>	66
Fumiquinazoline N	<i>Scopulariopsis</i> sp. (TA01-33)	Weak antibacterial activity against <i>B. subtilis</i> , <i>S. albus</i> , and <i>Vibrio parahaemolyticus</i> (MIC = 50 µM)	53
Fumiquinazoline S (25)	<i>Aspergillus</i> . sp. (F452)	Weak inhibition against Na <sup>+</sup> /K <sup>+</sup> -ATPase (IC <sub>50</sub> = 34 µM)	54

ED<sub>50</sub> = Effective dose causing 50% of maximum effect, IC<sub>50</sub> = Concentration causing 50% inhibitory effect, MIC= Minimum inhibitory concentration.

### 1.3.2.3 Fiscalins

Fiscalins have structures similar to gyantrypines and fumiquinazolines. The only difference between these groups is the substituents at C-1: while gyantrypines have an hydrogen atom and fumiquinazolines have a methyl group, fiscalins have an isopropyl group at the corresponding carbon. Some fiscalins display a gyantrypine-like structure, such as fiscalin B (**26**), others are fused with a pyrrolidinone ring system, like fiscalin A (**27**), neofiscalin A (**28**), and fiscalin C (**29**). Fiscalin A (**27**), B (**26**), and C (**29**) were firstly isolated from *Neosartorya fischeri* in 1993<sup>67</sup>. The spectroscopic and amino acids analyses disclosed that these three compounds contain an indolyl moiety linked to an Ant derived tricyclic system. Fiscalin A (**27**) and fumiquinazoline A (**21**) have similar features. Both compounds have in common the methyl imidazolone ring resulting from the coupling of indole nitrogen with alanine (Ala) an oxidative cyclization reaction. The only difference in both compounds is in the pyrazinoquinazolinone ring, with an isopropyl or a methyl group on C-1 of the pyrazine ring in fiscalin A (**27**) or fumiquinazoline A (**21**), respectively. The stereochemistry at C-18 is also different, being 18*R* in fiscalin A (**27**), and 18*S* in fumiquinazoline A (**21**)<sup>68</sup>. Recently, several other members of fiscalins were isolated from other fungi such as *Neosartorya siamensis* (KUFC 6349)<sup>69</sup> and *Xylaria humosa*<sup>70</sup> and evaluated for their biological activities. Fiscalin derivatives have been reported to be substance P antagonists, antibacterial, and antitumor agents. A summary of fiscalins derivatives and their biological activities is presented in Table 3.

**Table 3** : Summary of the sources and biological activities of naturally-occurring fiscalins.

Compounds	Sources	Biological Activities	Ref.
Fiscalin A ( <b>27</b> )	<i>Neosartorya fischeri</i> <i>N. siamensis</i> (KUFC 6349) <i>N. siamensis</i> (KUFA 0017) <i>Xylaria humosa</i>	Substance P inhibitor to NK-1 receptor ( $K_i = 57$ $\mu$ M)	67, 69, 71-73
<i>epi</i> -Fiscalin A	<i>N. siamensis</i> (KUFC 6349) <i>N. siamensis</i> (KUFA 0017) <i>X. humosa</i>	Weak cytotoxicity against MCF-7 cells ( $IC_{50} = 24.4$ $\mu$ g/mL)	69, 71- 73
Neofiscalin A ( <b>28</b> )	<i>N. siamensis</i> (KUFC 6349)	Potent antibacterial activity against <i>S. aureus</i> and <i>Enterococcus faecalis</i> (MIC = 8 $\mu$ g/mL)	69, 74- 75
<i>epi</i> -Neofiscalin A	<i>N. siamensis</i> (KUFC 6349) <i>N. siamensis</i> (KUFA 0017)	Not known	69, 72- 73
Fiscalin B ( <b>26</b> )	<i>N. fischeri</i> <i>Dichotomomyces cejprii</i> (BRF082)	Substance P inhibitor to NK-1 receptor ( $K_i = 174$ $\mu$ M)	67, 76- 78

Compounds	Sources	Biological Activities	Ref.
Fiscalin C (29)	<i>Corynascus setosus</i>		
	<i>N. fischeri</i>	Substance P inhibitor to NK-1 receptor ( $K_i = 68$ $\mu\text{M}$ )	69, 71
	<i>N. udagawae</i> (HDN13-313)		75-76
	<i>X. cf. cubensis</i> (PK108)	Weak cytotoxicity ( $\text{IC}_{50} = 21$ $\mu\text{g/mL}$ )	81-82
epi-Fiscalin C	<i>N. siamensis</i> (KUFC 6349)	Potential adjuvant in antimicrobial combined therapeutics	
	<i>X. cf. cubensis</i> (PK108)	Weak cytotoxicity against MCF-7 cells ( $\text{IC}_{50} = 21$ $\mu\text{g/mL}$ )	69, 71-
	<i>N. siamensis</i> (KUFC 6349)		73, 79
	<i>N. siamensis</i> (KUFA 0017)		
Fiscalin E	<i>X. humosa</i>		
	<i>N. udagawae</i> (HDN13-313)	No cytotoxicity against HL-60 cancer cell line ( $\text{IC}_{50} > 50$ $\mu\text{M}$ ) No antiviral activity against H1N1	80
Fiscalin F	<i>N. udagawae</i> (HDN13-313)	No cytotoxicity against HL-60 cancer cell line ( $\text{IC}_{50} > 50$ $\mu\text{M}$ ) No antiviral activity against H1N1	80
Cladoquinazoline	<i>Cladosporium</i> sp. PJX-41	Weakly active against Influenza A virus (H1N1) ( $\text{IC}_{50} = 100\text{-}150$ $\mu\text{M}$ )	47
epi-Cladoquinazoline	<i>Cladosporium</i> sp. PJX-41	Weakly active against Influenza A virus (H1N1) ( $\text{IC}_{50} = 100\text{-}150$ $\mu\text{M}$ )	47
Norquinadoline A	<i>Cladosporium</i> sp. PJX-41	Anti-H1N1 activity ( $\text{IC}_{50} = 82$ $\mu\text{M}$ )	47
Quinadoline A	<i>Cladosporium</i> sp. PJX-41	Weakly active against Influenza A virus (H1N1) ( $\text{IC}_{50} = 100\text{-}150$ $\mu\text{M}$ )	47

NK-1= Neurokinase-1,  $K_i$  = Inhibitory constant,  $\text{IC}_{50}$  = Concentration causing 50% inhibitory effect, MIC= Minimum inhibitory concentration.

### 1.3.3 Biosynthesis of quinazolinones

The pyrazino[2,1-*b*]quinazoline-3,6-dione core is assembled through the condensation of the  $\beta$ -amino acid anthranilate (Ant), tryptophan (Trp), and additional amino acids as shown in Figure 5.

Many of the pyrazinoquinazolinones are biosynthesized by the trimodular non-ribosomal peptide synthetase (NRPSs) which consists of adenylation (A), peptide carrier protein (PCP)/thiolation (T), and condensation (C) domains arranged in repeating units that assemble non-ribosomal peptides (NRP) by activating and joining amino acid building blocks. There are some variations on NRPSs at C domain responsible for epimerization (E), heterocyclization domains and specific domains for *N*-methylation or formylation being the most common. The general process of building peptidyl backbone

begins with A-domain-catalyzed activation of Ant to the corresponding anthranilyl-adenosine monophosphate (AMP) during phosphorylation.

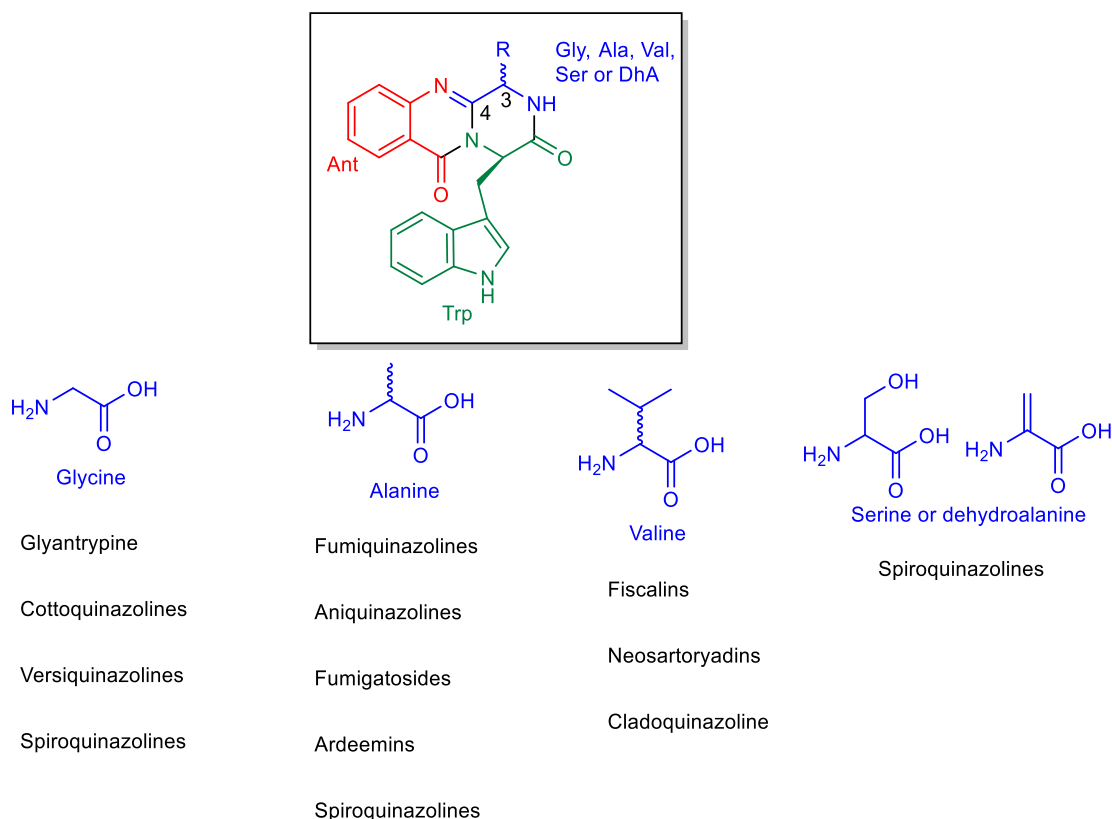
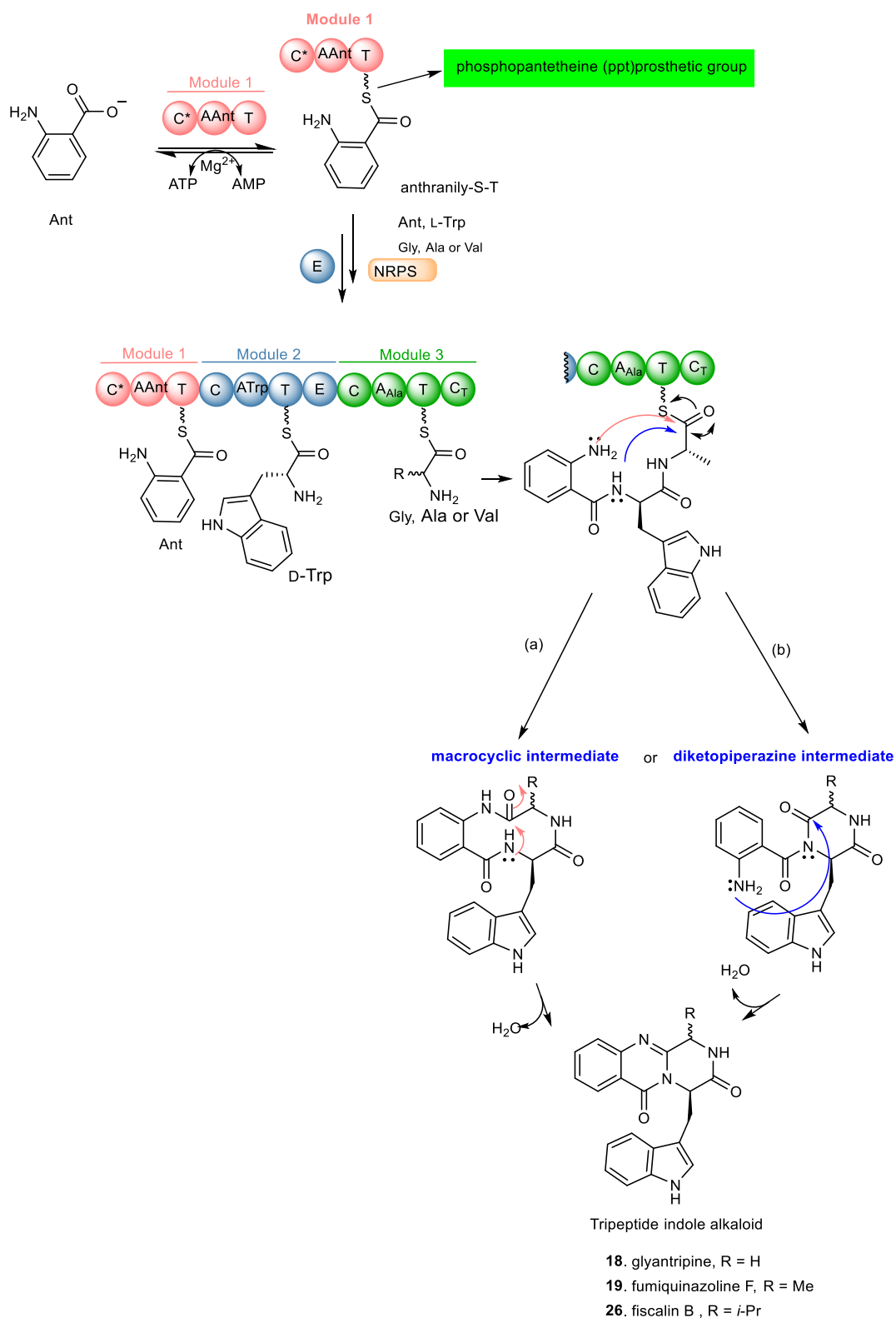


**Figure 5:** The components for model biosynthesis and synthesis of pyrazinoquinazoline alkaloids.

This domain mediates the attachment to the 4'-phosphonantethine (PPT) prosthetic arm of the T-domain, forming an acylthioester intermediate (Scheme 1). The anthranilate is always the first amino acid to be incorporated by the trimodular NRPS in module one, and usually Trp in module two being the third amino acid in module three. The Trp-activating module has an embedded epimerization domain, presumably to convert the L-Trp-S-T domain thioester into a mixture of D- and L-isomers. The condensation of the third amino acid gives a linear tripeptidyl acyl thioester tethered to the T-domain (Scheme 1). This domain catalyzes the cyclization and the release of the tripeptide either through the formation of a ten-membered macrolactam, that upon intramolecular cyclization yields the pyrazino[2,1-*b*]quinazoline-3,6-dinone core via intramolecular formation (a) or an Ant-diketopiperazine (b), followed by cyclization and dehydration to form the molecules of the referred alkaloids.





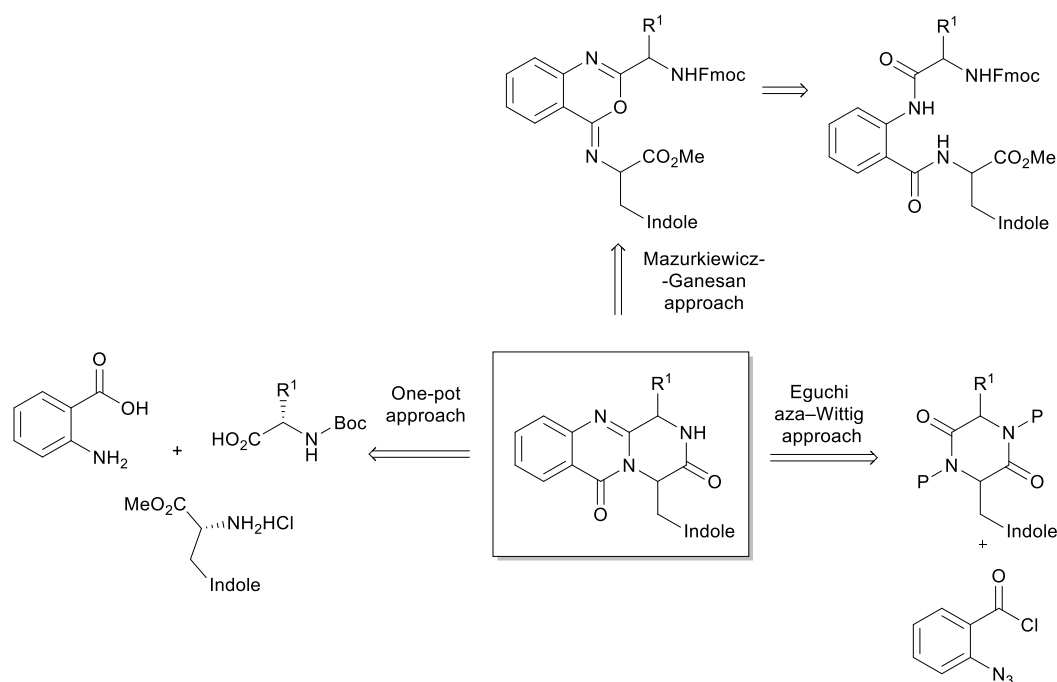
**Scheme 1** : Biosynthesis of **18**, **19**, **26**. Anthranilate activation (by adenylation (A), and anthranilyl transfer by thiolation (T) by the NRPS module 1 and the biosynthesis of tripeptide indole alkaloids. C = condensation domain, C<sub>T</sub> = Thioester domain, E= epimerization domain, T = Thiolation domain, Ala = Alanine, Gly = Glycine, Val = Valine, ATP = Adenosine triphosphate, AMP = Adenosine monophosphate.

### 1.3.4 Synthesis of quinazolinones

The chemistry of quinazolinone alkaloids is well documented in several comprehensive reviews and monographs and it is continuously updated in Natural Product Reports<sup>81-82</sup>. Recently from our research group, Resende *et al.*<sup>39</sup> published a review on the chemistry of quinazolinone containing alkaloids. The review represented the isolation, bioactivities, and synthesis of naturally-occurring quinazolinone alkaloids isolated from the last two decades with an emphasis on classical methods for their synthesis. Herein, these methods are briefly summarized due to their importance within the scope of this thesis.

The main synthetic routes to obtain quinazolinone compounds use 2-aminobenzoic acid (anthranilic acid, Ant) or its derivatives, 2-aminobenzamide, 2-aminobenzonitrile, isatoic anhydride, 2-carbomethoxyphenyl isocyanate, *N*-arylnitrilium salt, or 4*H*-3,1-benzoxazinone as precursors. Other important methods include coupling of *o*-methylbutyrolactam with Ant, cycloaddition of Ant iminoketene with methylbutyrolactam (via sulphonamide anhydride), reactions of Ant derivatives with a wide range of substrates including imidates (carboximidate) and imino halides, reaction of Ant and the appropriately substituted imidate in a facile one-pot procedure, and microwave-promoted reaction of Ant with amine and formic acid (or its *ortho* ester) and isatoic anhydride.

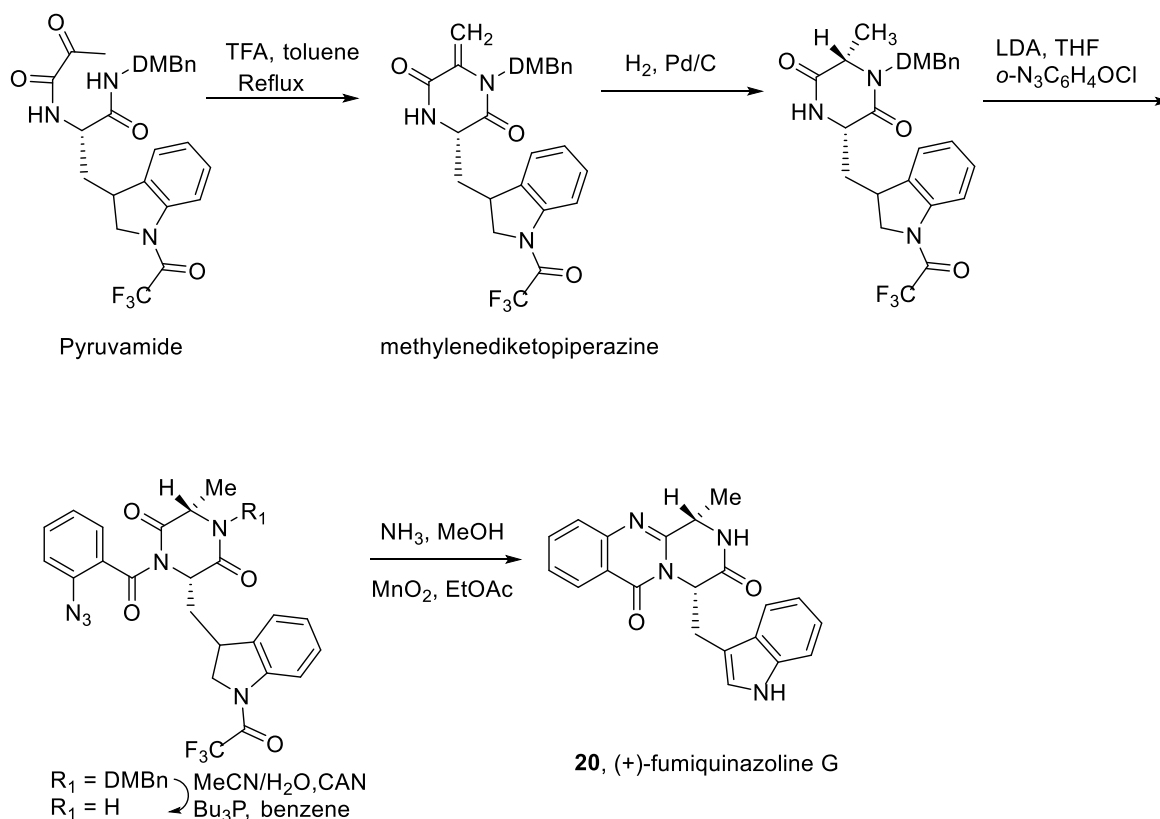
Although there are several approaches for the synthesis of compounds containing this kind of core structure<sup>83-89</sup>; the methodologies used to their syntheses are based on two main general approaches: i) the Eguchi-aza Wittig<sup>90-92</sup> that consists in a selective acylation of diketopiperazines with *o*-azido benzoyl chloride, followed by cyclization, and ii) the Mazurkiewicz-Ganesan approach<sup>93</sup> which involves a two-step sequence from linear dipeptide through isomerisation of 4-imino-4*H*-3,1-benzoxozines to the quinazoline-4-ones (Scheme 2)<sup>94-95</sup>. Additionally, a third approach, by a highly efficient three-component one-pot methodology promoted by microwave irradiation, was also reported by Liu *et al.*<sup>96</sup> for the total syntheses of gyantrypine (**18**), fumiquinazoline F (**19**), and fiscalin B (**26**).



**Scheme 2:** Approaches to the syntheses of the pyrazinoquinazoline alkaloids.

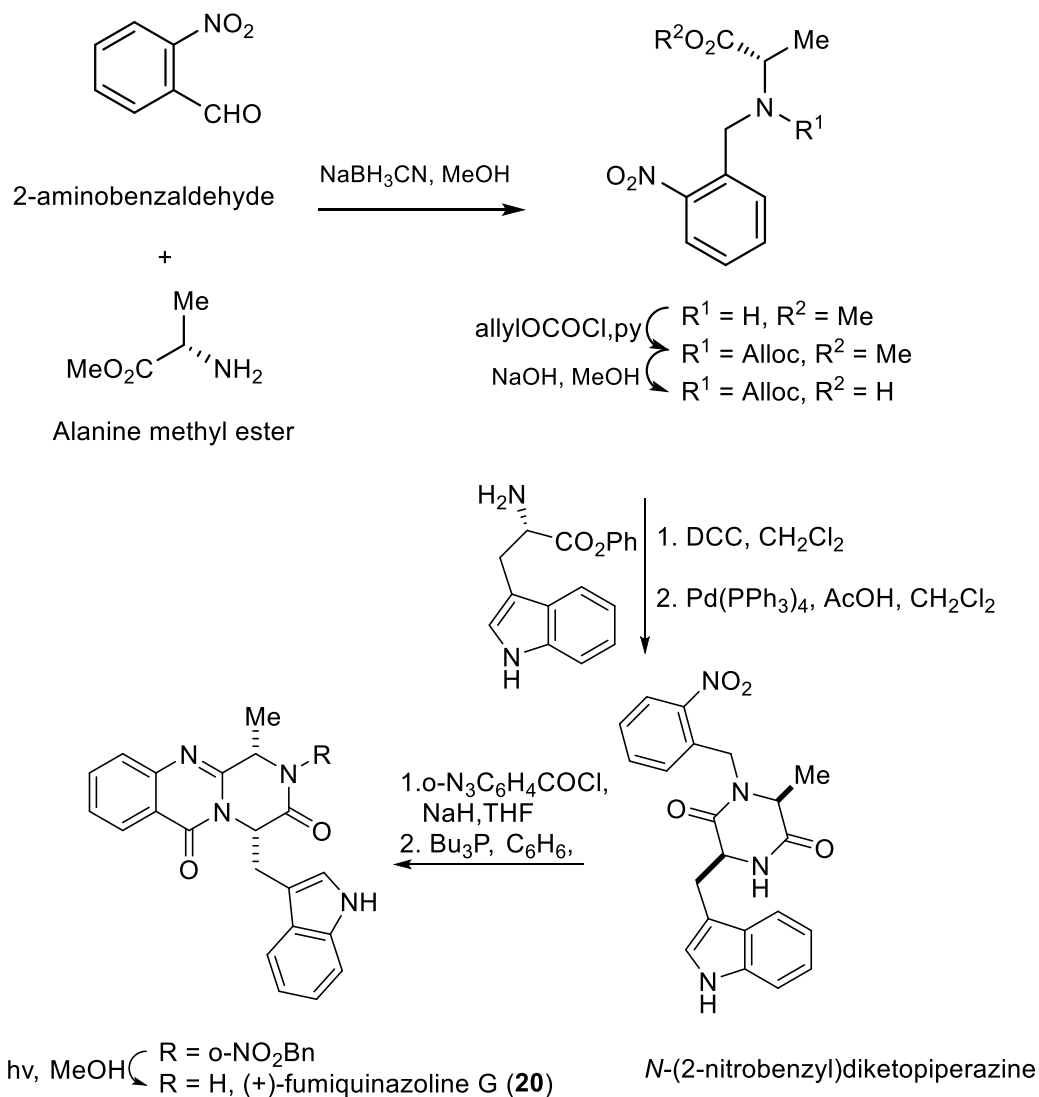
### 1.3.4.1 Eguchi-aza Wittig approach

Quinazolinone alkaloids like (+)-fumiquinazoline G (**20**) and (+)-dehydrofumiquinazoline were first synthesized by He and Snider in 1997<sup>97</sup>, using the Eguchi's procedure to accomplish the annulation of the quinazoline-4-one onto an amide (Scheme 3). The total synthesis started with the preparation of the pyruvamide from Cbz-L-Trp and dimethoxybenzylamine. The next step consisted of the reduction of the methylene group of the methylenediketopiperazine, obtained through dehydration of the intermediary enamide, and was followed by the acylation of the 4-substituted-2,5-piperazinedione with *o*-azidobenzoylchloride after formation of the amide anion with lithium diisopropylamide (LDA) in tetrahydrofuran (THF). Removal of the dimethoxybenzyl (DMBn) protecting group by oxidation with cerium(IV) ammonium nitrate (CAN), followed by a Staudinger reaction with a phosphine and subsequent cyclization of the corresponding phosphazene after oxidation of the indoline with MnO<sub>2</sub> in ethyl acetate (EtOAc), completed the total synthesis of (+)-fumiquinazoline G (**20**).



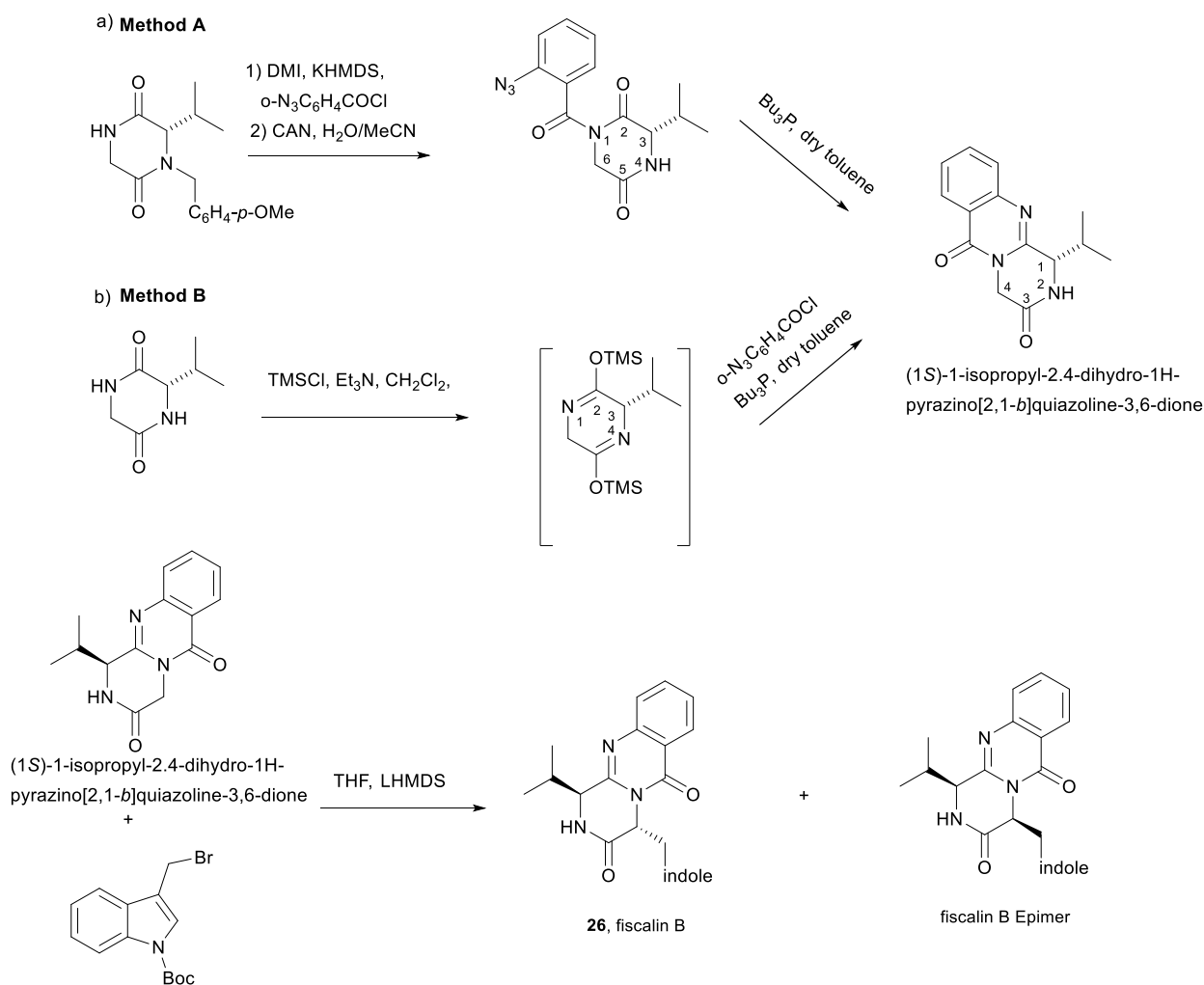
**Scheme 3:** Total synthesis of (+)-fumiquinazoline G (**20**). TFA = Trifluoroacetic acid, MDbn = 1,4-Dimethylbenzen, LDA = Lithium diisopropylamide, CAN = Cerium ammonium nitrate.

The synthesis of (+)-fumiquinazoline G (**20**), by Snider and Busuyek (Scheme 4) demonstrated the utility of their newly developed general procedure for the synthesis of *N*-(2-nitrobenzyl)diketopiperazines, previously reported for the formation of the benzodiazepinedione asperlicin<sup>51-52, 98-99</sup>. Reductive amination of 2-nitrobenzaldehyde with alanine methyl ester, followed by the coupling with allyl chloroformate, furnishing the intermediate which was submitted to the hydrolysis of the methyl ester. Condensation of the activated phenyl ester such as tryptophan phenyl ester using *N,N'*-dicyclohexylcarbodiimide (DCC) in  $\text{CH}_2\text{Cl}_2$  gave an intermediary dipeptide that, after deprotection of the allyloxycarbonyl (Alloc) group and subsequent cyclization, yielded the desired monoprotected diketopiperazine. The diketopiperazine can be further deprotected in methanol (MeOH) over irradiation at 254 nm. The use of the 2-nitrobenzyl group as a photochemically labile protecting group for the amide of the diketopiperazines allowed the utilization of this aza-Wittig procedure (Scheme 4). The acylation of diketopiperazine allowed to obtain (+)-fumiquinazoline G (**20**) in 87% yield.



**Scheme 4:** Total synthesis of (+)-fumiquinazoline G (**20**). DCC = *N,N'*-dicyclohexyl carbodiimide, THF = Tetrahydrofuran.

Regio- and diastereoselective alkylation at C-4 of (1*S*)-1-isopropyl-2,4-dihydro-1*H*-pyrazino[2,1-*b*]quinazoline-3,6-diones (Scheme 5) was used by Hernández *et al.*<sup>100</sup> for the synthesis of fiscalin B (**26**). The authors reported a method to synthesize 1,4-dialkyl derivatives of pyrazino[2,1-*b*]quinazoline-3,6-dione by using enantiomerically pure 1,3-dialkylpiperazine-2,5-diones via imino ether by condensation with Ant or alternatively from 1,6-dialkyl-, and 1,3,6-trialkylpiperazine-2,5-diones through *N*-acylation with *o*-azidobenzoyl chloride followed by an intramolecular Staudinger reaction.



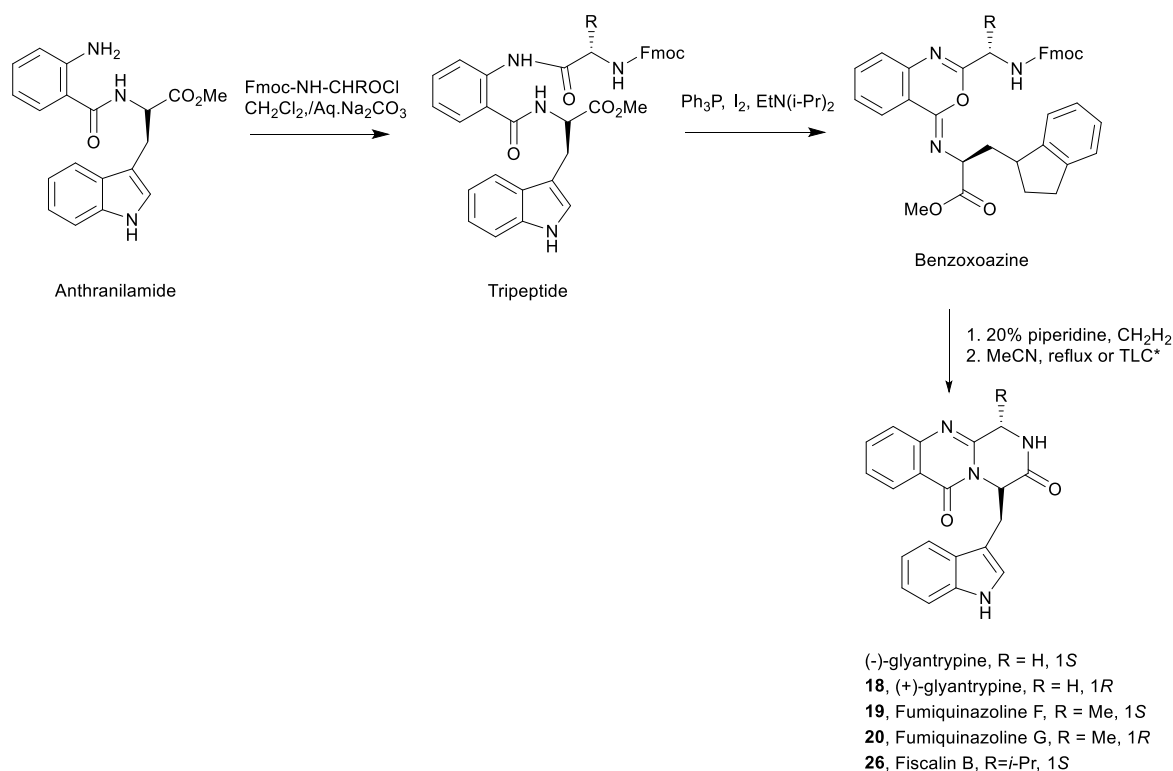
**Scheme 5:** Total synthesis of fiscalin B (**26**), and *epi*-fiscalin B. DMI = 1,3-Dimethyl-2-imidazolidinone, KHMS = Potassium bis(trimethylsilyl)amide CAN = Cerium ammonium nitrate, TMSCl = Trimethylsilyl chloride, LHMS = Lithium hexamethyldisilazide, THF = Tetrahydrofuran, Boc = *tert*-Buthyloxycarbonyl.

This approach started from the *N*-unsubstituted pyrazino[2,1-*b*]quinazoline-3,6-dione which was either prepared by oxidative debenzoylation of (3*S*)-3-methyl(isopropyl)-4-*p*-methoxybenzyl-1-*o*-azidobenzoylpiperazine-2,5-dione with CAN followed by intramolecular Staudinger reaction (Scheme 5, method A), or by acylation with *o*-azidobenzoyl chloride of (3*S*)-3-methyl(isopropyl)-2,5-bis(trimethylsilyloxy)-3,6-dihydropyrazine, followed by treatment with tributylphosphine (Scheme 9, method B). Both methods afforded 1-isopropyl-2,4-dihydro-1*H*-pyrazino[2,1-*b*]quinazoline-3,6-dione which was subjected to alkylation in the presence of lithium hexamethyldisilazide (LHMS). The authors found that there was a regio- and diastereoselective alkylation at C-4 and the basic conditions used did not affect the stereogenic center at C-1.

#### 1.3.4.2 Mazurkiewicz-Ganesan approach

Wang and Ganesan reported the total synthesis of gyantrypine (**18**) fumiquinazoline G (**20**), and fiscalin B (**26**), based on a key step that involved the cyclization of *N*-acylanthranilamide (Scheme 6)<sup>94</sup>. The authors used the Wipf's protocol, which involves the application of a Hunig's base, *N,N*-diisopropylethylamine (DIEA)<sup>93, 101</sup> with triphenylphosphine and iodine to give the cyclization product, initially described as 4-quinazolinone and which after was proved to be the 4-imino-4*H*-3,1-benzoxazine by He and Snider<sup>102</sup>. To accomplish a total synthesis, deprotection of the fluorenylmethyloxycarbonyl (Fmoc) group of 4-imino-4*H*-3,1-benzoxazine with piperidine afforded an intermediate that was converted to fumiquinazoline G (**20**) on preparative thin layer chromatography (TLC). Other two quinazolinones were obtained after refluxing the intermediates in acetonitrile. This methodology was widely applied to total syntheses of several natural alkaloids such as alantrypinone<sup>103-104</sup>, gyantrypine (**18**)<sup>95</sup>, anacine<sup>105</sup> verrucines A and B<sup>105</sup>, circumdatins C and F<sup>106</sup>, fiscalin B (**26**)<sup>94-95</sup>, and fumiquinazolines A (**21**), B, C (**22**), E, H (**23**), and I<sup>68, 95, 107-109</sup>.

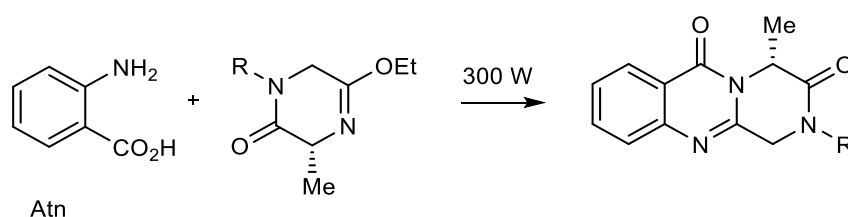
The referred authors, have also made use of the same methodology for the synthesis of more complex fumiquinazolines on solid support starting from Wang resin<sup>108</sup> as well as in solution<sup>95</sup>. The first step is the coupling of Ant with Trp methyl ester (solution-phase) or Fmoc-Trp (solid-phase) in the presence of 1-ethyl-3-(3-dimethylaminopropyl)carbodiimide (EDAC) as activating agent to form anthranilamide. Acylation of the amino group of the aniline moiety with Fmoc-protected amino acids chloride (Fmoc-Gly-Cl, Fmoc-Phe-Cl, Fmoc-Ala-Cl, and Fmoc-Val-Cl) provides linear tripeptides; and subsequent dehydrative cyclization of these compounds yields the benzoxazines intermediates. Finally, piperidine-mediated deprotection of the Fmoc group and rearrangement of the oxazine into 4-imino-4*H*-3,1-benzoxazines gives amidine carboxamides. After refluxing in acetonitrile to induce cyclative cleavage (+)-gyantrypine (**18**), (-)-gyantrypine, fumiquinazoline F (**19**), fumiquinazoline G (**20**), and fiscalin B (**26**) were obtained (Scheme 6).



**Scheme 6:** Total synthesis of glyantrypine (**18**), fumiquinazoline F (**19**), G (**20**), and fiscalin B (**26**) in the solution phase. \* Glyantrypine (**18**) was purified by thin layer chromatography (TLC).

### 1.3.4.3 Microwave assisted method

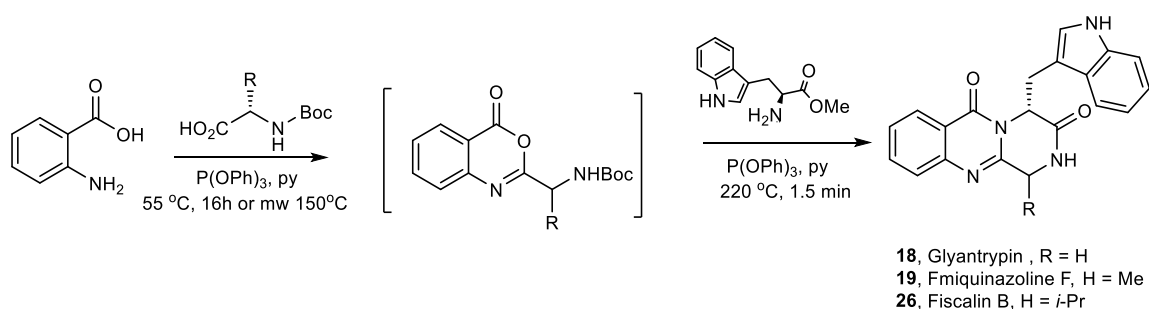
Cledera *et al.*<sup>110</sup> described the microwave-assisted synthesis of novel pyrazino[1,2-*b*]quinazoline-3,6-diones by a solvent free cyclocondensation of lactim ether with Ant (Scheme 7). The solvent-free reaction mixtures were irradiated in domestic oven containing an alumina bath. Since the temperature could not be measured, a comparison with conventional heating (120-140 °C) was made. The microwave-assisted reaction was much better than the thermal one regarding the yields and the short reaction times achieved. The authors also observed that this approach gave better stereochemical integrity compare to the conventional conditions.



**Scheme 7:** Microwave-assisted reaction synthesis of pyrazino[1,2-*b*]quinazoline-3,6-diones.



Liu *et al.*<sup>111</sup> reported an easy access to the core pyrazino[2,1-*b*]quinazoline-3,6-dione through a novel and highly efficient three-component one-pot reaction sequence promoted by microwave irradiation. The application of this synthetic strategy to the syntheses of glyantrypine (**18**), fumiquinazoline F (**19**), and fiscalin B (**26**) from readily available starting materials (Scheme 8) demonstrated the utility and versatility of this methodology. This work was performed under pressure at 300 W into a specifically designed platform (Smith synthesizer) producing controlled irradiation at 2450 MHz. The author reported that the enantiomeric excess of **18**, **19**, and **26** were 70, 72, and 50 %, respectively.



**Scheme 8:** Microwave synthesis of glyantrypine (**18**), fumiquinazoline F (**19**) and fiscalin B (**26**). mw = microwave, Boc = *tert*-butyloxycarbonyl, py= pyridine.

#### 1.4 Carbazole alkaloids

Another group of alkaloids containing indole is the class of carbazole alkaloids, aromatic heterocyclic organic compounds having a tricyclic structure, consisting of two phenyl rings fused on a five membered nitrogen-containing ring (**38**, Figure 6). The structure is based on the indole structure, but in which a second phenyl ring (A or C) is fused onto the five-member ring (B) at the 4a-9a or 4b-8a positions<sup>112</sup>. These alkaloids have been of interested since the first isolation of carbazole (**38**) from coal tar in 1872, and the isolation and evaluation of the antimicrobial murrayanine (3-formyl-1-methoxycarbazole, (**39**) from *Murraya koenigii* Spreng in 1965<sup>113</sup>. Most carbazole alkaloids have been isolated from the higher plants of Rutaceae family from genus *Clausena*, *Clycosmis*, and *Murraya*<sup>114</sup>, and other sources like lower plant (*Streptomyces* species), blue-green algae (*Hyella caespitosa*), *Aspergillus* species, *Actinomadura* species, and the ascidian (*Didemnum granulatum*)<sup>113</sup>.

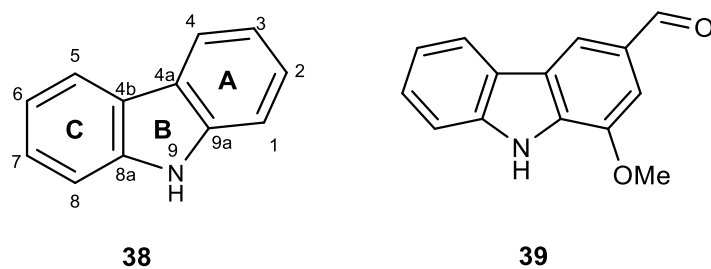


**Figure 6:** Carbazole alkaloid core (38) and murrayanine (39).

It has been reported that carbazole alkaloids exhibit a broad pharmacological profile, including antiplatelet aggregation and vasorelaxing<sup>115</sup>, antibacterial<sup>116</sup>, antifungal<sup>117</sup>, antiplasmodial<sup>118</sup>, anti-Alzheimer's<sup>119</sup>, antidiabetic, anti-HIV-1<sup>120</sup>, and antitumor activities<sup>121-125</sup>.

#### 1.4.1 Isolation and biological activities of carbazole alkaloids

Biologically-active carbazole alkaloids have been isolated from diverse natural sources and exhibit a broad range of different frameworks and functional groups. There are full reviews about occurring, biogenesis and synthesis of bioactive carbazole alkaloids<sup>113, 126</sup>. Regarding to the substitution pattern of ring A and ring C, carbazole alkaloids are divided as following: (1) tricyclic carbazoles, (2) pyranocarbazoles, (3) biscarbazoles, (4) carbazolelactones, (5) terpenoid carbazoles, (6) benzocarbazoles, (7) furocarbazoles, (8) pyrrolo[2,3-*c*]carbazoles, (9) pyrido[4,3-*b*]carbazoles, (10) quinolino[4,3-*b*]carbazoles, (11) indolocarbazoles, and (12) miscellaneous carbazoles. In this section the naturally-occurring (tricyclic) carbazole alkaloids sources and biological activities are discussed and summarized in Table 4. Compounds considered as non-oxygenated carbazoles refer to those having substituents besides the oxygen atom. Oxygenated tricyclic carbazoles are compounds in which one or more oxygen atoms are directly attached to the carbazole core and can be divided into six groups according to the position and number of oxygens containing on ring A and ring C of the carbazole nucleus: monooxygenated, dioxygenated, trioxygenated, carbazole-1,4-quinones, carbazole-1,4-quinols, and carbazole-3,4-quinone alkaloids.

**Table 4:** Summary of sources and biological activities of tricyclic carbazole alkaloids.

Compounds	Sources	Biological Activities	Ref
<b>Non-oxygenated carbazoles</b>			
Carbazole (38)	<i>Glycosmis pentaphylla</i>	Unknown	127
3-Methyl carbazole (40)	<i>Clausena spp.</i>	Unknown	128
	<i>G. pentaphylla</i>		127
	<i>Murraya koenigii</i>		129
	<i>M. euchrestifolia</i>		
3-Formylcarbazole (41)	<i>M. euchrestifolia</i>	Unknown	130
	<i>C. lansium</i>		
Methyl carbazole-3-carboxylate (43)	<i>C. lansium</i>	Unknown	
9-Formyl-3-methyl carbazole	<i>M. koenigii</i>	Weak cytotoxicity against mouse melanoma B16 and adriamycin-resistant P388 mouse leukemia cell lines	129
2,7-Dibromocarbazole	<i>Kyrtuthrix maculans</i>	Basis of the neuroprotective compound P7C3	131
3,6 -Dibromocarbazole	<i>K. maculans</i>	Unknown	131
3,6-Diiodocarbazole	Sediment	Unknown	131
1,3,6,8-Tetrabromocarbazole			132
<b>Monoxygenated carbazole alkaloids</b>			
Murrayafoline A (44)	<i>M. euchrestifolia</i>	Unknown	133
	<i>G. stenocarpa</i>		134
Koenoline (45)	<i>M. koenigii</i>	Unknown	135
Murrayanine (39)	<i>M. koenigii</i>	Cytotoxicity against KB, MCF-7, NCI-87 cell lines	136
	<i>C. heptaphylla</i>		137
	<i>G. stenocarpa</i>	Antimicrobial activity against human pathogenic fungi	134
	<i>C. excavata</i>		138
Clausamine D	<i>C. anisata</i>	Inhibits Epstein-Barr virus early antigen (EBV-EA) activation induced by TPA in Raji cells	139
Clausamine E	<i>C. anisata</i>	Unknown	139
Clausamine G	<i>C. anisata</i>	Antitumor against 1,3-5-triaza-7-phosphaadamantane-induced <i>in vitro</i> EBV	139
1-Hydroxy-3-methylcarbazole (48)	<i>M. koenigii</i>	Unknown	140
O-Demethylmurrayanine (49)	<i>C. anisata</i>	Strong cytotoxicity against MCF-7 and SMMC-7721 cell lines	141

Compounds	Sources	Biological Activities	Ref
Clausine E (50)	<i>C. excavata</i>	Detoxification agent	
	<i>C. vestita</i>	Cytotoxicity against HepG2 cell	115
		Induces cell cycle arrest in the S and G2/M	142
		Decreases F-actin staining and Rhodamine A activity and inhibits phosphorylation of PKC6 $\delta$	143
		Inhibition of rabbit platelet aggregation and vasoconstriction	144
	Moderate topoisomerase II inhibition		
Clausine D	<i>C. excavata</i>	Inhibition of platelet aggregation	145
Clausine F	<i>C. excavata</i>	Inhibition of platelet aggregation	145
Clausamine F	<i>C. anisata</i>	Antitumor activity	139
2-Methoxy-3-methylcarbazole (51)	<i>M. koenigii</i>	Unknown	
O-Methylmukonal or	<i>M. siamensis</i>	Anti-HIV-1	146
Glycosinine (52)	<i>G. pentaphylla</i>		147
	<i>C. excavata</i>		148
	<i>M. koenigii</i>		149
Clausine L (53)	<i>C. excavata</i>	Unknown	150
	<i>M. koenigii</i>		140
2-Hydroxy-3-methylcarbazole (54)	<i>M. koenigii</i>	Cytotoxicity against HepG2 cells	144
	<i>C. vestita</i>		
Mukonidine (56)	<i>M. koenigii</i>	Antiplatelet aggregation	150
Heptaphylline (57)	<i>C. heptaphylla</i>	Cytotoxicity against NCI-H187 cell line	151
	<i>C. harmadiana</i>	Induces apoptosis by Inhibition of the	152
	<i>C. anisata</i>	activation of NF-kB/p65(rel)	153-154
	<i>C. excavata</i>	Potent analgesic effect in rodent model	155
	<i>Rhodamnia dumetorum</i>	Moderate cytotoxicity against HepG2 cell line	156
Mukonal (55)	<i>C. harmadiana</i>	Strong cytotoxicity against NCI-H187 and KB cells lines	157
Clauszoline K	<i>C. harmadiana</i>	Strong cytotoxicity against NCI-H187 and KB cells lines	157
	<i>C. vestita</i>	Cytotoxicity against HepG2 cells	
Carazostatin	<i>Streptomyces</i>	Strong inhibitory activity against the free	158
	<i>chromofuscus</i>	radical-induced lipid peroxidation in liposomal membrane, antioxidant	159
Antiostatins	<i>S. cyaneus</i> 2007-SV1	Strong inhibitory activity against free radical-induced lipid peroxidation	160

Compounds	Sources	Biological Activities	Ref
Lipocarbazoles	<i>Tsukamurella pseudomonas</i> Acta1857	Antioxidation activity	161
3-Formyl-6-methoxycarbazole	<i>C. lansium</i> <i>Micromelum hirsutum</i>	Anti-tuberculosis (TB) activity against the H <sub>37</sub> Rv strain of <i>Mycobacterium tuberculosis</i>	162 163
8-Formyl-6-methoxy-3-methylcarbazole	<i>M. koenigii</i>	Inhibitory activity against Gram-negative bacteria and fungi	164
Micromeline	<i>M. hirsutum</i>	Anti-TB activity against H <sub>37</sub> Rv strain of <i>Mycobacterium tuberculosis</i> and against the Erdman strain of <i>M. tuberculosis</i> in a J77 mouse macrophage model	163
Siamenol	<i>M. siamensis</i>	Showed anti-HIV activity	165
<b>Dioxygenated carbazole alkaloids</b>			
Clausenine	<i>C. anisata</i>	Antibiotic activity	166
Clausanol	<i>C. anisata</i>	Antibiotic activity Nearly active against some bacteria as streptomycin	166
Clausine I	<i>C. excavata</i>	Shows inhibition of rabbit platelet aggregation and vasoconstriction	115
Causine Z	<i>C. excavata</i>	Exhibits an inhibitory activity against cyclin-dependent kinase 5 and shows a protective effect on cerebral granule neuron against free radical-induced cell death	167
Clausenal	<i>C. heptaphylla</i>	Exhibits promising antimicrobial activity against fungi and Gram-positive and Gram-negative bacteria	117
Carbalexin A	<i>G. pentaphylla</i> <i>G. parviflora</i>	Shows a strong antifungal activity in bioautographic test with <i>Cladosporium herbarum</i>	168
Glycozolidol	<i>G. pentaphylla</i>	Active against Gram-positive and Gram-negative bacteria	169
Glybomine B	<i>G. arborea</i>	Shows significant antitumor-promoting activity in conjunction with the tumor promoter TPA	170
Glybomine C			
Carbalexin C	<i>G. parviflora</i>	Shows a strong antifungal activity in bioautographic test	168
7-Methoxyheptaphylline (62)	<i>C. harmandiana</i>	Cytotoxicity against NCI-H187 and KB cell lines	152 125

Compounds	Sources	Biological Activities	Ref
2-Hydroxy-3-formyl-7-methoxycarbazole or 7-Methoxymukonal ( <b>63</b> )	<i>C. harmandiana</i> <i>R. dumetorum</i> <i>C. vestita</i>	Strong cytotoxicity against MCF-7 and KB cell lines Cytotoxicity against HepG2 cells Antimalarial activity and Anti-TB against <i>M. tuberculosis</i> H <sub>37</sub> Rv	152 156 144
Heptazoline	<i>C. harmandiana</i>	Moderate cytotoxicity against MCF-7 cells	171
Clausine H	<i>C. excavata</i>	Shows inhibition of rabbit platelet aggregation and vasoconstriction	172
Clausine K	<i>C. excavata</i>	Anti-HIV-1 activity Strong anticancer against HepG2 cells	148 155
Clausine-TY	<i>C. excavata</i>	Exhibits cytotoxicity against CEM-SS cell line	173
Carbalexin B	<i>G. parviflora</i>	Shows a strong antifungal activity in bioautographic test with <i>C. herbarum</i>	168
Carbazomycin A	<i>Streptoverticillium</i>	Inhibits the growth of phytopathogenic fungi	174
Carbazomycin B	<i>ehimense</i> H 1051-MY 10	and shows antibacterial and anti-yeast activity Inhibits 5-lipoxygenase and shows inhibitory activity against lipid peroxidation induced by free radicals	175 176
Streptoverticillin	<i>S. morookaense</i>	Shows antifungal activity against <i>Peronophythora litchi</i>	177
Neocarazostatin	<i>S. species</i> GP38	Exhibits a strong inhibitory activity against free radical-induced lipid peroxidation	178
Carbazomadurin A	<i>Actinomadura maduae</i>	Exhibits a strong neuronal cell protecting activity against L-glutamate-induced cell death	179
Carbazomadurin B	2808-SV1		
Epocarbazolin A	<i>S. anulatus</i> T688-8	Inhibits 5-lipoxygenase	180
Epocarbazolin B		Weak antibacterial activity	
6,7-Dimethoxy-1-hydroxy-3-methyl carbazole	<i>M. koenigii</i>	Exhibits high activity against Gram-positive and Gram-negative bacteria and against fungi	164
Carbazomycin C	<i>S. ehimense</i> 1051-MY 10	Inhibits 5-lipoxygenase	181

TB = Tuberculosis, TPA = 12-O-tetradecanoyl-phorbol-13-acetate, EBV = Epstein-Barr virus, HIV = Human immunocompromising virus,

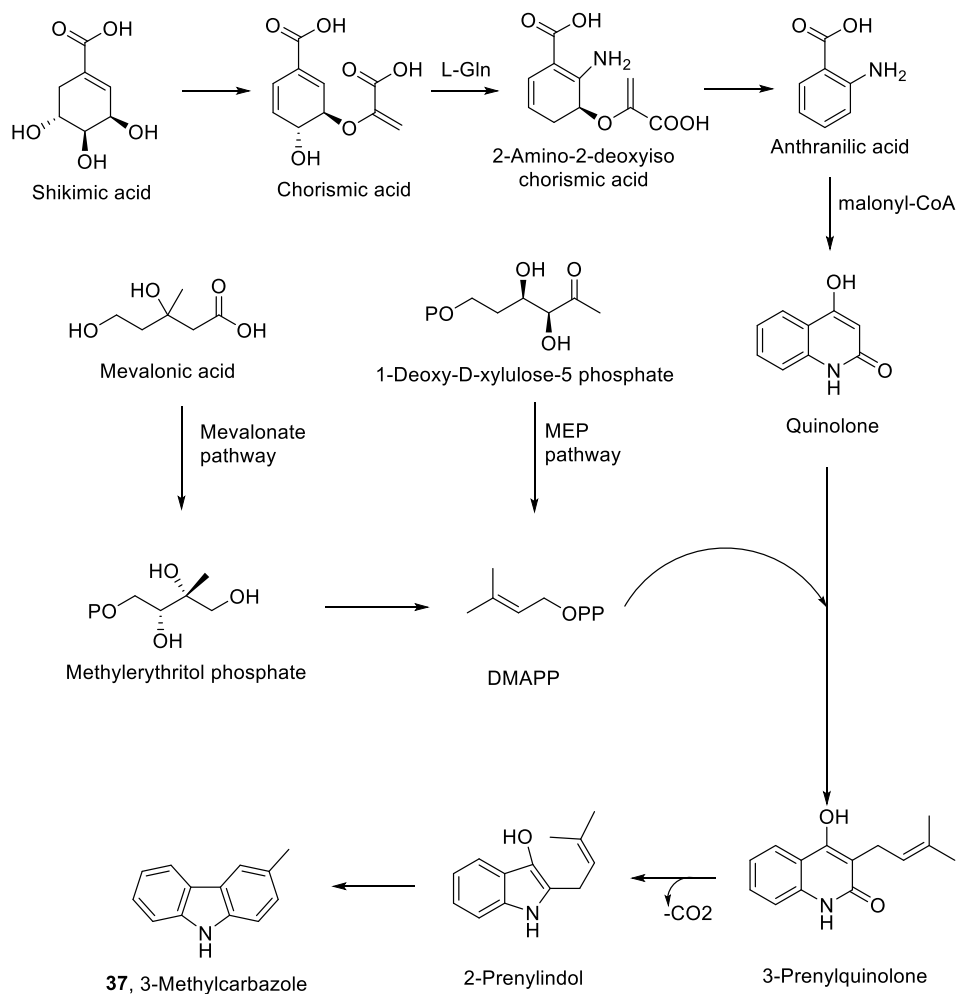
#### 1.4.2 Biosynthesis of carbazole alkaloids

Regarding their natural origin, carbazole alkaloids are classified into two groups. To the first group belong alkaloids isolated from higher plants generally featuring a C<sub>1</sub>-substituent at C-3 (a methyl group or its oxidized equivalents). For example, 3-methylcarbazole (**40**), 3-

formylcarbazole (**41**) (oxidized congener of **40**) and carbazole-3-carboxylate from Rutaceae family (genera: *Murraya*, *Clausena*, and *Glycosmic*), are biosynthesized via an oxidation of the methyl group, which was confirmed by photochemical oxidation<sup>113, 182</sup>. To the second group belong alkaloids isolated from other natural sources like microorganisms, which usually lack a C<sub>1</sub>-substituent at C-3. The biosynthesis of these members is not yet fully understood owing to the lack of experimental support. However, there are two proposed pathways for the biosynthesis of these carbazole alkaloids – anthranilic acid (Ant) pathway and L-tryptophan (Trp) pathway. Following, the Ant pathway is presented being the proposed for the carbazoles studied in the scope of this thesis.

#### 1.4.2.1 Biosynthesis of carbazole alkaloids based on the anthranilic acid pathway

To date, the so-called “anthranilic acid pathway”, which proceeds via the 3-prenylquinolone, represents the most widely accepted proposal for the biogenesis of carbazole alkaloids in higher plants. Thus, it has been suggested that the carbazole nucleus derives from shikimic acid and prenyl pyrophosphate as described in Scheme 9. The biosynthesis begins with the dehydration and reduction of 3-dehydroquinic acid to shikimic acid, observed in the Japanese plant *Illicium religiosum* Sieb (Japanese shikimi)<sup>183</sup>. The shikimic acid proceeds to the carbazole nucleus of the quinolone by the intermediates chorismic acid, 2-amino-deoxyisochorismic acid, and Ant (the most abundance in Rutaceae family). Later on, it provides the indole unit, being this pathway corresponding to the formation of rings B and C of the carbazole nucleus. Prenyl pyrophosphate provides the carbon atoms for ring A with a methyl substituent at C-3. 3-Methylcarbazole (**40**) is formed via the 3-prenylquinolone following 2-prenylindole<sup>184</sup>. Prenylation of quinolone at C-3 can be formed via two independent pathways – the mevalonate pathway, found in mammals and fungi derived from mevalonic acid, and the methylerythritol phosphate (MEP) pathway, found in plants, algae and bacteria, derived from 1-deoxy-D-xylulose 5-phosphate, affording the 3-prenylquinolone (Scheme 9). The last step of the biosynthesis of 3-methylcarbazole (**40**) is the *trans* decarboxylation of 3-prenylquinolone to 3-methylcarbazole (**40**) via extrusion of carbon monoxide and subsequent oxidative cyclization of the intermediate 2-prenylindole<sup>184</sup>.

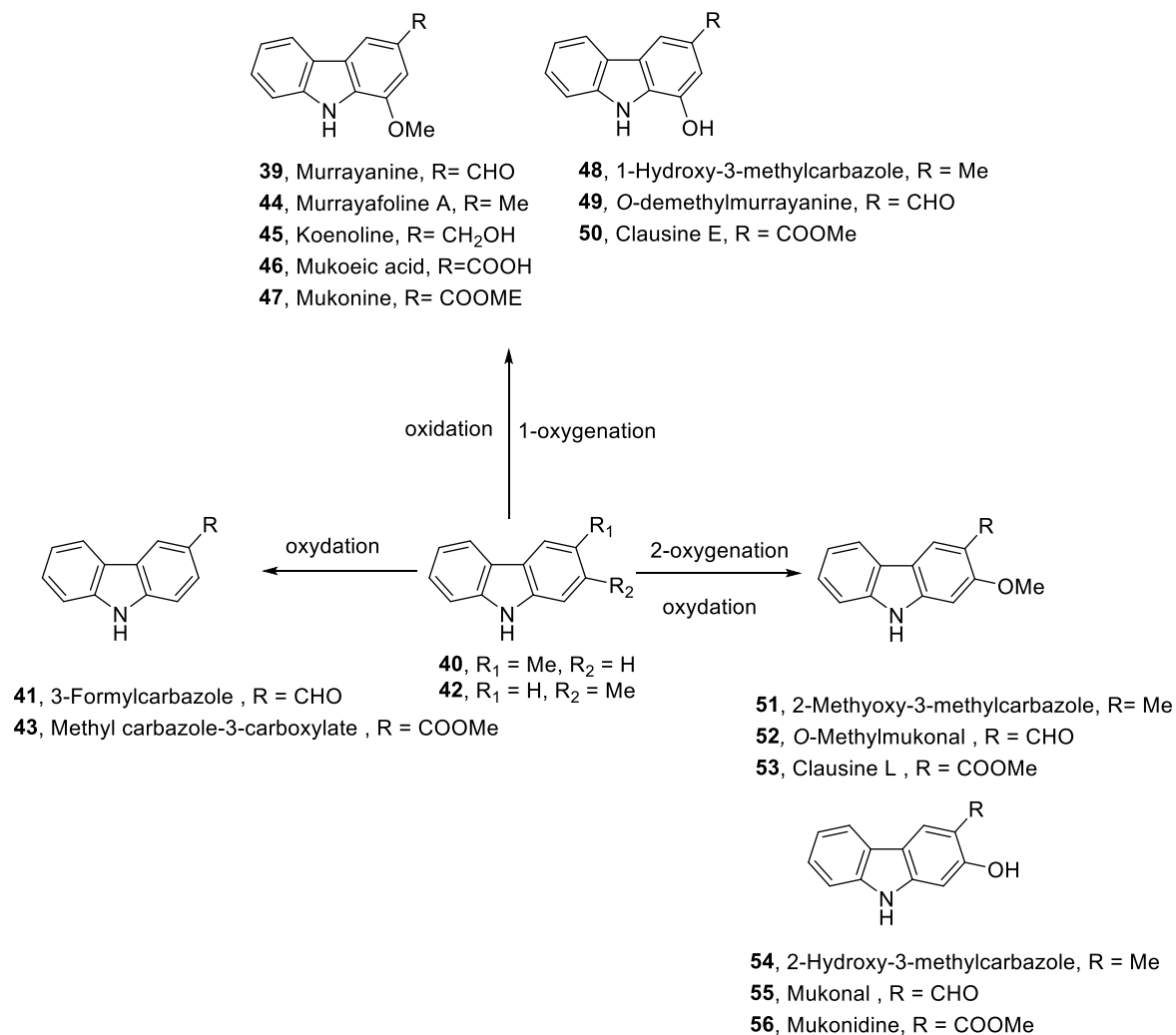


**Scheme 9:** Biosynthesis of 3-methylcarbazole (**37**) via anthranilic acid pathway. DMAPP = Dimethylallylpyrophosphate

The carbazole nucleus can be easily functionalized at 1-, 2-, 6-, and 9-positions. The structural heterogeneity provides a large variety of different physicochemical and biological properties. Based on the structural features of carbazole alkaloids isolated from the same sources 3-methylcarbazole (**40**) was suggested to be the key intermediate in their biosynthesis in higher plants. On the other hand, 2-methylcarbazole (**42**) appears to be the common biogenetic precursor of conventional tricyclic carbazole isolated from lower plants. The isolation of several 3-methylcarbazole derivatives from higher plant shows that the aromatic methyl group can be eliminated oxidatively from the key intermediate 3-methylcarbazole (**40**) via -CH<sub>2</sub>OH, CHO, and COOH<sup>113</sup>. 3-Methylcarbazole (**40**) is oxygenated and/or oxidized *in vivo* in different positions to generate murrayanine (**39**), 3-formylcarbazole (**41**), methylcarbazole-3-carboxylate (**43**), murrayazoline A (**44**), keonenoline (**45**), mukoeic acid (**46**), mukonine (**47**), 1-hydroxy-3-methylcarbazole (**48**), *O*-demethylmurrayanine (**49**), causine E (**50**), 2-methoxy-

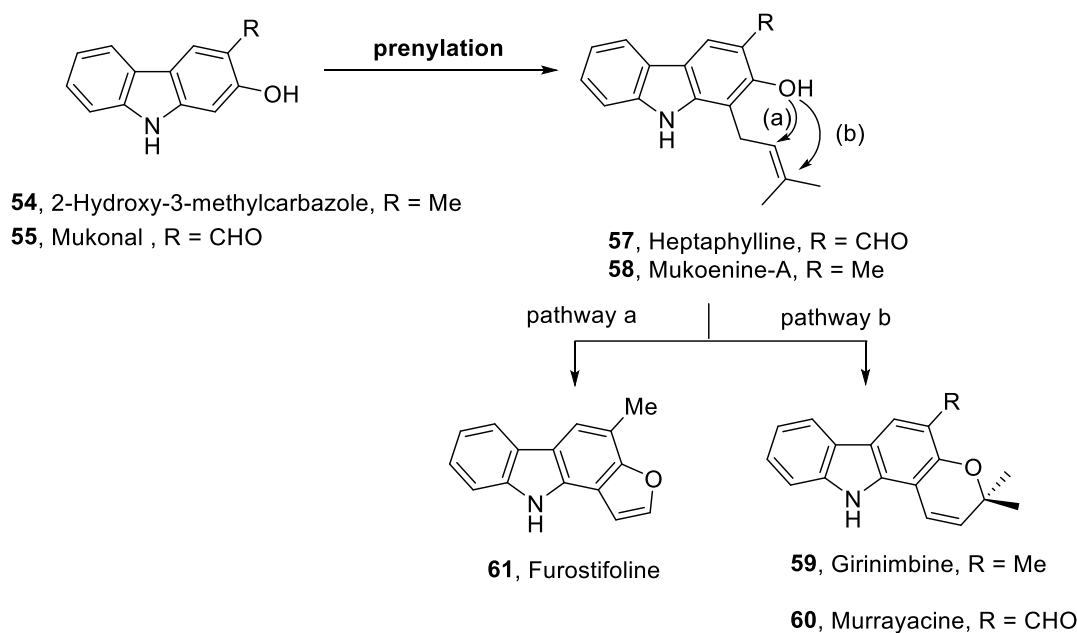


3-methylcarbazole (**51**), O-methylmukonal (**52**), causine L (**53**), 2-hydroxy-3-methylcarbazole (**54**), mukonal (**55**), and mukonidine (**56**) (Scheme 10).



**Scheme 10:** Biosynthetic oxygenation and oxidation of 3-methylcarbazole (**40**).

Compounds **54** and **55** are considered the precursors for pyranocarbazoles and furocarbazoles, proved by the isolation of heptaphylline (**57**), mukoenine A (**58**), girinimbine (**59**), murrayacine (**60**), and furostifoline (**61**). Mukoenine A (**58**) can be considered as precursor for furo[3,2-a]- and pyrano [3,2-a]carbazole alkaloids. The isolation of furostifoline (**61**) from *Murraya* supports the proposed biosynthesis for the origin of the furan ring which suggested to be formed via cyclization pathways (a) of prenylated mukoenine A (**58**) or cyclization pathway (b) of mukoenine A (**58**) or heptaphylline (**57**) (Scheme 11).



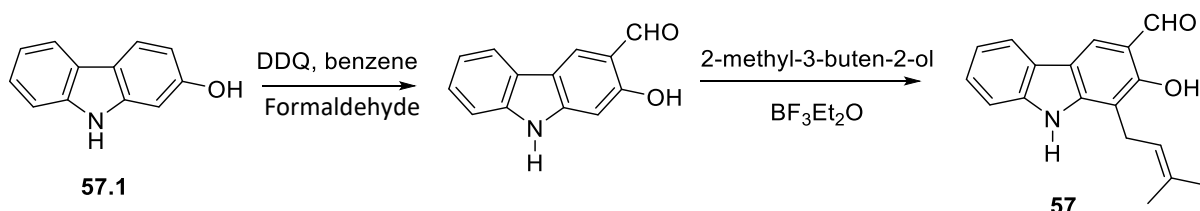
**Scheme 11:** Prenylation and cyclization of 2-hydroxy-3-methylcarbazole (**54**) and mukonal (**55**).

### 1.4.3 Synthesis of carbazole alkaloids

The synthesis of carbazole alkaloids has been reported<sup>113, 126</sup>. Generally, the total synthesis of carbazole alkaloids in past decades used both classical methods (i.e. Fischer-Borsche and the Graebe-Ullmann synthesis) and the nonclassical methods such as transition metal-mediated catalyzed processes<sup>185-186</sup>, cadogan syntheses<sup>187</sup>, electrocyclic reactions<sup>188</sup>, and other methods. Initially, the most used approach to carbazoles involved the dehydrogenation of 1,2,3,4-tetrahydrocarbazole. However, easier ways to access fully aromatized carbazoles involved the construction of the central pyrrole ring by cyclization of either biphenyls with an *ortho*-nitrogen substituent or diarylamines. Thus, the carbazole structure can be developed under mild reactions, affording good to excellent yields using either commercially available or easily prepared starting materials<sup>189</sup>. The synthesis of tricyclic oxygenated carbazole alkaloids closely related to compounds studied in this thesis – heptaphylline (**57**), 7-methoxyheptaphylline (**62**), and 7-methoxymukonal (**63**) are following described.

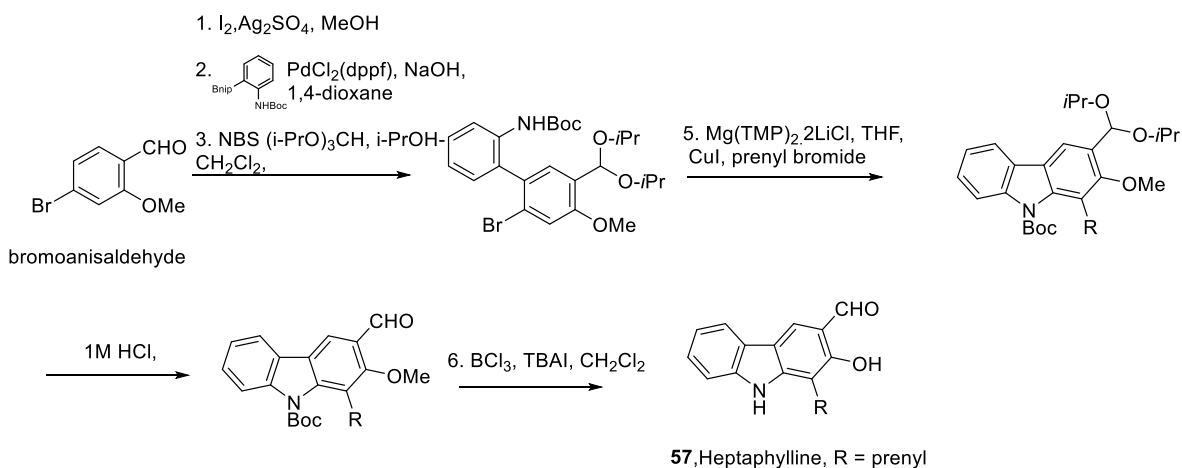
### 1.4.3.1 Synthesis of oxygenated carbazole alkaloids

In the early 80's, Sharma and Kapil<sup>190</sup> reported the synthesis of heptaphylline (**57**) and derivatives by oxidation. The synthesis of **57** was started from 2-hydrozycarbazole (**57.1**) through a formylation followed by a prenylation<sup>191</sup>.



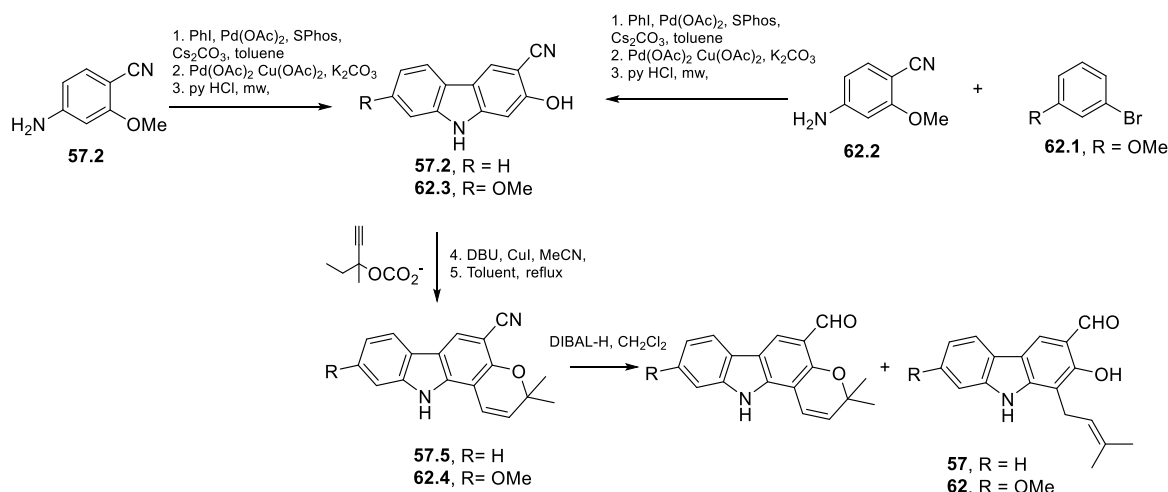
**Scheme 12:** Total synthesis of heptaphylline (**57**). DDQ = 2,3-Dichloro-5,6-dicyano-1,4-benzoquinone.

In 2013, Toshiharu *et al.*<sup>192</sup> and Okano *et al.*<sup>193</sup> reported the five-step synthesis of heptaphylline (**57**) via benzyne-mediated from substituted indolines and carbazoles. The reaction included the generation of benzyne using Mg(TMP)<sub>2</sub>LiCl as a base, cyclization and trapping the resulting organomagnesium intermediate with an electrophile from a bromoanisaldehyde. Prenylation, removal of the acetal moiety under acidic condition, and removal of the Boc protecting group yielded heptaphylline (**57**) in 16% (Scheme 13).



**Scheme 13:** Total synthesis of heptaphylline (**57**). NBS = *N*-Bromosuccinimide, dppf = 1,1'-Bis(diphenylphosphino)ferrocene, TMP = 2,2,6,6-Tetramethylpiperidide, THF = Tetrahydrofuran, TBAI = Tetrabutylammonium iodide.

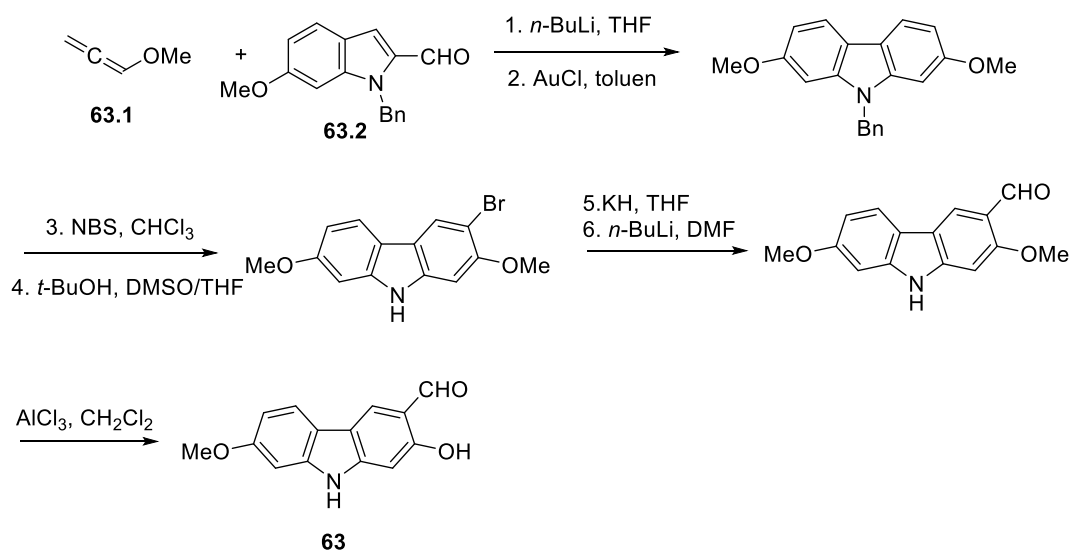
In 2014, Ronny *et al.*<sup>194</sup> developed the method to synthesize carbazole alkaloids including heptaphylline (**57**), 7-methoxyheptaphylline (**62**) using diisobutylaluminum hydride (DIBAL-H) promoted reductive pyran ring opening to provide the direct access of prenyl-substituted carbazoles like compounds **57** and **62**. The approach to heptaphylline (**57**) started with the Buchwald-Hartwig coupling of arylamine (**57.2**) followed by a palladium(II)-catalyzed oxidation cyclization to yield 2-hydroxycarbazole (**57.3**). The Godfrey's method followed by thermal induced rearrangement yielded pyrano[3,2-*a*]carbazole (**57.4**). Treatment of **57.4** with DIBAL-H afforded murrayacine (**64**) and heptaphylline (**57**) as a byproduct, due to reductive ring opening of pyran ring of **64** (Scheme 14). Using similar conditions, 7-methoxyheptaphylline (**62**) was obtained starting from bromoarene (**62.1**) and arylamine (**62.2**).



**Scheme 14:** Total synthesis of heptaphylline (**57**) and 7-methoxyheptaphylline (**62**). SPhos = 2-Dicyclohexylphosphino-2',6'-dimethoxybiphenyl, py = Pyridine, mw = Microwave, OAc = acetate, DBU = 1,8-Diazabicyclo[5.4.0]undec-7-ene, DIBAL-H = Diisobutylaluminum hydride, MeCN = acetonitrile,.

In 2015, Kalyan *et al.*<sup>195</sup> reported the synthesis of heptaphylline (**57**) and derivatives using ring-closing metathesis (RCM) and ring-rearrangement-aromatization (RRA) as the key step. This method based on the allyl Grignard addition provided 2,2-diallyl-3-oxindole derivatives via 1,2-allyl shift. Diallyl underwent the combination of RCM and RRA to yield heptaphylline (**57**) and derivatives.

Dengke *et al.*<sup>196</sup> first reported the synthesis of 7-methoxymukonal (**63**) using the Au-catalyzed cyclization route as the key step from methoxypropadiene (**63.1**) and 1-benzyl-6-methoxy-1*H*-indole-2-carbaldehyde (**63.2**) in six steps (Scheme 15).

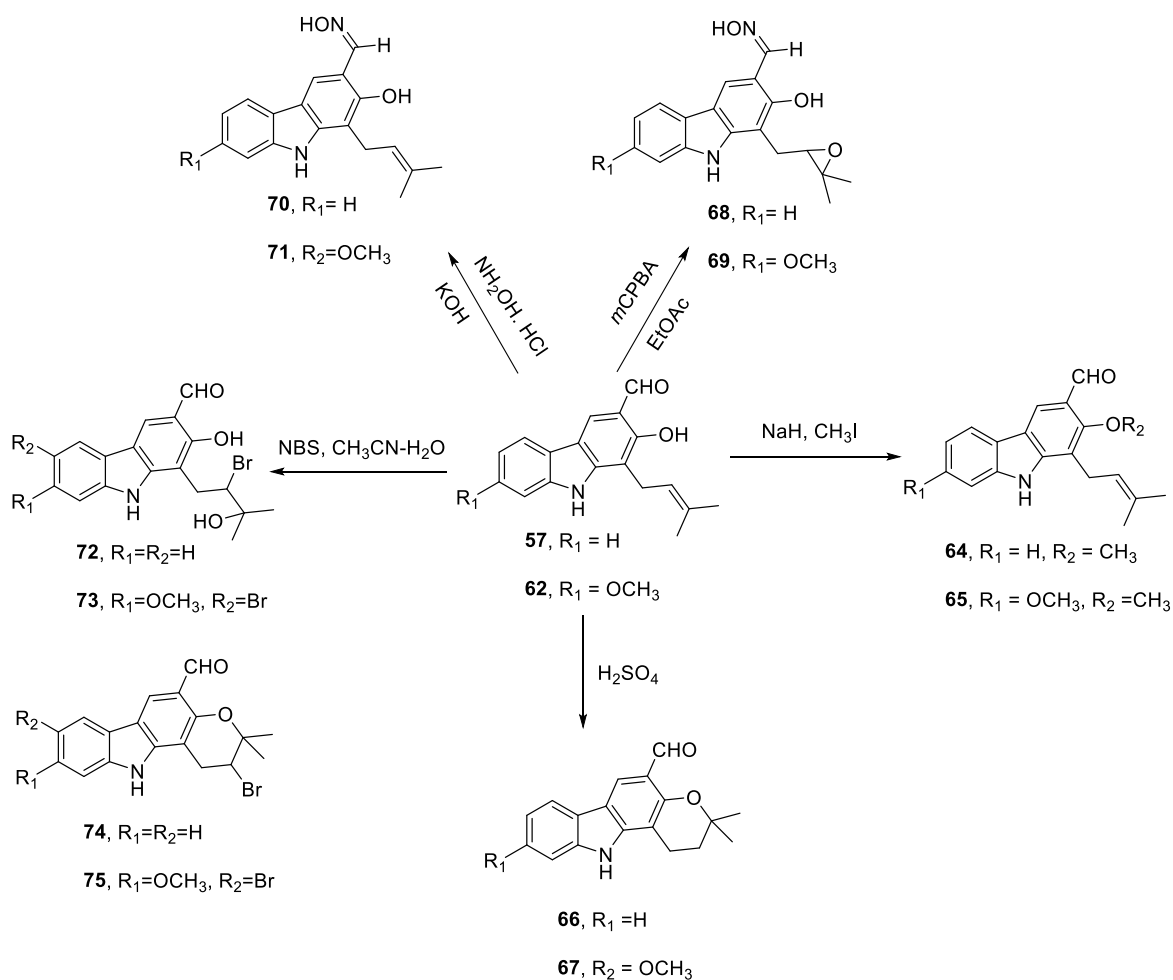


**Scheme 15:** The total synthesis of 7-methoxymukonal (**63**). Bu = Butyl, THF= Tetrahydrofuran, NBS= *N*-Bromosuccinimide, DMSO = Dimethyl sulfoxide, DMF = Dimethylformamide.

The challenges of this synthesis were the selective monobromination and the selective demethylation. The monobromination at C-3 was controlled by temperature while selective demethylation at C-2 was achieved by using the AlCl<sub>3</sub>.

#### 1.4.4 Semi-synthesis of carbazole alkaloids

Molecular modifications of NP carbazole alkaloid were reported to improve their biological activities. Thongthoom *et al.*<sup>125</sup> reported the modification of heptaphylline (**57**) and 7-methoxyheptaphylline (**62**) yielding derivatives showing better cytotoxicities (Figure 16.A). The modification process is shown in Scheme 16 and included (1) methylation using NaH/CH<sub>3</sub>I yielded compounds **64** and, (2) treatment with conc. H<sub>2</sub>SO<sub>4</sub> afforded pyran, compounds **66** and **67**, (3) epoxidation of the isolated double bond in the prenyl moiety of **57** and **62** using *m*-chloroperoxybenzoic acid (*m*CPBA) provided **68** and **69**, (4) treatment with NH<sub>2</sub>OH.HCl under basic conditions furnished oximes derivatives **70** and **71**, and (5) bromination using NBS in the present of aqueous conditions yielded compounds **72-75**. Most of the semisynthetic derivatives were cytotoxic and compound **72** was the most active about 138 and 10 folds compared to ellipticine standard tested in NCI-H187 and KB cell lines, respectively.



**Scheme 16:** (A) Semi-synthesis of heptaphylline (**57**) and 7-methoxyheptaphylline (**62**). (B) *In silicon* study of small molecule restoring p53, PhiKan083 (**76**). mCPBA = *m*-Chloroperoxybenzoic acid, NBS = *N*-Bromosuccinimide.

The molecular modification on NH of pyrrole ring was obtained by N-alkylation which was observed in the commercially available reagent such as Phikan083 (**76**, Figure 7), having restoring capacity on p53 obtained from *in silicon* study<sup>198</sup>.

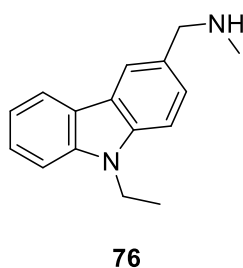


**Figure 7.** Structure of Phikan083 (**76**), mutant p53 restoring agent

## Aims of the thesis and work plan

Cancer and pathogenic diseases such as malaria are emergent health problems which cause significant mortality in developed and developing countries. Drug development to overcome those issues has been a concern since the development of drug resistance of disease-causing agents like resistant tumor cells and resistant pathogens. Secondary metabolites isolated from NPs provide an array of unique molecular architectures and play a dominant role in the discovery of leads for development of drugs for treatment of human diseases. Particularly, 83% anticancer approved drugs, 73% antibacterial approved drugs, and 90% antifungal approved drugs were either NPs based thereon, or mimicked NPs in one form or another<sup>5, 11</sup>. Two alkaloid scaffolds containing an indole moiety were within the scope of this thesis (1) quinazolinone alkaloids containing indolomethyl pyrazino [1,2-*b*]quinazoline-3,6-dione and (2) carbazole alkaloids. From the first scaffold, neofiscalin A (**28**), a complex chemical structure, showed a potent antibacterial activity against *Staphylococcus aureus* and *Enterococcus faecalis* (MIC = 8 µg/mL)<sup>69, 73, 197</sup> even in multi-resistant clinical isolates. This result disclosed by members of the Medicinal Chemistry and Natural Products group of CIIMAR research centre of University of Porto influenced the work of this thesis towards the synthesis of fiscalin B (**26**) and derivatives. While for the homologue fiscalin A (**27**) attempts toward the total synthesis failed, procedures were available for the syntheses of simpler quinazolinones like glyantrypine (**18**), fumiquinazoline F (**19**), or fiscalin B (**26**). This gave a very enthusiastic hint to explore the total syntheses and biological activities of their derivatives.

Concerning carbazole alkaloids, these abundant metabolites from plants, have reactive functional groups which are easily modified using a semi-synthetic approach. Some naturally-occurring carbazole alkaloids from *Clausena harmandiana*, namely heptaphylline (**57**), 7-methoxyheptaphylline (**62**), and 7-methoxymukonal (**63**) were available to perform molecular modifications. These molecules contain in their structure's aldehydes and hydroxyl groups. Chemical modifications to these molecules have already been reported, and included alkylation of nitrogen's indole<sup>122</sup>, esterification<sup>125</sup>, and cyclization at hydroxyl groups in order to explore their biological activities. For example, heptaphylline (**57**) showed cytotoxicity against tumor cell lines, and its oxime derivative, compound **68**, showed an excellent cell growth inhibitory effect against NCI-H187 cell line (IC<sub>50</sub> = 0.02 µM, 138 times stronger than ellipticine standard)<sup>125</sup>. On the other hand, Phikan083 (**76**, Figure 7), a small amino carbazole molecule was disclosed to activate p53, by stabilizing the structure of the mutant p53 and increasing the level of p53 in a wild-type conformation and activity. Based on the above considerations and in the interest in discovering p53 activators<sup>198</sup>, it was hypothesized that amino carbazole derivatives of **57**,

**62**, and **63** would give promising candidates for restoring p53 activity as well as tumor cell growth inhibitors. Until now, to the best of our knowledge, the synthesis of amino carbazole from **57**, **62**, and **63** has never been attempted before.

Therefore, two main objectives of this thesis were:

1. to synthesize a library of indolomethyl pyrazino [1,2-*b*]quinazoline-3,6-diones and explore their biological activities,
2. to synthesize semi-synthetic analogues of natural-isolated heptaphylline (**57**) and analogues and explore their biological activities.

The specific aims were:

1. to develop a library of quinazolinone alkaloids consisting of *syn* and *anti* analogues (using one-pot three components microwave assisted and Mazurkiewicz-Ganesan methods) and evaluated antitumor, antimicrobial, neuroprotective, and antimalarial activities also focusing on the problem of drug resistance,
2. to develop a library of amino carbazole analogues using reductive amination reaction and investigate their antitumor activity as well as p53 restoring activity.
3. to establish structure-activity relationship (SAR),
4. to separate enantiomers when useful for SAR studies,
5. to scale-up the synthesis of the most promising candidates.

The major findings of the thesis were divided in chapters corresponding to articles, briefly described as below:

- **Chapter 2:** a review on marine natural products with important role in circumventing multidrug resistance to anticancer drugs <sup>199</sup>.
- **Chapter 3:** a research article on the antitumor activity investigation of quinazolinone alkaloids based on marine natural products, which describes two synthetic approaches to obtain *anti* and *syn* enantiomers and their evaluation of tumor cell growth and modulatory activity of P-glycoprotein (P-gp) <sup>200</sup>.



- **Chapter 4:** a research article on the synthesis of new proteomimetic quinazolinone alkaloids and the evaluation of their neuroprotective and antitumor effects. The findings of this article were the establishment of a cell growth inhibition structure-activity relationship (SAR) of quinazolinone alkaloids and the confirmation that quinazolinone alkaloids have potential to develop compounds with neuroprotective effects <sup>201</sup>.
- **Chapter 5:** a research article on halogenated quinazolinone alkaloids with potent antibacterial and antifungal activities. This article presents the halogenated quinazolinone alkaloids with antibacterial and antifungal activities both in sensitive and resistant strains and allowed to develop a SAR study for antibacterial activity. Also, the enantioselective effect of these derivatives was emphasized with the *1S,4R*-enantiomer being the active eutomer.
- **Chapter 6:** a research article on antimalarial activity of the library of quinazolinone derivatives. This article describes, for the first time to the best of our knowledge, that quinazolinone alkaloids containing an indolomethyl pyrazino [1,2-*b*]quinazoline-3,6-dione scaffold exhibit antimalarial activity.
- **Chapter 7:** an unpublished work on the gram scale-up synthesis of synthetic fiscalin B (**78**) and other promising derivative (**99**) using the one-pot three component microwave assisted method. This finding highlights the increasing scope of the reaction.
- **Chapter 8:** a research article on the semi-synthesis of heptaphylline (**57**) and derivatives and their restoration of p53 activity. This article highlights the selectivity of semi-synthetic derivatives to inhibit cell growth on p53 mutant cell lines.

To accomplish these objectives, a working plan of this thesis was established as schematized in Figure 8.

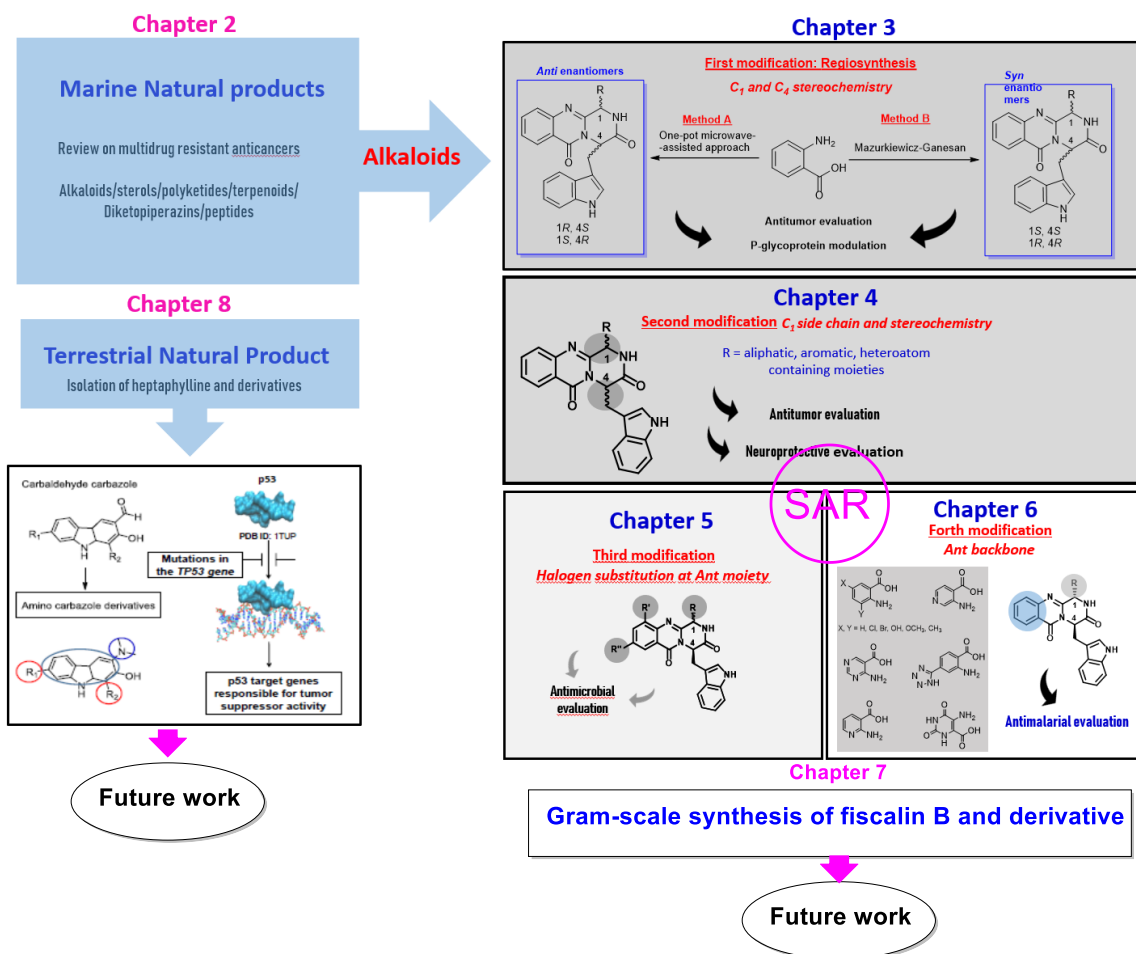
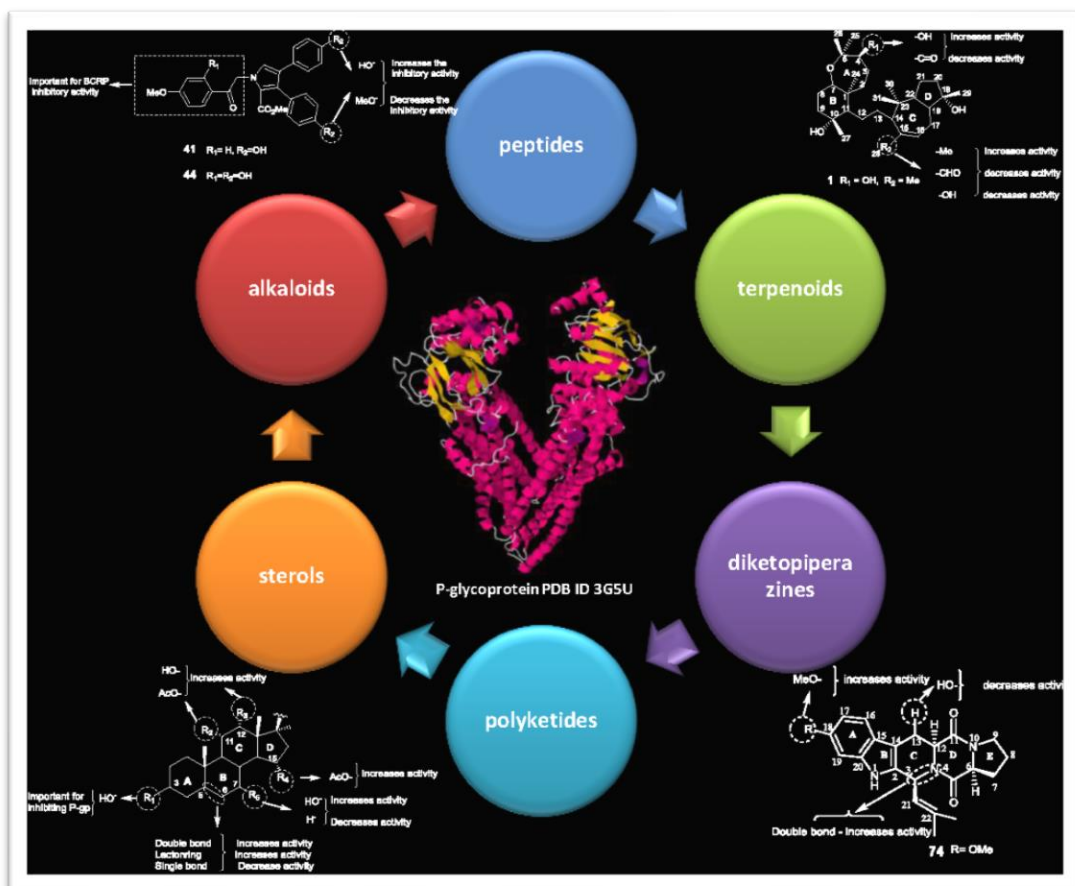


Figure 7: Schematic representation of research work in this thesis.

# Chapter 2

## Marine natural products as models to circumvent multidrug resistance

Graphical abstract





Review

# Marine natural products as models to circumvent multidrug resistance

Solida Long<sup>1</sup>, Emilia Sousa<sup>1,2\*</sup>, Anake Kijjoa<sup>2,3</sup>, and Madalena M.M. Pinto<sup>1,2</sup>

<sup>1</sup> Departamento de Química, Laboratório de Química Orgânica e Farmacêutica, Faculdade de Farmácia, Universidade do Porto, Portugal; up201502099@ff.up.pt (S.L.) ; esousa@ff.up.pt (E.S.) ; madalena@ff.up.pt (M.P.)

<sup>2</sup> Interdisciplinary Centre of Marine and Environmental Research (CIIMAR), Portugal ; ankijjoa@icbas.up.pt (A.K.)

<sup>3</sup> Instituto de Ciências Biomédicas Abel Salazar (ICBAS), Universidade do Porto, Portugal

\* Correspondence: esousa@ff.up.pt; Tel.: +351-220428689; Fax: +351-226093390

Academic Editor: Helena Vasconcelos

Received: 14 June 2016; Accepted: 1 July 2016; Published: 8 July 2016

**Abstract:** Multidrug resistance (MDR) to anticancer drugs is a serious health problem leading to more failure of cancer treatments. ATP binding cassette (ABC) transporter such as P-glycoprotein (P-gp) is responsible for MDR which leads to premature efflux of drugs from cancer cells. On the other hand, a strategy to search for modulators from natural products to overcome MDR had been set up in the last decades. However, nature limits the amount of some natural products which leads to the development of synthetic strategies to increase their availabilities. This review summarizes the research findings on marine natural products and derivatives mainly alkaloids, polyoxygenated sterols, polyketides, terpenoids, diketopiperazines, and peptides with P-gp inhibitory activity highlighting structure-activity relationships established. The synthetic pathways for the total synthesis of the most promising members and analogs are also presented. It is expected that the gathered data of the last decades concerning the synthesis and MDR-inhibiting activities will help

medicinal chemists to develop potential drug candidates using marine natural products as models which can deliver new ABC transporters inhibitor scaffolds.

**Keywords:** ABC transporters; P-glycoprotein modulators; marine natural products; multidrug resistance (MDR); synthesis; structure activity relationship (SAR)

## 1. Introduction

It is well known that cancer figures among the leading causes of morbidity and mortality [1]. Despite much advance in therapy, diagnosis, and prevention, cancer remains a deadly disease. Although cancer consists of many different diseases, most of the disseminated cancers share a common feature of not responding to available chemotherapies. The remorseless onset to resistance to a wide variety of structurally and mechanistically unrelated anticancer drugs, known as multidrug resistance (MDR), is the major obstacle for a successful therapy of human cancers [2]. This eventually leads to cancer relapse and death. Some cancers such as gastrointestinal and renal cancers are largely unresponsive to chemotherapy, i.e.; they have a high degree of intrinsic MDR, whereas leukemias, lymphomas, ovarian, and breast cancers often respond to initial treatment, but acquire MDR during the course of the disease [3]. MDR to anticancer drugs is therefore a serious health problem that dramatically affects the efficacy of cancer treatment [4]. MDR is a phenomenon by which cancer cells develop broad resistance to a wide variety of structurally and functionally unrelated compounds which may arise from several mechanisms [5,6] including: i) decreased cellular drug uptake, ii) activation of detoxifying enzymes, iii) alterations in the molecular targets of the drugs, iv) defective apoptotic pathways and, v) increased drug efflux [6-9]. One of the most prominent mechanisms of MDR to cytotoxic drugs is usually associated with the overexpression of ATP-binding cassette (ABC)-transporter proteins in the tumor cells. Due to the increased efflux out of cells, these pumps can lead to a reduced cellular accumulation of anticancer drugs. These proteins mediate MDR not only in drug entry, but also in drug sequestration by lysosomes, phase III metabolism, mechanisms activated after nuclear entry, apoptosis, microenvironment, and signal transduction pathways that lead to the overexpression of genes that codify these ABC transporters [10]. Such proteins belong to a large family of 49 genes, classified in seven subfamilies (A-G), with

several transporters involved in MDR [11]. These include P-glycoprotein (P-gp or ABCB1), multidrug resistance associated proteins 1-6 (MRP1-6 or ABCC1-6), and breast cancer resistance protein (BCRP or ABCG2) [12]. P-gp is the best characterized efflux pump mediating MDR due to its broadest substrate specificity and widest tissue and organ distribution. This 170 kDa glycoprotein acts as a drug efflux pump for a wide variety of anticancer agents such as anthracyclines and epidodophyllotoxins, thus limiting their bioavailability and activity. P-gp is encoded by the human *MDR-1* gene, which is located at chromosome 7. It contains 1280 amino acids, arranged in two halves, each encompassing a transmembrane domain (TMD) which spans the membrane and an intracellular nucleotide-binding domain (NBD) [13,14].

Several studies have already correlated P-gp expression with resistance to chemotherapeutic drugs, particularly in leukemia cells [15]. Furthermore, down-regulation of P-gp expression was shown to sensitize several tumor-resistant cell lines to chemotherapeutic drugs. Indeed, the use of antisense or ribozyme targeting *MDR-1* gene has led to the sensitization of acute myeloid leukemia (AML), ovarian, colon, and breast cancer cells to doxorubicin as well as to increase the sensitivity of chronic and AML cells to daunorubicin [16,17].

It was found that P-gp could be expressed in Chinese hamster ovary cells, selected for colchicine resistance, almost 40 years ago, and since then there has been an ongoing effort to develop therapies that could either block or inactivate this transporter to increase the concentration of anticancer drugs within cells [18]. First generation of P-gp inhibitors referred to drugs already in clinical use or under investigation for therapeutic ability e.g. verapamil, quinidine, and cyclosporine A [19]. However, most of the first generation P-gp inhibitors were found to lack selectivity for P-gp and being substrates for other transporters and enzyme systems; this promiscuity resulted in unpredictable pharmacokinetic interactions in the presence of anticancer drugs [20]. Moreover, low affinity for P-gp, associated with the original therapeutic activity, required the use of high doses which resulted in unacceptable toxicity [6,21]. Second generation of P-gp inhibitors were developed, based on the selective optimization of side activity (SOSA) approach, to increase the potency and reduce toxicity, many of which were single enantiomers of the first generation drugs. An example of these is dexverapamil which is an *R*-enantiomer of verapamil. Interestingly, many of the second generation P-gp inhibitors such as valspodar (PSC-833), elacridar (GF 120918), and biricodar, also entered clinical trials [6]. Although some of the second generation inhibitors showed better pharmacological profiles in clinical trials, they still had limited use as P-gp modulators since most of them were found to be substrates of cytochrome P450 3A, thus interfering with the metabolism and excretion of co-administered chemotherapeutic agents [22]. The third generation of P-gp inhibitors, which exhibited P-gp inhibitory activity at nanomolar concentrations, were developed to overcome the referred

problems through quantitative structure-activity relationships (QSAR) studies and combinatorial chemistry approaches [23]. Since the third generation of inhibitors that entered clinical trials did not interfere with cytochrome P450 3A4, they did not reveal any interference with pharmacokinetics of anticancer drugs [24]. One of the most popular third generation P-gp inhibitors is tariquidar, however, its phase III studies on non-small cell lung cancer patients were terminated due to its high toxicity [25]. The same unwanted results were observed with other third generation inhibitors like zosuquidar, elacridar, laniquidar, and ontogeny [20,26]. Although phase I and II trials were performed with some third generation P-gp inhibitors, an emerging consensus, in 2010, was that P-gp should be taken off the list of druggable targets due to the failure of zosuquidar clinical benefits in phase III clinical trials [27]. Until now, the existing P-gp inhibitors have demonstrated limited clinical success due to their limitations in potency and specificity and also to their interactions with anticancer drugs. Moreover, QSAR and docking studies also could not produce promising hits or leads for safe and effective compounds. As there is a permanent need to identify and validate new antitumor agents, with novel mechanisms of action, more efficient P-gp inhibitors are needed.

Recently, there has been a proposal of a new generation of ABC's inhibitors which focused on natural products and natural products mimics [28-30], peptidomimetics [31], surfactants and lipids [32], and dual ligands [20]. While the traditional sources of terrestrial plants and microbes will undoubtedly continue to yield valuable new bioactive agents, it is even more important to explore all available pools of molecular diversity. This strategy to seek out new ecosystems for bioprospecting brings with it the opportunity to discover unprecedented molecular structures, with bioactivities unencumbered by known (and evolving) mechanisms of drug resistance [33]. Marine natural products are one of the most interesting targets for global drug discovery since they not only possess structural and chemical uniqueness but also represent novel scaffolds for drug development [34]. Marine natural products have also been studied and tested alongside with synthetic compounds as ABC transporters inhibitors [29,35-38]. The development of anticancer drugs from marine compounds is one of the most promising approaches in drug discovery with therapeutic agents in clinical practice, such as the anticancer trabectedin [37]. Recently, marine natural products and their analogs with antitumor activity have been developed, and many of them have shown also ability for ABC modulation. Thus, marine natural products are revealing an interesting potential in this field not only for the possibility of being used in combination with other anticancer drugs but also as dual inhibitors of tumor cell growth and P-gp. Thus, they could be of value in the rational design of analogs with high potential and reduced pharmacokinetic interactions.

There are already several reviews which highlighted the importance of marine natural products in cancer and, in particular, as P-gp modulators [29,35,39-43]. However, this review aims



to describe not only the effects of the most valuable scaffolds from marine natural products and analogs in overcoming MDR but also their synthetic pathways. These data along with structure-activity relationship herein described could serve to guide medicinal chemists in pursuing innovative inhibitors of ABC transporters using marine natural products as models.

## 2. Marine natural products and derivatives as inhibitors of ABC transporters

### 2.1. Terpenoids

#### 2.1.1. Sipholane triterpenoids and derivatives

Sipholane triterpenes are compounds that contain a perhydrobenzoxepin (rings A and B) and a [5, 3, 0]bicyclodecane ring systems (rings C and D) linked together by an ethylene group (Figure 1). This class of triterpenes consists of sipholenol A (**1**), sipholenone E (**2**), sipholenol L (**3**), and siphonellinol D (**4**), isolated from the Red Sea sponge *Callyspongia siphonella* [44,45], and semisynthetic derivatives of sipholenol A such as sipholenol A-4-O-acetate (**5**), sipholenol A-4-O-isonicotinate (**6**) [39], sipholenol A-4-O-3',4'-dichlorobenzoate (**7**) [46], sipholenol A 4-O-4'-chlorobenzoate (**8**), and 19,20-anhydrosipholenol A 4-O-4'-chlorobenzoate (**9**) [47] that were synthesized using a ligand-based design approach. Natural and semisynthetic siphonane triterpenoids were shown to reverse MDR activities (**1-6**), and antimigratory and antiproliferative activities in breast cancer cell lines (**7-9**). Sipholenol A (**1**) showed to be potent in reversing MDR KB-C2 [48] and KB-V1 tumor cells with overexpressed P-gp, in a concentration-dependent manner. Compound **1** also inhibited P-gp-mediated drug efflux and did not alter the expression of P-gp after treatment in KB-C2 and KB-V1 cells. This compound stimulated the activity of ATPase, and also inhibited the photo-labeling transporter with [<sup>125</sup>I]-iodoarylazidoprazosin [44]. From SAR studies (Figure 1), it was demonstrated that substitution of the methyl group on C-15 by carbonyl or alcohol reduced the MDR-inhibitory activity, while changing from a hydroxyl to a ketone function at C-4 also reduced the activity [48]. Compounds **2**, **3**, and **4** also enhanced the cytotoxicity of several P-gp substrates including colchicine, vinblastine, and paclitaxel, and reversed the MDR-phenotype in P-gp-overexpressing MDR KB-C2 tumor cells, in a dose-dependent manner [45]. Compound **2** was reported as a better P-gp inhibitor than **1** in KB-3-1 and KB-C2 cell lines [49], while **3** and **4** also showed a reversal of MDR in the same tumor cells but did not reveal the effect on cells lacking P-gp expression or expressing MRP1, MRP7, or BCRP transporters [36,45,49].

The semisynthetic esters **5** and **6** were found to strongly reverse P-gp (ABCB1)-mediated MDR, however they showed no effect on MRP1/ABCC1 and BCRP/ABCG2-mediated MDR. These analogs increased the intracellular accumulation of paclitaxel through inhibition of its active efflux, and re-

sensitized cells that have developed drug-resistance to doxorubicin and paclitaxel. These two compounds stimulated more intensively the ATPase activity of P-gp membranes than **2**, **3**, and **4**. *In silico* molecular docking study, by the inspection of the virtual binding modes of compounds **5** and **6** into human homology model of P-gp, revealed that both compounds were overlapped but with different molecular orientation of ester substituents. Their strong affinity and specificity to P-gp expressing efflux protein indicated that compounds **5** and **6** may represent a potential reversal agent for treatment of MDR cancers [39].

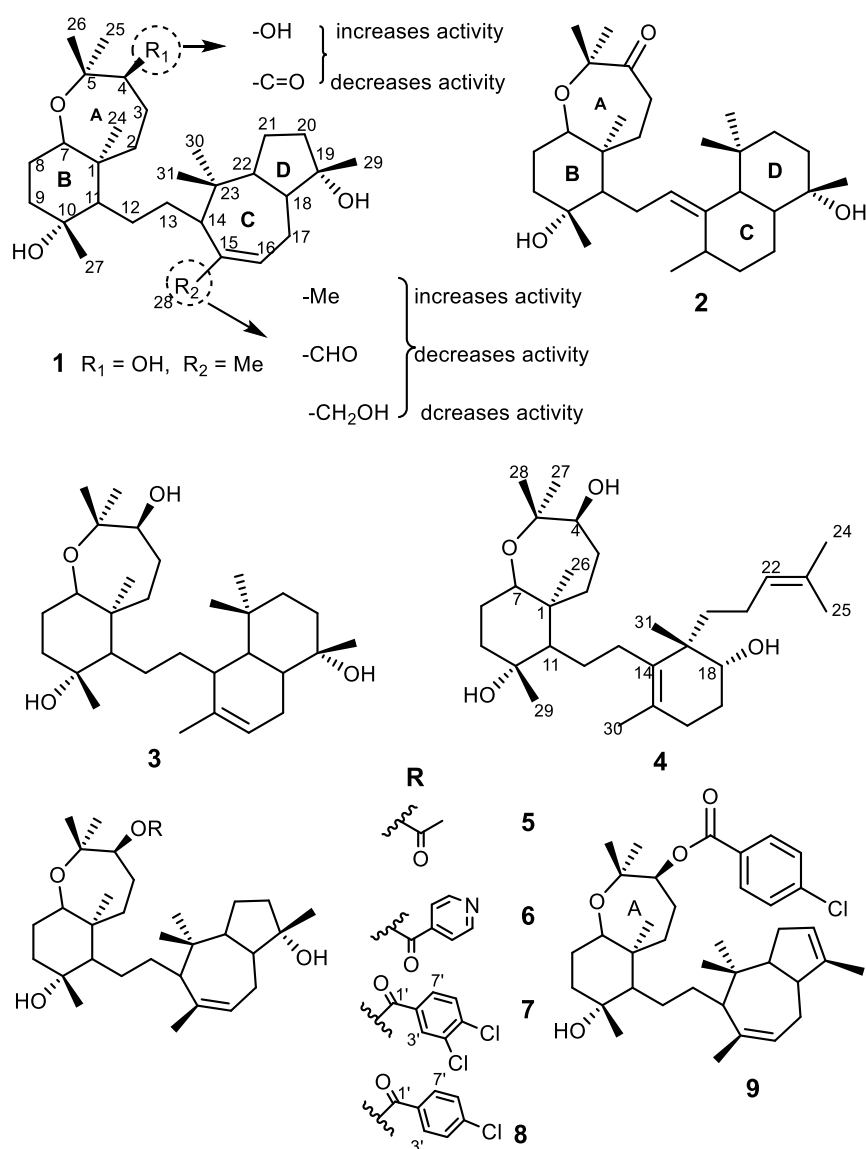
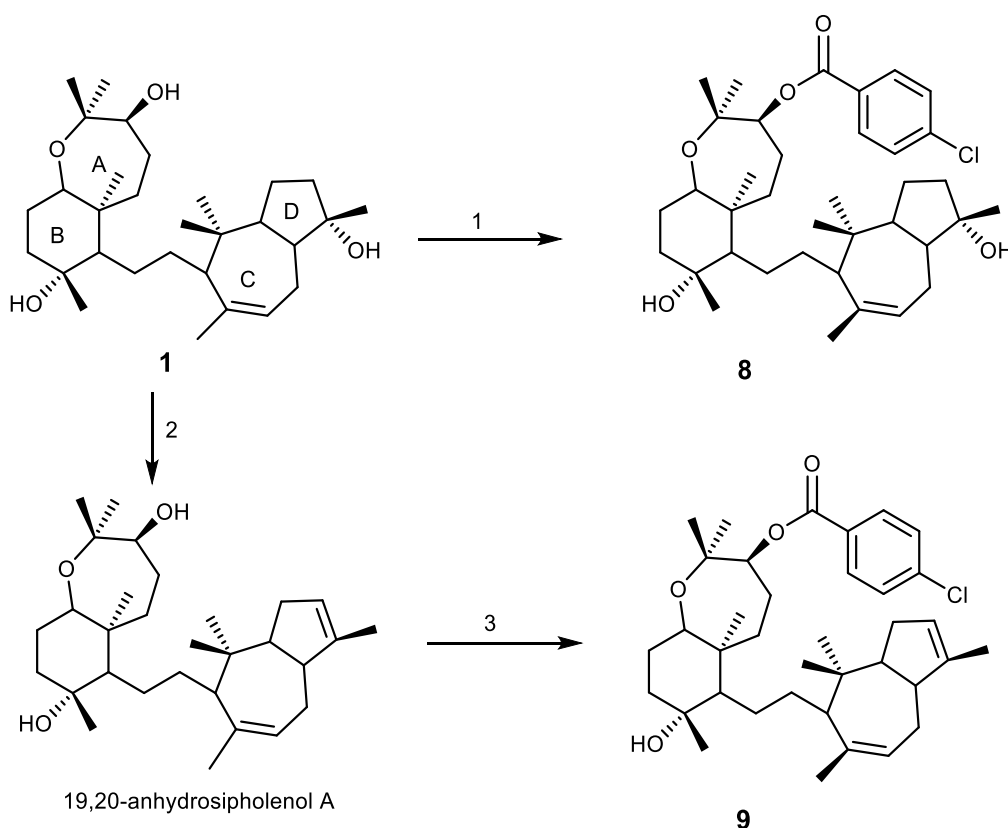


**Figure 1.** Structures of sipholane triterpenes **1-4** and their analogs **5-9**. Dashed circles indicate SAR studies performed for MDR activities.

In scheme 1, the synthesis of the ester analogs **8** and **9** is described to highlight the strategy involved (using a ligand-based design approach).



**Scheme 1.** The semi-synthesis transformation of siphophenol A (**1**) into analogs **8** and **9**. Reagents and conditions: 1) acid anhydride, MDAP, anhydrous  $\text{CH}_2\text{Cl}_2$ ; 2) *p*-toluenesulfonic acid,  $\text{CHCl}_3$ ; 3) acid anhydride, MDAP, anhydrous  $\text{CH}_2\text{Cl}_2$ .

### 2.1.2. Parguerenes and derivatives

Parguerenes I (**10**) and II (**11**) (Figure 2) are bromoditerpenes, isolated from the Australian red alga, *Laurencia filiformis* [50]. Other brominated diterpenes of the parguerenes and isoparguerenes were isolated from red alga *Jania rubens* were reported to have antitumor, anthelmintic and antimicrobial activities [51]. Parguerene derivatives have cytotoxic activity on P388 and HeLa cells due to an acetoxy group at C-2 and a bromine at C-15 [52]. Compounds **10** and **11** were non-cytotoxic and dose-dependent inhibitors of P-gp mediated drug efflux of verapamil and cyclosporine A. It was also reported that **10** and **11** are capable of reversing P-gp mediated vinblastine, doxorubicin, and paclitaxel in cells overexpressing both P-gp (SW620/ADV300, CEM/VLB100, and HEK93/ABCB1) and MRP1 (2008/MRP1), in a dose-dependent manner. However, their inhibitory effect did not extend to BCRP. Compounds **10** and **11** interact with P-gp by disturbing the

extracellular antibody binding epitope of P-gp differently from existing P-gp inhibitors [53]. Therefore, the use of this scaffold as a model for the synthesis of new MDR reversal agents could be of value. To the best of our knowledge, the synthesis of parguerenes has not yet been reported.

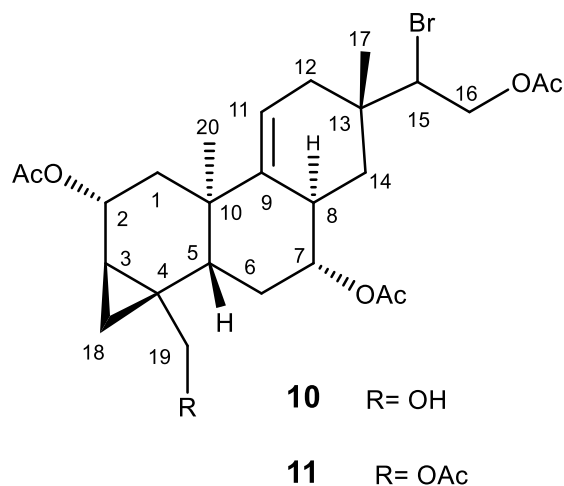


**Figure 2.** The structures of parguerene I (**10**) and II (**11**).

## 2.2. Sterols

### 2.2.1. Agosterol and derivatives

Agosterol A (**12**, Figure 3), a polyhydroxylated sterol acetate isolated from the marine sponge *Spongia sp.* [54], was found to completely reverse MDR to colchicine in human carcinoma cells KB-C2 and to vincristine in KB-CV60 (overexpressing MRP1) [55]. Compound **12** was reported to have a dual effect on MRP1 function by reducing MRP1-mediated [<sup>3</sup>H]-LTC<sub>4</sub> and enhancing the accumulation of [<sup>3</sup>H]-vincristine in KB/MRP cells to the control levels. It also enhances the ATP-dependent efflux and reduces glutathione intracellular concentration [56]. Therefore, **12** has inhibitory effects on both P-gp and MRP1. The effect of analogs of **12**, including agosterol B, C, A4, D2, A5 and C6, on MDR in tumor cells was also investigated. Agosterol C was found to be proteasome inhibitor [57]. From the SAR studies, it was possible to infer that the acetoxy groups on C-3, C-4, and C-6, and the hydroxyl groups on C-11 and C-12 were crucial for MDR reversal activity for binding to the C-terminal of MRP1 (Figure 3) [58,59]. 4-Deacetoxyagosterol A (**13**) showed a similar MDR-modulating activity against KB CV-60 cell overexpressing MRP [60].

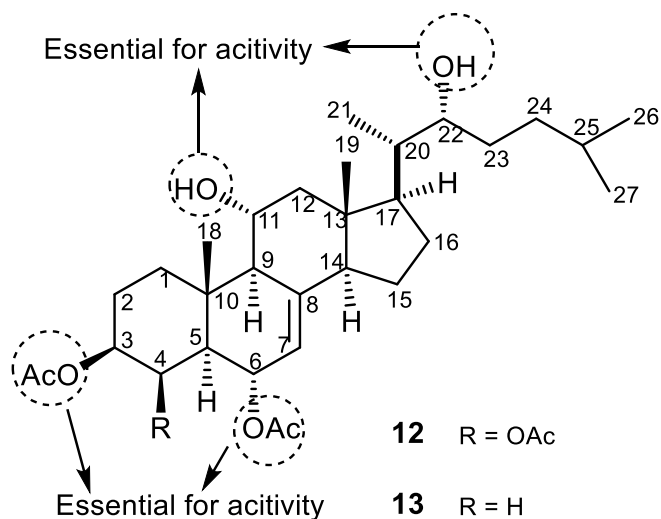
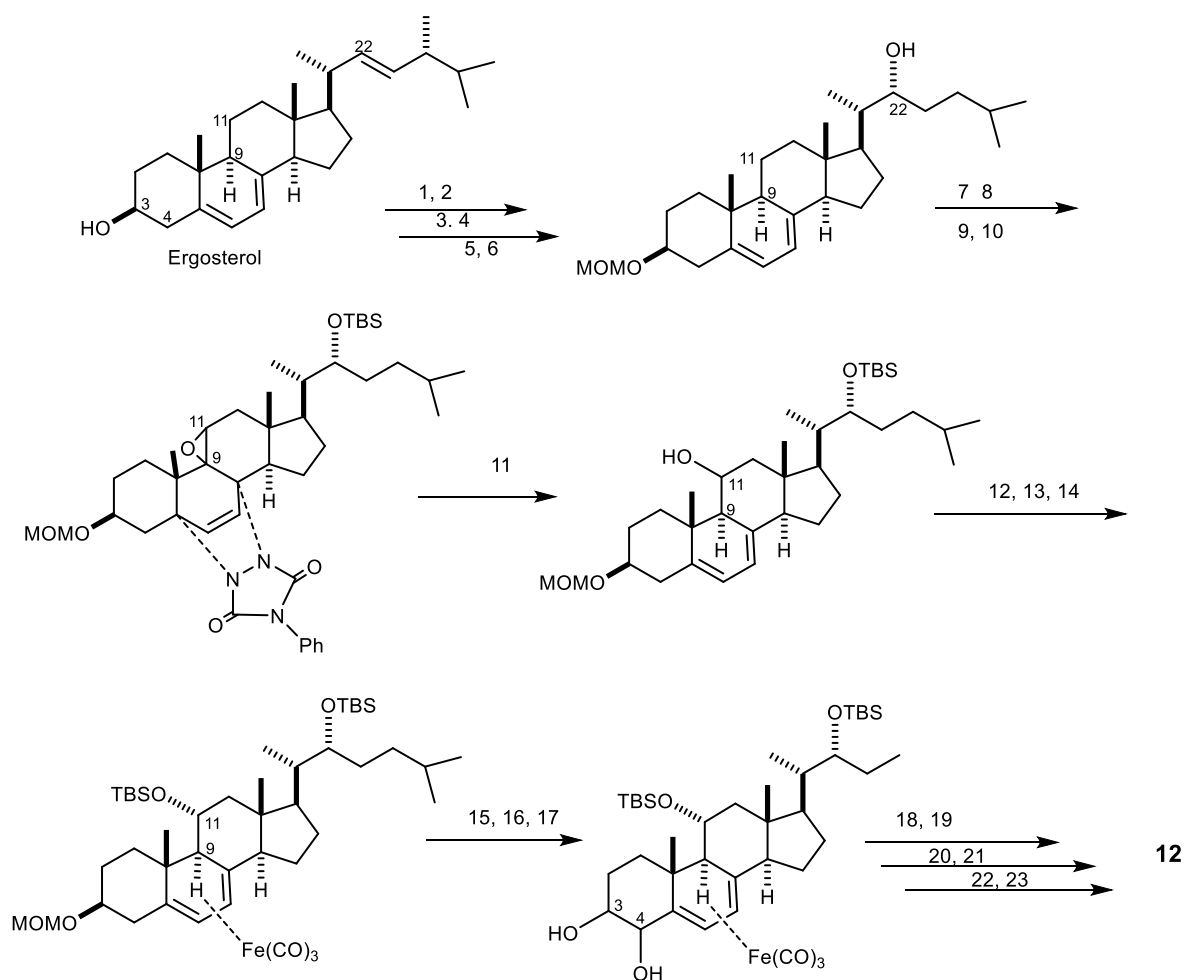


**Figure 3.** Structure of agosterol A (**12**) and 4-deacetoxyagosterol A (**13**). Dashed circles indicate the groups essential for reversing MDR activity.

The first synthesis of **12** from ergosterol, through 23 steps with 3.5% yield, by utilizing regioselective epoxy-cleavage and regioselective dehydroxylation as key reactions was reported in 2001 [61]. The synthetic pathway started with the oxidative cleavage of the C-22/C-23 double bond of ergosterol to introduce a hydroxyl group to C-22, followed by a regioselective reductive epoxy-cleavage of 9 $\alpha$ , 11 $\alpha$ -epoxide to form an 11 $\alpha$ -hydroxyl group. The next step was the introduction of a C-3/C-4 double bond which, after a selective dehydroxylation, afforded 3 $\beta$ ,4 $\beta$ -dihydroxyl groups. Finally, a differential removal of the protecting group and acetylation afforded **12** (Scheme 2). Compound **13** was also synthesized from ergosterol by reductive regioselective epoxy-cleavage reaction similar to that of **12** [60].



**Scheme 2.** The synthetic pathway of agosterol A (**12**). Reagents and conditions: 1) MOMCl, *i*Pr<sub>2</sub>NEt, CH<sub>2</sub>Cl<sub>2</sub>; 2) phthalhydrazide, Pb(OAc)<sub>4</sub>, CH<sub>2</sub>Cl<sub>2</sub>, AcOH, two steps; 3) O<sub>3</sub>, CH<sub>2</sub>Cl<sub>2</sub>, pyridine, then Me<sub>2</sub>S; 4) 3-methylbutylmagnesium bromide, THF, two steps; 5) TMAD, PMe<sub>3</sub>, *p*-OCH<sub>3</sub>BzOH, THF; 6) LiAlH<sub>4</sub>, THF; 7) (*S*)-(-)-MTPA[(*R*)-(+)-MTPA], EDCI.HCl, DMAP, CH<sub>2</sub>Cl<sub>2</sub>; 8) TBSOTf, 2,6-lutidine, DMF-CH<sub>2</sub>Cl<sub>2</sub>; 9) Hg(OAc)<sub>2</sub>, EtOH/CHCl<sub>3</sub>/AcOH; 10) 4-phenyl-1,2,4-triazoline-3,5-dione, CH<sub>2</sub>Cl<sub>2</sub>; 11) *m*CPBA, CHCl<sub>3</sub>; 12) LiAlH<sub>4</sub>, THF; 13) TBSOTf, 2,6-lutidine, toluene; 14) Fe(CO)<sub>5</sub>, 1-(4-methoxyphenyl)-4-phenyl-1-azabuta-(*E,E*)-1,3-diene, PhCH<sub>3</sub>; 15) MgBr<sub>2</sub>-Et<sub>2</sub>O, Me<sub>2</sub>S, CH<sub>2</sub>Cl<sub>2</sub>; 16) TsCl, pyridine, quant.; 17) DBN, PhH, quant.; 18) OsO<sub>4</sub>, pyridine, then aq. NaHSO<sub>3</sub>; 19) TESOTf, pyridine, quant.; 20) Me<sub>3</sub>NO, PhH; 21) BH<sub>3</sub>Me<sub>2</sub>S, THF, then H<sub>2</sub>O<sub>2</sub>, aq. NaOH; 22) TBAF, THF; 23) Ac<sub>2</sub>O, pyridine; HF, pyridine, THF.

### 2.2.2. Polyoxygenated steroids and derivatives

A number of polyoxygenated steroids has been isolated from gorgonians (*Isis hippuris* [62] and *Leptogorgia sarmentosa* [63]), soft corals (*Sarcophyton* sp. [64] and *Sinularia* sp. [65]), echinoderms, and sponges [62]. Interestingly, all the polyoxygenated steroids investigated for antitumor [66], antibacterial [64], antifungal [64], and reversing MDR [62] activities contain the characteristic

3 $\beta$ ,5 $\alpha$ ,6 $\beta$ -hydroxyl moiety. Among these derivatives are a spiroketal hippurinstanol (**14**), hippuristerone (**15**) which possesses a 3-keto group, and cyclopropane containing gorgosterols (**16-20**) (Figure 4) [62,64]. Polyoxygenated steroids **14-20** also differ in the side chains. Some of them (**16-20**) have been tested against KB-C2 overexpressing P-gp cells and showed moderate activity at the concentration of 3  $\mu$ M by inhibiting the growth of this resistance cell line. Compounds **17** and **18** were the most potent against KB-C2 cells [62].

Semi-synthetics of 3,16,20-polyoxygenated cholestanes, namely (20S)-hydroxycholestane-3,6-dione (**21**), (16S,20S)-dihydroxycholestan-3-one (**22**), (20S)-hydroxycholest-1-ene-3,16-dione (**23**), and (20S)-hydroxycholest-4-ene-3,16-dione (**24**) were tested for cytotoxicity against three tumor cell lines, i.e. human breast adenocarcinoma (MCF7), human small-cell lung carcinoma (NCI-H187), and human epidermoid carcinoma of cavity (KB). Compounds **23** and **24** showed strong activity against NCI-H187, and moderate activity against MCF-7 and KB, while compound **21** did not show any activity [63]. Although no MDR-reversal activities were described, these compounds provided a promising synthetic approach for natural polyoxygenated steroids. The synthesis of these four analogs, **21-24**, was conducted through four reaction steps, using-tigogenin as a starting material, as shown in Scheme 3. The synthetic pathway started with the transformation of a spiroketal functionality of tigogenin to a keto ester using the method previously described by Micovic *et al.* and modified by Fushs *et al.* [67]. The keto ester **I** was then transformed to a trihydroxyl intermediate **II** by Grignard reagent which, after oxidation, gave compounds **21** and **22**. Dehydrogenation of **21** then afforded **23** and **24** [63]. In addition, the introduction of epoxidation and dihydroxylation in suitable positions of steroid nucleus containing oxygenated functions was reported by using transition metal-based oxidants such as methyltrioxorhenium-hydrogen peroxide system, ruthenium tetroxide, osmium tetroxide, and potassium permanganate [68].

### 2.3. Polyketides

#### 2.3.1. Bryostatin and derivatives

Bryostatins are highly oxygenated marine macrolides with a polyacetate backbone [69], and more than 20 analogs have been isolated from the marine bryozoans *Bugula neritina* and *Amathia convoluta* [70]. Most of bryostatins possess antineoplastic activity in many cancer systems like M5076 sarcoma, L10AB cell, and mouse lymphogenous metastatic model SCID. Bryostatin 1 (**25**, Figure 5) was reported to down-regulate *MDR-1* and *BCL-2*, but up-regulates *BAX* (induction of apoptosis) [71,72]. Spitaler *et al.* reported that **25** interacted with the mutated *MDR-1-V185* and the wild-type

*MDR-1*-G185, but reversed *MDR* and inhibited drug efflux only in *P-gp*-V185 mutants [72]. The mechanism of regulating *MDR* for **25** was also reported as protein kinase C (*PKC*) independent, and it seems to interact directly with *MDR-1* encoded *P-gp* [73]. However, in human breast cancer cell line (MCF-7), **25** only decreases *P-gp* phosphorylation after 24 h treatment in a concentration of 100 nM but did not affect *P-gp* function in the intracellular accumulation of [<sup>3</sup>H]-vinblastine and rhodamine 123 [74].

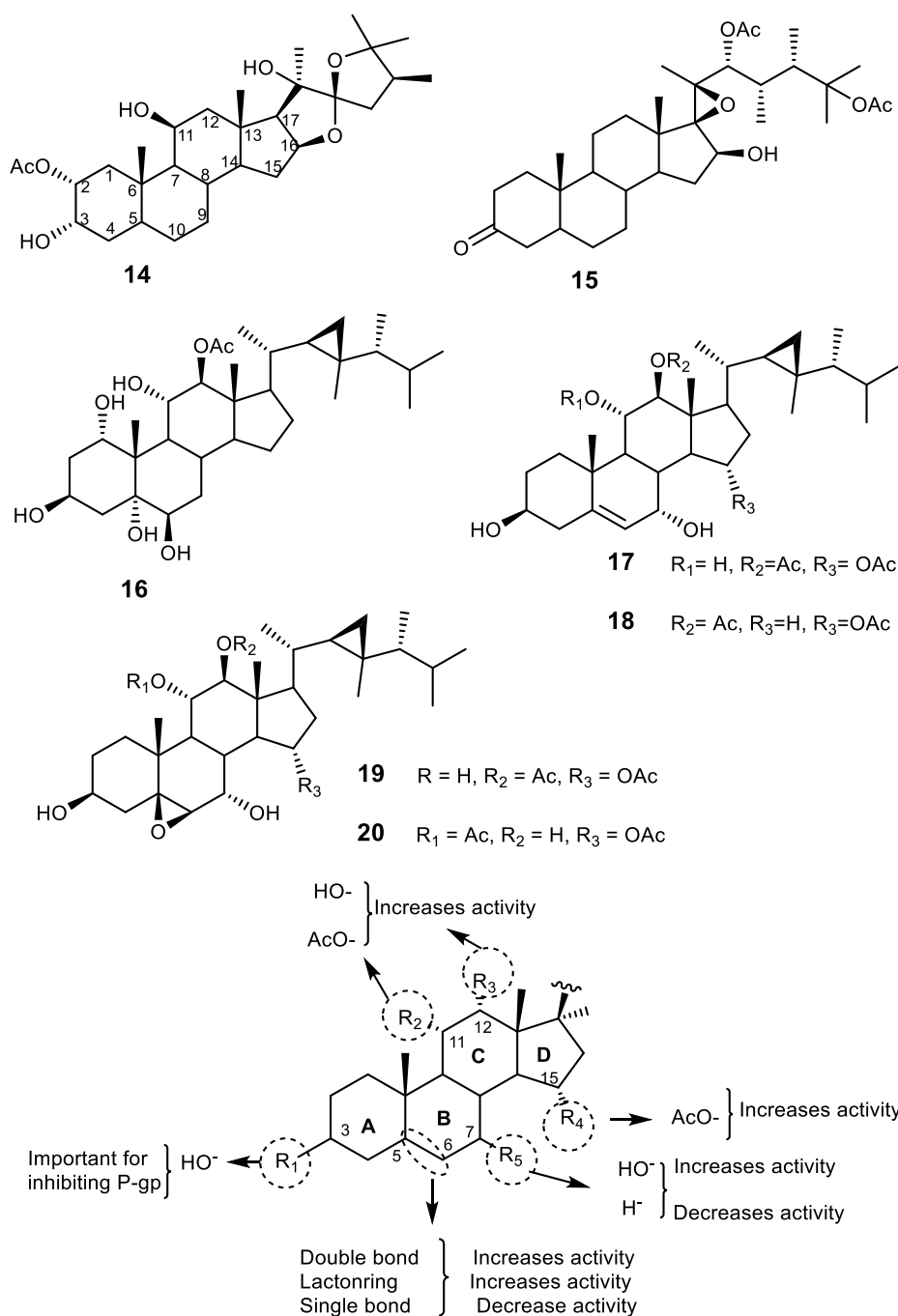
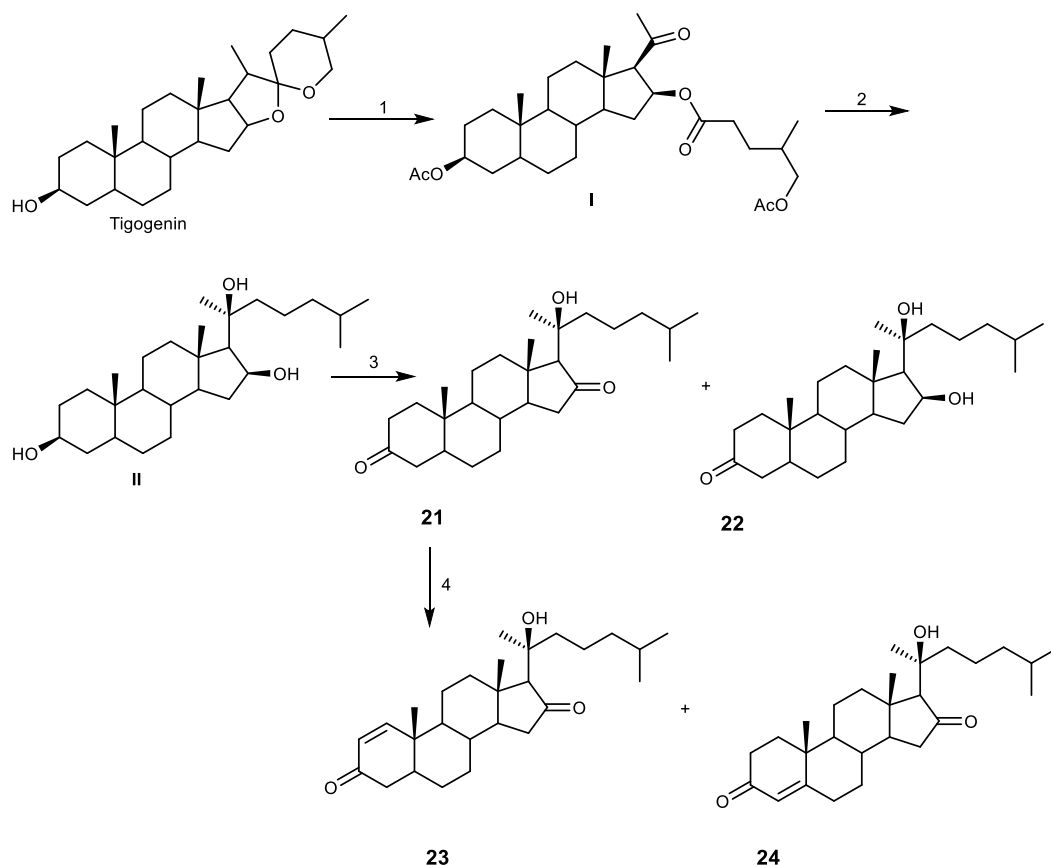


**Figure 4.** The structures of polyoxygenated steroids **14-20**, and SAR for polyoxygenated steroids with antitumor activity in overexpressing *P-gp* cells.





**Scheme 3.** The synthesis of 3, 16, 20-polyoxygenated steroids **21-24**. Reagents and conditions: 1) i.  $\text{NH}_4\text{Cl}$ , pyridine,  $\text{AcOH}$ ; ii.  $\text{CrO}_3$ ,  $\text{AcOH}$ ,  $\text{H}_2\text{O}$ ,  $(\text{CH}_2\text{Cl}_2)$ ; 2) 4-methylpentylmagnesiumbromide, THF; 3) PCC,  $\text{NaOAc}$ ,  $\text{CH}_2\text{Cl}_2$ ; (4)  $\text{Ph}_2\text{Se}_2$ , *m*-iodomybenzoic acid, toluene, reflux.

It was found that C-1 to C-9 segment of bryostatins is suitable for both synthetic and biological investigation, and this segment was prepared from an inexpensive and easily accessible compound 2,2-dimethyl-8-oxabicyclo[3,2,1]oct-6-en-3-one [69]. Merle 23 (**26**, Figure 5), is a synthetic analog of bryostatin and whose structure differs from that of bryostatin 1 (**25**) in four positions of the space domain fragment (Figure 5). Interestingly, merle 23 (**26**) showed a behavior of a phorbol ester and not of bryostatin in human prostate cancer cell line (LNCaP), and this finding provided a powerful tool to dissect bryostatins mechanisms and responses [75,76].

The synthesis of bryostatin analog **27** (Scheme 4.a) without ring A and with simplified ring B was carried out by a convergent esterification-macrotransacetalization procedure to couple the recognition (C-17-C-27) and the spacer (C-1-C-16) domain fragments (Figure 5) [70]. The synthetic pathway involves an allylation of an appropriate alcohol **I** to give the ether intermediate **II**. Hydroboration of the ether intermediate **II**, followed by oxidation gave the appropriate aldehyde **III**, which was then subjected to an oxidative cleavage reaction to furnish the spacer domain. The

Yamanguchi's esterification was used to produce the next intermediate **IV**, after which macrotranscetalization and deblocking of C-26 alcohol were accomplished to yield bryostatin analog **27** in 11 steps (Scheme 4.a) [77].

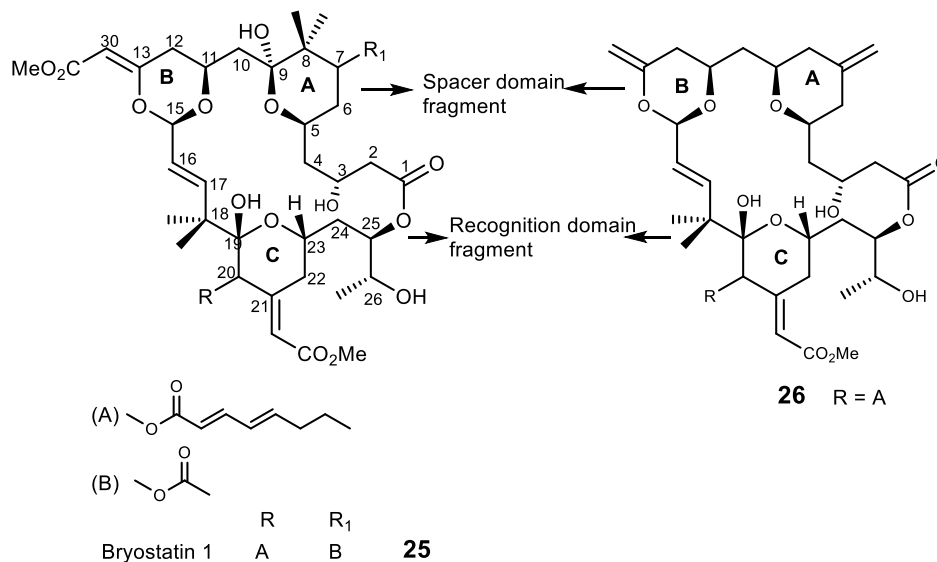
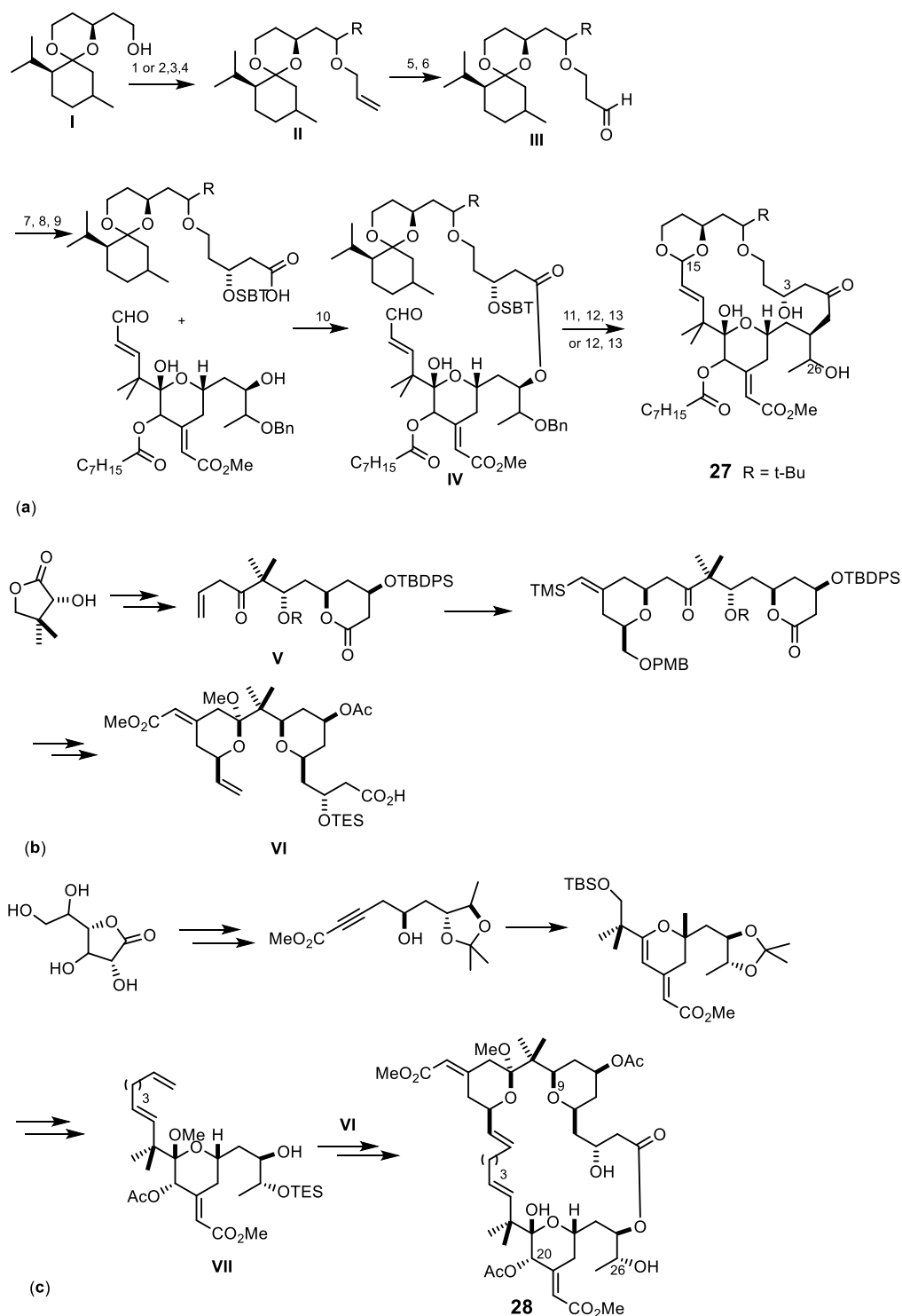


**Figure 5.** The structures of bryostatin 1 (**25**) and merle 23 (**26**).

Trost *et al.* reported the synthesis of the bryostatin analog **28** with cross-metathesis approach at C-16-C-17 bond using ruthenium and palladium coupling methodologies for the synthesis of B- and C-rings [78,79]. The synthetic pathway of the spacer domain started from (*R*)-pantolactone and a protected alcohol to produce the intermediate **V**. The coupling of the intermediate **V** with an alkyne afforded B-ring pyran. The A-ring ketal was formed by deprotection and cyclization reactions, and the spacer domain **VI** was formed by deprotection, oxidation, and olefination (Scheme 4.b). The C-ring fragment was prepared from a lactonized sugar using Roy's approach [80], and the recognized domain **VII** was obtained as described in Scheme 4.c. Finally, a Shiina esterification was used to join **VI** and **VII** to give **28** with 36% yield [79].

### 2.3.2. Discodermolide

Discodermolide (**29**, Figure 6) is a polyketide found in the marine sponge *Discodermia dissoluta*. This marine product was reported to have a mechanism of action similar to that of taxol, i.e. by blocking the cell cycle at G2/M checkpoint and inducing apoptosis against several cancer cell lines and against taxol-resistant cells.



**Scheme 4.** Synthesis of the methyl bryostatin 1 analogs **27** and **28**. Reagents and conditions: (a) 1) NaH, allylbromide, THF, rt; 2) Dess-Martin periodinene, CH<sub>2</sub>Cl<sub>2</sub>, rt; 3) *t*-BuLi, Et<sub>2</sub>O, -78°C, (1:1 mixture of diastereomer which can be recycled: Dess-Martin periodinane, CH<sub>2</sub>Cl<sub>2</sub>, rt, then NaBH<sub>4</sub>, CeCl<sub>3</sub>·7H<sub>2</sub>O, -40°C; 4) *t*-BuOH, allylbromide, THF, rt; 5) 9-BBN, THF, 66°C, then NaOH, H<sub>2</sub>O<sub>2</sub>; 6) Dess-Martin periodinane, CH<sub>2</sub>Cl<sub>2</sub>, rt; 7) (-)-(lpc)BOMe, allylmagnesium bromide, CH<sub>2</sub>Cl<sub>2</sub>, -78°C to rt; 8) TBSCl, imidazole, THF, rt; 9) catalytic KMnO<sub>4</sub>, NaIO<sub>4</sub>, rt; 10) 2,4,6-trichlorobenzoylchloride, Et<sub>3</sub>N, DMAP, CH<sub>2</sub>Cl<sub>2</sub>, rt; 11) HF.pyridine, CH<sub>3</sub>CN, rt; 12) Ambertyst-15 resin, CH<sub>2</sub>Cl<sub>2</sub>, rt; 13) Pd(OH)<sub>2</sub>, H<sub>2</sub>, EtOAc, 1atm.

Biological activities of **29** include immunosuppressive properties, antiproliferative and antimetabolic properties, potent inducer of accelerated cell senescence, neuroprotective agent, and promote tubulin assembly [81-84]. In addition, **29** was also found to decrease the MDR to taxol in paclitaxel-resistant colon carcinoma (SW60AD-300) and MDR ovarian carcinoma (A2780Ad) [85].

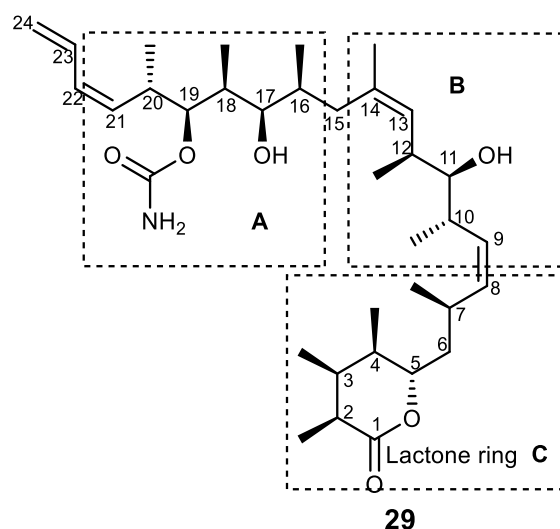
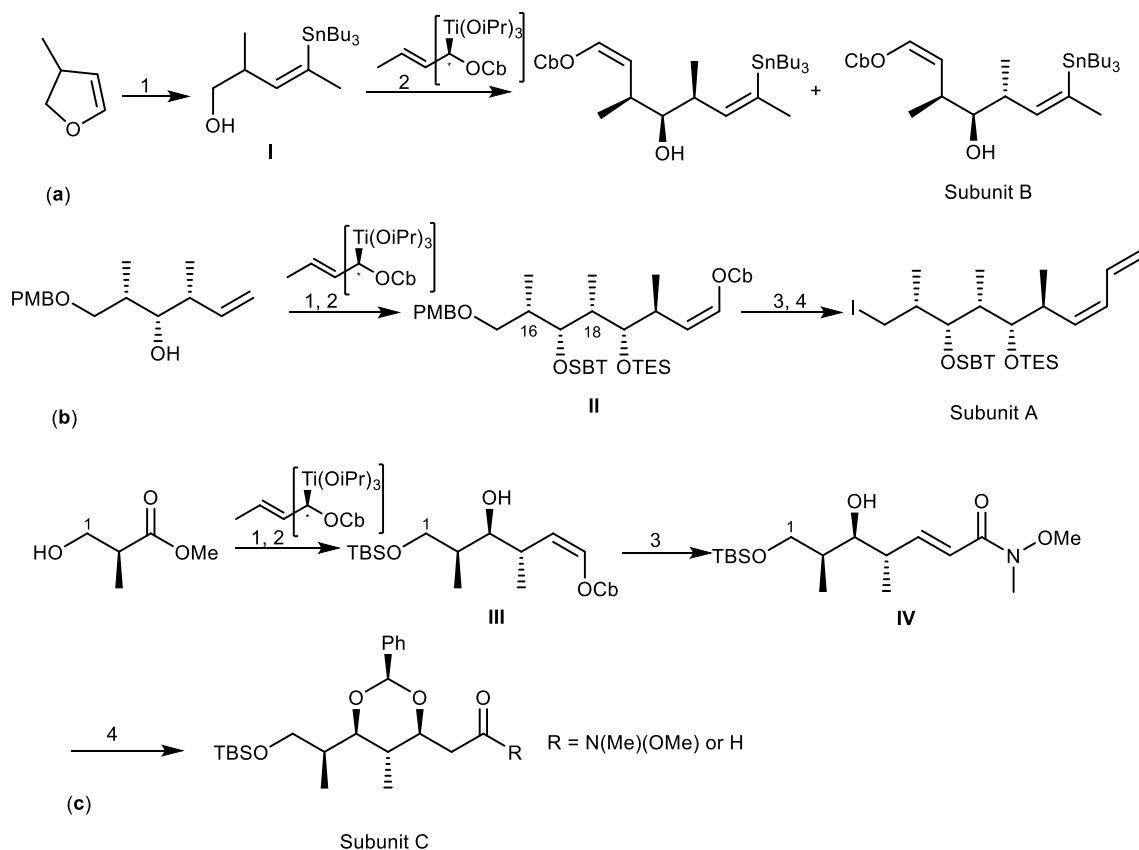


**Figure 6.** Structure of discodermolide (**29**) with highlighted subunits A, B, and C.

The strategy to synthesize (+)-discodermolide (**29**) and its analogs was achieved by preparing the three subunits: A (C-15-C-24), B (C-8-C-14), and C (C-1-C-7). The synthetic pathway was designed by two key disconnection points at C-7-C-8 and C-14-C-15 with the two *Z* double bonds at C-8-C-9 and C-13-C-14 being pivotal in this strategy. Formation of the C-7-C-8 bond was envisaged through an acetylide addition/reduction sequence, whereas formation of the C-14-C-15 linkage was accomplished by a Pd-catalyzed C(sp<sup>2</sup>)-C(sp<sup>3</sup>) cross-coupling reaction [86]. Subunit B was prepared in two main stages: a crotyl-titanation reaction for the installation of the stereotriad and a dyotropic rearrangement to build a *Z*-double bond **I** (Scheme 5.a). The synthesis of subunit A started with the preparation of the C-16-C-18 *syn-syn* stereotriad **II**, planned by means of a substrate-based crotylation reaction under Keck's conditions (Scheme 5.b). The third building block, C-1-C-7 subunit **C**, incorporates four stereocenters. The approach started with standard Brown crotylation of aldehyde to afford *syn-anti* homoallylic alcohol **III**. Then, the  $\alpha,\beta$ -unsaturated Weinreb amide was obtained through a classical Horner-Wadsworth-Emmons olefination. Finally, reaction of amide **IV** with benzaldehyde yielded subunit C (Scheme 5.c). The assembly of the three subunits by cross-coupling reaction and deprotection were the last steps to afford **29**. Recently, (+)-discodermolide (**29**) was synthesized by catalytic stereoselective diene hydroboration, and a strategy for alkylation of chiral enolate reaction was established through 36 steps with 13% yield [87].



**Scheme 5.** Total synthesis of subunits A, B, and C of (+)-discodermolide (**29**). Reactions and conditions: (a) 1)  $t\text{-BuLi}$ ,  $\text{Me}_2\text{CuLi}$ ,  $\text{LiCN}$ ,  $\text{Et}_2\text{O/DMS}$  then  $n\text{-Bu}_3\text{SnCl}$ ; 2) TEMPO, BAIB; (b) 1)  $\text{TBSOTf}$ ,  $2,6\text{-lutidine}$ ,  $\text{O}_3$ ,  $\text{sudan III}$  then  $\text{DMS}$ ; 2)  $\text{TBSOTf}$ ,  $2,6\text{-lutidine}$ , 3)  $\text{Ni}(\text{acac})_2$ ,  $(\text{CH}_2=\text{CH}_4)\text{Sn}$ ,  $\text{MeLi}$ ; (4)  $\text{DDQ}$ ,  $\text{CH}_2\text{Cl}_2/\text{H}_2\text{O}$ ,  $\text{I}_2$ ,  $\text{PPh}_3$ ; (c) 1)  $\text{TBSOTf}$ ,  $2,6\text{-lutidine}$ , 2)  $\text{O}_3$ ,  $\text{sudan III}$ ,  $(\text{EtO})_2\text{P}(\text{O})\text{CH}_2\text{C}(\text{O})\text{NMe}$ ,  $\text{NaH}$ ; (3)  $\text{O}_3$ ,  $\text{sudan III}$ ,  $(\text{EtO})_2\text{P}(\text{O})\text{CH}_2\text{C}(\text{O})\text{NMe}$ ,  $\text{NaH}$ ; (4)  $\text{PhCHO}$ ,  $\text{KHMDS}$ .

### 2.3.3. Halicondrin B and derivatives

The macrolide halichondrin B (**30**, Figure 7), a polyether isolated from the marine sponge *Halichondria okadai*, exhibited both *in vitro* and *in vivo* antitumor activity [88]. However, the very limited obtainability impairs this marine natural product for its therapeutic application [89]. Eribulin mesylate (E7389, or Halaven®, **31**), a synthetic analog of **30**, was approved in 2010 by FDA for the treatment of locally advanced and metastatic breast cancer by inhibiting the microtubules [89,90], and was reported as a P-gp substrate [91]. The structure of **31** (Figure 7) is complex, containing several oxygen heterocycles, two exocyclic methylene groups, a ketal group, and a pyran ring with *trans* ring junction, along with 15 stereogenic centers. Several molecular modifications of **31** have been performed, and SAR studies with semi-synthetic analogs revealed that the substituent on C-32 of **31** plays an important role in the P-gp mediated drug efflux. The presence of an amine function

in the substituents on C-32 in the analogs **32-35** led to a low susceptibility to P-gp-mediated drug efflux, and compounds **32-35** were active against MDR tumor cell line *in vitro* and in xenograft models *in vivo* [43,91]. Furthermore, treatment with eribulin in pretreated metastatic breast cancer patients was confirmed as feasible and safe in the real-world patients [92].

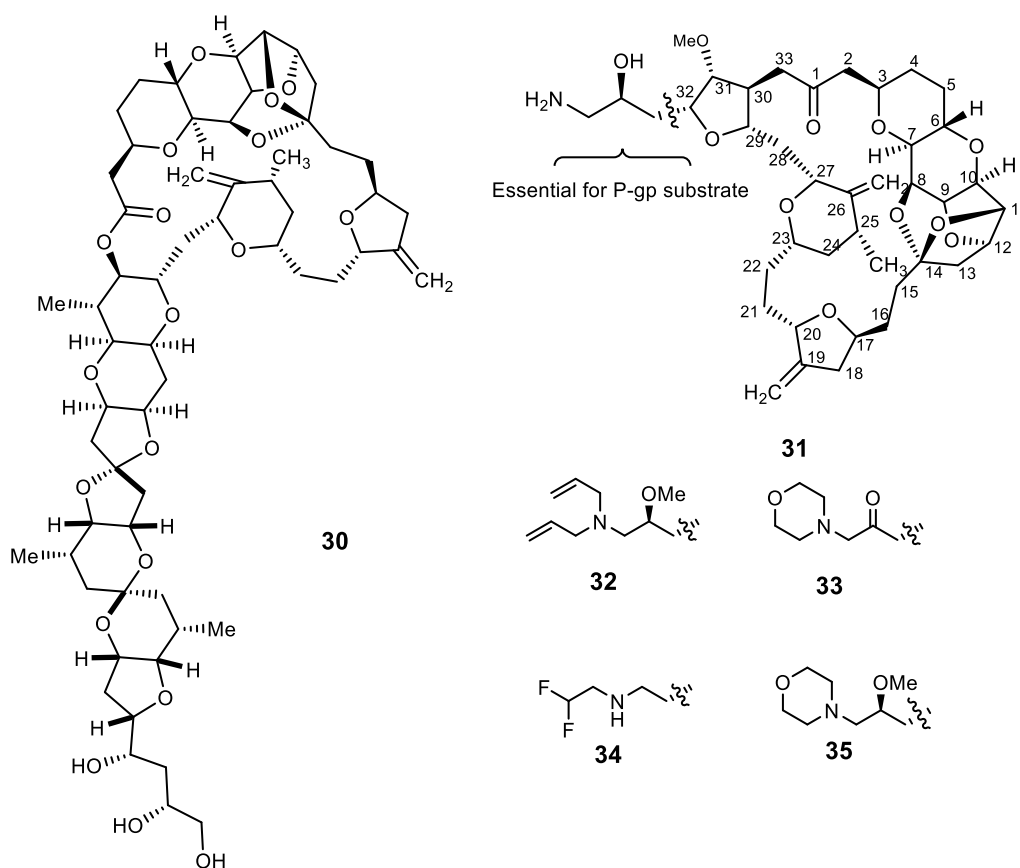
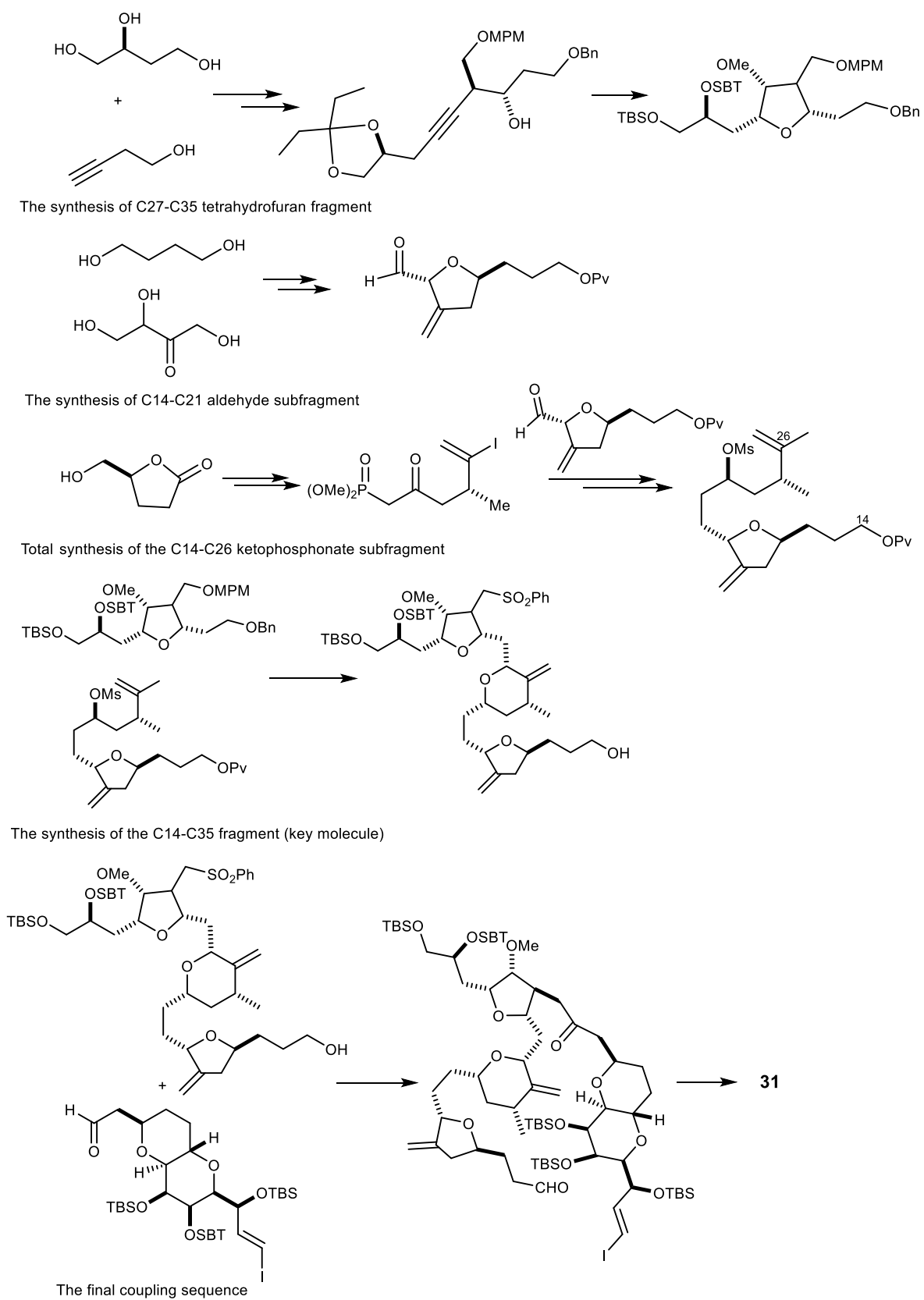


**Figure 7.** The structure of halichondrin B (**30**), eribulin (**31**), and the analogs **32-35**.

Different methods for the synthesis, to obtain milligram to gram amounts of **31** have been reported [75,93]. Generally, the synthetic pathway of **31** consists of preparation of two fragments, i.e. C-1–C-13 and C-14–C-26, as described by Kishi's group in 1992, and one key fragment (C-27 to C-35). The final assembly strategy is accomplished by the coupling reaction depicted in Scheme 6 [90,93].



**Scheme 6.** Schematic approach for the total synthesis of eribulin (**31**).

## 2.4. Alkaloids

### 2.4.1. Lamellarins and derivatives

Lamellarins are a group of polycyclic pyrrole-containing alkaloids possessing a common 14-phenyl-6*H*-[1]-benzopyrano[4',3',3,5]pyrrolo-[2,1- $\alpha$ ]isoquinoline ring system [94]. Lamellarins were isolated from many marine organisms such as prosobranch mollusk (*Lamellaria sp.*) [35,95], ascidian (*Daphniphyllum chartaceum*), sponge (*Dendrilla cactos*), and unidentified ascidians [35]. More than 50 lamellarins have been described and mainly differ in the number and position of hydroxyl and methoxy groups on the common chromenoindoles I scaffold (Figure 8) [96]. Some lamellarins possess interesting biological activities e.g. lamellarin L (**36**) which exhibited cytotoxicity against P388 and A549 cancer cell lines [97], lamellarin D (**37**) which is also an inhibitor of topoisomerase I-targeted antitumor agents and an antiproliferative agent [96,98] and the immunomodulating lamellarin  $\alpha$ -20 sulfate which inhibits also HIV [99]. Lamellarin I (**38**) was the most potent polycyclic pyrrole-containing alkaloid described as a MDR modulator. Methoxy-derivatives of lamellarin D (**37**), lamellarin K (**39**), and lamellarin N (**40**) (Figure 8), exhibit not only potent cytotoxicity against MDR cancer cell lines but also reverse their MDR at non-cytotoxic concentration [100,101]. Compound **38** was 16 folds more sensitive than verapamil in doxorubicin-resistant Lo Vo/Dx cell line, and it increased the cytotoxicity of doxorubin, vinblastine, and daunorubicine in MDR cells because it directly inhibited P-gp pump function and increased drug accumulation in the cells [102]. Lamellarin O (**41**) is relevant as a multiple P-gp, BCRP, and MRP1 inhibitor [96], but synthetic analogs of **41**, designed by QSAR studies and incorporating the methoxyacetophenone moiety unit, did not show BCRP inhibitory activity [103]. This study also allowed to establish some SAR features: bromo or mono-/dimethyl substituents on the indole moiety ( $R_2$ ) in lamellarin O (**41**) lead to a decrease in the BCRP inhibitory activity [103] (Figure 8).

The structures of lamellarins are categorized into three types (Figure 8) – type I-a (lamellarin D, **37**), type I-b (lamellarin L, **36**), and type II [lamellarins O (**41**), R (**42**), Q (**43**)]. The syntheses of these derivatives are illustrated by types as presented in the next subsections.

A total synthesis of a type-II lamellarins was described by Furstner in 1995. It was the first characterized pathway by a non-fused pyrrole moiety. The synthetic pathways started with the Sheffer-Weitz-epoxidation of an enone **I**, as depicted in Scheme 7.a, followed by a Lewis acid-mediated rearrangement and condensation with hydroxylamine to afford the corresponding isoxazole **II**. Cleavage of the N-O bond, condensation, and McMurry cyclization were the subsequent steps to yield lamellarin O dimethyl ester (Scheme 7.a) [104]. Another alternative for type-II lamellarin synthesis was performed by cross-coupling using Stille, Suzuki or Negishi



reactions which was described by Banwell *et al.* in 1997. In this process, the pyrrole was protected to form the intermediate which was suitable to afford dibromopyrrole 2-carboxylate. *N*-desilylation and cross-coupling with aryl stannane produced the coupling product which was subjected to *N*-alkylation, followed by desilylation to provide **41** with high yield of 45% in six steps (Scheme 7.b) [105]. The strategy of Banwell was employed by Alvarez *et al.* with variations on solid phase chemistry and gave lamellarin **43** (in 13% yield), and lamellarin **41** which could not be isolated [106]. In 2008, Iwao *et al.* used the Suzuki-Miyaura cross-coupling approach, used by Banwell, to synthesize type II lamellarins, yielding compounds **43**, **41**, and lamellarin P (**44**) in 7, 11, and 12% respectively, over eight steps [107]. Therefore, increasing the steps of reaction did not increase the reaction yield. Boger *et al.* described the synthesis of lamellarin **41** using an azadiene Diels-Alder reaction named as 1,2,4,5-tetrazine-1,2-diazine-pyrrole transformation with the overall yield of 34% within seven steps [108]. The pyrrole moiety was assembled by a [4+2] cycloaddition/cycloreversion reaction, followed by a reductive ring transformation. They started by forming the acetylenic precursor using Sonogashira-coupling from aryl acetylene and aryl iodide, followed by the cycloaddition of this precursor to give 1,2-diazine which was then subjected to a reductive ring contraction and *N*-alkylation. Selective hydrolysis of the symmetrical diester provided the monoacid. The subsequent hydrogenolysis afforded lamellarin **41** (Scheme 7.c) [108]. In 2012, Vazquez *et al.* used the Paal-Knorr pyrrole synthesis to synthesize **41** in 25% yield in seven steps, and **43** in 28% yield in six steps [94].

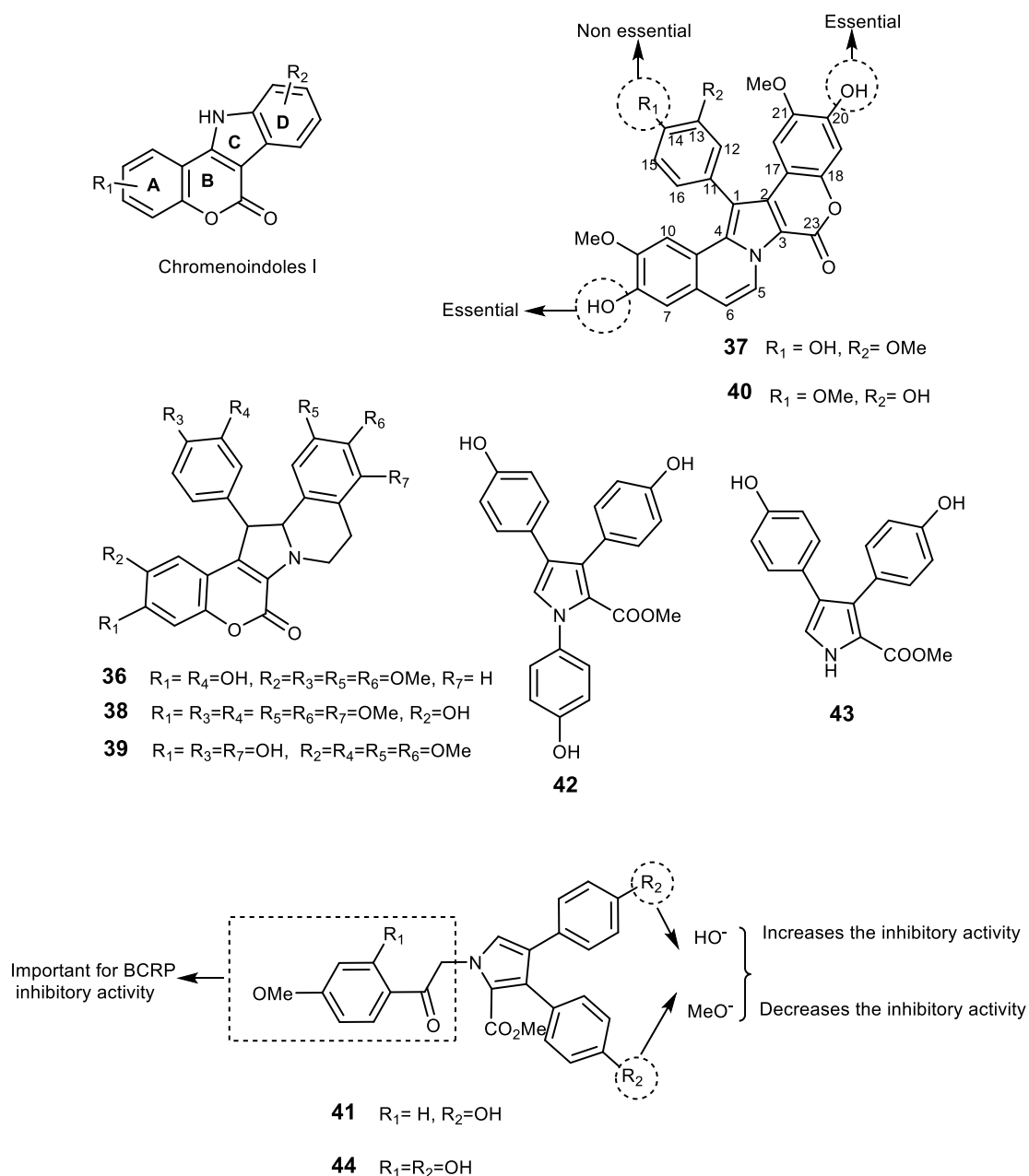
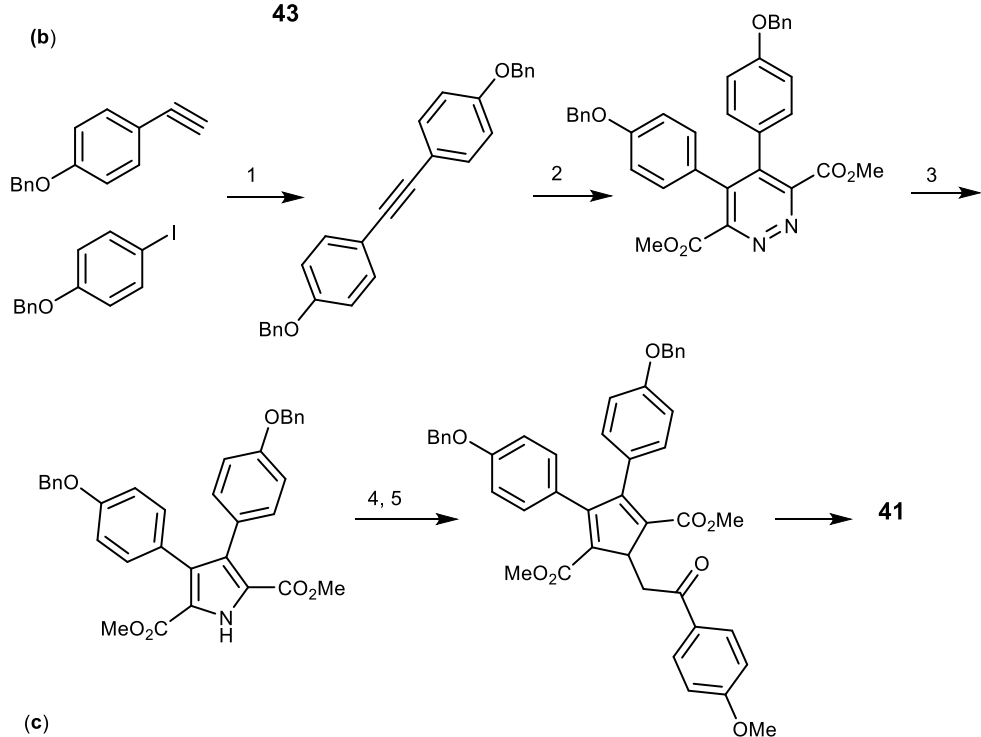
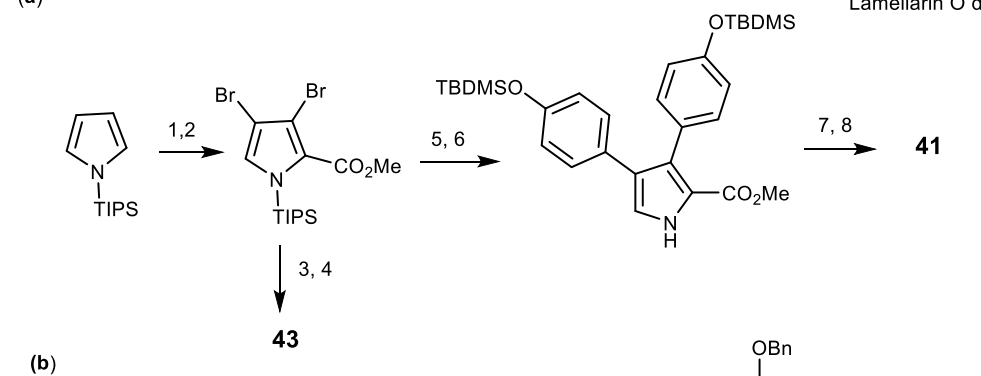
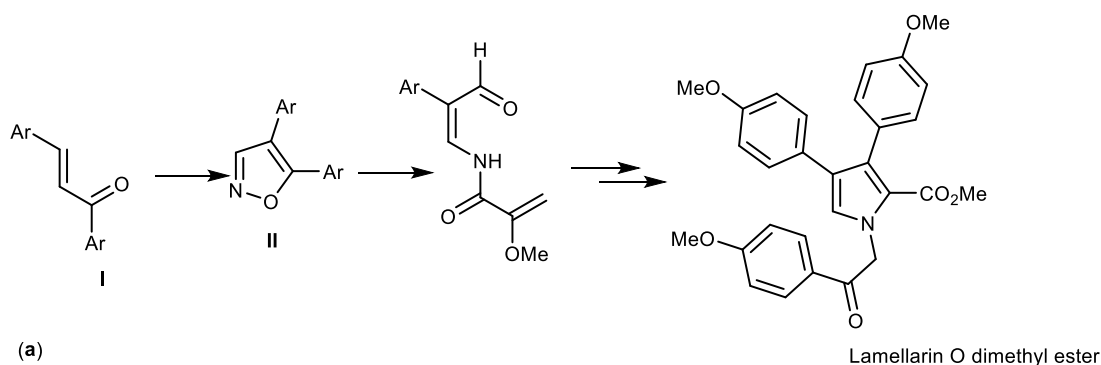


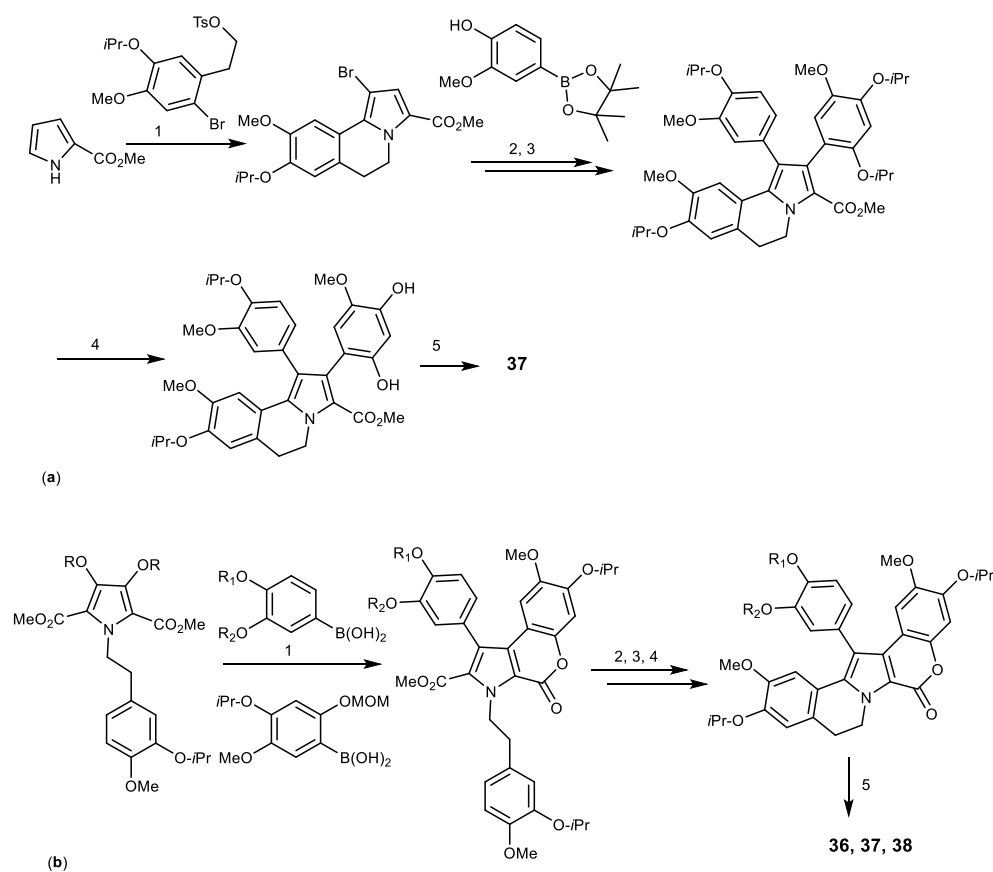
**Figure 8.** The scaffold of lamellarins and their representatives **36-44**. SAR studies for lamellarin D (**37**) and lamellarin O (**41**) regarding antitumor activity on BCRP overexpressing cells.

The synthesis of lamellarins type I-a was performed via different approaches such as the halogenation and cross-coupling reaction, *N*-ylide-mediated pyrrole ring formation, and other miscellaneous approaches. Lamellarin D (**37**) was synthesized by Alverz *et al.*, starting from the pyrrole ester. The A and B subunits of **37** were established by *N*-alkylation of pyrrole ester by Baeyer-Villiger oxidation, palladium-catalyzed Heck-type cyclization, followed by a regioselective bromination, providing the tricyclic building block which was subjected to Suzuki-Miyaura cross-coupling sequence *O*-isopropylation of the phenolic group and to a second bromination-Suzuki cross-coupling sequence. Introduction of a 5, 6-double bond was accomplished by oxidation.



**Scheme 7.** Synthesis of lamellarin O (**41**) and lamellarins type II. Reagents and conditions: (a) 1)  $\text{H}_2\text{O}_2$ , NaOH, EtOH/ $\text{H}_2\text{O}$ ; 2)  $\text{BF}_3 \cdot \text{Et}_2\text{O}$ , Et<sub>2</sub>O, reflux, then  $\text{NH}_2\text{OH} \cdot \text{HCl}$ , reflux, pyridine, EtOH; 3)  $\text{H}_2$ , Pd/C, THF; 4)  $\text{ClCOCO}_2\text{Me}$ , pyridine, THF; 5) Ti-graphide ( $\text{TiCl}_3:\text{C}_8\text{K}=1:2$ ), DME, reflux; *p*-MeO- $\text{C}_6\text{H}_4\text{COCH}_2\text{Br}$ ,  $\text{K}_2\text{CO}_3$ , acetone, reflux; (b) 1) NBS (3 eq), THF; 2) PhLi (1 eq), then  $\text{ClCO}_2\text{Me}$  (1.05 eq); 3)  $\text{Pd}(\text{PPh}_3)_2\text{Cl}_2$  (10 mol%), 1,4-dioxane, *p*-TBOMSO- $\text{C}_4\text{H}_6$ -SnMe<sub>3</sub> (2 eq); 4)  $\text{Bu}_4\text{NF}$  (1.1 eq), THF, then 0.5 M HCl; 5)  $\text{Bu}_4\text{NF}$  (1.1 eq), THF then 0.5 M HCl; 6)  $\text{PPd}(\text{PPh}_3)_2\text{Cl}_2$  (10 mol%), 1,4-dioxane, *p*-TBOMSO- $\text{C}_4\text{H}_6$ -SnMe<sub>3</sub> (2 eq); 7) *p*-MeO- $\text{C}_4\text{H}_6$ -COBr (3 eq),  $\text{K}_2\text{CO}_3$  (5 eq),  $\text{Bu}_4\text{NCl}$  (20 mol%), THF; 8)  $\text{Bu}_4\text{NF}$  (1.1 eq), THF, then 0.5 M HCl; (c) 1)  $\text{Pd}(\text{PP}_3)_2\text{Cl}_2$  (3 mol%), CuI (6 mol%), Et<sub>3</sub>N; 2) dimethyl 1,2,4,5-tetrazine-3,6-dicarboxylate, toluene, reflux; 3) Zn, HOAc; 4) *p*-MeO- $\text{C}_4\text{H}_6$ -COBr,  $\text{K}_2\text{CO}_3$ , DMF; 5) LiOH, THF/ $\text{CH}_3\text{OH}/\text{H}_2\text{O}$  (3:2:1); 6) TFA,  $\text{CH}_2\text{Cl}_2$ ; 7)  $\text{H}_2$ , Pd/C (0.1 wt%), EtOH.

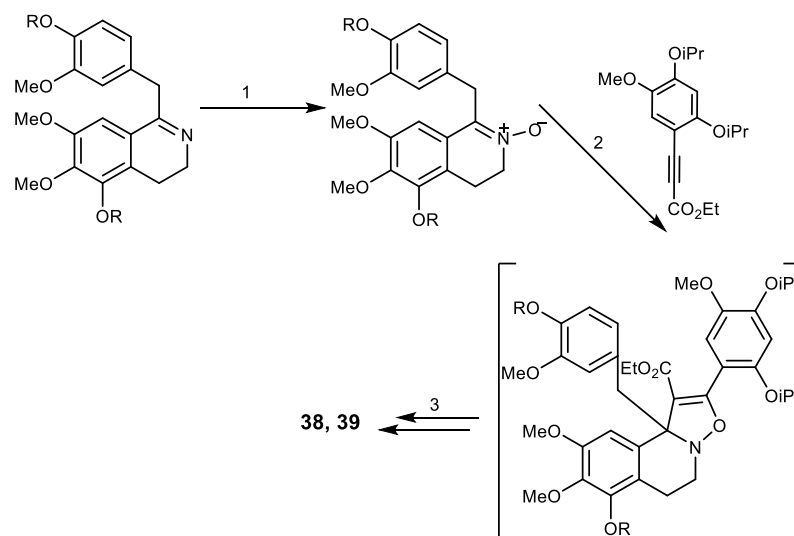
Finally, cleavage of isopropyl esters, followed by acidic lactonization, afforded **37** in 3% yield, over 16 steps (simplified in Scheme 8.a) [109]. In the same year, Pla *et al.* reported a sequential and regioselective bromination/Suzuki cross-coupling reaction to introduce the aryl group at position 1 of methyl 5,6-dihydropyrrolo[2,1-*a*]isoquinoline-2-carboxylate, with the combination of microwave-assisted 2,3-dichloro-5,6-dicyanobenzoquinone (DDQ) oxidation, followed by phenol deprotection and lactonization to give **37** in the 18% yield in 8 steps reaction [109]. Iwao *et al.* also reported the synthesis of **36**, **37**, and **40** in 19%, 18%, and 16% yields over 11, 12, and 12 steps, respectively. They started from isopropyl-protected isovanillin and applied a nitroaldol condensation, a *N*-dialkylation and Hinsberg pyrrole cyclization reactions (Scheme 8.b) [110].



**Scheme 8.** Synthesis of lamellarin D (**37**). Reagents and conditions: (a) 1) PdCl<sub>2</sub>(PPh<sub>3</sub>)<sub>2</sub>, PPh<sub>3</sub>, K<sub>2</sub>CO<sub>3</sub>, NaH, DMF; 2) PdCl<sub>2</sub>(PPh<sub>3</sub>)<sub>2</sub>, K<sub>2</sub>CO<sub>3</sub>, DMF; 3) NBS, THF; 4) DDQ, CHCl<sub>3</sub>, MW, AlCl<sub>3</sub>, CH<sub>2</sub>Cl<sub>2</sub>; 5) NaH, THF; (b) 1) Pd(PPh<sub>3</sub>)<sub>4</sub>, THF, reflux; 2) KOH-EtOH, reflux, then *p*-TsOH, CH<sub>2</sub>Cl<sub>2</sub>, reflux; 3) Cu<sub>2</sub>O, quinolone; 4) Pd(OAc)<sub>2</sub>, CH<sub>3</sub>CN, reflux; 5) BCl<sub>3</sub>, CH<sub>2</sub>Cl<sub>2</sub>.

In 2001, Diaz *et al.* constructed the pyrrole core in [3+2]-cycloaddition of nitron to synthesize **38** and **39** (Scheme 9). The *N*-oxides were prepared in moderate yields by reduction of 3,4-dihydro-1-

benzylisoquinolines, followed by disodium tungstate-catalyzed oxidation with hydrogen peroxide. Reaction of *N*-oxide with alkyne produced an intermediate through the 1,3-dipolar cycloaddition-thermal rearrangement. Selective removal of isopropyl group from the intermediate, with concomitant lactonization, gave lamellarins **38** and **39** in 4 and 6% yields, respectively [101]. In 2014, Yamaguchi *et al.* reported the synthesis of lamellarin I (**38**) using  $\beta$ -selective arylation of pyrroles with aryl iodides and a new double C-H/C-H coupling as a key step to afford **38** in 3% over 8 steps, starting from 2,3,4-trimethoxybenzaldehyde [111].



**Scheme 9.** Synthesis of lamellarin I (**38**) and K (**39**) via 1,3-dipolar cyclization of nitrones. Reagents and conditions: 1) NaBH<sub>4</sub>, MeOH, H<sub>2</sub>O<sub>2</sub>, Na<sub>2</sub>WO<sub>3</sub>, MeOH; 2) toluene, 120°C, 18h; 3) AlCl<sub>3</sub>.

#### 2.4.2. Ningalins and derivatives

Ningalins are members of 3,4-dihydroxyphenylalanine (DOPA)-derived *o*-catechol metabolites including the tunichromes [112]. Biological activities of ningalins was found to be HIV-1 integrase inhibition [113], Ningalin B (**45**, Figure 9), was isolated from an ascidian of the genus *Didemnum* by Boger *et al.* in 1999. Compound **45** lacks an intrinsic cytotoxicity which makes this alkaloid an interesting model as MDR reversal agent. Interestingly, the synthetic analogs **46-50** were shown to significantly sensitize the HCT116/VM46 human colorectal carcinoma cell overexpressing P-gp to vinblastine and doxorubicin better than the marine natural product **45** and verapamil [114]. Studies of the *N*-aryl homologs of **45** (**50-51**) revealed that increasing the carbon linker leads to increase in activity. The authors concluded that the *N*-alkylaryl substituent is necessary for activity, but the analogs which bear free phenolic groups and methyl esters are more cytotoxic and lack potent MDR reversal properties. Analogs of **45** containing tetra- or penta-substituted pyrroles showed the highest activity as MDR reversal agents [114-116] whereas those having 2- carboxylate or 2, 5-carboxylates

bearing 3,4-diaryl-substituted pyrrole showed reversal ability toward HCT116/VM46 cells. Compound **51** exhibited the greatest potential in reversing the MDR at 1 mM, and at 10 mM with about 4,000-folds increase in sensitivity against the vinblastine resistant MDR-leukemia cell line. This compound was also shown to compete with [<sup>3</sup>H]-azidopine for P-gp binding site and increased the intracellular accumulation and retention of MDR substrates. In nude mice-xenograft models, the combination of sub-optimal dose of paclitaxel with **51** not only leads to shrinkage the HCT116 tumor size but also to a complete therapeutic remission without increasing toxicity toward the host [116]. The amide analog **48** showed little or no effect of MDR on HCT116/VM46, while amine derivatives (dimers) were inactive as MDR reversal compounds [115]. The synthetic analog **46**, 1-[2-(4-methoxyphenyl)-2-oxoethyl]-3,4-bis (3,4-dimethoxyphenyl)-1*H*-pyrrole-2,5-dione (**52**) showed a remarkable enhancement of MDR reversal abilities in concentrations up to 1 μM [117,118]. Compound **53**, having a methoxy group on D-ring, showed a 18.2-fold increase in sensitizing cells towards paclitaxel at 1 μM concentration, and a 66-fold when 0.5 μM of **53** was combined with 0.5 μM of **54** [117]. It was found that increasing the number of the methoxy group on ring B of ningalin scaffold showed only low to moderate P-gp-modulating activity, while the addition of a benzyloxy group on the D ring enhanced the P-gp modulating activity [119]. SAR studies of a series of novel *N*-substituted derivatives of **45** on breast P-gp-overexpressing tumor cell line (LCC6MDR) showed that analogs containing one methoxy group and one benzyloxy group on ring C are the most potent P-gp modulators (1 μM desensitized cell line by 42.7 folds) without showing cytotoxicity IC<sub>50</sub> for L929 fibroblast > 100 μM) [117,119,120]. The analog containing dimethoxy groups on rings A and B, and tri-substitution on ring D with *o*-methoxyethyl morpholine, *m*-bromo and *p*-benzyloxy (**55**) showed an effect compatible with P-gp modulation with an effective concentration (EC<sub>50</sub>) of 423 μM in reversing paclitaxel resistance [118]. Figure 9 summarizes the SAR established for this class of compounds against P-gp modulation highlighting the most promising ningalin derivatives. The synthesis of ningalin B (**45**) was described by Boger *et al.* using the Diels-Alder reaction of the acetylene **I** with 1,2,4,5-tetrazine **II** to give the 1,2-diazine **III**. The synthetic pathway includes the transformation of 1,2-diazine **III** to the pyrrole **IV**, followed by *N*-alkylation, lactonization and decarboxylation, and demethylation to yield **45** (Scheme 10.a) [121,122].

Another synthesis of ningalin B (**45**) started from the aldehyde **V** and the amine **VI**, as depicted in Scheme 10.b, and was accomplished by oxidative coupling reaction to yield the pyrrole moiety, followed by Vilsmeier-Haack formylation under traditional heating to give the formylpyrrole **VII** which was subsequently converted to the lactone and then to ningalin B (**45**) [113].

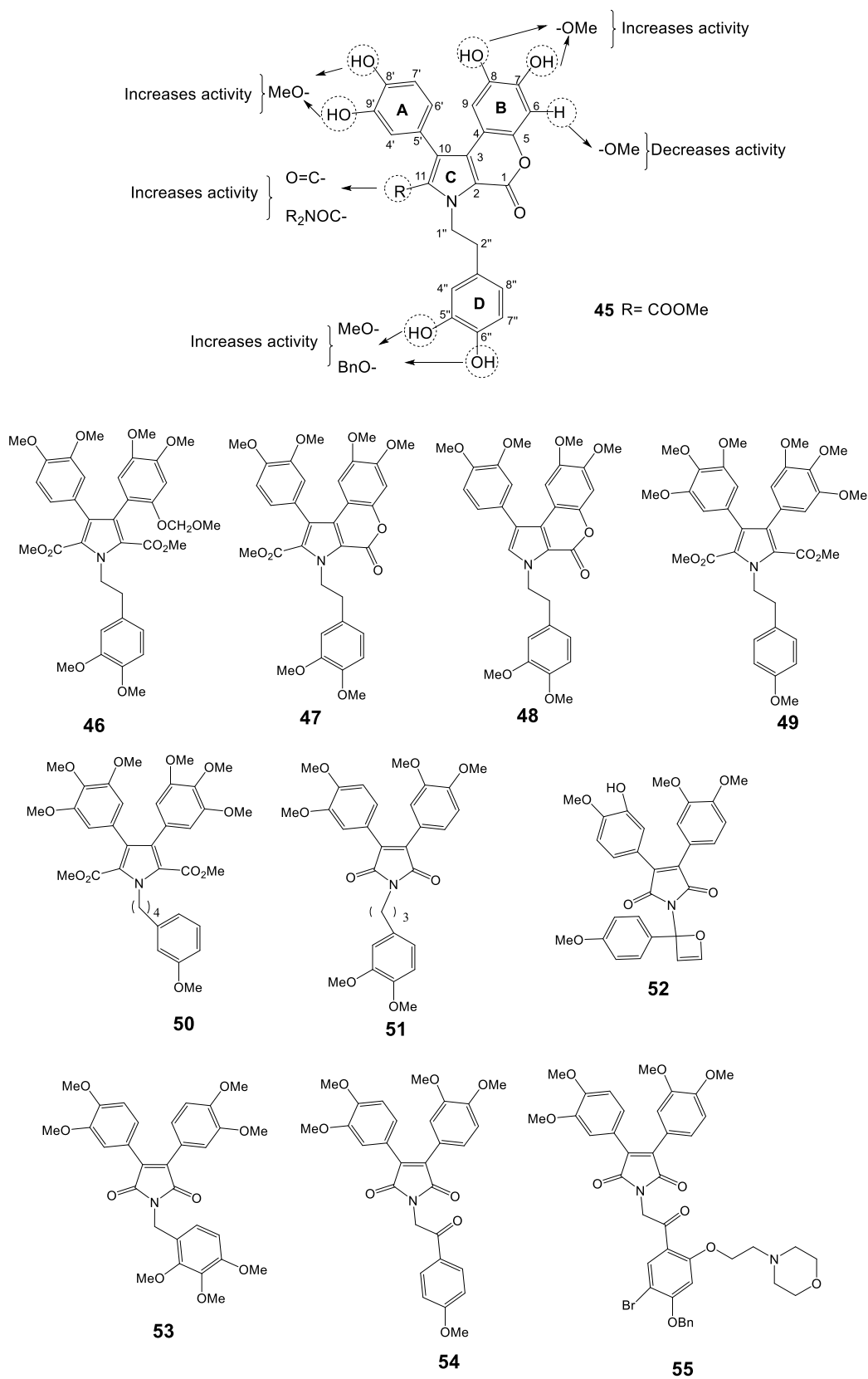


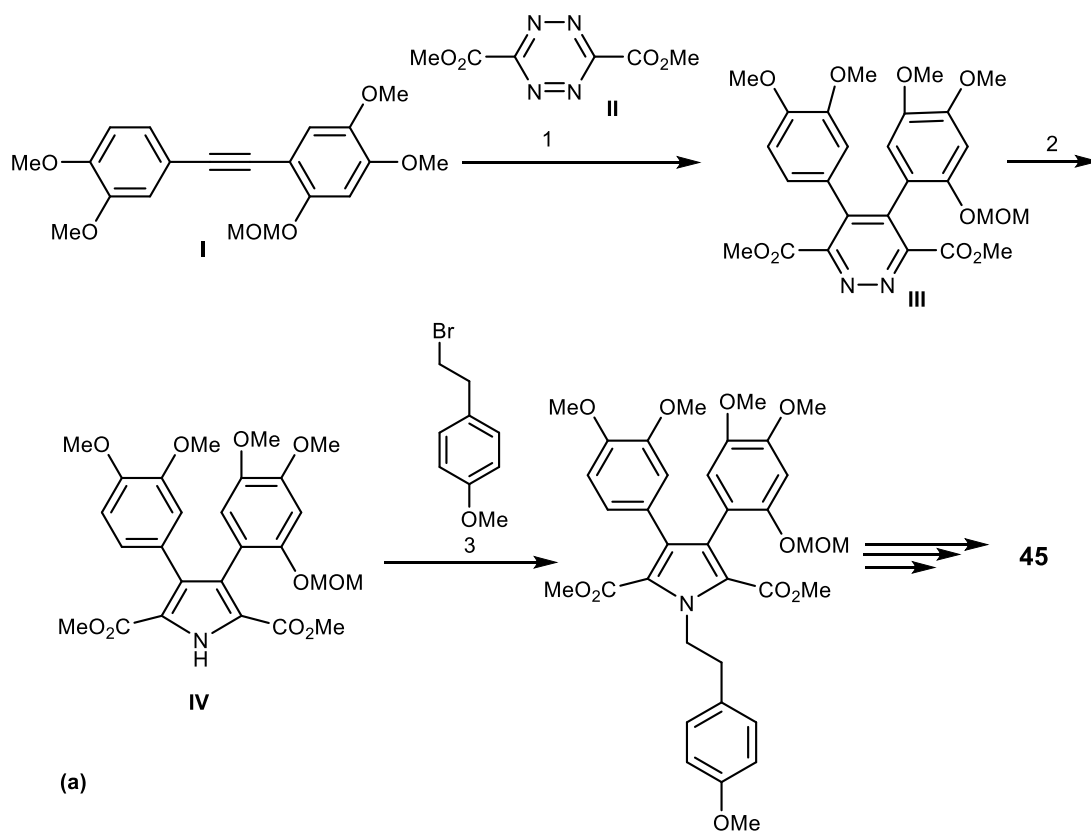
**Figure 9.** Structures of ningalin B (**45**), analogs **46-55**, and SAR studies for P-gp modulation.

### 2.4.3. Welwitindolinones and derivatives

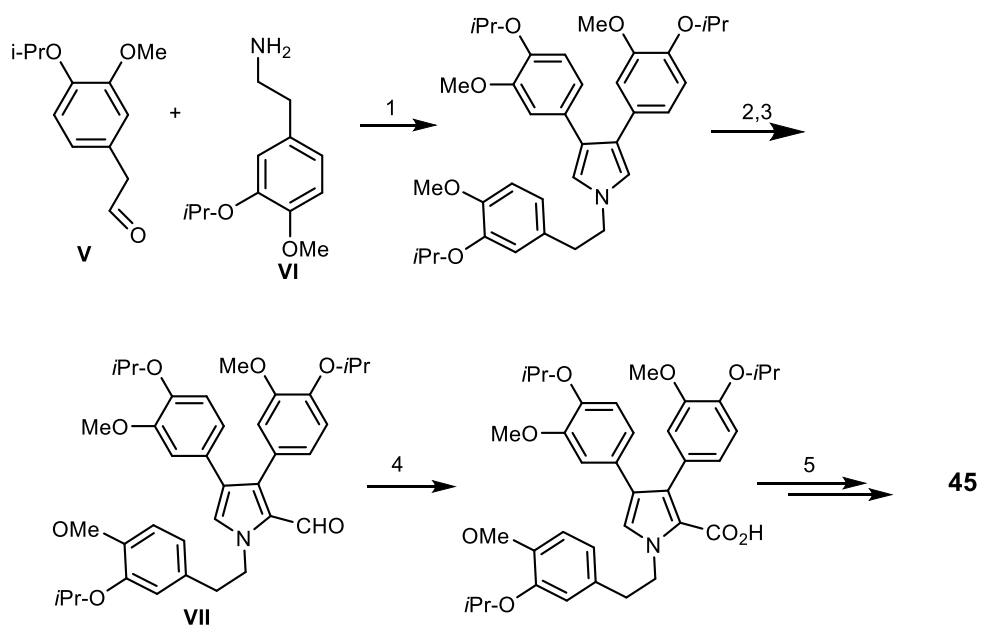
Welwitindolinones are alkaloids found in cyanobacteria *Hapalosiphon weltischii*, *Westiella intracta*, *Fischerella muscicola*, and *F. major* [123,124]. The extracts which significantly contain N-methylwelwitindolinone (**56**) were found to have potent biological activities including antifungal, larvicidal, and insecticidal properties [124]. Most of welwitindolinones possess a densely functionalized oxindole-fused bicyclo[4,3,1]decane ring system. The core structure of these alkaloids contains two contiguous stereogenic centers. These alkaloids exhibit a significant activity in reversing P-gp-mediated drug resistance in human tumor cells [125]. Among them, N-methylwelwitindolinone C (**56**) enhanced cytotoxicity of anticancer drugs like vinblastine, taxol, actinomycin D, colchicine, and daunomycin in MDR breast carcinoma cell line. The absence of the N-methyl group reduced the activity while the absence of the isothiocyanate group completely abolished the activity, as observed for welwitindolinone C isothiocyanate (**57**) and welwitindolinone isonitrile (**58**), respectively. Welwitindolinone **57** was found to be the most potent derivative in increasing the accumulation of [<sup>3</sup>H]-vinblastine and [<sup>3</sup>H]-paclitaxel by blocking P-gp in SK-VLB-1 cells. This compound also inhibits the P-gp photoaffinity labeling by [<sup>3</sup>H]-azidopine in MDR cells [36].

Compound **57** was synthesized by two different approaches – Gang's and Rawal's. In Gang's method, the synthetic pathway begins with coupling of a functional cyclohexanone using iodine promoted bromoindole addition, followed by ring closure to form the key intermediate compound **I**. Thereafter, **57** was formed by chlorination through vinyltrimethylstannane oxidation to oxindole, isotopically enhanced tethered nitrene insertion, and isothiocyanate introduction (Scheme 11.a) [126-128]. In Rawal's approach (Scheme 11.b), the coupling of silylenolether **II** with nucleophile bromoindole **III** was achieved by Lewis acid to form the corresponding cyclohexanone **IV** which then produces the key intermediate **V** by palladium-catalyzed enolate arylation [124,129]. The key intermediate compound **V** was subjected to aldehyde reduction via a hydrazine (oxidation to the oxindole), alcohol oxidation and oxime formation, and Curtius rearrangement of oxime to isothiocyanate to furnish **57**.





(a)



(b)

**Scheme 10.** Synthesis of ningalin B (**45**). Reagents and conditions: (a) 1)  $N_2$ ; 2) Zn, AcOH; 3)  $K_2CO_3$ ; (b) 1) AgOAc, NaOAc, THF; 2) POCl, DMF; 3) DMSO/ $H_2O$  or THF:*t*-BuOH: $H_2O$ ; 4)  $Pb(OAc)_4$ , EtOAc; 5)  $BBr_3$ ,  $CH_2Cl_2$ .

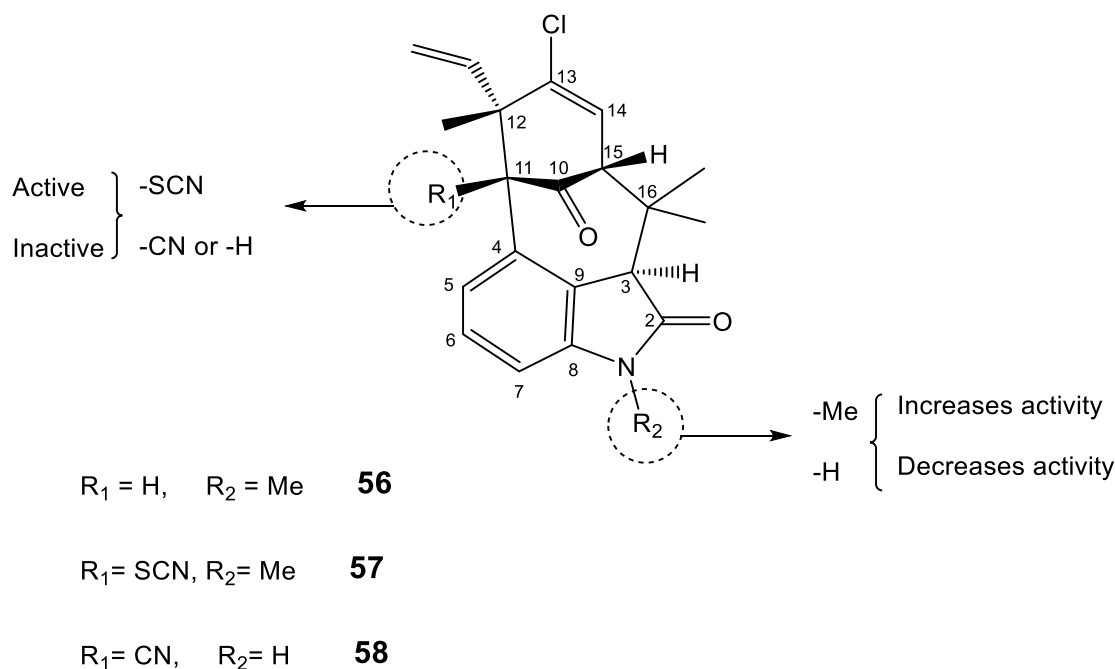
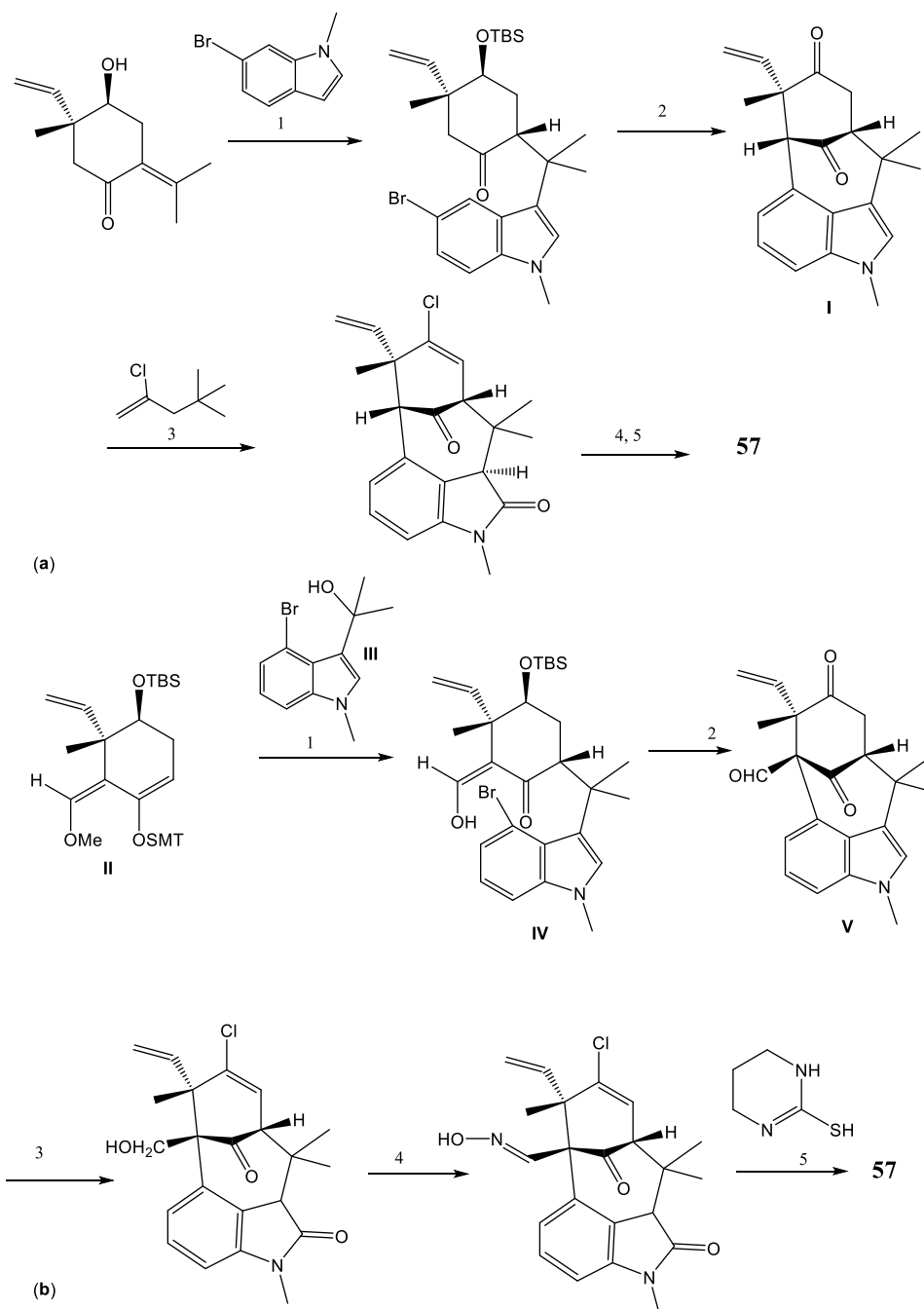


**Figure 10.** Structures of welwitindolinones **56-58** and SAR studies. The dashed circle indicates the groups important for P-gp.

#### 2.4.4. Harmine and derivatives

Harmine (**59**) is a  $\beta$ -carboline alkaloid found in plants, mammals, insects, and marine organisms [130], e.g. the marine brown alga *Melanothamnus afaqhusainii* [131,132]. The plant extracts containing **59** were traditionally used to treat alimentary tract cancer and malaria in Northwest China [133]. These extracts have a broad spectrum of biological activities, including antimicrobial, antifungal, antitumor, antiplasmodial, antioxidant, antimutagenic, antigenotoxic, as well as hallucinogenic properties [130]. Compound **59** also inhibits topoisomerase I, cyclin-dependent kinases, monoamine oxidase A, and intercalates into DNA [134]. Studies on the biological function of **59** reported this alkaloid as a potent antiproliferative and cytotoxic agent, with MDR reversal activity by inhibiting BCRP in a BCRP overexpressing breast cancer cell line (MDA-MB-123) and by reducing the resistance of mitoxantrone and camptothecin mediated by BCRP but did not inhibit *MDR-1* overexpressing cells growth [135]. More detailed studies of **59** revealed that this compound failed clinical applications due to low pharmacological effects and neurotoxicity [132,134]. To improve the therapeutic efficacy of **59**, several derivatives were synthesized by modification of substituents in positions 2, 7, and 9 of harmine (**59**) ring and with other two different groups – 2-amino-2-deoxy-D-glucose and methionine, two derivatives were obtained, 2DG-Har-01 (**60**) and MET-Har-02 (**61**), respectively. This study found that substitution at position 7 reduced natural

toxicity and increased tumor cell uptake ability, at position 9 enhanced cytotoxicity, and at position 2 enhanced the antiproliferative effect [132], and also showed that substituents at position 1 could be crucial to antitumor potency [136].



**Scheme 11.** Synthesis of *N*-methylwelwitindolinone C isothiocyanate (**57**) by Gang's approach (a) and Rawal's approach (b). Reagents and conditions: (a) 1) iodine promoted bromination, 2) NaNH<sub>2</sub>, *t*-BuOH, THF; 3) trimethylstannane; 4) LiEt<sub>3</sub>B-D, THF, Cl<sub>3</sub>CCONCO, CH<sub>2</sub>Cl<sub>2</sub>, K<sub>2</sub>CO<sub>3</sub>, MeOH; AgOTf, PhI(OAc)<sub>2</sub>, CH<sub>3</sub>CN, bathophenanthroline; 5) NaH, air, THF; (b) 1) TiCl<sub>4</sub>, toluene; 2) Pd(OAc)<sub>2</sub>, *P*-*t*Bu<sub>3</sub>, KO-*t*Bu, toluene; 3) NaBH(OMe)<sub>3</sub>, THF/EtOH then N<sub>2</sub>H<sub>4</sub>, AcOH, EtOH; NCS, pyridine; MMPP, TFA, AcOH; 4) Dess-Martin periodinane, NaHCO<sub>3</sub>, CH<sub>2</sub>Cl<sub>2</sub>; NH<sub>2</sub>OH.HCl, pyridine, MeOH; 5) NCS, DMF, THF, then Et<sub>3</sub>N.

SAR studies confirmed that substituents in position 2 and 9 displayed an important role in modulation of antitumor activities [134]. Derivatives of **59** that possess in R1, R2, and, R3 (Figure 11) a benzyl and 3'-fluorobenzyl groups are more likely to act as protein synthesis inhibitors [137].

The scaffold of harmine (**59**,  $\beta$ -carboline) was a model for the synthesis of novel compounds which are bivalent  $\beta$ -carbolines. The different number of methylene units in the linker between two  $\beta$ -carbolines produced agents which displayed good and selective cytotoxicity against 769-P and KB cell lines, being the six-methylene unit derivative **62** a potent antitumor compound against Lewis lung cancer in mice [136].

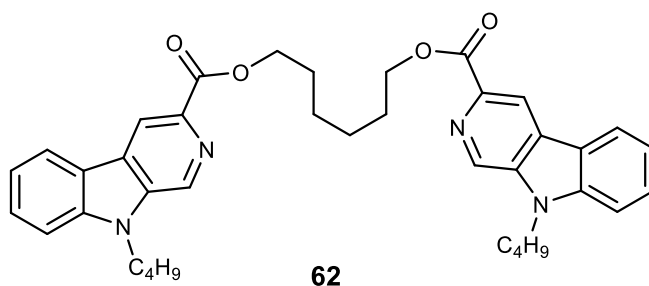
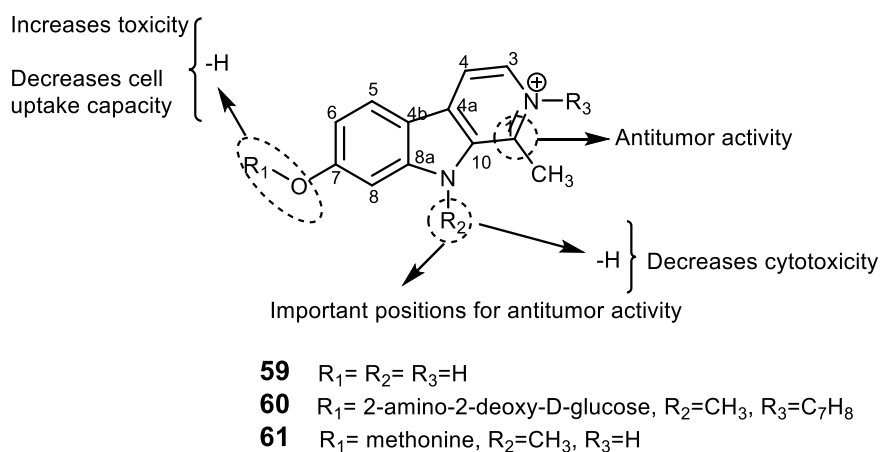


**Figure 11.** Harmine (**59**) and analogs **60-62**. The dashed circles indicate groups important for biological functions.

The synthesis of  $\beta$ -carboline-based alkaloids has been reported using tryptophan as starting material [138,139]. To the best of our knowledge, there is no report on the total synthesis of **59**. Most of the harmine analogs were synthesized from harmine scaffold using Friedel-Crafts reaction, molecular modifications, and *N*-oxidation [132,140-142].

#### 2.4.5. Indolcarbazoles and derivatives

Indolcarbazoles are alkaloids isolated from marine-derived actinomycetes strain Z039-2 which possess a broad spectrum of biological activities including anticancer activity [143]. The mechanisms of their antitumor effects include topoisomerase I poisoning, inhibition of PKC, PKA, pyruvate dehydrogenase kinase (PDK)/cyclin B, and cyclin-dependent kinase 5 (CDK5)/p5 [144,145]. The naturally occurring arcyriaflavin (**63**) and indolcarbazole K252c or staurosporin aglycone (**64**, Figure 12) showed the most potent effects in BCRP inhibition in the BCRP-transferred HEK-293 cell line, with low toxicity in BCRP-transfected cells, and reduced the relative resistance of ABCG2-transfected cells SN-38 [29,146]. Bisindolylmaleimide analogs **65-69** (Figure 12) were found to be able to inhibit [<sup>125</sup>I]iodoarylazidoprazosin labeling of BCRP by 65 to 80% at 20  $\mu$ M [146]. These findings revealed that indolcarbazole and bisindolylmaleimide analogs directly interact with BCRP protein and may increase oral bioavailability of BCRP substrates.

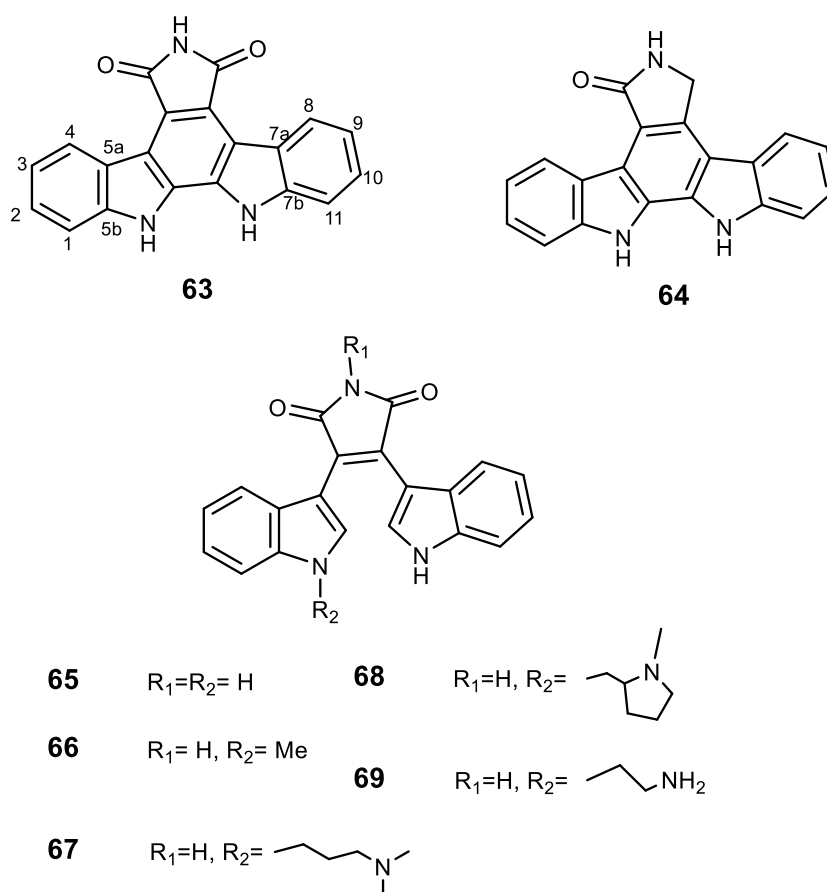
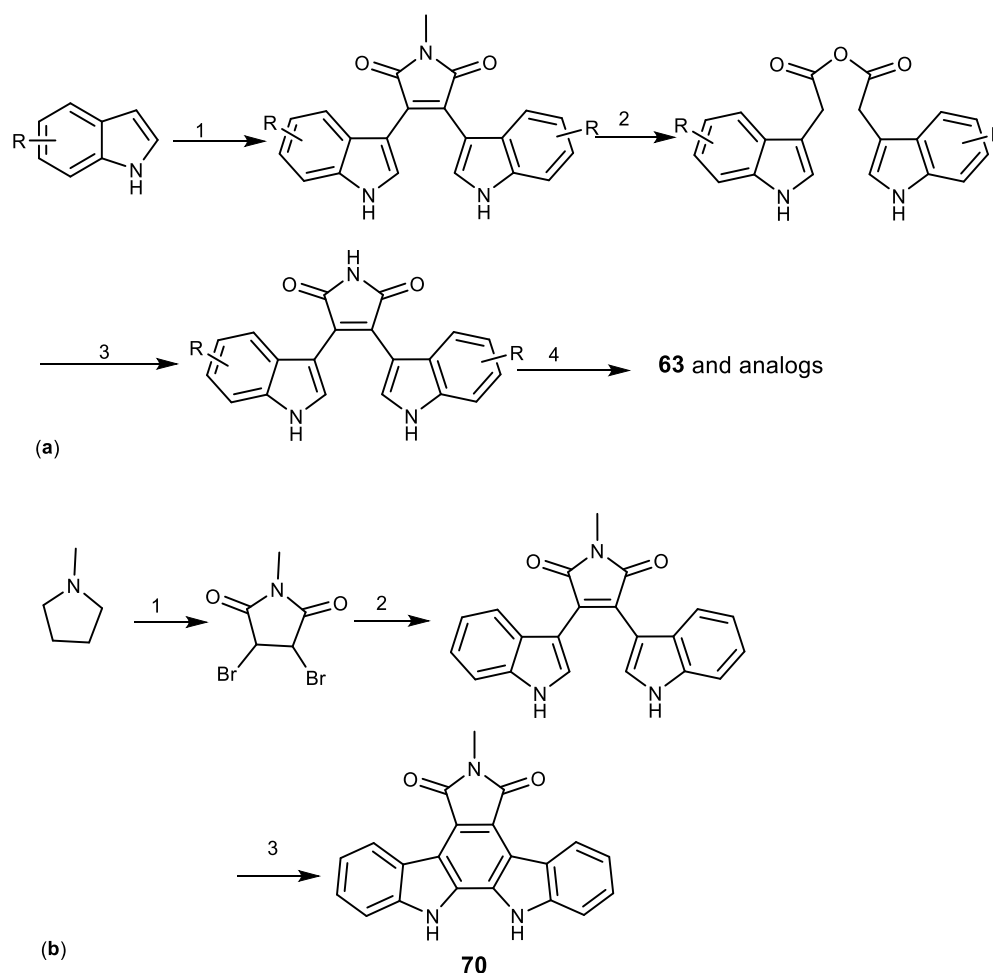


**Figure 12.** Structures of indolcarbazole derivatives **63-69**.

The indolcarbazole nucleus was prepared from bis-indolylmaleimides, followed an oxidative cyclisation to give indolcarbazole (Scheme 12.a). Another way to obtain indolcarbazole

nucleus was applied in the preparation of *N*-methyl indolcabazole (**70**) which was obtained from *N*-methyl-pyrrole by bromination and oxidation to give *N*-methyl-dibromomaleimide which was coupled with indolylmagnesium bromide to afford bis-indolylmaleimide. Oxidative cyclization of the later compound led to indolcabazole **70**, as depicted in Scheme 12.b [145,147,148].



**Scheme 12.** Synthesis of indolcabazole derivatives **63** and **70**. Reagents and conditions: (a) 1) i. EtMgBr, THF, benzene, ii. *N*-methylmaleimide; 2) KOH, MeOH or dioxane; 3) NH<sub>4</sub>OAc; 4) DDQ, PTSA, toluene; (b) 1) Br<sub>2</sub>, HNO<sub>3</sub>; 2) CH<sub>3</sub>CH<sub>2</sub>Br, Mg, THF, indole, toluene; 3) DDQ, toluene.

#### 2.4.6. Ecteinascidin 743 (trabectedin) and derivatives

Ecteinascidin 743 or trabectedin (**71**, Figure 13) is the anticancer tetrahydroisoquinolone alkaloid already approved by the FDA. This compound was first isolated from the Caribbean tunicate *Ecteinascidia turbinata* in a minute quantity. However, this compound could be synthesized from cyanosafrafin B, a starting material obtained from fermentation of *Pseudomonas fluorescens* [149]. It is a highly potent anticancer agent and has activity against a number of human solid tumor

cells. The compound was also showed to reverse the resistance to doxorubicin and vincristine in KB-C2 and KB-8-5 cells overexpressing P-gp in concentrations of 0.1 nM [150,151]. Trabectedin (**71**) was granted as Yondelis®, a medicine for treatment of advanced soft-tissue sarcomas and ovarian cancer. Although **71** is a substrate for P-gp, this potential mechanism of resistance has only been shown to be significant at concentrations exceeding clinically relevant values [151]. Moreover, this marine natural product also inhibits the activation of the *MDR-1* gene that encodes for P-gp [152]. Therefore, **71** could be considered a promising model to overcome MDR. For instance, the synthetic agent lurbinectedin or PM01183 (**72**), which was obtained by modification of the subunit C of **71**, showed a potent cytotoxic activity against tumor cell line of different origin, and it was introduced in phase I clinical trials for solid tumor, and phase II for metastatic pancreatic cancer. PM01183 (**72**) showed enhanced activity to cisplatin- and oxaliplatin-resistant cell line, and combination of **72** and cisplatin was the most synergistic toward parental and cisplatin-resistant ovarian carcinoma cells [153].

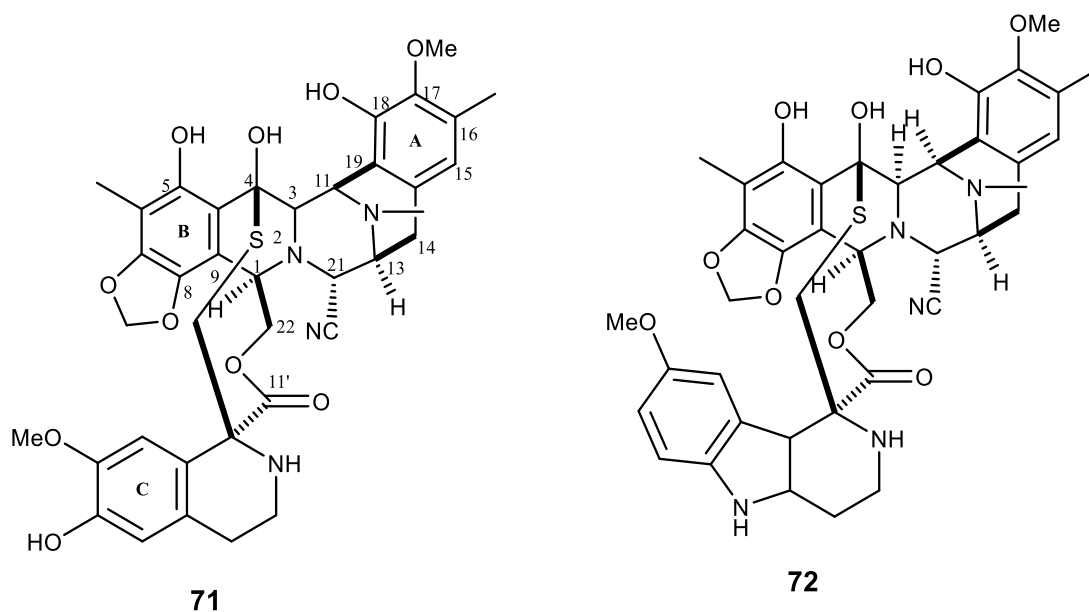
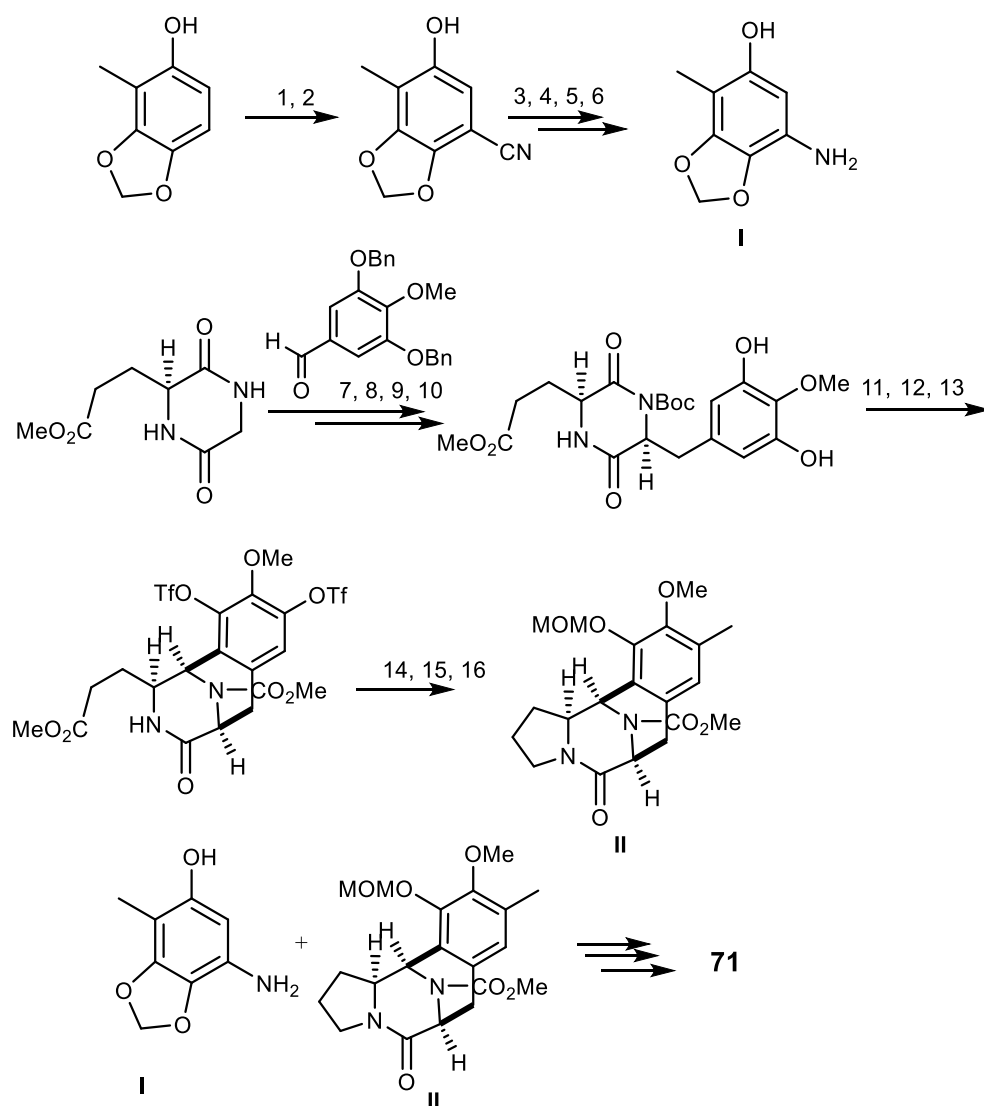


**Figure 13.** Structures of trabectedin (**71**) and lurbinectedin (**72**).

The synthesis of trabectedin (**71**) was described by many researchers. In summary, there are three important pathways (Scheme 13): (A) combination of two fragments (**I** and **II**) via an oxazolidine intermediate, (B) acid-promoted macrocyclization via creation of carbon-sulfur bond with concomitant formation of a 10-membered ring, and (C) the intramolecular Pictet-Spengler reaction to obtain **71** [154-157]. The straightforward synthesis of **71**, using 28 steps with 1.1% yield, started from L-glutamic acid as the single chiral source [158] while the 31 steps synthesis, with 1.7%

yield, began from 3-methyl catechol [159]. The first conditions lead to the B-ring formation by stereoselective Heck reaction between diazonium salt and enamide, oxidative cleavage of the resulting alkane and intramolecular *ortho* substitution of phenol by aldehyde. This pathway can form a diketopiperazine by Perkin condensation and the bicycle [3.3.3]system by an *N*-acyliminium ion-mediated cyclization, and a regioselective Suzuki-Miyaura coupling (Scheme 13) [158]. In 2000, Cuevas *et al.* established the synthesis of **71** and **72** from cyanosafrafrin B, which is an antibiotic obtained from fermentation of the bacterium *Pseudomonas fluorescens*.



**Scheme 13.** Total synthesis of trabectedin (**71**). Reagents and conditions: 1)  $\text{PhI}(\text{OAc})_2$ , MeOH; 2) NaCN, DMF/H<sub>2</sub>O; 3) BnBr, K<sub>2</sub>CO<sub>3</sub>, DMF; 4) aq H<sub>2</sub>O<sub>2</sub>, K<sub>2</sub>CO<sub>3</sub>, DMSO; 5)  $\text{PhI}(\text{OAc})_2$ , KOH, MeOH; 6) LiOH, EtOH/H<sub>2</sub>O, reflux; 7) *t*-BuOK, THF, DBU, 8) Boc<sub>2</sub>O, DMAP, THF, (2 steps); 9) H<sub>2</sub> (750psi), Pd/C, EtOAc; 10) H<sub>2</sub>NNH<sub>2</sub>·H<sub>2</sub>O, THF, evaporation; NaBH<sub>4</sub>, MeOH, (2 steps); 11) TFA, CF<sub>3</sub>CH<sub>2</sub>OH; evaporation; PhNTf<sub>2</sub>, DMAP, Cs<sub>2</sub>CO<sub>3</sub>, MeCN; 12) trimethylboroxine, Pd(PPh<sub>3</sub>)<sub>4</sub>, K<sub>3</sub>PO<sub>4</sub>, 1,4-dioxane; 13) HCl, EtOAc; ClCO<sub>2</sub>Me, NaHCO<sub>3</sub>, H<sub>2</sub>O; 14) L-selectride, THF; 15) CSA, toluene, reflux (2 steps).



Methoxy-*p*-quinone of cyanosafracin B was treated with bromochloromethane, followed by Edman degradation to form thiourea (Scheme 13). The critical substitution of the amino group by an alcohol group gave the key intermediate to yield **71** through Corey method [149].

## 2.5. Diketopiperazines

### 2.5.1. Nocardioazines

Nocardioazines are bridged diketopiperazine alkaloids which were isolated from a non-saline liquid culture of *Nocardioopsis sp.* (CMB-M0232). Nocardioazine A (**73**) is composed of cyclo-(L-Trp-L-Trp) and cyclo-(L-Trp-D-Trp), as shown in Figure 14. This compound has revealed an effect compatible with P-gp inhibition in a P-gp overexpressing colon cancer cell line (SW60Ad300) [160].

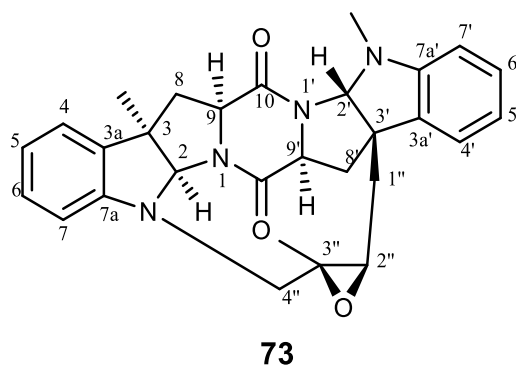
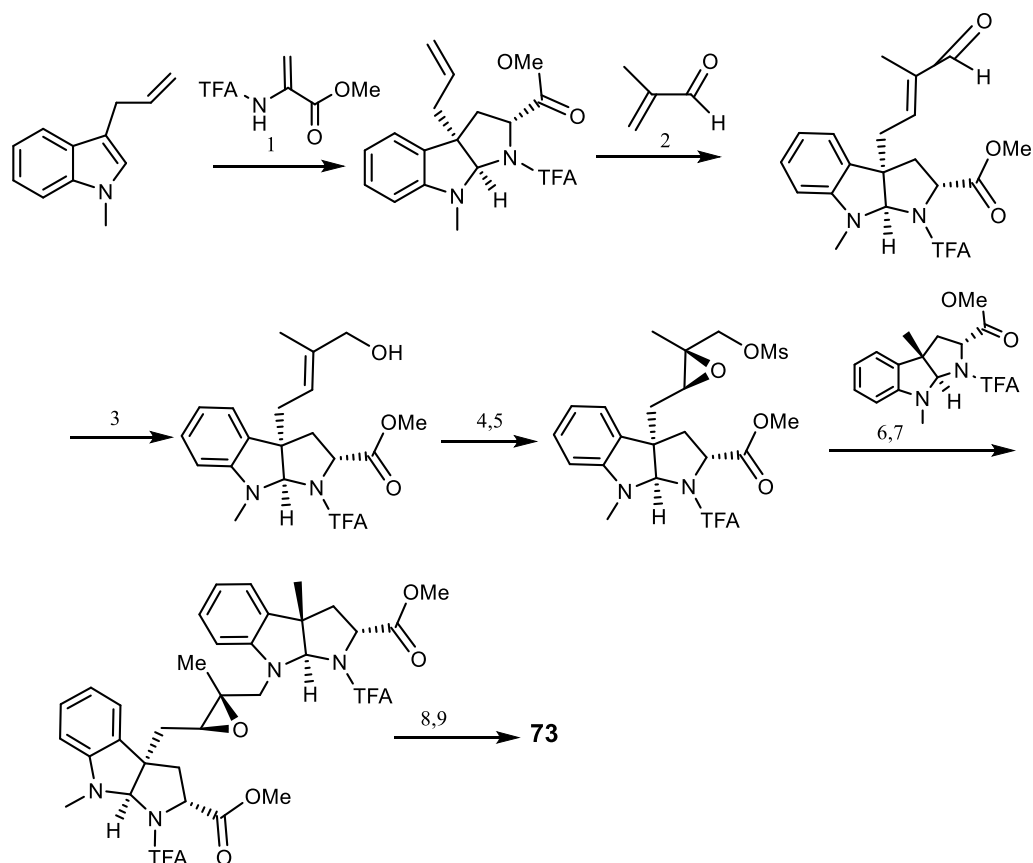


**Figure 14:** Structure of nocardioazine A (**73**).

The first synthesis of (+)-nocardioazine A (**73**) was reported in 2014 by Wang and Reisman. The synthetic pathway comprises the building of the pyrroloindoline unit from an enantioselective formal [3+2] cycloaddition, and an unusual intramolecular diketopiperazine formation. The synthesis was performed from 3-allylindole in 9 steps which gave the overall yield of 11% of **73** (Scheme 14) [161].



**Scheme 14.** Total synthesis of nocardioazine A (**73**). Reagents and conditions: 1) (S)-BINOL, SnCl<sub>4</sub>, DCM; 2) O<sup>i</sup>Pr-HG II, DCM, reflux; 3) NaBH<sub>4</sub>, CeCl<sub>3</sub>·7H<sub>2</sub>O, MeOH; 4) (+)-diethyltartrate, Ti(O<sup>i</sup>Pr)<sub>4</sub>, tBuOOH, 4Å MS, DMC; 5) MsCl, Et<sub>3</sub>N, THF; 6) TBAI, DIPEA, CH<sub>3</sub>CN; 7) Pd<sub>2</sub>(dba)<sub>3</sub>, dppb, DMBA, DEC; 8) LiOH, THF/H<sub>2</sub>O; 9) PyBrop, DIPEA, DMF.

### 2.5.2. Fumitremorgins and derivatives

Fumitremorgin C (FTC, **74**) is an indolyl diketopiperazine alkaloid found in several marine fungi such as the fungal strain BM939, fungal A-f-11, *Aspergillus sydowii*, and *Aspergillus fumigatus* (YK-7) [162]. Fumitremorgins were found to be tremorgenic mycotoxins by interfering the releasing neurotransmitters and also showed inhibitory activity on cell cycle [163]. Compound **74** was reported as a chemo sensitizing agent that could reverse a drug-resistant cell lines that do not overexpress P-gp and MRP [163,164]. This effect was shown to be due to BCRP expression in the S1-M1-3.2 cell line resistant to mitoxantrone, topotecan, and doxorubicin [164]. Fumitremorgin C (**74**) almost completely reversed resistance mediated by BCRP in MCF-7 cells transfected with this protein [165]. Moreover, **75** was found to inhibit nitrofurantoin and mitoxantrone (BCRP's substrates) transcellular transport in MDCKII and MEF3.8 cell lines [166]. The SAR study using the *ftm* gene cluster revealed that the moieties that are essential for inhibitory activity of **74** against BCRP

are the double bond between C-3 and N-4, as well as the methoxy group at C-18, however, the hydroxyl groups at C-12 and C-13 lead to a decrease in activity (Figure 15) [167]. Unfortunately, **74** was found to induce tremors or convulsion in mice and other animals [168]. Two derivatives, Ko132 (**75**) and Ko134 (**76**), were found to be potent inhibitors of the BCRP-mediated drug efflux in T6400 mouse and T8 human cell lines with low cytotoxicity at an effective concentration of 1  $\mu$ M [163,169]. In addition, **77** was the most effective inhibitor of BCRP, with very low activity against P-gp or other known drug transporters [168,170]. In addition, the stereospecificity was shown to be very critical in the Ko family, for example, compounds having the 3*S*,6*S*,12 *$\alpha$* *S* configuration were 18 times more potent than those with 3*S*,6*R*,12 *$\alpha$* *S* configuration in inhibiting BCRP; however, this stereoselective effect was not observed in P-gp and MRP-1 [171].

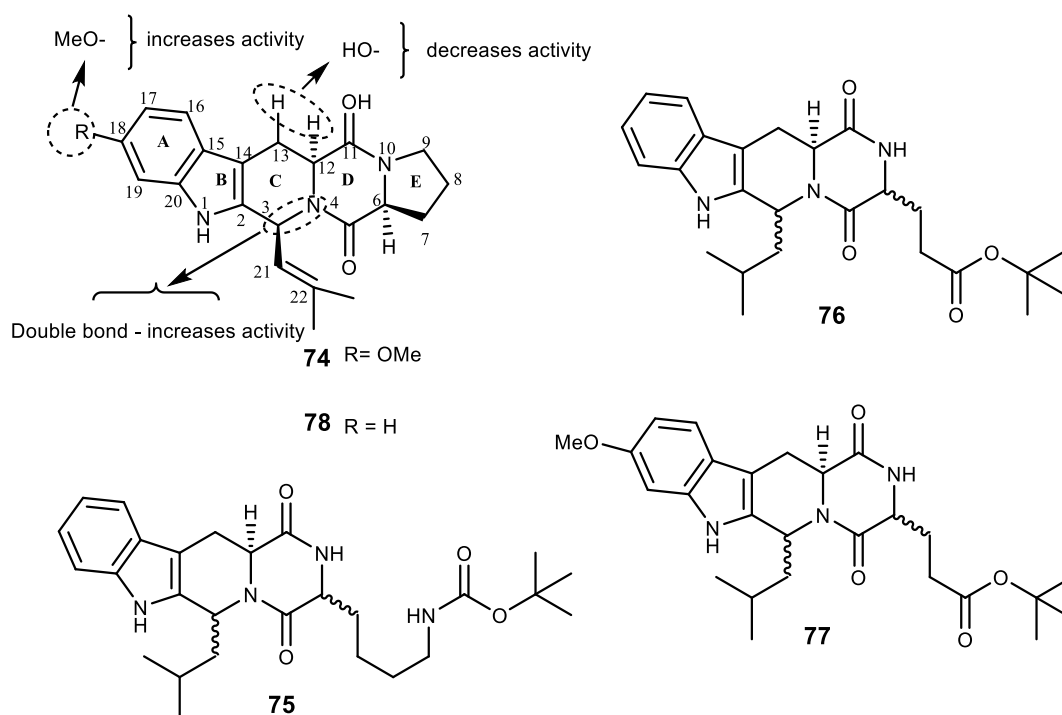


**Figure 15.** Structures of fumitremorgin C (**74**) and derivatives **75-78** and SAR for BCRP inhibition.

The first synthesis of **74** was reported by Hino *et al.* who prepared *N*-propyl-7-methoxy- $\beta$ -carboline as the key intermediate [172]. Loevezijn *et al.* reported a solid phase synthesis of demethoxy-FTC (**78**), also an inhibitor of BCRP-mediated MDR, by a cyclization/cleavage multiple parallel syntheses method (Scheme 15.a). This synthetic pathway was based on the formation of the diketopiperazine rings system, followed by simultaneous cleavage of solid support, which acted as a leaving group at the cyclization step. The reaction was performed by the Pictet-Spengler

condensation of the hydroxyethyl functionalized polystyrene resin linked L-tryptophan with excess of aldehyde (Scheme 15.a) [163,169].

Another alternative to obtain **78** was achieved by  $Mg(ClO_4)_2$ -catalyzed intramolecular allylic amination with carbamate or sulfonamide as nucleophiles to form substituted piperidine and pyrrolidine (Scheme 15.b) [173]. The synthesis of Ko143 (**77**), a potent BCRP inhibitor of the FTC series was accomplished and optimized by Yuexian *et al.* which involved ytterbium triflate-promoted coupling between 6-methoxyindole and optically active 1-benzyl-2-methyl-(S)-1,2-aziridinedicarboxylate (Scheme 15.c) [174].

### 2.5.3. Halimide and derivatives

Halimide, is a diketopiperazine secondary metabolite isolated from the marine fungus *Aspergillus ustus*. This compound exhibited potential *in vitro* cytotoxic activity against human colon and ovarian carcinoma cells [175]. Structurally, halimide is composed of a phenylalanine, a histidine, and a tertiary butyl group. An analog of halimide, plinabulin (KPU-2, **79**, Figure 16), that was obtained by molecular modification at the phenyl ring, has revealed a potent *in vitro* antitumor activity not only against various human tumor cell lines, but also against those with various MDR profiles [176]. Moreover, **79** was reported to have a similar mechanism of action to that of eribulin (**31**) as microtubule-disrupting agent with colchicine-like tubulin-depolymerizing activity, but the main problem concerning **79** is its poor solubility ( $<0.1 \mu M$ ), which can trigger further studies on this scaffold. The phase I/II clinical trial of **79** in combination with docetaxel was completed in patients with advanced non-small cell lung cancer, and compound **79** was shown to act synergistically with docetaxel in murine models of NSCLC [177].

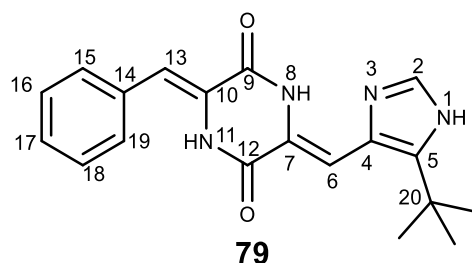
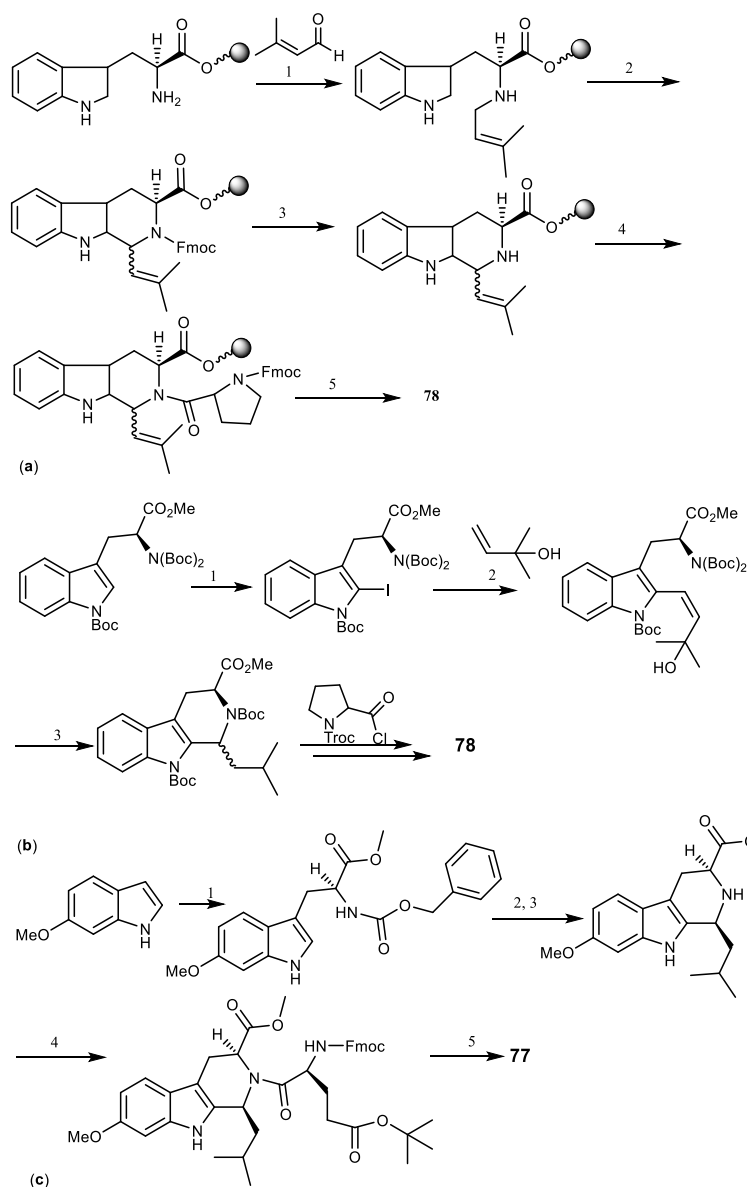


**Figure 16.** Structure of plinabulin (**79**).



**Scheme 15.** Total synthesis of FTC derivatives, dimethoxy-FTC (**78**) and Ko143 (**77**). Reagents and conditions: (a) 1) CH(OMe)<sub>3</sub>; 2) Fmoc-HCl, pyridine, CH<sub>2</sub>Cl<sub>2</sub>; 3) piperidine, DMF; 4) Fmoc-L-pro-OH, CIP, DiPEA, MNP; 5) piperidine, THF; (b) 1) Hg(OOCCF<sub>3</sub>)<sub>2</sub>, KI, I<sub>2</sub>, CH<sub>2</sub>Cl<sub>2</sub>, then Boc<sub>2</sub>O, DMAP, MeCN; 2) Pd(OAc)<sub>2</sub>, Ag<sub>2</sub>CO<sub>3</sub>, toluene; 3) Mg(ClO<sub>4</sub>)<sub>2</sub>, MeCN; (c) 1) 1-benzyl-2-methyl-(S)-1,2-aziridinedicarboxylate, ytterbium triflate, CH<sub>2</sub>Cl<sub>2</sub>; 2) H<sub>2</sub> balloon, MeOH, 10% Pd/C; 3) isovaleraldehyde, TFA, CH<sub>2</sub>Cl<sub>2</sub>; 4) N-Fmoc-5-*t*-butyl L-glutamic acid ester, diisopropylethylamine 2-chloro-1,3-dimethylimidazolium hexafluorophosphate, N-methylpyrrolidinone; 5) piperidine, THF.

## 2.6. Peptides

### 2.6.1. Hapalosin and derivatives

Hapalosin (**80**, Figure 17) is a cyclic depsipeptide, isolated from the lipophilic fraction of the extract of a cyanobacterium *Hapalosiphon welwitschii* W. & G.S West, and was found to reverse MDR

in a P-gp overexpressing, vinblastine-resistant human ovarian adenocarcinoma cell line with higher effect than the known P-gp inhibitor verapamil [178,179]. At 20  $\mu$ M concentration, compound **80** significantly enhanced the accumulation of [<sup>3</sup>H]-paclitaxel in SKVLB1 cell and exhibited a similar activity to verapamil in breast cancer cell MCF-7/ADR in the range of 1.5-10  $\mu$ M [180,181]. Several syntheses for **80** and respective analogs have been reported, with the purpose of obtaining compounds with similar or better MDR reversal activity. Some of the analogs did not fulfill this objective; for example, the glucose mimic of hapalosin (**80**) and 8-deoxyhapalosin, the triamide analogs, and *N*-demethylhapalosin **81** possessing a *trans*-amide, exhibited weak MDR reversal activity [180-182]. Through SAR studies, proline-containing congeners (**82** and **83**) were found to be more potent against MCF-7/ADR cells than **81** [182]. Substitution at C-12 in **80** furnished analogs **84-88**, which exhibited higher vincristine accumulation than verapamil and **80** in MDR 2780AD cells at 10  $\mu$ M [183]. It was postulated that the *cis*-peptide might be essential to express the MDR-reversing activity, and the bioactive function of **80** and analogs depends on the *S-cis* or *S-trans* configuration [182,184]. Also, a free hydroxyl and aromatic groups may be important for the anti-MDR activity of hapalosin (**80**) and its analogs.

The structure of hapalosin (**80**) was investigated for synthesis, and it was divided into 3 main domains: a  $\beta$ -hydroxy acid (A), a  $\gamma$ -amino- $\beta$ -hydroxy acid (B), and an  $\alpha$ -hydroxy acid (C). Hapalosin (**80**) was initially synthesized by macro lactonization and by cycloamidation [185]. Nobuki *et al.* reported the synthesis of **80** and analogs by cyclization, producing the peptide bond at the end of the process which allowed obtaining **80** in 44% yield. They used the coupling of *N*-propionyl-(4*S*, 5*R*)-4-methyl-5-phenyl-2-oxazolidinone with octanal (Scheme 16.a) [181,186]. Another synthesis of hapalosin (**80**) and its analogs was accomplished by a macro lactonization strategy [187-189]. The method was based on a chiral acetate reagent, which offered advantages to the aldol reaction and avoided intramolecular cyclization during amino group deprotection and segment coupling [189]. Shigeru *et al.* presented the synthesis of hapalosin (**80**) and derivatives with modification at C-12 by cyclization producing the peptide bond at the final stage [183]. According to their strategy, hapalosin (**80**) and derivatives were commenced by using  $\gamma$ -amino- $\beta$ -hydroxy acid **I** which was obtained by either Evans aldol/Curtius combination route [190] or asymmetric dihydroxylation route [191]. Then, the catalytic hydrogenation of the benzyl ester **II** was performed, and the generated carboxylic acid was coupled with an appropriate allyl  $\alpha$ -hydroxylate, leading to allyl ester **III**. After sequential deprotection, cyclization produced **80** and derivatives (Scheme 16.b). Kumar *et al.* also described a flexible and highly diastereoselective synthesis of hapalosin (**80**) with the addition of an organometallic reagent to *N-tert*-butanesulfinylimine, the non-aldol aldol reaction, and the Yamaguchi esterification as key steps in this strategy [192].

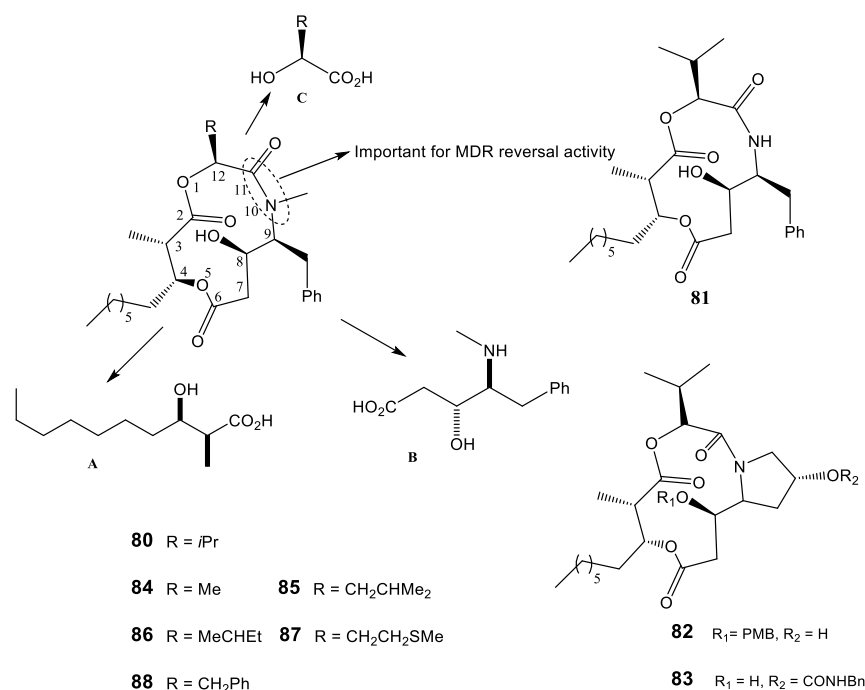
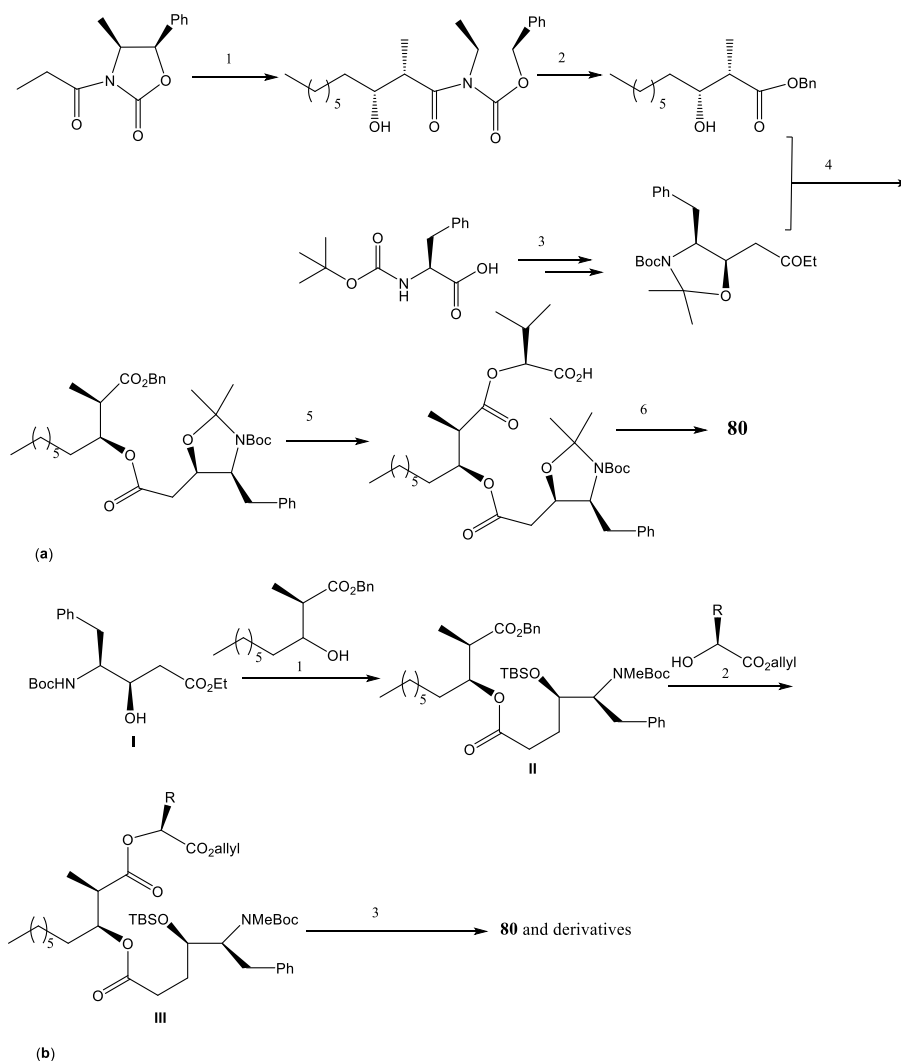


**Figure 17.** Structure of hapalosin (**80**) and analogs **81-88** highlighting the important domains for synthesis (A-C).

### 2.6.2. Botryllamides and derivatives

Botryllamides are a group of dehydrotyrosine derivatives, isolated from styelid ascidians *Botryllus sp.* [194,195]. Some botryllamides exhibited weak cytotoxicity against the HCT-116 cell [195]. Botryllamides exhibited selectivity toward BCRP but have different specificity to other ABC transporters. Two naturally occurring botryllamides, botryllamide I (**89**) and J (**90**) were reported to have activity against BCRP by inhibiting BCRP-mediated BODIPY FL prazosin transport in BCRP-transfected HEK293 cells (Figure 18). Both **89** and **90** competed with [<sup>125</sup>I]-iodoarylazidoprazosin labeling of BCRP and were shown to stimulate BCRP-associated ATPase activity, reversing BCRP-mediated resistance [196]. In a different study, botryllamide G (**91**) was reported as the most potent botryllamide BCRP inhibitor but did not inhibit the efflux of rhodamine out of P-gp overexpressing cells. In contrast, botryllamide A (**92**), which is less potent against BCRP, showed that activity against P-gp [197]. These differences were explained by the present or absent of an *o*-methyl group at C-15. The biological investigation of analogs of botryllamides **92** and **93** suggested that the 2-methoxy-*p*-coumaric acid moiety and the number of conjugated double bonds with this group were important for BCRP inhibition [197]. This study also found that: i) the phenolic hydroxyl group at C-7 was not important for activity, ii) the binding region with BCRP was between C-4 and C-9 (right side of figure 18) of the aryl ring, and iii) conjugation through C-1 to C-9 was necessary for activity, but extended

conjugation from C-10 to C-17 (left side of figure 18) of the aryl ring was not required, however, it might contribute to specificity of activity.



**Scheme 16.** Synthesis of hapalosin (**80**) and derivatives. Reagents and conditions: **(a)** 1)  $\text{Bu}_2\text{BOTf}$ ,  $\text{Et}_3\text{N}/\text{CH}_2\text{Cl}_2$ , then  $\text{Me}(\text{CH}_2)_6\text{CHO}$ ; 2)  $n\text{-BuLi}$ ,  $\text{BnOH}/\text{THF}$ ; 3) Ref. [193]; 4)  $\text{NaOH}$ ,  $\text{DCC}$ ,  $\text{DMAP}/\text{CH}_2\text{Cl}_2$ ; 5)  $\text{H}_2$ ,  $\text{Pd}(\text{OH})_2/\text{EtOH}$ , vinyl-2-hydroxy-3-methylbutanoate,  $\text{DCC}$ ,  $\text{DMAP}/\text{CH}_2\text{Cl}_2$ ; 6)  $\text{TFA}/\text{CH}_2\text{Cl}_2$ ,  $\text{DPPA}$ ,  $i\text{-Pr}_2\text{NEt}/\text{DMF}$ ; **(b)** 1) i.  $\text{DCC}$ ,  $\text{DMAP}/\text{CH}_2\text{Cl}_2$ , ii.  $\text{H}_2$ ,  $\text{Pd}(\text{OH})_2/\text{EtOH}$ , 2)  $\text{DCC}$ ,  $\text{DMAP}/\text{CH}_2\text{Cl}_2$ ; 3) i.  $\text{HF}$ -pyridine, ii.  $(\text{Ph}_3\text{P})_4\text{Pd}$ , morpholine, then  $\text{TFA}$ , iii.  $\text{DPPA}$ ,  $\text{EtNt-Pr}$ .

The syntheses of botryllamides **G** (**91**) and **F** (**93**) were already described and are depicted in Scheme 17. The strategy started with a condensation of octopamine with 2-methoxy-*p*-coumaric acid to generate an amide bond, followed by a dehydration of the adjacent hydroxyl group to provide the key enamine amide functionality [197].



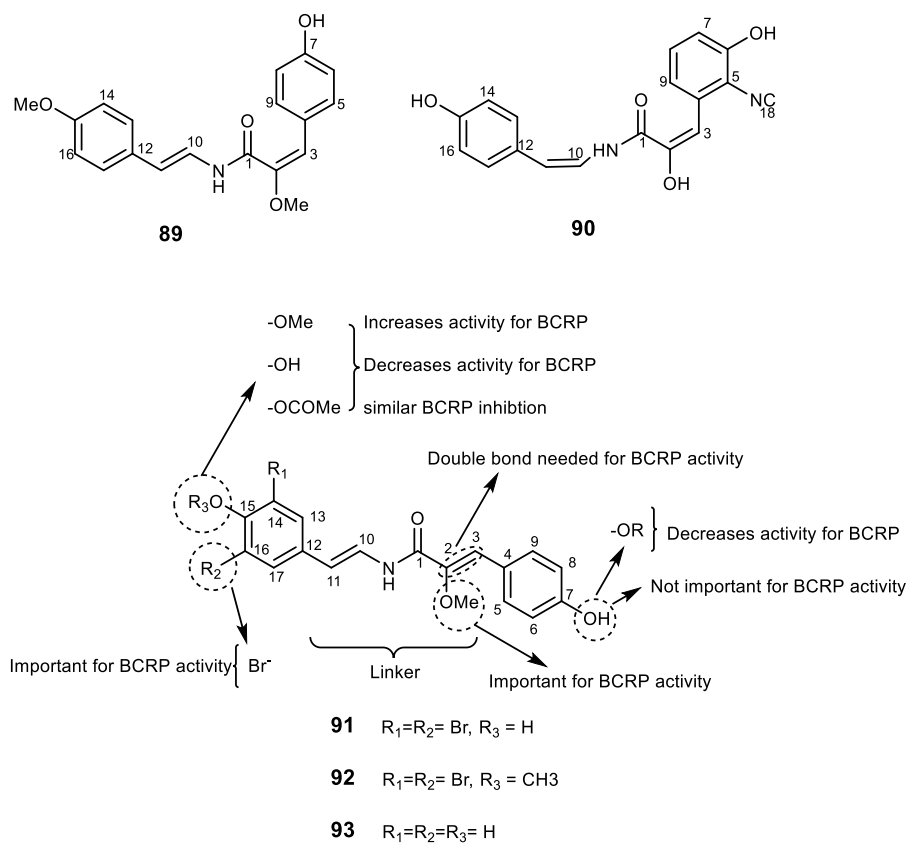
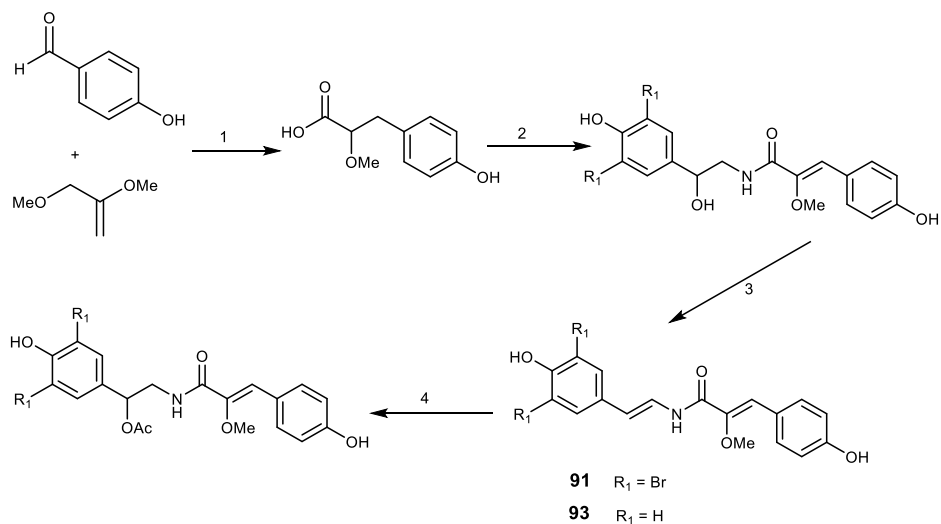


**Figure 18.** Botryllamides **89-93** and SAR studies on BCRP inhibitory activity.



**Scheme 17.** Synthesis of botryllamides **G (91)** and **F (93)**. Reagents and conditions: 1) NaOMe, MeOH, reflux, overnight; 2) octopamine.HCl or bis-brominated octopamine, WSCI, HOBt, Et<sub>3</sub>N; 3) Ac<sub>2</sub>O, pyridine; 4) K<sub>2</sub>CO<sub>3</sub>, DMSO.

### 2.6.3. Kendarimide

Kendarimide A (**94**, Figure 19) is an oligopeptide found in the Indonesian sponge *Haliclona sp.* This compound showed the potential of MDR reversal in human carcinoma (KB-C2) cell line overexpressing P-gp at the concentration of 6  $\mu\text{M}$ , however, it was not active against KB-3-1 at the same concentration. The combination of **94** (0.1 mg/mL) with colchicine (0.1 mg/mL) was found to inhibit KB-C2 cell growth by 87% [198]. Kendarimide A (**94**) is composed of several amino acids such as *N*-methylpyroglutamic acid (pyroMeGlu), *N*-methylated eight membered cysteinyl-cysteine (ox-[MeCys-MeCys]) together with many *N*-methyl amino acid residues, similar to cyclosporine A, a well-known P-gp inhibitor [199]. These data highlight that peptides can be considered as a valuable scaffold to reverse MDR. From our understanding the total synthesis of compound **94** has not yet been reported. L-pyroMeGlu-L-Phe-OEt is the moiety that was synthesized as a model compound to represent pyroMeGlu of **94** as described in Scheme 18.a [198]. Another synthetic model compound (*N*-methylcysteinyl-*N*-methylcysteine ring) to study the absolute stereostructure of the C-terminal tetrapeptides (N-MeCys-N-MeCys) in **94** was synthesized, and the absolute configuration of both of the two adjacent *N*-methylcysteines in **94**, which form an eight-membered disulfide ring, was elucidated to be L. The synthetic pathway was described in Scheme 18.b [199].

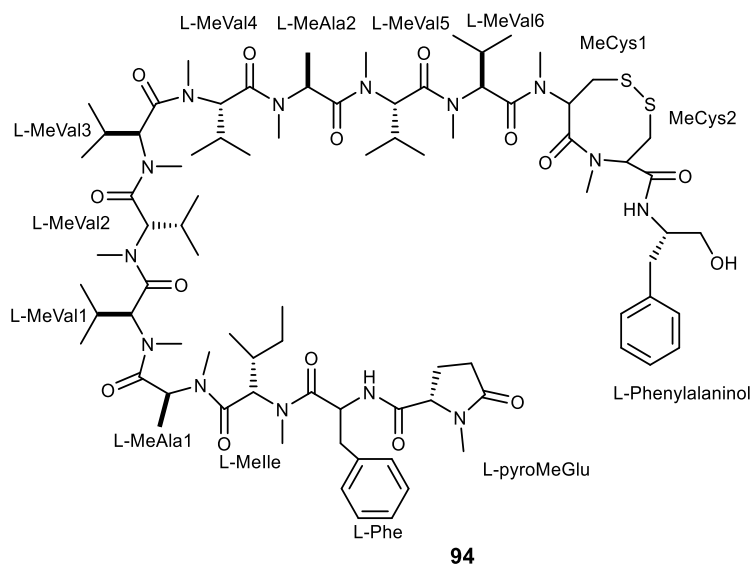
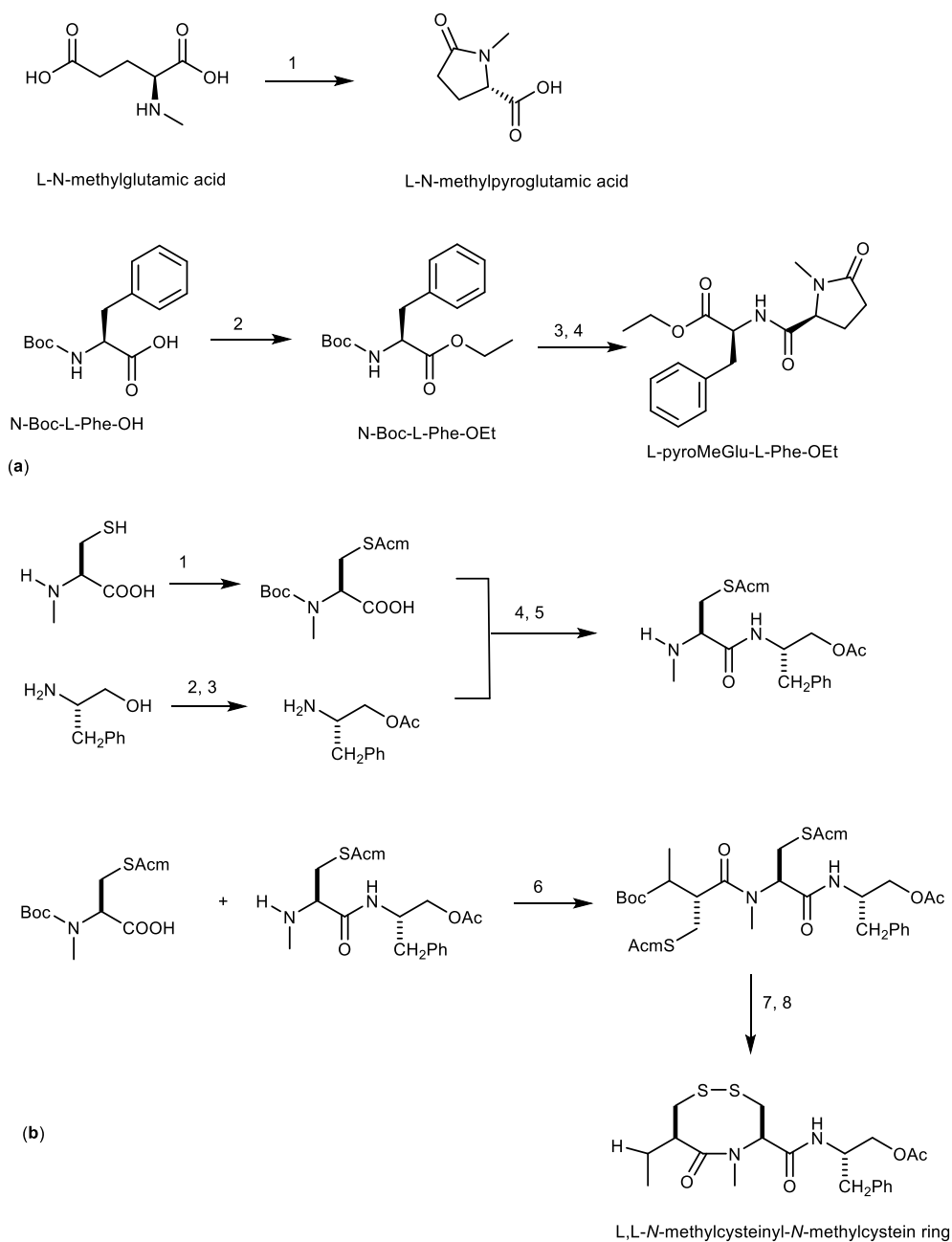


**Figure 19.** Structure of kendarimide A (**94**).



**Scheme 18.** Synthesis of L-pyroMeGlu-L-Phe-OEt (a) and L,L-N-methylcysteinyl-N-methylcystein ring (b). Conditions and reagents: (a) 1) H<sub>2</sub>O, 132°C, 1.9 kg/cm<sup>2</sup> (autoclave); 2) Na<sub>2</sub>HCO<sub>3</sub>, C<sub>2</sub>H<sub>5</sub>I, DMF; 3) TFA, CH<sub>2</sub>Cl<sub>2</sub>; 4) L-N-pyroMeGlu, DEPC, TEA, DMF, 0°C; (b) 1) acetamido methanol, conc. HCl, (Boc)<sub>2</sub>O, 1N NaOH; 2) (Boc)<sub>2</sub>O, 1N NaOH, Ac<sub>2</sub>O, pyridine; 3) TFA, CH<sub>2</sub>Cl<sub>2</sub>; 4) DEPC, Et<sub>3</sub>N, DMF; 5) TFA, CH<sub>2</sub>Cl<sub>2</sub>, quant.; 6) EDCl, HOAt, CH<sub>2</sub>Cl<sub>2</sub>/DMF; 7) I<sub>2</sub>, CH<sub>2</sub>Cl<sub>2</sub>/MeOH; 8) TFA, CH<sub>2</sub>Cl<sub>2</sub>, quant.

#### 2.6.4. Patellamide and derivatives

Patellamides are thiazole and oxazoline lipophilic cyclic peptides isolated from the tunicate *Lissoclinum patella*. These compounds exhibited cytotoxicity and reversed MDR in tumor cells. Patellamides B (**95**), C (**96**), and D (**97**) showed reversal activity and enhanced the activity of P-gp inhibitors such as vinblastine, colchicine, and doxorubicin in CEM/VLB100 cell line (Figure 20) [200,201]. Patellamide D (**97**) showed a better result than verapamil in modulating drug resistance *in vitro*, and colchicine cytotoxicity were enhanced by 2.8 folds. Doxorubicin toxicity was reduced from  $IC_{50} > 1000$  ng/mL to 110 ng/mL, by **97**. This result indicated that patellamide D (**97**) acts as a selective antagonist in MDR, and thus can be considered as a potential modulator for drug resistance [7].

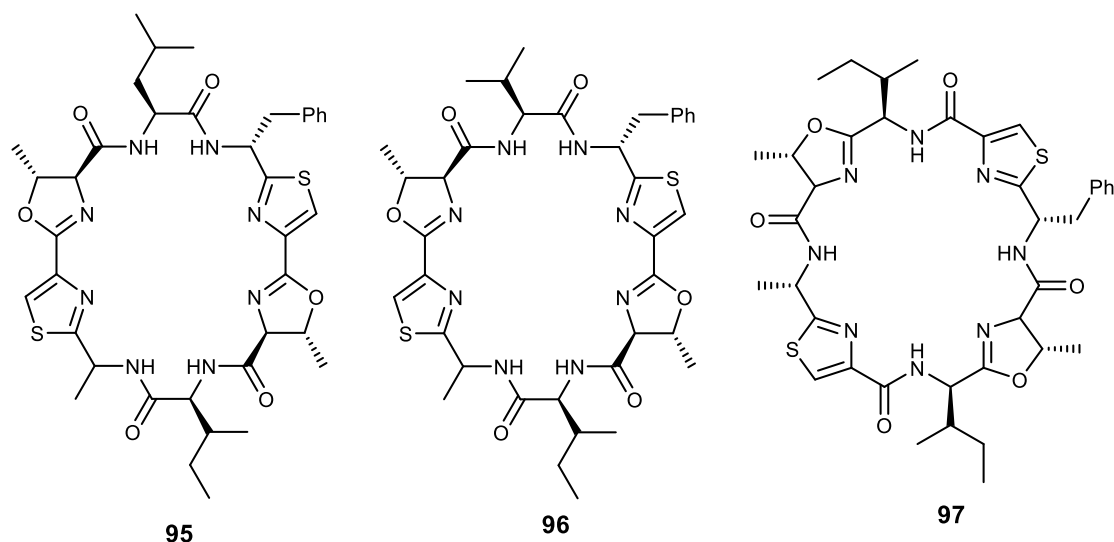
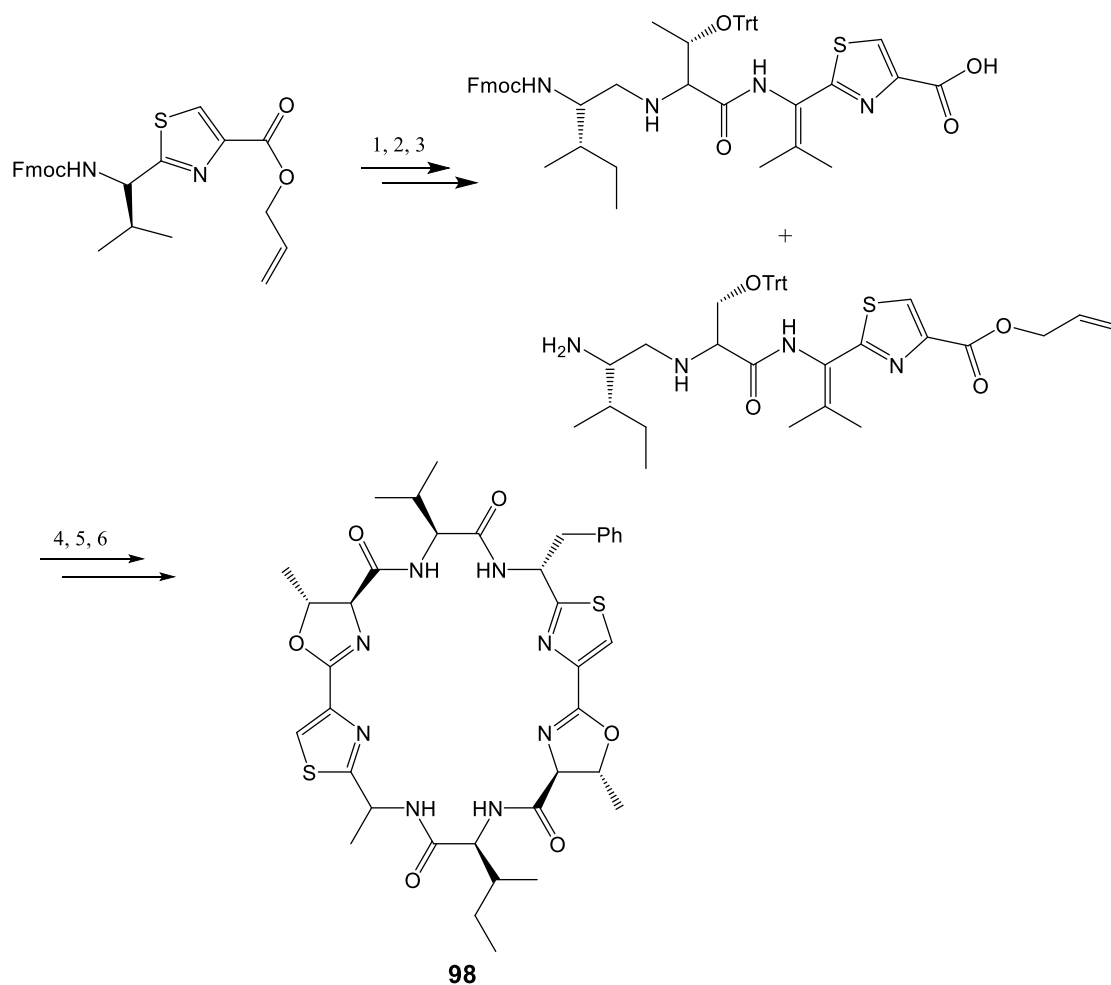


**Figure 20.** Structures of patellamides B (**95**), C (**96**), and D (**97**).

The synthesis of patellamide derivatives has been accomplished, using thiazole as starting material, via two contemporary heterocyclization approaches to form oxazolines and thiazoline via coupling and cyclodehydration reactions. The example illustrating the synthesis of patellamide A (**98**) is described in Scheme 19 [202].



**Scheme 19.** Synthesis of patellamide A (**98**). Reagents and conditions: 1) 20% piperidine/DMF, HOBt, HBTU, DIEA, Fmoc-L-Thr(Trt)-OH; 2) 20% piperidine/DMF, HOBt, HBTU, DIEA, Fmoc-Ile-OH; 3) Pd(PPh<sub>3</sub>)<sub>4</sub>, PhSiH<sub>3</sub>, CH<sub>2</sub>Cl<sub>2</sub>, 6h and 20% piperidine/DMF; 4) HOBt, HBTU, DIEA, CH<sub>2</sub>Cl<sub>2</sub>, 2% TFA, PhSH, CH<sub>2</sub>Cl<sub>2</sub>; 5) Burgess reagent, THF, 55°C, 1h then 77°C, 4h; 6) Pd(PPh<sub>3</sub>)<sub>4</sub>, PhSiH<sub>3</sub>, CH<sub>2</sub>Cl<sub>2</sub>, 2h.

## 2.7. Miscellaneous

### 2.7.1. Irciniasulfonic acid derivatives

Irciniasulfonic acids consist of ISA (compound **99-101**, [203]) and ISA-B (compound **102-103**, [204]). These acids are esters that were isolated from the marine sponge *Ircinia sp* [203], and deacyl irciniasulfonic acid was isolated from tropical *Coscinoderma sp* sponge (Figure 21) [205]. Irciniasulfonic acids **99-103** were found to reverse MDR against KB/VJ300 overexpressing P-gp at the concentration of 100 μM in the present of vincristine [203,204,206]. Compound **99-101** were shown to reverse MDR against KB/VJ300 overexpressing P-gp in the presence of verapamil at the concentration of 25 μM, and the simplified analog (deacyl ISA, **104**) showed to be 13-folds more potent than other irciniasulfonic acids in reversal the MDR phenotype [203,204].

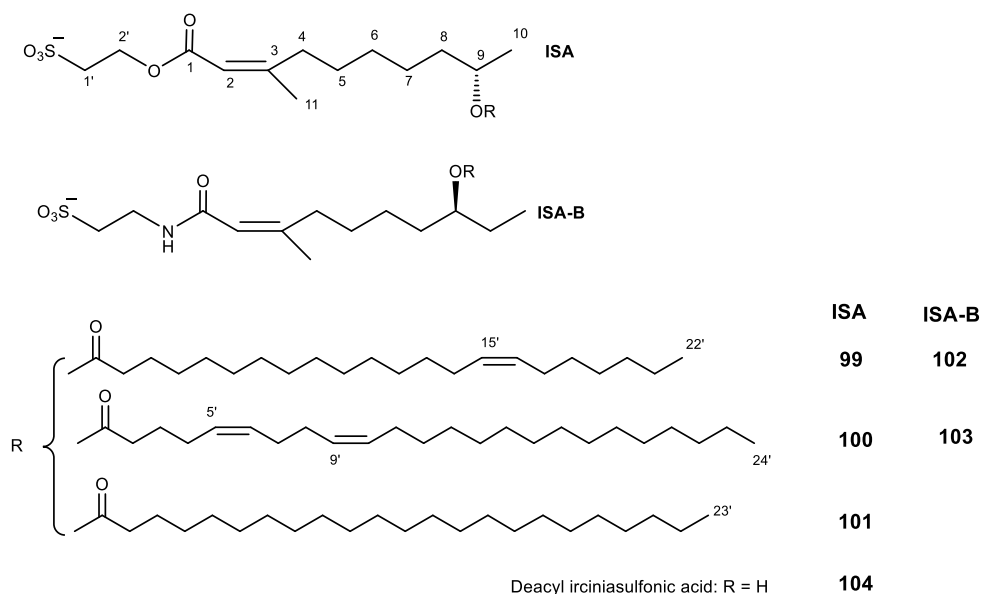
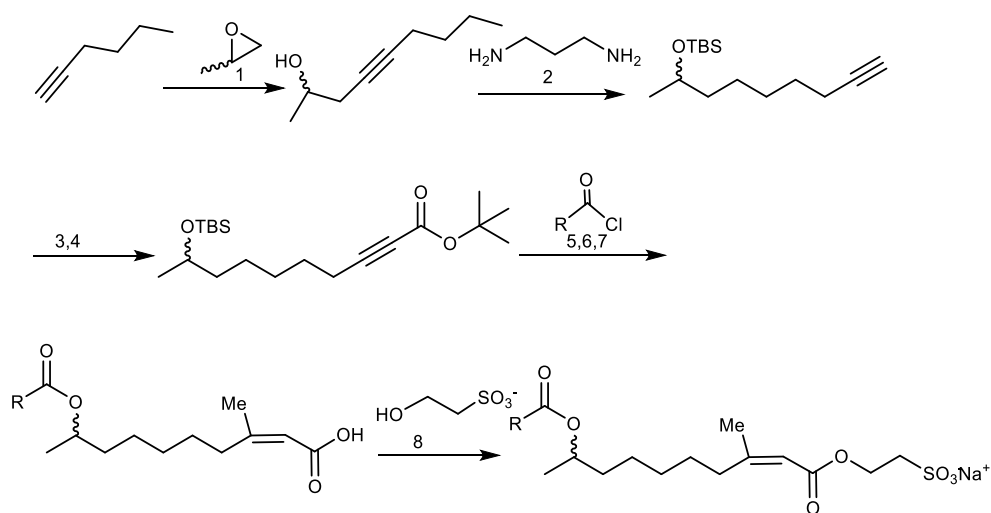


**Figure 21.** Structure of ISA (99-101), ISA-B (102-103), and deacyl ISA (104).

The synthesis of ISA derivatives was accomplished using propylene oxide as starting material via a convergent approach to achieve both enantiomers of the natural product and allowed also the incorporation of a range of side chains for optimization of their biological activity. The procedure of this synthesis is illustrated in Scheme 20 [207].



**Scheme 20.** The total synthesis of ISA derivatives. Reagents and conditions: 1) *n*-BuLi, Et<sub>2</sub>AlCl, toluene; 2) KH; 3) TBS-Cl, imidazole, DMAP, DMF; 4) *n*-BuLi, Boc<sub>2</sub>O; 5) CuBr<sub>2</sub>.SMe<sub>2</sub>, MeLi, THF; 6) HF-pyridine, 7) TFA, CH<sub>2</sub>Cl<sub>2</sub>; 8) (COCl)<sub>2</sub>, DMF cat, CH<sub>2</sub>Cl<sub>2</sub>, toluene, reflux.

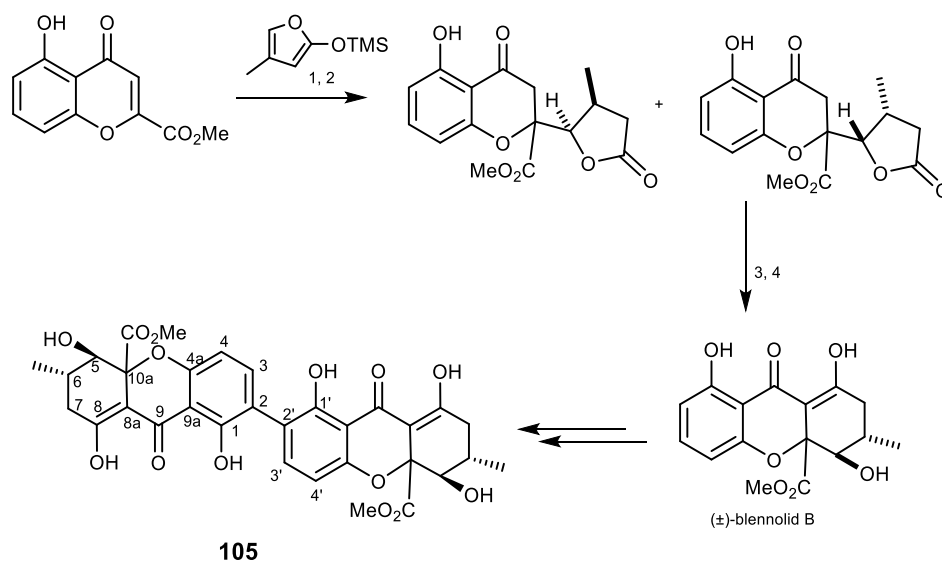
### 2.7.2. Secalonic acid D

Secalonic acid D (**105**, Scheme 21) is a mycotoxin isolated from the marine fungi *Penicillium oxalicum* [208] and *Gliocladium sp.* T31 [209], which was investigated for antitumor properties as a DNA topoisomerase I inhibitor [210]. This compound showed a potent cytotoxicity on MDR cells (P-gp, MRP1, and BCRP-overexpressing cells) and on their parental cells by down-regulating the expression of BCRP protein [211]. It also decreased the percentage of side population cell in lung cancer cells. These results highlight **105** as an interesting molecule that has a potent cytotoxic activity by enduring BCRP degradation and was considered as a lead compound for the development of new BCRP inhibitors [212].

Chemically, secalonic acid D (**105**) is the chiral dimeric natural product of ergochrome xanthone [213]. The synthesis of secalonic acid D (**105**) started from the intermediate compound ( $\pm$ )-blennolide B, which was synthesized from 5-hydroxychromone, with a construction of a hemisecalonic derivative, followed by the conversion with iodide and stannane. This reaction is a copper-catalyzed C–C bond-forming between the two molecules under oxidative conditions as the key dimerization step. This reaction is the first challenge to oxidize the xanthone framework which was previously shown as unsuitable for a direct oxidation. The iodide compound can be pre-activated at an *o*-position to make the dimerization regioselective. The total synthesis of secalonic acid D (**105**) is illustrated in Scheme 21 [213-216].

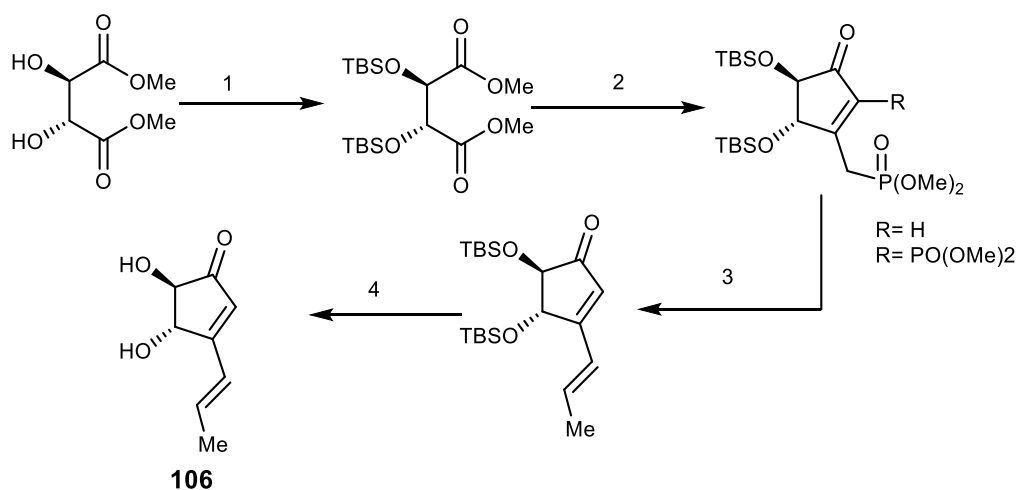
### 2.7.3. Terrein

Terrein (**106**, Scheme 22) is a fungal metabolite isolated from the marine-derived thermophilic fungus *Aspergillus terreus*. This metabolite has been already reported to inhibit cell proliferation, to induce cell cycle arrest in human ovarian tumor cells (SKOV3,) and to inhibit the proliferation of ovarian cancer stem-like cells [217], to inhibit the epidermal proliferation of skin [218], as well as to inhibit melanogenesis [219]. It also displayed a strong cytotoxicity against breast cancer (MCF-7) cell and suppressed the growth of MCF-7 expressing BCRP cells by inducing apoptosis caspase-7 pathway and inhibiting the Akt signaling pathway [220].



**Scheme 21.** Total synthesis of secalonic acid D (**105**). Reagents and conditions: 1) 2,6-lutidine,  $i\text{PrSi}(\text{OTf})_2$ ,  $\text{CH}_2\text{Cl}_2$ , then  $\text{Et}_3\text{N}\cdot 3\text{HF}$ ; 2)  $\text{Rh}/\text{Al}_2\text{O}_3$ ,  $\text{H}_2$ ,  $\text{MeOH}$ ; 3)  $\text{NaH}$ ,  $\text{THF}$ ; 4)  $\text{CH}_2\text{Cl}_2$ , then  $\text{NaH}$ ,  $\text{THF}$ .

A simple synthesis of (+)-terrein (**106**) was reported by using L-tartrate or dimethyl L-tartrate as starting materials. The whole process included cyclization, Horner-Wadsworth-Emmons, and deprotection of bis-*t*-butyldimethylsilyl (bis-TBS) group as shown in Scheme 22 [221].



**Scheme 22.** Synthesis of (+)-terrein (**106**). Reagents and conditions: 1)  $\text{TBSCl}$ , imidazole,  $\text{DMF}$ ; 2)  $n\text{-BuLi}$ ,  $\text{MePO}(\text{OMe})_2$ ,  $\text{THF}$ , then benzene- $\text{H}_2\text{O}$ , reflux; 3)  $\text{NaH}$ ,  $\text{MeCHO}$ ,  $\text{THF}$ ; 4) condition ( $\text{Et}_3\text{NCl}$ ),  $\text{MeCN}$  or  $\text{HF}\cdot\text{MeCN}$  or  $\text{TBAF}$ ,  $\text{MeCN}$ .



#### 2.7.4. Shornephine A

Shornephine A (**107**, Figure 22) is a diketomorpholine isolated from the marine fungus *Aspergillus sp.* (CMC-M081F) which was collected from marine sediment. This compound was described as a non-cytotoxic inhibitor of P-gp in MDR human colon tumor cells (SW60 Ad300) at the concentration of 20  $\mu$ M [222].

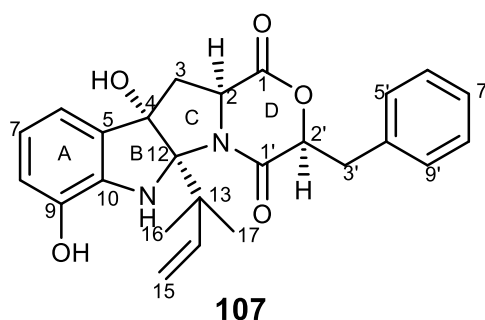


**Figure 22.** Structure of shornephine A (**107**).

### 3. Future Perspectives

We are now witnessing a renaissance of the interest in efflux transporters not only due to requirements in regulatory issues but also to the significant role of these carriers in the adsorption, distribution, metabolism, excretion, and toxicity (ADMET) process of drugs discovery. Therefore, P-gp and other ABC transporters that mediate drug efflux are recognized as a “team to beat”. Marine organisms have proven to be an important source in the discovery and development of interesting compounds, and, in particular, of anticancer agents. These marine-derived compounds, which can be grouped mainly as alkaloids, polyoxygenated sterols, terpenoids, and peptides have demonstrated a reversal effect of MDR by themselves. Some compounds showed to increase rather than decrease cytotoxicity towards MDR cell lines and can be defined as collateral sensitizing agents or this effect was shown in combination with anticancer drugs, being non-cytotoxic MDR reversal agents. The major sources of marine MDR reversal agents and mechanisms have been scarcely studied, and very little is known about their mechanism of action. Several marine compounds which have shown potent and selective MDR activity against cancer cell lines belong to alkaloids; however, they present some toxicity. Among marine natural products, trabectedin proved to be the most promising against MDR with *in vitro* and *in vivo* efficacy. Chemically, synthetic analogs of marine

compounds acting as inhibitors have been investigated to achieve higher activity, less toxicity and less pharmacokinetic interaction properties, and to establish SAR. With this diversity of scaffolds, it is not possible to extract common features essential for MDR reversal activity; however, most of the derivatives are highly lipophilic and contain fused rings and multiple chiral centers, which in turn reflect their complex total synthesis procedures. Among the synthetic analogs, eriburin has been shown to be the most promising P-gp modulator, active against MDR *in vitro* and with proved safety in clinical patients. These features also open new challenges for medicinal chemists to accomplish viable synthetic routes and new avenues in the design of analogs with suitable drug-like properties that could render potential drug candidates. Joining together all the pieces of the chemical-biological-pharmaceutical puzzle, we can anticipate more effective chemotherapies based on molecules from the sea.

**Acknowledgments:** The authors thank to national funds provided by FCT – Foundation for Science and Technology and European Regional Development Fund (ERDF) and COMPETE under the projects PEst-C/MAR/LA0015/2013, PTDC/MAR-BIO/4694/2014, and INNOVMAR - Innovation and Sustainability in the Management and Exploitation of Marine Resources, reference NORTE-01-0145-FEDER-000035, Research Line NOVELMAR. S.L. thanks Erasmus Mundus Action 2 (LOTUS+, LP15DF0205) for full PhD scholarship.

**Author Contributions:** The manuscript was conceived by E.S., S.L. collected the primary data and compiled draft manuscripts. E.S., A.K. and M.P. supervised development of the manuscript, and assisted in data interpretation, manuscript evaluation, and editing.

**Conflicts of Interest:** The authors declare no conflict of interest.

## References

1. Cancer. Available online <http://www.who.int/mediacentre/factsheets/fs297/en/> (Accessed on 16-03-2016),
2. Che, X.F.; Nakajima, Y.; Sumizawa, T.; Ikeda, R.; Ren, X.Q.; Zheng, C.L.; Mukai, M.; Furukawa, T.; Haraguchi, M.; Gao, H., *et al.* Reversal of p-glycoprotein mediated multidrug resistance by a newly synthesized 1,4-benzothiazipine derivative, jtv-519. *Cancer Lett.* **2002**, *187*, 111-119.
3. Gustav, L. P-glycoprotein as a drug target in the treatment of multidrug resistant cancer. *Curr. Drug Targets* **2000**, *1*, 85-99.

4. Higgins, C.F. Multiple molecular mechanisms for multidrug resistance transporters. *Nature* **2007**, *446*, 749-757.
5. Ambudkar, S.V.; Kim, I.-W.; Sauna, Z.E. The power of the pump: Mechanisms of action of p-glycoprotein (abcb1). *Eur. J. Pharm. Sci.* **2006**, *27*, 392-400.
6. Thomas, H.; Coley, H.M. Overcoming multidrug resistance in cancer: An update on the clinical strategy of inhibiting p-glycoprotein. *Cancer Control* **2003**, *10*, 159-165.
7. Williams, A.B.; Jacobs, R.S. A marine natural product, patellamide d, reverses multidrug resistance in a human leukemic cell line. *Cancer Lett.* **1993**, *71*, 97-102.
8. Xun, L.; Hongyu, Y.; Jifeng, W.; Jinpei, L.; Xianjun, Q.; Wenfang, X.; Wei, T. Strategies to overcome or circumvent p-glycoprotein mediated multidrug resistance. *Curr. Med. Chem.* **2008**, *15*, 470-476.
9. Li, X.; Li, J.P.; Yuan, H.Y.; Gao, X.; Qu, X.J.; Xu, W.F.; Tang, W. Recent advances in p-glycoprotein-mediated multidrug resistance reversal mechanisms. *Method. Find. Exp. Clin. Pharmacol.* **2007**, *29*, 607-617.
10. Baguley, B.C. Multiple drug resistance mechanisms in cancer. *Mol. Biotechnol.* **2010**, *46*, 308-316.
11. Gillet, J.-P.; Gottesman, M.M. Overcoming multidrug resistance in cancer: 35 years after the discovery of abcb1. *Drug Resist. Update.* **2012**, *15*, 2-4.
12. Ween, M.P.; Armstrong, M.A.; Oehler, M.K.; Ricciardelli, C. The role of abc transporters in ovarian cancer progression and chemoresistance. *Crit. Rev. Oncol. Hematol.* **2015**, *2*, 220-256.
13. Leslie, E.M.; Deeley, R.G.; Cole, S.P.C. Multidrug resistance proteins: Role of p-glycoprotein, mrp1, mrp2, and bcrp (abcg2) in tissue defense. *Toxicol. Appl. Pharm.* **2005**, *204*, 216-237.
14. Lopes-Rodrigues, V.; Seca, H.; Sousa, D.; Sousa, E.; Lima, R.T.; Vasconcelos, M.H. The network of p-glycoprotein and micromnas interactions. *Int. J. Cancer* **2014**, *135*, 253-263.
15. Rubnitz, J.E.; Gibson, B.; Smith, F.O. Acute myeloid leukemia. *Pediatr. Clin. N. Am.* **2008**, *55*, 21-51, ix.
16. Steinbach, D.; Legrand, O. Abc transporters and drug resistance in leukemia: Was p-gp nothing but the first head of the hydra? *Leukemia* **2007**, *21*, 1172-1176.

17. Rubnitz, J.E. How i treat pediatric acute myeloid leukemia. *Blood* **2012**, *119*, 5980-5988.
18. Kessel, D.; Botterill, V.; Wodinsky, I. Uptake and retention of daunomycin by mouse leukemic cells as factors in drug response. *Cancer Res.* **1968**, *28*, 938-941.
19. Srivastava, S.; Choudhary, B.S.; Sharma, M.; Malik, R. Pharmacophore modeling and 3d-qsar studies of galloyl benzamides as potent p-gp inhibitors. *Med. Chem. Res.* **2016**, *25*, 1140-1147.
20. Palmeira, A.; Sousa, E.; Vasconcelos, M.H.; Pinto, M.M. Three decades of p-gp inhibitors: Skimming through several generations and scaffolds. *Curr. Med. Chem.* **2012**, *19*, 1946-2025.
21. Perez-Victorias, F.J.; Conseil, G.; Munoz-Martinez, F.; Perez-Victoria, J.M.; Dayan, G.; Marsaud, V.; Castanys, S.; Gamarro, F.; Renoir, J.M.; Di Pietro, A. Ru49953: A non-hormonal steroid derivative that potently inhibits p-glycoprotein and reverts cellular multidrug resistance. *Cell. Mol. Life Sci.* **2003**, *60*, 526-535.
22. Modok, S.; Mellor, H.R.; Callaghan, R. Modulation of multidrug resistance efflux pump activity to overcome chemoresistance in cancer. *Curr. Opin. Pharmacol.* **2006**, *6*, 350-354.
23. Krishna, R.; Mayer, L.D. Multidrug resistance (mdr) in cancer - mechanisms, reversal using modulators of mdr and the role of mdr modulators in influencing the pharmacokinetics of anticancer drugs. *Eur. J. Pharm. Sci.* **2000**, *11*, 265-283.
24. Coley, H.M. Overcoming multidrug resistance in cancer: Clinical studies of p-glycoprotein inhibitors. In *Multi-drug resistance in cancer*, Zhou, J., Ed. Humana Press: Totowa, NJ, 2010; pp 341-358.
25. Discontinuation of two phase iii trials of tariquidar in non-small-cell lung cancer. *Inpharma Weekly* **2013**, *1387*, 10-10.
26. Wandel, C.; B. Kim, R.; Kajiji, S.; Guengerich, F.P.; Wilkinson, G.R.; Wood, A.J.J. P-glycoprotein and cytochrome p-450 3a inhibition: Dissociation of inhibitory potencies. *Cancer Res.* **1999**, *59*, 3944-3948.
27. Cripe, L.D.; Uno, H.; Paietta, E.M.; Litzow, M.R.; Ketterling, R.P.; Bennett, J.M.; Rowe, J.M.; Lazarus, H.M.; Luger, S.; Tallman, M.S. Zosuquidar, a novel modulator of p-glycoprotein, does not improve the outcome of older patients with newly

- diagnosed acute myeloid leukemia: A randomized, placebo-controlled trial of the eastern cooperative oncology group 3999. *Blood* **2010**, *116*, 4077-4085.
28. Chen, C.; Zhou, J.; Ji, C. Quercetin: A potential drug to reverse multidrug resistance. *Life Sci.* **2010**, *87*, 333-338.
  29. Cherigo, L.; Lopez, D.; Martinez-Luis, S. Marine natural products as breast cancer resistance protein inhibitors. *Mar. Drugs* **2015**, *13*, 2010-2029.
  30. Gomes, N.; Lefranc, F.; Kijjoo, A.; Kiss, R. Can some marine-derived fungal metabolites become actual anticancer agents? *Mar. Drugs* **2015**, *13*, 3950.
  31. Hoffmann, K.; Bekeredjian, R.; Schmidt, J.; Büchler, M.W.; Märten, A. Effects of the high-affinity peptide reversin 121 on multidrug resistance proteins in experimental pancreatic cancer. *Tumor Biol.* **2009**, *29*, 351-358.
  32. Bogman, K.; Erne-Brand, F.; Alsenz, J.; Drewe, J. The role of surfactants in the reversal of active transport mediated by multidrug resistance proteins. *J. Pharm. Sci.* **2003**, *92*, 1250-1261.
  33. Capon, R.J. Marine bioprospecting - trawling for treasure and pleasure. *Eur. J. Org. Chem.* **2001**, 633-645.
  34. Zhang, G.; Li, J.; Zhu, T.; Gu, Q.; Li, D. Advanced tools in marine natural drug discovery. *Curr. Opin. Biotech.* **2016**, *42*, 13-23.
  35. Lopez, D.; Martinez-Luis, S. Marine natural products with p-glycoprotein inhibitor properties. *Mar. Drugs* **2014**, *12*, 525-546.
  36. Abraham, I.; El Sayed, K.; Chen, Z.S.; Guo, H. Current status on marine products with reversal effect on cancer multidrug resistance. *Mar. Drugs* **2012**, *10*, 2312-2321.
  37. Kathawala, R.J.; Gupta, P.; Ashby, C.R.; Chen, Z.S. The modulation of abc transporter-mediated multidrug resistance in cancer: A review of the past decade. *Drug Resist. Updates* **2015**, *18*, 1-17.
  38. Stonik, V.A.; Fedorov, S.N. Marine low molecular weight natural products as potential cancer preventive compounds. *Mar. Drugs* **2014**, *12*, 636-671.
  39. Zhang, Y.; Zhang, Y.K.; Wang, Y.J.; Vispute, S.G.; Jain, S.; Chen, Y.; Li, J.; Youssef, D.T.A.; El Sayed, K.A.; Chen, Z.S. Esters of the marine-derived triterpene siphonolol a reverse p-gp-mediated drug resistance. *Mar. Drugs* **2015**, *13*, 2267-2286.

40. Shanthi, J.; Senthil, A.; Gopikrishnan, V.; Balagurunathan, R. Characterization of a potential  $\beta$ -lactamase inhibitory metabolite from a marine streptomyces sp. Pm49 active against multidrug-resistant pathogens. *Appl. Biochem. Biotech.* **2015**, *175*, 3696-3708.
41. Huang, X.C.; Kumar, P.; Anreddy, N.; Xiao, X.; Yang, D.H.; Chen, Z.S. P-gp inhibitory activity from marine sponges, tunicates and algae. In *Handbook of anticancer drugs from marine origin*, 2015; pp 593-619.
42. Dinić, J.; Podolski-Renić, A.; Stanković, T.; Banković, J.; Pešić, M. New approaches with natural product drugs for overcoming multidrug resistance in cancer. *Curr. Pharm. Design* **2015**, *21*, 5589-5604.
43. Patel, A.; Wang, D.-S.; Sim, H.-M.; Ambudkar, S.V.; Chen, Z.-S. Abc transporter modulatory drugs from marine sources: A new approach to overcome drug resistance in cancer. In *Resistance to targeted abc transporters in cancer*, Efferth, T., Ed. Springer International Publishing: Cham, 2015; pp 183-208.
44. Shi, Z.; Jain, S.; Kim, I.W.; Peng, X.X.; Abraham, I.; Youssef, D.T.A.; Fu, L.W.; El Sayed, K.; Ambudkar, S.V.; Chen, Z.S. Sipholenol a, a marine-derived sipholane triterpene, potently reverses p-glycoprotein (abcb1)-mediated multidrug resistance in cancer cells. *Cancer Sci.* **2007**, *98*, 1373-1380.
45. Abraham, I.; Jain, S.; Wu, C.P.; Khanfar, M.A.; Kuang, Y.; Dai, C.L.; Shi, Z.; Chen, X.; Fu, L.; Ambudkar, S.V., *et al.* Marine sponge-derived sipholane triterpenoids reverse p-glycoprotein (abcb1)-mediated multidrug resistance in cancer cells. *Biochem. Pharmacol.* **2010**, *80*, 1497-1506.
46. Akl, M.R.; Foudah, A.I.; Ebrahim, H.Y.; Meyer, S.A.; El Sayed, K.A. The marine-derived sipholenol a-4-o-3',4'-dichlorobenzoate inhibits breast cancer growth and motility in vitro and in vivo through the suppression of brk and fak signaling. *Mar. Drugs* **2014**, *12*, 2282-2304.
47. Foudah, A.I.; Sallam, A.A.; Akl, M.R.; El Sayed, K.A. Optimization, pharmacophore modeling and 3d-qsar studies of sipholanes as breast cancer migration and proliferation inhibitors. *Eur. J. Med. Chem.* **2014**, *73*, 310-324.

48. Jain, S.; Laphookhieo, S.; Shi, Z.; Fu, L.W.; Akiyama, S.I.; Chen, Z.S.; Youssef, D.T.A.; Van Soest, R.W.M.; El Sayed, K.A. Reversal of p-glycoprotein-mediated multidrug resistance by sipholane triterpenoids. *J. Nat. Prod.* **2007**, *70*, 928-931.
49. Jain, S.; Abraham, I.; Carvalho, P.; Kuang, Y.H.; Shaala, L.A.; Youssef, D.T.A.; Avery, M.A.; Chen, Z.S.; El Sayed, K.A. Sipholane triterpenoids: Chemistry, reversal of abcb1/p-glycoprotein-mediated multidrug resistance, and pharmacophore modeling. *J. Nat. Prod.* **2009**, *72*, 1291-1298.
50. Rochfort, S.J.; Capon, R.J. Parguerenes revisited: New brominated diterpenes from the southern Australian marine red alga *Laurencia filiformis*. *Aus. J. Chem.* **1996**, *49*, 19-26.
51. Awad, N.E. Bioactive brominated diterpenes from the marine red alga *Jania rubens* (L.) Lamouroux. *Phytother. Res.* **2004**, *18*, 275-279.
52. Takeda, S.; Kurosawa, E.; Komiyama, K.; Suzuki, T. The structures of cytotoxic diterpenes containing bromine from the marine red alga *Laurencia obtusa* (Hudson) Lamouroux. *Bull. Chem. Soc. Jpn.* **1990**, *63*, 3066-3072.
53. Huang, X.-c.; Sun, Y.-L.; Salim, A.A.; Chen, Z.-S.; Capon, R.J. Parguerenes: Marine red alga bromoditerpenes as inhibitors of p-glycoprotein (abcb1) in multidrug resistant human cancer cells. *Biochem. Pharmacol.* **2013**, *85*, 1257-1268.
54. Aoki, S.; Chen, Z.-S.; Higashiyama, K.; Setiawan, I.; Akiyama, S.-i.; Kobayashi, M. Reversing effect of agosterol A, a spongean sterol acetate, on multidrug resistance in human carcinoma cells. *Jpn. J. Cancer Res.* **2001**, *92*, 886-895.
55. Aoki, S.; Yoshioka, Y.; Miyamoto, Y.; Higuchi, K.; Setiawan, A.; Murakami, N.; Chen, Z.S.; Sumizawa, T.; Akiyama, S.; Kobayashi, M. Agosterol A, a novel polyhydroxylated sterol acetate reversing multidrug resistance from a marine sponge of *Spongia* sp. *Tetrahedron Lett.* **1998**, *39*, 6303-6306.
56. Chen, Z.-S.; Aoki, S.; Komatsu, M.; Ueda, K.; Sumizawa, T.; Furukawa, T.; Okumura, H.; Ren, X.-Q.; Belinsky, M.G.; Lee, K., *et al.* Reversal of drug resistance mediated by multidrug resistance protein (mrp) 1 by dual effects of agosterol A on mrp1 function. *Int. J. Cancer* **2001**, *93*, 107-113.
57. Mayer, A.M.S.; Rodríguez, A.D.; Berlinck, R.G.S.; Hamann, M.T. Marine pharmacology in 2003–4: Marine compounds with anthelmintic antibacterial,

anticoagulant, antifungal, anti-inflammatory, antimalarial, antiplatelet, antiprotozoal, antituberculosis, and antiviral activities; affecting the cardiovascular, immune and nervous systems, and other miscellaneous mechanisms of action. *Comp. Biochem. Physiol. C Toxicol. Pharmacol.* **2007**, *145*, 553-581.

58. Aoki, S.; Setiawan, A.; Yoshioka, Y.; Higuchi, K.; Fudetani, R.; Chen, Z.-S.; Sumizawa, T.; Akiyama, S.-i.; Kobayashi, M. Reversal of multidrug resistance in human carcinoma cell line by agosterols, marine spongean sterols. *Tetrahedron* **1999**, *55*, 13965-13972.
59. Mayer, A.M.S.; Gustafson, K.R. Marine pharmacology in 2001–2: Antitumour and cytotoxic compounds. *Eur. J. Cancer* **2004**, *40*, 2676-2704.
60. Murakami, N.; Sugimoto, M.; Morita, M.; Akiyama, S.-i.; Kobayashi, M. Synthesis and evaluation of 4-deacetoxyagosterol a as an mdr-modulator. *Bioorg. Med. Chem. Lett.* **2000**, *10*, 2521-2524.
61. Murakami, N.; Sugimoto, M.; Morita, M.; Kobayashi, M. Total synthesis of agosterol a: An mdr-modulator from a marine sponge. *Chem. Eur. J.* **2001**, *7*, 2663-2670.
62. Tanaka, J.; Trianto, A.; Musman, M.; Issa, H.H.; Ohtani, I.I.; Ichiba, T.; Higa, T.; Yoshida, W.Y.; Scheuer, P.J. New polyoxygenated steroids exhibiting reversal of multidrug resistance from the gorgonian isis hippuris. *Tetrahedron* **2002**, *58*, 6259-6266.
63. Boonananwong, S.; Kongkathip, B.; Kongkathip, N. First synthesis of 3,16,20-polyoxygenated cholestanes, new cytotoxic steroids from the gorgonian leptogorgia sarmentosa. *Steroids* **2008**, *73*, 1123-1127.
64. Wang, Z.; Tang, H.; Wang, P.; Gong, W.; Xue, M.; Zhang, H.; Liu, T.; Liu, B.; Yi, Y.; Zhang, W. Bioactive polyoxygenated steroids from the south china sea soft coral, sarcophyton sp. *Mar. Drugs* **2013**, *11*, 775-787.
65. Li, R.; Shao, C.L.; Qi, X.; Li, X.B.; Li, J.; Sun, L.L.; Wang, C.Y. Polyoxygenated sterols from the south china sea soft coral sinularia sp. *Mar. Drugs* **2012**, *10*, 1422-1432.
66. Wang, P.; Tang, H.; Liu, B.-S.; Li, T.-J.; Sun, P.; Zhu, W.; Luo, Y.-P.; Zhang, W. Tumor cell growth inhibitory activity and structure–activity relationship of polyoxygenated steroids from the gorgonian menella kanisa. *Steroids* **2013**, *78*, 951-958.



67. Kim, S.; Sutton, S.C.; Guo, C.; LaCour, T.G.; Fuchs, P.L. Synthesis of the north 1 unit of the cephalostatin family from hecogenin acetate<sup>1</sup>. *J. Am. Chem. Soc.* **1999**, *121*, 2056-2070.
68. Musumeci, D.; Sica, D.; Zollo, F. Synthesis of polyoxygenated steroids with transition metal-based oxidants: Methyltrioxorhenium-hydrogen peroxide system, ruthenium tetroxide, osmium tetroxide and potassium permanganate. *Curr. Org. Synth.* **2005**, *2*, 1-20.
69. Weiss, J.M.; Hoffmann, H.M.R. Synthesis of the c1-c9 segment of bryostatin. *Tetrahedron Asymmetry* **1997**, *8*, 3913-3920.
70. Ohmori, K.; Ogawa, Y.; Obitsu, T.; Ishikawa, Y.; Nishiyama, S.; Yamamura, S. Total synthesis of bryostatin 3. *Angew. Chem. Int. Ed.* **2000**, *39*, 2290-2294.
71. Pettit, G.R.; Herald, C.L.; Hogan, F. Chapter 12 - biosynthetic products for anticancer drug design and treatment: The bryostatins. In *Anticancer drug development*, Kerr, B.C.B.J., Ed. Academic Press: San Diego, 2002; pp 203-235.
72. Spitaler, M.; Utz, I.; Hilbe, W.; Hofmann, J.; Grunicke, H. Pkc-independent modulation of multidrug resistance in cells with mutant (v185) but not wild-type (g185) p-glycoprotein by bryostatin 1. *Biochem. Pharmacol.* **1998**, *56*, 861-869.
73. Utz, I.; Hofmann, J.; Grunicke, H. Bryostatin 1 regulates multi drug resistance by a pkc-independent mechanism. *Eur. J. Cancer* **1995**, *31*, Supplement 3, S13.
74. Scala, S.; Dickstein, B.; Regis, J.; Szallasi, Z.; Blumberg, P.M.; Bates, S.E. Bryostatin 1 affects p-glycoprotein phosphorylation but not function in multidrug-resistant human breast cancer cells. *Clin. Cancer Res.* **1995**, *1*, 1581-1587.
75. Kedei, N.; Telek, A.; Czap, A.; Lubart, E.S.; Czifra, G.; Yang, D.; Chen, J.; Morrison, T.; Goldsmith, P.K.; Lim, L., *et al.* The synthetic bryostatin analog merle 23 dissects distinct mechanisms of bryostatin activity in the lncap human prostate cancer cell line. *Biochem. Pharmacol.* **2011**, *81*, 1296-1308.
76. Kedei, N.; Telek, A.; Michalowski, A.M.; Kraft, M.B.; Li, W.; Poudel, Y.B.; Rudra, A.; Petersen, M.E.; Keck, G.E.; Blumberg, P.M. Comparison of transcriptional response to phorbol ester, bryostatin 1, and bryostatin analogs in lncap and u937 cancer cell lines provides insight into their differential mechanism of action. *Biochem. Pharmacol.* **2013**, *85*, 313-324.

77. Wender, P.A.; De Brabander, J.; Harran, P.G.; Hinkle, K.W.; Lippa, B.; Pettit, G.R. Synthesis and biological evaluation of fully synthetic bryostatin analogues. *Tetrahedron Lett.* **1998**, *39*, 8625-8628.
78. Trost, B.M.; Yang, H.; Dong, G. Total syntheses of bryostatins: Synthesis of two ring-expanded bryostatin analogues and the development of a new-generation strategy to access the c7-c27 fragment. *Chem. Eur. J.* **2011**, *17*, 9789-9805.
79. Trost, B.M.; Yang, H.; Thiel, O.R.; Frontier, A.J.; Brindle, C.S. Synthesis of a ring-expanded bryostatin analogue. *J. Am. Chem. Soc.* **2007**, *129*, 2206-2207.
80. Roy, R.; Rey, A.W.; Charron, M.; Molino, R. Enantiospecific synthesis of the c-17-c-20 and c-21-c-27 synthons of the antineoplastic macrolide bryostatins. *J. Chem. Soc. Chem. Commun.* **1989**, 1308-1310.
81. Honore, S.; Kamath, K.; Braguer, D.; Horwitz, S.B.; Wilson, L.; Briand, C.; Jordan, M.A. Synergistic suppression of microtubule dynamics by discodermolide and paclitaxel in non-small cell lung carcinoma cells. *Cancer Res.* **2004**, *64*, 4957-4964.
82. Loggley, R.E.; Ccddigan, D.; Harmody, D.; Gunasekera, M.; Gunasekera, S.P. Discodermolide-a new, marine-derived immunosuppressive compound: I. In vitro studies. *Transplantation* **1991**, *52*, 650-655.
83. Longley, R.E.; Gunasekera, S.P.; Faherty, D.; McLane, J.; Dumont, F. Immunosuppression by discodermolide. *Ann. N. Y. Acad. Sci.* **1993**, *696*, 94-107.
84. Dimri, G.P.; Lee, X.; Basile, G.; Acosta, M.; Scott, G.; Roskelley, C.; Medrano, E.E.; Linskens, M.; Rubelj, I.; Pereira-Smith, O. A biomarker that identifies senescent human cells in culture and in aging skin in vivo. *Proceedings of the National Academy of Sciences* **1995**, *92*, 9363-9367.
85. Kowalski, R.J.; Giannakakou, P.; Gunasekera, S.P.; Longley, R.E.; Day, B.W.; Hamel, E. The microtubule-stabilizing agent discodermolide competitively inhibits the binding of paclitaxel (taxol) to tubulin polymers, enhances tubulin nucleation reactions more potently than paclitaxel, and inhibits the growth of paclitaxel-resistant cells. *Mol. Pharmacol.* **1997**, *52*, 613-622.
86. Betzer, J.F.; Ardisson, J. Discodermolide: Total synthesis of natural product and analogues. In *Strategies and Tactics in Organic Synthesis*, 2015; Vol. 11, pp 51-84.

87. Yu, Z.; Ely, R.J.; Morken, J.P. Synthesis of (+)-discodermolide by catalytic stereoselective borylation reactions. *Angew. Chem. Int. Ed.* **2014**, *53*, 9632-9636.
88. Towle, M.J.; Salvato, K.A.; Budrow, J.; Wels, B.F.; Kuznetsov, G.; Aalfs, K.K.; Welsh, S.; Zheng, W.; Seletsky, B.M.; Palme, M.H., *et al.* In vitro and in vivo anticancer activities of synthetic macrocyclic ketone analogues of halichondrin b. *Cancer Res.* **2001**, *61*, 1013-1021.
89. Cortes, J.; Montero, A.J.; Glück, S. Eribulin mesylate, a novel microtubule inhibitor in the treatment of breast cancer. *Cancer Treat. Rev.* **2012**, *38*, 143-151.
90. Huyck, T.K.; Gradishar, W.; Manuguid, F.; Kirkpatrick, P. Eribulin mesylate. *Nat. Rev. Drug Discov.* **2011**, *10*, 173-174.
91. Narayan, S.; Carlson, E.M.; Cheng, H.; Du, H.; Hu, Y.; Jiang, Y.; Lewis, B.M.; Seletsky, B.M.; Tendyke, K.; Zhang, H., *et al.* Novel second generation analogs of eribulin. Part i: Compounds containing a lipophilic c32 side chain overcome p-glycoprotein susceptibility. *Bioorg. Med. Chem. Lett.* **2011**, *21*, 1630-1633.
92. Garrone, O.; Montemurro, F.; Saggia, C.; La Verde, N.; Vandone, A.M.; Airoidi, M.; De Conciliis, E.; Donadio, M.; Lucio, F.; Polimeni, M.A., *et al.* Eribulin in pretreated metastatic breast cancer patients: Results of the trotter trial—a multicenter retrospective study of eribulin in real life. *SpringerPlus* **2016**, *5*, 1-8.
93. Yu, M.J.; Zheng, W.; Seletsky, B.M. From micrograms to grams: Scale-up synthesis of eribulin mesylate. *Nat. Prod. Rep.* **2013**, *30*, 1158-1164.
94. Imbri, D.; Tauber, J.; Opatz, T. Synthetic approaches to the lamellarins - a comprehensive review. *Mar. Drugs* **2014**, *12*, 6142-6177.
95. Ishibashi, F.; Tanabe, S.; Oda, T.; Iwao, M. Synthesis and structure-activity relationship study of lamellarin derivatives. *J. Nat. Prod.* **2002**, *65*, 500-504.
96. Bailly, C. Anticancer properties of lamellarins. *Marine Drugs* **2015**, *13*, 1105-1123.
97. Ploypradith, P.; Jinaglueng, W.; Pavaro, C.; Ruchirawat, S. Further developments in the synthesis of lamellarin alkaloids via direct metal-halogen exchange. *Tetrahedron Lett.* **2003**, *44*, 1363-1366.
98. Facompre, M.; Tardy, C.; Bal-Mahieu, C.; Colson, P.; Perez, C.; Manzanares, I.; Cuevas, C.; Bailly, C. Lamellarin d: A novel potent inhibitor of topoisomerase i. *Cancer Res.* **2003**, *63*, 7392-7399.

99. Ridley, C.P.; Reddy, M.V.; Rocha, G.; Bushman, F.D.; Faulkner, D.J. Total synthesis and evaluation of lamellarin alpha 20-sulfate analogues. *Bioorg. Med. Chem.* **2002**, *10*, 3285-3290.
100. Ohta, T.; Fukuda, T.; Ishibashi, F.; Iwao, M. Design and synthesis of lamellarin d analogues targeting topoisomerase i. *J. Org. Chem.* **2009**, *74*, 8143-8153.
101. Díaz, M.; Guitián, E.; Castedo, L. Syntheses of lamellarins i and k by [3+2] cycloaddition of a nitron to an alkyne. *Synlett* **2001**, 1164-1166.
102. Quesada, A.R.; García Grávalos, M.D.; Fernández Puentes, J.L. Polyaromatic alkaloids from marine invertebrates as cytotoxic compounds and inhibitors of multidrug resistance caused by p-glycoprotein. *Br. J. Cancer* **1996**, *74*, 677-682.
103. Huang, X.C.; Xiao, X.; Zhang, Y.K.; Talele, T.T.; Salim, A.A.; Chen, Z.S.; Capon, R.J. Lamellarin o, a pyrrole alkaloid from an australian marine sponge, ianthella sp., reverses bcrp mediated drug resistance in cancer cells. *Mar. Drugs* **2014**, *12*, 3818-3837.
104. Fuerstner, A.; Weintritt, H.; Hupperts, A. A new, titanium-mediated approach to pyrroles: First synthesis of lukianol a and lamellarin o dimethyl ether. *J. Org. Chem.* **1995**, *60*, 6637-6641.
105. G. Banwell, M.; L. Flynn, B.; Hamel, E.; C. R. Hockless, D. Convergent syntheses of the pyrrolic marine natural products lamellarin-o, lamellarin-q, lukianol-a and some more highly oxygenated congeners. *Chem. Commun.* **1997**, 207-208.
106. Marfil, M.; Albericio, F.; Álvarez, M. Solid-phase synthesis of lamellarins q and o. *Tetrahedron* **2004**, *60*, 8659-8668.
107. Fukuda, T.; Sudo, E.-i.; Shimokawa, K.; Iwao, M. Palladium-catalyzed cross-coupling of n-benzenesulfonyl-3,4-dibromopyrrole and its application to the total syntheses of lamellarins o, p, q, and r. *Tetrahedron* **2008**, *64*, 328-338.
108. Boger, D.L.; Boyce, C.W.; Labroli, M.A.; Sehon, C.A.; Jin, Q. Total syntheses of ningalin a, lamellarin o, lukianol a, and permethyl storniamide a utilizing heterocyclic azadiene diels-alder reactions. *J. Am. Chem. Soc.* **1999**, *121*, 54-62.
109. Pla, D.; Marchal, A.; Olsen, C.A.; Albericio, F.; Álvarez, M. Modular total synthesis of lamellarin d. *J. Org. Chem.* **2005**, *70*, 8231-8234.

110. Fujikawa, N.; Ohta, T.; Yamaguchi, T.; Fukuda, T.; Ishibashi, F.; Iwao, M. Total synthesis of lamellarins d, l, and n. *Tetrahedron* **2006**, *62*, 594-604.
111. Ueda, K.; Amaike, K.; Maceiczky, R.M.; Itami, K.; Yamaguchi, J. B-selective c-h arylation of pyrroles leading to concise syntheses of lamellarins c and i. *J. Am. Chem. Soc.* **2014**, *136*, 13226-13232.
112. Kang, H.; Fenical, W. Ningalins a-d: Novel aromatic alkaloids from a western australian ascidian of the genus didemnum. *J. Org. Chem.* **1997**, *62*, 3254-3262.
113. Li, Q.; Jiang, J.; Fan, A.; Cui, Y.; Jia, Y. Total synthesis of lamellarins d, h, and r and ningalin b. *Org. Lett.* **2011**, *13*, 312-315.
114. Soenen, D.R.; Hwang, I.; Hedrick, M.P.; Boger, D.L. Multidrug resistance reversal activity of key ningalin analogues. *Bioorg. Med. Chem. Lett.* **2003**, *13*, 1777-1781.
115. Tao, H.; Hwang, I.; Boger, D.L. Multidrug resistance reversal activity of permethyl ningalin b amide derivatives. *Bioorg. Med. Chem. Lett.* **2004**, *14*, 5979-5981.
116. Chou, T.C.; Guan, Y.; Soenen, D.R.; Danishefsky, S.J.; Boger, D.L. Potent reversal of multidrug resistance by ningalins and its use in drug combinations against human colon carcinoma xenograft in nude mice. *Cancer Chemother. Pharmacol.* **2005**, *56*, 379-390.
117. Zhang, P.Y.; Wong, I.L.K.; Yan, C.S.W.; Zhang, X.Y.; Jiang, T.; Chow, L.M.C.; Wan, S.B. Design and syntheses of permethyl ningalin b analogues: Potent multidrug resistance (mdr) reversal agents of cancer cells. *J. Med. Chem.* **2010**, *53*, 5108-5120.
118. Wang, Z.; Wong, I.L.K.; Li, F.X.; Yang, C.; Liu, Z.; Jiang, T.; Jiang, T.F.; Chow, L.M.C.; Wan, S.B. Optimization of permethyl ningalin b analogs as p-glycoprotein inhibitors. *Bioorg. Med. Chem.* **2015**, *23*, 5566-5573.
119. Yang, C.; Wong, I.L.K.; Jin, W.B.; Jiang, T.; Chow, L.M.C.; Wan, S.B. Modification of marine natural product ningalin b and sar study lead to potent p-glycoprotein inhibitors. *Mar. Drugs* **2014**, *12*, 5209-5221.
120. Bin, J.W.; Wong, I.L.K.; Hu, X.; Yu, Z.X.; Xing, L.F.; Jiang, T.; Chow, L.M.C.; Biao, W.S. Structure-activity relationship study of permethyl ningalin b analogues as p-glycoprotein chemosensitizers. *J. Med. Chem.* **2013**, *56*, 9057-9070.
121. Hamasaki, A.; Zimpleman, J.M.; Hwang, I.; Boger, D.L. Total synthesis of ningalin d. *J. Am. Chem. Soc.* **2005**, *127*, 10767-10770.

122. Saracoglu, N. Recent advances and applications in 1,2,4,5-tetrazine chemistry. *Tetrahedron* **2007**, *63*, 4199-4236.
123. Fu, T.H.; McElroy, W.T.; Shamszad, M.; Martin, S.F. Formal syntheses of naturally occurring welwitindolinones. *Org. Lett.* **2012**, *14*, 3834-3837.
124. MacKay, J.A.; Bishop, R.L.; Rawal, V.H. Rapid synthesis of the n-methylwelwitindolinone skeleton. *Org. Lett.* **2005**, *7*, 3421-3424.
125. Smith, C.D.; Zilfou, J.T.; Stratmann, K.; Patterson, G.M.L.; Moore, R.E. Welwitindolinone analogues that reverse p-glycoprotein-mediated multiple drug resistance. *Mol. Pharmacol.* **1995**, *47*, 241-247.
126. Grundmann, A.; Kuznetsova, T.; Afiyatullof, S.; Li, S.M. Ftmpt2, an n-prenyltransferase from *aspergillus fumigatus*, catalyses the last step in the biosynthesis of fumitremorgin b. *Chembiochem* **2008**, *9*, 2059-2063.
127. Fu, T.H.; McElroy, W.T.; Shamszad, M.; Heidebrecht Jr, R.W.; Gullledge, B.; Martin, S.F. Studies toward welwitindolinones: Formal syntheses of n-methylwelwitindolinone c isothiocyanate and related natural products. *Tetrahedron* **2013**, *69*, 5588-5603.
128. Wood, J.L. Total synthesis: Welwitindolinone is well worth it. *Nat. Chem.* **2012**, *4*, 341-343.
129. Komine, K.; Nomura, Y.; Ishihara, J.; Hatakeyama, S. Total synthesis of (-)-n-methylwelwitindolinone c isothiocyanate based on a pd-catalyzed tandem enolate coupling strategy. *Org. Lett.* **2015**, *17*, 3918-3921.
130. Patel, K.; Gadewar, M.; Tripathi, R.; Prasad, S.K.; Patel, D.K. A review on medicinal importance, pharmacological activity and bioanalytical aspects of beta-carboline alkaloid "harmine". *Asian Pac. J. Trop. Biomed.* **2012**, *2*, 660-664.
131. Khan, A.M.; Noreen, S.; Imran, Z.P.; Atta ur, R.; Choudhary, M.I. A new compound, jolynamine, from marine brown alga *jolyna laminarioides*. *Nat. Prod. Res.* **2011**, *25*, 898-904.
132. Li, S.; Wang, A.; Gu, F.; Wang, Z.; Tian, C.; Qian, Z.; Tang, L.; Gu, Y. Novel harmine derivatives for tumor targeted therapy. *Oncotarget* **2015**, *6*, 8988-9001.

133. Chen, Q.; Chao, R.; Chen, H.; Hou, X.; Yan, H.; Zhou, S.; Peng, W.; Xu, A. Antitumor and neurotoxic effects of novel harmine derivatives and structure-activity relationship analysis. *Int. J. Cancer* **2005**, *114*, 675-682.
134. Cao, R.; Fan, W.; Guo, L.; Ma, Q.; Zhang, G.; Li, J.; Chen, X.; Ren, Z.; Qiu, L. Synthesis and structure-activity relationships of harmine derivatives as potential antitumor agents. *Eur. J. Med. Chem.* **2013**, *60*, 135-143.
135. Ma, Y.; Wink, M. The beta-carboline alkaloid harmine inhibits bcrp and can reverse resistance to the anticancer drugs mitoxantrone and camptothecin in breast cancer cells. *Phytother. Res.* **2010**, *24*, 146-149.
136. Wu, Q.; Bai, Z.; Ma, Q.; Fan, W.; Guo, L.; Zhang, G.; Qiu, L.; Yu, H.; Shao, G.; Cao, R. Synthesis and biological evaluation of novel bivalent  $\beta$ -carbolines as potential antitumor agents. *Med.Chem.Commun.* **2014**, *5*, 953-957.
137. Frédérick, R.; Bruyère, C.; Vancraeynest, C.; Reniers, J.; Meinguet, C.; Pochet, L.; Backlund, A.; Masereel, B.; Kiss, R.; Wouters, J. Novel trisubstituted harmine derivatives with original in vitro anticancer activity. *J. Med. Chem.* **2012**, *55*, 6489-6501.
138. Dighe, S.U.; Khan, S.; Soni, I.; Jain, P.; Shukla, S.; Yadav, R.; Sen, P.; Meeran, S.M.; Batra, S. Synthesis of  $\beta$ -carboline-based n-heterocyclic carbenes and their antiproliferative and antimetastatic activities against human breast cancer cells. *J. Med. Chem.* **2015**, *58*, 3485-3499.
139. Pohl, B.; Luchterhandt, T.; Bracher, F. Total syntheses of the chlorinated  $\beta$ -carboline alkaloids bauerine a, b, and c. *Synth. Commun.* **2007**, *37*, 1273-1280.
140. Nurmaganbetov, Z.S.; Shultz, E.E.; Chernov, S.V.; Turmukhambetov, A.Z.; Seydakhmetova, R.B.; Shakirov, M.M.; Tolstikov, G.A.; Adekenov, S.M. Synthesis of substituted indolizino[8,7-b]indoles from harmine and their biological activity. *Chem. Heterocycl. Comp.* **2011**, *46*, 1494-1499.
141. Mukusheva, G.K.; Nurmaganbetov, Z.S.; Ismagulova, N.M.; Ponamareva, O.A.; Burdel'naya, E.V.; Turmukhambetov, A.Z.; Kazantsev, A.V.; Adekenov, S.M. Synthesis and phagocytosis-stimulating activity of harmine and glaucine n-oxides. *Pharm. Chem. J.* **2011**, *45*, 458-460.

142. Begum, S.; Ali, S.; Farhat, F.; Hassan, S.; Siddiqui, B. A simple, rapid and mild one pot synthesis of benzene ring acylated and demethylated analogues of harmine under solvent-free conditions. *Molecules* **2008**, *13*, 1584.
143. Sanchez, C.; Mendez, C.; Salas, J.A. Indolocarbazole natural products: Occurrence, biosynthesis, and biological activity. *Nat. Prod. Rep.* **2006**, *23*, 1007-1045.
144. Prudhomme, M. Biological targets of antitumor indolocarbazoles bearing a sugar moiety. *Curr. Med. Chem. Anticancer Agents* **2004**, *4*, 509-521.
145. Li, Z.; Zhai, F.; Zhao, L.; Guo, Q.; You, Q. Design and synthesis of n-methylmaleimide indolocarbazole bearing modified 2-acetamino acid moieties as topoisomerase i inhibitors. *Bioorg. Med. Chem. Lett.* **2009**, *19*, 406-409.
146. Robey, R.W.; Shukla, S.; Steadman, K.; Obrzut, T.; Finley, E.M.; Ambudkar, S.V.; Bates, S.E. Inhibition of abcg2-mediated transport by protein kinase inhibitors with a bisindolylmaleimide or indolocarbazole structure. *Mol. Cancer Ther.* **2007**, *6*, 1877-1885.
147. Slater, M.J.; Cockerill, S.; Baxter, R.; Bonser, R.W.; Gohil, K.; Gowrie, C.; Robinson, J.E.; Littler, E.; Parry, N.; Randall, R., *et al.* Indolocarbazoles: Potent, selective inhibitors of human cytomegalovirus replication. *Bioorg. Med. Chem.* **1999**, *7*, 1067-1074.
148. Slater, M.J.; Baxter, R.; Bonser, R.W.; Cockerill, S.; Gohil, K.; Parry, N.; Robinson, E.; Randall, R.; Yeates, C.; Snowden, W., *et al.* Synthesis of n-alkyl substituted indolocarbazoles as potent inhibitors of human cytomegalovirus replication. *Bioorg. Med. Chem. Lett.* **2001**, *11*, 1993-1995.
149. Cuevas, C.; Pérez, M.; Martín, M.J.; Chicharro, J.L.; Fernández-Rivas, C.; Flores, M.; Francesch, A.; Gallego, P.; Zarzuelo, M.; De La Calle, F., *et al.* Synthesis of ecteinascidin et-743 and phthalascidin pt-650 from cyanosafraicin b. *Org. Lett.* **2000**, *2*, 2545-2548.
150. Kanzaki, A.; Takebayashi, Y.; Ren, X.Q.; Miyashita, H.; Mori, S.; Akiyama, S.; Pommier, Y. Overcoming multidrug drug resistance in p-glycoprotein/mdr1-overexpressing cell lines by ecteinascidin 743. *Mol. Cancer Ther.* **2002**, *1*, 1327-1334.
151. Beumer, J.H.; Buckle, T.; Ouwehand, M.; Franke, N.E.F.; Lopez-Lazaro, L.; Schellens, J.H.M.; Beijnen, J.H.; Van Tellingen, O. Trabectedin (et-743, yondelis™) is



- a substrate for p-glycoprotein, but only high expression of p-glycoprotein confers the multidrug resistance phenotype. *Invest. New Drugs* **2007**, *25*, 1-7.
152. Jin, S.; Gorfajn, B.; Faircloth, G.; Scotto, K.W. Ecteinascidin 743, a transcription-targeted chemotherapeutic that inhibits *mdr1* activation. *Proceedings of the National Academy of Sciences of the United States of America* **2000**, *97*, 6775-6779.
  153. Soares, D.G.; Machado, M.S.; Rocca, C.J.; Poindessous, V.; Ouaret, D.; Sarasin, A.; Galmarini, C.M.; Henriques, J.A.P.; Escargueil, A.E.; Larsen, A.K. Trabectedin and its c subunit modified analogue pm01183 attenuate nucleotide excision repair and show activity toward platinum-resistant cells. *Mol. Cancer Ther.* **2011**, *10*, 1481-1489.
  154. Chen, X.; Chen, J.; De Paolis, M.; Zhu, J. Synthetic studies toward ecteinascidin 743. *J. Org. Chem.* **2005**, *70*, 4397-4408.
  155. Enomoto, T.; Yasui, Y.; Takemoto, Y. Synthetic study toward ecteinascidin 743: Concise construction of the diazabicyclo[3.3.1]nonane skeleton and assembly of the pentacyclic core. *J. Org. Chem.* **2010**, *75*, 4876-4879.
  156. Zheng, S.; Chan, C.; Furuuchi, T.; Wright, B.J.; Zhou, B.; Guo, J.; Danishefsky, S.J. Stereospecific formal total synthesis of ecteinascidin 743. *Angew. Chem. Int. Ed. Engl.* **2006**, *45*, 1754-1759.
  157. Chen, J.; Chen, X.; Willot, M.; Zhu, J. Asymmetric total syntheses of ecteinascidin 597 and ecteinascidin 583. *Angew. Chem. Int. Ed. Engl.* **2006**, *45*, 8028-8032.
  158. Kawagishi, F.; Toma, T.; Inui, T.; Yokoshima, S.; Fukuyama, T. Total synthesis of ecteinascidin 743. *J. Am. Chem. Soc.* **2013**, *135*, 13684-13687.
  159. Chen, J.; Chen, X.; Bois-Choussy, M.; Zhu, J. Total synthesis of ecteinascidin 743. *J. Am. Chem. Soc.* **2006**, *128*, 87-89.
  160. Raju, R.; Piggott, A.M.; Huang, X.C.; Capon, R.J. Nocardioazines: A novel bridged diketopiperazine scaffold from a marine-derived bacterium inhibits p-glycoprotein. *Org. Lett.* **2011**, *13*, 2770-2773.
  161. Wang, H.; Reisman, S.E. Enantioselective total synthesis of (-)-lansai b and (+)-nocardioazines a and b. *Angew. Chem. Int. Ed.* **2014**, *53*, 6206-6210.
  162. Kato, N.; Suzuki, H.; Okumura, H.; Takahashi, S.; Osada, H. A point mutation in *ftmd* blocks the fumitremorgin biosynthetic pathway in *aspergillus fumigatus* strain af293. *Biosci. Biotechnol. Biochem.* **2013**, *77*, 1061-1067.

163. van Loevezijn, A.; van Maarseveen, J.H.; Stegman, K.; Visser, G.M.; Koomen, G.-J. Solid phase synthesis of fumitremorgin, verruculogen and tryprostatin analogs based on a cyclization/cleavage strategy. *Tetrahedron Lett.* **1998**, *39*, 4737-4740.
164. Rabindran, S.K.; He, H.; Singh, M.; Brown, E.; Collins, K.I.; Annable, T.; Greenberger, L.M. Reversal of a novel multidrug resistance mechanism in human colon carcinoma cells by fumitremorgin c. *Cancer Res.* **1998**, *58*, 5850-5858.
165. Rabindran, S.K.; Ross, D.D.; Doyle, L.A.; Yang, W.; Greenberger, L.M. Fumitremorgin c reverses multidrug resistance in cells transfected with the breast cancer resistance protein. *Cancer Res.* **2000**, *60*, 47-50.
166. Gonzalez-Lobato, L.; Real, R.; Prieto, J.G.; Alvarez, A.I.; Merino, G. Differential inhibition of murine bcrp1/abcg2 and human bcrp/abcg2 by the mycotoxin fumitremorgin c. *Eur. J. Pharmacol.* **2010**, *644*, 41-48.
167. Kato, N.; Suzuki, H.; Takagi, H.; Asami, Y.; Kakeya, H.; Uramoto, M.; Usui, T.; Takahashi, S.; Sugimoto, Y.; Osada, H. Identification of cytochrome p450s required for fumitremorgin biosynthesis in aspergillus fumigatus. *Chembiochem.* **2009**, *10*, 920-928.
168. Allen, J.D.; van Loevezijn, A.; Lakhai, J.M.; van der Valk, M.; van Tellingen, O.; Reid, G.; Schellens, J.H.; Koomen, G.J.; Schinkel, A.H. Potent and specific inhibition of the breast cancer resistance protein multidrug transporter in vitro and in mouse intestine by a novel analogue of fumitremorgin c. *Mol. Cancer Ther.* **2002**, *1*, 417-425.
169. van Loevezijn, A.; Allen, J.D.; Schinkel, A.H.; Koomen, G.J. Inhibition of bcrp-mediated drug efflux by fumitremorgin-type indolyl diketopiperazines. *Bioorg. Med. Chem. Lett.* **2001**, *11*, 29-32.
170. Weidner, L.D.; Zoghbi, S.S.; Lu, S.; Shukla, S.; Ambudkar, S.V.; Pike, V.W.; Mulder, J.; Gottesman, M.M.; Innis, R.B.; Hall, M.D. The inhibitor ko143 is not specific for abcg2. *J. Pharmacol. Exp. Ther.* **2015**, *354*, 384-393.
171. Szolomajer-Csikos, O.; Beery, E.; Kosa, L.; Rajnai, Z.; Jani, M.; Hetenyi, A.; Jakab, K.T.; Krajcsi, P.; Toth, G.K. Synthesis and abcg2 inhibitory activity of novel fumitremorgin c analogs--specificity and structure activity correlations. *Med. Chem.* **2013**, *9*, 494-509.

172. Hino, T.; Kawate, T.; Nakagawa, M. A synthesis of so-called fumitremorgin c. *Tetrahedron* **1989**, *45*, 1941-1944.
173. Jiang, D.; Xu, Z.; Jia, Y. Mg(clo<sub>4</sub>)<sub>2</sub>-catalyzed intramolecular allylic amination: Application to the total synthesis of demethoxyfumitremorgin c. *Tetrahedron* **2012**, *68*, 4225-4232.
174. Li, Y.; Hayman, E.; Plesescu, M.; Prakash, S.R. Synthesis of potent bcrp inhibitor?Ko143. *Tetrahedron Lett.* **2008**, *49*, 1480-1483.
175. Kanoh, K.; Kohno, S.; Asari, T.; Harada, T.; Katada, J.; Muramatsu, M.; Kawashima, H.; Sekiya, H.; Uno, I. (-)-phenylahistin: A new mammalian cell cycle inhibitor produced by aspergillus ustus. *Bioorg. Med. Chem. Lett.* **1997**, *7*, 2847-2852.
176. Nicholson, B.; Lloyd, G.K.; Miller, B.R.; Palladino, M.A.; Kiso, Y.; Hayashi, Y.; Neuteboom, S.T.C. Npi-2358 is a tubulin-depolymerizing agent: In-vitro evidence for activity as a tumor vascular-disrupting agent. *Anticancer Drugs* **2006**, *17*, 25-31.
177. Heist, R.; Aren, O.; Millward, M.; Mainwaring, P.; Mita, A.; Mita, M.; Bazhenova, L.; Blum, R.; Polikoff, J.; Gadgeel, S., *et al.* Abstract c30: Phase 1/2 study of the vascular disrupting agent (vda) plinabulin (npi-2358) combined with docetaxel in patients with non-small cell lung cancer (nsccl). *Mol. Cancer Ther.* **2009**, *8*, C30.
178. Stratmann, T.; Burgoyne, D.L.; Moore, R.E.; Patterson, G.M.L.; Smith, C.D. Hapalysin, a cyanobacterial cyclic depsipeptide with multidrug-resistance reversing activity (vol 59, pg 7222, 1994). *J. Org. Chem.* **1995**, *60*, 2950-2950.
179. Smith, C.D. New compounds from cyanobacteria to circumvent mdr. *Drug News Perspect.* **1995**, *8*, 423-425.
180. Dinh, T.Q.; Smith, C.D.; Du, X.; Armstrong, R.W. Design, synthesis, and evaluation of the multidrug resistance-reversing activity of d-glucose mimetics of hapalysin. *J. Med. Chem.* **1998**, *41*, 981-987.
181. Okuno, T.; Ohmori, K.; Nishiyama, S.; Yamamura, S.; Nakamura, K.; Houk, K.N.; Okamoto, K. Chemical study on hapalysin, a cyclic depsipeptide possessing multidrug resistance reversing activities: Synthesis, structure and biological activity. *Tetrahedron* **1996**, *52*, 14723-14734.

182. Dinh, T.Q.; Smith, C.D.; Armstrong, R.W. Analogs incorporating trans-4-hydroxy-l-proline that reverse multidrug resistance better than hapalosin. *J. Org. Chem.* **1997**, *62*, 790-791.
183. Kashihara, N.; To-e, S.; Nakamura, K.; Umezawa, K.; Yamamura, S.; Nishiyama, S. Synthesis and biological activities of hapalosin derivatives with modification at the c12 position. *Bioorg. Med. Chem. Lett.* **2000**, *10*, 101-103.
184. Dinh, T.Q.; Du, X.; Smith, C.D.; Armstrong, R.W. Synthesis, conformational analysis, and evaluation of the multidrug resistance-reversing activity of the triamide and proline analogs of hapalosin. *J. Org. Chem.* **1997**, *62*, 6773-6783.
185. Dinh, T.Q.; Du, X.H.; Armstrong, R.W. Synthesis and conformational analysis of the multidrug resistance-reversing agent hapalosin and its non-n-methyl analog. *J. Org. Chem.* **1996**, *61*, 6606-6616.
186. Ohmori, K.; Okuno, T.; Nishiyama, S.; Yamamura, S. Synthetic study on hapalosin, a cyclic depsipeptide possessing multidrug resistance reversing activities. *Tetrahedron Lett.* **1996**, *37*, 3467-3470.
187. Hermann, C.; Giammasi, C.; Geyer, A.; Maier, M.E. Syntheses of hapalosin analogs by solid-phase assembly of acyclic precursors. *Tetrahedron* **2001**, *57*, 8999-9010.
188. Hermann, C.; Pais, G.C.G.; Geyer, A.; Kuhnert, S.M.; Maier, M.E. Total synthesis of hapalosin and two ring expanded analogs. *Tetrahedron* **2000**, *56*, 8461-8471.
189. Palomo, C.; Oiarbide, M.; García, J.M.; González, A.; Pazos, R.; Odriozola, J.M.; Bañuelos, P.; Tello, M.; Linden, A. A practical total synthesis of hapalosin, a 12-membered cyclic depsipeptide with multidrug resistance-reversing activity, by employing improved segment coupling and macrolactonization†. *J. Org. Chem.* **2004**, *69*, 4126-4134.
190. Pais, G.C.G.; Maier, M.E. Efficient synthesis of the  $\gamma$ -amino- $\beta$ -hydroxy acid subunit of hapalosin. *J. Org. Chem.* **1999**, *64*, 4551-4554.
191. Maier, M.E.; Hermann, C. Synthesis of the gamma-amino-beta-hydroxy acid of hapalosin via an asymmetric dihydroxylation route. *Tetrahedron* **2000**, *56*, 557-561.
192. Kumar, H.; Reddy, A.S.; Yadav, J.S.; Reddy, B.V.S. A highly stereoselective formal synthesis of hapalosin. *Synlett* **2013**, *24*, 1415-1419.

193. Parkes, K.E.B.; Bushnell, D.J.; Crackett, P.H.; Dunsdon, S.J.; Freeman, A.C.; Gunn, M.P.; Hopkins, R.A.; Lambert, R.W.; Martin, J.A. Studies toward the large-scale synthesis of the hiv proteinase inhibitor ro 31-8959. *J. Org. Chem.* **1994**, *59*, 3656-3664.
194. McDonald, L.A.; Christopher Swersey, J.; Ireland, C.M.; Carroll, A.R.; Coll, J.C.; Bowden, B.F.; Fairchild, C.R.; Cornell, L. Botryllamides a-d, new brominated tyrosine derivatives from styelid ascidians of the genus botryllus. *Tetrahedron* **1995**, *51*, 5237-5244.
195. Rao, M.R.; Faulknert, D.J. Botryllamides e-h, four new tyrosine derivatives from the ascidian botrylloides tyreum. *J. Nat. Prod.* **2004**, *67*, 1064-1066.
196. Henrich, C.J.; Robey, R.W.; Takada, K.; Bokesch, H.R.; Bates, S.E.; Shukla, S.; Ambudkar, S.V.; McMahon, J.B.; Gustafson, K.R. Botryllamides: Natural product inhibitors of abcg2. *ACS Chem. Biol.* **2009**, *4*, 637-647.
197. Takada, K.; Imamura, N.; Gustafson, K.R.; Henrich, C.J. Synthesis and structure-activity relationship of botryllamides that block the abcg2 multidrug transporter. *Bioorg. Med. Chem. Lett.* **2010**, *20*, 1330-1333.
198. Aoki, S.; Cao, L.; Matsui, K.; Rachmat, R.; Akiyama, S.I.; Kobayashi, M. Kendarimide a, a novel peptide reversing p-glycoprotein-mediated multidrug resistance in tumor cells, from a marine sponge of haliclona sp. *Tetrahedron* **2004**, *60*, 7053-7059.
199. Kotoku, N.; Cao, L.; Aoki, S.; Kobayashi, M. Absolute stereo-structure of kendarimide a, a novel mdr modulator, from a marine sponge. *Heterocycles* **2005**, *65*, 563-578.
200. Fu, X.; Do, T.; Schmitz, F.J.; Andrusevich, V.; Engel, M.H. New cyclic peptides from the ascidian lissoclinum patella. *J. Nat. Prod.* **1998**, *61*, 1547-1551.
201. Schmidt, E.W.; Nelson, J.T.; Rasko, D.A.; Sudek, S.; Eisen, J.A.; Haygood, M.G.; Ravel, J. Patellamide a and c biosynthesis by a microcin-like pathway in prochloron didemni, the cyanobacterial symbiont of lissoclinum patella. *Proceedings of the National Academy of Sciences of the United States of America* **2005**, *102*, 7315-7320.
202. García-Reynaga, P.; VanNieuwenhze, M.S. A new total synthesis of patellamide a. *Org. Lett.* **2008**, *10*, 4621-4623.

203. Kawakami, A.; Miyamoto, T.; Higuchi, R.; Uchiumi, T.; Kuwano, M.; Van Soest, R.W.M. Structure of a novel multidrug resistance modulator, irciniasulfonic acid, isolated from a marine sponge, *ircinia* sp. *Tetrahedron Lett.* **2001**, *42*, 3335-3337.
204. Emura, C.; Higuchi, R.; Miyamoto, T. Irciniasulfonic acid b, a novel taurine conjugated fatty acid derivative from a japanese marine sponge, *ircinia* sp. *Tetrahedron* **2006**, *62*, 5682-5685.
205. Kim, C.K.; Song, I.H.; Park, H.Y.; Lee, Y.J.; Lee, H.S.; Sim, C.J.; Oh, D.C.; Oh, K.B.; Shin, J. Suvanine sesterterpenes and deacyl irciniasulfonic acids from a tropical *coscinoderma* sp. Sponge. *J. Nat. Prod.* **2014**, *77*, 1396-1403.
206. Emura, C.; Higuchi, R.; Miyamoto, T. Synthetic studies on the natural multidrug resistance modulator, irciniasulfonic acid b. *Chem. Lett.* **2010**, *39*, 1002-1003.
207. Adrian P. Dobbs, A.V., Laura A. Butler, Robert J. Parker. Document first total synthesis of the irciniasulfonic acids. *Synlett* **2005**, *4*, 4.
208. Steyn, P.S. The isolation, structure and absolute configuration of secalonic acid d, the toxic metabolite of *penicillium oxalicum*. *Tetrahedron* **1970**, *26*, 51-57.
209. Ren, H.; Tian, L.; Gu, Q.Q.; Zhu, W.M. Secalonic acid d; a cytotoxic constituent from marine lichen-derived fungus *gliocladium* sp t31. *Arch. Pharm. Res.* **2006**, *29*, 59-63.
210. Hong, R. Secalonic acid d as a novel DNA topoisomerase i inhibitor from marine lichen-derived fungus *gliocladium* sp. T31. *Pharm. Biol.* **2011**, *49*, 796-799.
211. Hu, Y.-p.; Tao, L.-y.; Wang, F.; Zhang, J.-y.; Liang, Y.-j.; Fu, L.-w. Secalonic acid d reduced the percentage of side populations by down-regulating the expression of *abcg2*. *Biochem. Pharmacol.* **2013**, *85*, 1619-1625.
212. Guru, S.K.; Pathania, A.S.; Kumar, S.; Ramesh, D.; Kumar, M.; Rana, S.; Kumar, A.; Malik, F.; Sharma, P.R.; Chandan, B.K., *et al.* Secalonic acid-d represses *hif1alpha*/vegf-mediated angiogenesis by regulating the akt/mTOR/p70s6k signaling cascade. *Cancer Res.* **2015**, *75*, 2886-2896.
213. Wezeman, T.; Masters, K.S.; Bräse, S. Double trouble - the art of synthesis of chiral dimeric natural products. *Angew. Chem. Int. Ed.* **2014**, *53*, 4524-4526.
214. Li, X.; Jiang, H.; Uffman, E.W.; Guo, L.; Zhang, Y.; Yang, X.; Birman, V.B. Kinetic resolution of secondary alcohols using amidine-based catalysts. *J. Org. Chem.* **2012**, *77*, 1722-1737.

215. Qin, T.; Porco, J.A., Jr. Total syntheses of secalonic acids a and d. *Angew. Chem. Int. Ed.* **2014**, *53*, 3107-3110.
216. Nising, C.F.; Schmid, U.K.; Nieger, M.; Bräse, S. A new protocol for the one-pot synthesis of symmetrical biaryls. *J. Org. Chem.* **2004**, *69*, 6830-6833.
217. Chen, Y.F.; Wang, S.Y.; Shen, H.; Yao, X.F.; Zhang, F.L.; Lai, D. The marine-derived fungal metabolite, terrein, inhibits cell proliferation and induces cell cycle arrest in human ovarian cancer cells. *Int. J. Mol. Med.* **2014**, *34*, 1591-1598.
218. Kim, D.S.; Cho, H.J.; Lee, H.K.; Lee, W.H.; Park, E.S.; Youn, S.W.; Park, K.C. Terrein, a fungal metabolite, inhibits the epidermal proliferation of skin equivalents. *J. Dermatol. Sci.* **2007**, *46*, 65-68.
219. Park, S.H.; Kim, D.S.; Kim, W.G.; Ryoo, I.J.; Lee, D.H.; Huh, C.H.; Youn, S.W.; Yoo, I.D.; Park, K.C. Terrein: A new melanogenesis inhibitor and its mechanism. *Cell. Mol. Life Sci.* **2004**, *61*, 2878-2885.
220. Liao, W.Y.; Shen, C.N.; Lin, L.H.; Yang, Y.L.; Han, H.Y.; Chen, J.W.; Kuo, S.C.; Wu, S.H.; Liaw, C.C. Asperjinone, a nor-neolignan, and terrein, a suppressor of abcg2-expressing breast cancer cells, from thermophilic aspergillus terreus. *J. Nat. Prod.* **2012**, *75*, 630-635.
221. Mandai, H.; Omori, K.; Yamamoto, D.; Tsumura, T.; Murota, K.; Yamamoto, S.; Mitsudo, K.; Ibaragi, S.; Sasaki, A.; Maeda, H., *et al.* Synthetic (+)-terrein suppresses interleukin-6/soluble interleukin-6 receptor induced-secretion of vascular endothelial growth factor in human gingival fibroblasts. *Bioorg. Med. Chem.* **2014**, *22*, 5338-5344.
222. Khalil, Z.G.; Huang, X.-c.; Raju, R.; Piggott, A.M.; Capon, R.J. Shornephine a: Structure, chemical stability, and p-glycoprotein inhibitory properties of a rare diketomorpholine from an australian marine-derived aspergillus sp. *J. Org. Chem.* **2014**, *79*, 8700-8705.

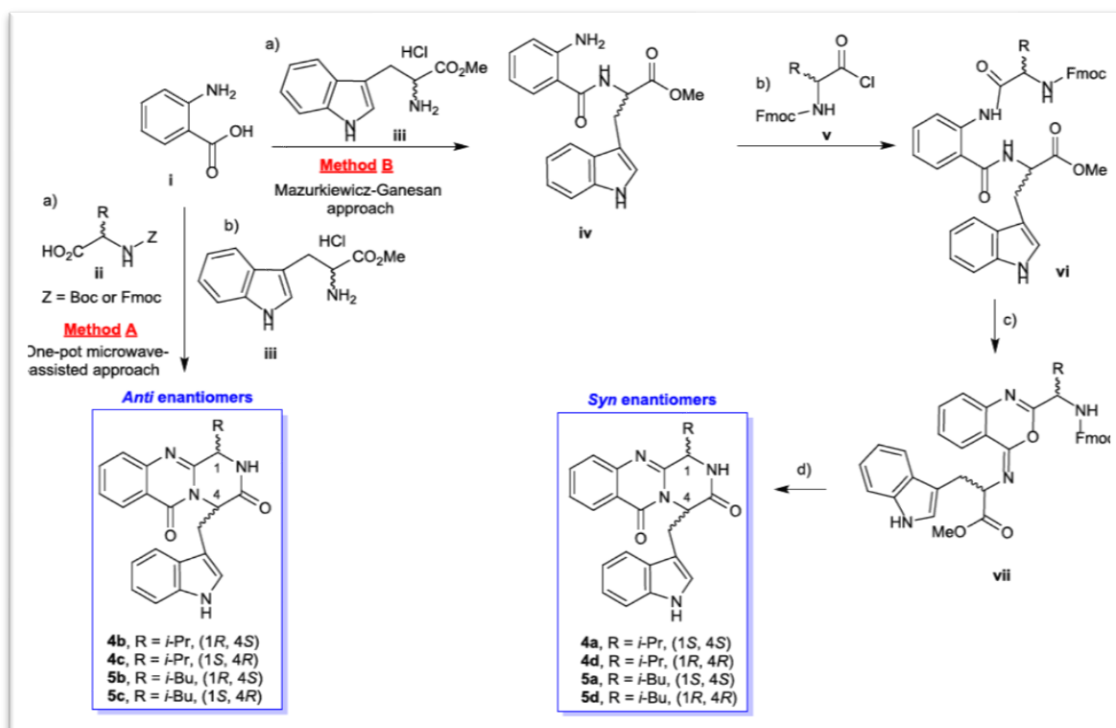




# Chapter 3

## Antitumor Activity of Quinazolinone Alkaloids Inspired by Marine Natural Products

Graphical abstract





Article

# Antitumor Activity of Quinazolinone Alkaloids Inspired by Marine Natural Products

Solida Long <sup>1</sup>, Diana I. S. P. Resende <sup>1,2</sup>, Anake Kijjoa <sup>2,3</sup>, Artur M. S. Silva <sup>4</sup>, André Pina <sup>5,6,7</sup>, Tamara Fernández-Marcelo <sup>5,6</sup>, M. Helena Vasconcelos <sup>5,6,8</sup>, Emília Sousa <sup>1,2\*</sup> and Madalena M. M. Pinto <sup>1,2</sup>

<sup>1</sup> Laboratório de Química Orgânica e Farmacêutica, Departamento de Ciências Químicas, Faculdade de Farmácia, Universidade do Porto, Rua de Jorge Viterbo Ferreira, 228, 4050-313 Porto, Portugal; up201502099@ff.up.pt\_(S.L.); dresende@ff.up.pt (D.I.S.P.R.); madalena@ff.up.pt (M.M.M.P).

<sup>2</sup> Interdisciplinary Centre of Marine and Environmental Research (CIIMAR), Terminal de Cruzeiros do Porto de Lexões, Av. General Norton de Matos s/n, 4450-208 Matosinhos, Portugal; ankijjoa@icbas.up.pt

<sup>3</sup> ICBAS—Instituto de Ciências Biomédicas Abel Salazar, Universidade do Porto, Rua de Jorge Viterbo Ferreira, 228, 4050-313 Porto, Portugal

<sup>4</sup> Química Orgânica, Produtos Naturais e Agroalimentares (QOPNA), Department of Chemistry, University of Aveiro, 3810-193 Aveiro, Portugal; artur.silva@ua.pt

<sup>5</sup> i3S—Instituto de Investigação e Inovação em Saúde, Universidade do Porto, 4200-135 Porto, Portugal; andre.fig.pina@gmail.com (A.P.), tamarafmarcelo\_@hotmail.com (T.F.-M.), hvasconcelos@ipatimup.pt (M.H.V.)

<sup>6</sup> Cancer Drug Resistance Group, IPATIMUP—Institute of Molecular Pathology and Immunology of the University of Porto, Porto, Portugal

<sup>7</sup> Department of Biochemistry, FCUP—Faculty of Sciences of the University of Porto, 4169-007 Porto, Portugal

<sup>8</sup> Laboratório de Microbiologia, Departamento de Ciências Biológicas, Faculdade de Farmácia, Universidade do Porto, 4050-313 Porto, Portugal

\* Correspondence: [esousa@ff.up.pt](mailto:esousa@ff.up.pt); Tel.: +351-2-2042-8689

Received: 11 June 2018; Accepted: 26 July 2018; Published: 31 July 2018

**Abstract:** Many fungal quinazolinone metabolites, which contain the methyl-indole pyrazino [1,2-*b*]quinazoline-3,6-dione core, have been found to possess promising antitumor activity. The purpose of this work was to synthesize the enantiomeric pairs of two members of this quinazolinone family, to explore their potential as antitumor and their ability to revert multidrug resistance. The marine natural product fiscalin B (**4c**), and *anti* enantiomers (**4b**, **5b**, and **5c**) were synthesized via a one-pot approach, while the *syn* enantiomers (**4a**, **4d**, **5a**, and **5d**) were synthesized by a multi-step procedure. These

strategies used anthranilic acid (i), chiral *N*-protected  $\alpha$ -amino acids (ii), and tryptophan methyl esters (iii) to form the core ring of pyrazino[2,1-*b*]quinazoline-3,6-dione scaffold. Four enantiomeric pairs, with different enantiomeric purities, were obtained with overall yields ranging from 7 to 40%. Compounds **4a–d** and **5a–d** were evaluated for their growth inhibitory effect against two tumor cell lines. Differences between enantiomeric pairs were noted and **5a–d** displayed GI<sub>50</sub> values ranging from 31 to 52  $\mu$ M, which are lower than those of **4a–d**. Nevertheless, no effect on P-glycoprotein (P-gp) modulation was observed for all compounds. This study disclosed new data for fiscalin B (**4c**), as well as for its analogues for a future development of novel anticancer drug leads.

**Keywords:** antitumor; enantiomers; fiscalins; quinazolinones; synthesis

## 1. Introduction

During the past ten years, great attention has been focused on drug development from Marine Natural Products (MNPs) as well as on their synthetic and semi-synthetic analogues. While terrestrial sources such as higher plants and microorganisms have reached the limelight, the marine environment increasingly becomes the newest and untapped resource of bioactive compounds [1]. A number of quinazolinone derivatives have played important roles in medicinal chemistry due to their broad spectrum of biological properties such as antibacterial, antifungal, anticonvulsant, anti-inflammatory, anti-HIV, anticancer, and analgesic activities [2,3]. One subclass of quinazolinone-derived Natural Products is the indolylmethyl pyrazinoquinazoline alkaloids (**1**) (Figure 1), characterized by a fused piperazine ring system linked to an indole moiety. So far, approximately 80 secondary metabolites of this subclass, covering structurally diverse compounds, have been isolated from fungi, mainly of marine origin. These include (i) compounds containing only a substituted piperazine ring such as glyantrypine (**2**), isolated from the culture broth of the mangrove-derived fungus *Cladosporium* sp. PJX-41 [4], fumiquinazoline F (**3**), isolated from the marine-derived fungus *Aspergillus fumigatus* strain H1-04 and *Aspergillus* sp. [5,6], and fiscalin B (**4**), isolated from the culture of the fungal strain

*Dichotomomyces cejpui* which was recovered from sediments of the Brazilian coast [7]; (ii) compounds with a more complex structure containing several rings such as fumiquinazoline K (**6**), isolated from the Mediterranean sponge-derived fungus *Aspergillus* sp., the soft coral (*Sinularia* sp.)-associated fungus *Aspergillus fumigatus* KMM 4631 [8], and a gorgonian-associated fungus [9]; (iii) *spiro* compounds such as fumiquinazoline C (**7**), isolated from the marine-derived fungus *Aspergillus fumigatus* strain H1-04, and *N*-formyllapatin A (**8**), isolated from the marine-derived fungus *Penicillium adametzioides* (AS-53) [10]; (iv) compounds with complex 3-indolyl groups such as cladoquinazoline (**9**) and epi-cladoquinazoline (**10**), isolated from the mangrove-derived fungus *Cladosporium* sp. PJX-41 [4], neofiscalin A (**11**) from *Neosartorya siamensis* KUFC 6349, which was isolated from a forest soil [11], as well as from *N. siamensis* KUFC 6349, isolated from the sea fan *Rumphella* sp. [12], and fumiquinazoline S (**12**), isolated from a solid-substrate culture of *Aspergillus* sp., collected from a marine-submerged wood [13]; or (v) compounds with indole glucosides such as fumigatoside A (**13**), isolated from *Aspergillus fumigatus* which was derived from the jellyfish *Nemopilema nomurai* [14].

Marine alkaloids containing indolymethyl pyrazinoquinazoline ring system can be considered conformationally constrained peptidomimetics exhibiting very interesting biological properties [15]. For instance, glyantrypine (**2**) is an antibacterial agent, active against *Vibrio harveyi* [16]; fumiquinazolines are antitumor compounds with moderate cytotoxicity [17]; fiscalins are substance P inhibitors and anticancer agents [7,18]; cladoquinazolines (**9** and **10**) are active against influenza A virus (H<sub>1</sub>N<sub>1</sub>); fumiquinazoline S (**12**) exhibits a weak inhibition against Na<sup>+</sup>/K<sup>+</sup>-ATPase, and *N*-acetylardeemin (**14**) is a potent inhibitor of multidrug resistant (MDR) tumor cells [4,13,19,20]. Moreover, the pyrazino[2,1-*b*]quinazoline ring system has been already ascribed as essential for the above-mentioned activities, and its enantioselective effects were observed for their antibacterial activity. For example, neofiscalin A (**11**) showed potent antibacterial activity against Gram-negative bacteria [12,21], whereas fiscalin C (**15**), epi-neofiscalin A (**16**), and epi-fiscalin C (**17**) were inactive in the same study. Interestingly, fiscalin C (**15**) displayed a synergistic effect against methicillin-resistant *Staphylococcus aureus* (MRSA) when combined with oxacillin [11,22]. Concerning antitumor activity, studies on quinazolinone compounds have mainly focused on natural or synthetic compounds with different substituents at the

stereogenic C-1 and C-4; however, there is no report on analogues with different configurations at C-1 and C-4.

Therefore, the aim of this study was to synthesize the diastereomers of fiscalin B (**4c**), *i.e.*, **4a–d**, and their homologues **5a–d**, to further explore their potential as growth inhibitors of tumor cells, their ability to revert MDR by inhibiting P-gp activity, as well as to perform the SAR study.

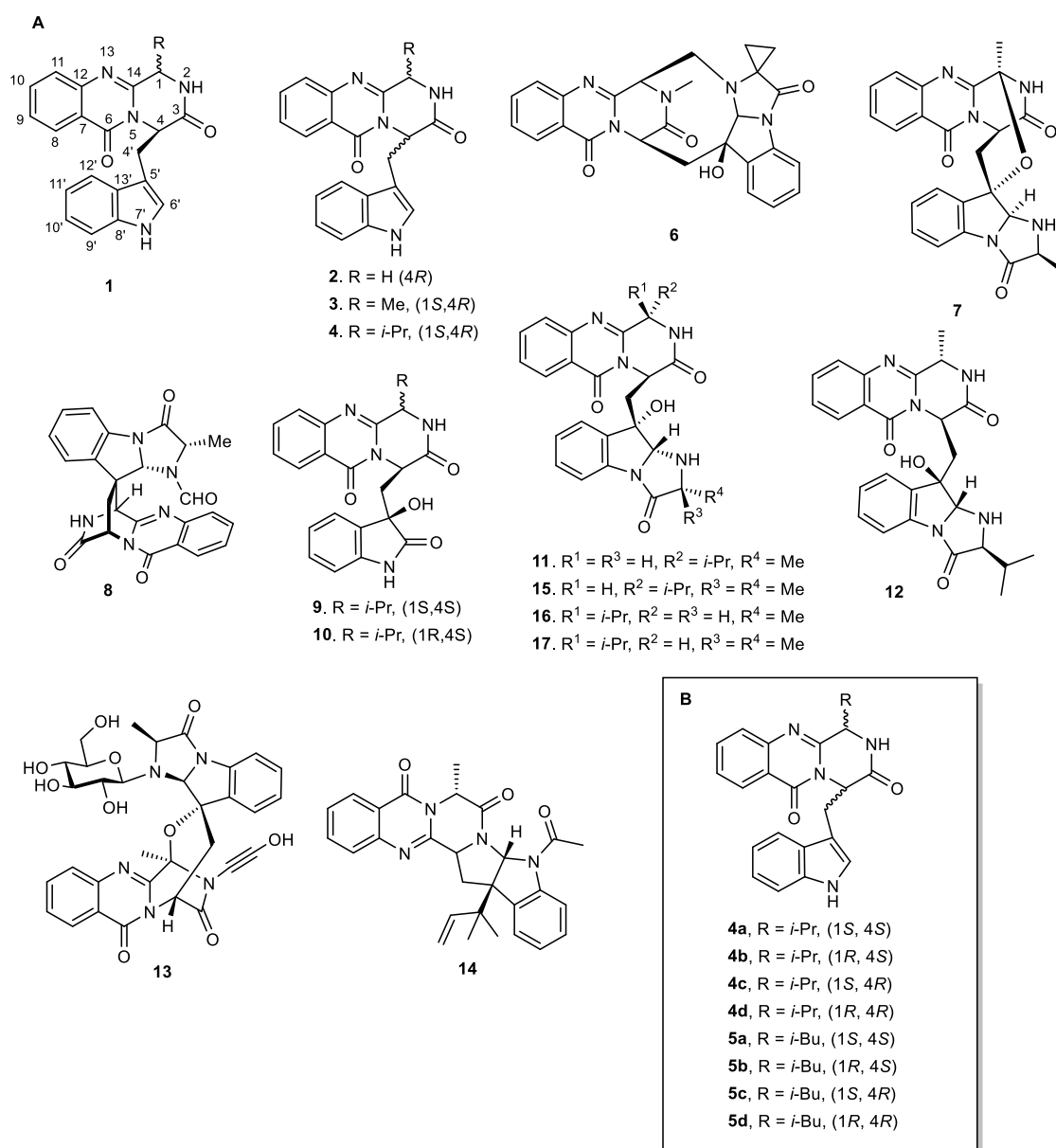


**Figure 1.** (A) Pyrazino[2,1-*b*]quinazoline-3,6-dione ring system (**1**) and some examples of the marine-derived quinazolinone containing alkaloids (**2–17**) and (B) synthesized diastereomers of fiscalin B and their homologues (**4–5**).

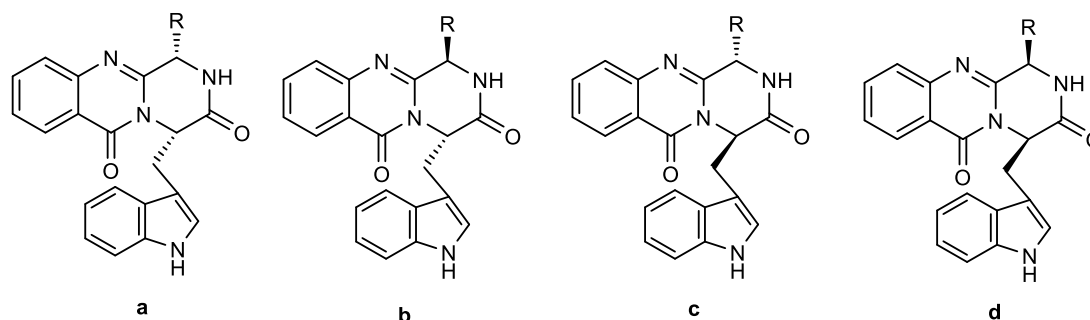
## 2. Results and Discussion

### 2.1. Synthesis of Pyrazinoquinazoline Alkaloids

The pyrazino[2,1-*b*]quinazoline-3,6-dione ring system (**1**) is the core structure of fumiquinazoline-derived group of alkaloids. There are two main methods to synthesize compounds containing this scaffold (i) the Eguchi-aza Wittig approach that consists of a selective acylation of diketopiperazines with *o*-azidobenzoyl chloride, followed by dehydrative cyclization [23]; and (ii) the Mazurkiewicz–Ganesan approach, consisting of coupling of linear tripeptides followed by the isomerization of 4-imino-4*H*-3,1-benzoxozines to obtain the corresponding quinazolin-4-ones [24,25]. In 2005, Liu et al. [26] reported a highly effective and environmentally friendly approach using a microwave-assisted multicomponent one-pot one step polycondensation of amino acids for the total syntheses of gyantrypine (**2**), fumiquinazoline F (**3**), and fiscalin B (**4**). With this procedure, the authors reported that the addition of a *N*-protected  $\alpha$ -amino acid (**ii**) to anthranilic acid (**i**), under a conventional heating condition at 55 °C with triphenylphosphite, (PhO)<sub>3</sub>P, generated the intermediate benzoxazin-4-one, followed by the addition of tryptophan (Trp) ester (**iii**), and then submitted to microwave irradiation at 220 °C for 1.5 min, to furnish the desired final products. Inspired by this simple and highly efficient methodology, we were able to prepare **4** and **5** (Scheme 1, method A). Attempts to obtain the syn enantiomers by this one-pot approach failed since only vestigial amounts could be detected due to the isomerization to the antienantiomers. The antienantiomers **4b/4c** and **5b/5c** were then obtained, starting from enantiomeric pure amino acids, from which no syn enantiomer were isolated (Entry 1–8, Table 1). Therefore, the syn enantiomers **4a/d** and **5a/d** were synthesized by the Mazurkiewicz–Ganesan method [25] (Scheme 1, method B) with some modifications. First, coupling of **i** with **iii**, using 1,1,3,3-tetramethylammonium tetrafluoroborate (TBTU) in basic conditions, afforded the dipeptide (**iv**). Coupling of **iv** with *N*-protected  $\alpha$ -amino acids chloride (**v**) [27] in a two-phase Schotten–Baumann condition yielded the tripeptides **vi**. The intermediates **vii** were obtained by adding the dehydrating agent, triphenylphosphine (Ph<sub>3</sub>P), to convert  $\beta$ -keto amides (**vi**) to the oxazoles (**vii**), followed by Fmoc-deprotection by 20% piperidine to afford **4a/d** and **5a/d** with a moderate yield of 21–40%. After purification by chromatographic techniques, the purity of

**4a–d** and **5a–d**, as determined by a reversed-phase HPLC (C18, MeOH: H<sub>2</sub>O; 60:40 or CH<sub>3</sub>CN:H<sub>2</sub>O; 50:50) was found to be higher than 90%. The enantiomers ratio was determined by the chiral HPLC equipped with amylose *tris*-3,5-dimethylphenylcarbamate column, using hexane: ethanol (80:20) as a mobile phase (Table 1).

**Table 1.** Enantiomers and diastereomers of the pyrazinoquinazolinone alkaloids **4** and **5**.



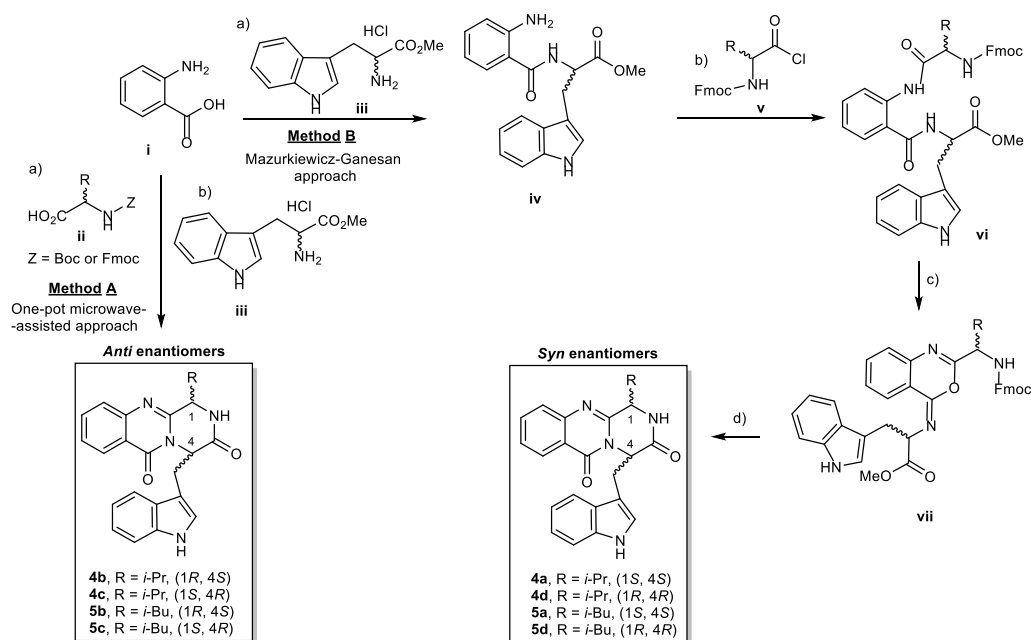
Entry	R <sup>a</sup>	Tryptophan	% <i>Anti</i> Compound	% <i>Syn</i> Compound	[α] <sub>D</sub> <sup>b</sup>	Enantiomeric Ratio <sup>c</sup>	Purity (%) <sup>d</sup>
1	L-valine	L-tryptophan	10 ( <b>4b</b> )	-	+63.8	40:60	87
2	D-valine	L-tryptophan	14 ( <b>4b</b> )	-	+65.2	39:61	89
3	L-valine	D-tryptophan	8 ( <b>4c</b> )	-	-248.1	62:37	90
4	D-valine	D-tryptophan	10 ( <b>4c</b> )	-	-100.0	63:37	91
5	L-leucine	L-tryptophan	7 ( <b>5b</b> )	-	+44.9	67:33	94
6	D-leucine	L-tryptophan	10 ( <b>5b</b> )	-	+89.7	50:50	94
7	L-leucine	D-tryptophan	8 ( <b>5c</b> )	-	-61.7	31:69	90
8	D-leucine	D-tryptophan	10 ( <b>5c</b> )	-	-142.9	46:54	86
9*	L-valine	L-tryptophan	-	28 ( <b>4a</b> )	+300.5	100:0	94
10*	D-valine	D-tryptophan	-	21( <b>4d</b> )	-210.5	7:93	89
11*	L-leucine	L-tryptophan	-	28 ( <b>5a</b> )	+81.8	90:10	89
12*	D-leucine	D-tryptophan	-	40 ( <b>5d</b> )	-186.0	17:83	85

<sup>a</sup> R residual of amino acid at C-1 position; <sup>b</sup> Optical rotation, concentration (g/100 mL); <sup>c</sup> Calculated from the peak area from chiral HPLC experiments (by using equation  $X \times 100 / X_n$  in which X is the peak area of each peak and X<sub>n</sub> is the total peak area); <sup>d</sup> Calculated from the peak area from reversed-phase HPLC experiments; \* Entry of Mazurkiewicz–Ganesan approach.

The overall yield of this one-step method ranged from 7 to 14% with different enantiomeric ratios (Table 1). The low yields of this one-pot reaction were attributed to a



high temperature applied in microwave irradiation to convert the intermediate Boc-protected-benzoxazin-4-one to the final products. Moreover, the steric hindrance at C-1 could also be a reason, as previously noted by Liu et al. [26] and Wang et al. [24] in the synthesis of similar compounds. Although a partial epimerization was observed under these conditions, this one-pot procedure was proved successful in providing the pyrazinoquinazolinone scaffold and a series of compounds for further biological investigations. On the other hand, the moderate yields of compounds obtained by Mazurkiewicz–Ganesan method were related to the mild conditions and a multistep approach (Table 1 entry 9–12).



**Scheme 1.** Synthesis of the pyrazinoquinazolinone alkaloids **4** and **5**. (Method A) One-pot microwave-assisted approach. Reagents and conditions: (a) dried-pyridine, (PhO)<sub>3</sub>P, 55 °C, 16–24 h; (b) dried-pyridine, (PhO)<sub>3</sub>P, 220 °C, 1.5 min; (Method B) Mazurkiewicz–Ganesan approach. Reagents and conditions (a) CH<sub>3</sub>CN, TBTU, Et<sub>3</sub>N, rt, 5 h; (b) CH<sub>2</sub>Cl<sub>2</sub>/aq.Na<sub>2</sub>CO<sub>3</sub>, rt, 3 h; (c) dried CH<sub>2</sub>Cl<sub>2</sub>, Ph<sub>3</sub>P, I<sub>2</sub>, EtN(*i*-Pr)<sub>2</sub>, rt, overnight; (d) piperidine in CH<sub>2</sub>CH<sub>2</sub>, rt, 12 min, then CH<sub>3</sub>CN, DMAP, reflux 19 h. *i*-Pr = isopropyl; *i*-Bu = isobutyl, Boc = *tert*-butyloxycarbonyl; Fmoc = fluorenylmethyloxycarbonyl; DMAP = 4-(dimethylamino)pyridine, TBTU = 1,1,3,3-tetramethylammonium tetrafluoroborate.

In this study, the coupling agent 1-ethyl-3-(3-dimethylaminopropyl)carbodiimide (ECD) was replaced by TBTU, which gave a similar yield for the dipeptide **iv** (81–94%) when compared to the previous reports. The tripeptides **vi** were also obtained in a very

high yield (84–94%). The bottleneck of this multistep approach was the conversion of the intermediates **vii** to the final products since their decomposition to form the precursors **vi**, similar to what has been previously reported by Ganesan et al. [25], was observed. Compounds **4a/d** and **5a/d** were purified by preparative TLC (EtOAc:CH<sub>2</sub>Cl<sub>2</sub>: MeOH: 50:47.5:2.5) after refluxing in CH<sub>3</sub>CN in the presence of 4-(dimethylamino)pyridine. The degrees of epimerization of **4a/d** and **5a/d** by Mazurkiewicz–Ganesan method were found to be lower than those obtained by the microwave method (Table 1). These results could be also associated with the mild conditions used in the multistep approach.

## 2.2. Structure Elucidation

The structures of the new compounds, **4a**, **4b**, and **4d**, and of the synthetic fiscalin B (**4c**) and their homologues **5a**, **5b**, **5d**, and **5c**, were established by extensive analyses of 1D and 2D NMR spectra and high-resolution mass spectrometry. The <sup>1</sup>H (Table 2) and <sup>13</sup>C NMR data (Table 3) of **4c** were in agreement with those reported in the literature for fiscalin B, which was obtained from the marine sources [24,25]. The chemical shift values of some key protons allowed the determination of the relative configurations of both stereogenic centres as well as the conformation of the piperazine ring in **4** and **5**, as shown in **4a**, **4b** and **4c**, **4d** (Figure 2). The substituent on C-4 is always in a pseudoaxial position while H-4 is shifted to  $\delta_{\text{H}}$  5.52–5.68 in all compounds, showing the characteristic anisotropic effect of the coplanar carbonyl group at C-14 on the quasi-equatorial proton, as explained by Hernández et al. [28]. The difference between *anti* and *syn* enantiomers were observed on H-1. In the *anti* enantiomers, the chemical shift value of the axial H-1 of **4b/c** and **5b/c** at  $\delta_{\text{H}}$  2.69–2.73 indicates the folding of the C-4-indolyl substituent over the piperazine ring and the isopropyl group. This phenomenon was also reported by Hernández and coworkers for H-1 signals of quinazolinones whose chemical shift values were *ca.* 3 ppm for the boat conformation and the *anti* enantiomers, due to the absence of the shielding effect by the aromatic ring [28]. Meanwhile, for the *syn* enantiomers, **4a/d** and **5a/d**, H-1 chemical shift values were at *ca.*  $\delta_{\text{H}}$  3.95–4.32, indicating the shielding effect from the aromatic ring over H-1. The chemical shifts of H-1' of the isopropyl group were also different between the *anti* and the *syn* enantiomers, being *ca.*  $\delta_{\text{H}}$  0.94–1.06 for **4a/d** and  $\delta_{\text{H}}$  2.61–2.66 for **4c/d**, indicating the different shielding effect of the aromatic ring on the group on C-1.

**Table 2.** <sup>1</sup>H NMR data (300 MHz, CDCl<sub>3</sub>) for **4** and **5**.

Position	$\delta_{\text{H}}$ (J in Hz)			
	4a	4b	4c	4d
H-1	3.95, dd (8.4,3.5)	2.69, d (2.4)	2.69, d (2.4)	3.95, dd (8.5, 3.6)
H-2	6.50, d (3.0)	5.85, br	5.80, br	6.39, d (3.2)
H-4	5.52, dd (6.3, 3.8)	5.68, dd (5.0, 2.8)	5.67, dd (5.0, 2.8)	5.52, dd (6.3, 3.8)
H-8	8.38, dd (8.0, 1.1)	8.37, dd (8.0, 1.1)	8.37, dd (8.0, 1.1)	8.38, dd (8.0, 1.2)
H-9	7.54, ddd (8.2, 7.2, 1.2)	7.54, ddd (7.9, 7.7, 1.8)	7.54, ddd (8.0, 6.2, 1.9)	7.54, ddd (8.1, 7.3, 1.1)
H-10	7.79, ddd (8.7, 7.7, 1.9)	7.77, ddd (7.9, 7.7, 1.9)	7.77, ddd (8.9, 6.2, 1.9)	7.79, ddd (8.5, 7.1, 1.2)
H-11	7.62, d (7.7)	7.57, d (7.7)	7.57, d (7.7)	7.62, d (7.7)
H-1'	1.06–0.94, m	2.66–2.61, m	2.66–2.61, m	1.06–0.94, m
H-2'	0.48, d (6.6)	0.63, d (2.3)	0.63, d (4.0)	0.48, d (6.6)
H-3'	0.75, d (6.8)	0.66, d (3.7)	0.65, d (4.3)	0.75, d (6.8)
H-4'a	3.72, dd (14.9, 3.7)	3.69, dd (15.0, 5.3)	3.69, dd (17.8, 4.0)	3.72, dd (14.8, 3.7)
H-4'b	3.80, dd (14.9, 6.3)	3.77, dd (15.0, 2.9)	3.77, dd (15.0, 2.8)	3.80, dd (14.8, 6.4)
H-6'	6.89, d (2.4)	6.60, d (2.3)	6.60, d (2.4)	6.90, d (2.3)
H-7'	8.06, br	8.03, br	8.03, br	8.03, br
H-9'	7.28, d (8.4)	7.28, d (8.2)	7.28, d (8.2)	7.28, d (7.8)
H-10'	7.10, ddd (8.6, 7.6, 1.0)	7.13, t (7.1)	7.13, t (7.1)	7.10, ddd (8.5, 7.5, 0.9)
H-11'	6.93, ddd (8.0, 7.1, 1.0)	6.93, t (7.5)	6.93, t (7.5)	6.94, ddd (8.2, 7.2, 1.0)
H-12'	7.49, d (7.9)	7.44, d (8.0)	7.44, d (8.1)	7.49, d (7.9)
	5a	5b	5c	5d
H-1	4.32, dt (10.7, 3.2)	2.73, dd (9.7, 3.4)	2.72, d (9.7)	4.31, dt (11.0, 3.2)
H-2	6.45, d (2.5)	5.75, br	5.75, br	6.21, d (2.5)
H-4	5.54, dd (5.2, 3.3)	5.68, dd (5.2, 3.0)	5.68, dd (5.0, 2.9)	5.55, dd (5.2, 3.3)
H-8	8.39, dd (8.0, 1.2)	8.37, d (8.0)	8.37, d (8.0)	8.39, dd (8.0, 1.1)
H-9	7.53, ddd (8.1, 7.1, 1.0)	7.55, ddd (8.5, 7.1, 1.5)	7.55, ddd (8.5, 7.1, 1.5)	7.53, ddd (8.2, 7.2, 1.1)
H-10	7.78, ddd (8.5, 7.2, 1.5)	7.78, ddd (8.5, 7.1, 1.5)	7.78, ddd (8.5, 7.1, 1.5)	7.79, ddd (8.5, 7.1, 1.6)
H-11	7.57, d (7.8)	7.60, d (7.8)	7.60, d (7.9)	7.59, d (7.8)
H-1'	2.84–2.44, m	1.43–1.33, m	1.44–1.36, m	2.89–2.56, m
H-2'	2.08–2.00, m	2.01, ddd (12.4, 12.5, 4.2)	2.01, dd (13.0, 9.4)	2.07–2.00, m
H-3'	0.75, d (6.0)	0.77, d (6.4)	0.77, d (6.3)	0.74, d (6.0)
H-3''	0.49, d (6.1)	0.28, d (6.5)	0.28, d (6.4)	0.49, d (6.0)
H-4'a	3.75, dd (15.0, 3.3)	3.65, dd (15.0, 5.3)	3.65, dd (14.9, 5.2)	3.75, dd (15.1, 3.4)
H-4'b	3.83, dd (15.0, 5.3)	3.77, dd (15.0, 2.6)	3.78, dd (15.1, 2.8)	3.84, dd (15.0, 5.3)
H-6'	6.68, d (2.3)	6.64, d (2.3)	6.64, d (2.0)	6.68, d (2.4)
H-7'	8.08, br	8.09, br	8.07, br	8.03, br
H-9'	7.28, d (8.1)	7.29, d (8.2)	7.29, d (8.2)	7.29, d (8.3)
H-10'	7.12, ddd (8.5, 7.1, 1.1)	7.13, t (7.6)	7.13, t (8.0)	7.12, ddd (8.1, 7.0, 1.1)
H-11'	6.97, ddd (8.5, 7.0, 1.1)	6.98, t (7.5)	6.98, t (7.5)	6.93, ddd (8.0, 7.1, 1.0)
H-12'	7.41, d (8.0)	7.50, d (8.0)	7.50, d (8.0)	7.42, d (8.0)

HMBC correlations were also used to distinguish the anti-isomers from the *syn* counterparts. For the *anti* isomer **4b** (whose indole moiety derived from L-Trp), H-4 exhibited correlations to C-14, C-5', C-4', and C-3 whereas H-1 showed correlations to C-14, C-2', C-3', and C-1'. On the contrary, in **4c** (whose indole moiety is derived from D-Trp), the

HMBC correlations from H-4 to C-14, C-5', C-4' and from H-1 to C-14, C-3', and C-2', were observed. For the *syn* isomer **4a** (whose indole moiety derived from L-Trp), the HMBC correlations from H-1 to C-14, and from H-4 to C-14, C-4', and C-5' were observed while the HMBC correlations from H-1 to C-3 and C-14 and from H-4 to only C-4' were observed in the *syn* isomer **4d**.

**Table 3.** <sup>13</sup>C NMR data (75 MHz, CDCl<sub>3</sub>) for **4** and **5**.

Position	$\delta_c$ , Type							
	<b>4a</b>	<b>4b</b>	<b>4c</b>	<b>4d</b>	<b>5a</b>	<b>5b</b>	<b>5c</b>	<b>5d</b>
C-1	61.9, CH	58.1	58.1	61.8	54.1, CH	50.8	50.8	54.1
C-3	167.8, CO	169.5	169.5	167.8	167.6, CO	169.4	169.4	167.5
C-4	57.5, CH	56.8	57.3	57.5	56.7, CH	57.3	57.3	56.7
C-6	161.4, CO	160.9	160.9	161.0	161.0, CO	160.8	160.8	161.1
C-7	120.2, C	120.2	120.2	120.2	120.4, C	120.3	120.3	120.0
C-8	126.8, CH	126.9	126.9	126.7	126.9, CH	126.9	126.9	126.8
C-9	127.1, CH	127.2	127.2	127.1	126.9, CH	127.4	127.4	126.8
C-10	134.7, CH	134.7	134.7	134.7	134.8, CH	134.6	134.6	134.7
C-11	127.1, CH	127.0	127.0	127.1	126.7, CH	127.1	127.1	126.7
C-12	146.8, C	147.1	147.1	146.1	147.2, C	147.0	147.0	147.2
C-14	149.3, C	150.3	150.3	149.8	151.3, C	151.5	151.5	151.3
C-1'	34.5, CH	29.4	29.5	34.8	45.8, CH <sub>2</sub>	40.2	40.2	45.8
C-2'	18.0, CH <sub>3</sub>	14.8	14.8	18.1	23.9, CH	24.1	24.1	23.9
C-3''	-	-	-	-	20.4, CH <sub>3</sub>	19.7	19.7	20.4
C-3'	19.6, CH <sub>3</sub>	18.8	18.8	19.8	22.9, CH <sub>3</sub>	23.3	23.3	22.9
C-4'	27.4, CH <sub>2</sub>	27.4	27.4	27.4	26.4, CH <sub>2</sub>	27.1	27.1	26.4
C-5'	110.2, C	109.3	109.3	110.2	107.9, C	109.7	109.7	107.9
C-6'	123.5, CH	123.6	123.6	123.6	123.6, CH	123.6	123.6	123.6
C-8'	136.0, C	136.0	136.0	135.9	137.1, C	136.1	136.1	137.1
C-9'	110.9, CH	111.1	111	111	110.2, CH	111.1	111.1	110.2
C-10'	122.3, CH	122.6	122.6	122.4	122.2, CH	122.8	122.8	122.2
C-11'	119.9, CH	120.0	120.0	119.9	119.9, CH	120.2	120.2	119.9
C-12'	118.7, CH	118.7	118.7	118.7	119.0, CH	118.8	118.8	119.1
C-13'	127.8, C	127.2	127.2	127.8	126.8, C	127.1	127.1	126.8

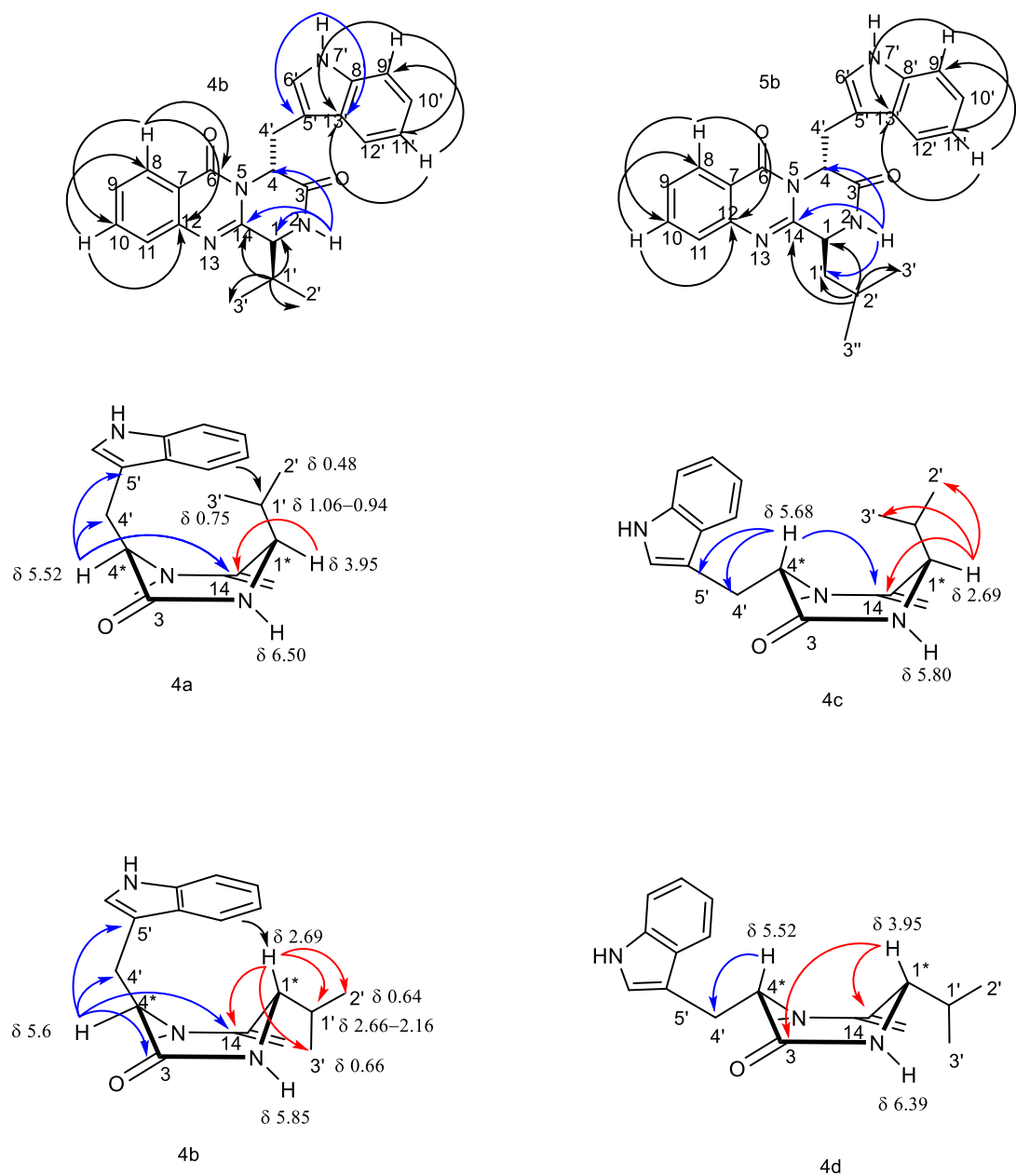


**Figure 2.** Most relevant chemical shifts and key HMBC correlations of the protons to the stereogenic centers on the piperazine ring of **4a-d**.

Moreover, the NOESY spectrum revealed the cross peak between the C-1' methyl groups and H-4 for the *anti* isomer **4c**, while for the *syn* isomer **4a** that correlation was absent. These observations support the identity/identification of the *syn* and *anti* conformational isomers.

### 2.3. Tumor Cell Growth Inhibitory Activity

Compounds **4a–d** and **5a–d** were tested for their tumor cell growth inhibitory activity against two human tumor cell lines: NCI-H460 (non-small cell lung cancer) and HCT-15 (colorectal adenocarcinoma), using the sulforhodamine B (SRB) colorimetric assay [29]. Five serial dilutions of each compound (at a maximum concentration of 150  $\mu\text{M}$ ) were tested for 48 h. Doxorubicin was used as a positive control, and the antitumor activity was reported as  $\text{GI}_{50}$  (drug concentration that inhibits the growth of cancer cells by 50%).

Compounds **4a–d**, **5a**, **5b**, and **5d** were also investigated for their possible modulatory activity of P-gp, a drug efflux pump associated with drug resistance. P-gp activity was determined by an assay which measures the mean fluorescence intensity of cells treated concomitantly with rhodamine 123 (Rh123, a substrate of P-gp), and the tested compounds [20]. The P-gp inhibitory activity of the compounds was tested on a drug resistant cell line which overexpresses P-gp (K562Dox), by measuring the intracellular accumulation of Rh123. After an incubation with the compounds and Rh123, cells were washed, and the fluorescence of Rh123 was detected by flow cytometry in the FL1 channel. The drug sensitive counterpart cells (K562) were used as control. The Rh123 accumulation ratio was calculated as:  $(\text{Mean FL1}_{\text{K562Dox+Compound}} - \text{Mean FL1}_{\text{K562Dox}}) / \text{Mean FL1}_{\text{K562Dox}}$  [30].

All the compounds tested showed weak to moderate activity, with the  $\text{GI}_{50}$  values ranging from 30 to 80  $\mu\text{M}$ . Some differences were observed among the groups of **4** and **5**. Compounds **4** were more potent in the HCT-15 cell line but exhibited higher  $\text{GI}_{50}$  values in the NCI-H460 cell lines. On the other hand, members of **5** were more potent than those of **4** in the NCI-H460 cell line. Compound **5c** was the most promising in this panel of cell lines (Table 4). The substituent at C-1 was found to influence the inhibitory effects observed in the NCI-H460 cell. For example, **4a–d**, whose C-1 bears the isopropyl group, exhibited  $\text{GI}_{50}$  values ranging from 57 to 81  $\mu\text{M}$ , while **5a–d**, whose C-1 bears the isobutyl group, displayed  $\text{GI}_{50}$  values ranging from 31 to 42  $\mu\text{M}$ . These findings are in accordance with the SAR obtained with the natural compounds *in vitro* antitumor assays. For instance, gyantrypine (**2**), whose C-1 bears a hydrogen atom, showed no antitumor activity ( $\text{GI}_{50} > 100 \mu\text{M}$ ) while the analogue, with the phenyl group on C-1, was more active ( $\text{GI}_{50} = 15 \mu\text{M}$ ) [25]. Moreover, fumiquinazolines F (**3**) and G (**4**), whose C-1 bears a methyl group, showed moderate activity against P-388 cells ( $\text{GI}_{50} = 13.5 \mu\text{M}$ ) [31]. Likewise, differences in the inhibitory

effects against the two cell lines were observed between enantiomeric pairs; i.e., **4a** (1*S*,4*S*)/**4d** (1*R*,4*R*) and **4b** (1*S*,1*R*)/**4c** (1*R*,4*S*). Significant differences were detected for GI<sub>50</sub> concentration values in the pair **4a/4d** in NCI-H460 cells ( $p = 0.026$ ). Among the fiscalin series such as *epi*-fiscalin A (**16**, 1*S*,4*S*), *epi*-fiscalin C (**17**, 1*S*,4*S*), fiscalin F (1*S*,4*S*), and fiscalin C (**15**, 1*R*,4*S*), the configurations of the stereogenic carbons of the isopropyl pyrazinone and imidazolone moieties have already been found to influence the antitumor activity [21,32]. Although this study brought insights into the antitumor activity of fiscalin B (**4c**) and the synthetic analogues, none of the compounds showed any effect on the intracellular accumulation of Rh123, when tested at 10  $\mu$ M concentrations using verapamil as a positive control for P-gp inhibition (Figure 3).

**Table 4.** The GI<sub>50</sub> of **4a–d** and **5a–d** in the NCI-H460 and HCT-15 human tumor cell lines.

Compound	GI <sub>50</sub> ( $\mu$ M)	
	NCI-H460	HCT-15
<b>4a</b>	81.33 $\pm$ 1.55	40.33 $\pm$ 3.12
<b>4b</b>	70.20 $\pm$ 3.15	38.15 $\pm$ 0.29
<b>4c</b>	57.62 $\pm$ 2.08	31.78 $\pm$ 1.21
<b>4d</b>	60.10 $\pm$ 2.61	33.30 $\pm$ 1.37
<b>5a</b>	32.52 $\pm$ 4.24	48.18 $\pm$ 2.51
<b>5b</b>	41.52 $\pm$ 2.52	51.94 $\pm$ 4.26
<b>5c</b>	31.19 $\pm$ 3.01	43.63 $\pm$ 0.25
<b>5d</b>	36.47 $\pm$ 3.98	47.00 $\pm$ 1.47

Values were determined with the SRB assay and are the mean  $\pm$  SEM of three independent experiments. Doxorubicin was used as a positive control, with the following GI<sub>50</sub> concentrations: 23.02  $\pm$  0.54 nM in NCI-H460 cells, 331.49  $\pm$  49 nM in HCT-15 cells.

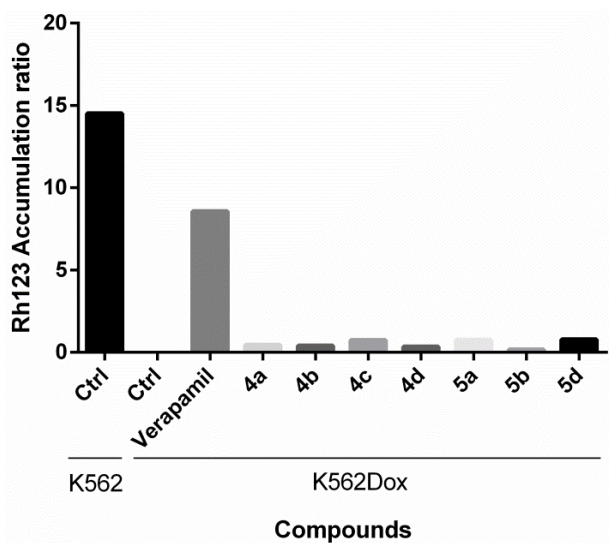


**Figure 3.** Accumulation ratio of Rh123 in K562 and K562Dox cell lines. Cells were incubated for 1 h with **4a–d**, **5a**, **5b**, and **5d** at a final concentration of 10  $\mu$ M. The activity of **5c** was not analyzed due to its quantity we have obtained. Verapamil (10  $\mu$ M) was used as a positive control (known P-gp inhibitor), and K562 cells were used as a negative control. The accumulation ratio in the untreated K562Dox cells was defined as zero; any value higher than that represents a potential inhibition of P-gp. Results are the mean of two independent experiments.

### 3. Materials and Methods

#### 3.1. General Procedure

All reagents were from analytical grade. Dried pyridine and triphenylphosphite were purchased from Sigma (Sigma-Aldrich Co. Ltd., Gillingham, UK). Protected amino acids (**ii**) and anthranilic acid (**i**) were purchased from TCI (Tokyo Chemical Industry Co. Ltd., Chuo-ku, Tokyo, Japan). Column chromatography purifications were performed using flash silica Merck 60, 230–400 mesh (EMD Millipore corporation, Billerica, MA, USA) and preparative TLC was carried out on precoated plates Merck Kieselgel 60 F<sub>254</sub> (EMD Millipore corporation, Billerica, MA, USA), spots were visualized with UV light (Vilber Lourmat, Marne-la-Vallée, France). Melting points were measured in a Köfler microscope and are uncorrected. Infrared spectra were recorded in a KBr microplate in a FTIR spectrometer Nicolet iS10 from Thermo Scientific (Waltham, MA, USA) with Smart OMNI-Transmission accessory (Software 188 OMNIC 8.3). <sup>1</sup>H and <sup>13</sup>C NMR spectra were recorded in CDCl<sub>3</sub> (Deutero GmbH, Kastellaun, Germany) at room temperature unless otherwise mentioned



on Bruker AMC instrument (Bruker Biosciences Corporation, Billerica, MA, USA), operating at 300 MHz for  $^1\text{H}$  and 75 MHz for  $^{13}\text{C}$ ). Carbons were assigned according to HSQC and or HMBC experiments. Optical rotation was measured at 25 °C using the ADP 410 polarimeter (Bellingham + Stanley Ltd., Tunbridge Wells, Kent, UK), using the emission wavelength of sodium lamp, concentrations are given in g/100 mL. Qualitative GC-MS analyses were performed on a Trace GC 2000 Series ThermoQuest gas chromatography (Thermo Fisher Scientific Inc., Austin, TX, USA) equipped with ion-trap GCQ Plus ThermoQuest Finnigan mass detector (Thermo Fisher Scientific Inc., Austin, TX, USA). Chromatographic separation was achieved using a capillary column (30 m  $\times$  0.25 mm  $\times$  0.25  $\mu\text{m}$ , cross-linked 5% diphenyl and 95% dimethyl polysiloxane) from Thermo Scientific™ (Thermo Fisher Scientific Inc., Austin, TX, USA) and high-purity helium C-60 as carrier gas. High resolution mass spectra (HRMS) were measured on a Bruker FTMS APEX III mass spectrometer (Bruker Corporation, Billerica, MA, USA) recorded as ESI (Electrospray) made in Centro de Apoio Científico e Tecnológico á Investigación (CACTI, University of Vigo, Pontevedra, Spain). The purity of synthesized compounds was determined by reversed-phase HPLC with diode array detector (DAD) using C18 column (Kimetex®, 2.6 EV0 C18 100 Å, 150  $\times$  4.6 mm), and the mobile phase was methanol: water (60:40) or acetonitrile:water (50:50). Enantiomeric ratio was determined by chiral HPLC (LCMS-2010EV, Shimadzu, Lisbon, Portugal), employing a system equipped with a chiral column (Lux® 5  $\mu\text{m}$  Amylose-1, 250  $\times$  4.6 mm) and UV-detection at 254 nm, mobile phase was hexane:ethanol (80:20) and the flow rate was 0.5 mL/min.

### 3.2. General Conditions for the Synthesis of 4-(1H-indol-3-ylmethyl)-1-isopropyl-2H-pyrazino[2,1-b]quinazoline-3,6-(1H,4H)-diones (**4b/4c**)

In a closed vial, anthranilic acid (**i**) (28 mg, 200  $\mu\text{mol}$ ), *N*-Boc-L-valine (**ii**a) for **4c** or *N*-Boc-D-valine (**ii**b) for **4b** (44 mg, 200  $\mu\text{mol}$ ), and triphenylphosphite (63  $\mu\text{L}$ , 220  $\mu\text{mol}$ ) were added along with 1 mL of dried pyridine. The vial was heated in heating block with stirring at 55 °C for 16–24 h. After cooling the mixture to room temperature, L-tryptophan methyl ester hydrochloride (**iii**a) for **4b** or D-tryptophan methyl ester hydrochloride (**iii**b) for **4c** (51 mg, 200  $\mu\text{mol}$ ) was added, and the mixture was irradiated in the microwave at a constant temperature at 220 °C for 1.5 min. Four reaction mixtures were prepared in the

same conditions and treated in parallel. After removing the solvent with toluene, the crude product was purified by flash column chromatography using hexane: EtOAc (60:40) as a mobile phase. The preparative TLC was performed using CH<sub>2</sub>Cl<sub>2</sub>:Me<sub>2</sub>CO (95:5) as mobile phase. The major compound appeared as a black spot with no fluorescence under the UV light. The desired compounds **4b/c** were collected as yellow solids. Before analysis, compounds were recrystallized from methanol.

### 3.2.1. (1*R*,4*S*)-4-(1*H*-indol-3-ylmethyl)-1-isopropyl-2*H*-pyrazino[2,1-*b*]quinazoline-3,6-(1*H*,4*H*)-dione (**4b**)

Yield: 14%; mp: 168–169 °C; [ $\alpha$ ]<sub>D</sub> = +65.21 (*c* 0.46; CHCl<sub>3</sub>); IR  $\nu_{max}$  (KBr) 3411, 3066, 1684, 1596, 1471, 1389, 1293 cm<sup>-1</sup>; <sup>1</sup>H NMR see Table 2; <sup>13</sup>C NMR see Table 3; *m/z* (rel. intensity, %): 385.9 (M<sup>+</sup>, 2), 257.1 (29), 214.1 (3), 202.0 (7), 171.1 (10), 143.1 (4), 130.1 (100), 103.0 (18), 77.0 (16); (+)-HRESIMS *m/z* 387.1810 (M + H)<sup>+</sup> (calculated for C<sub>23</sub>H<sub>22</sub>N<sub>4</sub>O<sub>2</sub>, 387.1776).

### 3.2.2. (1*S*,4*R*)-4-(1*H*-indol-3-ylmethyl)-1-isopropyl-2*H*-pyrazino[2,1-*b*]quinazoline-3,6-(1*H*,4*H*)-dione (**4c**)

Yield: 8%; mp: 168–169 °C; [ $\alpha$ ]<sub>D</sub> = -248.1 (*c* 0.43; CHCl<sub>3</sub>); IR  $\nu_{max}$  (KBr) 3346, 3066, 1683, 1596, 1471, 1389, 1293 cm<sup>-1</sup>; <sup>1</sup>H NMR see Table 2; <sup>13</sup>C NMR see Table 3; *m/z* (rel. intensity, %): 385.9 (M<sup>+</sup>, 5), 257.1 (32), 298.9 (37), 284.2 (6), 254.0 (15), 238.8 (12), 201.8 (18), 189.0 (35), 171.1 (25), 149.1 (32), 130.1 (100), 103.0 (9), 77.0 (13); (+)-HRESIMS *m/z* 387.1809 (M + H)<sup>+</sup> (calculated for C<sub>23</sub>H<sub>22</sub>N<sub>4</sub>O<sub>2</sub>, 387.1776).

### 3.3. General Condition for the Synthesis of 4-(1*H*-indol-3-ylmethyl)-1-isobutyl-2*H*-pyrazino[2,1-*b*]quinazoline-3,6-(1*H*,4*H*)-diones (**5b/5c**)

In a closed vial, anthranilic acid (**i**) (28 mg, 200  $\mu$ mol), *N*-Fmoc-L-leucine (**ii**c) for **5c** or *N*-Fmoc-D-leucine (**ii**d) for **5b** (70.68 mg, 200  $\mu$ mol), and triphenylphosphite (63  $\mu$ L, 220  $\mu$ mol) were added along with 1 mL of dried pyridine. The vial was heated in heating block at 55 °C for 16–24 h. After cooling the mixture to room temperature, we added L-tryptophan methyl ester hydrochloride (**iii**a) for **5b** (51 mg, 200  $\mu$ mol), or D-tryptophan methyl ester hydrochloride (**iii**b) **5d** (51 mg, 200  $\mu$ mol), and the mixture was irradiated in the microwave at a constant temperature at 220 °C for 1.5 min. Four reaction mixtures were prepared in

the same conditions and treated in parallel. After removing the solvent with toluene, the mixture was purified by flash column chromatography using hexane: EtOAc (60:40) as a mobile phase. The preparative TLC was performed using CH<sub>2</sub>Cl<sub>2</sub>:Me<sub>2</sub>CO (95:5) as a mobile phase. The major compound appeared as a black spot with no fluorescence under UV light. The desired compounds, **5b/5c**, were collected as yellow solids. Before analysis, compounds were recrystallized from methanol.

### 3.3.1. (1*R*,4*S*)-4-(1*H*-indol-3-ylmethyl)-1-isobutyl-2*H*-pyrazino[2,1-*b*]quinazoline-3,6-(1*H*,4*H*)-dione (**5b**)

Yield: 10%; mp: 220 °C; [ $\alpha$ ]<sub>D</sub> = +89.74 (*c* 0.52; CHCl<sub>3</sub>); IR  $\nu_{max}$  (KBr) 3334, 3060, 1686, 1457, 1386, 1291 cm<sup>-1</sup>; <sup>1</sup>H NMR see Table 2; <sup>13</sup>C NMR see Table 3; (+)-HRESIMS *m/z* 401.1967 (M + H)<sup>+</sup> (calculated for C<sub>24</sub>H<sub>24</sub>N<sub>4</sub>O<sub>2</sub>, 401.1933).

### 3.3.2. (1*S*,4*R*)-4-(1*H*-indol-3-ylmethyl)-1-isobutyl-2*H*-pyrazino[2,1-*b*]quinazoline-3,6-(1*H*,4*H*)-dione (**5c**)

Yield: 8%; mp: 219 °C; [ $\alpha$ ]<sub>D</sub> = -61.72 (*c* 0.54; CHCl<sub>3</sub>); IR  $\nu_{max}$  (KBr) 3334, 3060, 1682, 1587, 1396, 1298 cm<sup>-1</sup>; <sup>1</sup>H NMR see Table 2; <sup>13</sup>C NMR see Table 3; (+)-HRESIMS *m/z* 401.1966 (M + H)<sup>+</sup> (calculated for C<sub>24</sub>H<sub>24</sub>N<sub>4</sub>O<sub>2</sub>, 401.1933).

## 3.4. General Condition for the Synthesis of Compounds **4a** and **5a**

### 3.4.1. Synthesis of *N*-(2-aminobenzoyl)-*L*-tryptophan methyl ester (**iv-a**)

To a mixture of anthranilic acid (287 mg, 2.39 mmol) and TBTU (920 mg, 2.86 mmol, 1.2 equiv) in acetonitrile (20 mL) was added Et<sub>3</sub>N (833  $\mu$ L, 4.78 mmol, 2 equiv) and *L*-tryptophan methyl ester (521 mg, 2.39 mmol) at room temperature. After stirring for 5 h, the reaction mixture was concentrated under reduced pressure. The residue was dissolved in CH<sub>2</sub>Cl<sub>2</sub> and washed with 1 M HCl, extracted with CH<sub>2</sub>Cl<sub>2</sub> (3  $\times$  100 mL), dried with Na<sub>2</sub>SO<sub>4</sub>, filtered, and concentrated. The residue was purified by flash chromatography (eluent 1% MeOH in CH<sub>2</sub>Cl<sub>2</sub>) to yield **iv-a** as a white solid (675.5 mg, 96%), mp 134–135 °C, IR  $\nu_{max}$  (KBr): 3424, 1746, 1727, 1645, 1611, 1581; <sup>1</sup>H NMR (300, MHz, CDCl<sub>3</sub>): 8.15 (s, 1H), 7.56 (d, 1H, *J* = 7.9 Hz), 7.35 (d, 1H, *J* = 8.1 Hz), 7.19–7.15 (m, 3H), 7.09 (t, 1H, *J* = 7.4 Hz), 7.01 (d, 1H, *J* = 2.3 Hz), 6.65 (dd, 1H, *J* = 8.7 and 1.1 Hz), 6.56 (ddd, 1H, *J* = 7.5 and 0.8 Hz), 5.08

(dt, 1H,  $J = 7.5$  and  $5.3$  Hz), 3.71 (s, 3H), 3.43 (m, 2H);  $^{13}\text{C}$  NMR (75, MHz,  $\text{CDCl}_3$ ) 172.6 (CO), 168.8 (CO), 148.8 (C), 136.1 (C), 132.6 (CH), 127.6 (CH), 127.6 (C), 122.8 (CH), 122.3 (CH), 119.8 (CH), 118.7 (CH), 117.3 (CH), 116.7 (CH), 115.3 (C), 111.3 (CH), 110.1 (C), 53.1 (CH), 52.7 ( $\text{CH}_3$ ), 27.7 ( $\text{CH}_2$ ).

#### 3.4.2. Synthesis of *N*-[9*H*-fluoren-9-ylmethoxy]carbonyl]-L-valinyl-2-aminobenzoyl-L-tryptophan methyl ester (**vi-a**)

To a solution of **iv-a** (160 mg, 0.474 mmol) in dried  $\text{CH}_2\text{Cl}_2$  (10 mL) was added *N*-Fmoc-L-valine-Cl [27] (**v-a**, 182 mg, 0.5 mmol). The mixture was stirred for 30 min, followed by addition of aqueous  $\text{Na}_2\text{CO}_3$  (1 M, 8 mL, 8 mmol). After continuous stirring for 3 h, the mixture was extracted with  $\text{CH}_2\text{Cl}_2$  (4  $\times$  100 mL), dried with  $\text{Na}_2\text{SO}_4$ , filtered, and concentrated. The residue was purified by flash chromatography (eluent: 5% MeOH in  $\text{CH}_2\text{Cl}_2$ ) to give **vi-a** as a white solid (296.4 mg, 95%), mp: 194.4–196.3  $^\circ\text{C}$ ,  $[\alpha]^{30}_{\text{D}} = +13.22$  (c 0.126,  $\text{CHCl}_3$ ), IR  $\nu_{\text{max}}$  (KBr) 3318, 1727, 1698, 1588  $\text{cm}^{-1}$ ;  $^1\text{H}$  NMR (300, MHz,  $\text{CDCl}_3$ ): 11.4 (s, 1H), 8.50 (d, 1H,  $J = 8.3$  Hz), 8.24 (s, 1H), 7.67 (d, 2H,  $J = 7.4$  Hz), 7.57 (d, 1H,  $J = 7.4$  Hz), 7.51 (d,  $J = 7.3$ ), 7.43–7.19 (m, 8H), 7.08 (t, 1H,  $J = 7.4$  Hz), 6.97 (t, 1H,  $J = 7.4$  Hz), 6.91 (d, 1H,  $J = 7.5$  Hz), 6.87 (s, 1H), 6.68 (d, 1H,  $J = 7.6$  Hz), 5.50 (d, 1H,  $J = 8.5$  Hz), 4.97 (dd, 1H,  $J = 12.7$  and  $5.2$  Hz), 4.32 (dt, 3H,  $J = 17.5$  and  $10.4$  Hz), 4.20 (dt, 1H,  $J = 13.6$  and  $6.1$  Hz), 3.72 (s, 3H), 3.38 (dd, 1H,  $J = 15.0$  and  $5.2$  Hz), 3.31 (dd, 1H,  $J = 14.9$  and  $5.3$  Hz), 1.82 (m, 1H), 0.97 (d, 1H,  $J = 6.7$  Hz), 0.90 (d, 6H,  $J = 6.8$  Hz)  $^{13}\text{C}$  NMR (75, MHz,  $\text{CDCl}_3$ ) 172.1 (CO), 170.3 (CO), 168.3 (CO), 156.6 (C), 144.1 (2C), 141.3 (2C), 138.9 (C), 136.1 (C), 132.8 (CH), 127.7 (2CH), 127.5 (C), 127.1 (2CH), 127.1 (2CH), 127.0 (CH), 125.3 (CH), 125.2 (CH), 123.2 (CH), 122.8 (CH), 122.3 (CH), 121.4 (C), 120.0 (2CH), 119.8 (CH), 118.4 (C), 111.4 (CH), 109.6 (C), 67.3 ( $\text{CH}_2$ ), 61.4 (CH), 53.4 (CH), 52.6 ( $\text{CH}_3$ ), 47.3 (CH), 31.3 (CH), 27.3 ( $\text{CH}_2$ ), 19.4 ( $\text{CH}_3$ ), 17.6 ( $\text{CH}_3$ ).

#### 3.4.3. Synthesis of (1*S*,4*S*)-4-(1*H*-indol-3-ylmethyl)-1-isopropyl-2*H*-pyrazino[2,1-*b*]quinazolin-3,6-(1*H*, 4*H*)-dione (**4a**)

To a solution of **vi-a** (290 mg, 0.440 mmol) in dried  $\text{CH}_2\text{Cl}_2$  (20 mL) was added  $\text{Ph}_3\text{P}$  (576 mg, 2.2 mmol, 5 equiv),  $\text{I}_2$  (448 mg, 2.16 mmol, 4.9 equiv), and *N,N*-diisopropylethylamine (774  $\mu\text{L}$ , 4.44 mmol, 10 equiv). The reaction mixture was stirred at room temperature for 5 h, quenched with aqueous  $\text{Na}_2\text{CO}_3$ , and extracted with  $\text{CH}_2\text{Cl}_2$  (3  $\times$  100 mL), dried with  $\text{Na}_2\text{SO}_4$ , filtered and concentrated. Hexane was added to remove an

excess of Ph<sub>3</sub>P, the precipitate was filtered and treated with CH<sub>2</sub>Cl<sub>2</sub> (10 mL) and piperidine (2.5 mL, 20%) at room temperature for 20 min, followed by solvent evaporation to provide the solid which was triturated with hexane (1 × 200 mL), CH<sub>2</sub>Cl<sub>2</sub>/PhMe (1 × 200 mL), and hexane (1 × 200 mL). The vacuum-dried crude residue was dissolved in CH<sub>3</sub>CN (10 mL) in the presence of DMAP (64 mg, 0.53 mmol) and refluxed for 19 h. The reaction mixture was purified by preparative TLC (EtOAc: MeOH: CH<sub>2</sub>Cl<sub>2</sub>, 50:2.5:47.5) to afford **4a** (45.5 g, 28%); mp: 112.8–114.1 °C, [ $\alpha$ ]<sub>D</sub><sup>30</sup> = +300.55 (*c* 0.061, CHCl<sub>3</sub>), IR  $\nu_{max}$  (KBr) 3417, 3068, 1683, 1594, 1471, 1387, 1333 cm<sup>-1</sup>; <sup>1</sup>H NMR see Table 2; <sup>13</sup>C NMR see Table 3; *m/z* (rel. intensity, %): 386.3 (M<sup>+</sup>, 8), 341.0 (5), 315 (10), 282.0 (8), 257.1 (55), 241.9 (7), 217.1 (17), 186.1 (10), 171.0 (18), 130.1 (100), 103.0 (14), 77.0 (16); (+)-HRESIMS *m/z* 387.1810 (M + H)<sup>+</sup> (calculated for C<sub>23</sub>H<sub>22</sub>N<sub>4</sub>O<sub>2</sub>, 387.1776).

#### 3.4.4. Synthesis of *N*-[9*H*-fluoren-9-ylmethoxy)carbonyl]-*L*-methylpentanyl-2*H*-aminobenzoyl-*L*-tryptophan methyl ester (**vi-b**)

To a solution of compound **iv-a** (129 mg, 0.382 mmol) in dried CH<sub>2</sub>Cl<sub>2</sub> (10 mL) was added *N*-Fmoc-*L*-leucine-Cl [27] (**v-b**, 171 mg, 0.458 mmol). The mixture was stirred for 30 min, followed by addition of aqueous Na<sub>2</sub>CO<sub>3</sub> (1 M, 7.6 mL, 7.6 mmol). After being stirred for a total 3 h, the mixture was extracted with CH<sub>2</sub>Cl<sub>2</sub> (4 × 100 mL), dried with Na<sub>2</sub>SO<sub>4</sub>, filtered, and concentrated. The residue was purified by flash chromatography (eluent 5% MeOH in CH<sub>2</sub>Cl<sub>2</sub>) to give **vi-b** as a white solid (231.7 mg, 92%), mp: 193.7–194.9 °C, [ $\alpha$ ]<sub>D</sub><sup>30</sup> = +18.42 (*c* 0.398, CHCl<sub>3</sub>), IR  $\nu_{max}$  (KBr) 3405, 1744, 1695, 1586 cm<sup>-1</sup>; <sup>1</sup>H NMR (300, MHz, CDCl<sub>3</sub>): 11.4 (s, 1H), 8.59 (d, 1H, *J* 8.3 Hz), 8.19 (s, 1H), 7.76 (d, 2H, *J* 7.4 Hz), 7.65 (d, 1H, *J* 7.3 Hz), 7.59 (d, 1H, *J* 7.4 Hz), 7.52–7.28 (m, 8H), 7.17 (t, 1H, *J* 7.3 Hz), 7.06 (d, 1H, *J* 7.4 Hz), 7.00 (d, 1H, 7.7 Hz) 6.96 (s, 1H), 6.73 (d, 1H, *J* 7.6 Hz), 5.55 (d, 1H, *J* 8.5 Hz), 5.05 (dd, 1H, *J* 12.6 and 5.2 Hz), 4.39 (d, 2H, *J* 6.6 Hz), 4.28 (m, 2H), 3.72 (s, 3H), 3.38 (m, 2H), 2.33 (dt, 1H *J* 13.0 and 6.4 Hz), 1.06 (d, 3H, *J* 6.8 Hz), 0.98 (d, 3H, *J* 6.8 Hz); <sup>13</sup>C NMR (75, MHz, CDCl<sub>3</sub>): 172.1 (CO), 170.2 (CO), 168.3 (CO), 156.5 (CO), 143.8 (2C), 141.3 (2C), 139.0 (C), 136.1 (C), 132.9 (CH), 127.7 (2CH), 127.5 (C), 127.1 (2CH), 127.1 (2CH), 126.9 (CH), 125.3 (CH), 125.2 (CH), 123.2 (CH), 122.8 (CH), 122.4 (CH), 121.4 (C), 120.2 (2CH), 119.8 (CH), 118.5 (C), 111.4 (CH), 109.7 (CH), 67.2 (CH<sub>2</sub>), 61.3 (CH), 53.3 (CH), 52.6 (CH<sub>3</sub>), 38.6 (CH), 47.3 (CH<sub>2</sub>), 31.4 (CH), 27.3 (CH<sub>2</sub>), 19.4 (CH<sub>3</sub>), 17.5 (CH<sub>3</sub>).

### 3.4.5. Synthesis of (1*S*,4*S*)-4-(1*H*-indol-3-ylmethyl)-1-isobutyl-2*H*-pyrazino[2,1-*b*]quinazolin-3,6-(1*H*, 4*H*)-dione (**5a**)

To a solution of **vi-b** (232 mg, 0.344 mmol) in dried CH<sub>2</sub>Cl<sub>2</sub> (20 mL) was added Ph<sub>3</sub>P (451 mg, 1.72 mmol, 5 equiv), I<sub>2</sub> (428 mg, 1.68 mmol, 4.9 equiv), and *N,N*-diisopropylethylamine (605 μL, 3.47 mmol, 10 equiv). The reaction mixture was stirred at room temperature for 5 h, quenched with aqueous Na<sub>2</sub>CO<sub>3</sub>, and extracted with CH<sub>2</sub>Cl<sub>2</sub> (3 × 100 mL), dried with Na<sub>2</sub>SO<sub>4</sub>, filtered and concentrated. Hexane was added to remove an excess of Ph<sub>3</sub>P, the precipitate was filtered and treated with CH<sub>2</sub>Cl<sub>2</sub> (10 mL) and piperidine (2.5 mL, 20%) at room temperature for 20 min, followed by solvent evaporation to provide the solid which was triturated with hexane (1 × 200 mL), CH<sub>2</sub>Cl<sub>2</sub>/PhMe (1 × 200 mL), and hexane (1 × 200 mL). The vacuum-dried crude residue was dissolved in CH<sub>3</sub>CN (10 mL) in the presence of DMAP (80 mg, 0.66 mmol) and refluxed for 19 h. The reaction mixture was purified by preparative TLC (EtOAc:MeOH:CH<sub>2</sub>Cl<sub>2</sub>, 50:2.5:47.5) to afford **5a** (39 mg, 28%); mp: 105.9–106.3 °C, [α]<sub>D</sub><sup>30</sup> = +81.76 (*c* 0.106, CHCl<sub>3</sub>), IR  $\nu_{max}$  (KBr) 3435, 3060, 1686, 1602, 1387, 1292 cm<sup>-1</sup>; <sup>1</sup>H NMR see Table 2; <sup>13</sup>C NMR see Table 3; (+)-HRESIMS *m/z* 401.1933 (M + H)<sup>+</sup> (calculated for C<sub>24</sub>H<sub>24</sub>N<sub>4</sub>O<sub>2</sub>, 401.1933).

## 3.5. General Condition for the Synthesis Compound **4d** and **5d**

### 3.5.1. Synthesis of *N*-(2-aminobenzoyl)-D-tryptophan methyl ester (**iv-b**)

To a mixture of anthranilic acid (287 mg, 2.39 mmol) and TBTU (920 mg, 2.86 mmol, 1.2 equiv) in CH<sub>3</sub>CN (20 mL) was added Et<sub>3</sub>N (833 μL, 4.78 mmol, 2 equiv) and D-tryptophan methyl ester (521 mg, 2.39 mmol) at room temperature with stirring. After being stirred for 5 h, the reaction mixture was concentrated under reduced pressure. The residue was dissolved in CH<sub>2</sub>Cl<sub>2</sub> and washed with 1M HCl, extracted with CH<sub>2</sub>Cl<sub>2</sub> (3 × 100 mL), dried with Na<sub>2</sub>SO<sub>4</sub>, filtered and concentrated. The residue was purified by flash chromatography (eluent: 1% MeOH in CH<sub>2</sub>Cl<sub>2</sub>) to yield **iv-b** as a white solid (569.7 mg, 81%), mp 131.9–134.3 °C, IR  $\nu_{max}$  (KBr) 3423, 1746, 1644 cm<sup>-1</sup>, <sup>1</sup>H NMR (300, MHz, CDCl<sub>3</sub>): 8.14 (s, 1H), 7.56 (d, 1H, *J* = 7.9 Hz), 7.35 (d, 1H, *J* = 8.1 Hz), 7.19–7.15 (m, 3H), 7.10 (ddd, 1H, *J* = 8.0, 7.1, and 1.1 Hz), 7.01 (d, 1H, *J* = 2.4 Hz), 6.65 (dd, 1H, *J* = 8.7 and 1.1), 6.60 (s, 1H), 6.59–6.52 (ddd, 2H, *J* = 7.5 and 0.8 Hz), 5.08 (dt, 1H, *J* = 7.5 and 5.3 Hz), 3.72 (s, 3H), 3.43 (m, 2H); <sup>13</sup>C NMR (75, MHz, CDCl<sub>3</sub>): 172.6 (CO), 168.8 (CO), 148.8 (C), 136.1 (C), 132.6 (CH), 127.6 (CH), 127.5 (C), 122.8

(CH), 122.3 (CH), 119.8 (CH), 118.7 (CH), 117.3 (CH), 116.7 (CH), 115.3 (C), 111.3 (CH), 110.1 (C), 53.1 (CH), 52.5 (CH<sub>3</sub>), 27.7(CH<sub>2</sub>).

### 3.5.2. Synthesis of *N*-[9*H*-fluoren-9-ylmethoxy)carbonyl]-*D*-valinyl-2-aminobenzoyl-*D*-tryptophan methyl ester (**vi-c**)

To a solution of **iv-b** (140 mg, 0.416 mmol) in dried CH<sub>2</sub>Cl<sub>2</sub> (10 mL) was added *N*-Fmoc-*D*-valine-Cl [27] (**v-c**, 182 mg, 0.5 mmol). The mixture was stirred for 30 min, followed by addition of aqueous Na<sub>2</sub>CO<sub>3</sub> (1 M, 8 mL, 8 mmol). After continuous stirring for 3 h, the mixture was extracted with CH<sub>2</sub>Cl<sub>2</sub> (4 × 100 mL), dried with Na<sub>2</sub>SO<sub>4</sub>, filtered, and concentrated. The residue was purified by flash chromatography (eluent: 5% MeOH in CH<sub>2</sub>Cl<sub>2</sub>) to give **vi-c** as a white solid (220.4 mg, 84%), mp: 197.8–200.2 °C, [α]<sup>30</sup><sub>D</sub> = -22.72 (c 0.088, CHCl<sub>3</sub>), IR  $\nu_{max}$  (KBr) 3423, 1724, 1670, 1589 cm<sup>-1</sup>; <sup>1</sup>H NMR (300, MHz, CDCl<sub>3</sub>): 11.42 (s, 1H), 8.59 (d, 1H, *J* = 8.3 Hz), 8.18 (s, 1H), 7.76 (d, 2H, *J* = 7.4 Hz), 7.66 (d, 1H, *J* = 7.3 Hz), 7.60 (d, 1H, *J* = 7.3 Hz); 7.53–7.28 (m, 9H), 7.17 (t, 1H, *J* = 7.3 Hz), 7.08 (d, 1H, *J* = 7.4 Hz), 7.02 (m, 1H), 6.96 (s, 1H), 6.72 (d, 1H, *J* = 7.6 Hz), 5.55 (d, 1H, *J* = 8.5 Hz), 5.06 (dd, 1H, *J* = 12.5 and 5.2 Hz), 4.40 (d, 1H, *J* = 6.6 Hz), 4.32–4.24 (m, 1H), 3.73 (s, 3H), 3.45–3.31 (m, 2H), 1.65 (s, 3H) 2.40–2.31 (m, 1H), 1.06 (d, 3H, *J* = 6.8 Hz), 0.98 (d, 3H, *J* = 6.9 Hz); <sup>13</sup>C NMR (75, MHz, CDCl<sub>3</sub>) 172.0 (CO), 170.2 (CO), 168.3 (CO), 156.5 (C), 144.1 (2C), 141.3 (2C), 139.0 (C), 136.1 (C), 132.9 (CH), 127.7 (2CH), 127.5 (C), 127.1 (2CH), 127.1(2CH), 126.9 (CH), 125.3 (CH), 125.2 (CH), 123.2 (CH), 122.8 (CH), 122.4 (CH), 121.4 (C), 120.2 (2CH), 119.8 (CH), 118.5 (C), 111.4 (CH), 109.7 (C), 67.2 (CH<sub>2</sub>), 61.3 (CH), 53.3 (CH), 52.6 (CH<sub>3</sub>), 47.3 (CH), 31.3 (CH), 27.3 (CH<sub>2</sub>), 19.4 (CH<sub>3</sub>), 17.6 (CH<sub>3</sub>).

### 3.5.3. Synthesis of (1*R*,4*R*)-4-(1*H*-indol-3-ylmethyl)-1-isopropyl-2*H*-pyrazino[2,1-*b*]quinazolin-3,6-(1*H*, 4*H*)-dione (**4d**)

To a solution of **vi-c** (183 mg, 0.278 mmol) in dried CH<sub>2</sub>Cl<sub>2</sub> (20 mL) was added Ph<sub>3</sub>P (365 mg, 1.4 mmol, 5 equiv), I<sub>2</sub> (345 mg, 1.36 mmol, 4.9 equiv), and *N,N*-diisopropylethylamine (489 μL, 2.81 mmol, 10 equiv). The reaction mixture was stirred at room temperature for 5 h, quenched with aqueous Na<sub>2</sub>CO<sub>3</sub>, and extracted with CH<sub>2</sub>Cl<sub>2</sub> (3 × 100 mL), dried with Na<sub>2</sub>SO<sub>4</sub>, filtered, and concentrated. Hexane was added to remove an excess of Ph<sub>3</sub>P, the precipitate was filtered and treated with CH<sub>2</sub>Cl<sub>2</sub> (10 mL) and piperidine (2.5 mL, 20%) at room temperature for 20 min, followed by solvent evaporation to provide

the solid which was triturated with hexane (1 × 200mL), CH<sub>2</sub>Cl<sub>2</sub>/PhMe (1 × 200 mL), and hexane (1 × 200 mL). The vacuum-dried crude residue was dissolved in CH<sub>3</sub>CN (10 mL) in the presence of DMAP (64 mg, 0.53 mmol) and refluxed for 19 h. The reaction mixture was purified by preparative TLC (EtOAc:MeOH:CH<sub>2</sub>Cl<sub>2</sub>, 50:2.5:47.5) to afford **4d** (22.4 mg, 21%), mp: 111.9–113.0 °C,  $[\alpha]_{D}^{30} = -210.53$  (*c* 0.114, MeOH), IR  $\nu_{max}$  (KBr) 3321, 3068, 1683, 1593, 1471, 1387, 1291 cm<sup>-1</sup>; <sup>1</sup>H NMR see Table 2; <sup>13</sup>C NMR see Table 3; *m/z* (rel. intensity, %): 385.9 (M<sup>+</sup>, 12), 257.1 (29), 214.1 (3), 202.0 (7), 171.1 (10), 143.1 (4), 130.1 (100), 103.0 (18), 77 (16); (+)-HRESIMS *m/z* 389.1776 (M + H)<sup>+</sup> (calculated for C<sub>23</sub>H<sub>22</sub>N<sub>4</sub>O<sub>2</sub>, 387.1809).

#### 3.5.4. Synthesis of *N*-[9*H*-fluoren-9-ylmethoxy)carbonyl]-*D*-methylpentyl-2-aminobenzoyl-*D*-tryptophan methyl ester (**vi-d**)

To a solution of **iv-b** (130 mg, 0.386 mmol) in dried CH<sub>2</sub>Cl<sub>2</sub> (10 mL) was added *N*-Fmoc-*D*-leucine-Cl [27] (**v-d**, 172.5 mg, 0.464 mmol). The mixture was stirred for 30 min, followed by addition of aqueous Na<sub>2</sub>CO<sub>3</sub> (1 M, 7.7 mL, 7.7 mmol). After continuous stirring for 3 h, the mixture was extracted with CH<sub>2</sub>Cl<sub>2</sub> (4×), dried with Na<sub>2</sub>SO<sub>4</sub>, filtered, and concentrated. The residue was purified by flash chromatography (eluent: 5% MeOH in CH<sub>2</sub>Cl<sub>2</sub>) to give **vi-d** as a white solid (251 mg, 98%), mp: 194.9–196.3 °C,  $[\alpha]_{D}^{30} = -31.75$  (*c* 0.105, CHCl<sub>3</sub>), IR  $\nu_{max}$  (KBr) 1740, 1645, 1584 cm<sup>-1</sup>; <sup>1</sup>H NMR (300, MHz, CDCl<sub>3</sub>): 11.5 (s, 1H), 8.58 (d, 1H, *J* = 8.3 Hz), 8.23 (s, 1H), 7.76 (d, 2H, *J* = 7.4 Hz), 7.66 (d, 1H, *J* = 7.4 Hz), 7.57 (d, 1H, *J* = 7.4 Hz), 7.51–7.26 (m, 8H), 7.16 (t, 1H, *J* = 7.4 Hz), 7.07 (d, 1H, *J* = 7.4 Hz), 7.00 (t, 1H, *J* = 7.5 Hz), 6.93 (s, 1H), 6.74 (d, 1H, *J* = 7.6 Hz), 5.43 (d, 1H, *J* = 7.9 Hz), 5.04 (dd, 1H, *J* = 12.7 and 5.2 Hz), 4.41 (dt, 3H, *J* = 17.5 and 10.4 Hz), 4.25 (t, 1H, *J* = 7.0 Hz), 3.72 (s, 3H), 3.38 (dd, 1H, *J* = 15.0 and 5.2 Hz), 3.31 (dd, 1H, *J* = 14.9 and 5.3 Hz), 1.82 (m, 1H), 1.00 (d, 6H, *J* = 6.2 Hz); <sup>13</sup>C NMR (75 MHz, CDCl<sub>3</sub>): 172.1 (CO), 170.2 (CO), 168.3 (CO), 156.4 (CO), 143.8 (2C), 141.3 (2C), 139.0 (C), 136.1 (C), 132.9 (CH), 127.7 (2CH), 127.5 (C), 127.1 (2CH), 127.1 (2CH), 126.9 (CH), 125.3 (CH), 125.2 (CH), 123.2 (CH), 122.8 (CH), 122.4 (CH), 121.4 (C), 120.2 (2CH), 119.8 (CH), 118.5 (C), 111.4 (CH), 109.7 (CH), 67.2 (CH<sub>2</sub>), 61.3 (CH), 53.3 (CH), 52.6 (CH<sub>3</sub>), 47.3 (CH<sub>2</sub>), 38.6 (CH), 31.4 (CH), 27.3 (CH<sub>2</sub>), 19.4 (CH<sub>3</sub>), 17.5 (CH<sub>3</sub>).

#### 3.5.5. Synthesis of (1*R*,4*R*)-4-(1*H*-indol-3-ylmethyl)-1-isobutyl-2*H*-pyrazino[2,1-*b*]quinazolin-3,6-(1*H*, 4*H*)-dione (**5d**)



To a solution of **vi-d** (251 mg, 0.373 mmol) in dried CH<sub>2</sub>Cl<sub>2</sub> (20 mL) was added Ph<sub>3</sub>P (489 mg, 1.9 mmol, 5 equiv), I<sub>2</sub> (464 mg, 1.83 mmol, 4.9 equiv), and *N,N*-diisopropylethylamine (656 μL, 3.77 mmol, 10 equiv). The reaction mixture was stirred at room temperature for 5 h, quenched with aqueous Na<sub>2</sub>CO<sub>3</sub>, and extracted with CH<sub>2</sub>Cl<sub>2</sub> (3 × 100 mL), dried with Na<sub>2</sub>SO<sub>4</sub>, filtered, and concentrated. Hexane was added to remove an excess of Ph<sub>3</sub>P, the precipitate was filtered and treated with CH<sub>2</sub>Cl<sub>2</sub> (10 mL) and piperidine (2.5 mL, 20%) at room temperature for 20 min, followed by solvent evaporation to provide the solid which was triturated with hexane (1 × 200 mL), CH<sub>2</sub>Cl<sub>2</sub>/PhMe (1 × 200 mL), and hexane (1 × 200 mL). The vacuum-dried crude residue was dissolved in CH<sub>3</sub>CN (10 mL in the presence of DMAP (84 mg, 0.82 mmol) and refluxed for 19 h. The reaction mixture was purified by preparative TLC (EtOAc:MeOH:CH<sub>2</sub>Cl<sub>2</sub>, 50:2.5:47.5) to afford **5d** (61.6 mg, 40%), mp: 103.2–105.6 °C, [α]<sup>30D</sup> = -186.04 (*c* 0.086, CHCl<sub>3</sub>), IR  $\nu_{max}$  (KBr) 3333, 3061, 1687, 1603, 1296 cm<sup>-1</sup>; <sup>1</sup>H NMR see Table 2; <sup>13</sup>C NMR see Table 3; (+)-HRESIMS *m/z* 401.1966 (M + H)<sup>+</sup> (calculated for C<sub>24</sub>H<sub>24</sub>N<sub>4</sub>O<sub>2</sub>, 401.1933).

#### 3.4. Screening Test for Antitumor and Anti-P-Glycoprotein Activity

Compounds **4a–d** and **5a–d** were reconstituted in sterile DMSO to the final concentration of 60 mM, and several aliquots were made and stored at -20 °C to avoid repeated freeze-thaw cycles. For experiments, the compounds were freshly diluted in medium to the desired concentration. Screening for tumor cell growth inhibition was carried out in two human tumor cell lines (NCI-H460 and HCT-15), with the sulforhodamine B (SRB) assay, as previously described [30]. Briefly, tumor cells were plated in 96-well plates, incubated at 37 °C for 24 h, and then treated for 48 h with 5 serial dilutions (1:2) of each compound (ranging from 150 μM to 9.375 μM). The effect of the vehicle solvent (DMSO) was also analyzed as a control. Cells were fixed with 10% ice-cold trichloroacetic acid, washed with water and stained with SRB. Finally, the plates were washed with 1% acetic acid and the bound SRB was solubilized with 10 mM Tris Base. Absorbance was measured in a microplate reader (Synergy Mx, Biotek Instruments Inc., Winooski, VT, USA) at 510 nm. For each compound, the corresponding GI<sub>50</sub> (concentration which inhibited 50% of net cell growth) was determined, as previously described [33]. For the screening of compounds for drug-efflux inhibitory activity, the flow cytometry determination of

rhodamine-123 cellular accumulation was carried out as previously described [34]. Briefly, K562 and K562Dox cells were incubated for 1 h at 37 °C with 20 µM of the compounds, and 1 µM of rhodamine-123 (Rh123, from Sigma, USA). Verapamil was used as a positive control. Cells were then washed, resuspended in ice cold PBS, and analyzed in a BD Accuri™ C6 Flow Cytometer (BD Biosciences, San Jose, CA, USA). Data were analyzed using the FlowJo software (version 7.6.1, Tree Star, Inc.). The ratio of Rh123 accumulation in the cells was then calculated as  $MFI_{K562Dox+Compound} - MFI_{K562Dox} / MFI_{K562Dox}$  [30].

#### 4. Conclusions

Inspired by the marine-derived fiscalin B (**4c**), quinazolinone alkaloid derivatives were synthesized using two different methodologies: a highly efficient and straightforward three-component one-pot microwave-assisted approach and also a multistep Mazurkiewicz–Ganesan approach. While the former proved to be efficient and practical for broad screening libraries of the compounds, the latter, although with a more intricate methodology, proved to be a good approach for the synthesis of the syn enantiomers. Moreover, we have found that partial epimerization under the reaction conditions could occur. In vitro growth inhibitory activity of two tumor cell lines revealed that among this series of synthesized compounds, six new analogues were found to exhibit tumor cell growth inhibitory activity. Consequently, this marine-inspired synthesis can bring new insights into discovery of new lead compounds in the oncology area.

**Supplementary Materials:** The following are available online at <http://www.mdpi.com/1660-3397/16/8/261/s1>.

**Author Contributions:** E.S. and A.K. conceived the study design. S.L. synthesized the compounds and elucidated their structure and, A.M.S.S., E.S., and M.M.M.P. analysed the data. D.I.S.P.R. performed the HPLC analysis. A.P. and T.F.-M. performed the cytotoxicity and anti-Pgp assays, and T.F.-M. and M.H.V. analyzed the data and discussed results. S.L. and E.S. wrote the manuscript, while all authors gave significant contributions in discussion and revision. All authors agreed to the final version of the manuscript.

**Funding:** This research was partially supported by the Strategic Funding UID/Multi/04423/2013 through national funds provided by FCT—Foundation for Science and Technology and European Regional Development Fund (ERDF), in the framework of the program PT2020. The authors thank to national funds provided by FCT—Foundation for Science and Technology and European Regional

Development Fund (ERDF) and COMPETE under the Strategic Funding UID/Multi/04423/2013, the projects POCI-01-0145-FEDER-028736, PTDC/MAR-BIO/4694/2014 (POCI-01-0145-FEDER-016790; 3599-PPCDT), and INNOVMAR—Innovation and Sustainability in the Management and Exploitation of Marine Resources, reference NORTE-01-0145-FEDER-000035, Research Line NOVELMAR. The work was also funded by FEDER—Fundo Europeu de Desenvolvimento Regional através do COMPETE 2020—Programa Operacional para a Competitividade e Internacionalização (POCI), Portugal 2020, and by Portuguese fundings through FCT—Fundação para a Ciência e a Tecnologia/Ministério da Ciência, Tecnologia e Inovação, no âmbito do projeto “Instituto de Investigação e Inovação em Ciências da Saúde “(POCI—01-0145-FEDER—007274)”.

**Acknowledgments:** S.L. thanks Erasmus Mundus Action 2 (LOTUS+, LP15DF0205) for full PhD scholarship. To Sara Cravo for technical support. To Centro de Apoio Científico e Tecnológico á Investigation (CACTI, University of Vigo, Pontevedra, Spain) for HRMS analysis.

**Conflicts of Interest:** The authors declare no conflicts of interest.

## References

1. Montaser, R.; Luesch, H. Marine natural products: A new wave of drugs? *Future Med. Chem.* **2011**, *3*, 1475-1489. doi:10.4155/fmc.11.118
2. Panda, S.; Tripathy, U.P. Quinazolone: A molecule of significant pharmacological and biological activity. *Res. J. of Pharm. Technol.* **2013**, *6*, 849-855.
3. Eguchi, S. Quinazoline alkaloids and related chemistry. In *Bioactive heterocycles i*, Eguchi, S., Ed. Springer Berlin Heidelberg: Berlin, Heidelberg, 2006; pp 113-156.
4. Peng, J.; Lin, T.; Wang, W.; Xin, Z.; Zhu, T.; Gu, Q.; Li, D. Antiviral alkaloids produced by the mangrove-derived fungus *cladosporium* sp. Pjx-41. *J. Nat. Prod.* **2013**, *76*, 1133-1140. doi:10.1021/np400200k
5. Zhou, Y.; Debbab, A.; Mándi, A.; Wray, V.; Schulz, B.; Müller, W.E.G.; Kassack, M.; Lin, W.; Kurtán, T.; Proksch, P., *et al.* Alkaloids from the sponge-associated fungus *aspergillus* sp. *Eur. J. Org. Chem.* **2013**, *2013*, 894-906. doi:10.1002/ejoc.201201220
6. He, F.; Han, Z.; Peng, J.; Qian, P.Y.; Qi, S.H. Antifouling indole alkaloids from two marine derived fungi. *Nat. Prod. Commun.* **2013**, *8*, 329-332.
7. Rodrigues, B.S.F.; Sahm, B.D.B.; Jimenez, P.C.; Pinto, F.C.L.; Mafezoli, J.; Mattos, M.C.; Rodrigues-Filho, E.; Pfenning, L.H.; Abreu, L.M.; Costa-Lotufo, L.V., *et al.*

- Bioprospection of cytotoxic compounds in fungal strains recovered from sediments of the brazilian coast. *Chem. Biodivers.* **2015**, *12*, 432-442. doi:10.1002/cbdv.201400193
8. Afiyatullof, S.S.; Zhuravleva, O.I.; Antonov, A.S.; Kalinovskiy, A.I.; Pivkin, M.V.; Menchinskaya, E.S.; Aminin, D.L. New metabolites from the marine-derived fungus *aspergillus fumigatus*. *Nat. Prod. Commun.* **2012**, *7*, 497-500.
  9. Shao, C.L.; Xu, R.F.; Wei, M.Y.; She, Z.G.; Wang, C.Y. Structure and absolute configuration of fumiquinazoline 1, an alkaloid from a gorgonian-derived *scopulariopsis* sp. Fungus. *J. Nat. Prod.* **2013**, *76*, 779-782. doi:10.1021/np4002042
  10. Liu, Y.; Li, X.M.; Meng, L.H.; Wang, B.G. N-formyllapatin a, a new n-formylspiroquinazoline derivative from the marine-derived fungus *penicillium adametzioides* as-53. *Phytochem. Lett.* **2014**, *10*, 145-148. doi:10.1016/j.phytol.2014.08.018
  11. Zin, W.W.M.; Prompanya, C.; Buttachon, S.; Kijjoa, A. Bioactive secondary metabolites from a thai collection of soil and marine-derived fungi of the genera *neosartorya* and *aspergillus*. *Curr. Drug Deliv.* **2016**, *13*, 378-388.
  12. Prata-Sena, M.; Ramos, A.A.; Buttachon, S.; Castro-Carvalho, B.; Marques, P.; Dethoup, T.; Kijjoa, A.; Rocha, E. Cytotoxic activity of secondary metabolites from marine-derived fungus *neosartorya siamensis* in human cancer cells. *Phytother. Res.* **2016**, *30*, 1862-1871. doi:10.1002/ptr.5696
  13. Liao, L.; You, M.; Chung, B.K.; Oh, D.-C.; Oh, K.-B.; Shin, J. Alkaloidal metabolites from a marine-derived *aspergillus* sp. Fungus. *J. Nat. Prod.* **2015**, *78*, 349-354. doi:10.1021/np500683u
  14. Liu, J.; Wei, X.; Kim, E.L.; Lin, X.; Yang, X.W.; Zhou, X.; Yang, B.; Jung, J.H.; Liu, Y. Erratum: Fumigatosides a-d, four new glucosidated pyrazinoquinazoline indole alkaloids from a jellyfish-derived fungus *aspergillus fumigatus* (org. Lett. (2014)). *Org. Lett.* **2014**, *16*, 2574. doi:10.1021/ol500243k
  15. Martine, D.; Isabelle, B. Survey of recent literature related to the biologically active 4(3h)-quinazolinones containing fused heterocycles. *Curr. Med. Chem.* **2013**, *20*, 794-814. doi:10.2174/0929867311320060006
  16. Penn, J.; Purcell, M.; Mantle, P.G. Biosynthesis of gyantrypine by *aspergillus clavatus*. *FEMS Microbiol. Lett.* **1992**, *92*, 229-233. doi:10.1016/0378-1097(92)90714-Y

17. Takahashi, C.; Matsushita, T.; Doi, M.; Minoura, K.; Shingu, T.; Kumeda, Y.; Numata, A. Fumiquinazolines a-g, novel metabolites of a fungus separated from a pseudolabrus marine fish. *J. Chem. Soc. Perkin Trans. 1* **1995**, 2345-2353. doi:10.1039/P19950002345
18. Wong, S.M.; Musza, L.L.; Kydd, H.G.C.; Kullnig, R.; Gillum, A.M.; Cooper, R. Fiscalins: New substance p inhibitors produced by the fungus neosartorya fischeri taxonomy, fermentation, structures, and biological properties. *J. Antibiot.* **1993**, *46*, 545-553. doi:10.7164/antibiotics.46.545
19. Avendaño, C.; Caballero, E.; Méndez-Vidal, C.; De Quesada, A.R.; Menéndez, J.C. Mdr reversal by deprenylated tetracyclic and hexacyclic analogues of n-acetylardeemin: Confirmation of the ardeemin pharmacophore. *Lett. Drug Des. Discov.* **2006**, *3*, 369-377. doi:10.2174/157018006777805558
20. Hayashi, D.; Tsukioka, N.; Inoue, Y.; Matsubayashi, Y.; Iizuka, T.; Higuchi, K.; Ikegami, Y.; Kawasaki, T. Synthesis and abcg2 inhibitory evaluation of 5-n-acetylardeemin derivatives the paper is dedicated to professor amos b. Smith, iii on the occasion of his 70th birthday. *Bioorg. Med. Chem.* **2015**, *23*, 2010-2023. doi:10.1016/j.bmc.2015.03.017
21. Buttachon, S.; Chandrapatya, A.; Manoch, L.; Silva, A.; Gales, L.; Bruyère, C.; Kiss, R.; Kijjoa, A. Sartorymensin, a new indole alkaloid, and new analogues of tryptoquivaline and fiscalins produced by neosartorya siamensis (kufc 6349). *Tetrahedron* **2012**, *68*, 3253-3262. <http://dx.doi.org/10.1016/j.tet.2012.02.024>
22. Bessa, L.J.; Buttachon, S.; Dethoup, T.; Martins, R.; Vasconcelos, V.; Kijjoa, A.; da Costa, P.M. Neofiscalin a and fiscalin c are potential novel indole alkaloid alternatives for the treatment of multidrugresistant gram-positive bacterial infections. *FEMS Microbiol. Lett.* **2016**, *363*. doi:10.1093/femsle/fnw150
23. Cledera, P.; Avendaño, C.; Menéndez, J.C. A new route toward 4-substituted pyrazino[2,1-b]quinazoline-3,6-dione systems. Total synthesis of glyantrypine. *J. Org. Chem.* **2000**, *65*, 1743-1749. doi:10.1021/jo991626e
24. Wang, H.; Ganesan, A. Total synthesis of the quinazoline alkaloids (-)-fumiquinazoline g and (-)-fiscalin b. *J. Org. Chem.* **1998**, *63*, 2432-2433.

25. Wang, H.; Ganesan, A. Total synthesis of the fumiquinazoline alkaloids: Solution-phase studies. *J. Org. Chem.* **2000**, *65*, 1022-1030. 10.1021/jo9914364
26. Liu, J.F.; Ye, P.; Zhang, B.; Bi, G.; Sargent, K.; Yu, L.; Yohannes, D.; Baldino, C.M. Three-component one-pot total syntheses of gyantrypine, fumiquinazoline f, and fiscalin b promoted by microwave irradiation. *J. Org. Chem.* **2005**, *70*, 6339-6345. doi:10.1021/jo0508043
27. Kantharaju; Patil, B.S.; Suresh Babu, V.V. Synthesis of fmoc-amino acid chlorides assisted by ultrasonication, a rapid approach. *Int. J. Pept. Res. Ther.* **2002**, *9*, 227-229.
28. Hernández, F.; Buenadicha, F.L.; Avendao, C.; Söllhuber, M. 1-alkyl-2,4-dihydro-1h-pyrazino[2,1-b]quinazoline-3,6-diones as glycine templates. Synthesis of fiscalin b. *Tetrahedron Asymmetry* **2002**, *12*, 3387-3398. doi:10.1016/S0957-4166(02)00027-7
29. Vichai, V.; Kirtikara, K. Sulforhodamine b colorimetric assay for cytotoxicity screening. *Nat. Protoc.* **2006**, *1*, 1112-1116. doi:10.1038/nprot.2006.179
30. Lopes-Rodrigues, V.; Oliveira, A.; Correia-da-Silva, M.; Pinto, M.; Lima, R.T.; Sousa, E.; Vasconcelos, M.H. A novel curcumin derivative which inhibits p-glycoprotein, arrests cell cycle and induces apoptosis in multidrug resistance cells. *Bioorg.Med. Chem.* **2017**, *25*, 581-596. doi:10.1016/j.bmc.2016.11.023
31. Han, X.-x., XU Xiao-yan, CUI Cheng-bin, Gu Qian-qun. Alkaloidal compounds produced by a marine-derived fungus, *aspergillus fumigatus* h1-04, and their antitumor activities. *J. Chin. Med. Chem.* **2007**, *4*, 232.
32. Yu, G.; Zhou, G.; Zhu, M.; Wang, W.; Zhu, T.; Gu, Q.; Li, D. Neosartoryadins a and b, fumiquinazoline alkaloids from a mangrove-derived fungus *neosartorya udagawae* hdn13-313. *Org. Lett.* **2016**, *18*, 244-247. doi:10.1021/acs.orglett.5b02964
33. Kijjoa, A.; Santos, S.; Dethoup, T.; Manoch, L.; Almeida, A.P.; Vasconcelos, M.H.; Silva, A.; Gales, L.; Herz, W. Sartoryglabrin, analogs of ardeemins, from *neosartorya glabra*. *Nat. Prod. Commun.* **2011**, *6*, 807-812.
34. Palmeira, A.; Vasconcelos, M.H.; Paiva, A.; Fernandes, M.X.; Pinto, M.; Sousa, E. Dual inhibitors of p-glycoprotein and tumor cell growth: (re)discovering thioxanthenes. *Biochem. Pharmacol.* **2012**, *83*, 57-68. doi:10.1016/j.bcp.2011.10.004



© 2018 by the authors. Licensee MDPI, Basel, Switzerland. This article is an open access article distributed under the terms and conditions of the Creative Commons Attribution (CC BY) license (<http://creativecommons.org/licenses/by/4.0/>).

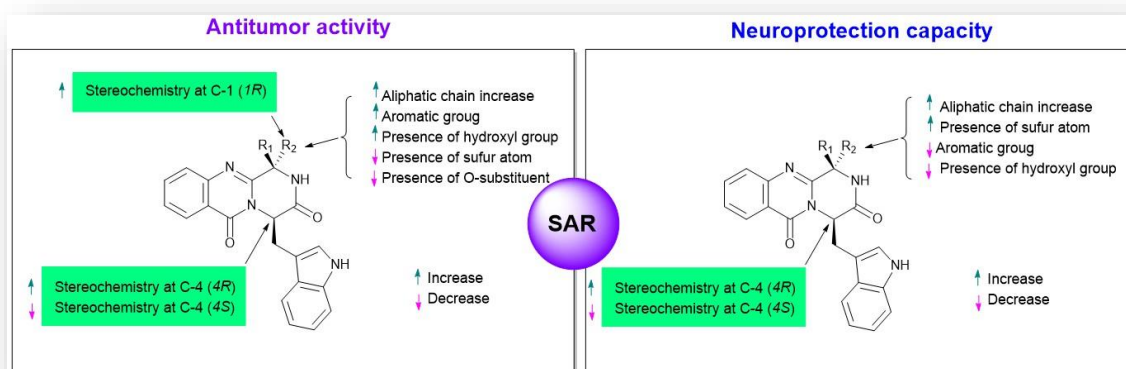




# Chapter 4

## Synthesis of new proteomimetic quinazolinone alkaloids and evaluation of their neuroprotective and antitumor effects

Graphical abstract





Article

# Synthesis of New Proteomimetic Quinazolinone Alkaloids and Evaluation of Their Neuroprotective and Antitumor Effects

Solida Long <sup>1</sup>, Diana I. S. P. Resende <sup>1,2</sup>, Anake Kijjoa <sup>2,3</sup>, Artur M. S. Silva <sup>4</sup>, Ricardo Fernandes <sup>5,6</sup>, Cristina P. R. Xavier <sup>5,6</sup>, M. Helena Vasconcelos <sup>5,6,7</sup>, Emília Sousa <sup>1,2,\*</sup> and Madalena M. M. Pinto <sup>1,2</sup>

<sup>1</sup> Laboratory of Organic and Pharmaceutical Chemistry (LQOF), Department of Chemical Sciences, Faculty of Pharmacy, University of Porto, Rua de Jorge Viterbo Ferreira, 228, 4050-313 Porto, Portugal; up201502099@ff.up.pt (S.L.); dresende@ff.up.pt (D.I.S.P.R.); madalena@ff.up.pt (M.M.M.P)

<sup>2</sup> Interdisciplinary Centre of Marine and Environmental Research (CIIMAR), 4450-208 Matosinhos, Portugal

<sup>3</sup> ICBAS-Instituto de Ciências Biomédicas Abel Salazar, University of Porto, 4050-313 Porto, Portugal; ankijjoa@icbas.up.pt

<sup>4</sup> Organic Chemistry and Natural Products Unit (QOPNA), Department of Chemistry, University of Aveiro, 3810-193 Aveiro, Portugal; artur.silva@ua.pt

<sup>5</sup> Instituto de Investigação e Inovação em Saúde (i3S), University of Porto, 4200-135 Porto, Portugal; ricardojorgefernandes@gmail.com (R.F.); hvasconcelos@ipatimup.pt (M.H.V.)

<sup>6</sup> Cancer Drug Resistance Group, Institute of Molecular Pathology and Immunology of the University of Porto (IPATIMUP), 4200-135, Porto, Portugal; cristinax@ipatimup.pt

<sup>7</sup> Laboratory of Microbiology, Department of Biological Sciences, Faculty of Pharmacy, University of Porto, 4050-313 Porto, Portugal

\* Correspondence: [esousa@ff.up.pt](mailto:esousa@ff.up.pt); Tel.: +351-2-2042-8689

Received: 8 January 2019; Accepted: 30 January 2019; Published: 1 February 2019

**Abstract:** New quinazolinone derivatives of the marine-derived alkaloids fiscalin B (**3**) and fumiquinazoline G (**1**), with neuroprotective and antitumor effects, were synthesized. Eleven quinazolinone-containing indole alkaloids were synthesized, proceeding the *anti* analogs via a one-pot method, and the *syn* analogs by the Mazurkiewicz-Ganesan approach. The neuroprotection capacity of these compounds on the rotenone-damage human neuroblastoma cell SH-SY5y was evaluated using the MTT assay. Compounds **1**, **3**, **5**, and **7** showed more than 25% protection. The antitumor activity was investigated using the sulforhodamine B assay and some compounds were tested on the non-malignant

MCF-12A cells. Fumiquinazoline G (**1**) was the most potent compound, with GI<sub>50</sub> values lower than 20 μM. Compounds **5**, **7**, and **11** were more active in all tumor cell lines when compared to their enantiomers. Compounds **5**, **7**, **10**, and **11** had very little effect in the viability of the non-malignant cells. Differences between enantiomeric pairs were also noted as being essential for these activities the *R*-configuration at C-4. These results reinforce the previously described activities of the fiscalin B (**3**) as substance P inhibitor and fumiquinazoline G (**1**) as antitumor agent showing potential as lead compounds for the development of drugs for treatment of neurodegenerative disorders and cancer, respectively.

**Keywords:** antitumor; neuroprotection; quinazolinones; fiscalin B; fumiquinazoline; enantioselectivity.

---

## 1. Introduction

The pathophysiology of neurodegenerative diseases is poorly understood, and there are few therapeutic options, making neuroprotective drug discovery appealing for medicinal chemists. Although cancer and neurodegeneration have very distinct pathological disorders, over recent years growing evidence indicates that they share common molecular pathways [1]. Furthermore, it is recognized that several drugs used in the treatment of neurodegenerative diseases display antitumor effects while some antitumor drugs are neuroprotective [2].

Marine-derived indolylmethylpyrazinoquinazoline alkaloids, with a pyrazino[2,1-*b*]quinazoline-3,6-dione linked to an indole moiety (Figure 1), have attracted our attention due to their promising antitumor activities [3], with *epi*-fiscalin A [4], fumiquinazoline A [5–9], fumiquinazoline G [7], and versiquinazolines [10] as the most active analogs. Moreover, the response of fiscalins A–C [11] and (–)-spiroquinazoline [12] (Figure 1A) as substance P inhibitors was also reported as a novel neuroprotective therapy in the intrastriatal 6-hydroxydopamine model of early stage of Parkinson’s disease (PD) [13]. It is

well known that among compounds implicated in neurodegeneration, non-proteinogenic amino acids may cause significant collateral neurodegenerative damage [14].

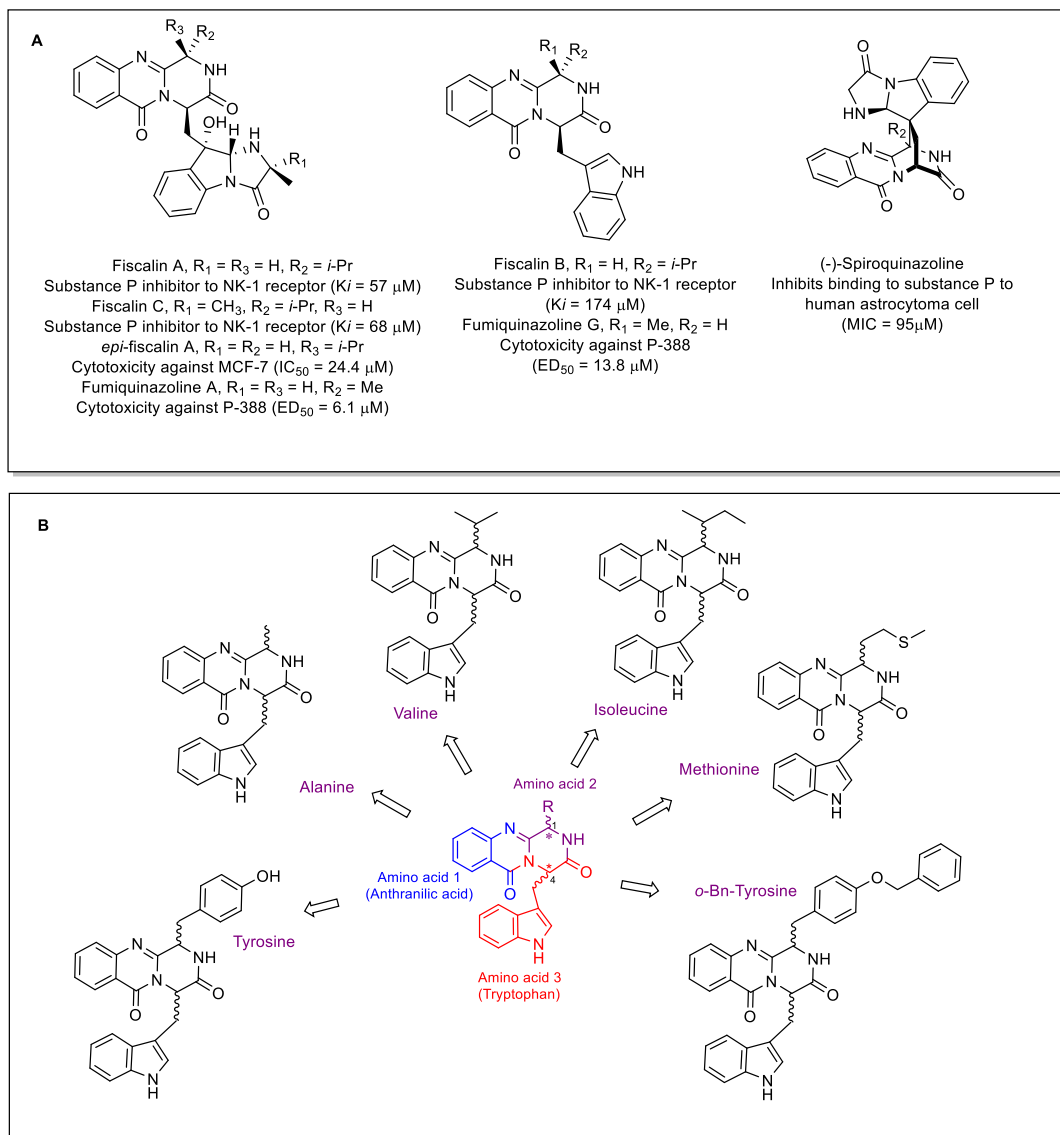


**Figure 1:** (A) Structure of natural quinazolinone-containing piperazine linked to an indole moiety such as substance P receptor antagonists and antitumor agents. (B) Proposed conformation constraint peptidomimetics synthetic quinazolinone alkaloids with different substituents at C-1.2.

Rodgers *et al.* [15] reported that proteomimetic L-tyrosine of L-DOPA is cytotoxic *in vitro* and capable of generating protein aggregation, whereas non-protein amino acid  $\beta$ -methylamino-L-alanine (BMAA) has been linked to neurological diseases such as amyotrophic lateral sclerosis (ALS) and PD since BMAA was detected in brain protein of

LAS and PD patients. In the previous work, we have described syntheses of a series of fiscalin B derivatives, which showed weak to moderate antitumor activity against non-small cell lung cancer (NCI-H460) and colorectal adenocarcinoma (HCT-15) cell lines [16]. These findings led us to develop a small library of proteomimetic quinazolinone-derived compounds (Figure 1B) with different configurations at C-1 and C-4 to investigate their action on neurodegenerative disorders as well as to further explore their potential as tumor cell growth inhibitors, putting in evidence the influence of the stereochemistry of the derivatives.

## 2. Results

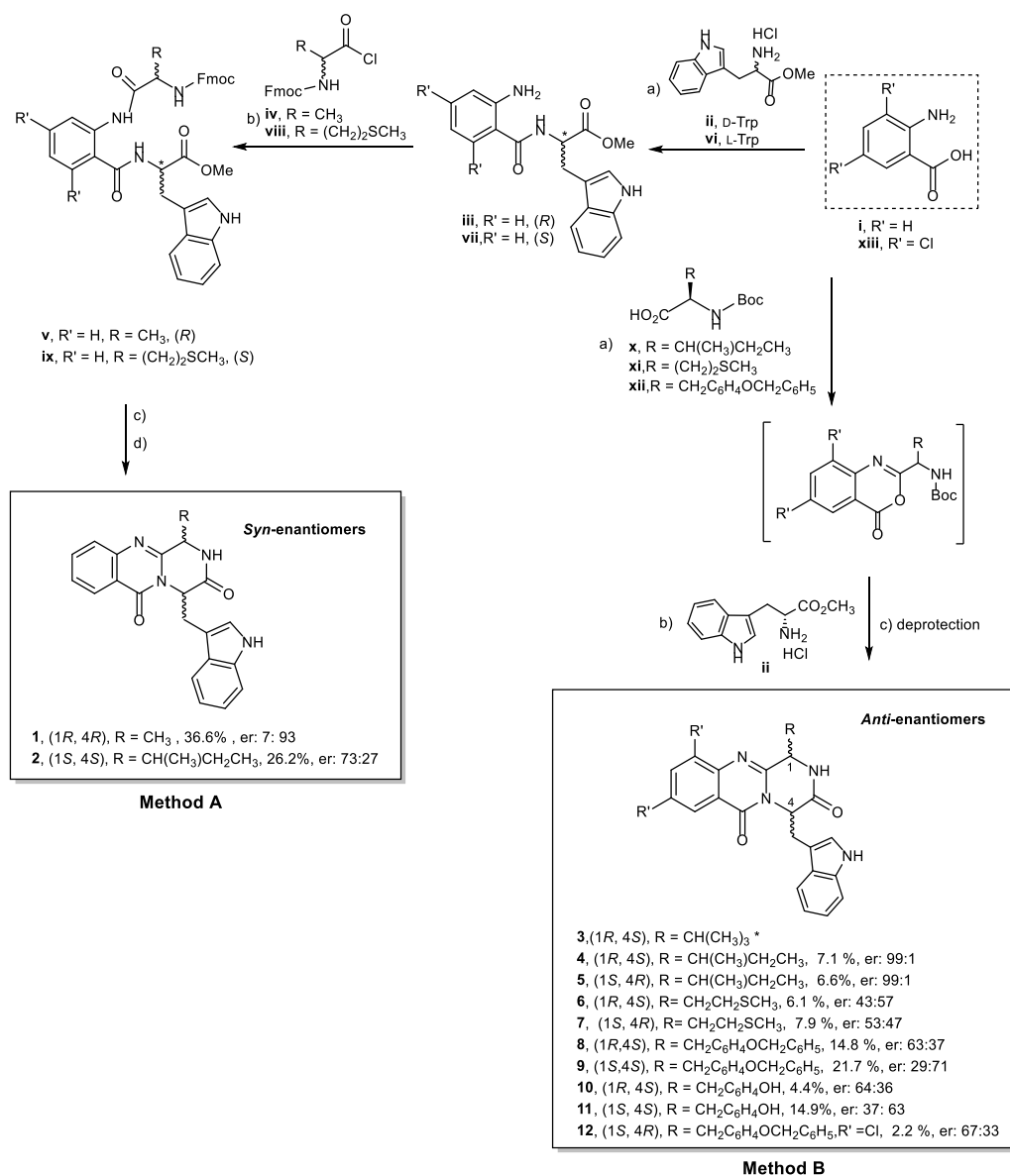
### 2.1. Chemistry

Two synthetic approaches were used to prepare the *syn* and *anti* enantiomers of quinazolinone alkaloids. The *syn* enantiomers **1** (fumiquinazoline G) and **2** were synthesized by the Mazurkiewicz-Ganesan procedure [17] (Scheme 1.A) by coupling anthranilic acid (**i**) with D-tryptophan methyl ester (**ii**) for **1** or with L-tryptophan methyl ester (**vi**) for **2**, using 1,1,3,3-tetramethylammonium tetrafluoroborate (TBTU) in alkaline condition to obtain the dipeptide **iii** or **vii**. Then, the coupling of **iii** or **vii** with N-protected  $\alpha$ -amino acid chloride in a two-phase Schotten-Baumann condition yielded a tripeptide (dehydrate  $\beta$ -keto amides) **v** or **ix**. The oxazole intermediates were obtained by adding the dehydrating agent, triphenylphosphine (Ph<sub>3</sub>P), and I<sub>2</sub> to dehydrate  $\beta$ -keto amide **v** or **ix**, and N-deprotection by 20% piperidine afforded **1** and **2**. On the other hand, a highly effective and environmentally friendly approach using a microwave-assisted multicomponent polycondensation of amino acids was used to prepare a series of the *anti* enantiomers of pyrazinoquinazoline alkaloids [18], as described in our previous work [16]. This methodology was used to synthesize new derivatives of fiscalin B (**3**) and fumiquinazoline G (**1**), **4**, **5**, **6**, **7**, and **8** (Scheme 1.B). The *syn* isomer **9** was obtained along with **8**, and both were isolated by preparative thin layer chromatography (TLC). Diastereoisomers of **10** and **11** were obtained after deprotection of O-benzyl group from **8** and **9**, respectively, using boron trichloride, according to Okaya et al. [20] with a slight modification. Compound **12** was also synthesized using microwave irradiation from 3,5-

dichloroanthranilic acid (**xiii**). The purity of the compounds was determined by a reversed-phase liquid chromatography (LC, C18, MeOH:H<sub>2</sub>O; 60:40 or CH<sub>3</sub>CN:H<sub>2</sub>O; 50:50) and was found to be higher than 90%. The enantiomeric ratio (er) was determined by a chiral LC equipped with amylose tris-3,5-dimethylphenylcarbamate column, using hexane:EtOH (80:20) or (70:30) as a mobile phase.

The reaction carried out using microwave with high temperature resulted not only in low yields of the products in the range of 2.2 to 21.7%, but also with a high degree of epimerization (Scheme 1). Contrary to what has been found in our previous study [16] that the reaction under a microwave irradiation was regioselective and yielded only *anti* isomers, the synthesis of **8**, by a microwave irradiation, produced also its *syn* epimer, **9** [4-(benzyloxy)-1-methylbenzyl at C-1], with a 22% yield. This study suggested that microwave irradiation is beneficial for the synthesis of quinazolinone alkaloids with bulky substituents at C-1 which was previously reported as unsuccessful by Mazurkiewicz-Ganesan method [17]. However, this methodology failed for the synthesis of *syn* enantiomers as described in the experimental section for **4** and **6**. The *syn* enantiomers of **1** and **2** were synthesized by Mazurkiewicz-Ganesan approach [17] and gave moderate yields (37 and 26%, respectively). Compounds **10** and **11** were obtained by deprotection in good yields (30 and 69%, respectively).

Moreover, the methodology involving microwave irradiation was characterized by producing partial epimerizations. Surprisingly, **4** and **5**, with three stereogenic centers, gave a higher enantiomeric ratio (er) of 99%. Similar to the previous report for fiscalin B analogs [16], the multi-step approach gave a better yield and, in most cases, higher enantiomeric ratios due to milder conditions; nonetheless, the one-pot reaction is a faster alternative to provide *anti* enantiomers with diversity of substituents at C-1.



**Scheme 1. (A)** Mazurkiewicz-Ganesan approach for **1** and **2**. Reagents and conditions (a) CH<sub>3</sub>CN, TBTU, Et<sub>3</sub>N, rt, 5 h; (b) CH<sub>2</sub>Cl<sub>2</sub>/aq.Na<sub>2</sub>CO<sub>3</sub>, rt, 3 h; (c) dried CH<sub>2</sub>Cl<sub>2</sub>, Ph<sub>3</sub>P, I<sub>2</sub>, EtN(i-Pr)<sub>2</sub>, rt, overnight; (d) piperidine in CH<sub>2</sub>CH<sub>2</sub>, rt, 12 min, then CH<sub>3</sub>CN, DMAP, reflux 19 h. Fmoc = fluorenylmethyloxycarbonyl; DMAP = 4-(dimethylamino)pyridine, TBTU = 1,1,3,3-tetramethylammonium tetrafluoroborate. **(B)** One-pot synthesis of pyrazinoquinazolinone alkaloids **3**, **4**, **5**, **6**, **7**, **8**, **9**, **10**, **11**, and **12**. Reagents and conditions: a) dried pyridine, (PhO)<sub>3</sub>P, 55 °C, 16-24 h; b) dried pyridine, (PhO)<sub>3</sub>P, 220 °C, 1.5 min; c) BCl<sub>3</sub>, CH<sub>2</sub>Cl<sub>2</sub>, -78 °C for 10 min then 25 °C for 6 h; Boc = tert-butyloxycarbonyl, R' = H when no mentioned; er = enantiomeric ratio calculated from the peak area from chiral LC experiments (by using equation  $X \times 100/X_n$  in which X is the peak area of each peak and X<sub>n</sub> is the total peak area. \* referred to previous work [16].



## 2.2. Structure Elucidation

A series of 1D and 2D NMR experiments and HRMS were used to confirm the structures of all the new compounds (Supplementary information, Figures S1–S57). The amide proton (H-2) appeared as a broad singlet (*brs*) in the *anti* isomers, i.e., **4**, **5**, **6**, **7**, **8**, **10**, and **12**, but as a doublet (*d*) in the *syn* isomers, i.e., **1**, **2**, **9**, and **11** (Supplementary information, Figure S1-21). Each stereoisomer exhibited different chemical shift values for H-2, H-4, and H-1. For example, for isomers **2**, **4**, and **5**, with the isobutyl group at C-1, the *syn* and the *anti* isomers were distinguished by the chemical shift values of H-1 and H-1'; which were *ca.*  $\delta_{\text{H}}$  4.03 and 0.93, respectively for the *syn* isomer (**2**), and at *ca.*  $\delta_{\text{H}}$  2.80 and 2.3, respectively, for the *anti* isomers (**4** and **5**), due to the absence of the shielding effect by the aromatic ring of the indole moiety [20].

This assignment was also confirmed by HMBC correlations which distinguished between the isomers of **2**, **4**, and **5** by the presence or absence of correlations from H-2 to C-3, C-4, and C-14. In **2**, H-2 showed no correlation to C-3, C-4, and C-14 whereas in **4** and **5**, H-2 showed correlations to those three carbons. H-4 also showed correlations to different carbons among isomers. H-4 showed correlations to C-3 and C-4' in **2**, but to C-3, C-14, C-4', and C-5' in **4**, while there were no such correlations observed in **5**. H-1 of the *syn* isomer of **2** showed correlation only to C-14 while in the *anti* isomer of **4** and **5**, it displayed correlations to C-14, C-1' and C-3'' (Figure 2). In contrast, in **1**, H-2 and H-4 showed no correlations to carbons that are two or three bonds away ( $^2J$  or  $^3J$ ), and H-1 showed cross peaks to C-3 and C-14. Furthermore, H-8 and H-10 of **12** (with Cl at C-9 and C-11) appeared as two doublets ( $\delta_{\text{H}}$  8.26,  $J = 2.4$  Hz and  $\delta_{\text{H}}$  7.85,  $J = 2.4$  Hz, respectively) while in other compounds H-8 appeared as a double doublet and H-10 as double-double doublet. The NOESY spectrum for compound **6** with an *anti* configuration (*1R*, *4S*) showed correlations from H-1 to H-1' and H-3' (methyl group attached to S atom) and H-2, while H-4 showed cross peak to H-4' (Supplementary information, Figure S56). The NOESY spectrum for the *syn* configuration compound **2** (*1S*, *4S*) exhibited correlations between H-1 and H-1', H-2', H-3'', and H-2 as well as from H-4 to H-4'. Also, correlations between H-4' and H-1' in the *syn* configuration compound **2** could be noted while these were absent in the *anti* configuration compound **6** (Supplementary information, Figure S-57). These observations were similar to the previously described for fiscalin B isomers [16].

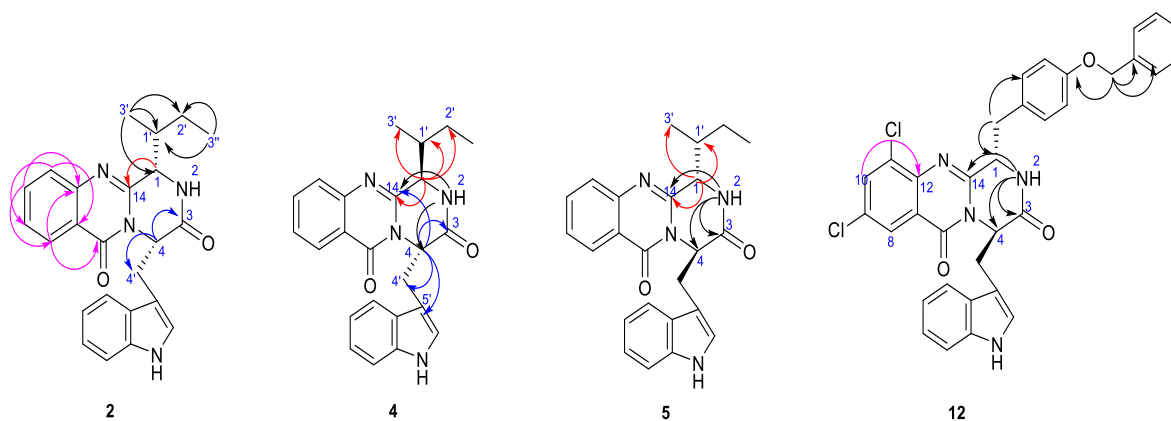


**Figure 2.** Key HMBC correlations for **2**, **4**, **5**, and **12**.

### 2.3 Neuroprotection Activity

The neuroprotection assay was performed on human neuroblastoma cell SH-SY5y treated with rotenone, a toxin that acts by interfering with the electron transport chain in mitochondria, inhibiting the transfer of electron from iron-sulfur centers in complex I to ubiquinone. This in turn interferes with NADH, therefore creating reactive oxygen species (ROS), which can damage DNA and other components, leading to cell death [21,22]. In animal experimentation, rotenone reproduces features of PD, including selective nigrostriatal dopaminergic degeneration and alpha-synuclein-positive cytoplasmic inclusions [23]. Furthermore, rotenone triggers mitochondrial impairment, oxidative damage, and cell death in neuronal culture, phenomena that are common in neurodegenerative diseases [24].

In this assay, the SH-SY5y cells were treated with 2  $\mu$ M of rotenone for 24 h. The MTT assay, which assesses cell metabolic activity through the activity of NAD(P)H-dependent cellular oxidoreductase enzyme that reflect the number of viable cells [24], was used for quantifying the cell death. The cellular protection of **1**, **2**, **4**, **5**, **6**, **7**, **8**, **9**, **10**, **11**, and **12** against the toxin was determined by MTT assay and expressed as percentage referred to the cell treated with rotenone at 10 different concentrations to produce the dose-dependent curve. Synthetic fiscalin B (**3**), previously obtained by some of us [16] and was reported as a substance P antagonist [12], was also tested in this assay for comparison.

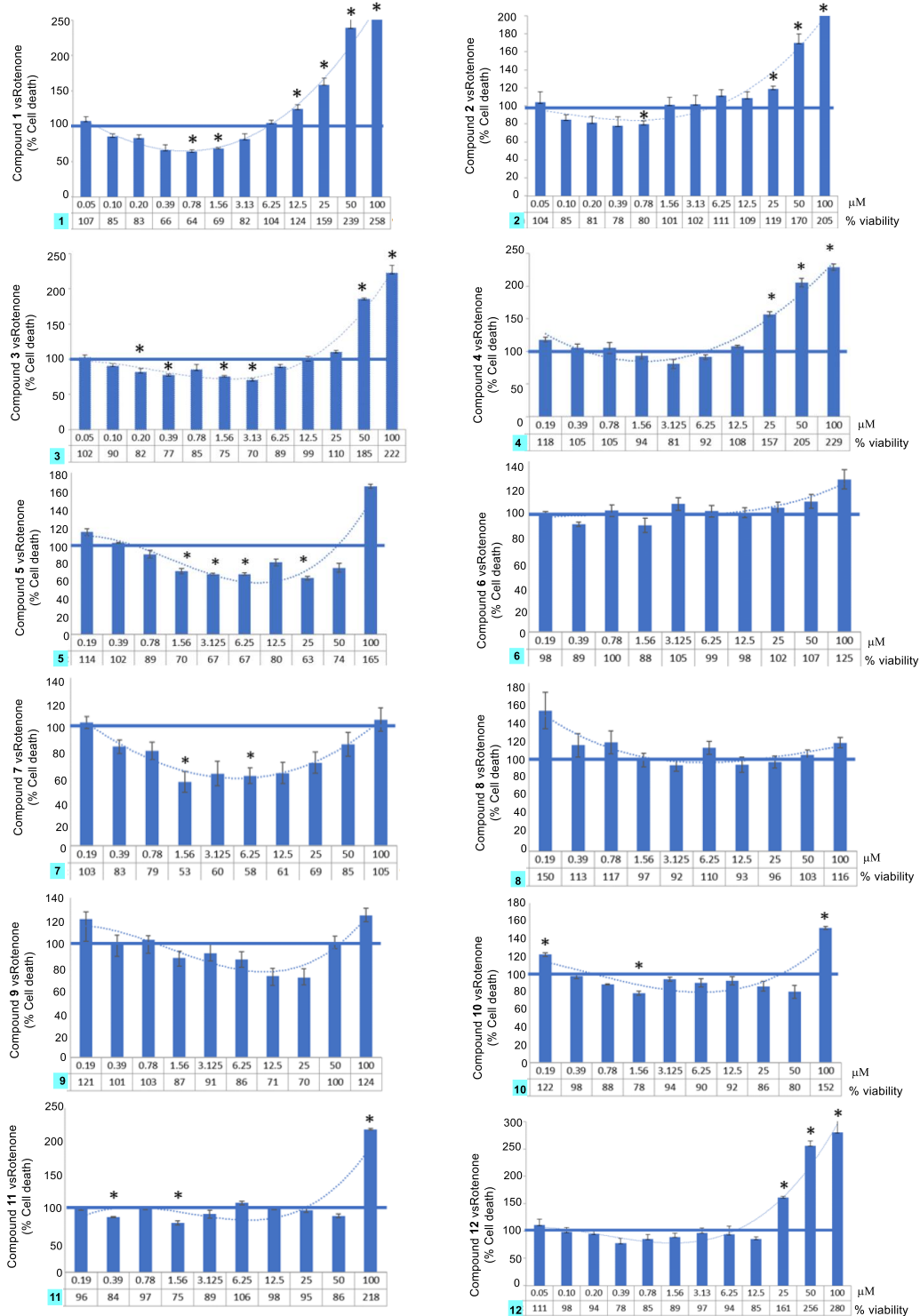


**Figure 3.** Neuroprotective effect of 1–12 against rotenone-induced neuron cell death. Neuroblastoma cells were treated with 2  $\mu$ M rotenone to induce cell injury. Compounds were assayed at several concentrations (0.1 to 100  $\mu$ M) for 24 h. Cell death was determined using MTT test. The data represent the percentage of rotenone-induced cell death (means and errors), performed in triplicate. Statistical significance of differences from rotenone-treated cells was examined with the Student’s t-test (\* $p < 0.05$ ).

Compounds considered as neuroprotective must have (i) more than 25% of protection, (ii) statistically significant difference, and (iii) protection is more than one dose [23,24].

Most of the compounds, at the highest concentration tested (100  $\mu\text{M}$ ), were found to increase toxicity, which ensures that the compounds were assayed at their maximal tolerated dose (MTD). Compounds **1**, **2**, **3**, **4**, **5**, **10**, **11**, and **12** showed high toxicity at 100  $\mu\text{M}$  and some of them also at 50  $\mu\text{M}$ . The compounds which showed neuroprotective activity in rotenone-treated *in vitro* model were **1**, **3**, **5**, and **7**. Additionally, some neuroprotective effect was also observed for **11** while **2**, **4**, **6**, **8**, **9**, **10**, and **12** did not display any neuroprotection (Figure 3). Compound **1**, **3**, **5**, and **7** showed more than 25% of protection of the cell death at least in one concentration. Compound **7** exhibited the best neuroprotective activity, with rotenone inhibitory of 47, 40, 42, 39, and 31% at the concentrations of 1.56, 3.13, 6.25, 12.5, and 25  $\mu\text{M}$ , respectively.

#### 2.4. Tumor Cell Growth Inhibitory Activity

Compounds **1–2**, **4–8**, **10** and **11** were tested for tumor cell growth inhibitory activity on three human tumor cell lines: NCI-H460 (non-small cell lung cancer), BxPC3 (human pancreatic adenocarcinoma), and PANC1 (human pancreatic adenocarcinoma) using the sulforhodamine B (SRB) colorimetric assay [16,25]. Cells were exposed to five concentrations of each compound (at a maximum concentration of 25, 150 or 200  $\mu\text{M}$ , depending on the compound) for 48 h. Doxorubicin was used as a positive control for NCI-H460 cell line, and gemcitabine was used as a positive control for the BxPC3 and PANC1 cell lines. The antitumor activity was reported as  $\text{GI}_{50}$  concentration (drug concentration that inhibits the growth of cancer cells by 50%).

Compounds **2**, **4–8**, **10**, and **11** showed weak to moderate growth inhibitory, with  $\text{GI}_{50}$  ranking from  $27.93 \pm 0.8$  to  $151.07 \pm 2.9$   $\mu\text{M}$  (Table 2). In general, compounds with the indolylmethyl substituent on C-4 whose configuration of C-4 is *R* showed better antitumor activity in all cell lines when compared to those with *4S* configuration. This was evidenced by stronger antitumor activities of **1**, **5**, and **7** than those of **2**, **4**, and **6**. Only fumiquinazoline **G (1)** with *R*-configuration for both C-1 and C-4 showed strong growth inhibitory effect in all cancer cell lines tested ( $\text{GI}_{50}$  ranging from  $7.62 \pm 0.7$  to  $17.34 \pm 1.7$   $\mu\text{M}$ ). In addition, these

results agree with those reported in our previous publication in which enantiomers with *R*-configuration at C-1 and C-4 showed better antitumor activity than enantiomers with *S*-configuration [16]. Unfortunately, **9** and **12** tested in this study could not be evaluated regarding their tumor cell growth inhibitory activity due to contamination of the compounds (data not shown).

**Table 2:** Growth inhibition ( $GI_{50}$ ) concentration of **1–2**, **4–8**, **10**, and **11** against NCI-H460, BxPC3, and PANC1 human tumor cell lines.

Compounds	$GI_{50}$ ( $\mu$ M)		
	NCI-H460	BxPC3	PANC1
<b>1</b>	7.62 $\pm$ 0.7	17.34 $\pm$ 1.7	10.06 $\pm$ 0.8
<b>2</b>	65.38 $\pm$ 4.0	104.77 $\pm$ 10.9	86.30 $\pm$ 11.1
<b>4</b>	69.26 $\pm$ 2.9	88.81 $\pm$ 9.6	78.17 $\pm$ 8.4
<b>5</b>	40.11 $\pm$ 5.0	57.44 $\pm$ 4.7	60.68 $\pm$ 4.8
<b>6</b>	151.07 $\pm$ 2.9	126.06 $\pm$ 21.5	112.44 $\pm$ 12.7
<b>7</b>	61.37 $\pm$ 2.3	99.10 $\pm$ 5.8	76.65 $\pm$ 4.8
<b>8</b>	72.68 $\pm$ 6.2	115.42 $\pm$ 12.1	74.90 $\pm$ 7.2
<b>10</b>	38.00 $\pm$ 1.5	50.59 $\pm$ 2.3	34.13 $\pm$ 1.8
<b>11</b>	46.25 $\pm$ 5.8	29.87 $\pm$ 3.7	27.93 $\pm$ 0.8
<b>Gemcitabine</b>	-	0.20 $\pm$ 0.08	0.73 $\pm$ 0.22
<b>Doxorubicin</b>	0.0124 $\pm$ 0.0018	-	-

The  $GI_{50}$  concentrations ( $\mu$ M) were determined by the SRB assay and results are the mean of  $\pm$  SEM of three independent experiments. Gemcitabine was used as a positive control for the BxPC3 and PANC1 cell lines, and doxorubicin as a positive control for the NCI-H460 cell line. (-) indicates not-determined.

### 2.5. Activity in Non-Tumor Cells

Compounds presenting the best neuroprotection and/or antitumor effects, namely **5**, **7**, **10**, and **11**, were also evaluated against the non-malignant MCF-12A human breast epithelial cells. For that, one concentration of each compound (corresponding to approximately the highest  $GI_{50}$  value obtained in the cell growth inhibitory activity assay)

was tested and the percentage of cell growth inhibition was determined by the SRB assay. In this assay, the duration of the SRB assay had to be longer since non-malignant cells have a much slower growth rate than tumor cells. This longer duration of the assay also allowed to evaluate possible delayed effects of the compounds in these non-malignant cells. Therefore, the assay in the MCF-12A cells was performed following 7 days of treatment with compounds (48 h with compound incubation plus 5 days without the compounds). As shown in Table 3, all the tested compounds caused a small effect in the growth of these non-malignant cells, meaning that the cell growth inhibition detected in MCF-12A cells after 7 days of treatment was much lower than that detected in the tumor cell lines after 2 days of treatment (when tested at the same concentration).

**Table 3.** The percentage of cell growth inhibition (relative to the control) of **5**, **7**, **10**, and **11** in the non-malignant MCF-12A human breast epithelial cells.

<b>Compounds</b>	<b>Concentration (<math>\mu\text{M}</math>) *</b>	<b>% Cell growth inhibition (relative to the control)</b>
<b>5</b>	65	71.69 $\pm$ 7.9
<b>7</b>	100	89.56 $\pm$ 3.7
<b>10</b>	50	75.63 $\pm$ 4.7
<b>11</b>	50	71.15 $\pm$ 2.0

\*These concentrations correspond to approximately the highest GI<sub>50</sub> concentrations determined in the tumor cell lines tested (from Table 2). The values were determined by the SRB assay and results are the mean of  $\pm$  SEM of three independent experiments.

### 3. Structural-Activity Relationship (SAR)

Structure-activity relationship analysis showed that the obtained results were consistent with data previously reported for the natural product fumiquinazoline G [26] and fiscalin B [11,27–29] and their derivatives [16] (Figure 4). Moreover, it was found that the configurations of C-1 and C-4 have strong influence on antitumor activity since fumiquinazoline G (**1**), with *R*-configurations at C-1 and C-4, showed the strongest antitumor effect against NCI-H460, BxPC3, and PANC1 cell lines. Comparing the enantiomeric pairs **4** and **5**, compound **5** with also *R*-configuration at C-4 and *S* at C-1

showed stronger antitumor effect. In contrast, their isomer, compound **2**, with *S*-configurations both at C-1 and C-4 were *S* exhibited the weakest inhibitory effect on all cell lines. In addition, the substituent at C-1 also affected the antitumor activity. Alkyl residues (isoleucine residues) in **2**, **4**, and **5** showed better antitumor activity than that found in compounds with a sulfur atom (methionine residues) such as **6** and **7**. Aromatic groups such as the tyrosine residue present in **10** and **11** produced good antitumor activity, with GI<sub>50</sub> values ranging from 27.93 ± 0.8 to 50.59 ± 2.3 μM, but the substitution by benzyl groups as in the case of **8** caused a 2-fold decrease in the antitumor activity. Regarding neuroprotection capacity, SAR suggests that the *R*-configuration at C-4 is also important (when comparing compounds **6** and **7**, Figure 2); however, increasing the molecular weight of C-1 substituent has a negative effect in neuroprotection. In addition, this study confirmed that quinazolinone alkaloids which act as substance P inhibitors (i.e., fiscalin B, **3**), showed a potential as neuroprotective agents. Therefore, the studied fumiquinazoline-derived alkaloids showed promising antitumor and neuroprotection effects and deserves to be further explored.

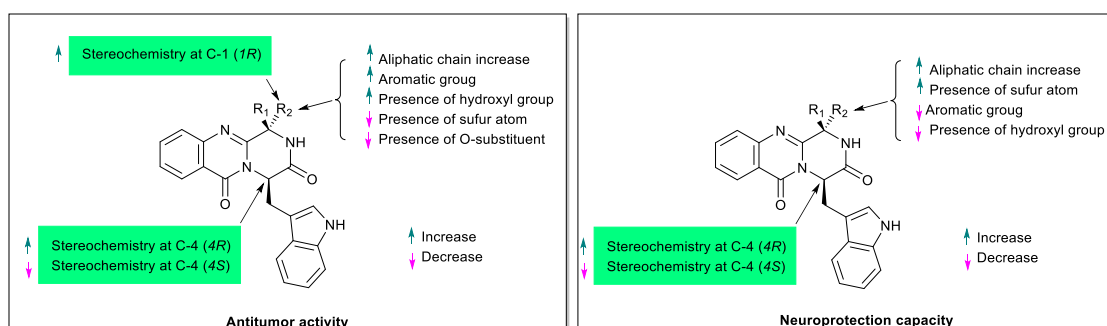


**Figure 4.** Structure-activity relationship studies of quinazolinone alkaloids **1–12** with antitumor and neuroprotective activities.

## 4. Materials and Methods

### 4.1. General Procedure

All reagents were from analytical grade. Dried pyridine and triphenylphosphite were purchased from Sigma (Sigma-Aldrich Co. Ltd., Gillingham, UK). Anthranilic acid (**i**) and

Protected amino acids (**ii** and **vii**) were purchased from TCI (Tokyo Chemical Industry Co. Ltd., Chuo-ku, Tokyo, Japan). Column chromatography purifications were performed using flash silica Merck 60, 230–400 mesh (EMD Millipore corporation, Billerica, MA, USA) and preparative TLC was carried out on precoated plates Merck Kieselgel 60 F<sub>254</sub> (EMD Millipore corporation, Billerica, MA, USA), spots were visualized with UV light (Vilber Lourmat, Marne-la-Vallée, France). Melting points were measured in a Köfler microscope and are uncorrected. Infrared spectra were recorded in a KBr microplate in a FTIR spectrometer Nicolet iS10 from Thermo Scientific (Waltham, MA, USA) with Smart OMNI-Transmission accessory (Software 188 OMNIC 8.3, Thermo Fisher Scientific Inc., Austin, TX, USA). <sup>1</sup>H and <sup>13</sup>C NMR spectra were recorded in CDCl<sub>3</sub> or DMSO-d<sub>6</sub> (Deutero GmbH, Kastellaun, Germany) at room temperature unless otherwise mentioned on Bruker AMC instrument (Bruker Biosciences Corporation, Billerica, MA, USA), operating at 300 MHz for <sup>1</sup>H and 75 MHz for <sup>13</sup>C). Carbons were assigned according to HSQC and or HMBC experiments. Optical rotation was measured at 25 °C using the ADP 410 polarimeter (Bellingham + Stanley Ltd., Royal Tunbridge Wells, Kent, UK), using the emission wavelength of sodium lamp, concentrations are given in g/100 mL. Qualitative GC-MS analyses were performed on a Trace GC 2000 Series ThermoQuest gas chromatography (Thermo Fisher Scientific Inc., Austin, TX, USA) equipped with ion-trap GCQ Plus ThermoQuest Finnigan mass detector (Thermo Fisher Scientific Inc.). Chromatographic separation was achieved using a capillary column (30 m × 0.25 mm × 0.25 μm, cross-linked 5% diphenyl and 95% dimethyl polysiloxane) from Thermo Scientific™ (Thermo Fisher Scientific Inc.) and high-purity helium C-60 as carrier gas. High resolution mass spectra (HRMS) were measured on a Bruker FTMS APEX III mass spectrometer (Bruker Corporation, Billerica, MA, USA) recorded as ESI (Electrospray) made in Centro de Apoyo Científico e Tecnológico á Investigación (CACTI, University of Vigo, Pontevedra, Spain). The purity of synthesized compounds was determined by reversed-phase LC with diode array detector (DAD) using C18 column (Kimetex®, 2.6 EV0 C18 100 Å, 150 × 4.6 mm), and the mobile phase was methanol:water (60:40) or acetonitrile:water (50:50). Enantiomeric ratio was determined by chiral LC (LCMS-2010EV, Shimadzu, Lisbon, Portugal), employing a system equipped with a chiral column (Lux® 5 μm Amylose-1, 250 × 4.6 mm) and UV-detection at 254 nm, mobile phase was hexane:ethanol (80:20) and the flow rate



was 0.5 mL/min. Compound **3** was obtained according to previous described method [17]. Neuroprotection studies were performed in Fundación Centro de Excelencia en Investigación de Medicamentos Innovadores en Andalucía, MEDINA (Granada, Spain).

#### 4.2. General Conditions for the Synthesis of Compound (1*R*,4*R*)-4-((1*H*-indol-3-yl)methyl)-1-((*R*)-methyl)-1,2-dihydro-6*H*-pyrazino[2,1-*b*]quinazoline-3,6(4*H*)-dione (**1**)

To a mixture of anthranilic acid (**i**, 287 mg, 2.39 mmol) and TBTU (920 mg, 2.86 mmol, 1.2 equiv) in acetonitrile (20 mL) was added Et<sub>3</sub>N (833 μL, 4.78 mmol, 2 equiv) and *D*-tryptophan methyl ester (**ii**, 521 mg, 2.39 mmol) at room temperature. After stirring for 5 h, the reaction mixture was concentrated under reduced pressure. The residue was dissolved in CH<sub>2</sub>Cl<sub>2</sub> and washed with 1 M HCl, extracted with CH<sub>2</sub>Cl<sub>2</sub> (3 × 100 mL), dried with Na<sub>2</sub>SO<sub>4</sub>, filtered, and concentrated. The residue was purified by flash chromatography (eluent 1% MeOH in CH<sub>2</sub>Cl<sub>2</sub>) to yield **iii** as a white solid. <sup>1</sup>H NMR and <sup>13</sup>C NMR referred to the previous work [16]. To a solution of **iii** (140 mg, 0.416 mmol) in dried CH<sub>2</sub>Cl<sub>2</sub> (10 mL) *N*-Fmoc-*D*-alanine-Cl [30] (**iv**, 182 mg, 0.5 mmol) was added. The mixture was stirred for 30 min, followed by the addition of aqueous Na<sub>2</sub>CO<sub>3</sub> (1 M, 8 mL, 8 mmol). After continuous stirring for 3 h, the mixture was extracted with CH<sub>2</sub>Cl<sub>2</sub> (4 × 100 mL), dried with Na<sub>2</sub>SO<sub>4</sub>, filtered, and concentrated. The residue was purified by flash chromatography (eluent: 5% MeOH in CH<sub>2</sub>Cl<sub>2</sub>) to give **v** (220.4 mg, 84.2%) as a white solid. <sup>1</sup>H NMR (300 MHz, CDCl<sub>3</sub>) δ 11.48 (s, 1H), 8.58 (d, 1H, *J* = 8.4 Hz), 8.13 (s, 1H), 7.76 (d, 2H, *J* = 7.5 Hz), 7.66 (d, 1H, *J* = 7.1 Hz), 7.59 (t, 1H, *J* = 7.4 Hz), 7.49-7.26 (m, 8H), 7.17 (t, 1H, *J* = 7.2 Hz), 7.06 (t, 1H, *J* = 7.6 Hz), 7.00 (t, 1H, *J* = 7.7 Hz), 6.97 (s, 1H), 6.71 (d, 1H, *J* = 7.6 Hz), 5.55 (d, 1H, *J* = 6.8), 5.03 (dt, 1H, *J* = 7.6, 5.3 Hz), 4.44 (m, 2H), 4.36 (1m, 1H), 4.26 (t, 1H, *J* = 7.0 Hz), 3.73 (s, 3H), 3.40 (dd, 1H, *J* = 15.3, 5.8 Hz), 3.34 (dd, 1H, *J* = 15.3, 5.3 Hz), 1.53 (d, 3H, *J* = 7.0 Hz) and <sup>13</sup>C NMR (75 MHz, CDCl<sub>3</sub>) 172.7, 172.2, 168.8, 156.6, 144.2, 143.8, 141.4, 138.6, 136.4, 132.8, 127.8, 127.4, 127.2, 125.3, 123.4, 123.3, 122.1, 121.6, 120.9, 120.0, 119.5, 118.3, 111.7, 109.2, 67.3, 53.6, 52.7, 52.2, 47.3, 27.3, 18.4 (See in [31]). To a solution of **v** (183.2 mg, 0.278 mmol) in dried CH<sub>2</sub>Cl<sub>2</sub> (20 mL) Ph<sub>3</sub>P (365 mg, 1.39 mmol, 5 equiv), I<sub>2</sub> (345 mg, 1.36 mmol, 4.9 equiv), and *N,N*-diisopropylethylamine (489 μL, 2.81 mmol, 10 equiv) were added. The reaction mixture was stirred at room temperature for 5 h, quenched with aqueous Na<sub>2</sub>CO<sub>3</sub>, and extracted with CH<sub>2</sub>Cl<sub>2</sub> (3 × 100 mL), dried with Na<sub>2</sub>SO<sub>4</sub>, filtered, and concentrated. Hexane was added

to remove an excess of  $\text{Ph}_3\text{P}$ , the precipitate was filtered and was treated with  $\text{CH}_2\text{Cl}_2$  (10 mL) and piperidine (2.5 mL, 20%) at room temperature for 20 min, followed by solvent evaporation to provide the solid which was triturated with hexane (1 × 200 mL),  $\text{CH}_2\text{Cl}_2/\text{PhMe}$  (1 × 200 mL), and hexane (1 × 200 mL). The vacuum-dried crude residue was dissolved in  $\text{CH}_3\text{CN}$  (10 mL) in the presence of DMAP (64 mg, 0.53 mmol) and refluxed for 19 h. The reaction mixture was purified by preparative TLC ( $\text{EtOAc}:\text{MeOH}:\text{CH}_2\text{Cl}_2$ , 50:2.5:47.5) to afford **1**. Yield: 22.4 mg, 21.11%; *er* = 7:93; mp: 105.9-106.5 °C;  $[\alpha]_D^{30} = -117.64$  (*c* 0.034;  $\text{CHCl}_3$ );  $\nu_{\text{max}}$  (KBr) 3406, 2924, 2852, 1678, 1473, 1329, and 1261  $\text{cm}^{-1}$ ;  $^1\text{H}$  NMR (300 MHz,  $\text{CDCl}_3$ ):  $\delta$  8.38 (dd, 1H, *J* = 8.0 and 1.1 Hz, CH), 8.18 (br, 1H, NH-Trp), 7.78 (ddd, 1H, *J* = 8.5, 7.1, and 1.6 Hz, CH), 7.57 (d, 1H, *J* 7.4 Hz, CH), 7.54 (dd, 1H, *J* = 8.0 and 1.0 Hz, CH), 7.29 (d, 1H, *J* = 3.1 Hz, CH-Trp), 7.27 (d, 1H, *J* = 2.0 Hz, CH-Trp), 7.08 (ddd, 1H, *J* = 9.5, 7.0 and 0.9 Hz, CH-Trp), 6.83 (ddd, 1H, *J* = 8.7, 7.1 and 1.0 Hz, CH-Trp), 6.73 (d, 1H, *J* = 2.3 Hz, CH-Trp), 6.70 (d, 1H, *J* = 2.0 Hz, NH-amide), 5.54 (dd, 1H *J* = 5.2 and 3.6 Hz,  $\text{CH}^*\text{-Trp}$ ), 4.46 (qd, 1H, *J* = 6.9 and 2.8 Hz,  $\text{CH}^*\text{-ala}$ ), 3.78 (dd, 1H, *J* = 14.9 and 5.3 Hz,  $\text{CH}_2\text{-Trp}$ ), 3.70 (dd, 1H, *J* = 14.9 and 3.4 Hz,  $\text{CH}_2\text{-Trp}$ ), 0.58 (d, 3H, *J* = 7.0 Hz,  $\text{CH}_3\text{-ala}$ );  $^{13}\text{C}$  NMR (75 MHz,  $\text{CDCl}_3$ ):  $\delta$  167.3 (C=O), 161.0 (C=O), 151.2 (C=N), 147.2 (C), 135.7 (C-Trp), 134.9 (CH), 127.9 (C-Trp), 126.9 (CH), 126.8 (CH), 126.7 (CH), 123.7 (CH-Trp), 122.3 (CH-Trp), 120.1 (C), 119.9 (CH-Trp), 118.7 (CH-Trp), 111.1 (CH-Trp), 109.4 (C-Trp), 56.9 ( $\text{CH}^*\text{-Trp}$ ), 51.9 ( $\text{CH}^*\text{-ala}$ ), 27.1 ( $\text{CH}_2\text{-Trp}$ ), 22.8 ( $\text{CH}_3\text{-ala}$ ). (+)-HRMS-ESI *m/z* 359.1505 ( $\text{M} + \text{H}^+$ ), (calculated for  $\text{C}_{21}\text{H}_{18}\text{N}_4\text{O}_2$ , 358.1430).

#### 4.3. General Conditions for the Synthesis of Compound (1*S*,4*S*)-4-((1*H*-indol-3-yl)methyl)-1-((*S*)-*sec*-butyl)-1,2-dihydro-6*H*-pyrazino[2,1-*b*]quinazoline-3,6(4*H*)-dione (**2**)

To a mixture of anthranilic acid (**i**, 287 mg, 2.39 mmol) and TBTU (920 mg, 2.86 mmol, 1.2 equiv) in acetonitrile (20 mL),  $\text{Et}_3\text{N}$  (833  $\mu\text{L}$ , 4.78 mmol, 2 equiv) and L-tryptophan methyl ester (**vi**, 521 mg, 2.39 mmol) were added at room temperature. After stirring for 5 h, the reaction mixture was concentrated under reduced pressure. The residue was dissolved in  $\text{CH}_2\text{Cl}_2$  and washed with 1 M HCl, extracted with  $\text{CH}_2\text{Cl}_2$  (3 × 100 mL), dried with  $\text{Na}_2\text{SO}_4$ , filtered, and concentrated. The residue was purified by flash chromatography (eluent 1% MeOH in  $\text{CH}_2\text{Cl}_2$ ) to yield **vii** as a white solid.  $^1\text{H}$  NMR and  $^{13}\text{C}$  NMR referred to the previous work [16]. To a solution of **vii** (304 mg, 0.901 mmol) in dried  $\text{CH}_2\text{Cl}_2$  (30

mL), *N*-Fmoc-L-isoleucine-Cl [30] (**viii**, 395 mg, 1.08 mmol) was added. The mixture was stirred for 30 min, followed by addition of aqueous Na<sub>2</sub>CO<sub>3</sub> (1 M, 16 mL, 16 mmol). After continuous stirring for 3 h, the mixture was extracted with CH<sub>2</sub>Cl<sub>2</sub> (4 × 100 mL), dried with Na<sub>2</sub>SO<sub>4</sub>, filtered, and concentrated. The residue was purified by flash chromatography (eluent: 5% MeOH in CH<sub>2</sub>Cl<sub>2</sub> to give **ix** (475.8 mg, 86.2%) as a white solid. <sup>1</sup>H NMR (300 MHz, CDCl<sub>3</sub>): δ 11.43 (s, 1H), 8.59 (d, 1H, *J* = 8.3 Hz), 8.19 (s, 1H), 7.76 (d, 2H, *J* = 7.4 Hz), 7.69-7.56 (m, 2H), 7.53-7.28 (m, 7H), 7.17 (t, 1H, *J* = 7.3 Hz), 7.06 (t, 1H, *J* = 7.4 Hz), 7.01 (d, 1H, *J* = 7.6 Hz), 6.96 (d, 1H, *J* = 3.5 Hz), 6.72 (d, 1H, *J* = 7.6 Hz), 5.55 (d, 1H, *J* = 8.4 Hz), 5.06 (dd, 1H, *J* = 12.6 and 5.2 Hz), 4.39 (dd, 2H, *J* = 16.4 and 9.1 Hz), 3.73 (s, 3H), 3.37 (m, 2H), 2.11-2.00 (m, 1H), 1.68-1.48 (m, 2H), 1.03 (d, 3H, *J* = 6.8 Hz), 0.96 (t, 3H, *J* = 7.3 Hz) and <sup>13</sup>C NMR (75 MHz, CDCl<sub>3</sub>) 172.1, 170.2, 168.6, 144.1, 143.8, 141.3, 139.0, 136.1, 132.9, 127.7, 127.5, 127.1, 127.1, 126.9, 125.3, 125.2, 123.2, 122.8, 122.4, 121.4, 120.2, 120.0, 119.8, 118.5, 111.4, 109.7, 67.2, 61.3, 53.3, 52.6, 47.3, 37.9, 31.4, 27.3, 15.8, 11.7. To a solution of **ix** (291.5 mg, 0.432 mmol) in dried CH<sub>2</sub>Cl<sub>2</sub> (20 mL) Ph<sub>3</sub>P (565 mg, 2.16 mmol, 5 equiv), I<sub>2</sub> (448 mg, 2.12 mmol, 4.9 equiv), and *N,N*-diisopropylethylamine (753 μL, 4.32 mmol, 10 equiv) were added. The reaction mixture was stirred at room temperature for 5 h, quenched with aqueous Na<sub>2</sub>CO<sub>3</sub>, and extracted with CH<sub>2</sub>Cl<sub>2</sub> (3 × 100 mL), dried with Na<sub>2</sub>SO<sub>4</sub>, filtered, and concentrated. Hexane was added to remove an excess of Ph<sub>3</sub>P, the precipitate was filtered and was treated with CH<sub>2</sub>Cl<sub>2</sub> (10 mL) and piperidine (2.5 mL, 20%) at room temperature for 20 min, followed by solvent evaporation to provide the solid which was triturated with hexane (1 × 200 mL), CH<sub>2</sub>Cl<sub>2</sub>/PhMe (1 × 200 mL), and hexane (1 × 200 mL). The vacuum-dried crude residue was dissolved in CH<sub>3</sub>CN (10 mL) in the presence of DMAP (158 mg, 1.39 mmol) and refluxed for 19 h. The reaction mixture was purified by preparative TLC (EtOAc: MeOH: CH<sub>2</sub>Cl<sub>2</sub>, 50:2.5:47.5) to afford **2**. Yield: 36 mg, 36.2%; enantiomeric ratio (er) = 73:27; m.p: 181-183 °C; [ $\alpha$ ]<sub>D</sub><sup>30</sup> = +346.40 (*c* 0.051; CHCl<sub>3</sub>);  $\nu_{max}$  (KBr) 3375, 3187, 2880, 1684, 1662, 1472, 1434, and 1261 cm<sup>-1</sup>; <sup>1</sup>H NMR (300 MHz, CDCl<sub>3</sub>): δ 8.38 (dd, 1H, *J* = 8.0 and 1.1 Hz, CH), 8.07 (br, 1H, NH-Trp), 7.79 (ddd, 1H, *J* = 8.5, 7.1, and 1.6 Hz, CH), 7.62 (dd, *J* = 8.2 and 0.5 Hz, CH), 7.54 (ddd, 1H, *J* = 8.2, 7.2, and 1.2 Hz, CH), 7.48 (d, 1H, *J* 7.9 Hz, CH-Trp), 7.28 (d, 1H, *J* = 8.5 Hz, CH-Trp), 7.12 (ddd, 1H, *J* = 8.1, 7.1 and 1.1 Hz, CH-Trp), 6.94 (ddd, 1H, *J* = 8.0, 7.1 and 1.0 Hz, CH-Trp), 6.87 (d, 1H, *J* = 2.3 Hz, CH-Trp), 6.55 (d, 1H, *J* = 3.1 Hz, NH-amide), 5.52 (dd, 1H, *J* = 6.4 and 3.6 Hz, CH\*-Trp), 4.03 (dd, 1H, *J* = 8.0 and 3.5 Hz, CH-Ile), 3.83 (dd, 1H, *J* = 14.9

and 6.4 Hz, CH<sub>2</sub>-Trp), 3.73 (dd, 1H, *J* = 14.8 and 3.5 Hz, CH<sub>2</sub>-Trp), 0.99 – 0.85 (m, 1H, CH\*-Ile), 0.85 – 0.69 (m, 2H, CH<sub>2</sub>-Ile), 0.66 (d, 3H, *J* = 6.5 Hz, CH<sub>3</sub>-Ile), 0.58 (t, 3H *J* = 7.1 Hz, CH<sub>3</sub>-Ile); <sup>13</sup>C NMR (75 MHz, CDCl<sub>3</sub>): δ 167.8 (C=O), 161.4 (C=O), 149.4 (C=N), 146.8 (C), 135.9 (C-Trp), 134.7 (CH), 127.9 (C-Trp), 127.1 (CH), 127.1 (CH), 126.8 (CH), 123.5 (CH-Trp), 122.3 (CH-Trp), 120.3 (C), 120.0 (CH-Trp), 119.0 (CH-Trp), 111.0 (CH-Trp), 110.2 (C-Trp), 60.8 (CH\*-Ile), 57.6 (CH\*-Trp), 40.8 (CH\*-Ile), 27.1 (CH<sub>2</sub>-Trp), 24.3 (CH<sub>2</sub>-Ile), 15.3 (CH<sub>3</sub>-Ile), 10.4 (CH<sub>3</sub>-Ile); (+)-HREM-ESI *m/z* 401.1967 (M + H)<sup>+</sup>, 423.1787 (M + Na)<sup>+</sup> (calculated for C<sub>24</sub>H<sub>25</sub>N<sub>4</sub>O<sub>2</sub>, 400.1899).

#### 4.4. General Conditions for the Synthesis of Quinazolinone-3,6-(4H)-Diones Compound **4**, **5**, **6**, **7**, **8**, and **9**

In a closed vial anthranilic acid (**i**, 28 mg, 200 μmol), *N*-Boc-L-isoleucine (**x**, 44 mg, 200 μmol) for **4** and **5**, or *N*-Boc-L-methionine (**xi**, 46 mg, 200 μmol) for **6** and **7**, or *N*-Boc-*o*-Bn-Tyrosine (**xii**, 74 mg, 200 μmol) for **8** and **9**, and triphenylphosphite (63 μL, 220 μmol) were added along with 1 mL of dried pyridine. The vial was heated in heating block with stirring at 55 °C for 16–24 h. After cooling the mixture to room temperature, D-tryptophan methyl ester hydrochloride (**ii**) for **5**, and **7**, L-tryptophan methyl ester hydrochloride (**vi**) for **4**, **6**, **8** and **9** (51 mg, 200 μmol) was added, and the mixture was irradiated in the microwave at the constant temperature at 220 °C for 1.5 min. Reaction mixtures were prepared in the same conditions and treated in parallel. After removing the solvent with toluene, the crude product was purified by flash column chromatography using hexane:EtOAc (60:40) as a mobile phase. The preparative TLC was performed using CH<sub>2</sub>Cl<sub>2</sub>:Me<sub>2</sub>CO (95:5) as mobile phase. The major compound appeared as a black spot with no fluorescence under the UV light (366 nm). The desirable compounds **4**, **5**, **6**, **7**, **8**, and **9** were collected as yellow solids. Before analysis, compounds were recrystallized from methanol.

(1*R*,4*S*)-4-((1*H*-indol-3-yl)methyl)-1-((*S*)-*sec*-butyl)-1,2-dihydro-6*H*-pyrazino[2,1-*b*]quinazoline-3,6(4*H*)-dione (**4**). Yield: 29.2 mg, 7.1%; *er* = 3:97; m.p: 220–221 °C; [α]<sub>D</sub><sup>30</sup> = + 484.7 (*c* 0.037; CHCl<sub>3</sub>); *v*<sub>max</sub> (KBr) 3373, 3059, 2880, 1684, 1662, 1472, 1434, and 1261 cm<sup>-1</sup>; <sup>1</sup>H NMR (300 MHz, CDCl<sub>3</sub>): δ 8.38 (dd, 1H, *J* = 7.9 and 1.2 Hz, CH), 8.07 (br, 1H, NH-Trp), 7.78 (ddd, 1H, *J* = 8.4, 7.1, and 1.6 Hz, CH), 7.57 (d, *J* = 8.0 Hz, CH), 7.52 (d, 1H, *J* = 6.0 Hz, CH), 7.47 (d, 1H, *J* = 8.0 Hz, CH-Trp), 7.28 (d, 1H, *J* = 8.2 Hz, CH-Trp), 7.12 (t, 1H, *J* = 7.1 Hz, CH-Trp), 6.96 (t, 1H, *J*

= 7.5 Hz, CH-Trp), 6.57 (d, 1H,  $J = 2.4$  Hz, CH-Trp), 5.68 (dd, 1H,  $J = 5.2$  and  $2.7$  Hz, CH\*-Trp), 5.64 (s, 1H, NH-amide), 3.76 (dd, 1H,  $J = 14.8$  and  $2.7$  Hz, CH<sub>2</sub>-Trp), 3.63 (dd, 1H,  $J = 14.9$  and  $5.3$  Hz, CH<sub>2</sub>-Trp), 2.80 (d, 1H,  $J = 2.4$  Hz, CH\*-Ile), 2.36 (dt, 1H,  $J = 14.9$  and  $7.5$  Hz, CH\*-Ile), 0.98 (m, 2H, CH<sub>2</sub>-Ile), 0.88 (d, 3H,  $J = 6.5$  Hz, CH<sub>3</sub>-Ile), 0.64 (t, 3H,  $J = 6.4$  Hz, CH<sub>3</sub>-Ile); <sup>13</sup>C NMR (75 MHz, CDCl<sub>3</sub>):  $\delta$  169.5 (C=O), 160.9 (C=O), 150.7 (C=N), 147.1 (C), 136.1 (C-Trp), 134.7 (CH), 127.2 (CH), 127.1 (CH), 127.0 (C-Trp), 126.9 (CH), 123.6 (CH-Trp), 122.8 (CH-Trp), 120.2 (C), 120.1 (C-Trp), 118.8 (CH-Trp), 111.1 (CH-Trp), 109.4 (C-Trp), 56.8 (CH\*-Trp), 55.1 (CH\*-Ile), 35.8 (CH\*-Ile), 27.4 (CH<sub>2</sub>-Trp), 25.8 (CH<sub>2</sub>-Ile), 13.2 (CH<sub>3</sub>-Ile), 11.0 (CH<sub>3</sub>-Ile; (+)-HRMS-ESI  $m/z$  401.1964 (M + H)<sup>+</sup> (calculated for C<sub>24</sub>H<sub>25</sub>N<sub>4</sub>O<sub>2</sub>, 400.1899).

(1*S*,4*R*)-4-((1*H*-indol-3-yl)methyl)-1-((*S*)-sec-butyl)-1,2-dihydro-6*H*-pyrazino[2,1-*b*]quinazoline-3,6(4*H*)-dione (5). Yield: 27.2 mg, 6.6%; *er* = 3:97; m.p: 218–220 °C;  $[\alpha]_D^{30} = -372.6$  (c 0.034; CHCl<sub>3</sub>);  $\nu_{max}$  (KBr) 3373, 3059, 2880, 1684, 1662, , 1472, 1434, 1261 cm<sup>-1</sup>; <sup>1</sup>H NMR (300 MHz, CDCl<sub>3</sub>):  $\delta$  8.37 (dd, 1H,  $J = 7.9$  and  $1.2$  Hz, CH), 8.07 (br, 1H, NH-Trp), 7.78 (ddd, 1H,  $J = 8.4$ , 7.1, and  $1.6$  Hz, CH), 7.57 (d,  $J = 8.0$  Hz, CH), 7.52 (d, 1H,  $J = 6.0$  Hz, CH), 7.47 (d, 1H,  $J = 8.0$  Hz, CH-Trp), 7.28 (d, 1H,  $J = 8.2$  Hz, CH-Trp), 7.12 (t, 1H,  $J = 7.1$  Hz, CH-Trp), 6.96 (t, 1H,  $J = 7.5$  Hz, CH-Trp), 6.57 (d, 1H,  $J = 2.4$  Hz, CH-indole), 5.68 (dd, 1H,  $J = 5.2$  and  $2.7$  Hz, CH\*-Trp), 5.52 (s, 1H, NH-amide), 3.76 (dd, 1H,  $J = 14.8$  and  $2.7$  Hz, CH<sub>2</sub>-Trp), 3.63 (dd, 1H,  $J = 14.9$  and  $5.3$  Hz, CH<sub>2</sub>-Trp), 2.80 (d, 1H,  $J = 2.4$  Hz, CH\*-Ile), 2.37 (dt, 1H,  $J = 14.9$  and  $7.5$  Hz, CH\*-Ile), 0.88 (m, 2H,  $J = 6.7$  Hz, CH<sub>2</sub>-Ile), 0.62 (d, 3H,  $J = 6.5$  Hz, CH<sub>3</sub>-Ile), 0.46 (t, 3H,  $J = 6.4$  Hz, CH<sub>3</sub>-Ile); <sup>13</sup>C NMR (75 MHz, CDCl<sub>3</sub>):  $\delta$  169.4 (C=O), 160.9 (C=O), 150.1 (C=N), 147.1 (C), 136.1 (C-Trp), 134.7 (CH), 127.2 (CH), 127.2 (CH), 127.0 (CH-Trp), 126.9 (CH), 123.6 (CH-Trp), 122.7 (CH-Trp), 120.2 (C), 120.1 (C-Trp), 118.8 (CH-Trp), 111.1 (CH-Trp), 109.4 (C-indol), 56.8 (CH\*-Trp), 55.5 (CH\*-Ile), 35.6 (CH\*-Ile), 27.4 (CH<sub>2</sub>-Trp), 25.9 (CH<sub>2</sub>-Ile), 13.2 (CH<sub>3</sub>-Ile), 11.0 (CH<sub>3</sub>-Ile; (+)-HRMS-ESI  $m/z$  401.1973 (M + H)<sup>+</sup> (calculated for C<sub>24</sub>H<sub>25</sub>N<sub>4</sub>O<sub>2</sub>, 400.1899).

(1*R*,4*S*)-4-((1*H*-indol-3-yl)methyl)-1-(2-(methylthio)ethyl)-1,2-dihydro-6*H*-pyrazino[2,1-*b*]quinazoline-3,6(4*H*)-diones (6). Yield: 27 mg, 6.1%; m.p: 198–200.7 °C;  $[\alpha]_D^{30} = +74.1$  (c 0.045; CHCl<sub>3</sub>);  $\nu_{max}$  (KBr) 3295, 3067, 2915, 1682, 1600, 1470, 770, and 697 cm<sup>-1</sup>; <sup>1</sup>H NMR (300 MHz, CDCl<sub>3</sub>):  $\delta$  8.37 (dd, 1H,  $J = 8.0$  and  $1.2$  Hz, CH), 8.07 (br, 1H, NH-Trp), 7.78 (ddd, 1H,  $J = 8.4$ , 7.0, and  $1.5$  Hz, CH), 7.57 (d, 1H,  $J = 2.5$  Hz, CH), 7.53 (dd, 1H,  $J = 8.2$  and  $1.1$  Hz, CH), 7.41 (d, 1H,  $J = 8.0$  Hz, CH-Trp), 7.30 (d, 1H,  $J = 8.3$  Hz, CH-Trp), 7.13 (t, 1H,  $J = 7.7$  Hz, CH-Trp),

6.93 (t, 1H,  $J = 7.0$  Hz, CH-Trp), 6.71 (d, 1H,  $J = 2.4$  Hz, CH-Trp), 6.37 (s, 1H, NH-amide), 5.67 (dd, 1H,  $J = 5.2$  and  $3.0$  Hz, CH\*-Trp), 3.74 (dd, 1H,  $J = 15.0$  and  $3.0$  Hz, CH<sub>2</sub>-Trp), 3.65 (dd, 1H,  $J = 14.9$  and  $5.3$  Hz, CH<sub>2</sub>-Trp), 2.99 (dd, 1H,  $J = 6.6$  and  $3.6$  Hz, CH\*-Met), 2.49-2.13 (m, 4H, CH<sub>2</sub>-Met), 1.96 (s, 3H, CH<sub>3</sub>-Met); <sup>13</sup>C NMR (75 MHz, CDCl<sub>3</sub>):  $\delta$  169.3 (C=O), 161.1 (C=O), 150.3 (C=N), 147.1 (C), 136.0 (C-Trp), 134.7 (CH), 127.2 (CH), 127.2 (C-Trp), 126.9 (CH), 123.5 (CH-Trp), 122.7 (CH-Trp), 120.2 (C), 120.2 (C-Trp), 118.7 (CH-Trp), 111.1 (CH-Trp), 109.5 (C-Trp), 57.2 (CH\*Trp), 52.8 (CH\*-Met), 30.7 (CH<sub>2</sub>-S-Met), 29.7 (CH<sub>2</sub>-Met), 27.2 (CH<sub>2</sub>-Trp), 15.3 (CH<sub>3</sub>-Met); HRMS-ESI  $m/z$  419.1544 (M + H)<sup>+</sup> (calculate for C<sub>23</sub>H<sub>23</sub>N<sub>4</sub>O<sub>2</sub>S, 418.1463).

(1*S*,4*R*)-4-((1*H*-indol-3-yl)methyl)-1-(2-(methylthio)ethyl)-1,2-dihydro-6*H*-pyrazino[2,1-*b*]quinazoline-3,6(4*H*)-diones (7). Yield: 34.8 mg, 7.9%; *er* = 49: 51; m.p.: 197-200 °C;  $[\alpha]_D^{30} = -56.9$  (*c* 0.041; CHCl<sub>3</sub>);  $\nu_{max}$  (KBr) 3290, 3058, 2918, 2854, 1684, 1670, 1602, 773, and 695 cm<sup>-1</sup>; <sup>1</sup>H NMR (300 MHz, CDCl<sub>3</sub>):  $\delta$  8.37 (dd, 1H,  $J = 8.0$  and  $1.1$  Hz, CH), 8.12 (br, 1H, NH-Trp), 7.78 (ddd, 1H,  $J = 8.4, 7.2,$  and  $1.5$  Hz, CH), 7.57 (d,  $J = 8.3$  Hz, CH), 7.54 (d, 1H,  $J = 7.0$  Hz, CH), 7.40 (d, 1H,  $J = 8.0$  Hz, CH-Trp), 7.30 (d, 1H,  $J = 8.2$  Hz, CH-Trp), 7.12 (t, 1H,  $J = 7.1$  Hz, CH-Trp), 6.92(t, 1H,  $J = 7.0$  Hz, CH-Trp), 6.71 (d, 1H,  $J = 2.4$  Hz, CH-Trp), 5.67 (dd, 1H,  $J = 5.4$  and  $3.1$  Hz, CH\*-Trp), 6.54 (s, 1H, NH-amide), 3.73 (dd, 1H,  $J = 15.0$  and  $2.9$  Hz, CH<sub>2</sub>-Trp), 3.65 (dd, 1H,  $J = 15.1$  and  $5.5$  Hz, CH<sub>2</sub>-Trp), 3.01 (dd, 1H,  $J = 6.6$  and  $3.6$  Hz, CH\*-Met), 2.48-2.20 (m, 4H, CH<sub>2</sub>-Met), 1.96 (s, 3H, CH<sub>3</sub>-Met); <sup>13</sup>C NMR (75 MHz, CDCl<sub>3</sub>):  $\delta$  169.5 (C=O), 161.0 (C=O), 150.6 (C=N), 146.9 (C), 136.1 (C-Trp), 134.7 (CH), 127.2 (C-Trp), 127.2 (CH), 126.9 (CH), 123.5 (CH-Trp), 122.6 (CH-Trp), 120.2 (C), 120.1 (C-Trp), 118.7 (CH-Trp), 111.2 (CH-Trp), 109.5 (C-Trp), 57.2 (CH\*-Trp), 52.8 (CH\*-Met), 30.7 (CH<sub>2</sub>-S-Met), 29.7 (CH<sub>2</sub>-Met), 27.2 (CH<sub>2</sub>-Trp), 15.3 (CH<sub>3</sub>-Met); (+)-HRMS-ESI  $m/z$  419.1526 (M + H)<sup>+</sup>, (calculated for C<sub>23</sub>H<sub>23</sub>N<sub>4</sub>O<sub>2</sub>S, 418.1463).

(1*R*,4*S*)-4-((1*H*-indol-3-yl)methyl)-1-(4-(benzyloxy)benzyl)-1,2-dihydro-6*H*-pyrazino[2,1-*b*]quinazoline-3,6(4*H*)-diones (8). Yield: 81.9 mg, 14.8%; *er* = 63:37; m.p.: 226.9-227.9 °C;  $[\alpha]_D^{30} = +46.7$  (*c* 0.05; CHCl<sub>3</sub>);  $\nu_{max}$  (KBr) 3393, 3268, 2954, 1671, 1611, 1511, 1465, 1240, 772, and 697 cm<sup>-1</sup>; <sup>1</sup>H NMR (300 MHz, CDCl<sub>3</sub>):  $\delta$  8.39 (dd, 1H,  $J = 8.0$  and  $1.2$  Hz, CH), 8.05 (br, 1H, NH-Trp), 7.80 (ddd, 1H,  $J = 8.5, 7.2$  and  $1.5$  Hz, CH), 7.62 (d,  $J = 8.0$  Hz, CH), 7.56 (dt, 1H,  $J = 7.3, 7.7,$  and  $1.1$  Hz, CH), 7.45-7.39 (m, 5H, CH-Bz), 7.32 (d, 2H,  $J = 8.0$  Hz, CH-Trp), 7.17 (t, 1H,  $J = 7.5$  Hz, CH-Trp), 6.88 (t, 1H,  $J = 7.5$  Hz, CH-Trp), 6.76 (d, 2H,  $J = 9.0$  Hz, CH-Tyr), 6.61 (d,

1H, *J* = 3.0 Hz, CH-Trp), 6.39 (d, 2H, *J* = 8.5 Hz, CH-Tyr), 5.64 (dd, 1H, *J* = 5.2 and 2.7, CH\*-Trp), 5.35 (s, 1H, NH-amide), 5.05 (s, 2H, CH<sub>2</sub>-Bz), 3.76 (dd, 1H, *J* = 14.9 and 2.6 Hz, CH<sub>2</sub>-Trp), 3.67 (dd, 1H, *J* = 15.0 and 5.3 Hz, CH<sub>2</sub>-Trp), 3.52 (dd, 1H, *J* = 14.7 and 3.6 Hz, CH<sub>2</sub>-Tyr), 2.89 (dd, *J* = 11.1 and 3.6 Hz, CH\*-Tyr), 2.46 (dd, 1H, *J* = 14.7 and 11.2 Hz, CH<sub>2</sub>-Tyr); <sup>13</sup>C NMR (75 MHz, CDCl<sub>3</sub>): δ 169.2 (C=O), 160.7 (C=O), 157.9 (C-Tyr), 151.0 (C=N), 147.0 (C), 137.0 (C-Trp), 136.1 (C-Bz), 134.8 (CH), 128.7 (CH-Tyr (2)), 128.6 (CH-Bz (2)), 128.0 (C-Tyr), 127.4 (CH-Bz), 127.3 (CH-Trp), 127.2 (CH), 127.1 (CH-Bz (2)), 127.0 (CH), 126.9 (CH), 123.8 (CH-Trp), 122.8 (CH-Trp), 120.6 (C), 120.4 (CH-Trp), 119.0 (CH-Trp), 115.5 (CH-Tyr (2H)), 111.1 (CH-Trp), 109.7 (C-Trp), 70.1 (CH<sub>2</sub>-Bz), 57.4 (CH\*-Trp), 52.9 (CH\*-Tyr), 37.1 (CH<sub>2</sub>-Tyr), 29.7 (CH<sub>2</sub>-Trp); (+)-HRMS-ESI *m/z* 541.2232 (M + H)<sup>+</sup>, (calculated for C<sub>34</sub>H<sub>29</sub>N<sub>4</sub>O<sub>3</sub>, 540.2161).

(1*S*,4*S*)-4-((1*H*-indol-3-yl)methyl)-1-(4-(benzyloxy)benzyl)-1,2-dihydro-6*H*-pyrazino[2,1-*b*]quinazoline-3,6(4*H*)-diones (**9**). Yield: 119.9 mg, 21.7%; *er* = 29:71; m.p.: 165.9-166.6 °C; [ $\alpha$ ]<sub>D</sub><sup>30</sup> = +205.8 (c 0.076; CHCl<sub>3</sub>);  $\nu_{\text{max}}$  (KBr) 3489, 3364, 2923, 1674, 1612, 1512, 1467, 1249, 774, and 695 cm<sup>-1</sup>; <sup>1</sup>H NMR (300 MHz, CDCl<sub>3</sub>): δ 8.42 (dd, 1H, *J* = 8.0 and 1.1 Hz, CH), 8.08 (br, 1H, NH-Trp), 7.83 (ddd, 1H, *J* 8.5, 7.1, and 1.5 Hz, CH), 7.66 (d, *J* 7.7 Hz, CH), 7.62-7.52 (m, 2H, CH), 7.39 (t, 4H, *J* = 2.6 Hz, CH-Bz), 7.35 (ddd, *J* = 6.2, 3.4, and 1.5 Hz, 1H, CH-Bz), 7.30 (d, 1H, *J* = 8.1 Hz, CH-Trp), 7.20 (td, 1H, *J* = 7.6 and 1.1 Hz, CH-Trp), 6.10 (td, 1H, *J* = 7.5 and 1.0 Hz, CH-Trp), 6.74 (d, 2H, *J* = 8.7 Hz, CH-Tyr), 6.60 (d, 1H, *J* = 2.3 Hz, CH-Trp), 6.23 (d, 2H, *J* = 8.6 Hz, CH-Tyr), 5.56 (t, 1H, *J* = 4.2 Hz, CH\*-Trp), 5.55 (s, 1H, NH-amide), 4.99 (s, 2H, CH<sub>2</sub>-Bz), 4.33 (dt, 1H, *J* = 11.7 and 2.8 Hz, CH\*-Tyr), 3.86 (dd, 1H, *J* = 14.9 and 3.0 Hz, CH<sub>2</sub>-Trp), 3.80 (dd, 1H, *J* = 14.9 and 4.4 Hz, CH<sub>2</sub>-Trp), 2.95 (dd, 1H, *J* = 13.3 and 3.1 Hz, CH<sub>2</sub>-Tyr), 0.53 (dd, *J* = 13.1 and 11.9 Hz, CH<sub>2</sub>-Tyr); <sup>13</sup>C NMR (75 MHz, CDCl<sub>3</sub>): δ 166.5 (C=O), 160.9 (C=O), 158.0 (C-Tyr), 150.2 (C=N), 147.2 (C), 136.9 (C-Trp), 135.8 (C-Bn), 134.9 (CH), 130.28 (CH-Tyr (2)), 128.6 (CH-Bz (2)), 128.1 (C-Tyr), 128.0 (CH-Bz), 127.7 (C-Trp), 127.4 (CH), 127.0 (CH-Bz (2)), 126.9 (CH), 123.5 (CH-Trp), 122.8 (CH-Trp), 120.5 (C), 120.2 (C-Trp), 119.5 (CH-Trp), 115.2 (CH-Tyr (2)), 111.4 (CH-Trp), 109.7 (C-Trp), 70.0 (CH<sub>2</sub>-Bz), 57.9 (CH\*-Tyr), 56.8 (CH\*-Trp), 42.0 (CH<sub>2</sub>-Tyr), 26.6 (CH<sub>2</sub>-Trp); (+)-HRMS-ESI *m/z* 541.2221 (M + H)<sup>+</sup>, (calculated for C<sub>34</sub>H<sub>29</sub>N<sub>4</sub>O<sub>3</sub>, 540.2161).

4.5. General Conditions for the Synthesis of (1*S*)-4-((1*H*-indol-3-yl)methyl)-1-(4-hydroxybenzyl)-1,2-dihydro-6*H*-pyrazino[2,1-*b*]quinazoline-3,6(4*H*)-dione (**10** and **11**).

In an oven-dried round-bottomed flash equipped with Teflon-coated magnetic stir bar, a rubber septum, a glass stopper, and nitrogen gas inlet compound **8** or **9** (50 mg, 0.092 mmol) dissolved with anhydrous CH<sub>2</sub>Cl<sub>2</sub> (5 mL) was added. After cooled the mixture to -78 °C, 1M boron trichloride in CH<sub>2</sub>Cl<sub>2</sub> (190 μL, 0.19 mmol, 2eq) was added dropwise over 5 min at -78 °C. After stirring for 45 min at -78 °C, the mixture was quenched by syringe addition of CHCl<sub>3</sub>/MeOH (10/1, 10 mL) at -78 °C and was warmed to ambient temperature. The solvent was evaporated, and the content was purified by flash column chromatography using hexane: EtOAc (6:4) as mobile phase. Compounds **10** or **11** were obtained as pale-yellow solids. Before analysis, compounds were recrystallized from methanol.

(1*R*,4*S*)-4-((1*H*-indol-3-yl)methyl)-1-(4-hydroxybenzyl)-1,2-dihydro-6*H*-pyrazino[2,1-*b*]quinazoline-3,6(4*H*)-dione (**10**). Yield: 12.5 mg, 30%; *er* = 36:65; m.p.: 134–136 °C;  $[\alpha]_D^{30} = +39.5$  (*c* 0.034; CH<sub>3</sub>OH);  $\nu_{max}$  (KBr) 3427, 1677, 1603, 1515, 1468, 1159, 1025, 998, and 765 cm<sup>-1</sup>; <sup>1</sup>H NMR (300 MHz, DMSO-*d*<sub>6</sub>):  $\delta$  10.48 (s, 1H, NH-Trp), 8.89 (d, 1H, *J* = 4.9 Hz, OH-Tyr), 8.32 (dd, 1H, *J* = 8.0 and 1.2 Hz, CH), 7.81 (dd, 1H, *J* = 7.7 and 1.6 Hz, CH), 7.61 (d, *J* = 7.9 Hz, CH), 7.56 (dd, 1H, *J* = 12.7 and 7.2 Hz, CH), 7.39 (dd, 1H, *J* = 8.0 and 5.4 Hz, CH-Trp), 7.34 (dt, 1H, *J* = 8.1 Hz, CH), 7.13 (dd, 1H, *J* = 13.4 and 6.7 Hz, CH-Trp), 6.84 (dd, 1H, *J* = 13.4 and 6.7 Hz, CH-Trp), 6.60 (d, 1H, *J* = 3.4 Hz, CH-Trp), 6.58 (dd, 2H, *J* = 8.5 and 6.0 Hz, CH-Tyr), 6.53 (d, 1H, *J* = 4.4 Hz, NH-amide), 6.46 (dd, 2H, *J* = 7.9 and 5.7 Hz, CH-Tyr), 5.44 (dd, 1H, *J* = 5.0 and 2.8 Hz, CH\*-Trp), 3.64 (dd, 1H, *J* = 14.8 and 2.7 Hz, CH<sub>2</sub>-Trp), 3.56 (dd, 1H, *J* = 14.9 and 5.3 Hz), 3.26 (dt, *J* = 13.4 and 3.6 Hz, CH<sub>2</sub>-Tyr), 3.03 (dt, 1H, *J* = 8.9 and 4.7 Hz, CH\*-Tyr), 2.67 (dt, 1H, *J* = 13.3 and 10.5 Hz); <sup>13</sup>C NMR (75 MHz, CDCl<sub>3</sub>):  $\delta$  168.1 (C=O), 160.0 (C=O), 150.5 (C-Tyr), 146.3 (C), 135.8 (C-Trp), 134.1 (CH), 129.4 (CH-Tyr (2)), 126.7 (C-Trp), 126.6 (CH), 126.4 (CH), 126.1 (CH), 124.9 (C-Tyr), 123.7 (CH-Trp), 121.2 (CH-Trp), 119.6 (CH-Trp), 118.9 (CH-Trp), 115.0 (C-Tyr), 111.2 (CH-Trp), 108.0 (C-Trp), 56.6 (CH\*-Trp), 52.8 (CH\*-Tyr), 36.3 (CH<sub>2</sub>-Tyr), 26.5 (CH<sub>2</sub>-Trp); (+)-HRMS-ESI *m/z* 451.1766 (M + H)<sup>+</sup>, 473.1576 (M + Na)<sup>+</sup> (calculated for C<sub>27</sub>H<sub>23</sub>N<sub>4</sub>O<sub>3</sub>, 450.1692).

(1*S*,4*S*)-4-((1*H*-indol-3-yl)methyl)-1-(4-hydroxybenzyl)-1,2-dihydro-6*H*-pyrazino[2,1-*b*]quinazoline-3,6(4*H*)-dione (**11**). Yield: 25.7 mg, 68.7%; *er* = 61:39; m.p.: 102–103 °C;  $[\alpha]_D^{30} = +75.9$  (*c* 0.079; CH<sub>3</sub>OH);  $\nu_{max}$  (KBr) 3428, 2927, 1667, 1610, 1592, 1474, 1337, 1232, 772, and 699 cm<sup>-1</sup>; <sup>1</sup>H NMR (300 MHz, DMSO-*d*<sub>6</sub>):  $\delta$  10.54 (s, 1H, NH-Trp), 8.86 (s, 1H, OH-Tyr), 8.34 (dd, 1H, *J* = 8.0 and 1.2 Hz, CH), 7.83 (dd, 1H, *J* = 7.7, and 1.6 Hz, CH), 7.62 (d, *J* = 7.9 Hz, CH),



7.56 (dt, 1H,  $J = 7.6, 7.6,$  and  $0.6$  Hz, CH), 7.49 (d, 1H,  $J = 7.9$  Hz, CH-Trp), 7.30 (d, 1H,  $J = 8.1$  Hz, CH), 7.20 (d, 1H,  $J = 3.3$  Hz, NH-amide), 7.09 (dt, 1H,  $J = 7.6$  and  $0.6$  Hz, CH-Trp), 6.94 (dt, 1H,  $J = 7.5$  and  $0.5$  Hz, CH-Trp), 6.66 (d, 1H,  $J = 2.3$  Hz, CH-Trp) 6.57(d, 2H,  $J = 5.6$  Hz, CH-Tyr), 6.45 (d, 2H,  $J = 8.4$  Hz, CH-Tyr), 5.37 (dd, 1H,  $J = 5.2$  and  $3.3$  Hz, CH\*-Trp), 4.36 (dt, 1H,  $J = 10.5$  and  $3.4$  Hz, CH\*-Tyr), 3.63 (dd, 1H,  $J = 14.8$  and  $3.1$  Hz, CH<sub>2</sub>-Trp), 3.55 (dd, 1H,  $J = 14.9$  and  $5.4$  Hz, CH<sub>2</sub>-Trp), 2.69 (dd,  $J = 13.4$  and  $3.6$  Hz CH<sub>2</sub>-Tyr), 0.86 (dd, 1H,  $J = 13.3$  and  $10.5$  Hz, CH<sub>2</sub>-Tyr); <sup>13</sup>C NMR (75 MHz, CDCl<sub>3</sub>):  $\delta$  165.8 (C=O), 160.2 (C=O), 155.8 (C-Tyr), 150.4 (C=N), 146.7 (C), 135.6 (C-Trp), 134.2 (CH), 129.9 (CH-Tyr (2)), 127.4 (CH-Trp), 126.3 (CH), 126.2 (CH), 126.1 (CH-Trp), 125.9 (C-Tyr), 123.7 (CH-Trp), 121.1 (CH-Trp), 119.5 (CH-Trp), 118.7 (CH-Trp), 114.9 (CH-Tyr (2)), 111.2 (CH-Trp), 108.0 (C-Trp), 57.2 (CH\*-Trp), 56.3 (CH\*-Tyr), 41.8 (CH<sub>2</sub>-Tyr), 26.1 (CH<sub>2</sub>-Trp); (+)-HRMS-ESI  $m/z$  451.1771 (M + H)<sup>+</sup>, 473.1564 (M + Na)<sup>+</sup> (calculated for C<sub>27</sub>H<sub>23</sub>N<sub>4</sub>O<sub>3</sub>, 450.1692).

#### 4.6. General Conditions for the Synthesis of (1S,4R)-4-((1H-indol-3-yl)methyl)-1-(4-(benzyloxy)benzyl)-8,10-dichloro-1,2-dihydro-6H-pyrazino[2,1-b]quinazoline-3,6(4H)-dione (**12**)

In a closed vial 3,5-dichloro anthranilic acid (**xiii**, 41 mg, 200  $\mu$ mol), *N*-Boc-*o*-Bn-Tyrosine (**xii**, 74 mg, 200  $\mu$ mol), and triphenylphosphite (63  $\mu$ L, 220  $\mu$ mol) were added along with 1 mL of dried pyridine. The vial was heated in heating block with stirring at 55 °C for 16–24 h. After cooling the mixture to room temperature, *D*-tryptophan methyl ester hydrochloride (**ii**, 51 mg, 200  $\mu$ mol) was added, and the mixture was irradiated in the microwave at the constant temperature at 220 °C for 1.5 min. Reaction mixtures were prepared in the same conditions and treated in parallel. After removing the solvent with toluene, the crude product was purified by flash column chromatography using hexane: EtOAc (60:40) as a mobile phase. The preparative TLC was performed using CH<sub>2</sub>Cl<sub>2</sub>:Me<sub>2</sub>CO (95:5) as mobile phase. The major compound appeared as a black spot with no fluorescence under the UV light (366 nm). Compound **12** was collected as orange solids. Before analysis, compound was recrystallized from methanol. Yield: 26.2 mg, 2.2%; *er* 67:33; m.p.: 233–235 °C;  $[\alpha]_D^{30} = +244.44$  (c 0.045; CH<sub>3</sub>OH);  $\nu_{\max}$  (KBr) 3424, 3334, 2921, 1681, 1593, 1511, 1455, 1247, 1012, 695, and 420 cm<sup>-1</sup>; <sup>1</sup>H NMR (300 MHz, CDCl<sub>3</sub>):  $\delta$  8.26 (d, 1H,  $J = 2.4$  Hz, CH), 8.09 (br, 1H, NH-Trp), 7.85 (d, 1H,  $J = 2.4$  Hz, CH), 7.44 (dd, 5H,  $J = 6.4$  and  $2.0$  Hz, CH-Bz), 7.39 (d, 2H,  $J = 8.2$  Hz, CH-Trp), 7.19 (t, 1H,  $J = 7.7$  Hz, CH-Trp), 6.96 (t, 1H,  $J = 7.5$  Hz, CH-Trp),

6.75 (d, 2H,  $J = 8.7$  Hz, CH-Tyr), 6.62 (d, 1H,  $J = 2.3$  Hz, CH-Trp), 6.40 (d, 2H,  $J = 8.5$  Hz, CH-Tyr), 5.56 (dd, 1H,  $J = 5.2$  and  $2.6$ , CH\*-Trp), 5.41 (s, 1H, NH-amide), 5.06 (s, 2H, CH<sub>2</sub>-Bz), 3.77 (dd, 1H,  $J = 15.0$  and  $2.6$  Hz, CH<sub>2</sub>-Trp), 3.62 (dd, 1H,  $J = 15.6$  and  $4.1$  Hz, CH<sub>2</sub>-Trp), 3.50 (dd, 1H,  $J = 17.5$  and  $4.4$  Hz, CH<sub>2</sub>-Tyr), 2.95 (dd,  $J = 10.8$  and  $3.6$  Hz, CH\*-Tyr), 2.51 (dd, 1H,  $J = 14.8$  and  $10.9$  Hz, CH<sub>2</sub>-Tyr); <sup>13</sup>C NMR (75 MHz, CDCl<sub>3</sub>):  $\delta$  168.7 (C=O), 159.2 (C=O), 158.0 (C-Tyr), 152.0 (C=N), 142.4 (C), 136.9 (C-Bz), 136.1 (C-Trp), 135.1 (CH), 133.2 (C-Cl), 132.6 (C-Cl), 129.6 (CH-Tyr (2)), 128.7 (CH-Bz (2)), 128.1 (CH-Bz), 127.4 (CH-Bz(2)), 126.9 (C-Trp), 126.6 (C-Tyr), 125.2 (CH), 123.7 (CH-Trp), 122.9 (CH-Trp), 122.4 (C), 118.9 (CH-Trp), 115.5 (CH-Tyr (2H)), 111.2 (CH-Trp), 109.4 (C-Trp), 70.1 (CH<sub>2</sub>-Bz), 57.6 (CH\*-Trp), 53.1 (CH\*-Tyr), 36.9 (CH<sub>2</sub>-Tyr), 27.1 (CH<sub>2</sub>-Trp). (+)-HRMS-ESI  $m/z$  609.1427 (M + H)<sup>+</sup>, (calculated for C<sub>34</sub>H<sub>27</sub>N<sub>4</sub>O<sub>3</sub>Cl<sub>2</sub>, 608.1382).

#### 4.7. Neuroprotection Assay

Compounds **1**, **2**, **4**, **5**, **6**, **7**, **8**, **9**, **10**, **11**, and **12c** together with fiscalin B (**3**) were assayed in co-treatment with rotenone at eight concentrations per triplicate. The SH-SY5y cells (ATCC Ref.: CRL-2266) were seeded at a density of 40,000/well in a 96-well plate and were incubated in a humidified atmosphere at 37 °C with 5% CO<sub>2</sub> for overnight. The compounds were dissolved in DMSO at the concentration of 10 mM and the higher concentration assayed was 100  $\mu$ M. The negative control was 1% DMSO. After 24 h of co-treatment, plates were treated with MTT (3-(4,5-dimethylthiazol-2-yl)-2,5-diphenyltetrazolium bromide) at 5  $\mu$ g/mL in Minimum Essential Medium Eagle (MEM) for 3 h at the standard culture condition. Then, DMSO was added to the plates to solubilizing the formazan crystal formed in viable cells and plates were put in the stirring for 5 min to homogenize the solution. Absorbance at 570 nm was measured by VICTOR Multilabel Plate Reader (PerkinElmer).

#### 4.8. Screening Test for Antitumor Activity

Compounds **1**, **2**, **4**, **5**, **6**, **7**, **8**, **10**, and **11** were reconstituted in sterile DMSO to the final concentration of 60 mM, and several aliquots were made and stored at -20 °C to avoid repeated freeze-thaw cycles. For experiments, the compounds were freshly diluted in medium to the desired concentration. Screening for tumor cell growth inhibitory activity was carried out in three human tumor cell lines (NCI-H460, BxPC3 and PANC1), with the sulforhodamine B (SRB) assay, as previously described [34]. Briefly, tumor cells were plated

in 96-well plates, incubated at 37 °C for 24 h, and then treated for 48 h with 5 serial dilutions (1:2) of each compound (ranging from 25 μM to 1.5625 μM, 150 μM to 9.375 μM or 200 μM to 12.5 μM, depending on the compound and for reasons related with solubility). The effect of the vehicle solvent (DMSO) was also analyzed as a control. Cells were fixed with 10% ice-cold trichloroacetic acid, washed with water, and stained with SRB. Finally, the plates were washed with 1% acetic acid and the bound SRB was solubilized with 10 mM Tris Base. Absorbance was measured in a microplate reader (Synergy Mx, Biotek Instruments Inc., Winooski, VT, USA) at 510 nm. For each compound, the corresponding GI<sub>50</sub> (concentration which inhibited 50% of net cell growth) was determined, as previously described [33].

#### 4.9. Testing Effect of Compounds on Non-malignant Breast Cells

Compounds **5**, **7**, **10** and **11** (which presented simultaneously the best neuroprotection and antitumor effects) were tested against the non-malignant MCF-12A human breast epithelial cells. For that, cells were incubated with specific concentrations of each compound (corresponding to approximately the highest GI<sub>50</sub> concentration obtained in the antitumor activity screening) for 48 h, followed by removal of the compound, addition of new medium to the cells and then 5 more days in culture. At the end of the 7 days in total, the sulforhodamine B (SRB) assay was performed, as previously described [32].

## 5. Conclusions

New quinazolinone alkaloid derivatives with *anti* and *syn* stereochemistry were synthesized by combining both a one-pot microwave-assisted reaction and a multi-step approach. Interestingly, fumiquinazoline G (**1**) presented a better antitumor activity in all the tumor cell lines tested, with GI<sub>50</sub> values lower than 20 μM. The antitumor activity of the remaining compounds was not relevant, with GI<sub>50</sub> values higher than 20 μM in the tested cell lines. The effect of the synthesized compounds in the growth of the tested non-malignant cells was smaller than the effect on the studied tumor cells. It is worth noting that among the compounds tested, only **1**, **3**, **5**, and **7** showed potential for neuroprotection in a PD in vitro model. This finding highlights new insights into marine natural products belonging to the proteomimetic quinazolinone alkaloids.

**Supplementary Materials:** The following are available online Figures S1–S57.

**Author Contributions:** E.S. conceived the study design. S.L. synthesized the compounds and elucidated their structure and, A.S., E.S., A.K. and M.M.M.P. analyzed the data. D.I.S.P.R. performed the LC analysis. R.F. and C.X. performed the cytotoxic studies in tumor cells and non-malignant breast cells. C.X. and M.H.V. analyzed data from the cytotoxic studies, discussed and wrote those results. S.L. and E.S. wrote the manuscript, while all authors gave significant contributions in discussion and revision. All authors agreed with the final version of the manuscript.

**Funding:** This research was partially supported by the Strategic Funding UID/Multi/04423/2013 through national funds provided by FCT—Foundation for Science and Technology and European Regional Development Fund (ERDF), in the framework of the program PT2020. The authors thank to national funds provided by FCT—Foundation for Science and Technology and European Regional Development Fund (ERDF) and COMPETE under the Strategic Funding UID/Multi/04423/2013, the projects POCI-01-0145-FEDER-028736 and PTDC/MAR-BIO/4694/2014 (POCI-01-0145-FEDER-016790; 3599-PPCDT).

**Acknowledgments:** S.L. thanks Erasmus Mundus Action 2 (LOTUS+, LP15DF0205) for full PhD scholarship. D. I. S. P. R. thanks for her postdoctoral scholarship (NOVELMAR/BPD\_2/2016-019). To Sara Cravo for technical support.

**Conflicts of Interest:** The authors declare no conflicts of interest.

## References

1. Plun-Favreau, H.; Lewis, P.A.; Hardy, J.; Martins, L.M.; Wood, N.W. Cancer and neurodegeneration: Between the devil and the deep blue sea. *PLOS Genet.* **2010**, *6*, e1001257.
2. Klus, P.; Cirillo, D.; Botta Orfila, T.; Tartaglia, G.G. Neurodegeneration and cancer: Where the disorder prevails. *Sci. Rep.* **2015**, *5*, 15390.
3. Resende, D.I.S.P.; Boonpothong, P.; Sousa, E.; Kijjoa, A.; Pinto, M.M.M. Chemistry of the fumiquinazolines and structurally related alkaloids. *Nat. Prod. Rep.* **2019**, *36*, 7–34.
4. Buttachon, S.; Chandrapatya, A.; Manoch, L.; Silva, A.; Gales, L.; Bruyère, C.; Kiss, R.; Kijjoa, A. Sartorymensin, a new indole alkaloid, and new analogues of

- tryptoquivaline and fiscalins produced by neosartorya siamensis (kufc 6349). *Tetrahedron* **2012**, *68*, 3253–3262.
5. Tamiya, H.; Ochiai, E.; Kikuchi, K.; Yahiro, M.; Toyotome, T.; Watanabe, A.; Yaguchi, T.; Kamei, K. Secondary metabolite profiles and antifungal drug susceptibility of aspergillus fumigatus and closely related species, aspergillus lentulus, aspergillus udagawae, and aspergillus viridinutans. *J. Infect. Chemother.* **2015**, *21*, 385-391.
  6. He, F.; Sun, Y.-L.; Liu, K.-S.; Zhang, X.-Y.; Qian, P.-Y.; Wang, Y.-F.; Qi, S.-H. Indole alkaloids from marine-derived fungus aspergillus sydowii scsio 00305. *J. Antibiot.* **2012**, *65*, 109–111.
  7. Takahashi, C.; Matsushita, T.; Doi, M.; Minoura, K.; Shingu, T.; Kumeda, Y.; Numata, A. Fumiquinazolines a–g, novel metabolites of a fungus separated from a pseudolabrus marine fish. *J. Chem. Soc. Perkin Trans. 1* **1995**, *18*, 2345–2353.
  8. Numata, A.; Takahashi, C.; Matsushita, T.; Miyamoto, T.; Kawai, K.; Usami, Y.; Matsumura, E.; Inoue, M.; Ohishi, H.; Shingu, T. Fumiquinazolines, novel metabolites of a fungus isolated from a saltfish. *Tetrahedron Lett.* **1992**, *33*, 1621–1624.
  9. Han, X.-x.; Xu, X.-y.; Cui, C.-b.; Gu, Q.-q. Alkaloidal compounds produced by a marine-derived fungus, aspergillus fumigatus h1-04, and their antitumor activities. *Chinese J. Org. Chem.* **2007**, *17*, 232–237.
  10. Cheng, Z.; Lou, L.; Liu, D.; Li, X.; Proksch, P.; Yin, S.; Lin, W. Versiquinazolines a–k, fumiquinazoline-type alkaloids from the gorgonian-derived fungus aspergillus versicolor lzd-14-1. *J. Nat. Prod.* **2016**, *79*, 2941–2952.
  11. Wong, S.M.; Musza, L.L.; Kydd, G.C.; Kullnig, R.; Gillum, A.M.; Cooper, R. Fiscalins: New substance p inhibitors produced by the fungus neosartorya fischeri. Taxonomy, fermentation, structures, and biological properties. *J. Antibiot.* **1993**, *46*, 545–553.

12. Barrow, C.J.; Sun, H.H. Spiroquinazoline, a novel substance p inhibitor with a new carbon skeleton, isolated from aspergillus flavipes. *J. Nat. Prod.* **1994**, *57*, 471–476.
13. Thornton, E.; Vink, R. Treatment with a substance p receptor antagonist is neuroprotective in the intrastriatal 6-hydroxydopamine model of early parkinson's disease. *PLoS ONE* **2012**, *7*.
14. Dunlop, R.A.; Cox, P.A.; Banack, S.A.; Rodgers, K.J. The non-protein amino acid bmaa is misincorporated into human proteins in place of l-serine causing protein misfolding and aggregation. *PLOS ONE* **2013**, *8*, e75376.
15. Rodgers, K.J. Non-protein amino acids and neurodegeneration: The enemy within. *Exp. Neurol.* **2014**, *253*, 192–196.
16. Long, S.; Resende, D.I.S.P.; Kijjoa, A.; Silva, A.M.S.; Pina, A.; Fernández-Marcelo, T.; Vasconcelos, M.H.; Sousa, E.; Pinto, M.M.M. Antitumor activity of quinazolinone alkaloids inspired by marine natural products. *Mar. Drugs* **2018**, *16*, 261.
17. Wang, H.; Ganesan, A. Total synthesis of the fumiquinazoline alkaloids: Solution-phase studies. *J. Org. Chem.* **2000**, *65*, 1022–1030.
18. Liu, J.F.; Ye, P.; Zhang, B.; Bi, G.; Sargent, K.; Yu, L.; Yohannes, D.; Baldino, C.M. Three-component one-pot total syntheses of gyantrypine, fumiquinazoline f, and fiscalin b promoted by microwave irradiation. *J. Org. Chem.* **2005**, *70*, 6339–6345.
19. Okaya, S.; Okuyama, K.; Okano, K.; Tokuyama, H. Trichloroboron-promoted deprotection of phenolic benzyl ether using pentamethylbenzene as a non lewis-basic cation scavenger. *Organic Syntheses*; Wiley: Hoboken, NJ, USA, 2016; Volume 93, pp. 63–74.
20. Hernández, F.; Buenadicha, F.L.; Avendao, C.; Söllhuber, M. 1-alkyl-2,4-dihydro-1h-pyrazino[2,1-b]quinazoline-3,6-diones as glycine templates. Synthesis of fiscalin b. *Tetrahedron Asymmetr.* **2002**, *12*, 3387–3398.

21. Campos, A.C.; Fogaça, M.V.; Sonego, A.B.; Guimarães, F.S. Cannabidiol, neuroprotection and neuropsychiatric disorders. *Pharmacol. Res.* **2016**, *112*, 119–127.
22. Bagli, E.; Goussia, A.; Moschos, M.M.; Agnantis, N.; Kitsos, G. Natural compounds and neuroprotection: Mechanisms of action and novel delivery systems. *In Vivo* **2016**, *30*, 535–547.
23. Cannon, J.R.; Tapias, V.; Na, H.M.; Honick, A.S.; Drolet, R.E.; Greenamyre, J.T. A highly reproducible rotenone model of parkinson's disease. *Neurobiol. Dis.* **2009**, *34*, 279–290.
24. Condello, S.; Currò, M.; Ferlazzo, N.; Caccamo, D.; Satriano, J.; Ientile, R. Agmatine effects on mitochondrial membrane potential and nfn-κb activation protect against rotenone-induced cell damage in human neuronal-like sh-sy5y cells. *J. Neurochem.* **2011**, *116*, 67–75.
25. Vichai, V.; Kirtikara, K. Sulforhodamine b colorimetric assay for cytotoxicity screening. *Nat. protoc.* **2006**, *1*, 1112–1116.
26. Zhou, Y.; Debbab, A.; Mándi, A.; Wray, V.; Schulz, B.; Müller, W.E.G.; Kassack, M.; Lin, W.; Kurtán, T.; Proksch, P.; et al. Alkaloids from the sponge-associated fungus *aspergillus* sp. *Eur. J. Org. Chem.* **2013**, *5*, 894–906.
27. Rodrigues, B.S.F.; Sahm, B.D.B.; Jimenez, P.C.; Pinto, F.C.L.; Mafezoli, J.; Mattos, M.C.; Rodrigues-Filho, E.; Pfenning, L.H.; Abreu, L.M.; Costa-Lotufo, L.V.; et al. Bioprospection of cytotoxic compounds in fungal strains recovered from sediments of the brazilian coast. *Chem. Biodivers.* **2015**, *12*, 432–442.
28. Fujimoto, H.; Negishi, E.; Yamaguchi, K.; Nishi, N.; Yamazaki, M. Isolation of new tremorgenic metabolites from an ascomycete, *corynascus setosus*. *Chem. Pharm. Bull.* **1996**, *40*, 1843–1848.
29. Wu, B.; Chen, G.; Liu, Z.-g.; Pei, Y. Two new alkaloids from a marine-derived fungus *neosartorya fischeri*. *Rec. Nat. Prod.* **2015**, *9*, 271–275.

30. Kantharaju, B.S.P.; Suresh Babu, V.V. Synthesis of fmoc-amino acid chlorides assisted by ultrasonication, a rapid approach. *Int. J. Pept. Res. Ther.* **2002**, *9*, 227–229.
31. Wang, H.; Ganesan, A. Total synthesis of the quinazoline alkaloids (–)-fumiquinazoline g and (–)-fiscalin b. *J. Org. Chem.* **1998**, *63*, 2432–2433.
32. Lopes-Rodrigues, V.; Oliveira, A.; Correia-da-Silva, M.; Pinto, M.; Lima, R.T.; Sousa, E.; Vasconcelos, M.H. A novel curcumin derivative which inhibits p-glycoprotein, arrests cell cycle and induces apoptosis in multidrug resistance cells. *Bioorg. Med. Chem.* **2017**, *25*, 581–596.
33. Kijjoa, A.; Santos, S.; Dethoup, T.; Manoch, L.; Almeida, A.P.; Vasconcelos, M.H.; Silva, A.; Gales, L.; Herz, W. Sartoryglabrin, analogs of ardeemins, from *neosartorya glabra*. *Nat. Prod. Commun.* **2011**, *6*, 807–812.

**Sample Availability:** Samples of the compounds **1–12** are available from the authors.



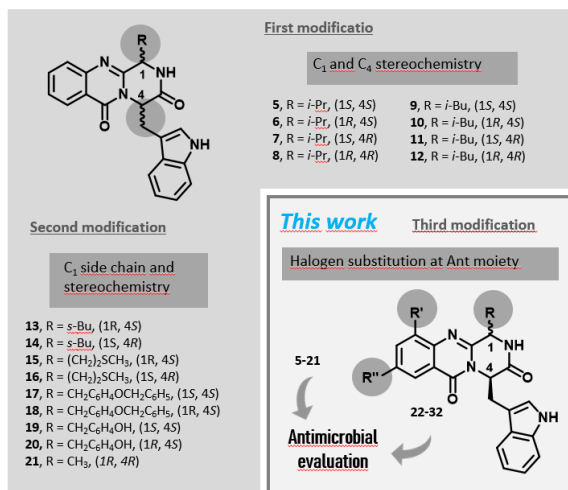
© 2019 by the authors. Submitted for possible open access publication under the terms and conditions of the Creative Commons Attribution (CC BY) license (<http://creativecommons.org/licenses/by/4.0/>).



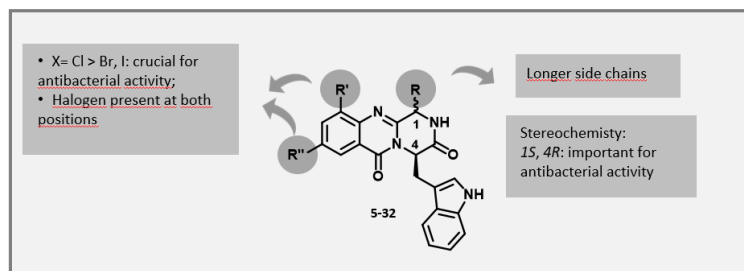
# Chapter 5

## Synthesis and Characterization of Antimicrobial Activities of Marine-Derived Indolymethyl Pyrazinoquinazoline Alkaloids

Graphical abstract



Structure-activity relationship





# Synthesis and Characterization of Antimicrobial Activities of Marine-Derived Indolymethyl Pyrazinoquinazoline Alkaloids

*Solida Long<sup>1</sup>, Patrícia Pereira-Terra<sup>2,3</sup>, Joana Freitas-Silva<sup>2,3</sup>, Diana I. S. P. Resende<sup>1,2</sup>, Anake Kijjoa<sup>2,3</sup>, Artur M. S. Silva<sup>4</sup>, Maria Elizabeth Tiritan<sup>1,2,5</sup>, Eugénia Pinto<sup>2,6</sup>, Paulo Martins da Costa<sup>2,3\*</sup>, Emília Sousa<sup>1,2,\*</sup> and Madalena M. M. Pinto<sup>1,2</sup>*

<sup>1</sup>LQOF - Laboratório de Química Orgânica e Farmacêutica, Departamento de Ciências Químicas, Faculdade de Farmácia, Universidade do Porto, Rua de Jorge Viterbo Ferreira, 228, 4050-313 Porto, Portugal

<sup>2</sup>CIIMAR - Centro Interdisciplinar de Investigação Marinha e Ambiental, Terminal de Cruzeiros do Porto de Leixões, Av. General Norton de Matos S/N, 4450-208 Matosinhos, Portugal

<sup>3</sup>ICBAS - Instituto de Ciências Biomédicas Abel Salazar, Universidade do Porto, Rua de Jorge Viterbo Ferreira, 228, 4050-313 Porto, Portugal

<sup>4</sup>QOPNA - Química Orgânica, Produtos Naturais e Agroalimentares, Departamento de Química, Universidade de Aveiro, 3810-193 Aveiro, Portugal

<sup>5</sup>CESPU, Instituto de Investigação e Formação Avançada em Ciências e Tecnologias da Saúde (IINFACETS), Rua Central de Gandra, 1317, 4585-116 Gandra PRD, Portugal

<sup>6</sup>Laboratório de Microbiologia, Departamento de Ciências Biológicas, Faculdade de Farmácia, Universidade do Porto, Rua de Jorge Viterbo Ferreira, 228, 4050-313 Porto, Portugal

\*Corresponding authors: [esousa@ff.up.pt](mailto:esousa@ff.up.pt), [pmcosta@icbas.up.pt](mailto:pmcosta@icbas.up.pt)

**KEYWORDS:** Alkaloids, antimicrobial, resistance, enantioselective, fiscalins.

**ABSTRACT.** A series of halogenated indolomethyl pyrazino [1,2-*b*]quinazoline-3,6-diones was synthesized by a highly effective and environmentally friendly approach using a one-pot microwave-

assisted multicomponent polycondensation of amino acids. All the synthesized compounds were evaluated for their antimicrobial activity against a panel of nine bacterial strains and five fungal strains. Out of all prepared analogs, compounds **26** and **27** (with MIC values of 4 µg/mL) were the most effective against *Staphylococcus aureus* ATCC 29213 reference strain and a methicillin-resistant isolate (MRSA) with MIC values of 8 µg/mL. Following enantioselective preparative LC, it was possible to infer that enantiomer (-)-**26** was responsible for the antibacterial activity (MIC 4 µg/mL) while (+)-**26** had no activity. Compounds **26**, **28**, and **29** showed a weak antifungal activity against clinical isolate *Trichophyton rubrum* with MIC 128 µg/mL and presented a synergistic effect with fluconazole. Generally, chloro-quinazolinones were the most promising regarding both antibacterial and antifungal activities compared to bromo and iodo derivatives.

## INTRODUCTION

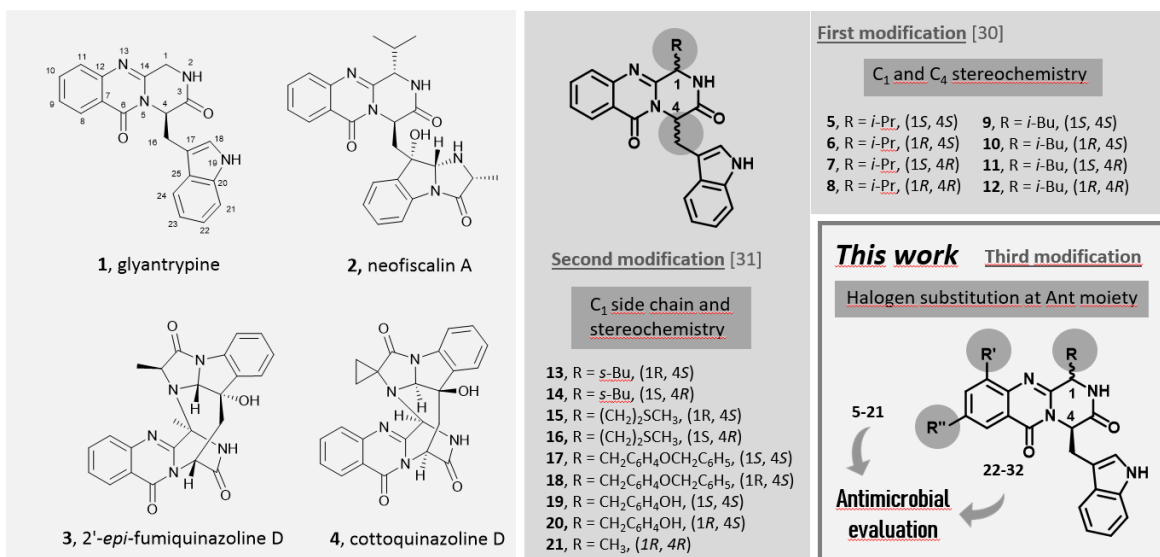
Infectious diseases caused by microorganisms stand as a major threat to public health<sup>1-2</sup>. Since antibiotics were first introduced as medicines, these drugs have been used to prevent or treat infections in several applications<sup>3-4</sup>. Nonetheless, antibacterial resistance has increased dramatically, becoming an emergency in healthcare during the last 40 years<sup>5</sup>. Among 50 emerging infectious agents that have been identified, 10% have developed resistance to multiple drugs including antibiotics such as vancomycin<sup>6-7</sup>, methicillin<sup>8</sup>, carbapenems<sup>9</sup>, and cephalosporins<sup>10-12</sup>. Despite enormous efforts, the number of therapeutically useful compounds that aim for circumventing the resistance is continuously decreasing and no truly novel class of compounds has been introduced into therapy, causing the world to face the “post-antibiotic era”<sup>13-14</sup>. In order to make stop the clinical consequences of the development and spread of antimicrobial resistance both the preservation of current antimicrobials through their appropriate use, as well as the discovery and development of new agents are mandatory<sup>15</sup>.

Several reports emphasized the discovery of new sophisticated antimicrobials from marine sources as a promising strategy to overcome the ever increasing drug-resistant infectious diseases<sup>16-19</sup>. In the last years, fungal alkaloids containing a indolomethyl pyrazino[1,2-*b*]quinazoline-3,6-dione scaffold

were isolated from marine organisms and presented very interesting antimicrobial activities. For instance, glyantypine (**1**, **Figure 1**) isolated from *Cladosporium* sp. PJX-41, exhibited moderate inhibitory activity against bacteria *Vibrio harveyi* (MIC = 32  $\mu\text{g/mL}$ )<sup>20-23</sup> and neofiscalin A (**2**) found in *Neosartorya siamensis* KUFC 6349 exhibited a potent antibacterial activity against *Staphylococcus aureus* and *Enterococcus faecalis* (MIC = 8  $\mu\text{g/mL}$ )<sup>24-26</sup>. Regarding antifungal activity, 2'-*epi*-fumiquinazoline D (**3**), obtained from culture of *Aspergillus fumigatus* LN-4 showed good activity (MIC = 12.5-50  $\mu\text{g/mL}$ )<sup>27</sup> and cottoquinazoline D (**4**), obtained from *Aspergillus versicolor* LCJ-5-4 showed moderate antifungal activity against *Candida albicans* (MIC = 22.6  $\mu\text{M}$ )<sup>28</sup>. Inspired by these marine models and the need for new antimicrobial agents to fight resistance, in the last years we have committed to coursing in the synthesis of fumiquinazolines and related alkaloids<sup>29</sup>. Our first approach (**Figure 1**) was to synthesize enantiomeric pairs of two members of this quinazolinone family (structural modifications at C-1 and C-4 stereochemistry), including the marine-derived alkaloid fiscalin B (**7**)<sup>30</sup>. The second approach (**Figure 1**) consisted in the synthesis of other derivatives of these natural alkaloids, but this time with modification of the C-1 side chain and stereochemistry, by using different amino acids<sup>31</sup>. Influenced by the high amount of halogenated marine natural products with interesting antimicrobial activities isolated over the last few years<sup>32-33</sup>, in the present work (**Figure 1**) we present a third approach in the synthesis of indolomethyl pyrazino[1,2-*b*]quinazoline-3,6-dione analogues: the introduction of halogen atoms in the aromatic ring of the anthranilic acid (Ant) and further antimicrobial evaluation of the new as well as previously obtained libraries of synthesized compounds<sup>30-31</sup>.

## Marine antimicrobials

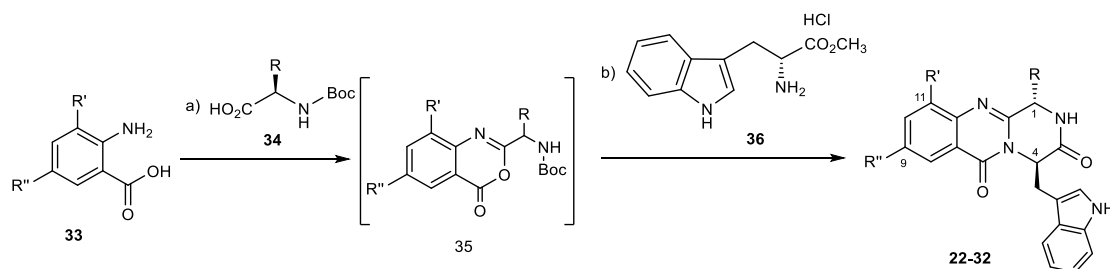
## Previous work



**Figure 1.** Marine antimicrobials **1-4** and rational of this work.

## RESULTS AND DISCUSSIONS

**Chemistry.** The eleven new indolomethyl pyrazino[1,2-*b*]quinazoline-3,6-dione derivatives were synthesized by a previously described approach using a microwave assisted multicomponent polycondensation of amino acids (**Table 1**)<sup>30-31,34</sup>. The coupling of halogenated commercial anthranilic acids (**33**) to *N*-protected L- $\alpha$ -amino acids (**34**), and further dehydrative cyclization using triphenyl phosphite [(PhO)<sub>3</sub>P], generated the intermediates benzoxazin-4-ones **35** which, followed by the addition of D-tryptophan methyl ester (**36**) under microwave irradiation, furnished the desirable final products **22-32** (2-14 % yield) with partial epimerization (**Table 1**).

**Table 1.** Synthesis of halogenated quinazolinone derivatives **22-32**<sup>a</sup>

Compound	R	R'	R''	Yield (%)	$[\alpha]_D^{25}$ <sup>b</sup>	<i>e.r.</i> <sup>c</sup>	% <sup>d</sup>
22	<i>i</i> -Pr	Cl	H	5	-273	56:44	99
23	<i>i</i> -Bu	Cl	H	3	+154	44:56	92
24	<i>s</i> -Bu	Cl	H	2	+130	46:54	92
25	<i>i</i> -Pr	Cl	Cl	5	+140	43:57	92
26	<i>i</i> -Bu	Cl	Cl	4.5	-169	60:40	92
27	<i>s</i> -Bu	Cl	Cl	2.6	-264	71:29	99
28	<i>i</i> -Pr	I	H	4.1	-175	51:49	90
29	<i>i</i> -Pr	Br	H	1.2	-170	50:50	99
30	<i>i</i> -Bu	I	H	11.8	-165	51:49	90
31	<i>i</i> -Bu	Br	H	13.8	-243	51:49	91
32	<i>i</i> -Bu	I	I	3.5	-229	54:46	91

<sup>a</sup> Reaction conditions: a) dried-pyridine, (PhO)<sub>3</sub>P, 55 °C, 16-24 h; b) dried-pyridine, (PhO)<sub>3</sub>P, 220 °C, 1.5 min; <sup>b</sup> Optical rotation; <sup>c</sup> *e.r.* = enantiomeric ratio determined by enantioselective LC (column: amylose, Lux® 5 m Amylose-1, 250 x 4.6 mm, flow rate: 0.5ml/min, mobile phase: hexane/EtOH, 9:1), <sup>d</sup> = % purity determined by RP-LC.

Using this methodology only anti isomers were produced (1*S*, 4*R*) and the different side chains at C-1 were obtained by selecting diverse L- $\alpha$  amino acids – valine, leucine, and isoleucine. The purities of the compounds were determined by reversed-phase liquid chromatography, (RP-LC, C18, MeOH: H<sub>2</sub>O; 60:40 or CH<sub>3</sub>CN:H<sub>2</sub>O; 50:50) and was found to be higher than 90 %.

## Microbiology

**Antibacterial susceptibility testing.** An initial screening of the antibacterial activity of the compounds **5-32** against different reference strains of Gram-positive, Gram-negative bacteria, as well as clinically relevant multidrug-resistant (MDR) strains was performed by the disk diffusion method<sup>35-36</sup>. This primary assessment was followed by the determination of minimal inhibitory concentrations (MIC) of reference strains. For active compounds, this determination was also made for MDR strains. In the range of concentrations tested, none of the compounds was active against Gram-negative bacteria, and none of **5-21, 28, 29 and 32** was active against any of the tested strains (results not shown). The results of antibacterial activity on Gram-positive strains regarding all other compounds are presented in **Table 2**. None of halogenated derivatives exhibit antibacterial activity against Gram-negative, similarly to the described for the natural isolated neofiscalin A (**2**). Regarding antimicrobial activity against Gram-positive bacteria, **22, 23, and 24** had an inhibitory effect on both *Enterococcus faecalis* ATCC 29212 and *Staphylococcus aureus* ATCC 29213 reference strains, while **25, 26, 27, 30, and 31** only showed an inhibitory effect on *S. aureus* ATCC 29213. The most effective compounds against *S. aureus* reference strain were **26** and **27**, with MIC values of 4 µg/mL. All of those compounds presented a bacteriostatic activity, with minimal bactericidal concentrations (MBC) greater than 64 µg/mL (**Table 2**). Analogue **24** was the most effective, with MIC values of 32 µg/mL and 16 µg/mL against *E. faecalis* ATCC 29212 and *S. aureus* ATCC 29213, respectively. When tested against *vancomycin-resistant Enterococcus* (VRE) that was sensitive to ampicillin, the MICs obtained for **22, 23 and 24** were higher than those obtained for the reference strain (64 µg/mL as opposed to 32 µg/mL). In the range of concentrations tested, all these compounds were ineffective against *E. faecalis* B3/101, a VRE strain that was also resistant to ampicillin (**Table 2**). Regarding *S. aureus*, **22, 23 and 24** inhibited the growth of the strain 40/61/24 (MIC 64 µg/mL), which is sensitive to the most commonly used antibiotic families, but not of methicillin-resistant *S. aureus* (MRSA) 66/1. More importantly, compounds **26** and **27** showed a greater inhibitory capacity on both sensitive (40/61/24) and methicillin-resistant *S. aureus* (66/1) strains, with MIC values of 8 µg/mL.



Synergistic effects with vancomycin and oxacillin were evaluated for MDR strains, but no effect was found. These antibiotics are relevant in the treatment of infections caused by *Enterococcus* spp. and *Staphylococcus aureus*, respectively.

**Table 2.** Antibacterial activity of quinazolinones **22-27, 30, 31** on Gram-positive reference and clinically relevant strains.

	<i>S. aureus</i> ATCC 29213		<i>S. aureus</i> 40/61/24		<i>S. aureus</i> 66/1 (MRSA)		<i>E. faecalis</i> ATCC 29212		<i>E. faecalis</i> A5/102 (VRE)		<i>E. faecalis</i> B3/101 (VRE)	
	MIC	MBC	MIC	MBC	MIC	MBC	MIC	MBC	MIC	MBC	MIC	MBC
<b>22</b>	<b>32</b>	> 64	<b>64</b>	>64	>64	>64	<b>64</b>	>64	<b>64</b>	>64	>64	>64
<b>22a</b>	>64	>64	ND	ND	ND	ND	>64	>64	ND	ND	ND	ND
<b>22b</b>	>64	>64	ND	ND	ND	ND	>64	>64	ND	ND	ND	ND
<b>23</b>	<b>32</b>	> 64	<b>64</b>	>64	>64	>64	<b>32</b>	>64	<b>64</b>	>64	>64	>64
<b>23b</b>	>64	ND	ND	ND	ND	ND	>64	>64	ND	ND	ND	ND
<b>24</b>	<b>16</b>	> 64	<b>64</b>	>64	>64	>64	<b>32</b>	>64	<b>64</b>	>64	>64	>64
<b>25</b>	<b>16</b>	> 64	>64	>64	>64	>64	>64	>64	ND	ND	ND	ND
<b>26</b>	<b>4</b>	> 64	<b>8</b>	>64	<b>8</b>	>64	>64	>64	ND	ND	ND	ND
<b>26a</b>	<b>4</b>	>64	<b>4</b>	>64	<b>4</b>	>64	>64	>64	ND	ND	ND	ND
<b>26b</b>	>64	>64	ND	ND	ND	ND	>64	>64	ND	ND	ND	ND
<b>27</b>	<b>4</b>	> 64	<b>8</b>	>64	<b>8</b>	>64	>64	>64	ND	ND	ND	ND
<b>30</b>	<b>16</b>	> 64	<b>64</b>	>64	>64	>64	>64	>64	ND	ND	ND	ND
<b>31</b>	<b>16</b>	> 64	>64	>64	>64	>64	>64	>64	ND	ND	ND	ND

MIC, minimal inhibitory concentration; MBC, minimal bactericidal concentration; VRE, vancomycin-resistant *Enterococcus*; MRSA, methicillin-resistant *Staphylococcus aureus*; ND, not determined. MIC and MBC are expressed in µg/mL. Cefotaxime (CTX) was used as control with the concentrations range 0.031-16µg/mL.

The compounds showed activity only for Gram-positive strains and, overall, this activity was greater for reference strains than for clinically relevant strains, whether MDR or not. Regarding Gram-positive strains, the range was not equal for all compounds, with a greater number of compounds being active against *S. aureus* than *E. faecalis*. Whereas for *E. faecalis* there appeared to

exist an inverse relationship between compound activity and resistance against clinically important antibiotics, there was not a clear tendency for *S. aureus*. It would be interesting to further study the promising inhibitory effect of compounds **26** and **27** on MRSA.

**Antifungal activity.** The antifungal activity of the test compounds was evaluated against *Candida albicans*, *Aspergillus fumigatus* and *Trichophyton rubrum* by determining MICs<sup>37-38</sup>. None of the compounds tested showed activity against *C. albicans* nor *A. fumigatus* strains. Nevertheless, compounds **26**, **28**, and **29** presented a weak inhibitory effect on a dermatophyte strain (*T. rubrum* FF5) with MIC values of 128 µg/mL and a minimal fungicidal concentration (MFC) higher than 128 µg/mL, suggesting that this compound has fungistatic activity (**Table 3**). Given these results, **26**, **28** and **29** were tested against two additional dermatophyte strains (*Microsporum canis* FF1 and *Epidermophyton floccosum* FF9), but no activity was observed (**Table 3**). Compounds **26**, **28**, and **29** were also evaluated for synergistic effects for *T. rubrum*. A synergistic effect was observed for **28** and **29** with fluconazole (data not shown).

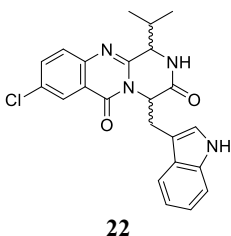
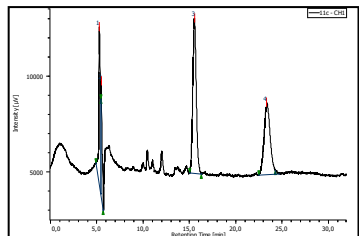
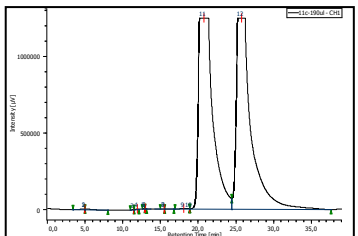
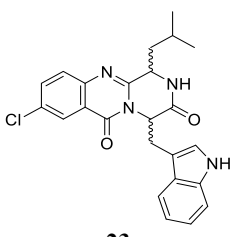
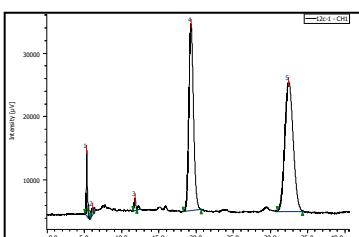
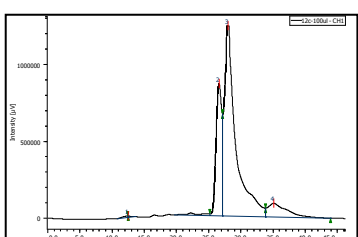
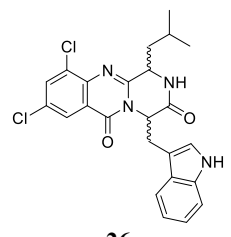
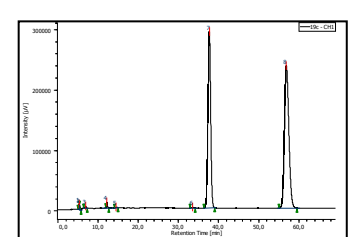
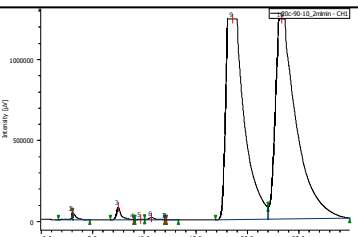
**Table 3.** Antifungal activity of quinazolines **26**, **28**, **29** against dermatophyte strains.

	<i>T. rubrum</i> FF5		<i>M. canis</i> FF1		<i>E. floccosum</i> FF9	
	MIC	MFC	MIC	MFC	MIC	MFC
<b>26</b>	<b>128</b>	>128	>128	>128	>128	>128
<b>26a</b>	>128	>128	ND	ND	ND	ND
<b>26b</b>	>128	>128	ND	ND	ND	ND
<b>28</b>	<b>128</b>	>128	>128	>128	>128	>128
<b>29</b>	<b>128</b>	>128	>128	>128	>128	>128

MIC, minimum inhibitory concentration; MFC, minimum fungicidal concentration; ND, not determined. MIC and MFC are expressed in µg/mL. Voriconazole MIC for *Candida krusei* ATCC 6258 was used as quality control.

**Enantioselective liquid chromatography.** In order to evaluate the *in vitro* activities, such as antibacterial and antifungal, the most promising derivatives **22**, **23**, and **26**, were obtained in milligram scale by semipreparative enantioselective liquid chromatography, employing a *tris*-3,5-dimethylphenylcarbamate amylose column with multiple injection in a 200  $\mu$ L loop. The analytical method presented good separation ( $\alpha > 1.2$ ) and resolution values ( $R_s > 8$ ) for all compounds to allow the scale-up to the preparative mode. The semipreparative separation was optimized by adjusting the sample volume from the analytical method. The optimized mobile phase of analytical system (hexane: EtOH, 90:10) was transferred without any modification to semipreparative mode and 245 was chosen as minimum wavelength absorption.

**Table 4:** Separation performance on the amylose *tris*-3,5 dimethylphenylcarbamate phase for compounds **22**, **23**, and **26**.

Compounds structure	Analytical column <sup>a</sup>	Semipreparative column <sup>b</sup>
 <p><b>22</b></p>	 <p>(<math>k_I = 1.95</math>, <math>\alpha = 1.76</math> <math>R_s = 8.43</math>)</p>	
 <p><b>23</b></p>	 <p>(<math>k_I = 2.64</math>, <math>\alpha = 1.94</math> <math>R_s = 8.15</math>)</p>	
 <p><b>26</b></p>	 <p>(<math>k_I = 5.60</math>, <math>\alpha = 1.75</math> <math>R_s = 11.69</math>)</p>	

<sup>a</sup> Flow rate: 0.5 mL/min, loop 20  $\mu$ L, detection: 245 nm, column: Lux® 5  $\mu$ m Amylose-1, (250 mm x 4.6 mm), mobile phase hexane: EtOH, 90:10.  $k$  = Retention factor,  $R_s$  = Resolution,  $\alpha$  = Separation factor  
<sup>b</sup> Flow rate: 2 mL/min, loop 200  $\mu$ L, loading *ca.* 1.5 mg/mL in hexane:EtOH (50:50), detection 245 nm, column: amylose *tris*-3,5-dimethylphenylcarbamate coated with Nucleosil (200 mm x 7 mm); mobile phase *n*-hexane: EtOH, 90:10.

The column diameter was enlarged to a scale-up factor of 2. The flow rate was increase from 0.5 to 2 mL/min, and the retention times were between 15 to 50 min. The loading effect in semipreparative mode was examined by keeping the concentration of the feed solution at the maximum (1.5 mg/mL) and by varying the volume (100 to 200  $\mu$ L). The mobile phase composition, chromatograms, and chromatographic parameter are summarized in **Table 4** at analytical and semipreparative scales. The elution order, specific rotation, and enantiomeric ratio (*e.r*) of resolved enantiomers were measured and the data is presented in **Table 5**. The *e.r* was greater than 97% for each enantiomer.

**Table 5:** Elution order, specific rotation, and enantiomeric excess (*e.r*) of the resolved compound **22**, **23**, and **26** enantiomers.

Enantiomer	Elution order	$[\alpha]_D$ (c) <sup>a</sup>	<i>e.r</i> (%) <sup>b</sup>
(-)- <b>22</b> ( <b>22a</b> )	First	-0.06 (0.08)	99:1
(+)- <b>22</b> ( <b>22b</b> )	Second	+0.04 (0.10)	99:1
(-)- <b>23</b> ( <b>23a</b> )	First	-0.08 (0.05)	99:1
(+)- <b>23</b> ( <b>23b</b> )	Second	+0.22 (0.12)	99:1
(-)- <b>26</b> ( <b>26a</b> )	First	-0.16 (0.03)	97:3
(+)- <b>26</b> ( <b>26b</b> )	Second	+0.15 (0.03)	99:1

<sup>a</sup> Specific rotation in methanol with c = concentration in g/mL

<sup>b</sup> Enantiomeric ratio (*e.r*) determined by enantioselective LC under condition

The pure enantiomers of **22**, **23**, and **26** were evaluated for antibacterial and antifungal activity. Enantiomer **26a** showed a MIC of 4  $\mu$ g/mL for reference strain *S. aureus* ATCC 29213, sensitive clinical isolate *S. aureus* 40/61/24, and methicillin-resistant strain *S. aureus* 66/1, while enantiomer **26b** showed no effect (**Table 2**). Noteworthy, these derivatives showed higher potency than the natural product neofiscalin A (**2**), (tested by the group with the same conditions)<sup>24-26</sup>. None of the pure enantiomers was active against the fungi tested.

**Structure-activity relationship (SAR) study.** Regarding antibacterial activity, SAR suggested that the presence of a halogen atom at positions C-9 or C-11 plays a crucial role for this activity, since all the non-halogenated compounds were inactive against all the tested strains (**Figure 2**). In fact, compounds containing chlorine atoms at one or both positions exhibited better antibacterial activity compared to those having bromine and iodine. Higher antibacterial activities were obtained when the halogen atom is present at both C-9 and C-11 positions (i.e., compound **25**, **26**, **27** and **32**) and/or the presence of longer side chains at C-1. Compounds **26**, **28**, and **29** were also evaluated for synergistic effects for *T. rubrum*. A synergistic effect was observed for compounds **28** and **29** with fluconazole (data not shown). The enantiopure compound **26a** showed significant antibacterial effect against a resistant strain of *S. aureus* while its antipode (**26b**) did not. This emphasizes that configuration (*1S,4R*) is crucial for antibacterial activity of quinazolinone scaffold.

### Structure-activity relationship

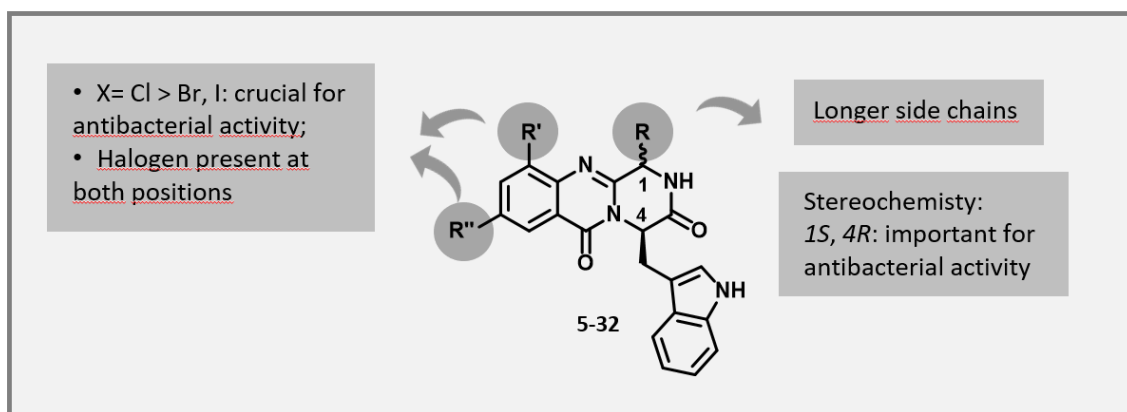


**Figure 2.** Structure-activity relationship for antibacterial activity of the library of quinazolinones.

### CONCLUSIONS

A series of halogenated and non-halogenated indolomethyl pyrazino [1,2-*b*]quinazoline-3,6-diones was designed and synthesized. Among all the obtained compounds, **26** and **27** exhibited a potent antibacterial activity against *S. aureus* strains, with MIC values of 4 µg/mL for a reference strain and MIC values of 8 µg/mL for a sensitive clinical isolate (*S. aureus* 40/61/24) and a

methicillin-resistant strain (*S. aureus* 66/1). Isolation of the enantiomers of **26** revealed that only enantiomer (*1S, 4R*), **26a**, was active, indicating that stereochemistry is vital for the referred activity. Comparing with the marine natural product neofiscalin A (**2**), a two-fold reduction in the MIC was observed. Regarding structure complexity and synthetic pathways, the excellent and inspiring results obtained in the present study show that simpler molecules than neofiscalin A (**2**) are a promising way to find new MDR agents. The presence of five stereocenters in neofiscalin A (**2**) makes its synthesis a challenge, while with this one-pot microwave-assisted multicomponent polycondensation of amino acids, highly active compounds were obtained in one single step.

## MATERIALS AND METHODS

**General Procedure.** All reagents were from analytical grade. Dried pyridine and triphenylphosphite were purchased from Sigma (Sigma-Aldrich Co. Ltd., Gillingham, UK). Anthranilic acids (**33**) and protected amino acids **34** and **36** were purchased from TCI (Tokyo Chemical Industry Co. Ltd., Chuo-ku, Tokyo, Japan). Column chromatography purifications were performed using flash silica Merck 60, 230–400 mesh (EMD Millipore corporation, Billerica, MA, USA) and preparative TLC was carried out on precoated plates Merck Kieselgel 60 F<sub>254</sub> (EMD Millipore corporation, Billerica, MA, USA), spots were visualized with UV light (Vilber Lourmat, Marne-la-Vallée, France). Melting points were measured in a Köfler microscope and are uncorrected. Infrared spectra were recorded in a KBr microplate in a FTIR spectrometer Nicolet iS10 from Thermo Scientific (Waltham, MA, USA) with Smart OMNI-Transmission accessory (Software 188 OMNIC 8.3). <sup>1</sup>H and <sup>13</sup>C NMR spectra were recorded in CDCl<sub>3</sub> (Deutero GmbH, Kastellaun, Germany) at room temperature unless otherwise mentioned on Bruker AMC instrument (Bruker Biosciences Corporation, Billerica, MA, USA), operating at 300 MHz for <sup>1</sup>H and 75 MHz for <sup>13</sup>C). Carbons were assigned according to HSQC and or HMBC experiments. Optical rotation was measured at 25 °C using the ADP 410 polarimeter (Bellingham + Stanley Ltd., Tunbridge Wells, Kent, UK), using the emission wavelength of sodium lamp, concentrations are given in g/100 mL. High resolution mass spectra (HRMS) were measured on a Bruker FTMS APEX III mass

spectrometer (Bruker Corporation, Billerica, MA, USA) recorded as ESI (Electrospray) made in Centro de Apoio Científico e Tecnológico à Investigação (CACTI, University of Vigo, Pontevedra, Spain). The purity of synthesized compounds was determined by reversed-phase LC with diode array detector (DAD) using C18 column (Kimetex<sup>®</sup>, 2.6 EV0 C18 100 Å, 150 × 4.6 mm), the mobile phase was MeOH: H<sub>2</sub>O (50:50), and flow rate was 1 mL/min. Enantiomeric ratio was determined by enantioselective LC (LCMS-2010EV, Shimadzu, Lisbon, Portugal), employing a system equipped with a chiral column (Lux<sup>®</sup> 5 µm Amylose-1, 250 × 4.6 mm) and UV-detection at 254 nm, mobile phase was hexane:EtOH (90:10) and the flow rate was 0.5 mL/min. For semipreparative chromatography, a HPLC system consisted of a Shimadzu LC-6AD pump with a 200 µL loop was used with an amylose tris-3,5-dimethylphenylcarbamate coated with Nucleosil (500 Å, 7 µm, 20%, w/w) packed into a stainless-steel (200 mm x 7 mm I.D. size) column, prepared in the UFSCar laboratory<sup>39</sup>.

**General conditions for the synthesis of compounds 22-32.** In a closed vial, 5-chloro anthranilic acid, **33a**, 34 mg, 200 µmol for **22**, **23**, and **24**, or 3,5-dichloro anthranilic acid, (**33b**, 41 mg, 200 µmol) for **25**, **26**, and **27**, or 5-iodoanthranilic acid, (**33c**, 53 mg, 200 µmol) for **28** and **30**, or 5-bromo anthranilic acid, (**33d**, 43 mg, 200 µmol) for **29** and **31**, or 3,5-diodo anthranilic acid (**33e**, 78 mg, 200 µmol) for **32**; was added *N*-Boc-L-valine (**34a**, 44 mg, 200 µmol) for **22**, **25**, **28** and **29**, or *N*-Boc-L-leucine (**34c**, 46 mg, 200 µmol) for **23**, **26**, **30**, and **32**, or *N*-Boc-L-isoleucine (**34d**, 46 mg, 200 µmol) for **24** and **27** (as present in Table 1), and triphenylphosphite (63 µL, 220 µmol) were added along with 1 mL of dried pyridine. The vial was heated in heating block with stirring at 55 °C for 16–24 h. After cooling the mixture to room temperature, D-tryptophan methyl ester hydrochloride (**36**, 51 mg, 200 µmol) was added, and the mixture was irradiated in the microwave at a constant temperature at 220 °C for 1.5 min. Four reaction mixtures were prepared in the same conditions and treated in parallel. After removing the solvent with toluene, the crude product was purified by flash column chromatography using hexane: EtOAc (60:40) as a mobile phase. The preparative TLC was performed using CH<sub>2</sub>Cl<sub>2</sub>:Me<sub>2</sub>CO (95:5) as mobile phase. The major compound appeared as a black

spot with no fluorescence under the UV light. The desired compounds were collected as yellow solids. Before analysis, compounds were recrystallized from methanol.

**(1*S*,4*R*)-4-((1*H*-indol-3-yl)methyl)-8-chloro-1-isopropyl-1,2-dihydro-6*H*-pyrazino[2,1-  
b]quinazoline-3,6(4*H*)-dione (22).** Yield: 39.8 mg, 7%; er = 56:44; mp: 200.3-202.4 °C;  $[\alpha]_D^{30} = -273$  (*c* 0.05; CHCl<sub>3</sub>);  $\nu_{max}$  (KBr) 3277, 2924, 1682, 1592, 1470, 1323, 741 cm<sup>-1</sup>; <sup>1</sup>H NMR (300 MHz, CDCl<sub>3</sub>):  $\delta$  8.33 (d, 1H, *J* = 2.4 Hz, CH), 8.33 (br, 1H, NH-indol), 7.70 (dd, 1H, *J* = 8.7 and 2.5 Hz, CH), 7.50 (d, *J* = 8.7 Hz, CH), 7.39 (d, 1H, *J* = 8.0 Hz, CH-Trp), 7.30 (d, *J* = 8.2 Hz, CH-Trp), 7.12 (t, 1H, *J* = 7.6 Hz, CH-Trp), 6.92 (t, 1H, *J* = 7.5 Hz, CH-Trp), 6.63 (d, 1H, *J* = 2.3 Hz, CH-indol), 5.64 (dd, 1H, *J* = 5.3 and 2.7, CH\*-Trp), 5.72 (s, 1H, NH-amidee), 3.73 (dd, 1H, *J* = 15.0 and 2.7 Hz, CH<sub>2</sub>-Trp), 3.63 (dd, 1H, *J* = 15.0 and 5.4 Hz, CH<sub>2</sub>-Trp), 2.76 (d, *J* = 2.3 Hz, CH\*-val), 2.60 (dtd, 1H, *J* = 13.9, 6.9, and 2.3 Hz, CH-val), 0.64 (d, 6H, *J* = 6.1 Hz, CH<sub>3</sub>-val); <sup>13</sup>C NMR (75 MHz, CDCl<sub>3</sub>):  $\delta$  169.2 (C=O), 159.9 (C=O), 150.6 (C=N), 145.6 (C), 136.1 (C-Trp), 135.7 (CH), 132.8 (C), 128.9 (CH), 127.2 (C-Trp), 126.2 (CH), 123.6 (CH-indol), 122.5 (CH-Trp), 121.2 (C), 119.9 (CH-Trp), 118.6 (CH-Trp), 111.1 (CH-Trp), 109.1 (C-indol), 57.0 (CH\*-Trp), 58.0 (CH\*-val), 29.3 (CH-val), 27.3 (CH<sub>2</sub>-Trp), 18.8 (CH<sub>3</sub>-val), 14.8 (CH<sub>3</sub>-val); (+)-HRMS-ESI *m/z*: 421.1442 (M + H)<sup>+</sup>, 443.1264 (M + Na)<sup>+</sup> (calculated for C<sub>23</sub>H<sub>22</sub>N<sub>4</sub>O<sub>2</sub>Cl, 421.1432; C<sub>23</sub>H<sub>21</sub>N<sub>4</sub>O<sub>2</sub>ClNa, 443.1252).

**(1*S*,4*R*)-4-((1*H*-indol-3-yl)methyl)-8-chloro-1-isobutyl-1,2-dihydro-6*H*-pyrazino[2,1-  
b]quinazoline-3,6(4*H*)-dione (23).** Yield: 12.3 mg, 3%; er = 44:56; mp: 208.8-210.1 °C;  $[\alpha]_D^{30} = +154$  (*c* 0.15; CHCl<sub>3</sub>);  $\nu_{max}$  (KBr) 3277, 2924, 1682, 1592, 1470, 1323, 741 cm<sup>-1</sup>; <sup>1</sup>H NMR (300 MHz, CDCl<sub>3</sub>):  $\delta$  8.33 (d, 1H, *J* = 2.4 Hz, CH), 8.07 (br, 1H, NH-indol), 7.70 (dd, 1H, *J* = 8.7 and 2.5 Hz, CH), 7.54 (d, *J* = 8.7 Hz, CH), 7.46 (d, 1H, *J* = 8.0 Hz, CH-Trp), 7.29 (d, *J* = 8.2 Hz, CH-Trp), 7.13 (t, 1H, *J* = 7.6 Hz, CH-Trp), 6.98 (t, 1H, *J* = 7.5 Hz, CH-Trp), 6.65 (d, 1H, *J* = 2.2 Hz, CH-indol), 5.71 (s, 1H, NH-amide), 5.65 (dd, 1H, *J* = 5.2 and 2.8, CH\*-Trp), 3.76 (dd, 1H, *J* = 15.1 and 2.7 Hz, CH<sub>2</sub>-Trp), 3.63 (dd, 1H, *J* = 15.1 and 5.4 Hz, CH<sub>2</sub>-Trp), 2.70 (dd, *J* = 9.7 and 2.3 Hz, CH\*-Leu), 1.97 (ddd, 1H, *J* = 11.8, 7.7, and 2.1 Hz, CH-Leu), 1.39—1.30 (m, 2H), 0.77 (d, 3H, *J* = 6.4 Hz, CH<sub>3</sub>-Leu), 0.28 (d, 3H, *J* = 6.5 Hz, CH<sub>3</sub>-Leu); <sup>13</sup>C NMR (75 MHz, CDCl<sub>3</sub>):  $\delta$  169.1 (C=O), 159.8



(C=O), 151.9 (C=N), 145.5 (C), 136.0 (C-Trp 135.1 (CH), 132.9 (C), 129.1 (CH), 127.2 (C-tyr), 126.2 (CH), 123.6 (CH-indol), 122.7 (CH-Trp), 121.2 (C), 120.2 (CH-Trp), 118.7 (CH-Trp), 111.1 (CH-Trp), 109.5 (C-indol), 57.5 (CH\*-Trp), 50.8 (CH\*-Leu), 40.2 (CH<sub>2</sub>-Leu), 27.2 (CH<sub>2</sub>-Trp), 24.1 (CH-Leu), 23.3 (CH<sub>3</sub>-Leu), 19.7 (CH<sub>3</sub>-Leu); (+)-HRMS-ESI *m/z*: 435.1579 (M + H)<sup>+</sup>, 457.1206 (M + Na)<sup>+</sup> (calculated for C<sub>24</sub>H<sub>24</sub>N<sub>4</sub>O<sub>2</sub>Cl, 435.1588; C<sub>24</sub>H<sub>23</sub>N<sub>4</sub>O<sub>2</sub>ClNa, 457.1408).

**(1*S*,4*R*)-4-((1*H*-indol-3-yl)methyl)-1-((*S*)-sec-butyl)-8-chloro-1,2-dihydro-6*H*-pyrazino[2,1-*b*]quinazoline-3,6(4*H*)-dione (24).** Yield: 16.7 mg, 3%; er = 46:54; mp: 209.1-211.2 °C; [ $\alpha$ ]<sub>D</sub><sup>30</sup> = +130 (*c* 0.03; CHCl<sub>3</sub>);  $\nu_{max}$  (KBr) 3277, 2924, 1682, 1592, 1470, 1323, 741 cm<sup>-1</sup>; <sup>1</sup>H NMR (300 MHz, CDCl<sub>3</sub>):  $\delta$  8.33 (d, 1H, *J* 2.4 Hz, CH), 8.05 (br, 1H, NH-indol), 7.70 (dd, 1H, *J* = 8.7 and 2.4 Hz, CH), 7.49 (d, *J* = 8.7 Hz, CH), 7.38 (d, 1H, *J* = 8.0 Hz, CH-Trp), 7.29 (d, *J* = 8.2 Hz, CH-Trp), 7.13 (t, 1H, *J* = 7.9 Hz, CH-Trp), 6.92 (t, 1H, *J* = 7.8 Hz, CH-Trp), 6.63 (d, 1H, *J* = 2.4 Hz, CH-indol), 5.64 (dd, 1H, *J* = 5.2 and 2.8, CH\*-Trp), 5.80 (s, 1H, NH-amide), 3.72 (dd, 1H, *J* = 15.1 and 2.7 Hz, CH<sub>2</sub>-Trp), 3.62 (dd, 1H, *J* = 15.0 and 5.4 Hz, CH<sub>2</sub>-Trp), 2.29 (ddd, 1H, *J* = 11.6, 7.9, and 4.8 Hz, CH-Ile), 2.69 (d, *J* = 2.2 Hz, CH\*-Ile), 0.99—0.79 (m, 2H), 0.70 (d, 3H, *J* = 7.4 Hz, CH<sub>3</sub>-Ile), 0.63 (d, 3H, *J* = 7.2 Hz, CH<sub>3</sub>-Ile); <sup>13</sup>C NMR (75 MHz, CDCl<sub>3</sub>):  $\delta$  169.1 (C=O), 159.9 (C=O), 150.7 (C=N), 145.5 (C), 136.0 (C-Trp 135.1 (CH), 132.8 (C), 128.9 (CH), 127.2 (C-tyr), 126.2 (CH), 123.5 (CH-indol), 122.7 (CH-Trp), 121.1 (C), 120.1 (CH-Trp), 118.6 (CH-Trp), 111.1 (CH-Trp), 109.2 (C-indol), 58.3 (CH\*-Ile), 57.0 (CH\*-tyr), 36.2 (CH-Leu), 27.3 (CH<sub>2</sub>-Trp), 23.1 (CH<sub>2</sub>-Ile), 15.6 (CH<sub>3</sub>-Ile), 12.0 (CH<sub>3</sub>-Ile); (+)-HRMS-ESI *m/z*: 435.1580 (M + H)<sup>+</sup>, 457.1394 (M + Na)<sup>+</sup> (calculated for C<sub>24</sub>H<sub>24</sub>N<sub>4</sub>O<sub>2</sub>Cl, 434.1588; C<sub>24</sub>H<sub>23</sub>N<sub>4</sub>O<sub>2</sub>ClNa, 457.1408).

**(1*S*,4*R*)-4-((1*H*-indol-3-yl)methyl)-8,10-dichloro-1-isopropyl-1,2-dihydro-6*H*-pyrazino[2,1-*b*]quinazoline-3,6(4*H*)-dione (25).** Yield: 22.1 mg, 5%; er = 43:57; mp: 232.9-235.1 °C; [ $\alpha$ ]<sub>D</sub><sup>30</sup> = +140 (*c* 0.038; CHCl<sub>3</sub>);  $\nu_{max}$  (KBr) 3293, 2954, 1671, 1611, 1511, 1465, 1240, 772, and 697 cm<sup>-1</sup>; <sup>1</sup>H NMR (300 MHz, DMSO-*d*<sub>6</sub>):  $\delta$  10.2 (br, 1H, NH-indol), 8.20 (d, 1H, *J* 2.4 Hz, CH), 7.83 (d, 1H, *J* = 2.4 Hz, CH), 7.37 (d, 1H, *J* = 8.1 Hz, CH-Trp), 7.33 (d, *J* = 8.1 Hz, CH-Trp), 7.11 (s, 1H, NH-amide), 7.07 (t, 1H, *J* = 7.7 Hz, CH-Trp), 6.87 (t, 1H, *J* = 7.5 Hz, CH-Trp), 6.66 (d, 1H, *J* = 2.3 Hz,

CH-indol), 5.50 (dd, 1H,  $J = 5.2$  and  $2.9$ , CH\*-Trp), 3.69 (dd, 1H,  $J = 14.9$  and  $3.0$  Hz, CH<sub>2</sub>-Trp), 3.58 (dd, 1H,  $J = 14.9$  and  $5.4$  Hz, CH<sub>2</sub>-Trp), 2.76 (d,  $J = 2.2$  Hz, CH\*-val), 2.60- 254 (m, 1H, CH-val), 0.71 (dd, 6H,  $J = 8.4$  and  $7.2$  Hz, CH<sub>3</sub>-val); <sup>13</sup>C NMR (75 MHz, CDCl<sub>3</sub>):  $\delta$  169.2 (C=O), 159.9 (C=O), 150.6 (C=N), 145.7 (C), 136.0 (C-Trp), 135.1 (CH), 132.8 (C), 128.9 (CH), 127.2 (C-Trp), 126.2 (CH), 123.6 (CH-indol), 122.7 (CH-Trp), 121.2 (C), 120.1 (CH-Trp), 118.6 (CH-Trp), 111.1 (CH-Trp), 109.2 (C-indol), 58.1 (CH\*-val), 57.0 (CH\*-Trp), 29.3 (CH-val), 27.3 (CH<sub>2</sub>-Trp), 18.8 (CH<sub>3</sub>-val), 14.8 (CH<sub>3</sub>-val; (+)-HRMS-ESI  $m/z$ : 455.1436 (M + H)<sup>+</sup> (calculated for C<sub>23</sub>H<sub>21</sub>N<sub>4</sub>O<sub>2</sub>Cl<sub>2</sub>, 455.1041).

**(1*S*,4*R*)-4-((1*H*-indol-3-yl)methyl)-8,10-dichloro-1-isobutyl-1,2-dihydro-6*H*-pyrazino[2,1-*b*]quinazoline-3,6(4*H*)-dione (26).** Yield: 41.8 mg, 4.5%; er = 60:40; mp: 253.4-254.3 °C; [ $\alpha$ ]<sub>D</sub><sup>30</sup> = -169 (*c* 0.04; CHCl<sub>3</sub>);  $\nu_{max}$  (KBr) 3289, 2960, 1680, 1600, 1556, 1315, 757, 720 cm<sup>-1</sup>; <sup>1</sup>H NMR (300 MHz, DMSO-*d*<sub>6</sub>): 10.22 (br, 1H, NH-indol),  $\delta$  8.13 (d, 1H,  $J$  2.4 Hz, CH), 7.75 (d, 1H,  $J = 2.4$  Hz, CH), 7.33 (d, 1H,  $J = 8.0$  Hz, CH-Trp), 7.25 (d,  $J = 8.2$  Hz, CH-Trp), 7.19 (br, NH-amide), 7.00 (t, 1H,  $J = 8.0$  Hz, CH-Trp), 6.82 (t, 1H,  $J = 7.8$  Hz, CH-Trp), 6.60 (d, 1H,  $J = 2.4$  Hz, CH-indol), 5.42 (dd, 1H,  $J = 5.3$  and  $2.9$ , CH\*-Trp), 3.63 (dd, 1H,  $J = 15.0$  and  $2.9$  Hz, CH<sub>2</sub>-Trp), 3.50 (dd, 1H,  $J = 15.0$  and  $5.4$  Hz, CH<sub>2</sub>-Trp), 2.68 (dd,  $J = 7.3$  and  $4.9$  Hz, CH\*-Leu), 1.94-1.86 (m, 1H CH<sub>2</sub>-Leu), 1.50 (tt, 1H,  $J = 13.2$  and  $6.5$  Hz, CH-Leu), 1.29-1.22 (m, 1H, CH<sub>2</sub>-Leu), 0.56 (d, 3H,  $J = 6.6$  Hz, CH<sub>3</sub>-Leu), 0.35 (d, 3H,  $J = 6.6$  Hz, CH<sub>3</sub>-Leu); <sup>13</sup>C NMR (75 MHz, DMSO-*d*<sub>6</sub>):  $\delta$  168.4 (C=O), 158.8 (C=O), 152.8 (C=N), 142.0 (C), 135.9 (C-Trp), 134.1 (CH), 132.6 (C), 131.4 (C), 126.5 (C-Trp), 124.3 (CH), 123.5 (CH-indol), 121.6 (CH-Trp), 121.5 (C), 118.9 (CH-Trp), 117.7 (CH-Trp), 111.1 (CH-Trp), 107.7 (C-indol), 57.3 (CH\*-Trp), 50.6 (CH\*-Leu), 39.6 (CH<sub>2</sub>-Leu), 26.2 (CH<sub>2</sub>-Trp), 23.8 (CH-Leu), 22.1 (CH<sub>3</sub>-Leu), 20.5 (CH<sub>3</sub>-Leu); (+)-HRMS-ESI  $m/z$ : 469.1186 (M + H)<sup>+</sup>, 491.1008 (M + Na)<sup>+</sup> (calculated for C<sub>24</sub>H<sub>23</sub>N<sub>4</sub>O<sub>2</sub>Cl<sub>2</sub>, 469.1198; C<sub>24</sub>H<sub>22</sub>N<sub>4</sub>O<sub>2</sub>Cl<sub>2</sub>Na, 491.1018).

**(1*S*,4*R*)-4-((1*H*-indol-3-yl)methyl)-1-((*S*)-sec-butyl)-8,10-dichloro-1,2-dihydro-6*H*-pyrazino[2,1-*b*]quinazoline-3,6(4*H*)-dione (27).** Yield: 22.4 mg, 2.6%; er = 71:29; mp: 252.9-254.7 °C; [ $\alpha$ ]<sub>D</sub><sup>30</sup> = -264 (*c* 0.034; CHCl<sub>3</sub>);  $\nu_{max}$  (KBr) 3373, 3074, 2922, 1698, 1609, 1550, 1450, 1262,

794 cm<sup>-1</sup>; <sup>1</sup>H NMR (300 MHz, CDCl<sub>3</sub>): δ 8.33 (d, 1H, *J* 2.4 Hz, CH), 8.05 (br, 1H, NH-indol), 7.70 (dd, 1H, *J* = 8.7 and 2.4 Hz, CH), 7.38 (d, 1H, *J* = 8.0 Hz, CH-Trp), 7.29 (d, *J* = 8.2 Hz, CH-Trp), 7.13 (t, 1H, *J* = 7.9 Hz, CH-Trp), 6.92 (t, 1H, *J* = 7.8 Hz, CH-Trp), 6.63 (d, 1H, *J* = 2.4 Hz, CH-indol), 5.64 (dd, 1H, *J* = 5.2 and 2.8, CH\*-Trp), 5.80 (s, 1H, NH-amide), 3.72 (dd, 1H, *J* = 15.1 and 2.7 Hz, CH<sub>2</sub>-Trp), 3.62 (dd, 1H, *J* = 15.0 and 5.4 Hz, CH<sub>2</sub>-Trp), 2.29 (ddd, 1H, *J* = 11.6, 7.9, and 4.8 Hz, CH-Ile), 2.69 (d, *J* = 2.2 Hz, CH\*-Ile), 0.99—0.79 (m, 2H), 0.70 (d, 3H, *J* = 7.4 Hz, CH<sub>3</sub>-Ile), 0.63 (d, 3H, *J* = 7.2 Hz, CH<sub>3</sub>-Ile); <sup>13</sup>C NMR (75 MHz, CDCl<sub>3</sub>): δ 168.9 (C=O), 159.5 (C=O), 151.3 (C=N), 142.5 (C), 136.1 (C-Trp) 135.0 (CH), 133.2 (C), 132.4 (C), 127.1 (C-tyr), 125.1 (CH), 123.5 (CH-indol), 122.9 (CH-Trp), 122.1 (C), 120.2 (CH-Trp), 118.6 (CH-Trp), 111.1 (CH-Trp), 109.2 (C-indol), 58.2 (CH\*-Ile), 57.3 (CH\*-tyr), 36.2 (CH-Leu), 27.1 (CH<sub>2</sub>-Trp), 23.6 (CH<sub>2</sub>-Ile), 15.5 (CH<sub>3</sub>-Ile), 12.1 (CH<sub>3</sub>-Ile); (+)-HRMS-ESI *m/z*: 469.1186 (M + H)<sup>+</sup>, 491.1024 (M + Na)<sup>+</sup> (calculated for C<sub>24</sub>H<sub>23</sub>N<sub>4</sub>O<sub>2</sub>Cl<sub>2</sub>, 469.1198; C<sub>24</sub>H<sub>22</sub>N<sub>4</sub>O<sub>2</sub>Cl<sub>2</sub>Na, 491.1018).

**(1*S*,4*R*)-4-((1*H*-indol-3-yl)methyl)-8-iodo-1-isopropyl-1,2-dihydro-6*H*-pyrazino[2,1-*b*]quinazoline-3,6(4*H*)-dione (28)**. Yield: 21.2 mg, 4.1%; er = 51:49; mp: 246.5-248.2 °C; [ $\alpha$ ]<sub>D</sub><sup>30</sup> = -175 (*c* 0.041; CHCl<sub>3</sub>);  $\nu_{max}$  (KBr) 3311, 3192, 2963, 1681, 1655, 1588, 1464, 1246, 828, and 741 cm<sup>-1</sup>; <sup>1</sup>H NMR (300 MHz, CDCl<sub>3</sub>): δ 8.71 (d, 1H, *J* 2.4 Hz, CH), 8.04 (br, 1H, NH-indol), 8.02 (dd, 1H, *J* = 8.6 and 2.1 Hz, CH), 7.41 (d, 1H, *J* = 8.0 Hz, CH-Trp), 7.30 (d, *J* = 8.4 Hz, CH) 7.29 (d, *J* = 8.4 Hz, CH-Trp), 7.13 (ddd, 1H, *J* = 8.0, 7.1 and 0.9 Hz, CH-Trp), 6.94 (ddd, 1H, *J* = 8.0, 7.1 and 0.9 Hz, CH-Trp), 6.61 (d, 1H, *J* = 2.4 Hz, CH-indol), 5.64 (dd, 1H, *J* = 5.4 and 2.8, CH\*-Trp), 5.67 (s, 1H, NH-amide), 3.73 (dd, 1H, *J* = 14.9 and 2.7 Hz, CH<sub>2</sub>-Trp), 3.61 (dd, 1H, *J* = 15.1 and 5.4 Hz, CH<sub>2</sub>-Trp), 2.64 (d, *J* = 2.4 Hz, CH\*-val), 2.63-2.56 (m, 1H, CH-val), 0.63 (d, 6H, *J* = 6.8 Hz, CH<sub>3</sub>-val); <sup>13</sup>C NMR (75 MHz, CDCl<sub>3</sub>): δ 169.1 (C=O), 159.5 (C=O), 151.0 (C=N), 146.3 (C), 143.5 (CH), 136.0 (C-Trp) 135.7 (CH), 129.0 (CH), 127.2 (C-Trp), 123.5 (CH-indol), 122.7 (CH-Trp), 121.7 (C), 120.2 (CH-Trp), 118.7 (CH-Trp), 111.1 (CH-Trp), 109.3 (C-indol), 91.4 (C), 58.1 (CH\*-val), 57.0 (CH\*-Trp) 29.7 (CH-val), 27.3 (CH<sub>2</sub>-Trp), 18.8 (CH<sub>3</sub>-val), 14.8 (CH<sub>3</sub>-val); (+)-HRMS-ESI *m/z*: 513.0778 (M + H)<sup>+</sup> (calculated for C<sub>23</sub>H<sub>22</sub>N<sub>4</sub>O<sub>2</sub>I, 513.0787).

**(1*S*,4*R*)-4-((1*H*-indol-3-yl)methyl)-8-bromo-1-isopropyl-1,2-dihydro-6*H*-pyrazino[2,1-*b*]quinazoline-3,6(4*H*)-dione (29).** Yield: 10.9 mg, 1.2%; er = 50:50; mp: 236.5-238.0 °C;  $[\alpha]_D^{30} = -170$  (*c* 0.03; CHCl<sub>3</sub>);  $\nu_{max}$  (KBr) 3292, 3193, 2958, 1681, 1666, 1592, 1466, 1237, 832, and 742 cm<sup>-1</sup>; <sup>1</sup>H NMR (300 MHz, CDCl<sub>3</sub>):  $\delta$  8.50 (d, 1H, *J* 2.2 Hz, CH), 8.05 (br, 1H, NH-indol), 7.84 (dd, 1H, *J* = 8.7 and 2.3 Hz, CH), 7.41 (t, *J* = 8.0 Hz, CH), 7.41 (t, *J* = 8.0 Hz, CH-Trp), 7.29 (d, *J* = 8.2 Hz, CH-Trp), 7.13 (ddd, 1H, *J* = 8.0, 7.1 and 1.0 Hz, CH-Trp), 6.93 (ddd, 1H, *J* = 8.0, 7.1 and 1.1 Hz, CH-Trp), 6.62 (d, 1H, *J* = 2.4 Hz, CH-indol), 5.64 (dd, 1H, *J* = 5.4 and 3.0, CH\*-Trp), 5.63 (s, 1H, NH-amide), 3.73 (dd, 1H, *J* = 14.9 and 2.7 Hz, CH<sub>2</sub>-Trp), 3.62 (dd, 1H, *J* = 15.0 and 5.4 Hz, CH<sub>2</sub>-Trp), 2.66 (d, *J* = 2.4 Hz, CH\*-val), 2.60 (m, 1H, CH-val), 0.65 (d, 3H, *J* = 6.5 Hz, CH<sub>3</sub>-val), 0.63 (d, 3H, *J* = 6.4 Hz, CH<sub>3</sub>-val); <sup>13</sup>C NMR (75 MHz, CDCl<sub>3</sub>):  $\delta$  169.1 (C=O), 159.7 (C=O), 150.9 (C=N), 145.9 (C), 138.1 (CH), 136. (C-Trp), 129.4 (C), 129.1 (CH), 127.2 (C-tyr), 123.5 (CH-indol), 122.7 (CH-Trp), 121.5 (C), 120.6 (CH-Trp), 120.2 (C), 118.7 (CH-Trp), 111.1 (CH-Trp), 109.3 (C-indol), 57.0 (CH\*-tyr), 53.8 (CH\*-val), 29.7 (CH-val), 27.3 (CH<sub>2</sub>-Trp), 18.8 (CH<sub>3</sub>-val), 14.8 (CH<sub>3</sub>-val); (+)-HRMS-ESI *m/z*: 465.0987 (M + H)<sup>+</sup>, 487.0726 (M + Na)<sup>+</sup> (calculated for C<sub>23</sub>H<sub>22</sub>N<sub>4</sub>O<sub>2</sub>Br: 465.0926; C<sub>23</sub>H<sub>21</sub>N<sub>4</sub>O<sub>2</sub>BrNa: 487.0746).

**(1*S*,4*R*)-4-((1*H*-indol-3-yl)methyl)-8-iodo-1-isobutyl-1,2-dihydro-6*H*-pyrazino[2,1-*b*]quinazoline-3,6(4*H*)-dione (30).** Yield: 62.4 mg, 11.8%; er = 51:49; mp: 192.1-194.3 °C;  $[\alpha]_D^{30} = -165$  (*c* 0.038; CHCl<sub>3</sub>);  $\nu_{max}$  (KBr) 3318, 2956, 1671, 1686, 1593, 1464, 1247, 790, and 740 cm<sup>-1</sup>; <sup>1</sup>H NMR (300 MHz, CDCl<sub>3</sub>):  $\delta$  8.70 (d, 1H, *J* 2.0 Hz, CH), 8.03 (br, 1H, NH-indol), 8.03 (dd, 1H, *J* = 8.6 and 2.1 Hz, CH), 7.44 (d, *J* = 7.9 Hz, CH-Trp), 7.33 (d, 1H, *J* = 8.6 Hz, CH), 7.29 (d, *J* = 8.2 Hz, CH-Trp), 7.13 (t, 1H, *J* = 7.8 Hz, CH-Trp), 6.98 (t, 1H, *J* = 7.8 Hz, CH-Trp), 6.68 (d, 1H, *J* = 2.4 Hz, CH-indol), 5.96 (s, 1H, NH-amide), 5.65 (dd, 1H, *J* = 5.2 and 2.8, CH\*-Trp), 3.76 (dd, 1H, *J* = 15.0 and 2.8 Hz, CH<sub>2</sub>-Trp), 3.63 (dd, 1H, *J* = 15.0 and 5.3 Hz, CH<sub>2</sub>-Trp), 2.69 (dd, *J* = 9.6 and 3.3 Hz, CH\*-Leu), 2.02-1.92 (m, 1H, CH-Leu), 1.40-1.30 (m, 2H, CH<sub>2</sub>-Leu), 0.79 (d, 3H, *J* = 6.5 Hz, CH<sub>3</sub>-Leu), 0.29 (d, 3H, *J* = 6.4 Hz, CH<sub>3</sub>-Leu); <sup>13</sup>C NMR (75 MHz, CDCl<sub>3</sub>):  $\delta$  169.5 (C=O), 159.4 (C=O), 152.1 (C=N), 146.3 (C), 143.4 (CH), 136.1 (C-Trp), 135.7 (C), 129.2 (CH), 127.1 (C-tyr), 123.5 (CH-indol), 122.9 (CH-Trp), 121.8 (C), 120.4 (CH-Trp), 118.7 (CH-Trp), 111.2 (CH-Trp),

109.5 (C-indol), 91.5 (C), 57.4 (CH\*-tyr), 51.0 (CH\*-Leu), 40.1 (CH<sub>2</sub>-Leu), 27.1 (CH<sub>2</sub>-Trp), 24.1 (CH-Leu), 23.3 (CH<sub>3</sub>-Leu), 19.7 (CH<sub>3</sub>-Leu); (+)-HRMS-ESI *m/z*: 527.0936 (M + H)<sup>+</sup>, 549.0748 (M + Na)<sup>+</sup> (calculated for C<sub>24</sub>H<sub>24</sub>N<sub>4</sub>O<sub>2</sub>I, 527.0944; C<sub>24</sub>H<sub>23</sub>N<sub>4</sub>O<sub>2</sub>INa, 549.0764).

**(1*S*,4*R*)-4-((1*H*-indol-3-yl)methyl)-8-bromo-1-isobutyl-1,2-dihydro-6*H*-pyrazino[2,1-*b*]quinazoline-3,6(4*H*)-dione (31)**. Yield: 64.6 mg, 13.8%; er = 51:49; mp: 227.0-228.2 °C; [ $\alpha$ ]<sub>D</sub><sup>30</sup> = -243 (*c* 0.037; CHCl<sub>3</sub>);  $\nu_{max}$  (KBr) 3284, 2959, 1686, 1658, 1599, 1433, 1245, 746, and 684 cm<sup>-1</sup>; <sup>1</sup>H NMR (300 MHz, CDCl<sub>3</sub>):  $\delta$  8.50 (d, 1H, *J* 2.3 Hz, CH), 8.06 (br, 1H, NH-indol), 7.84 (dd, 1H, *J* = 8.7 and 2.3 Hz, CH), 7.47 (dd, *J* = 8.2 and 1.9 Hz, CH), 7.47 (dd, 1H, *J* = 8.2 and 1.9 Hz, CH-Trp), 7.29 (d, *J* = 8.2 Hz, CH-Trp), 7.14 (t, 1H, *J* = 7.9 Hz, CH-Trp), 6.92 (t, 1H, *J* = 7.8 Hz, CH-Trp), 6.65 (d, 1H, *J* = 2.4 Hz, CH-indol), 5.65 (dd, 1H, *J* = 5.2 and 2.9, CH\*-Trp), 5.71 (s, 1H, NH-amide), 3.76 (dd, 1H, *J* = 15.0 and 2.8 Hz, CH<sub>2</sub>-Trp), 3.63 (dd, 1H, *J* = 15.0 and 5.3 Hz, CH<sub>2</sub>-Trp), 2.70 (dd, *J* = 9.7 and 3.3 Hz, CH\*-Leu), 2.07-1.89 (m, 1H, CH-Leu), 1.38—1.21 (m, 2H, CH<sub>2</sub>-Leu), 0.77 (d, 3H, *J* = 6.3 Hz, CH<sub>3</sub>-Leu), 0.28 (d, 3H, *J* = 6.5 Hz, CH<sub>3</sub>-Leu); <sup>13</sup>C NMR (75 MHz, CDCl<sub>3</sub>):  $\delta$  169.1 (C=O), 159.7 (C=O), 152.0 (C=N), 145.8 (C), 137.8 (CH), 136.8 (C-Trp), 129.4 (C), 129.2 (CH), 127.1 (C-Trp), 123.8 (CH-indol), 122.9 (CH-Trp), 121.6 (C), 120.6 (CH), 120.4 (CH-Trp), 118.7 (CH-Trp), 111.2 (CH-Trp), 109.6 (C-indol), 57.5 (CH\*-Trp), 50.8 (CH\*-Leu), 40.1 (CH<sub>2</sub>-Leu), 27.1 (CH<sub>2</sub>-Trp), 24.1 (CH-Leu), 23.3 (CH<sub>3</sub>-Leu), 19.7 (CH<sub>3</sub>-Leu); (+)-HRMS-ESI *m/z*: 479.1086 (M + H)<sup>+</sup>, 501.0912 (M + Na)<sup>+</sup> (calculated for C<sub>24</sub>H<sub>24</sub>N<sub>4</sub>O<sub>2</sub>Br, 479.1082; C<sub>24</sub>H<sub>23</sub>N<sub>4</sub>O<sub>2</sub>BrNa, 501.0900).

**(1*S*,4*R*)-4-((1*H*-indol-3-yl)methyl)-8,10-diiodo-1-isobutyl-1,2-dihydro-6*H*-pyrazino[2,1-*b*]quinazoline-3,6(4*H*)-dione (32)**. Yield: 22.5 mg, 3.5%; er = 54:46; mp: 242.8-243.8 °C; [ $\alpha$ ]<sub>D</sub><sup>30</sup> = -229 (*c* 0.032; CHCl<sub>3</sub>);  $\nu_{max}$  (KBr) 3313, 2955, 1681, 1599, 1462, 1261, 772, and 669 cm<sup>-1</sup>; <sup>1</sup>H NMR (300 MHz, DMSO-*d*<sub>6</sub>): 10.17 (br, 1H, NH-indol),  $\delta$  8.62 (d, 1H, *J* 1.9 Hz, CH), 8.55 (d, 1H, *J* = 1.9 Hz, CH), 7.41 (d, 1H, *J* = 8.0 Hz, CH-Trp), 7.33 (d, *J* = 8.0 Hz, CH-Trp), 7.11 (br, NH-amide), 7.09 (t, 1H, *J* = 7.9 Hz, CH-Trp), 6.91 (t, 1H, *J* = 7.5 Hz, CH-Trp), 6.68 (d, 1H, *J* = 2.3 Hz, CH-indol), 5.50 (dd, 1H, *J* = 5.1 and 2.9, CH\*-Trp), 3.72 (dd, 1H, *J* = 14.9 and 2.9 Hz, CH<sub>2</sub>-Trp), 3.58 (dd, 1H, *J* = 15.0 and 5.3 Hz, CH<sub>2</sub>-Trp), 2.75 (dd, *J* = 6.6 and 5.3 Hz, CH\*-Leu), 1.68-1.53 (m, 1H CH<sub>2</sub>-Leu),

1.38-1.23 (m, 2H,  $J = 13.2$  and  $6.5$  Hz, CH<sub>2</sub>-Leu), 0.62 (t, 3H,  $J = 6.5$  Hz, CH<sub>3</sub>-Leu), 0.47 (d, 3H,  $J = 6.6$  Hz, CH<sub>3</sub>-Leu); <sup>13</sup>C NMR (75 MHz, DMSO-d<sub>6</sub>):  $\delta$  168.4 (C=O), 162.0 (C=O), 153.0 (C=N), 151.1 (C), 136.2 (C-Trp), 135.9 (C), 127.1 (C-Trp), 123.4 (CH-indol), 121.8 (C), 121.5 (CH-Trp), 119.0 (CH-Trp), 117.8 (CH-Trp), 111.0 (CH-Trp), 107.8 (C-indol), 91.5 (CH), 89.2 (CH), 57.4 (CH\*-Trp), 50.5 (CH\*-Leu), 39.4 (CH<sub>2</sub>-Leu), 26.3 (CH<sub>2</sub>-Trp), 23.9 (CH-Leu), 21.8 (CH<sub>3</sub>-Leu), 20.6 (CH<sub>3</sub>-Leu); (+)-HRMS-ESI  $m/z$ : 652.9915 (M + H)<sup>+</sup>, 674.9746 (M + Na)<sup>+</sup> (calculated for C<sub>24</sub>H<sub>23</sub>N<sub>4</sub>O<sub>2</sub>Cl<sub>2</sub>, 652.9910; C<sub>24</sub>H<sub>22</sub>N<sub>4</sub>O<sub>2</sub>Cl<sub>2</sub>Na, 674.9730).

## Microbiology

**Microbial strains and growth conditions.** In the present study, two Gram-positive – *Staphylococcus aureus* ATCC 29213 and *Enterococcus faecalis* ATCC 29212– and two Gram-negative – *Escherichia coli* ATCC 25922 and *Pseudomonas aeruginosa* ATCC 27853 – reference bacterial strains were used. When it was possible to determine a minimal inhibitory concentration (MIC) value for these strains, clinically relevant strains were also used. These included methicillin-resistant *S. aureus* (MRSA) 66/1, isolated from public buses<sup>40</sup>, as well as a isolate sensitive to the most commonly used antibiotic families (*S. aureus* 40/61/24); and two *vancomycin-resistant Enterococcus (VRE) strains isolated from river water*<sup>41</sup>, *E. faecalis* B3/101 and *E. faecalis* A5/102, which is sensitive to ampicillin. Frozen stocks of all strains were grown on Mueller-Hinton agar (MH – BioKar Diagnostics, Allone, France) at 37 °C for 24 h. All bacterial strains were sub-cultured on MH agar and incubated overnight at 37 °C before each assay, in order to obtain fresh cultures. For the antifungal activity screening, a yeast reference strain *Candida albicans* ATCC 10231, a filamentous fungi reference strain *Aspergillus fumigatus* ATCC 46645, and a dermatophyte clinical strain *Trichophyton rubrum* FF5 were used. For compounds showing some activity in the dermatophyte *T. rubrum*, the activity was enlarged to other species of dermatophytes (*Microsporum canis* FF1 and *Epidermophyton floccosum* FF9). Frozen stocks of all fungal strains were sub-cultured in Sabouraud Dextrose Agar (SDA - BioMérieux, Marcy L'Etoile, France) before each test, to ensure optimal growth conditions and purity. Stock solutions of each compound (10 mg/mL) were prepared

in dimethylsulfoxide (DMSO – Alfa Aesar, Kandel, Germany). In the experiments, the final in-test concentration of DMSO was kept below 1%, as recommended by the CLSI <sup>42</sup>.

### **Antimicrobial susceptibility testing**

**Antibacterial activity.** An initial screening of the antibacterial activity of the compounds was performed by the Kirby-Bauer disk diffusion method, as recommended by the Clinical and Laboratory Standards Institute (CLSI).<sup>43-44</sup> Briefly, sterile 6 mm blank paper disks (Oxoid, Basingstoke, England) impregnated with 15 µg of each compound were placed on inoculated MH agar plates. A blank disk with DMSO was used as a negative control. MH inoculated plates were incubated for 18-20 hours at 37 °C. At the end of incubation, the inhibition halos were measured. The minimal inhibitory concentration (MIC) was used to determine the antibacterial activity of each compound, in accordance with the recommendations of the CLSI <sup>45</sup>. Two-fold serial dilutions of the compounds were prepared in Mueller-Hinton Broth 2 (MHB2 – Sigma-Aldrich, St. Louis, MO, USA) within the concentration range of 0.062-64 µg/mL. Cefotaxime (CTX) ranging between 0.031-16 µg/mL was used as a control. Sterility and growth controls were included in each assay. Purity check and colony counts of the inoculum suspensions were also performed in order to ensure that the final inoculum density closely approximates the intended number ( $5 \times 10^5$  CFU/mL). The MIC was determined as the lowest concentration at which no visible growth was observed. The minimal bactericidal concentration (MBC) was assessed by spreading 10 µL of culture collected from wells showing no visible growth on MH agar plates. The MBC was determined as the lowest concentration at which no colonies grew after 16-18 hours incubation at 37 °C. These assays were performed in duplicate.

**Antifungal activity.** The MIC of each compound was determined by the broth microdilution method, according to CLSI guidelines (reference documents M27-A3 <sup>46</sup> for yeasts and M38-A2 <sup>47</sup> for filamentous fungi). Briefly, cell or spore suspensions were prepared in RPMI-1640 broth medium supplemented with MOPS (Sigma-Aldrich, St. Louis, MO, USA) from fresh cultures of the different strains of fungi. In the case of filamentous fungi, the inoculum was adjusted to  $0.4-5 \times 10^4$  CFU/mL

for *A. fumigatus* ATCC 46645 and to  $1-3 \times 10^3$  CFU/mL for the dermatophytes. The inoculum of *C. albicans* was adjusted to  $0.5-2.5 \times 10^3$  CFU/mL. Two-fold serial dilutions of the compounds were prepared in RPMI-1640 broth medium supplemented with MOPS within the concentration range of 1-128  $\mu\text{g/mL}$ , with maximum DMSO concentration not exceeding 2.5% (v/v). Sterility and growth controls were also included in each assay. The plates were incubated for 48 hours at 35 °C (*C. albicans* and *A. fumigatus*) or during 5 days at 25 °C (*T. rubrum*, *M. canis* and *E. floccosum*). MICs were recorded as the lowest concentrations resulting in 100% growth inhibition in comparison to the compound-free controls. Voriconazole MIC for *Candida krusei* ATCC 6258 was used as quality control<sup>37-38</sup>. The assay was validated when results obtained were within the recommended limits. The minimal fungicidal concentration (MFC) was determined by spreading 20  $\mu\text{L}$  of culture collected from wells showing no visible growth on SDA plates. The MFC was determined as the lowest concentration showing 100% growth inhibition after 48 hours at 35 °C (for *C. albicans* and *A. fumigatus*) or 5 days incubation at 25 °C (*T. rubrum*, *M. canis* and *E. floccosum*). All the experiments were repeated independently at least two times.

### **Antimicrobial synergy testing**

**Antibiotic synergy.** In order to evaluate the combined effect of the compounds and clinically relevant antimicrobial drugs, a screening was conducted using the disk diffusion method, as previously described<sup>42, 48</sup>. A set of antibiotic disks (Oxoid, Basingstoke, England) to which the isolates were resistant was selected: cefotaxime (CTX, 30  $\mu\text{g}$ ) for extended spectrum beta-lactamase-producer *E. coli* SA/2, oxacillin (OX, 1  $\mu\text{g}$ ) for *S. aureus* 66/1, and vancomycin (VA, 30  $\mu\text{g}$ ) for *E. faecalis* B3/101. Antibiotic disks alone (controls) and antibiotic disks impregnated with 15  $\mu\text{g}$  of each compound were placed on MH agar plates seeded with the respective bacteria. Sterile 6 mm blank papers impregnated with 15  $\mu\text{g}$  of each compound alone were also tested. A blank disk with DMSO was used as a negative control. MH inoculated plates were incubated for 18-20 hours at 37 °C. Potential synergism was recorded when the halo of an antibiotic disk impregnated with a compound was greater than the halo of the antibiotic or compound-impregnated blank disk alone.



**Antifungal synergy.** In order to evaluate the combined effect of the compounds and clinically relevant antifungal drugs, checkerboard assay was conducted, as previously described<sup>48</sup>. Fluconazole was used in a range between (0.062 - 4 µg/mL) and compounds were tested in a range between their MIC and progressive two-fold dilutions. Fractional inhibitory concentrations (FIC) were calculated as follows: FIC of compound = MIC of compound in combination with antifungal / MIC of compound alone and FIC of antifungal = MIC of antifungal in combination with compound / MIC of antifungal alone. The FIC index (FICI) was calculated as sum of each FIC and interpreted as follows:  $FICI \leq 0.5$ , synergy;  $0.5 < FICI \leq 4$ , no interaction;  $4 > FICI$ , antagonism<sup>49</sup>.

#### AUTHOR INFORMATION

##### **Corresponding Author**

\* Emília Sousa; email: [esousa@ff.up.pt](mailto:esousa@ff.up.pt),

\* Paulo Martins da Costa: [pmcosta@icbas.up.pt](mailto:pmcosta@icbas.up.pt)

##### **Author Contributions**

E.S. and A.K. conceived the study design. S.L. synthesized the compounds and elucidated their structure and, A.M.S.S., E.S., and M.M.M.P. analysed the data. D.I.S.P.R. performed the HPLC analysis. P.P-T., J. F-S., E.P., and P.M.C. evaluated the antimicrobial activity. S.L. and E.S. wrote the manuscript, while all authors gave significant contributions in discussion and revision. All authors agreed to the final version of the manuscript.

##### **Funding Sources**

This research was partially supported by the Strategic Funding UID/Multi/04423/2019 through national funds provided by FCT-Foundation for Science and Technology and European Regional Development Fund (ERDF), in the framework of the program PT2020. This research was developed under Project No. POCI-01-0145-FEDER-028736 and PTDC/MAR-BIO/4694/2014 (POCI-01-

0145-FEDER-016790; 3599-PPCDT), co-financed by COMPETE 2020, Portugal 2020 and the European Union through the ERDF, and by FCT through national funds and also by CESPU (CHIRALBIOACTIVE-PI-3RL-IINFACTS-2019)

## ACKNOWLEDGMENTS

S.L. thanks Erasmus Mundus Action 2 (LOTUS+, LP15DF0205) for full PhD scholarship. To Sara Cravo for technical support. To Centro de Apoio Científico e Tecnológico à Investigação (CACTI, University of Vigo, Pontevedra, Spain) for HRMS analysis.

## ABBREVIATIONS

SDA, Sabouraud Dextrose Agar; CFU, Colony forming unit; CLSI, Clinical Standards and Laboratory Institute; FIC, Fractional inhibitory concentration; HPLC, high performance liquid chromatography; MFC, Minimal fungicidal concentration; MBC, Minimal bactericidal concentration; MDR, multidrug-resistant; MIC, Minimal inhibitory concentration; MH, Mueller-Hinton agar; MHB2, Mueller-Hinton Broth 2; MRSA, methicillin-resistant *Staphylococcus aureus* TLC, Thin layer chromatography; VRE, vancomycin-resistant *Enterococcus*; Ant, anthranilic acid; Rs, resolution values; *e.r.*, enantiomeric ratio; SAR, structure-activity relationship; DMSO, dimethylsulfoxide;

## REFERENCES

1. Reardon, S., Phage therapy gets revitalized. *Nature* **2014**, *510* (7503), 15-16.
2. Gyawali, R.; Ibrahim, S. A., Natural products as antimicrobial agents. *Food Control* **2014**, *46*, 412-429.
3. Shankar, P., Piryani, R., Piryani, S., The state of the world's antibiotics 2015. *J. Chitwan Med Col.* **2017**, *6* (4), 2.
4. Ventola, C. L., The antibiotic resistance crisis: part 1: causes and threats. *P & T: a peer-reviewed J. Formul Manag* **2015**, *40* (4), 277-283.

5. Butler, M. S.; Blaskovich, M. A.; Cooper, M. A., Antibiotics in the clinical pipeline in 2013. *J. Antibiot* **2013**, *66*, 571.
6. McGuinness, W. A.; Malachowa, N.; DeLeo, F. R., Vancomycin Resistance in *Staphylococcus aureus*. *The Yale J. Bio Med* **2017**, *90* (2), 269-281.
7. Courvalin, P., Vancomycin Resistance in Gram-Positive Cocci. *Clin Infec Dis* **2006**, *42* (Supplement\_1), S25-S34.
8. Stapleton, P. D.; Taylor, P. W., Methicillin resistance in *Staphylococcus aureus*: mechanisms and modulation. *Sci Progr* **2002**, *85* (1), 57-72.
9. Codjoe, F. S.; Donkor, E. S., Carbapenem Resistance: A Review. *Med Sci (Basel, Switzerland)* **2017**, *6* (1), 1.
10. Park, S. H., Third-generation cephalosporin resistance in gram-negative bacteria in the community: a growing public health concern. *Korean J. Inter Med* **2014**, *29* (1), 27-30.
11. WHO. Published list of bacteria for which new antibiotics are urgently needed. **2017** World Health Organization: Geneva, 2017 (<http://www.who.int/mediacentre/news/releases/2017/bacteria-antibiotics-needed/en/>) (available on 21 February 2017)
12. Russell, A. D., Antibiotic and biocide resistance in bacteria: Introduction. *J. Appl Microbiol Sym Suppl* **2002**, *92* (1), 1S-3S.
13. Michael, C. A.; Dominey-Howes, D.; Labbate, M., The antimicrobial resistance crisis: causes, consequences, and management. *Front Public Health* **2014**, *2*, 145-145.
14. WHO. Global antimicrobial resistance surveillance system (GLASS) report: early implementation 2016-2017, **2017**. World Health Organization: Geneva, 2017.
15. Powers, J. H., Antimicrobial drug development – the past, the present, and the future. *Clin Microbiol Infect* **2004**, *10*, 23-31.
16. Hughes, C. C.; Fenical, W., Antibacterials from the sea. *Chemistry (Weinheim an der Bergstrasse, Germany)* **2010**, *16* (42), 12512-12525.
17. Kasanah, N.; Hamann, M. T., Development of antibiotics and the future of marine microorganisms to stem the tide of antibiotic resistance. *Curr Opin Inves Drugs (London, England : 2000)* **2004**, *5* (8), 827-837.

18. Eom, S.-H.; Kim, Y.-M.; Kim, S.-K., Marine bacteria: potential sources for compounds to overcome antibiotic resistance. *Appl Microbiol Biotechnol* **2013**, *97* (11), 4763-4773.
19. Tortorella, E.; Tedesco, P.; Palma Esposito, F.; January, G. G.; Fani, R.; Jaspars, M.; de Pascale, D., Antibiotics from Deep-Sea Microorganisms: Current Discoveries and Perspectives. *Mar Drugs* **2018**, *16* (10), 355.
20. Penn, J.; Mantle, P. G.; Bilton, J. N.; Sheppard, R. N., Gyantrypine, a novel anthranilic acid-containing metabolite of *Aspergillus clavatus*. *J. Chem Soc Perkin Trans I* **1992**, 1495-1496.
21. Peng, J.; Lin, T.; Wang, W.; Xin, Z.; Zhu, T.; Gu, Q.; Li, D., Antiviral alkaloids produced by the mangrove-derived fungus *Cladosporium* sp. PJX-41. *J Nat Prod* **2013**, *76* (6), 1133-1140.
22. Liu, Y.; Li, X.-M.; Meng, L.-H.; Wang, B.-G., N-Formyllapatin A, a new N-formylspiroquinazoline derivative from the marine-derived fungus *Penicillium adametzioides* AS-53. *Phytochem Lett* **2014**, *10*, 145-148.
23. Fan, Y.-Q.; Li, P.-H.; Chao, Y.-X.; Chen, H.; Du, N.; He, Q.-X.; Liu, K.-C., Alkaloids with cardiovascular effects from the marine-derived fungus *Penicillium expansum* Y32. *Mar Drugs* **2015**, *13* (10), 6489-6504.
24. Buttachon, S.; Chandrapatya, A.; Manoch, L.; Silva, A.; Gales, L.; Bruyère, C.; Kiss, R.; Kijjoa, A., Sartorymensin, a new indole alkaloid, and new analogues of tryptoquivaline and fiscalins produced by *Neosartorya siamensis* (KUFC 6349). *Tetrahedron* **2012**, *68* (15), 3253-3262.
25. Bessa, L. J.; Buttachon, S.; Dethoup, T.; Martins, R.; Vasconcelos, V.; Kijjoa, A.; da Costa, P. M., Neofiscalin A and fiscalin C are potential novel indole alkaloid alternatives for the treatment of multidrug-resistant Gram-positive bacterial infections. *FEMS Microbiol Lett* **2016**, *363* (15), 1-5.
26. War May Zin, W.; Prompanya, C.; Buttachon, S.; Kijjoa, A., Bioactive Secondary Metabolites from a Thai Collection of Soil and Marine-Derived Fungi of the Genera *Neosartorya* and *Aspergillus*. *Curr Drug Deliv* **2016**, *13* (3), 378-388.
27. Li, X.-J.; Zhang, Q.; Zhang, A.-L.; Gao, J.-M., Metabolites from *Aspergillus fumigatus*, an Endophytic Fungus Associated with *Melia azedarach*, and Their Antifungal, Antifeedant, and Toxic Activities. *J Agric Food Chem* **2012**, *60* (13), 3424-3431.

28. Zhuang, Y.; Teng, X.; Wang, Y.; Liu, P.; Li, G.; Zhu, W., New Quinazolinone Alkaloids within Rare Amino Acid Residue from Coral-Associated Fungus, *Aspergillus versicolor* LCJ-5-4. *Org Lett* **2011**, *13* (5), 1130-1133.
29. Resende, D. I. S. P.; Boonpothong, P.; Sousa, E.; Kijjoa, A.; Pinto, M. M. M., Chemistry of the fumiquinazolines and structurally related alkaloids. *Nat Prod Rep* **2019**, *36* (1), 7-34.
30. Long, S.; Resende, D. I. S. P.; Kijjoa, A.; Silva, A. M. S.; Pina, A.; Fernández-Marcelo, T.; Vasconcelos, M. H.; Sousa, E.; Pinto, M. M. M., Antitumor Activity of Quinazolinone Alkaloids Inspired by Marine Natural Products. *Mar Drugs* **2018**, *16* (8).
31. Long, S.; Resende, D. I. S. P.; Kijjoa, A.; Silva, A. M. S.; Fernandes, R.; Xavier, C. P. R.; Vasconcelos, M. H.; Sousa, E.; Pinto, M. M. M., Synthesis of New Proteomimetic Quinazolinone Alkaloids and Evaluation of Their Neuroprotective and Antitumor Effects. *Molecules* **2019**, *24* (3), 534.
32. Gribble, W. G., Biological Activity of Recently Discovered Halogenated Marine Natural Products. *Mar Drugs* **2015**, *13* (7).
33. Resende, D. I. S. P.; Pereira-Terra, P.; Inácio, A. S.; Da Costa, P. M.; Pinto, E.; Sousa, E.; Pinto, M. M. M., Lichen xanthenes as models for new antifungal agents. *Molecules* **2018**, *23* (10).
34. Liu, J. F.; Ye, P.; Zhang, B.; Bi, G.; Sargent, K.; Yu, L.; Yohannes, D.; Baldino, C. M., Three-component one-pot total syntheses of gyantrypine, fumiquinazoline F, and fiscalin B promoted by microwave irradiation. *J Org Chem* **2005**, *70* (16), 6339-6345.
35. Gomes, N. M.; Bessa, L. J.; Buttachon, S.; Costa, P. M.; Buaruang, J.; Dethoup, T.; Silva, A. M. S.; Kijjoa, A., Antibacterial and antibiofilm activities of tryptoquivalines and meroditerpenes isolated from the marine-derived fungi *Neosartorya paulistensis*, *N. laciniosa*, *N. tsunodae*, and the soil fungi *N. fischeri* and *N. siamensis*. *Mar Drugs* **2014**, *12* (2), 822-839.
36. Bessa, L. J.; Palmeira, A.; Gomes, A. S.; Vasconcelos, V.; Sousa, E.; Pinto, M.; Da Costa, P. M., Synergistic effects between thioxanthenes and oxacillin against methicillin-resistant staphylococcus aureus. *Microb Drug Resist* **2015**, *21* (4), 404-415.
37. Garzón, D.; Cabezas, R.; Vega, N.; Ávila-Rodríguez, M.; Gonzalez, J.; Gómez, R. M.; Echeverria, V.; Aliev, G.; Barreto, G. E., Novel Approaches in Astrocyte Protection: from Experimental Methods to Computational Approaches. *J. Mol Neurosci* **2016**, *58* (4), 483-492.

38. Aureli, M.; Mauri, L.; Ciampa, M. G.; Prinetti, A.; Toffano, G.; Secchieri, C.; Sonnino, S., GM1 Ganglioside: Past Studies and Future Potential. *Mol Neurobio* **2016**, *53* (3), 1824-1842.
39. Matlin, S. A.; Tiritan, M. E.; Crawford, A. J.; Cass, Q. B.; Boyd, D. R., HPLC with carbohydrate carbamate chiral phases: Influence of chiral phase structure on enantioselectivity. *Chirality* **1994**, *6* (2), 135-140.
40. Simões, R. R.; Aires-de-Sousa, M.; Conceição, T.; Antunes, F.; da Costa, P. M.; de Lencastre, H., High Prevalence of EMRSA-15 in Portuguese Public Buses: A Worrisome Finding. *PLOS ONE* **2011**, *6* (3), e17630.
41. Bessa, L. J.; Barbosa-Vasconcelos, A.; Mendes, Â.; Vaz-Pires, P.; Martins da Costa, P., High prevalence of multidrug-resistant *Escherichia coli* and *Enterococcus* spp. in river water, upstream and downstream of a wastewater treatment plant. *J Water Health* **2014**, *12* (3), 426-435.
42. CLSI, Performance standards for antimicrobial susceptibility testing. 27th ed. Clinical and Laboratory Standards Institute: Wayne, PA, USA, 2017.
43. Gomes, N.; Bessa, L.; Buttachon, S.; Costa, P.; Buaruang, J.; Dethoup, T.; Silva, A.; Kijjoa, A., Antibacterial and Antibiofilm Activities of Tryptoquivalines and Meroditerpenes Isolated from the Marine-Derived Fungi *Neosartorya paulistensis*, *N. laciniosa*, *N. tsunodae*, and the Soil Fungi *N. fischeri* and *N. siamensis*. *Mar Drugs* **2014**, *12* (2), 822.
44. Bessa, L. J.; Palmeira, A.; Gomes, A. S.; Vasconcelos, V.; Sousa, E.; Pinto, M.; Martins da Costa, P., Synergistic Effects Between Thioxanthenes and Oxacillin Against Methicillin-Resistant *Staphylococcus aureus*. *Microb Drug Resist* **2015**, *21* (4), 404-415.
45. Solomos, A. C.; Rall, G. F., Get It through Your Thick Head: Emerging Principles in Neuroimmunology and Neurovirology Redefine Central Nervous System "immune Privilege". *ACS Chem Neurosci* **2016**, *7* (4), 435-441.
46. CLSI, Reference Method for Broth Dilution Antifungal Susceptibility Testing of Yeasts, Approved Standard-Third Edition. Clinical and Laboratory Standards Institute: Wayne, PA, USA, 2008.
47. CLSI, Reference Method for Broth Dilution Antifungal Susceptibility Testing of Filamentous Fungi, Approved Standard-Second Edition. Clinical and Laboratory Standards Institute: Wayne, PA, USA, 2008.

48. CLSI, Performance Standards for Antimicrobial Disk Susceptibility Tests. 11th ed. Clinical and Laboratory Standards Institute: Wayne, PA, USA, 2012.
49. CLSI, Methods for Dilution Antimicrobial Susceptibility Tests for Bacteria That Grow Aerobically, Approved Standard-Tenth Edition. Clinical and Laboratory Standards Institute: Wayne, PA, USA, 2015.

Supplementation information

# Synthesis and Characterization of Antimicrobial Activities of Marine-Derived Indolymethyl Pyrazinoquinazoline Alkaloids

*Solida Long<sup>1</sup>, Patrícia Pereira-Terra<sup>2,3</sup>, Joana Freitas-Silva<sup>2,3</sup>, Diana I. S. P. Resende<sup>1,2</sup>, Anake Kijjoa<sup>2,3</sup>, Artur M. S. Silva<sup>4</sup>, Maria Elizabeth Tiritan<sup>1,2,5</sup>, Eugénia Pinto<sup>2,6</sup>, Paulo Martins da Costa<sup>2,3\*</sup>, Emília Sousa<sup>1,2,\*</sup> and Madalena M. M. Pinto<sup>1,2</sup>*

<sup>1</sup>LQOF - Laboratório de Química Orgânica e Farmacêutica, Departamento de Ciências Químicas, Faculdade de Farmácia, Universidade do Porto, Rua de Jorge Viterbo Ferreira, 228, 4050-313 Porto, Portugal

<sup>2</sup>CIIMAR - Centro Interdisciplinar de Investigação Marinha e Ambiental, Terminal de Cruzeiros do Porto de Leixões, Av. General Norton de Matos S/N, 4450-208 Matosinhos, Portugal

<sup>3</sup>ICBAS - Instituto de Ciências Biomédicas Abel Salazar, Universidade do Porto, Rua de Jorge Viterbo Ferreira, 228, 4050-313 Porto, Portugal

<sup>4</sup>QOPNA - Química Orgânica, Produtos Naturais e Agroalimentares, Departamento de Química, Universidade de Aveiro, 3810-193 Aveiro, Portugal

<sup>5</sup>CESPU, Instituto de Investigação e Formação Avançada em Ciências e Tecnologias da Saúde (IINFACETS), Rua Central de Gandra, 1317, 4585-116 Gandra PRD, Portugal

<sup>6</sup>Laboratório de Microbiologia, Departamento de Ciências Biológicas, Faculdade de Farmácia, Universidade do Porto, Rua de Jorge Viterbo Ferreira, 228, 4050-313 Porto, Portugal

\*Corresponding authors: [esousa@ff.up.pt](mailto:esousa@ff.up.pt), [pmcosta@icbas.up.pt](mailto:pmcosta@icbas.up.pt)



**Table S1.** Antibacterial activity of quinazolinones **5-32** on Gram-positive and Gram-negative sensitive strains. MIC and MBC are expressed in  $\mu\text{g}/\text{mL}$ . Inhibition halos are expressed in mm.

	Gram-positive						Gram-negative					
	<i>S. aureus</i> ATCC 29213			<i>E. faecalis</i> ATCC 29212			<i>E. coli</i> ATCC 25922			<i>P. aeruginosa</i> ATCC 27853		
	Halo	MIC	MBC	Halo	MIC	MBC	Halo	MIC	MBC	Halo	MIC	MBC
<b>5</b>	0	>64	ND	0	>64	ND	0	>64	ND	0	>64	ND
<b>6</b>	0	>64	ND	0	>64	ND	0	>64	ND	0	>64	ND
<b>7</b>	0	>64	ND	0	>64	ND	0	>64	ND	0	>64	ND
<b>8</b>	0	>64	ND	0	>64	ND	0	>64	ND	0	>64	ND
<b>9</b>	0	>64	ND	0	>64	ND	0	>64	ND	0	>64	ND
<b>10</b>	0	>64	ND	0	>64	ND	0	>64	ND	0	>64	ND
<b>11</b>	0	>64	ND	0	>64	ND	0	>64	ND	0	>64	ND
<b>12</b>	0	>64	ND	0	>64	ND	0	>64	ND	0	>64	ND
<b>13</b>	0	>64	ND	0	>64	ND	0	>64	ND	0	>64	ND
<b>14</b>	0	>64	ND	0	>64	ND	0	>64	ND	0	>64	ND
<b>15</b>	0	>64	ND	0	>64	ND	0	>64	ND	0	>64	ND
<b>16</b>	0	>64	ND	0	>64	ND	0	>64	ND	0	>64	ND
<b>17</b>	0	>64	ND	0	>64	ND	0	>64	ND	0	>64	ND
<b>18</b>	0	>64	ND	0	>64	ND	0	>64	ND	0	>64	ND
<b>19</b>	0	>64	ND	0	>64	ND	0	>64	ND	0	>64	ND
<b>20</b>	0	>64	ND	0	>64	ND	0	>64	ND	0	>64	ND
<b>21</b>	0	>64	ND	<b>9*</b>	>64	ND	0	>64	ND	0	>64	ND
<b>22</b>	<b>9</b>	<b>&gt;32</b>	> 64	0	>64	>64	0	>64	ND	0	>64	ND
<b>22a</b>	<b>9</b>	>64	ND	0	>64	ND	0	>64	ND	0	>64	ND
<b>22b</b>	<b>9</b>	>64	ND	0	>64	ND	0	>64	ND	0	>64	ND
<b>23</b>	<b>9</b>	<b>&gt;32</b>	> 64	0	<b>&gt;32</b>	>64	0	>64	ND	0	>64	ND
<b>23b</b>	<b>10</b>	>64	ND	0	>64	ND	0	>64	ND	0	>64	ND
<b>24</b>	<b>9</b>	<b>&gt;16</b>	> 64	0	<b>&gt;32</b>	>64	0	>64	ND	0	>64	ND
<b>25</b>	<b>11</b>	<b>&gt;16</b>	> 64	<b>9.5*</b>	>64	ND	<b>8*</b>	>64	ND	0	>64	ND
<b>26</b>	<b>11</b>	<b>&gt;4</b>	> 64	<b>11*</b>	>64	ND	<b>8*</b>	>64	ND	0	>64	ND
<b>26a</b>	<b>11</b>	<b>&gt;4</b>	>64	<b>9</b>	>64	ND	0	>64	ND	0	ND	ND
<b>26b</b>	<b>11</b>	>64	ND	<b>8.5</b>	>64	ND	0	>64	ND	0	ND	ND
<b>27</b>	<b>10</b>	<b>&gt;4</b>	> 64	<b>10*</b>	>64	ND	<b>8*</b>	>64	ND	0	>64	ND
<b>28</b>	<b>9*</b>	> 64	ND	0	>64	ND	<b>8.5*</b>	>64	ND	<b>8.5*</b>	>64	ND
<b>29</b>	0	> 64	ND	0	>64	ND	0	>64	ND	<b>8.5*</b>	>64	ND
<b>30</b>	<b>9.5</b>	<b>&gt;16</b>	> 64	<b>9.5*</b>	>64	ND	<b>8</b>	>64	ND	0	>64	ND
<b>31</b>	<b>9.5</b>	<b>&gt;16</b>	> 64	<b>10*</b>	>64	ND	<b>8</b>	>64	ND	0	>64	ND
<b>32</b>	<b>9</b>	> 64	ND	<b>11*</b>	>64	ND	0	>64	ND	0	>64	ND

MIC, minimum inhibitory concentration; MBC, minimum bactericidal concentration; \* halo of partial inhibition; ND, not determined

**Table S2.** Antibacterial activity of quinazolinones **5-32** on five different bacterial strains. MIC and MBC are expressed in µg/mL. Inhibition halos are expressed in mm.

	<i>S. aureus</i> 66/1 (MRSA)			<i>S. aureus</i> 40/61/24			<i>E. faecalis</i> B3/101 (VRE)			<i>E. coli</i> SA/2			<i>E. faecalis</i> A5/102 (VRE)		
	Hal o	MI C	MB C	Hal o	MI C	MB C	Hal o	MI C	MB C	Hal o	MI C	MB C	Hal o	MI C	MB C
<b>5</b>	0	>64	ND	-	-	-	0	>64	ND	0	>64	ND	-	-	-
<b>6</b>	0	>64	ND	-	-	-	0	>64	ND	0	>64	ND	-	-	-
<b>7</b>	0	>64	ND	-	-	-	0	>64	ND	0	>64	ND	-	-	-
<b>8</b>	0	>64	ND	-	-	-	0	>64	ND	0	>64	ND	-	-	-
<b>9</b>	0	>64	ND	-	-	-	0	>64	ND	0	>64	ND	-	-	-
<b>10</b>	0	>64	ND	-	-	-	0	>64	ND	0	>64	ND	-	-	-
<b>11</b>	0	>64	ND	-	-	-	0	>64	ND	0	>64	ND	-	-	-
<b>12</b>	0	>64	ND	-	-	-	0	>64	ND	0	>64	ND	-	-	-
<b>13</b>	0	>64	ND	-	-	-	7	>64	ND	7	>64	ND	-	-	-
<b>14</b>	0	>64	ND	-	-	-	8	>64	ND	0	>64	ND	-	-	-
<b>15</b>	0	>64	ND	-	-	-	8	>64	ND	0	>64	ND	-	-	-
<b>16</b>	0	>64	ND	-	-	-	8	>64	ND	0	>64	ND	-	-	-
<b>17</b>	0	>64	ND	-	-	-	0	>64	ND	0	>64	ND	-	-	-
<b>18</b>	0	>64	ND	-	-	-	0	>64	ND	0	>64	ND	-	-	-
<b>19</b>	0	>64	ND	-	-	-	0	>64	ND	0	>64	ND	-	-	-
<b>20</b>	0	>64	ND	-	-	-	0	>64	ND	0	>64	ND	-	-	-
<b>21</b>	0	>64	ND	-	-	-	0	>64	ND	0	>64	ND	-	-	-
<b>22</b>	0	>64	ND	ND	64	>64	9	>64	ND	7	ND	ND	ND	>64	>64
<b>22a</b>	9	ND	ND	-	-	-	0	ND	ND	0	ND	ND	-	-	-
<b>22b</b>	9	ND	ND	-	-	-	0	ND	ND	0	ND	ND	-	-	-
<b>23</b>	0	>64	ND	ND	64	>64	8	>64	ND	7	ND	ND	ND	>64	>64
<b>23b</b>	0	ND	ND	-	-	-	0	ND	ND	0	ND	ND	-	-	-
<b>24</b>	9	>64	ND	ND	64	>64	8	>64	ND	7	ND	ND	ND	>64	>64
<b>25</b>	10	>64	ND	ND	>64	ND	0	ND	ND	0	ND	ND	ND	ND	ND
<b>26</b>	10	>8	>64	ND	>8	>64	0	ND	ND	0	ND	ND	ND	ND	ND
<b>26a</b>	0	>4	>64	ND	>4	>64	0	ND	ND	0	ND	ND	ND	ND	ND
<b>26b</b>	0	ND	ND	-	-	-	0	ND	ND	0	ND	ND	-	-	-
<b>27</b>	9.5	>8	>64	ND	>8	>64	0	ND	ND	9	ND	ND	ND	ND	ND
<b>28</b>	10	ND	ND	-	-	-	0	ND	ND	0	ND	ND	-	-	-
<b>29</b>	0	ND	ND	-	-	-	0	ND	ND	0	ND	ND	-	-	-
<b>30</b>	9*	>64	ND	ND	64	>64	0	ND	ND	0	ND	ND	ND	ND	ND
<b>31</b>	10*	>64	ND	ND	>64	ND	0	ND	ND	8.5	ND	ND	ND	ND	ND
<b>32</b>	0	ND	ND	-	-	-	0	ND	ND	0	ND	ND	-	-	-

MIC, minimum inhibitory concentration; MBC, minimum bactericidal concentration; \* halo of partial inhibition; ND, not determined

**Table S3.** Antifungal activity of quinazolines **5-32** against a panel of yeast and filamentous fungi. MIC and MFC are expressed in  $\mu\text{g/mL}$ .

	<i>C. albicans</i> ATCC 10231		<i>A. fumigatus</i> ATCC 46645		<i>T. rubrum</i> FF5		<i>M. canis</i> FF1		<i>E. floccosum</i> FF9	
	MIC	MFC	MIC	MFC	MIC	MFC	MIC	MFC	MIC	MFC
<b>5</b>	> 128	ND	> 128	ND	> 128	ND	<b>ND</b>	ND	ND	ND
<b>6</b>	> 128	ND	> 128	ND	> 128	ND	ND	ND	ND	ND
<b>7</b>	> 128	ND	> 128	ND	> 128	ND	ND	ND	ND	ND
<b>8</b>	> 128	ND	> 128	ND	> 128	ND	ND	ND	ND	ND
<b>9</b>	> 128	ND	> 128	ND	> 128	ND	ND	ND	ND	ND
<b>10</b>	> 128	ND	> 128	ND	> 128	ND	ND	ND	ND	ND
<b>11</b>	> 128	ND	> 128	ND	> 128	ND	ND	ND	ND	ND
<b>12</b>	> 128	ND	> 128	ND	> 128	ND	ND	ND	ND	ND
<b>13</b>	> 128	ND	> 128	ND	> 128	ND	ND	ND	ND	ND
<b>14</b>	> 128	ND	> 128	ND	> 128	ND	ND	ND	ND	ND
<b>15</b>	> 128	ND	> 128	ND	> 128	ND	ND	ND	ND	ND
<b>16</b>	> 128	ND	> 128	ND	> 128	ND	ND	ND	ND	ND
<b>17</b>	> 128	ND	> 128	ND	> 128	ND	ND	ND	ND	ND
<b>18</b>	> 128	ND	> 128	ND	> 128	ND	ND	ND	ND	ND
<b>19</b>	> 128	ND	> 128	ND	> 128	ND	ND	ND	ND	ND
<b>20</b>	> 128	ND	> 128	ND	> 128	ND	ND	ND	ND	ND
<b>21</b>	> 128	ND	> 128	ND	> 128	ND	ND	ND	ND	ND
<b>22</b>	> 128	ND	> 128	ND	> 128	ND	ND	ND	ND	ND
<b>22a</b>	> 128	ND	> 128	ND	> 128	ND	ND	ND	ND	ND
<b>22b</b>	> 128	ND	> 128	ND	> 128	ND	ND	ND	ND	ND
<b>23</b>	> 128	ND	> 128	ND	> 128	ND	ND	ND	ND	ND
<b>23b</b>	> 128	ND	> 128	ND	> 128	ND	ND	ND	ND	ND
<b>24</b>	> 128	ND	> 128	ND	> 128	ND	ND	ND	ND	ND
<b>25</b>	> 128	ND	> 128	ND	> 128	ND	ND	ND	ND	ND
<b>26</b>	> 128	ND	> 128	ND	<b>128</b>	>128	>128	ND	>128	ND
<b>26a</b>	>128	ND	>128	ND	>128	ND	ND	ND	ND	ND
<b>26b</b>	>128	ND	>128	ND	>128	ND	ND	ND	ND	ND
<b>27</b>	> 128	ND	> 128	ND	> 128	ND	ND	ND	ND	ND
<b>28</b>	> 128	ND	> 128	ND	<b>128</b>	>128	>128	ND	>128	ND
<b>29</b>	> 128	ND	> 128	ND	<b>128</b>	>128	>128	ND	>128	ND
<b>30</b>	> 128	ND	> 128	ND	> 128	ND	ND	ND	ND	ND
<b>31</b>	> 128	ND	> 128	ND	> 128	ND	ND	ND	ND	ND
<b>32</b>	> 128	ND	> 128	ND	> 128	ND	ND	ND	ND	ND

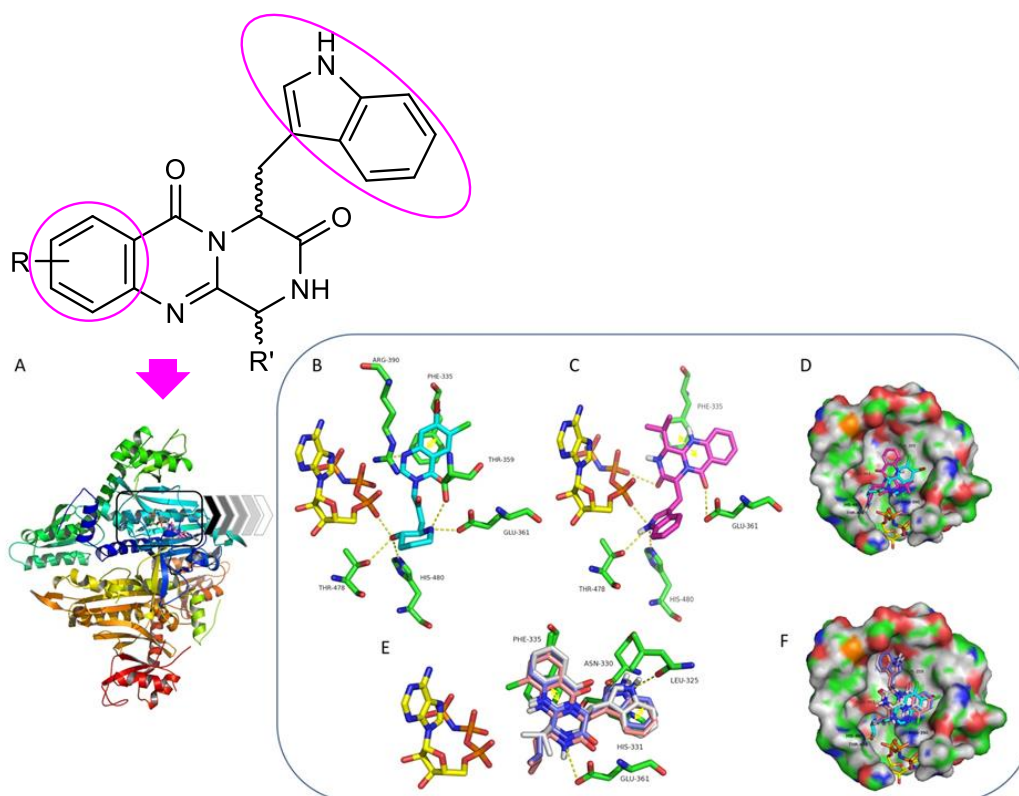
MIC, minimum inhibitory concentration; MFC, minimum fungicidal concentration; ND, not determined



# Chapter 6

## Discovery of indole-containing pyrazino[2,1-*b*]quinazoline-3,6-diones as promising antimalarial agents

Graphical abstract





# Discovery of indole-containing pyrazino[2,1-*b*]quinazoline-3,6-diones as promising antimalarial agents

*Solida Long*<sup>1</sup>, *Vera C. F. Camões*<sup>2</sup>, *Rafael Oliveira*<sup>2</sup>, *Diana I. S. P. Resende*<sup>1,3</sup>, *Andreia Palmeira*<sup>1</sup>, *Artur M. S. Silva*<sup>4</sup>, *Rui Moreira*<sup>5</sup>, *Anake Kijjoa*<sup>3,6</sup>, *Fátima Nogueira*<sup>2,\*</sup>, *Emília Sousa*<sup>1,3,\*</sup>, *Madalena M. M. Pinto*<sup>1,3</sup>

<sup>1</sup> Laboratório de Química Orgânica e Farmacêutica, Faculdade de Farmácia, Universidade do Porto, Rua de Jorge Viterbo Ferreira, 228, 4050-313 Porto, Portugal.

<sup>2</sup> Global Health and Tropical Medicine, GHTM, Unidade de Ensino e Investigação de Parasitologia Médica, Instituto de Higiene e Medicina Tropical, IHMT, Universidade Nova de Lisboa, UNL, Rua da Junqueira no 100, 1349-008 Lisbon, Portugal.

<sup>3</sup> CIIMAR - Centro Interdisciplinar de Investigação Marinha e Ambiental, Terminal de Cruzeiros do Porto de Leixões, 4450-208 Matosinhos, Portugal.

<sup>4</sup> QOPNA - Química Orgânica, Produtos Naturais e Agroalimentares, Departamento de Química, Universidade de Aveiro, Campus Universitário de Santiago, 3810-193 Aveiro, Portugal.

<sup>5</sup> Research Institute for Medicines and Pharmaceutical Sciences (iMed.UL), Faculdade de Farmácia, Universidade de Lisboa, Av. Prof. Gama Pinto, 1649-019 Lisboa, Portugal.

<sup>6</sup> ICBAS-Instituto de Ciências Biomédicas Abel Salazar, Universidade do Porto, Rua de Jorge Viterbo Ferreira, 228, 4050-313 Porto, Portugal.

\* Correspondence: [esousa@ff.up.pt](mailto:esousa@ff.up.pt); Tel.: +351-220428689; [FNogueira@ihmt.unl.pt](mailto:FNogueira@ihmt.unl.pt);

Tel.: +351-213652600

**Abstract:** Malaria is still among the main public health problems in least developed regions of the world and, despite severe efforts amongst the scientific community in order to control and eradicate this disease, new antimalarial compounds will not become available in the upcoming years. Four series of pyrazino[2,1-*b*]quinazoline-3,6-dione containing indole alkaloids were synthesized and investigated for their antimalarial activity. Compounds **8** (fiscalin B), **9**, **12**, and **21** were the most potent against the sensitive strain *P. falciparum* 3D7 with IC<sub>50</sub> values of 0.1, 0.15, 0.05, and 0.2 μM, respectively. Structure-activity relationship shows that *anti*-isomers (*1S,4R*) possess excellent antimalarial activity and the presence of a substituent on the anthranilic acid moiety has a negative effect on the activity. Derivatives with this scaffold are considered with acceptable therapeutic windows for the development of antimalarial drugs with SI >10. Although, the *hit* compounds did not inhibit β-hematin, they were predicted *in silico* to interact with prolyl-tRNA synthetase, in a similar mode to halofuginone. These results represent the discovery of a potential new chemotype for further optimization towards novel and affordable antimalarial drugs of fiscalin B.

**Keywords:** Pyrazino[2,1-*b*]quinazoline-3,6-dione, fiscalin B, antimalarial, *P. falciparum*, prolyl-tRNA



## 1. Introduction

Malaria represents a major threat to the public health worldwide, with over 219 million clinical cases in 2017 with 435 thousand of deaths [1]. Though the number of cases has shown a decrease since 2010 [2], evidences of slower *Plasmodium falciparum* parasite clearance [3] have appear in some countries in Southeast Asia especially at Greater Mekong Subregion (GMS) including Lao PDR, Thailand, Cambodia, Myanmar, and Vietnam [1, 4, 5]. These represent a serious threat to global malaria control and eradication. The frontline therapies for the treatment of symptomatic malaria are artemisinin (**1**) combination therapies (ACTs) for *P. falciparum* infections and in the case of infections with *P. vivax*, chloroquine (CQ, **2**) or ACTs are usually employed. This evidence, along with widespread resistance to other historical antimalarials, highlights the need to identify new chemical diversity, ideally with novel antimalarial modes of action.

Strategies used for the development of novel antimalarial drugs include the discovery of new active molecules from natural products [6], repurposing of commercially available drugs, development of hybrid compounds [7], and rational drug design with molecular modifications of existing antimalarial and hits [8]. The malarial chemotherapy has always been successfully influenced by natural products [6] and nature is still an important source of antimalarial drugs. Recently, the analysis of Tres Cantos Antimalarial Set (TCAMS) [9] suggested that indole-based antimalarials are the key core for the development of the next generation of antimalarial drugs since the indole scaffold is known as an important moiety present in several lead drug candidates with new mechanisms of action, such as the spiroindolone **3** and aminoindole derivatives [10-12]. For example, TCMDC-134281 (**4**) exhibited very potent antiplasmodial properties against *P. falciparum* 3D7 strain ( $EC_{50} = 34$  nM) [13]. However, although this compound showed no significant cytotoxicity against human HepG2 hepatoma cell line ( $EC_{50} > 10$   $\mu$ M), the presence of the 4-aminoquinolyl

moiety (an essential pharmacophore of CQ) might be responsible for cross-resistance with CQ (**2**) and poor-drug-like properties.

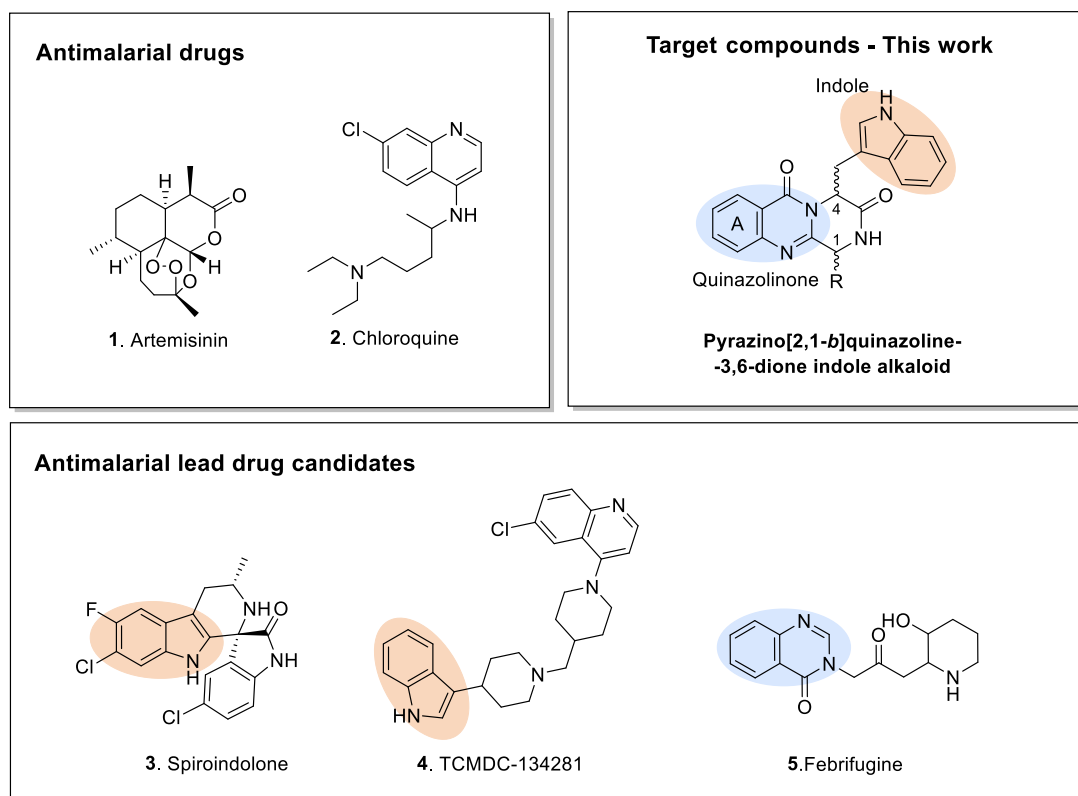


**Figure 1.** Current antimalarial drugs **1** and **2**, indole containing antimalarial compounds **3** and **4**, natural antimalarial compound **5**, and the scaffold of the target compounds, **6-34** an indole-containing pyrazino[2,1-*b*]quinazoline-3,6-dione.

Indole-containing pyrazino[2,1-*b*]quinazoline-3,6-diones (Figure 1) constitute a subclass of alkaloids mostly isolated from marine and terrestrial sources [14]. These structurally unique alkaloids contain simultaneously a quinazolinone core which can be found in the structure of the natural febrifugine (**5**) and an indole moiety commonly found in several drug lead candidates such as spiroindolone (**3**) and TCMDC-134281 (**4**). This hybrid structure, containing both moieties, led us to hypothesize the antimalarial potential of

derivatives with this scaffold and their ability to overcome the observed cross-resistance with CQ and ACTs (Figure 1).

In our previous works, three series of indole-containing pyrazino[2,1-*b*]quinazoline-3,6-diones were synthesized through a microwave-assisted multicomponent polycondensation of amino acids in which three modifications were introduced (Figure 2): (1) structural modifications at C-1 and C-4 stereochemistry [15]; (2) C-1 side chain and stereochemistry [16], and (3) introduction of halogen atoms in the aromatic ring of anthranilic acid (to be submitted to publication). In the present study, we introduce a fourth modification consisting of ring A variations on the pyrazino[2,1-*b*]quinazoline-3,6-dione scaffold or with an additional indole moiety (Figure 2). Herein, all the four synthesized series, in a total of 29 compounds **6-34**, were assayed against the CQ-sensitive *P. falciparum* 3D7 strain at fixed 5  $\mu$ M concentrations.

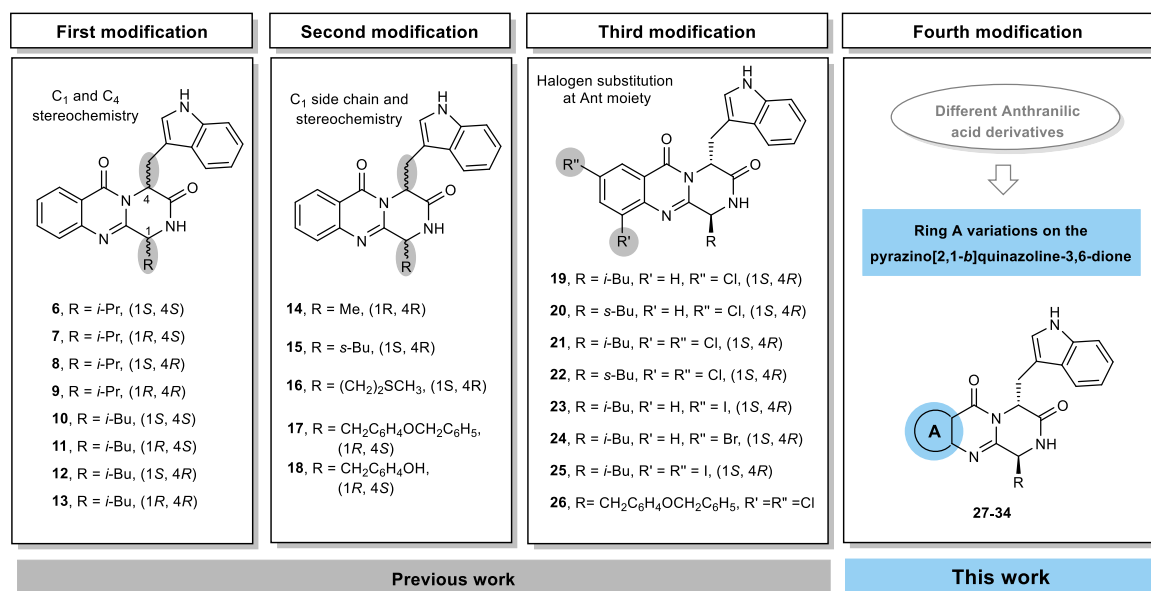


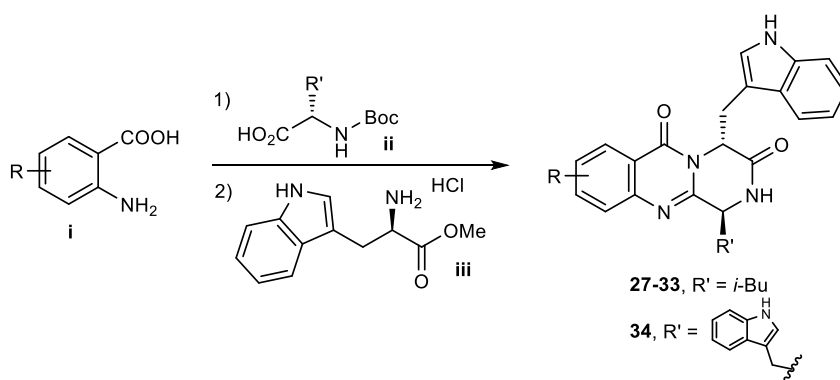
**Figure 2.** Structures of the three series of indole-containing pyrazino[2,1-*b*]quinazoline-3,6-diones previously synthesized and fourth modification planned.

## 2. Results and discussion

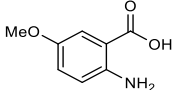
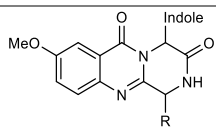
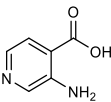
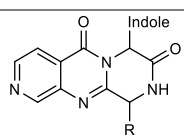
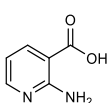
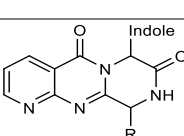
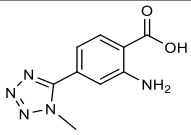
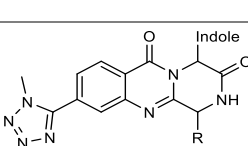
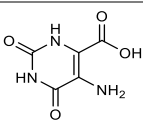
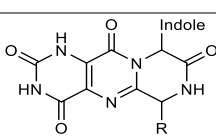
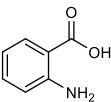
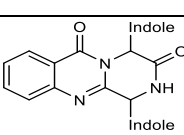
### 2.1 Chemistry

Indole-containing pyrazino[2,1-*b*]quinazoline-3,6-diones **27-34** were synthesized via a highly effective and environmentally friendly microwave-assisted multicomponent polycondensation of amino acids. This methodology allowed us to prepare the fourth series of pyrazinoquinazoline alkaloids through treatment of the anthranilic acid (**i**) derivatives with *N*-Boc-L-amino acids (**ii**) and (PhO)<sub>3</sub>P at 55 °C for 16-20 h. Later, D-tryptophan methyl ester hydrochloride (**iii**) was added, and the mixture was stirred under microwave irradiation (300 W) at 220 °C for 1.5 min to furnish the final products **27-34** (Table 1).

**Table 1:** Microwave-assisted multicomponent synthesis of indole-containing quinazolinone alkaloids **27-34**.



Anthranilic acid	Product	Compound	CLogP <sup>a</sup>	MW	Yield <sup>b</sup> / <i>er</i> <sup>c</sup>
		<b>27</b>	3.671	416.48	6.9/47:53
		<b>28</b>	4.088	414.51	3.1/42:58

Anthranilic acid	Product	Compound	CLogP <sup>a</sup>	MW	Yield <sup>b</sup> / <i>er</i> <sup>c</sup>
		<b>29</b>	3.814	430.51	5.8/30:70
		<b>30</b>	2.456	401.47	9.4/46:54
		<b>31</b>	2.456	401.47	12.1/46:54
		<b>32</b>	3.082	482.55	1.0/47:53
		<b>33</b>	1.277	434.55	2.3/57:43
		<b>34</b>	3.690	473.54	5.7/99:1

Reagents and conditions: 1) (PhO)<sub>3</sub>P, py, 55 °C, 24 h, 2) (PhO)<sub>3</sub>P, py, 220 °C, 1.5 min, a) calculated based on Cambio Draw, b) obtained after purification, c) determined by enantioselective liquid chromatography.

MW = molecular weight

## 2.2 Biology

### 2.2.1 *In vitro* susceptibility assay of *P. falciparum*

The principle of the *in vitro* susceptibility test to malaria is to assess the degree of development of parasites *P. falciparum* in the presence of different concentrations of the compounds. In this assay, *P. falciparum* 3D7, a CQ-susceptible strain, was used to evaluate

the antimalarial activity of the 29 quinazolinones. Activity was described in term of IC<sub>50</sub> (concentration that inhibits the growth of 50 % of *P. falciparum* parasite present in the culture) for 14 compounds (Table 2). The remaining 15, exhibited non-appreciable antiparasitic activity, they fail to produce dose-response curves and/or displayed > 75 % survival at 10 μM (data not shown).

To evaluate the antimalarial potential of the pyrazino[2,1-*b*]quinazoline-3,6-dione scaffold, our first approach was to screen the first series of compounds (**6-13**), having 4 types of stereoisomers (Figure 2). We observed that anti-isomers *1S*, *4R*, like compounds **8** (fiscalin B) and **12**, exhibited the highest antimalarial activity while *syn*-isomers *1S*, *4S* were inactive (compounds **6** and **10**) and *syn*-isomers *1R*, *4R* had decreased activity (compounds **9** and **13**). Compounds in the 1<sup>st</sup> series demonstrated that increasing the size of the C-1 substituent increased the antimalarial activity, for example, compound **12** with C-1 having an isobutyl the same position). Compounds **8**, **9**, **12**, and **13** showed the highest antimalarial activity against *P. falciparum* strain 3D7. To further evaluate the effect of C-1 substituent on the activity, the 2<sup>nd</sup> series of compounds (**14-18**) was evaluated, and SAR indicates that a sulfur substituent at C-1 do not favour activity (compounds **16**). In the investigation of the 3<sup>rd</sup> series of compounds (**19-26**) with different substituents on A ring, only compound **21** having chlorine atom at position 9 and 11 showed favourable antimalarial activity with an IC<sub>50</sub> value of 0.2 μM (weaker than compounds **8** and **12**), while other derivatives (substituted with Br or I) showed to be inactive. This result was concordant with other studies reporting the effect of halogen substituents [17]. For the 4<sup>th</sup> series of pyrazino[2,1-*b*]quinazoline-3,6-diones (**17-34**), isosteric substitutions with the nitrogen atom at different positions of ring A (positions 9, 10, 11), led to a decrease/inactivation of the antimalarial activity (compounds **30** and **31**). Compounds **27** and **29** each bearing a hydroxy or methoxy group at position 9 of ring A also showed a decrease in activity. Contrary to other reports of febrifugine

derivatives [18-21], compound **32** with a tetrazole group at position 10 also showed a weak activity against *P. falciparum*.

**Table 2.** In vitro activity against *Plasmodium falciparum* 3D7 strain.

<i>P. falciparum</i> (3D7)			
Compounds	IC <sub>50</sub> [μM]	Compounds	IC <sub>50</sub> [μM]
<b>8</b>	0.10 ± 0.02	<b>21</b>	0.20 ± 0.14
<b>9</b>	0.15 ± 0.05	<b>22</b>	1.51 ± 0.53
<b>11</b>	2.00 ± 0.32	<b>26</b>	4.00 ± 0.02
<b>12</b>	0.05 ± 0.02	<b>27</b>	0.73 ± 0.07
<b>13</b>	0.47 ± 0.22	<b>30</b>	4.00 ± 0.02
<b>14</b>	3.68 ± 0.62	<b>31</b>	3.76 ± 0.60
<b>18</b>	4.18 ± 0.03	<b>32</b>	1.02 ± 0.27
<b>CQ (2)*</b>	15.08 ± 0.08		

\* The IC<sub>50</sub> value of CQ is in nM.

### 2.2.2 In vitro cytotoxicity against mammalian cells

An important criterion in evaluating active antimalarial compounds is their cytotoxicity in mammalian host cells. Compounds that showed the lowest IC<sub>50</sub> values against *P. falciparum* (**8**, **12**, and **21**) were selected to evaluate their cytotoxicity. The cell lines used for *in vitro* cytotoxicity assay were the V79 from non-tumor cell line of Chinese hamster lung fibroblasts [22] and CQ (**2**) was used as control. The results showed relatively low LD<sub>50</sub> values (LD<sub>50</sub> concentration that inhibits the growth of 50 % of cells present in the culture) when compared to CQ (**2**) (Table 3). Nonetheless, the selectivity index (SI; calculated by

LD<sub>50</sub>/IC<sub>50</sub>) for compounds **8**, **12**, and **21** were between 19-70 (Table 3) and within the acceptable safety range (SI values greater than 10 indicates that a compound has an acceptable therapeutic window for the development of antimalarial drugs) [23, 24]. In general, the higher the SI, the more promising as an antimalarial are the compounds, due to its selective action against the parasite [25].

**Table 3.** Cytotoxicity against mammalian cells of compounds **8**, **12**, and **21**.

Compounds	<i>P. falciparum</i>	Mammalian cells	
	(3D7)	(V79)	SI
	IC <sub>50</sub> (μM)	DL <sub>50</sub> (μM)	
<b>8</b>	0.10 ± 0.02	1.91 ± 0.44	19
<b>12</b>	0.05 ± 0.02	1.78 ± 0.47	34
<b>21</b>	0.20 ± 0.14	14.00 ± 1.41	70
<b>CQ*</b>	15.08 ± 0.80*	167.00 ± 42.00	11074

\* the IC<sub>50</sub> value of CQ is in nM; SI - Selectivity Index; The results of IC<sub>50</sub> and LD<sub>50</sub> are presented as mean ± standard deviation.

### 2.2.3 Evaluation of hemotoxicity *in vitro*

The *in vitro* hemolysis assay evaluates the release of hemoglobin in the medium (as an indicator of lysis of erythrocytes) after exposure to the test compounds. Drug-induced hemolysis can occur by two mechanisms: allergic hemolysis (toxicity caused by an immunological reaction in patients previously sensitized to a drug) and toxic hemolysis (direct toxicity of the drug, its metabolite or an excipient in the formulation) [26]. This test was intended to determine the potential toxic hemolytic effect of the hit compounds **8**, **12**,



and **21** on healthy/non-parasitized erythrocytes (Figure 3). The % of hemolysis induced by the compounds was also determined under standard culture conditions of *P. falciparum*.

The % of hemolysis of healthy erythrocytes induced by **8**, **12**, and **21** was lower than 6% (Figure 3) and within the range of that of CQ (**2**). Compounds **8**, **12**, and **21** and CQ (**2**) had no hemolytic activity at  $\leq 10 \mu\text{M}$ . CQ (**2**) is considered a non-hemolytic antimalarial drug in healthy human erythrocytes [27]. Compounds **8**, **12**, and **21** did not present hemolytic activity, since the % hemolysis was  $<10\%$  (% hemolysis  $> 25\%$  is considered as indicative of risk of hemolysis [28]).

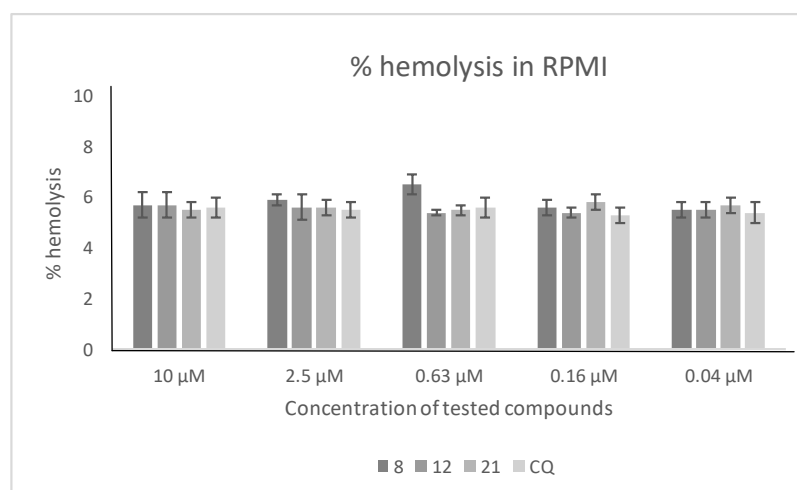


**Figure 3.** Hemolysis of healthy erythrocytes *in vitro* induced by the compounds. The error bars represent the mean  $\pm$  standard deviation of % hemolysis of the compounds relative to the positive control obtained by action of Triton® X-100.

#### 2.2.4 Evaluation of inhibition of polymerization of hemozoin ( $\beta$ -hematin) *in vitro*

The assay of inhibition of the polymerization of hemozoin ( $\beta$ -hematin) *in vitro* was based on the protocol of Basilico *et al.*[29] with some modifications and was carried out for compounds **8**, **12**, **21** and CQ (**2**) by using a hemin solution (ferriprotoporphyrin IX

chloride). In this assay, CQ (**2**) was used as a positive control to evaluate the quality of the test since **2** binds to portions of hemozoin produced from the proteolytic process of hemoglobin in infected erythrocytes, thus interfering with hemozoin detoxification. Compounds, **8**, **12**, and **21** did not show to inhibit the polymerization of  $\beta$ -hematin *in vitro* (Figure S1, supplementary material). Febrifugine (**5**) significantly inhibits the formation of hemozoin required for the maturation of the parasite *Plasmodium spp.* in the trophozoite stage via axial ligand or  $\pi$ - $\pi$  interaction to heme. Even though pyrazino[2,1-*b*]quinazoline-3,6-diones **8**, **12**, and **21** possess structure similarities with febrifugine (**5**), results suggested that the mechanism of action of these derivatives might be different from febrifugine (**5**).

### 2.3. Computational docking study on inhibitory effect of prolyl-tRNA synthetase

Recently, the cytoplasmic prolyl-tRNA synthetase of *P. falciparum* (PfcPRS), a member of the aminoacyl-tRNA synthetase (aaRS) family that drive protein translation, has been identified as the functional target of febrifugine (**5**) and analogues, such as halofuginone (HF) [30-33], a semisynthetic analogue in clinical trials [34]. Therefore, a putative target for this series of new antimalarials could be the PfcPRS and this hypothesis was explored with *in silico* studies. The binding affinity of twenty-nine pyrazinoquinazolinones (**6-34**) to PRS enzyme target was predicted using computational docking AutodockTools [35]. The positive controls were febrifugine (**5**, FF), HF, tetrahydroquinazolinone febrifugine (ThFF), and 6-fluorofebrifugine (6FFF) that were predicted as having high binding affinity to PRS, with docking scores between -9.3 and 9.7 kcal.mol<sup>-1</sup>, whereas the negative control, CQ (**2**), revealed a docking score of -7.4 kcal.mol<sup>-1</sup>. The most active antimalarials *in vitro*, compounds **8**, **9**, **12**, and **21** presented docking score from -9.1 to -11.4 kcal.mol<sup>-1</sup>, predicted as forming complexes with PRS enzyme (Table 4,

Figure 3A). The docking score of all the tested compounds range from -5.7 to 11.4 kcal/mol (Table S1, supplementary material).

**Table 4.** Docking scores of the test compounds and controls onto 4ydq PRS binding site.

<b>Compounds</b>	<b>Docking scores (kcal/mol)</b>
<b>8</b>	-9.1
<b>9</b>	-11.4
<b>12</b>	-10.0
<b>21</b>	-9.9
<b>Febrifugine (5, FF)</b>	-9.5
<b>Halofuginone (HF)</b>	-9.3
<b>ThFF</b>	-9.5
<b>6FFF</b>	-9.7
<b>CQ (2)</b>	-7.4

Halofuginone (HF) is described as being mimetic of the enzyme substrates L-Pro and adenine-76 of tRNA, binding into the active site pockets simultaneously with ATP [31, 33, 36]. Other quinazolinone-based compounds such as FF, 6FFF, and ThFF have also been described as specific for PfPRS, when in the presence of the ATP analogue adenosine 5'-( $\beta,\gamma$ -imido)triphosphate (AMPPNP) [32]. The structure of the ternary complex of PfPRS-AMPPNP-HF reveals hydrogen interactions with Thr359, Glu361, Arg390, Thr478, and His480, and  $\pi$ - $\pi$  stacking interactions with Phe335 [32] (Figure 3 B). Compound **9** fits the same binding pocket as HF, binding with some of the same residues as HF. The N atom of the indole ring forms hydrogen bonds with Thr478 and His480, and with AMPPNP phosphate groups; and the pyrazinoquinazolinone ring of **9** is mainly stabilized by hydrogen interactions with Glu361 and  $\pi$ - $\pi$  stacking contacts with Phe335, but does not establish polar

interactions with Arg390, suggesting chemical spaces available for additional modifications or derivatizations (Figure 3 C and D).

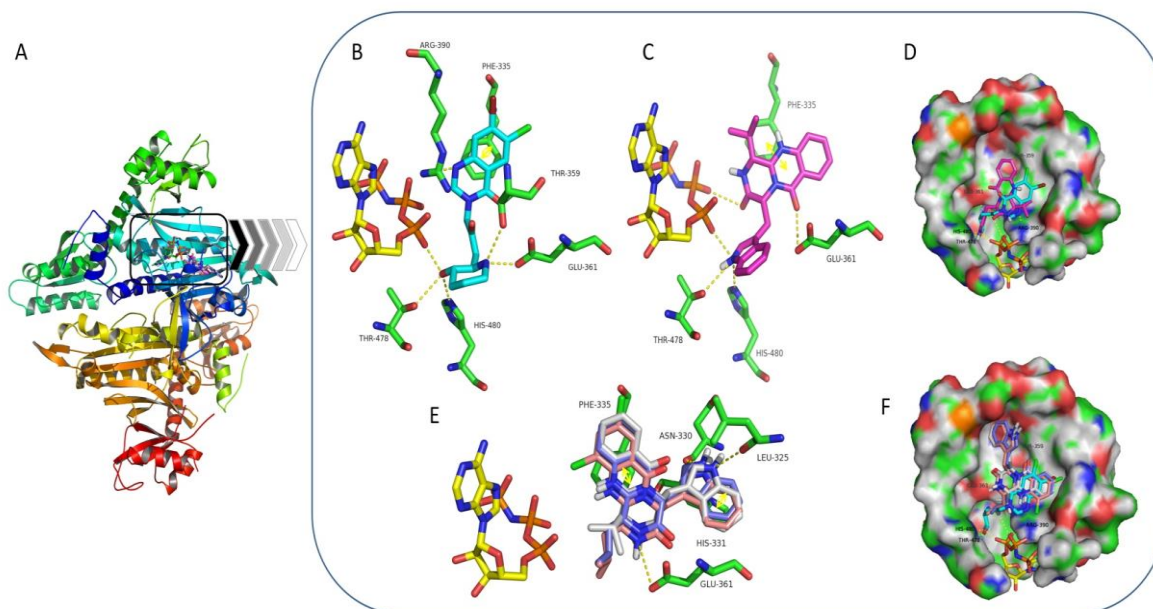


**Figure 3.** (A) Ribbon representation of Prolyl-tRNA Synthetase (PRS) (PDB code: 4YDQ) with crystallographic HF and top scored test molecules **8**, **9**, **12**, and **21**. (B) Crystallographic HF (light blue sticks); (C) **9** (pink sticks), (E) **8** (white sticks), **12** (dark blue sticks), and **21** (salmon sticks) docked into PRD active site. Relevant amino acids are represented in capped sticks and labeled. AMPPNP is represented as yellow sticks. Polar interactions are represented in yellow broken lines. Capped surface representation of PRS with docked conformations of (D) crystallographic HF and **9**, and (F) crystallographic HF, **8**, **12**, and **21**. Some PRS residues are omitted for simplification. AMPPNP = yellow; crystallographic HF = light blue; **9** = pink; **12** = blue; **21** = salmon; **8** = white. Polar interactions are represented in yellow broken lines. In the surface, carbons, oxygens, nitrogens, and hydrogens are represented in green, red, blue, and grey, respectively.

Compounds **8**, **12**, and **21** bind in the same positions in the PRS cavity but do not establish hydrogen interactions with AMPPNP. Hydrogen interactions are formed with

residues Glu361, Leu325, and Asn330;  $\pi$ - $\pi$  stacking interactions are established with Phe335 and His331 (Figure 3 E and F). The indole ring of **8**, **12**, and **21** dock into a lateral cavity flanked by His-331, that is not occupied by HF (Figure 3 F). The binding pose of **9**, different from the binding poses of **8**, **12**, and **21**, provides a hint on the relevance of chirality in the affinity of the binding to PRS target.

### 3. Conclusions

The pyrazino[2,1-b]quinazoline-3,6-dione scaffold showed productive derivatives which demonstrated good antimalarial activity *in vitro* against *P. falciparum* strain 3D7. The compounds were not shown to be cytotoxic *in vitro* against non-tumor mammalian cells V79. These compounds did not show significant hemolytic activity in healthy human erythrocytes also did not inhibit  $\beta$ -hematin *in vitro*. These new antimalarial compounds were hypothesized to interact with the prolyl-tRNA similarly to halofuginone. These finding reveals that quinazolinones have characteristics with potential for further optimizations and development of new antimalarial drugs.

## 4. Experimental

### 4.1 Chemistry

#### 4.1.1 General procedure

All reagents were from analytical grade. Dried pyridine and triphenylphosphite were purchased from Sigma (Sigma-Aldrich Co. Ltd., Gillingham, UK). Anthranilic acids **i** (Table 1) were purchased from TCI (Tokyo Chemical Industry Co. Ltd., Chuo-ku, Tokyo, Japan). Column chromatography purifications were performed using flash silica Merck 60, 230–400 mesh (EMD Millipore corporation, Billerica, MA, USA) and preparative TLC was carried

out on precoated plates Merck Kieselgel 60 F<sub>254</sub> (EMD Millipore corporation, Billerica, MA, USA), spots were visualized with UV light (Vilber Lourmat, Marne-la-Vallée, France). Melting points were measured in a Köfler microscope and are uncorrected. Infrared spectra were recorded in a KBr microplate in a FTIR spectrometer Nicolet iS10 from Thermo Scientific (Waltham, MA, USA) with Smart OMNI-Transmission accessory (Software 188 OMNIC 8.3). <sup>1</sup>H and <sup>13</sup>C NMR spectra were recorded in CDCl<sub>3</sub> or DMSO-d<sub>6</sub> (Deutero GmbH, Kastellaun, Germany) at room temperature unless otherwise mentioned on Bruker AMC instrument (Bruker Biosciences Corporation, Billerica, MA, USA), operating at 300 MHz for <sup>1</sup>H and 75 MHz for <sup>13</sup>C). Carbons were assigned according to HSQC and or HMBC experiments. Optical rotation was measured at 25 °C using the ADP 410 polarimeter (Bellingham + Stanley Ltd., Tunbridge Wells, Kent, UK), using the emission wavelength of sodium lamp, concentrations are given in g/100 mL. Chromatographic separation was achieved using a capillary column (30 m × 0.25 mm × 0.25 μm, cross-linked 5% diphenyl and 95% dimethyl polysiloxane) from Thermo Scientific™ (Thermo Fisher Scientific Inc., Austin, TX, USA) and high-purity helium C-60 as carrier gas. Enantiomeric ratio was determined by enantioselective liquid chromatography (LCMS-2010EV, Shimadzu, Lisbon, Portugal), employing a system equipped with a chiral column (Lux® 5 μm Amylose-1, 250 × 4.6 mm) and UV-detection at 254 nm, mobile phase was hexane:ethanol (80:20) and the flow rate was 0.5 mL.min<sup>-1</sup>.

#### *4.1.2. General conditions for the synthesis of quinazolinone-3,6-(4H)-diones compounds 27-34*

In a closed vial, 5-hydroxy-anthranilic acid (**ia**, 184 mg, 1.2 mmol) for **27**, 5-methyl-anthranilic acid (**ib**, 181 mg, 1.2 mmol) for **28**, 5-methoxy-anthranilic acid (**ic**, 200 mg, 1.2 mmol) for **29**, 3-aminoisonicotinic acid (**id**, 116 mg, 1.2 mmol) for **30**, 2-aminoisonicotinic

acid (**ie**, 116 mg, 200  $\mu$ mol) for **31**, 4-triazole-anthranilic acid (**if**, 124 mg, 1.2 mmol) for **32**, or 5-aminoindole-3-pyruvate (**ig**, 205 mg, 1.2 mmol) for **33**, or anthranilic acid (**ih**, 140 mg, 1.2 mmol) for **34** with *N*-Boc-L-leucine (**iiia**, 299 mg, 1.2 mmol) for **27-33** or *N*-Boc-L-tryptophan, (**iiib**, 365 mg, 1.2 mmol) for **34** and triphenyl phosphite (495  $\mu$ L, 1.44 mmol) were added along with 6 mL of dried pyridine. The vial was heated in heating block with stirring at 55  $^{\circ}$ C for 16-24 h. After cooling the mixture to room temperature, D-tryptophan methyl ester hydrochloride (**iii**, 306 mg, 1.2 mmol) was added, and the mixture was divided into 3 individual vials, and irradiated in the microwave at the constant temperature at 220  $^{\circ}$ C for 1.5 min. After removing the solvent with toluene, the crude product was purified by flash column chromatography using *n*-hexane: EtOAc (60:40) as a mobile phase. The preparative TLC was performed using CH<sub>2</sub>Cl<sub>2</sub>:Me<sub>2</sub>CO (95:5) as mobile phase. The major compound appeared as a black spot with no fluorescence under the UV light. The desirable compounds **27-34** were collected as yellow solids. Before analysis, compounds were recrystallized from methanol.

(1*S*,4*R*)-4-((1*H*-indol-3-yl)methyl)-8-hydroxy-1-isobutyl-1,2-dihydro-6*H*-pyrazino[2,1-*b*]quinazoline-3,6(4*H*)-dione (**27**). Yield: 38.5 mg, 6.9 %; mp: 162.4-163.5  $^{\circ}$ C (MeOH);  $[\alpha]_D^{30} = -74.60$  (*c* 0.042; CHCl<sub>3</sub>);  $\nu_{max}$  (KBr) 3185, 3070, 1666, 1617, 1431, 1247 and 776 cm<sup>-1</sup>; <sup>1</sup>H NMR (300 MHz, CDCl<sub>3</sub>):  $\delta$  8.63 (d, 1H, *J* = 3.6 Hz, CH), 8.02 (s, 1H, NH-Trp), 7.73 (d, 1H, *J* = 2.9 Hz, OH), 7.53 (d, 2H, *J* = 8.9 Hz, CH(2)), 7.34 (dd, 2H, *J* = 7.7 and 4.0 Hz, CH-Trp (2)), 7.14 (t, 1H, *J* = 7.1 Hz, CH-Trp), 7.00 (t, 1H, *J* = 7.2 Hz, CH-Trp), 6.64 (d, 1H, *J* = 2.3 Hz, CH-Trp), 5.66 (dd, 1H, *J* = 5.3 and 3.0 Hz, CH\*-Trp), 5.60 (s, 1H, NH-amide), 3.76 (dd, 1H, *J* = 14.9 and 2.8 Hz, CH<sub>2</sub>-Trp), 3.64 (dd, 1H, *J* = 15.3 and 5.4 Hz, CH<sub>2</sub>-Trp), 2.70 (dd, 1H, *J* = 8.3 and 4.0 Hz, CH\*-Leu), 1.70-1.59 (m, 1H, CH-Leu), 1.42-1.33 (m, 2H, CH<sub>2</sub>-Leu) 0.77 (d, 3H, *J* = 6.3 Hz, CH<sub>3</sub>-Leu), 0.27 (d, 3H, *J* = 6.4 Hz, CH<sub>3</sub>-Leu); <sup>13</sup>C NMR (75

MHz, Acetone d<sub>6</sub>):  $\delta$  169.7 (C=O), 161.1 (C=O), 157.2 (C-OH), 150.1 (C=N), 141.6 (C), 137.3 (C-Trp), 129.9 (CH), 128.3 (C-Trp), 124.9 (CH-Trp), 124.7 (CH), 122.5 (CH-Trp), 122.3 (C), 119.9 (CH-Trp), 119.1 (CH-Trp), 112.1 (CH-Trp), 110.0 (CH), 109.8 (C-Trp), 58.5 (CH\*-Trp), 51.4 (CH\*-Leu), 40.7 (CH-Leu), 27.4 (CH<sub>2</sub>-Trp), 24.8 (CH<sub>2</sub>-Leu), 23.3 (CH<sub>3</sub>-Leu), 21.1 (CH<sub>3</sub>-Leu).

*(1S,4R)-4-((1H-indol-3-yl)methyl)-1-isobutyl-8-methyl-1,2-dihydro-6H-pyrazino[2,1-b]quinazoline-3,6(4H)-dione (28)*. Yield: 15.6 mg, 3.1%; mp: 156.7-157.0 °C (MeOH);  $[\alpha]_D^{30} = -182$  (c 0.055; CHCl<sub>3</sub>);  $\nu_{max}$  (KBr) 3067, 2915, 1682, 1470, and 770 cm<sup>-1</sup>; <sup>1</sup>H NMR (300 MHz, CDCl<sub>3</sub>):  $\delta$  8.16 (s, 1H, CH), 8.04 (br, 1H, NH-Trp), 7.59 (dd, 1H, *J* 8.3, 2.0 Hz, CH), 7.50 (d, 2H, *J* 8.2 Hz, CH & CH-Trp), 7.28 (d, 1H, *J* 8.2 Hz, CH-Trp), 7.13 (t, 1H, *J* 7.6 Hz, CH-Trp), 6.99 (t, 1H, *J* 7.9 Hz, CH-Trp), 6.63 (d, 1H, *J* 2.3 Hz, CH-Trp), 5.70 (s, 1H, NH-amide), 5.68 (dd, 1H, *J* 5.4 and 2.9 Hz, CH\*-Trp), 3.76 (dd, 1H, *J* 15.0 and 2.8 Hz, CH<sub>2</sub>-Trp), 3.65 (dd, 1H, *J* 15.1 and 5.4 Hz, CH<sub>2</sub>-Trp), 2.71 (dd, 1H, *J* 9.8 and 3.3 Hz, CH\*-Leu), 2.53 (s, 3H, CH<sub>3</sub>), 1.99 (ddd, 1H, *J* 13.7, 10.4, and 3.2 Hz, CH-Leu), 1.40-1.27 (m, 2H, CH<sub>2</sub>-Leu), 0.77 (d, 3H, *J* 6.4 Hz, CH<sub>3</sub>-Leu), 0.27 (d, 3H, *J* 6.5 Hz, CH<sub>3</sub>-Leu); <sup>13</sup>C NMR (75 MHz, CDCl<sub>3</sub>):  $\delta$  169.5 (C=O), 160.9 (C=O), 150.6 (C=N), 145.0 (C), 137.3 (C), 136.2 (CH), 136.1 (C-Trp), 127.2 (CH), 126.2 (CH), 123.5 (CH-Trp), 122.8 (CH-Trp), 120.3 (C), 119.9 (CH-Trp), 118.9 (CH-Trp), 111.1 (CH-Trp), 109.8 (C-Trp), 57.2 (C\*-Trp), 50.7 (C\*-Leu), 40.2 (CH<sub>2</sub>-Leu), 27.1 (CH<sub>2</sub>-Trp), 24.13 (CH-Leu), 23.3 (CH<sub>3</sub>-Leu), 21.4 (CH<sub>3</sub>), 19.7 (CH<sub>3</sub>-Leu).

*(1S,4R)-4-((1H-indol-3-yl)methyl)-1-isobutyl-8-methoxy-1,2-dihydro-6H-pyrazino[2,1-b]quinazoline-3,6(4H)-dione (29)*. Yield: 36.6 mg, 5.83 %; mp: 152.7-153.3 °C (MeOH);



$[\alpha]_D^{30} = -222.22$  ( $c$  0.06;  $\text{CHCl}_3$ );  $\nu_{\text{max}}$  (KBr) 3184, 2956, 1666, 1617, 1464, 1247, and 776  $\text{cm}^{-1}$ ;  $^1\text{H NMR}$  (300 MHz,  $\text{DMSO-d}_6$ ):  $\delta$  10.35 (s, 1H, NH-Trp), 7.69 (d, 1H,  $J$  2.7 Hz, CH), 7.52 (d, 1H,  $J$  8.9 Hz, CH-Trp), 7.38 (d, 1H,  $J$  8.0 Hz, CH), 7.36 (dd, 1H,  $J$  7.9 and 4.0 Hz, CH), 7.31 (d, 1H,  $J$  8.1 Hz, CH-Trp), 7.21 (s, 1H, NH-amide), 7.05 (t, 1H,  $J$  7.1 Hz, CH-Trp), 6.87 (t, 1H,  $J$  7.4 Hz, CH-Trp), 6.68 (d, 1H,  $J$  2.3 Hz, CH-Trp), 5.56 (dd, 1H,  $J$  5.1 and 3.1 Hz, CH\*-Trp), 3.97 (s, 3H, O- $\text{CH}_3$ ), 3.68 (dd, 1H,  $J$  14.8 and 3.0 Hz,  $\text{CH}_2$ -Trp), 3.60 (dd, 1H,  $J$  14.9 and 5.3 Hz,  $\text{CH}_2$ -Trp), 2.77 (dd, 1H,  $J$  8.6 and 3.8 Hz, CH\*-Leu), 2.08-1.87 (m, 1H, CH-Leu), 1.58-1.26 (m, 2H,  $\text{CH}_2$ -Leu), 0.69 (d,  $J$  6.5 Hz,  $\text{CH}_3$ -Leu), 0.37 (d, 3H,  $J$  6.5 Hz,  $\text{CH}_3$ -Leu);  $^{13}\text{C NMR}$  (75 MHz,  $\text{DMSO-d}_6$ ):  $\delta$  168.6 (C=O), 160.0 (C=O), 157.9 (C-O), 150.0 (C=N), 141.2 (C), 136.2 (C), 128.9 (CH), 127.1 (C-Trp), 124.3 (CH-Trp), 121.4 (CH-Trp), 120.7 (C), 118.8 (CH-Trp), 118.8 (CH), 117.9 (CH-Trp), 111.5 (CH-Trp), 108.2 (C-Trp), 57.3 (C\*-Trp), 55.7 ( $\text{CH}_3$ ), 50.3 (C\*-Leu), 39.3 ( $\text{CH}_2$ -Leu), 26.4 ( $\text{CH}_2$ -Trp), 23.6 (CH-Leu), 22.9 ( $\text{CH}_3$ -Leu), 20.9 ( $\text{CH}_3$ -Leu).

(1*S*,4*R*)-4-((1*H*-indol-3-yl)methyl)-1-isobutyl-1,2-dihydro-6*H*-pyrazino[1,2-*a*]pyrido[3,4-*d*]pyrimidine-3,6(4*H*)-dione (**30**). Yield: 45.2 mg, 9.37 %; mp: 115.3-116.6 °C (MeOH);  $[\alpha]_D^{30} = -176.30$  ( $c$  0.043;  $\text{CHCl}_3$ );  $\nu_{\text{max}}$  (KBr) 3265, 2956, 1682, 1469, 1233, and 741  $\text{cm}^{-1}$ ;  $^1\text{H NMR}$  (300 MHz,  $\text{CDCl}_3$ ):  $\delta$  9.05 (s, 1H, CH), 8.74 (d, 1H,  $J$  5.2 Hz, CH), 8.14 (s, 1H, NH-Trp), 8.13 (d,  $J$  4.9 Hz, CH), 7.45 (d, 1H,  $J$  8.0 Hz, CH-Trp), 7.31 (d, 1H,  $J$  8.2 Hz, CH-Trp), 7.15 (dt, 1H,  $J$  7.6 and 0.8 Hz, CH-Trp), 6.97 (dt, 1H,  $J$  7.6 and 0.8 Hz, CH-Trp), 6.66 (d, 1H,  $J$  2.1 Hz, CH-Trp), 5.73 (s, 1H, NH-amide), 5.66 (dd, 1H,  $J$  5.2 and 1.9 Hz, CH\*-Trp), 3.79 (dd, 1H,  $J$  15.1 and 2.8 Hz,  $\text{CH}_2$ -Trp), 3.63 (dd, 1H,  $J$  15.1 and 5.3 Hz,  $\text{CH}_2$ -Trp), 2.75 (dd, 1H,  $J$  9.6 and 3.3 Hz, CH\*-Leu), 2.08-1.87 (m, 1H, CH-Leu), 1.45-1.28 (m, 2H,  $\text{CH}_2$ -Leu), 0.78 (d,  $J$  6.3 Hz,  $\text{CH}_3$ -Leu), 0.30 (d, 3H,  $J$  6.5 Hz,  $\text{CH}_3$ -Leu);  $^{13}\text{C NMR}$  (75 MHz,  $\text{CDCl}_3$ ):  $\delta$  168.8 (C=O), 159.8 (C=O), 153.81 (C=N), 151.2 (CH), 146.4 (CH), 136.2 (C-

Trp), 127.0 (C-Trp), 123.5 (CH-Trp), 123.0 (CH-Trp), 120.5 (CH-Trp), 118.7 (CH), 118.6 (CH-Trp), 111.3 (CH-Trp), 109.4 (C-Trp), 57.7 (C\*-Trp), 50.9 (C\*-Leu), 40.2 (CH<sub>2</sub>-Leu), 27.0 (CH<sub>2</sub>-Trp), 24.2 (CH-Leu) 23.3 (CH-Leu), 19.7 (CH<sub>3</sub>-Leu).

*(7R,10S)-7-((1H-indol-3-yl)methyl)-10-isobutyl-9,10-dihydro-5H-pyrazino[1,2-a]pyrido [2,3-d]pyrimidine-5,8(7H)-dione (31)*. Yield: 58.3 mg, 12.1%; mp: 111.3-111.5 °C (MeOH);  $[\alpha]_D^{30} = -153.15$  (c 0.037; CHCl<sub>3</sub>);  $\nu_{max}$  (KBr) 3295, 3067, 2915, 1682, 1600, 1470, 770, and 697 cm<sup>-1</sup>; <sup>1</sup>H NMR (300 MHz, CDCl<sub>3</sub>):  $\delta$  9.01 (d, 1H, *J* 4.6 Hz, CH), 8.71 (d, 1H, *J* 7.9 Hz, CH), 8.07 (s, 1H, NH-Trp), 7.54 (d, 1H, *J* 7.8 Hz, CH-Trp), 7.51 (dd, 1H, *J* 7.9 and 4.5 Hz, CH), 7.31 (d, 1H, *J* 8.2 Hz, CH-Trp), 7.15 (dt, 1H, *J* 7.6 and 0.8 Hz, CH-Trp), 7.01 (dt, 1H, *J* 7.6 and 0.8 Hz, CH-Trp), 6.61 (d, 1H, *J* 2.4 Hz, CH-Trp), 5.69 (s, 1H, NH-amide), 5.64 (dd, 1H, *J* 5.3 and 2.8 Hz, CH\*-Trp), 3.81 (dd, 1H, *J* 15.1 and 2.6 Hz, CH<sub>2</sub>-Trp), 3.61 (dd, 1H, *J* 15.0 and 5.3 Hz, CH<sub>2</sub>-Trp), 2.76 (dd, 1H, *J* 10.4 and 3.1 Hz, CH\*-Leu), 1.21-1.14 (m, 1H, CH-Leu), 1.05-0.98 (m, 2H, CH<sub>2</sub>-Leu), 0.78 (d, *J* 6.5 Hz, CH<sub>3</sub>-Leu), 0.22 (d, 3H, *J* 6.5 Hz, CH<sub>3</sub>-Leu); <sup>13</sup>C NMR (75 MHz, CDCl<sub>3</sub>):  $\delta$  169.1 (C=O), 160.0 (C=O), 153.81 (C=N), 147.1 (CH), 138.6 (CH), 136.1 (C-Trp), 127.2 (C-Trp), 123.4 (CH-Trp), 121.1 (CH-Trp), 119.8 (CH), 118.4 (CH-Trp), 111.3 (CH-Trp), 109.4 (C-Trp), 57.5 (C\*-Trp), 51.0 (C\*-Leu), 40.2 (CH<sub>2</sub>-Leu), 27.2 (CH<sub>2</sub>-Trp), 24.1 (CH-Leu) 23.5 (CH-Leu), 19.6 (CH<sub>3</sub>-Leu).

*(1S,4R)-4-((1H-indol-2-yl)methyl)-1-isobutyl-9-(1-methyl-1H-tetrazol-5-yl)-1,2-dihydro-6H-pyrazino [2,1-b]quinazoline-3,6(4H)-dione (32)*. Yield: 5.8 mg, 1 %; mp: 202.8-203.2 °C (MeOH);  $[\alpha]_D^{30} = -125.68$  (c 0.061; CHCl<sub>3</sub>);  $\nu_{max}$  (KBr) 3356, 3119, 3053, 1671, 1457, 1261, and 740 cm<sup>-1</sup>; <sup>1</sup>H NMR (300 MHz, CDCl<sub>3</sub>):  $\delta$  8.47 (d, 1H, *J* 8.3 Hz, CH), 8.41 (d, 1H, *J* 1.1 Hz, CH), 8.27 (dd, 1H, *J* 8.3 and 1.5 Hz, CH), 8.10 (s, 1H, NH-Trp), 7.50 (d, 1H, *J* 8.0

Hz, CH-Trp), 7.30 (d, 1H, *J* 8.3 Hz, CH-Trp), 7.13 (t, 1H, *J* 7.6 Hz, CH-Trp), 6.98 (d, 1H, *J* 7.5 Hz, CH-Trp), 6.67 (d, 1H, *J* 2.3 Hz, CH-Trp), 5.75 (s, 1H, NH-amide), 5.68 (dd, 1H, *J* 5.1 and 2.8 Hz, CH\*-Trp), 4.45 (s, 3H, CH<sub>3</sub>-N), 3.79 (dd, 1H, *J* 15.0 and 2.8 Hz, CH<sub>2</sub>-Trp), 3.66 (dd, 1H, *J* 15.1 and 5.3 Hz, CH<sub>2</sub>-Trp), 2.74 (dd, 1H, *J* 9.2 and 3.4 Hz, CH\*-Leu), 2.09-1.96 (m, 1H, CH-Leu), 1.43-1.30 (m, 2H, CH<sub>2</sub>-Leu), 0.76 (d, 3H, *J* 6.2 Hz, CH<sub>3</sub>-Leu), 0.31 (d, 3H, *J* 6.4 Hz, CH<sub>3</sub>-Leu) ; <sup>13</sup>C NMR (75 MHz, CDCl<sub>3</sub>): δ 169.3 (C=O), 164.2 (C=N-Tetrazol), 160.5 (C=O), 152.35 (C=N), 147.4 (C), 136.1 (C-Trp), 133.2 (C-Ctriazole), 127.8 (CH), 127.1 (C-Trp), 125.7 (CH), 125.0 (CH), 123.6 (CH-Trp), 122.8 (CH-Trp), 121.2 (C), 120.4 (CH-Trp), 118.7 (CH-Trp), 111.2 (CH-Trp), 109.6 (C-Trp), 57.4 (CH\*-Trp), 50.9 (CH\*-Leu), 40.7 (CH-Leu), 39.7 (CH<sub>3</sub>), 27.1 (CH<sub>2</sub>-Trp), 24.2 (CH<sub>2</sub>-Leu), 23.2 (CH<sub>3</sub>-Leu), 19.9 (CH<sub>3</sub>-Leu).

(6*S*,9*R*)-9-((1*H*-indol-3-yl)methyl)-6-isobutyl-6,7-dihydro-1*H*-pyrimido[5,4-*d*]pyrimidine-2,4,8,11 (3*H*,9*H*)-tetraone (**33**). Yield: 11.6 mg, 2.3 %; mp: 306-306.5 °C (MeOH); [ $\alpha$ ]<sub>D</sub><sup>30</sup> = -226.7 (*c* 0.025; CHCl<sub>3</sub>);  $\nu_{max}$  (KBr) cm<sup>-1</sup>; 3384, 2956, 1670, 1457, 1322, and 1095; <sup>1</sup>H NMR (300 MHz, CDCl<sub>3</sub>): δ 8.21 (s, 1H, NH-Trp), 7.65 (d, 1H, *J* 7.8 Hz, CH-Trp), 7.39 (d, 1H, *J* 8.0 Hz, CH-Trp), 7.22 (dd, *J* 8.1 and 1.1 Hz, CH-Trp), 7.18-7.12 (m, 1H, CH-Trp), 7.11 (d, 1H, *J* 2.3 Hz, CH-Trp), 6.73 (s, 1H, NH-amide), 5.98 (s, 1H, NH-Ant), 5.96 (s, 1H, NH-Ant), 4.28 (m, 1H, CH\*-Trp), 3.52 (dd, 1H, *J* 14.6 and 3.6 Hz, CH<sub>2</sub>-Trp), 3.44 (m, 1H, CH\*-Leu), 3.19 (dd, 1H, *J* 14.7 and 8.5 Hz, CH<sub>2</sub>-Trp), 1.69 (m, 1H, CH-Leu), 1.54 (m, 2H, CH<sub>2</sub>-Leu), 0.90 (d, *J* 6.1 Hz, CH<sub>3</sub>-Leu), 0.76 (d, 3H, *J* 6.1 Hz, CH<sub>3</sub>-Leu); <sup>13</sup>C NMR (75 MHz, CDCl<sub>3</sub>): δ 168.7 (C=O), 168.2 (C=O), 165.9 (C=O), 160.2 (C=O), 150.5 (C=N), 146.9 141.74 (C), 136.5 (C-Trp), 126.7 (C-Trp), 123.9 (CH-Trp), 122.8 (CH-Trp), 122.3 (C), 120.2 (CH-Trp), 118.8 (CH-Trp), 111.4 (CH-Trp), 109.3 (C-Trp), 54.7 (C\*-Trp), 53.1 (C\*-Leu), 42.1 (CH<sub>2</sub>-Leu), 29.9 (CH<sub>2</sub>-Trp), 24.0 (CH-Leu), 23.1 (CH-Leu), 20.8 (CH<sub>3</sub>-Leu).

(1*S*,4*R*)-1,4-bis((1*H*-indol-3-yl)methyl)-1,2-dihydro-6*H*-pyrazino[2,1-*b*]quinazoline-3,6(4*H*)-dione (**34**). Yield: 27.4 mg, 5.7%; *er* = 99:0; mp: 177.4-178.2 °C (MeOH);  $[\alpha]_D^{30} = -66.17$  (*c* 0.13; CHCl<sub>3</sub>);  $\nu_{max}$  (KBr): 3404, 3060, 2923, 1681, 1597, 1455, 695 and 668 cm<sup>-1</sup>; <sup>1</sup>H NMR (300 MHz, CDCl<sub>3</sub>):  $\delta$  8.41 (dd, 1H, *J* 8.0 and 1.3, CH), 8.10 (s, 1H, NH-Trp), 8.04 (s, 1H, NH-Trp), 7.82 (ddd, 1H, *J* 8.5, 7.2 and 1.5 Hz, CH), 7.66 (d, 1H, *J* 7.7 Hz, CH), 7.57 (ddd, 1H, *J* 8.1, 7.5 and 1.2 Hz, CH), 7.36 (d, 2H, *J* 8.1 Hz, CH-Trp), 7.34 (d, 2H, *J* 8.0 Hz, CH-Trp), 7.22 (ddd, 1H, *J* 8.1, 7.5 0.8 Hz, CH-Trp), 7.14 (t, 1H, *J* 7.3 Hz, CH-Trp), 7.08 (ddd, 1H, *J* 8.1, 7.5 0.8 Hz, CH-Trp), 6.80 (t, 1H *J* 7.3, CH-Trp), 6.65 (d, 1H *J* 2.3 Hz, CH-Trp), 6.42 (d, 1H *J* 1.9 Hz, CH-Trp), 5.68 (s, 1H, NH-amide), 5.66 (dd, 1H, *J* 7.8, 3.8 Hz, CH\*-Trp), 3.73 (dd, *J* 2.3 Hz, CH\*-Trp), 3.67 (dd, 2H, *J* 18.1 and 3.7 Hz, CH<sub>2</sub>-Trp), 3.11 (dd, 1H, *J* 11.0 and 3.4 Hz- CH<sub>2</sub>-Trp), 2.75 (dd, 15.1 and 11.1 Hz, CH<sub>2</sub>-Trp); <sup>13</sup>C NMR (75 MHz, CDCl<sub>3</sub>):  $\delta$  169.6 (C=O), 161.7 (C=O), 154.6, (C=N), 146.2 (C), 136.2 (C-Trp), 135.9 (C-Trp), 134.9 (CH), 133.3 (CH), 131.4 (CH), 127.8 (CH), 127.5 (C-Trp), 127.3 (C-Trp), 123.9 (CH), 123.7 (CH), 122.4 (CH-Trp), 122.3 (CH-Trp), 121.6 (CH-Trp), 119.7 (C-Trp(2)), 118.2 (CH-Trp), 114.1 (CH-Trp), 111.4 (CH-Trp), 110.1 (C-Trp), 64.6 (CH\*-Trp), 54.0 (CH\*-Trp), 30.9 (CH<sub>2</sub>-Trp), 25.1 (CH<sub>2</sub>-Trp).

## 4.2 Biology

### 4.2.1 Sample preparation

Each compound was lyophilized and solubilized in DMSO (Sigma-Aldrich) to obtain a final concentration of 5 mM. Some intermediate dilutions were made to achieve the final concentration of 10  $\mu$ M in the first well of the plate. Chloroquine (CQ; Sigma-Aldrich) was

prepared with RPMI-1640 (Invitrogen™) supplemented with AlbuMAXII (Invitrogen™) to obtain a final concentration of 10 µM.

#### 4.2.2 Culture of *P. falciparum*

Laboratory-adapted *P. falciparum* 3D7 (chloroquine and mefloquine sensitive), were continuously cultured using the method of Trager and Jensen, with previously described modifications (Nogueira *et al*, 2010). Parasites were cultivated at 5 % hematocrit, 37 °C and atmosphere with 5 % of CO<sub>2</sub>, human serum was replaced with 0.5 % AlbuMAXII (Invitrogen™) in the culture medium. Synchronized cultures were obtained by treatments with a 5 % (m/v) solution of D-sorbitol (Sigma-Aldrich) [48].

#### 4.2.3 *In vitro* susceptibility assay of *P. falciparum* using SYBR Green I

All compounds were screened for their *in vitro* antimalarial activity against chloroquine-susceptible (3D7) *P. falciparum* strain, using the Whole cell SYBR Green I assay as previously described [37] with modifications. Briefly, early ring stage parasites (>80 % of rings, 3 % haematocrit and 1 % parasitaemia) were tested in duplicate in a 96-well plate and incubated with the compounds for 48 h (37 °C, 5 % CO<sub>2</sub>), parasite growth was assessed with SYBRGreenI (Thermo Fisher Scientific). Each compound was tested in concentrations ranging from 10 to 0.001 µM. Fluorescence intensity was measured with a microplate reader with excitation and emission wavelengths of 485 and 535 nm, respectively, and analysed by nonlinear regression using GraphPad Prism 5 demo version to determine IC<sub>50</sub>.

#### 4.2.4 Cytotoxicity in vitro against mammalian cell

Cytotoxicity was assessed on the mammalian cell line V79 (Chinese hamster lung), using a MTT based assay, as previously described [38]. Tests were conducted in triplicate for each compound, at a range of concentrations (800  $\mu$ M to 0.0512  $\mu$ M), and with culture media containing 0.5 % DMSO (no drug control); incubation time 24 h. Absorbance was read at 570 nm on a multi-mode microplate reader, to produce a log dose-dependence curve. The LD<sub>50</sub> value for each compound was estimated by non-linear interpolation of the dose-dependence curve (GraphPad Software).

#### 4.2.5 Evaluation of hemotoxicity in vitro

In a 96-flat bottom plate was added of 3 % HTC, 20  $\mu$ L of 20 % Triton X-100, and 20  $\mu$ L of PBS or RPMIc in 2 % DMSO. Compounds were tested in a 1:4 serial dilution in concentrations ranging from 10  $\mu$ M to 0.04  $\mu$ M. After the incubation for 60 minutes, the plate was centrifuged at 2000 rpm for 5 minutes. 100 mL of Supernatant was transferred to a flat bottom plate. The absorbance reading was made at 450 nm in a Mode (Triad, Dynex Technologies). Two independent tests were carried out in triplicate. The results are presented in the form of a percentage of hemolysis-% hemolysis, obtained by the following formula: % Hemolysis =  $ABS(\text{sample})/abs(C+) \times 100$ . Whereas C + is a Triton X-100 to 20 % solution RPMIc.

#### 4.2.6 Evaluation of inhibition of polymerization of hemozoin

100  $\mu$ L of a freshly prepared solution of hemin (ferriprotoporphyrin IX chloride; Sigma-Aldrich) 4mM dissolved in 0.1 M NaOH (Sigma-Aldrich) was mixed with 50  $\mu$ L of acetic acid (Sigma-Aldrich) and 50  $\mu$ L of each tested compound. The mixture was incubated

during 24 h at 37 °C in a U-bottom 96 well plate. Compounds were tested at the following doses: **8** and **12** 48.0 μM, 24.0 μM and e 12.0 μM and **21** 96.0 μM, 48.0 μM and 24.0). After incubation, the resulting solution was spun down for 15 min at 4000 rpm, the supernatant discarded and the pellet was washed with 200 μL of DMSO (3 washes) after an additional final wash with water (200 μL), the pellet was dissolved in 0.1 M NaOH (200 μL). 50 μL of the solution was transferred to a flat-bottom 96 well clean plate and mixed with 150 μL of water and absorption measured at 405 nm using a multi microplate reader plate reader (Triad, Dynex Technologies).

#### 4.3 Virtual screening

Crystal structure of Prolyl-tRNA Synthetase (PRS) (PDB code: 4YDQ), downloaded from the protein databank (PDB) [39], was used for the study. Structure files of 60 test molecule, four positive (halofuginone (HF), febrifugine (FF, **5**), 6-fluorofebrifugine (6F-FF), and tetrahydro quinazolinone febrifugine (Th-FF)) and one negative (chloroquine, CQ, **2**) controls were created and minimized using the chemical structure drawing tool Hyperchem 7.5 (Hypercube, FL, USA) [35] and prepared for docking using AutodockTools [35]. Structure-based docking was carried out using AutoDock Vina (Molecular Graphics Lab, CA, USA) [40]. The active site was defined by a grid box (X: 19 Å; Y:14 Å; Z: 15 Å) drawn around the PRS crystallographic ligand HF. Default settings for small molecule-protein docking were used throughout the simulations. Top 9 poses were collected for each molecule and the lowest docking score value was associated with the more favorable binding conformation. PyMol1.3 (Schrödinger, NY, USA) [41] was used for visual inspection of results and graphical representations. To validate the docking approach for the protein structure used, the respective co-crystallized inhibitor HF was docked to the active site using Autodock Vina (Figure 2S, supplementary material).

**Supplementary Materials:** The supplementary materials are presented in a following section.

**Author Contributions:** E.S. and R.M. conceived the study design. S.L. synthesized the compounds and elucidated their structure and, A.M.S.S., E.S., A.K., and M.M.M.P. analyzed the data. D.I.S.P.R. performed the HPLC analysis. V.C and R.O performed the *in vitro* susceptibility test and non-tumoral cell V7. F. N. analyzed data from the cytotoxic studies, discussed and wrote those results. S.L. and E.S. wrote the manuscript, while all authors gave significant contributions in discussion and revision. All authors agreed to the final version of the manuscript.

**Funding:** This research was partially supported by the Strategic Funding UID/Multi/04423/2019 through national funds provided by FCT-Foundation for Science and Technology and European Regional Development Fund (ERDF), in the framework of the program PT2020 and was developed under project No. POCI-01-0145-FEDER-028736 and PTDC/MAR-BIO/4694/2014 (POCI-01-0145-FEDER-016790; 3599-PPCDT), co-financed by COMPETE 2020, Portugal 2020 and the European Union through the ERDF, and by FCT through national funds.

**Acknowledgments:** S.L. thanks Erasmus Mundus Action 2 (LOTUS+, LP15DF0205) for full PhD scholarship. To Sara Cravo for technical support.

**Conflicts of Interest:** The authors declare no conflicts of interest.

## 5. References



1. WHO: World Malaria Report 2018. Geneva: World Health Organization: World Health Organization. **2018**.
2. WHO: Global report on antimalarial efficacy and drug resistance: 2000-2010. **2010**:121.
3. Ines P, Richard E, Michael L: Drug-resistant malaria: Molecular mechanisms and implications for public health. *FEBS Letters* **2011**, 585(11):1551-1562.
4. WHO: World malaria report 2017. **2017**:196.
5. WHO: Eliminating malaria in the Greater Mekong Subregion: united to end a deadly disease. **2016**, Geneva: World Health Organization; 2016.
6. Fernández-Álvaro E, Hong WD, Nixon GL, O'Neill PM, Calderón F: Antimalarial Chemotherapy: Natural Product Inspired Development of Preclinical and Clinical Candidates with Diverse Mechanisms of Action. *Journal of Medicinal Chemistry* **2016**, 59(12):5587-5603.
7. Oliveira R, Guedes RC, Meireles P, Albuquerque IS, Gonçalves LM, Pires E, Bronze MR, Gut J, Rosenthal PJ, Prudêncio M *et al*: Tetraoxane-pyrimidine nitrile hybrids as dual stage antimalarials. *Journal of Medicinal Chemistry* **2014**, 57(11):4916-4923.
8. Flannery EL, Chatterjee AK, Winzeler EA: Antimalarial drug discovery-approaches and progress towards new medicines. *Nature Reviews Microbiology* **2013**, 11(12):849-862.
9. Almela MJ, Lozano S, Lelièvre J, Colmenarejo G, Coterón JM, Rodrigues J, Gonzalez C, Herreros E: A New Set of Chemical Starting Points with Plasmodium falciparum Transmission-Blocking Potential for Antimalarial Drug Discovery. *PLOS ONE* **2015**, 10(8):e0135139.
10. Rottmann M, McNamara C, Yeung BKS, Lee MCS, Zou B, Russell B, Seitz P, Plouffe DM, Dharia NV, Tan J *et al*: Spiroindolones, a potent compound class for the treatment of malaria. *Science* **2010**, 329(5996):1175-1180.
11. Cully M: Trial watch: Next-generation antimalarial from phenotypic screen shows clinical promise. *Nature Reviews Drug Discovery* **2014**, 13(10):717.

12. Barker Jr RH, Uргаonkar S, Mazitschek R, Celatka C, Skerlj R, Cortese JF, Tyndall E, Liu H, Cromwell M, Sidhu AB *et al*: Aminoindoles, a novel scaffold with potent activity against Plasmodium falciparum. *Antimicrobial Agents and Chemotherapy* **2011**, 55(6):2612-2622.
13. Gamo FJ, Sanz LM, Vidal J, De Cozar C, Alvarez E, Lavandera JL, Vanderwall DE, Green DVS, Kumar V, Hasan S *et al*: Thousands of chemical starting points for antimalarial lead identification. *Nature* **2010**, 465(7296):305-310.
14. Resende DISP, Boonpothong P, Sousa E, Kijjoa A, Pinto MMM: Chemistry of the fumiquinazolines and structurally related alkaloids. *Natural Product Reports* **2018**.
15. Long S, Resende DISP, Kijjoa A, Silva AMS, Pina A, Fernández-Marcelo T, Vasconcelos MH, Sousa E, Pinto MMM: Antitumor Activity of Quinazolinone Alkaloids Inspired by Marine Natural Products. *Marine Drugs* **2018**, 16(8).
16. Long S, Resende DISP, Kijjoa A, Silva AMS, Fernandes R, Xavier CPR, Vasconcelos MH, Sousa E, Pinto MMM: Synthesis of New Proteomimetic Quinazolinone Alkaloids and Evaluation of Their Neuroprotective and Antitumor Effects. *Molecules* **2019**, 24(3):534.
17. Pathak M, Ojha H, Tiwari AK, Sharma D, Saini M, Kakkar R: Design, synthesis and biological evaluation of antimalarial activity of new derivatives of 2,4,6-s-triazine. *Chemistry Central Journal* **2017**, 11(1):132-132.
18. Zhu S, Wang J, Chandrashekar G, Smith E, Liu X, Zhang Y: Synthesis and evaluation of 4-quinazolinone compounds as potential antimalarial agents. *European Journal of Medicinal Chemistry* **2010**, 45(9):3864-3869.
19. Zhu S, Zhang Q, Gudise C, Wei L, Smith E, Zeng Y: Synthesis and biological evaluation of febrifugine analogues as potential antimalarial agents. *Bioorganic and Medicinal Chemistry* **2009**, 17(13):4496-4502.
20. Zhu S, Meng L, Zhang Q, Wei L: Synthesis and evaluation of febrifugine analogues as potential antimalarial agents. *Bioorganic and Medicinal Chemistry Letters* **2006**, 16(7):1854-1858.
21. McLaughlin NP, Evans P, Pines M: The chemistry and biology of febrifugine and halofuginone. *Bioorganic and Medicinal Chemistry* **2014**, 22(7):1993-2004.

22. Villarreal W, Colina-Vegas L, Rodrigues de Oliveira C, Tenorio JC, Ellena J, Gozzo FC, Cominetti MR, Ferreira AG, Ferreira MAB, Navarro M *et al*: Chiral Platinum(II) Complexes Featuring Phosphine and Chloroquine Ligands as Cytotoxic and Monofunctional DNA-Binding Agents. *Inorganic Chemistry* **2015**, 54(24):11709-11720.
23. Katsuno K, Burrows JN, Duncan K, Van Huijsduijnen RH, Kaneko T, Kita K, Mowbray CE, Schmatz D, Warner P, Slingsby BT: Hit and lead criteria in drug discovery for infectious diseases of the developing world. *Nature Reviews Drug Discovery* **2015**, 14(11):751-758.
24. Cargnin ST, Staudt AF, Medeiros P, de Medeiros Sol Sol D, de Azevedo dos Santos AP, Zanchi FB, Gosmann G, Puyet A, Garcia Teles CB, Gnoatto SB: Semisynthesis, cytotoxicity, antimalarial evaluation and structure-activity relationship of two series of triterpene derivatives. *Bioorganic and Medicinal Chemistry Letters* **2018**, 28(3):265-272.
25. Jonville MC, Kodja H, Humeau L, Fournel J, De Mol P, Cao M, Angenot L, Frédérick M: Screening of medicinal plants from Reunion Island for antimalarial and cytotoxic activity. *Journal of Ethnopharmacology* **2008**, 120(3):382-386.
26. Dausset J, Contu L: Drug-Induced Hemolysis. *Annual Review of Medicine* **1967**, 18(1):55-70.
27. Chou AC, Fitch CD: Hemolysis of mouse erythrocytes by ferriprotoporphyrin IX and chloroquine. Chemotherapeutic implications. *Journal of Clinical Investigation* **1980**, 66(4):856-858.
28. Amin K, Dannenfelser RM: In vitro hemolysis: Guidance for the pharmaceutical scientist. *Journal of Pharmaceutical Sciences* **2006**, 95(6):1173-1176.
29. Basilico N, Pagani E, Monti D, Olliaro P, Taramelli D: A microtitre-based method for measuring the haem polymerization inhibitory activity (HPIA) of antimalarial drugs. *Journal of Antimicrobial Chemotherapy* **1998**, 42(1):55-60.
30. Derbyshire ER, Mazitschek R, Clardy J: Characterization of Plasmodium Liver Stage Inhibition by Halofuginone. *ChemMedChem* **2012**, 7(5):844-849.

31. Keller TL, Zocco D, Sundrud MS, Hendrick M, Edenius M, Yum J, Kim YJ, Lee HK, Cortese JF, Wirth DF *et al*: Halofuginone and other febrifugine derivatives inhibit prolyl-tRNA synthetase. *Nature chemical biology* **2012**, 8(3):311-317.
32. Jain V, Yogavel M, Oshima Y, Kikuchi H, Touquet B, Hakimi MA, Sharma A: Structure of Prolyl-tRNA Synthetase-Halofuginone Complex Provides Basis for Development of Drugs against Malaria and Toxoplasmosis. *Structure* **2015**, 23(5):819-829.
33. Son J, Lee EH, Park M, Kim JH, Kim J, Kim S, Jeon YH, Hwang KY: Conformational changes in human prolyl-tRNA synthetase upon binding of the substrates proline and ATP and the inhibitor halofuginone. *Acta crystallographica Section D, Biological crystallography* **2013**, 69(Pt 10):2136-2145.
34. Herman JD, Pepper LR, Cortese JF, Estiu G, Galinsky K, Zuzarte-Luis V, Derbyshire ER, Ribacke U, Lukens AK, Santos SA *et al*: The cytoplasmic prolyl-tRNA synthetase of the malaria parasite is a dual-stage target of febrifugine and its analogs. *Science translational medicine* **2015**, 7(288):288ra277-288ra277.
35. Froimowitz M: HyperChem: a software package for computational chemistry and molecular modeling. *BioTechniques* **1993**, 14(6):1010-1013.
36. Zhou H, Sun L, Yang XL, Schimmel P: ATP-directed capture of bioactive herbal-based medicine on human tRNA synthetase. *Nature* **2013**, 494(7435):121-124.
37. Nogueira F, Diez A, Radfar A, Pérez-Benavente S, Rosario VEd, Puyet A, Bautista JM: Early transcriptional response to chloroquine of the Plasmodium falciparum antioxidant defence in sensitive and resistant clones. *Acta Tropica* **2010**, 114(2):109-115.
38. Santos SA, Lukens AK, Coelho L, Nogueira F, Wirth DF, Mazitschek R, Moreira R, Paulo A: Exploring the 3-piperidin-4-yl-1H-indole scaffold as a novel antimalarial chemotype. *European Journal of Medicinal Chemistry* **2015**, 102:320-333.
39. Burley SK, Berman HM, Kleywegt GJ, Markley JL, Nakamura H, Velankar S: Protein Data Bank (PDB): The Single Global Macromolecular Structure Archive. *Methods in molecular biology* **2017**, 1607:627-641.

40. Jaghoori MM, Bleijlevens B, Olabarriaga SD: 1001 Ways to run AutoDock Vina for virtual screening. *Journal of computer-aided molecular design* **2016**, 30(3):237-249.
41. Seeliger D, de Groot BL: Ligand docking and binding site analysis with PyMOL and Autodock/Vina. *Journal of computer-aided molecular design* **2010**, 24(5):417-422.

## Supplementary Material

# Discovery of indole-containing pyrazino[2,1-*b*]quinazoline-3,6-diones as promising antimalarial agents

*Solida Long*<sup>1</sup>, *Vera C. F. Camões*<sup>2</sup>, *Rafael Oliveira*<sup>2</sup>, *Diana I. S. P. Resende*<sup>1,3</sup>, *Andreia Palmeira*<sup>1</sup>, *Artur M. S. Silva*<sup>4</sup>, *Rui Moreira*<sup>5</sup>, *Anake Kijjoa*<sup>3,6</sup>, *Fátima Nogueira*<sup>2,\*</sup>, *Emília Sousa*<sup>1,3,\*</sup>, *Madalena M. M. Pinto*<sup>1,3</sup>

<sup>1</sup> Laboratório de Química Orgânica e Farmacêutica, Faculdade de Farmácia, Universidade do Porto, Rua de Jorge Viterbo Ferreira, 228, 4050-313 Porto, Portugal.

<sup>2</sup> Global Health and Tropical Medicine, GHTM, Unidade de Ensino e Investigação de Parasitologia Médica, Instituto de Higiene e Medicina Tropical, IHMT, Universidade Nova de Lisboa, UNL, Rua da Junqueira no 100, 1349-008 Lisbon, Portugal.

<sup>3</sup> CIIMAR - Centro Interdisciplinar de Investigação Marinha e Ambiental, Terminal de Cruzeiros do Porto de Leixões, 4450-208 Matosinhos, Portugal.

<sup>4</sup> QOPNA - Química Orgânica, Produtos Naturais e Agroalimentares, Departamento de Química, Universidade de Aveiro, Campus Universitário de Santiago, 3810-193 Aveiro, Portugal.

<sup>5</sup> Research Institute for Medicines and Pharmaceutical Sciences (iMed.UL), Faculdade de Farmácia, Universidade de Lisboa, Av. Prof. Gama Pinto, 1649-019 Lisboa, Portugal.

<sup>6</sup> ICBAS-Instituto de Ciências Biomédicas Abel Salazar, Universidade do Porto, Rua de Jorge Viterbo Ferreira, 228, 4050-313 Porto, Portugal.

\* Correspondence: [esousa@ff.up.pt](mailto:esousa@ff.up.pt); Tel.: +351-220428689; [FNogueira@ihmt.unl.pt](mailto:FNogueira@ihmt.unl.pt); Tel.: +351-213652600

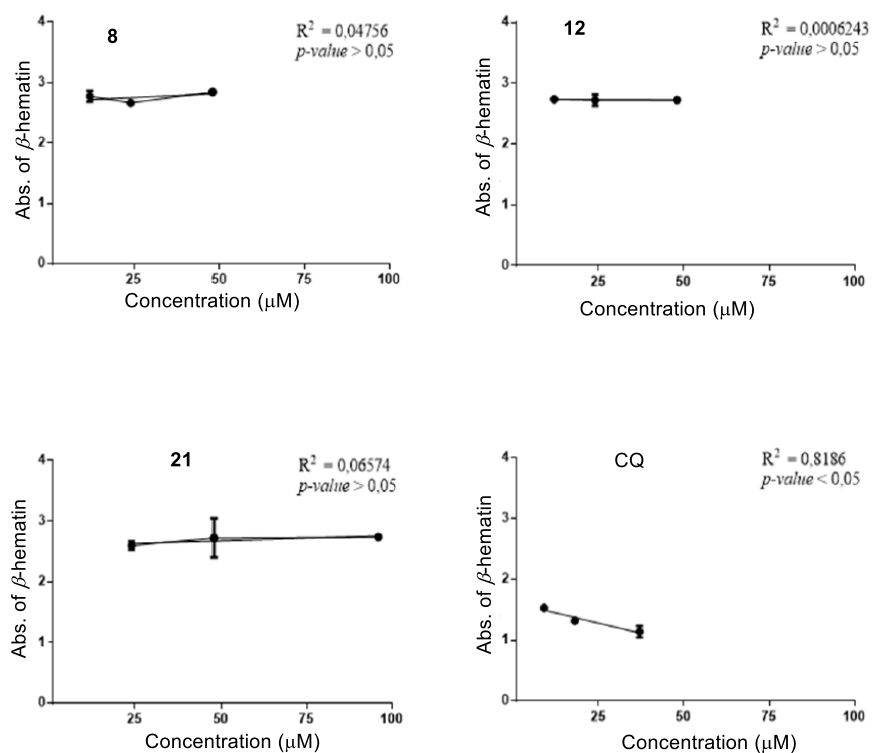


**Figure S1.** The inhibition of polymerization of hemozoin in vitro of compound **8**, **12**, **21**, and CQ.

The error bars represent a mean  $\pm$  SD.

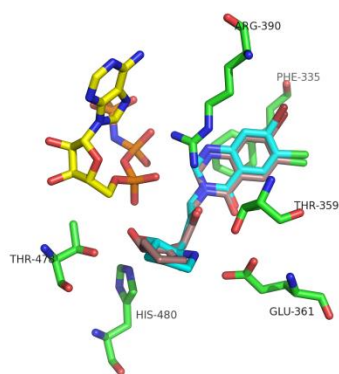


**Figure S2.** Crystallographic (light blue) and docked (brown) HF in binding pocket of PRS (RMSD = 0.582 Å). The RMSD value is < 2.0 Å, value usually considered a good threshold value for validating a structure for use in molecular docking. This is strong evidence that AutoDock Vina can predict docking poses accurately.

**Table S1.** Docking scores of test compounds and controls onto PRS (4ydq) HF binding site

<b>4ydq_chainA_AMP</b>	<b>Docking scores (kcal.mol<sup>-1</sup>)</b>
6	-10.7
7	-8.9
8	-9.1
9	-11.4
10	-9.9
11	-7.8
12	-10.0
13	-11.5
14	-10.3
15	-10.1
16	-9.4
17	-7.3
18	-7.7
19	-9.4
20	-7.6
21	-9.9
22	-8.9
23	-7.3
24	-8.6
25	-5.7
26	-8.3
27	-8.4
28	-8.6
29	-9.7
30	-10.1
31	-9.4
32	-7.8



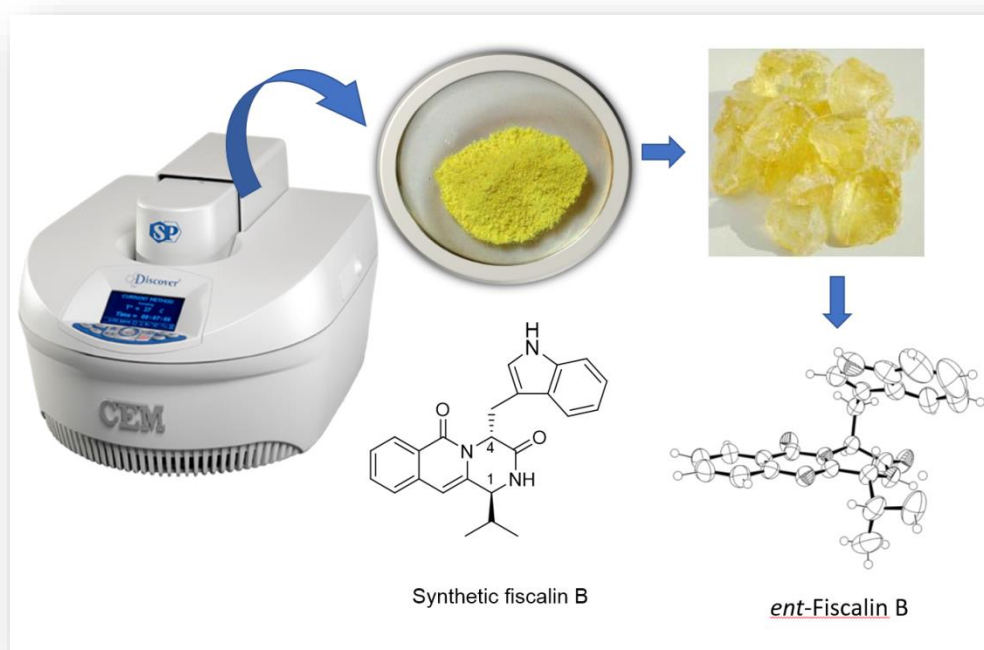
<b>4ydq_chainA_AMP</b>	<b>Docking scores (kcal.mol<sup>-1</sup>)</b>
<b>33</b>	-10.1
<b>34</b>	-11.5
<b>Febrifugine (5)</b>	-9.5
<b>Halofuginone</b>	-9.3
<b>ThFF</b>	-9.5
<b>6FFF</b>	-9.7
<b>Chloriquine (2)</b>	-7.4



# Chapter 7

## Microwave-assisted gram-scale synthesis of fiscalin B and a chloro derivative

Graphical abstract





# Microwave-assisted gram-scale synthesis of fiscalin B and a chloro derivative

Solida Long<sup>1</sup>, Diana I. S. P. Resende<sup>1,2</sup>, Artur M. S. Silva<sup>3</sup>, Luis Gales<sup>4,5</sup>, Emília Sousa<sup>1,2,\*</sup>, and Madalena M. M. Pinto<sup>1,2</sup>

<sup>1</sup> LQOF - Laboratório de Química Orgânica e Farmacêutica, Departamento de Ciências Químicas, Faculdade de Farmácia, Universidade do Porto, Rua de Jorge Viterbo Ferreira, 228, 4050-313 Porto, Portugal.

<sup>2</sup> CIIMAR - Centro Interdisciplinar de Investigação Marinha e Ambiental, Terminal de Cruzeiros do Porto de Leixões, Av. General Norton de Matos S/N, 4450-208 Matosinhos, Porto, Portugal.

<sup>3</sup> QOPNA - Química Orgânica, Produtos Naturais e Agroalimentares, Departamento de Química, Universidade de Aveiro, 3810-193 Aveiro, Portugal.

<sup>4</sup> ICBAS - Instituto de Ciências Biomédicas Abel Salazar, Universidade do Porto, Portugal

<sup>5</sup> i3S-IBMC-Instituto de Biologia Molecular e Celular, Universidade do Porto, Porto, Portugal.

\*Corresponding author: [esousa@ff.up.pt](mailto:esousa@ff.up.pt)

**Abstract:** The synthetic (-)-fiscalin B (**1**) of the naturally-occurring quinazolinone disclosed with antimalarial activity and its chloro derivative, 1*S*,4*R*-4-((1*H*-indol-3-yl)methyl)-8,10-dichloro-1-isobutyl-1,2-dihydro-6*H*-pyrazino[2,1-*b*]quinazoline-3,6(4*H*)-dione, (**2**), disclosed as antibacterial agent, were synthesized on a gram scale using a one-pot three component microwave-assisted polycondensation reaction with 22% and 17% isolated yields, respectively. The crystal structure of *ent*-fiscalin B, (+)-**1**, is also reported. This single

step reaction proved to be a feasible approach for gram synthesis of quinazolinone alkaloids when compared with a multistep approach.

**Keywords:** Fiscalin B, Gram-scale synthesis, one-pot synthesis.

## 1. Introduction

Studies on the isolation, biosynthesis, synthesis and biological studies of the pyrazino[2,1-*b*]quinazoline-3,6-dione core linked to an indole moiety have been increasing greatly in the last 20 years [1-4]. Structurally, these quinazolinone alkaloids have been classified from simple to complex structures and consist of three different building blocks – anthranilic acid,  $\alpha$ -amino acids, and tryptophanyl moieties that merge into a simple piperazine ring system [5]. The simplest structures are gyantrypine, fumiquinazolines F and G, and fiscalin B (**1**) which were reported in several synthetic studies [6-9]. Fiscalin B (**1**) was first isolated from a strain of *Aspergillus fumigatus* growth in the intestine of the marine fish *Pseudolabrus japonicus*, in 1992, and later from the ethyl acetate extract of cell mass from fungal culture of *Neosartorya fischeri* collected from We Fung Chi, Taiwan, in 1993 [10-13]. Fiscalin B (**1**) has been reported for its substance P inhibition [14], neuroprotective [15], antitumor [16], and antimalarial effects (Chapter 6).

Owing to the growing interest of **1** in medicinal and organic chemistry, some synthetic procedures enabling its facile production to have been developed in the last 20 years [6,8,9,17]. The first total synthesis of **1** was accomplished by Ganesan and coworkers in 1998 using Wipf oxazole synthesis and mild procedures with simple reagents for accomplishing dehydration via oxazine intermediates [8,9]. Later, in 2002, Hernández *et al.* reported the synthesis of **1** using the alkylation at C-4 of 1-methyl(isopropyl)-2,4-dihydro-

1*H*-pyrazino[2,1-*b*]quinazolino-3,6-dione regio- and diastereoselective, which was possible by the Eguchi-aza approach with *N*-Boc-3-indolymethyl bromide followed by deprotection [7].

Non-conventional chemical synthesis using microwave irradiation has been developed as a green chemistry methodology since first reported in 1986 [18]. The use of microwave heating technique has become common applicable in all areas of synthetic organic chemistry, including solvent-free, and water-mediated reactions [19,20]. Microwave heating has been described to solve cases of conventional heating reported failures in terms of chemo-, regio-, and stereo selective syntheses [21,22]. Recent innovation in microwave reactor technology allows controlled parallel and automated sequential processing under sealed-vessel conditions and the use of continuous or stop-flow reactors for scale-up purposes [23]. The increasing use of microwave methods was reported among the synthesis of privileged natural products and particularly with a quinazolinone scaffold [24-26]. In 2005, Lui *et al.* developed a novel microwave-assisted domino method using a three-component one-pot reaction to synthesize fiscalin B (**1**, Figure 1) via a *N*-protected benzoxazine-4-one intermediate [6]. This approach allowed an easy access to quinazolinone natural product template and libraries for screenings [22]. The work was performed under pressure at 300 W into a specifically designed platform (Smith synthesizer <sup>TM</sup>) producing controlled irradiation at 2450 MHz. Reaction temperature and pressure were determined using the built-in IR and pressure sensor. The authors also report a gram scale synthesis of (1*S*)-1-methyl-2,4-dihydro-1*H*-pyrazino[2,1-*b*]quinazoline-3,6-dione in a moderate yield of 53% starting from 10 mmol of anthranilic acid, *N*-Boc-L-alanine, and glycine methyl ester hydrochloride [6]. Herein, we report the concise total synthesis of fiscalin B (**1**) and its derivative, 1*S*,4*R*-4-((1*H*-indol-3-yl)methyl)-8,10-dichloro-1-isobutyl-1,2-dihydro-6*H*-pyrazino[2,1-*b*]quinazoline-3,6(4*H*)-dione, **2**, on gram scale using commercial microwave equipment.

The strategies employed involved quinazoline dehydration followed by diketopiperazine-like cyclization after *N*-deprotection.

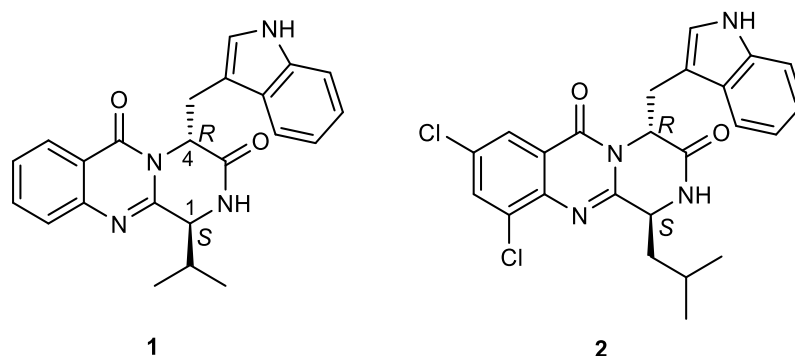


**Figure 1:** Structures of target compounds for gram syntheses, fiscalin B (**1**) and 1*S*,4*R*-4-((1*H*-indol-3-yl)methyl)-8,10-dichloro-1-isobutyl-1,2-dihydro-6*H*-pyrazino[2,1-*b*]quinazolinone-3,6(4*H*)-dione (**2**).

## 2. Results and discussion

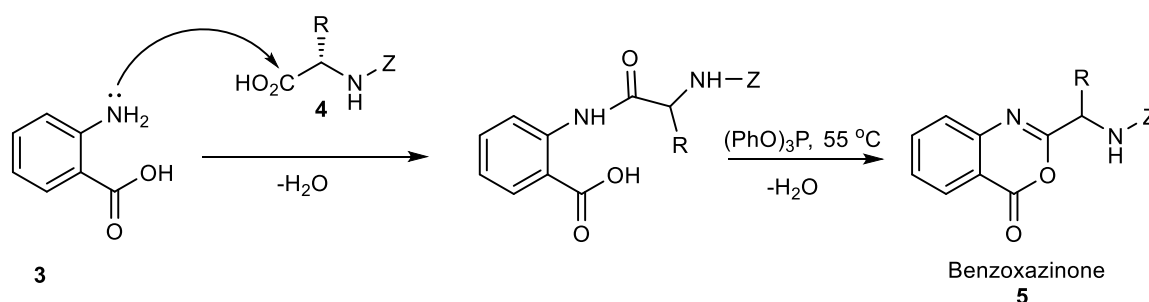
### 2.1 Chemistry background

Following the retrosynthetic analysis described by Lui *et al.*, we reasoned that the construction of the pyrazino[2,1-*b*]quinazolinone-3,6-dinone core is the key step in the synthesis of these targeted alkaloids, **1** and **2** [6]. The selection of the protecting group of the  $\alpha$ -amino acids was targeted to *tert*-butyloxycarbonyl (Boc) and fluorenylmethyloxycarbonyl (Fmoc) groups, which were reported to produce the lowest number of by-products.

The reaction begins with the condensation of the amine group of the anthranilic acid (**3**, 1.0 equiv.) with the carboxyl group of *N*-protected-amino acid (**4**, 1.0 equiv.) in pyridine

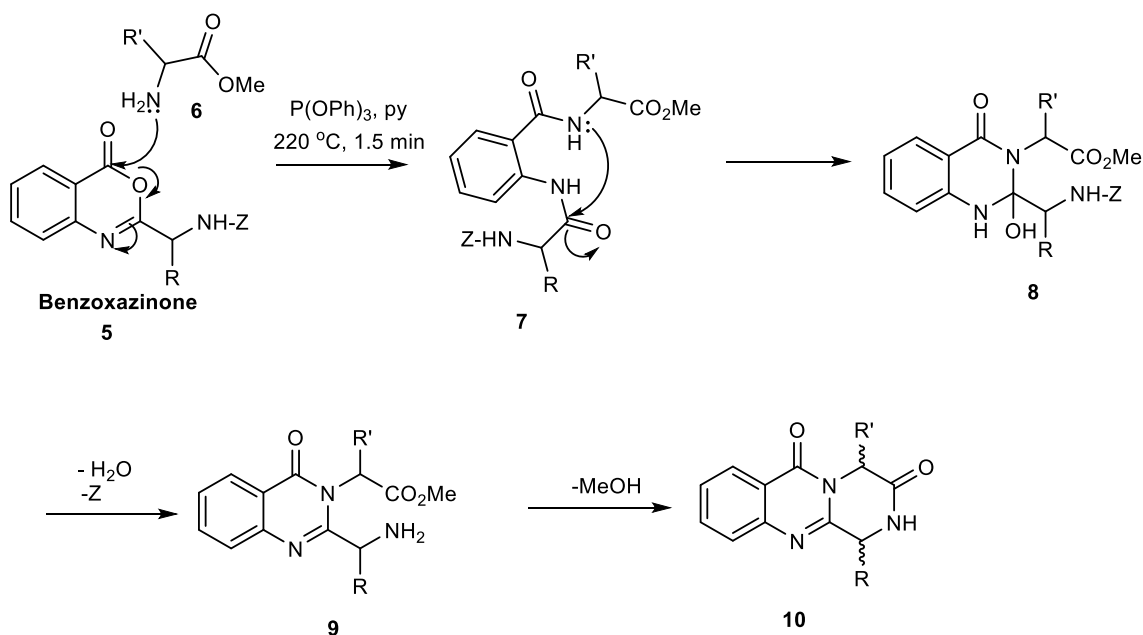


followed by dehydration to form the intermediate benzoxazinone **5** under conventional heating at 55 °C with a coupling-dehydrating agent, triphenyl phosphite (PhO)<sub>3</sub>P (1.2 equiv.) (Scheme 1).



**Scheme 1:** Condensation-cyclization reaction of anthranilic acid (**3**) and *N*-protected-amino acid **4**.

Subsequent addition of  $\alpha$ -amino acid methyl ester **6** under microwave irradiation at 220 °C provides the mixture of diamide **7** as a minor component and 2,3-disubstituted-3*H*-quiazolin-4-one (**9**) as the major component [27] (Scheme 2). The conversion of **7** and **9** to the final product, the pyrazino[1,2-*b*]quinazoline-3,6-dione (**10**) is accomplished by a nucleophilic substitution of **5** with amine group of **6** to form diamine **7** which undergoes an intramolecular condensation followed by removing of a protecting group, reported by Siro *et al.* [28] and Vanier *et al.* [29], to afford **9**, and finally removing of methanol under microwave irradiation to furnish the final product **10**.



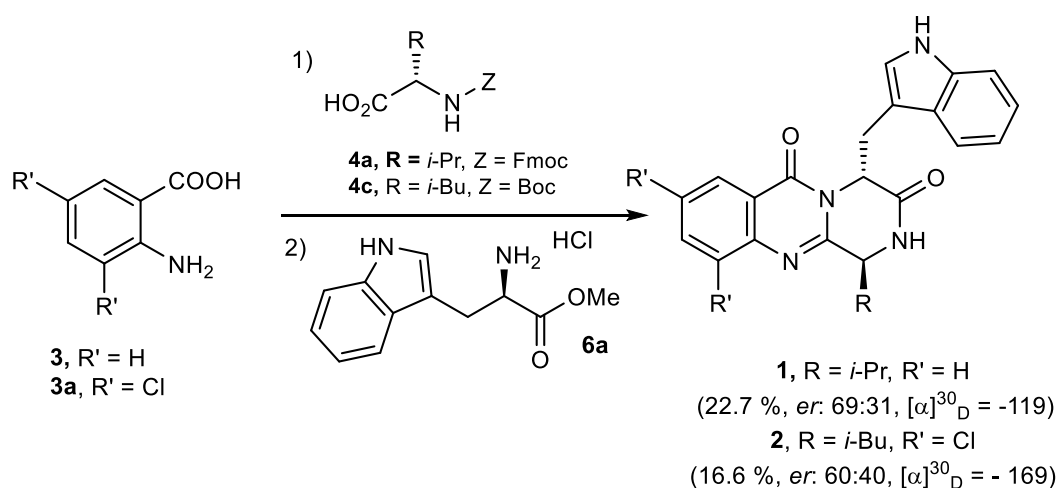
**Scheme 2:** Synthesis of pyrazino[2,1-*b*]quinazolinone-3,6-dione **10** by condensation-cyclization reaction of benzoxazinone **5** and amino acid ester **6**.

The work of Lui *et al.* [6,27] clearly indicated that microwave irradiation played a critical role in driving this reaction to be completed and providing access to a uniquely substituted quinazolinone scaffold which was not available from conventional heating.

## 2.2 Gram-scale synthesis of fiscalin B (**1**)

The first attempt to obtain gram amount of fiscalin B (**1**) followed the protocol used in the gram-scale synthesis of (1*S*)-1-methyl-2,4-dihydro-1*H*-pyrazino[2,1-*b*]quinazolinone-3,6-dione. The reaction was carried out at  $210\text{ }^\circ\text{C}$  for 10 min after the first condensed-cyclization (Scheme 1,  $\text{R} = i\text{-Pr}$ ), but did not proceed to form fiscalin B (**1**) (data not shown). This failure was attributed to the steric hindrance caused by the groups at C-4 and C-1 which was also reported by Lui *et al.* [6]. Therefore, the strategy to achieve gram scale synthesis was adopted from the milligram scale synthesis of fiscalin B (**1**) [16].

The reaction was performed in a closed two-neck round bottle flask. To the mixture of anthranilic acid (**3**, 4.2 g, 0.03 mol) in dried pyridine (150 mL), *N*-Fmoc-L-valine (**4a**, 10.4 g, 0.03 mol) and (PhO)<sub>3</sub>P (11.81 mL, 0.45 mol, 1.5 equiv) were added. The mixture was heated at 55 °C for 48 h to furnish benzoxazinone (**5a**) (Scheme 1, R = *i*-Pr) which was not subjected to purification/isolation. To the reaction mixture, D-tryptophan methyl ester hydrochloride (**6a**, 7.65 g, 0.03 mol) was added and the mixture was divided into 30 microwavable vials seal with cap. The parallel syntheses under microwave irradiation at 220 °C under the power of 300 W for 2 min were performed to yield the desirable product **1** using commercial microwave CEM (Scheme 3). After finished, the combined reaction products were evaporated under reduced pressure to remove pyridine and dried under nitrogen. The residue was purified by silica gel flash chromatography (CH<sub>2</sub>Cl<sub>2</sub>:EtOAc:MeOH = 50:48:2) followed by preparative TLC (CH<sub>2</sub>Cl<sub>2</sub>:Me<sub>2</sub>CO = 95:5) to give synthetic fiscalin B (**1**) as a pale-yellow solid (1.79 g, 22.7 %). The byproducts of the reaction were also isolated and included tripeptides and dipeptides (data not shown).



**Scheme 3:** One-pot synthesis of fiscalin B (**1**) and derivative **2**.

The enantiomeric ratio analysis of the synthetic fiscalin B (**1**) was performed by using enantioselective liquid chromatography employing a system equipped with a chiral column Whelk-O1-*S,S* (250 x 4.6 mm) and UV-detection at 245 nm, the mobile phase was MeOH/MeCN = 50:50 and the flow rate was 1.0 mL/min. The enantiomeric ratio (*er*) was calculated by the percentage of peak area. The *er* of fiscalin B (**1**) was found to be 69:31 in which 69 % was fiscalin B, (-)-**1**, and 31 % was *ent*-fiscalin B, (+)-**1**, confirmed by the specific rotation of a synthetic fiscalin B (**1**) obtained previously in a milligram scale [16] and that was enantiomerically purified ( $[\alpha]_D^{30} = -452$ , *er* = 99:1 and  $[\alpha]_D^{30} = +255$ , *er* = 99:1) (Chapter 6). Under the same conditions of temperature, pressure, and time in the CEM microwave equipment, synthetic fiscalin B (**1**) obtained in this scale-up process showed lower enantiomeric excess (*ee*), 38 %, when compared to the 50 % *ee* obtained by Lui *et al.* when the reaction was carried out in a Personal Chemistry™ Creator and Smith stations [30]. In the previously performed milligram-scale synthesis of fiscalin B (**1**) [16], Boc-L-valine was employed, and fiscalin B (**1**) was reported to have a 26 % of *ee* or a 63:37 of *er*, while in this gram-scale synthesis, using Fmoc-L-valine, the *ee* improved to 38 %.

### 2.3 Crystal structure of *ent*-fiscalin B, (+)-**1**

From the mixture of synthetic (-)-fiscalin B (**1**) in CHCl<sub>3</sub> and (Me)<sub>2</sub>CO, a crystal form of *ent*-fiscalin B or (+)-**1** was obtained. The X-ray crystallographic structure of compound (+)-**1** is presented in Figure 2. The Ortep diagram confirmed the structure of (+)-**1** with the *anti* configuration (*1R*, *4S*), the piperazine ring in boat conformation. The C-4 substituent (indole moiety) and C-1 proton are in a flagpole position to the piperazine ring, with the C-4 proton and the C-1 substituent (*i*-Pr) being in a bowsprit position to the piperazine ring, and with N-2 proton being in an equatorial position. The C-4 proton shows

to be affected by the characteristic anisotropic effect of the coplanar carbonyl group at C-6. The five-member ring of indole showed to be parallel to the piperazine ring, causing the shielding effect to C-1 and N-2 protons.  $^1\text{H}$  NMR and  $^{13}\text{C}$  NMR spectra of (-)-**1** and (+)-**1** were in accordance to the previous reported [16]. The optical rotation value for (+)-**1** was found to be  $[\alpha]_D^{30} = +255$  (Chapter 6).

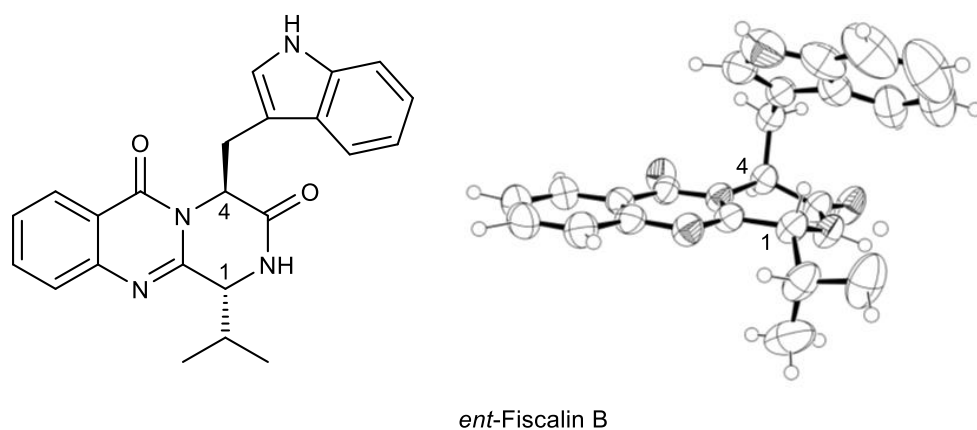


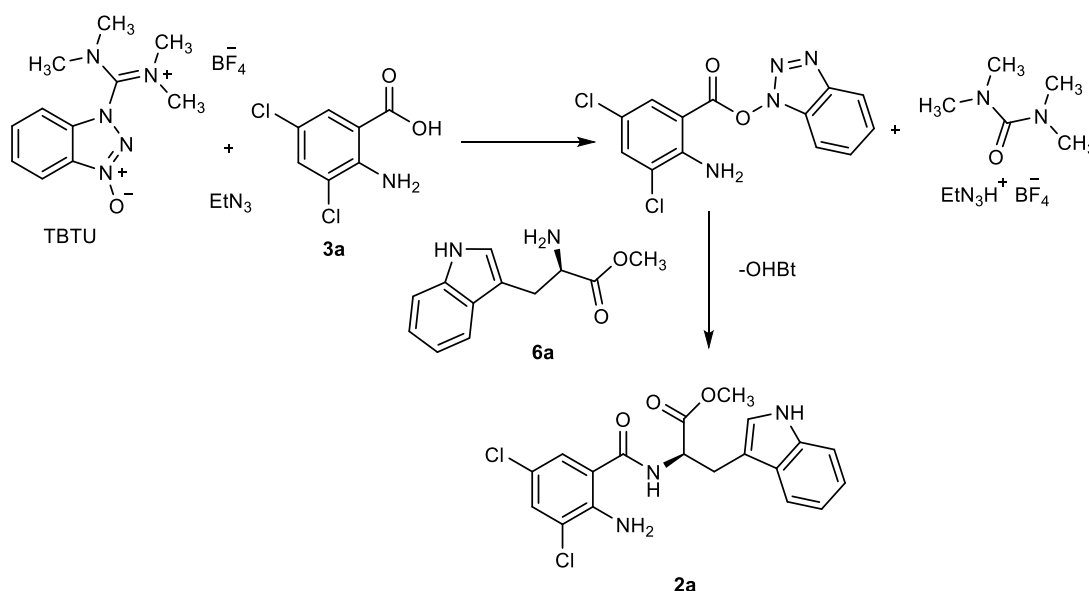
**Figure 2:** The structure of *ent*-fiscalin B or (+)-**1** with the Ortep view.

## 2.4 Gram-scale synthesis of the chloro derivative **2**

Following the successful result of the gram-scale synthesis of fiscalin B (**1**), the synthesis of 1*S*,4*R*-4-((1*H*-indol-3-yl)methyl)-8,10-dichloro-1-isobutyl-1,2-dihydro-6*H*-pyrazino[2,1-*b*]quinazoline-3,6(4*H*)-dione (**2**) reported as the most potent antimicrobial derivative from a library of fiscalin analogues (unpublished results, Chapters 5 and 6) was attempted. The yield of compound **2** was reported as 4.5 % from the one-pot multicomponent milligram synthesis as described in Chapters 5 and 6 [15,16]. Therefore, to achieve a better yield, the multi-step procedure was firstly applied to obtain compound **2** in gram amounts.

### 2.4.1 Dipeptide synthesis of tryptophanyl anthranilate

The first step of this approach is the synthesis of the dipeptide of 3,5-dichloroanthranilic acid (**3a**) with D-tryptophan methyl ester (**6a**). In this study the coupling agent *N*-(3-dimethylaminopropyl)-*N'*-ethylcarbodiimide (EDC) was replaced by 2-(1*H*-benzotriazol-1-yl)-*N,N,N',N'*-tetramethylammonium tetrafluoroborate (TBTU) in basic conditions to afford the dipeptide **2a** in a very excellent yield, 98 %, without purification (Scheme 4). The reaction begins with the activation of the hydroxyl group of **3a** by TBTU before condensation with the amine moiety of **6a**.

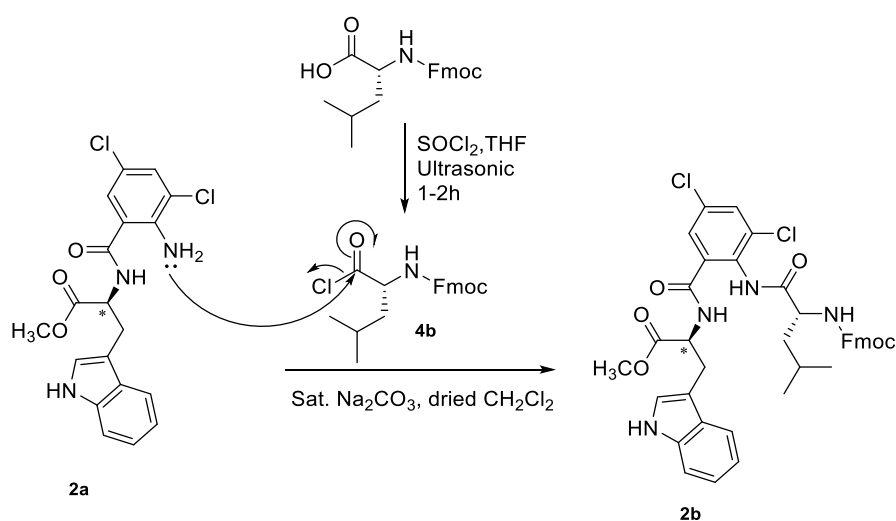


**Scheme 4:** Dipeptide **2a** synthesis by condensation with TBTU.

### 2.4.2 Linear tripeptide synthesis

Linear tripeptide **2b** is an important intermediate for the further first cyclization step. Tripeptide **2b** was obtained by condensation of dipeptide **2a** with activated *N*-Fmoc-L-leucine chloride (**4b**) under two-phase Schotten-Baumann consisting of dried dichloromethane and saturated  $\text{Na}_2\text{CO}_3$  conditions [31,32]. Activated *N*-Fmoc-L-leucine

chloride (**4b**) was produced by a rapid, easy, and efficient method under ultrasonic conditions of *N*-Fmoc-L-leucine with  $\text{SOCl}_2$  in dried tetrahydrofuran (THF) [33]. In the first step, the acyl chloride **4b** reacted with the amine of **2a**, forming a tripeptide **2b**. The base within the water phase neutralized the acid generated in this reaction while starting materials and product **2b** remained in the organic phase (Scheme 5).

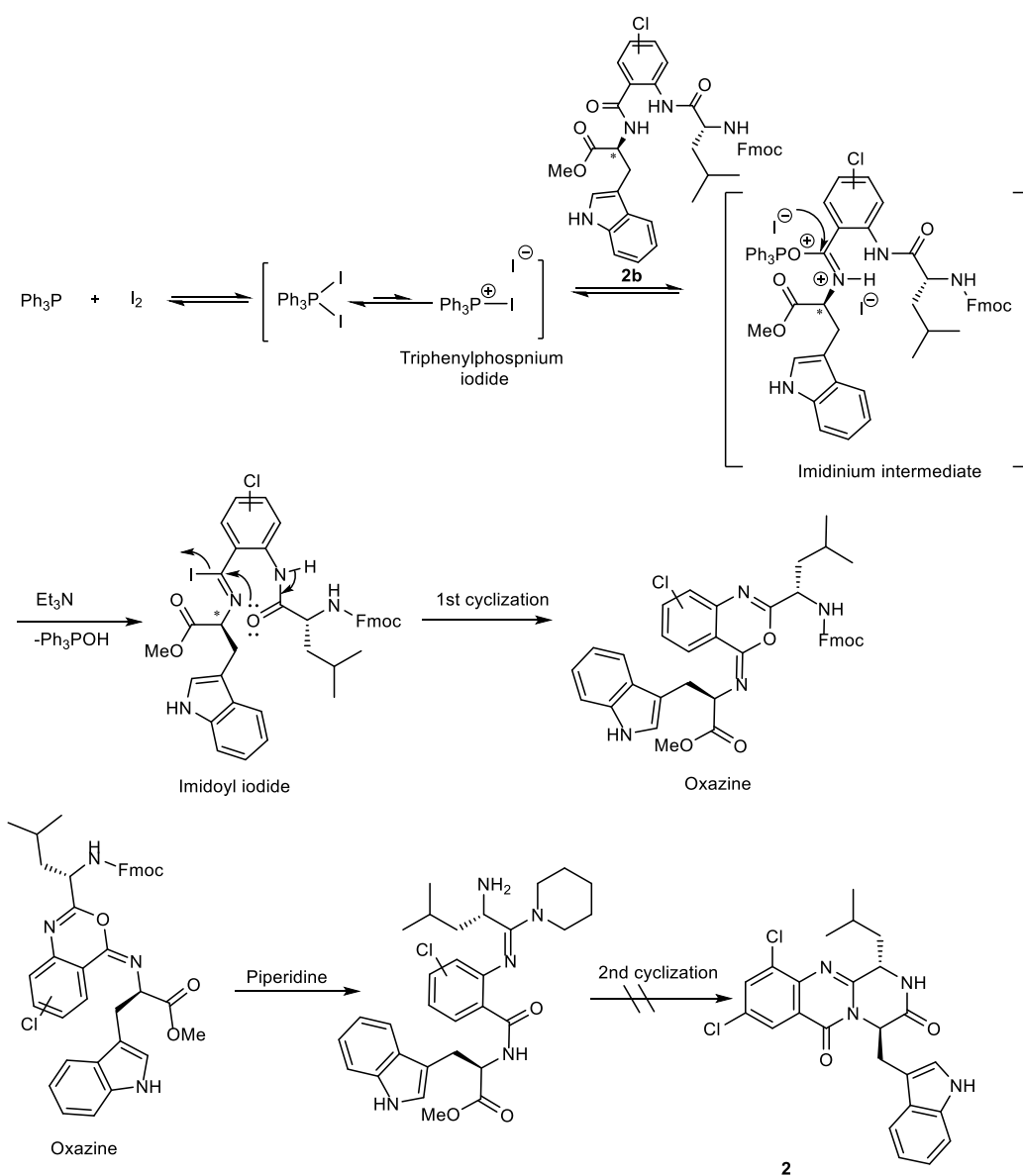


**Scheme 5:** Synthesis of tripeptide **2b** by the Schotten-Baumann reaction.

### 2.4.3 The double cyclization reactions

The transformation of linear peptide **2b** to quinazolinone is highly susceptible to steric hindrance around the cyclizing amide group. Wang *et al.* [9] report a suitable approach to reach the quinazolinone scaffold by selecting the dehydrating agent to be the  $\text{Ph}_3\text{P}/\text{I}_2$ /tertiary amine combination to dehydrate  $\beta$ -keto amide **2b** to an oxazine via cyclization (Scheme 6). The mechanism of the first cyclization reaction was proposed by Phakhodee *et al.* [34]. The reaction begins with the treatment of  $\text{Ph}_3\text{P}$  and  $\text{I}_2$  to provide reactive triphenylphosphonium iodide, and phosphorylation at the oxygen atom of amide yields imidinium intermediate. This species is then converted into imidoyl iodide in the presence of

base. Displacement of iodide of imidoyl iodide with an electron pair of oxygen of the amide leads to oxazine. Oxazine is difficult to isolate due to the steric hindrance of the group at C-1 and its relative instability. In this study, we followed this approach and considered not to isolate the oxazine. After removing  $\text{Ph}_3\text{P}$  by hexane in excess, the crude material was treated with 20% of piperidine to remove the Fmoc group, while refluxing the content with 4-dimethylaminopyridine (DMAP) in acetonitrile to afford product **2** (Scheme 6).



**Scheme 6:** Tentative synthesis of compound **2** by a dehydrative double cyclization approach.



Unfortunately, the cyclization product **2** was not formed/isolated under these conditions.

#### 2.4.4 Gram-scale synthesis of compound **2** via the three-component reaction

The failure of the multi-step led to the synthesis of compound **2** now using the microwave-assisted procedure from 3,5-dichloroanthranilic (**3a**) acid with *N*-Boc-L-leucine (**4c**, Scheme 3) and D-tryptophan methyl ester hydrochloride (**6a**) which was a successful approach to give compound **2** as a pale-yellow solid a 0.78 g amount (16.6% from 0.01 mol of the starting materials). The yield of this gram-scale of compound **2** was higher than in the milligram scale probably due to the prolonged reaction time of the first condensation and with the increase amount of the coupling agent from 1.2 equiv. to 1.5 equiv.. This increase in yield was also observed in the gram scale synthesis of fiscalin B (**1**). The enantiomeric ratio of compound **2** was found to be 60:40 using the same conditions as described for **1**.

Structure elucidation of compound **2** by  $^1\text{H}$  NMR and  $^{13}\text{C}$  NMR spectroscopy (Table 1) was in accordance to the previously reported in Chapter 5 and the correlations of key protons are presented in Figure 2.

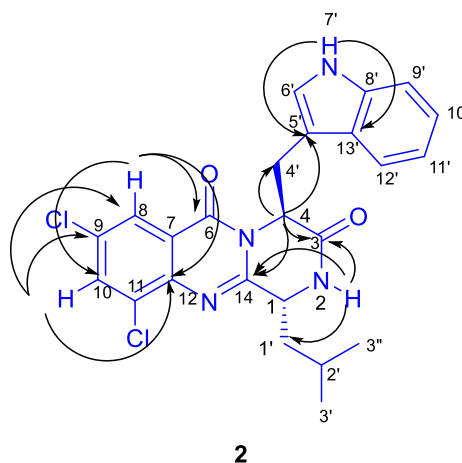


**Figure 2:** Key HMBC correlations for compound **2**.

**Table 1:**  $^1\text{H}$  NMR (300 MHz, DMSO- $d_6$ ) and  $^{13}\text{C}$  NMR data (75 MHz, DMSO- $d_6$ ) for compound 2.

Position	$\delta_{\text{H}}$ , Type (J)	Position	$\delta_{\text{C}}$ , Type
H-1	2.68, dd (7.3, 4.9)	C-1	50.6
H-2	7.19, br	C-3	168.4
H-4	5.42, dd (5.3, 2.9)	C-4	57.3
H-8	8.13, d (2.4)	C-6	158.8
H-9	-	C-7	121.6
H-10	7.75, d (2.4)	C-8	124.3
H-11	-	C-9	132.6
H-1'a	1.94-1.86, m	C-10	134.1
H-1'b	1.29-1.22, m	C-11	131.4
H-2'	1.50, tt (13.2, 6.5)	C-12	142.0
H-3'	0.56, d (6.6)	C-14	152.8
H-3'	0.35, d (6.6)	C-1'	39.6
H-4'a	3.63, dd (15.0, 2.9)	C-2'	23.8
H-4'b	3.50, dd (15.0, 5.4)	C-3'	22.1
H-6'	6.60, d (2.4)	C-3''	20.5
H-7'	10.22, br	C-4'	26.2
H-9'	7.25, d (8.2)	C-5'	107.7
H-10'	7.00, t (8.0)	C-6'	123.5
H-11'	6.82, t (7.8)	C-8'	135.9
H-12'	7.33, d (8.0)	C-9'	111.1
		C-10'	121.5
		C-11'	118.9
		C-12'	117.7

$\delta$  is measured in ppm,  $J$  is measured in Hz

Due to the effect of the two chlorine atoms at positions 9 and 11, protons H-8 and H-10 of the anthranilic acid moiety of compound **2** appeared as narrow doublets with  $\delta$  values of 8.13 and 7.75 ppm, respectively. The splitting of proton H-1' of L-leucine moiety in compound **2** into two different  $\delta$  values was also observed (Table 1), related to the effect of the chlorine atom at position 11. The signal corresponding to the H-2 proton appeared as broad singlet with  $\delta$  value of 7.14 ppm (the chemical shift in DMSO- $d_6$ ) while H-1 signal appeared as a doublet-doublet with  $\delta$  value of 2.68 ppm. These attributes reveal that compound **2** corresponded to the *anti*-isomer.

### 3. Conclusions

In summary, we have described for the first time a gram scale synthesis using parallel one-pot reactions of the quinazolinone alkaloid fiscalin B (**1**) and its derivative **2**. We also reported for the first time the crystal structure of *ent*-fiscalin B (+)-**1**. These syntheses constitute an expeditious approach to this family of natural products with potential application to a large-scale compounds production for potential medicinal studies.

### 4. Experimental section

**4.1 Gram scale synthesis of (1S,4R)-4-(1H-Indol-3-ylmethyl)-1-isopropyl-2H-pyrazino[2,1-b]quinazoline-3,6(4H)-dione (fiscalin B, 1).** In a closed two-neck round bottle, anthranilic acid (**3**, 4.2 g, 0.03 mol), *N*-Fmoc-L-valine (**4a**, 10.4 g, 0.03 mol), and triphenyl phosphite (11.81 mL, 0.045 mol) were added along with 150 mL of dried pyridine. The flask was heated in heating block with stirring at 55 °C for 48 h. After cooling the mixture to room

temperature, D-tryptophan methyl ester hydrochloride (**6a**, 7.65 g, 0.03 mol) was added, and the reactions mixture was divided into 5 mL mixtures in 30 microwavable vials that were further irradiated in the microwave at a constant temperature at 220 °C for 2 min in parallel. The reaction were gathered and the work-up and purifications were as described in previous report [16]. The desired compound **1** was collected as a yellow solid. Yield: 1.79 g, 22.7 %; er = 69:31; mp: 168-169 °C;  $[\alpha]_D^{30} = -119$  (*c* 0.045; CHCl<sub>3</sub>); IR  $\nu_{max}$ : <sup>1</sup>H NMR, <sup>13</sup>C NMR, and (+)-HRMS-ESI (See in [16]). The light-yellow cubical crystals of *ent*-fiscalin B, (+)-**1**, were obtained after recrystallization of **1** from the mixture of CHCl<sub>3</sub> and (Me)<sub>2</sub>CO.

**(1R,4S)-4-(1H-Indol-3-ylmethyl)-1-isopropyl-2H-pyrazino[2,1-b]quinazoline-3,6(4H)-dione (ent-fiscalin B,(+)-1)**. Yield:0.253g, 3.3% mp: 169-169.3 °C;  $[\alpha]_D^{30} = +78$  (*c* 0.06; CHCl<sub>3</sub>); IR  $\nu_{max}$ , <sup>1</sup>H NMR, <sup>13</sup>C NMR (See in [16]). The crystal of (+)-**1** was mounted on a cryoloop using paratone. X-ray diffraction data were collected at room temperature with a Gemini PX Ultra equipped with CuK<sub>α</sub> radiation ( $\lambda = 1.54184$  Å). The structure was solved by direct methods using SHELXS-97 and refined with SHELXL-97 [35]. Crystal was monoclinic, space group P2<sub>1</sub>/c, cell volume 2047.89(15) Å<sup>3</sup> and unit cell dimensions *a* = 18.0056(9) Å, *b* = 9.3592(3) Å and *c* = 12.7126(6) Å and  $\beta = 107.074(5)^\circ$  (uncertainties in parentheses). Non-hydrogen atoms were refined anisotropically. Hydrogen atoms were either placed at their idealized positions using appropriate HFIX instructions in SHELXL and included in subsequent refinement cycles or were directly found from difference Fourier maps and were refined freely with isotropic displacement parameters. The refinement converged to R (all data) = 12.46% and wR2 (all data) = 29.12%.

## 4.2 General procedure of the gram scale synthesis of compound 2

### 4.2.1 Synthesis of *N*-(2-(3,5-dichloro)aminobenzoyl)-D-tryptophan methyl ester (2a)

To a mixture of 3,5-dichloroanthranilic acid (**3a**, 2.06 g, 0.01 mol) and TBTU (3.85 g, 0.012 mol, 1.2 equiv.) in acetonitrile (100 mL) and D-tryptophan methyl ester (**5**, 2.54 g, 0.01 mol) were added Et<sub>3</sub>N (2.9 mL, 0.03 mol, 3 equiv.) at room temperature. After stirring for 48 h, the reaction mixture was concentrated under reduced pressure. The residue was dissolved in CH<sub>2</sub>Cl<sub>2</sub> and washed with 1 M HCl, extracted with CH<sub>2</sub>Cl<sub>2</sub> (3 × 500 mL), dried with Na<sub>2</sub>SO<sub>4</sub>, filtered, and concentrated to yield **2a** as a white solid (4.24 g, 97%), mp 175.1–175.2 °C,  $[\alpha]_D^{30} = -140$  (*c* 0.095, CHCl<sub>3</sub>), IR  $\nu_{max}$  (KBr): 3431, 3381, 3313, 1747, 1737, 1632; <sup>1</sup>H NMR (300, MHz, CDCl<sub>3</sub>): <sup>1</sup>H NMR (300 MHz, DMSO-d<sub>6</sub>)  $\delta$ : 10.37 (s, 1H), 8.34 (d, *J* = 7.5 Hz, 1H), 7.58 (d, *J* = 7.6 Hz, 1H), 7.50 (d, *J* = 2.3 Hz, 1H), 7.36 (d, *J* = 7.9 Hz, 1H), 7.30 (d, *J* = 2.3 Hz, 1H), 7.13 (d, *J* = 2.3 Hz, 1H), 7.12 – 7.05 (m, 1H), 7.07 – 6.99 (m, 1H), 6.17 (s, 1H), 4.82 (td, *J* = 8.0, 5.5 Hz, 1H), 3.72 (s, 3H), 3.44 – 3.36 (dd, *J* = 14.3, 2.9 Hz, 1H), 3.32 (dd, *J* = 13.3, 4.7 Hz, 1H). <sup>13</sup>C NMR (75, MHz, DMSO-d<sub>6</sub>) 172.6 (CO), 168.8 (CO), 148.8 (C), 136.1 (C-Trp), 134.6 (CH), 132.3 (C), 131.0 (C), 127.6 (C-Trp), 124.6 (CH), 122.8 (CH-Trp), 120.3 (C), 119.8 (CH-Trp), 118.7 (CH-Trp), 117.3 (CH-Trp), 116.7 (CH-Trp), 108.1 (C-Trp), 53.1 (CH\*-Trp), 52.7 (CH<sub>3</sub>), 27.7 (CH<sub>2</sub>-Trp).

#### ***4.2.2 Synthesis of N-[9H-fluoren-9-ylmethoxy]carbonyl-L-leucine-2-(-3,5-dichloro)aminobenzoyl-D-tryptophan methyl ester (2b)***

To a solution of **2a** (2 g, 4.92 mmol) in dried CH<sub>2</sub>Cl<sub>2</sub> (100 mL), *N*-Fmoc-L-leucine-Cl was added [33] (**4b**, 2.20 g, 5.91 mmol, 1.2 equiv.). The mixture was stirred for 3 h, followed by addition of aqueous Na<sub>2</sub>CO<sub>3</sub> (1 M, 14 mL, 14 mmol) and 56 mL of water. After continuous stirring for 24 h, the mixture was extracted with CH<sub>2</sub>Cl<sub>2</sub> (4 times), dried with Na<sub>2</sub>SO<sub>4</sub>, filtered, and concentrated to give **2b** as a white solid (4.12 g, 72%), mp: 181.9–182.5 °C,  $[\alpha]_D^{30} = -98$  (*c* 0.044, CHCl<sub>3</sub>), IR  $\nu_{max}$  (KBr): 3318, 1740, 1645, 1584 cm<sup>-1</sup>; <sup>1</sup>H NMR (300 MHz, DMSO):  $\delta$  9.92 (s, 1H), 9.35 (s, 1H), 7.80 (s, 1H), 7.76 (s, 1H), 7.73 (s, 1H), 7.63 (d, *J* = 7.4 Hz, 1H), 7.58 (d, *J* = 7.4 Hz, 1H), 7.54 – 7.47 (m, 4H), 7.40–7.32 (m

4H), 7.26 (t,  $J = 7.4$  Hz, 1H), 7.09 (d,  $J = 2.3$  Hz, 1H), 7.01 (t,  $J = 7.4$  Hz, 1H), 6.54 (s, 1H), 4.89 (dd,  $J = 13.4$  and  $6.3$  Hz, 1H), 4.51 – 4.28 (m, 2H), 4.21 (d,  $J = 7.0$  Hz, 1H), 3.67 (s, 3H), 3.43 – 3.25 (m, 2H), 1.81-1.65 (m, 1H), 0.94 (d,  $J = 5.1$  Hz, 6H).  $^{13}\text{C}$  NMR (75 MHz, DMSO- $d_6$ ): 172.1 (CO), 170.2 (CO), 168.3 (CO), 156.4 (CO), 143.8 (2C), 141.3 (2C), 139.0 (C), 136.1 (C), 134.0 (CH), 132.9 (C), 131.5 (C), 127.7 (2CH), 127.5 (C), 127.1 (2CH), 127.1 (2CH), 125.3 (CH), 125.2 (CH), 123.2 (CH), 122.8 (CH), 122.4 (CH), 121.4 (C), 120.2 (2CH), 119.8 (CH), 118.5 (C), 111.4 (CH), 109.7 (CH), 67.2 (CH $_2$ ), 61.3 (CH), 53.3 (CH), 52.6 (CH $_3$ ), 47.3 (CH $_2$ ), 38.6 (CH), 31.4 (CH), 27.3 (CH $_2$ ), 19.4 (CH $_3$ ), 17.5 (CH $_3$ ).

#### **4.3 General procedure of the gram scale synthesis of (1S,4R)-4-((1H-indol-3-yl)methyl)-8,10-dichloro-1-isopropyl-1,2-dihydro-6H-pyrazino[2,1-b]quinazoline-3,6(4H)-dione (2).**

In a closed two-neck round bottle, 3,5-dichloroanthranilic acid (**3a**, 2.06 g, 0.01 mol), *N*-Boc-L-leucine (**4c**, 2.3 g, 0.01 mol), and triphenyl phosphite (3.9 mL, 0.015 mol) were added along with 50 mL of dried pyridine. The flask was heated in heating block with stirring at 55 °C for 48 h. After cooling the mixture to room temperature, D-tryptophan methyl ester hydrochloride (**6a**, 2.55 g, 0.01 mol) was added, and the reaction mixture was divided into 5 mL mixtures in 30 microwavable vials that were irradiated in the microwave at a constant temperature at 220 °C for 2 min in parallel. After removing the solvent with toluene, the crude product was purified by flash column chromatography using *n*-hexane: EtOAc (60:40) as a mobile phase. The preparative TLC was performed using CH $_2$ Cl $_2$ :Me $_2$ CO (95:5) as mobile phase. The major compound appeared as a black spot with no fluorescence under the UV light. The desired compound **2** was collected as a yellow solid. Yield: 0.78 g, 16.62 %; er = 60:40; mp: 254.7-255.1 °C;  $[\alpha]_D^{30} = -169$  ( $c$  0.056; CHCl $_3$ );  $^1\text{H}$  NMR,  $^{13}\text{C}$  NMR (See Table 1);  $\nu_{\text{max}}$ , and (+)-HRMS-ESI (See in Chapter 5).

**Author Contributions:** E.S. conceived the study design. S.L. synthesized the compounds and elucidated their structure and A.M.S.S., E.S., and M.M.M.P. analyzed the data. D.I.S.P.R. performed the HPLC analysis. S.L. and L.G. wrote the manuscript.

**Acknowledgments:** This research was partially supported by the Strategic Funding UID/Multi/04423/2019 through national funds provided by FCT-Foundation for Science and Technology and European Regional Development Fund (ERDF), in the framework of the program PT2020. This research was developed under Project No. POCI-01-0145-FEDER-028736, co-financed by COMPETE 2020, Portugal 2020 and the European Union through the ERDF, and by FCT through national funds, and Erasmus-Lotus+ program (LOTUS+, LP15DF0205). S.L. thanks Erasmus Mundus Action 2 (LOTUS+, LP15DF0205) for full PhD scholarship. To Sara Cravo for technical support.

**Conflicts of Interest:** The authors declare no conflicts of interest

## 5. References

1. Resende, D.I.S.P.; Boonpothong, P.; Sousa, E.; Kijjjoa, A.; Pinto, M.M.M. Chemistry of the fumiquinazolines and structurally related alkaloids. *Nat. Prod. Rep.* **2018**.10.1039/C8NP00043C
2. Khan, I.; Zaib, S.; Batool, S.; Abbas, N.; Ashraf, Z.; Iqbal, J.; Saeed, A. Quinazolines and quinazolinones as ubiquitous structural fragments in medicinal chemistry: An update on the development of synthetic methods and pharmacological

- diversification. *Bioorg. Med. Chem.* **2016**, *24*, 2361-2381.10.1016/j.bmc.2016.03.031
3. Khan, I.; Ibrar, A.; Ahmed, W.; Saeed, A. Synthetic approaches, functionalization and therapeutic potential of quinazoline and quinazolinone skeletons: The advances continue. *Eur. J. Med. Chem.* **2015**, *90*, 124-169.10.1016/j.ejmech.2014.10.084
  4. Hameed, A.; Al-Rashida, M.; Uroos, M.; Ali, S.A.; Arshia; Ishtiaq, M.; Khan, K.M. Quinazoline and quinazolinone as important medicinal scaffolds: A comparative patent review (2011–2016). *Exp. Opin. Therap. Patents* **2018**, *28*, 281-297.10.1080/13543776.2018.1432596
  5. Mhaske, S.B.; Argade, N.P. The chemistry of recently isolated naturally occurring quinazolinone alkaloids. *Tetrahedron* **2006**, *62*, 9787-9826.10.1016/j.tet.2006.07.098
  6. Liu, J.F.; Ye, P.; Zhang, B.; Bi, G.; Sargent, K.; Yu, L.; Yohannes, D.; Baldino, C.M. Three-component one-pot total syntheses of gyantrypine, fumiquinazoline f, and fiscalin b promoted by microwave irradiation. *J. Org. Chem.* **2005**, *70*, 6339-6345.10.1021/jo0508043
  7. Hernández, F.; Buenadicha, F.L.; Avendao, C.; Söllhuber, M. 1-alkyl-2,4-dihydro-1h-pyrazino[2,1-b]quinazoline-3,6-diones as glycine templates. Synthesis of fiscalin b. *Tetrahedron Asymm.* **2002**, *12*, 3387-3398.10.1016/S0957-4166(02)00027-7
  8. Wang, H.; Ganesan, A. Total synthesis of the fumiquinazoline alkaloids: Solution-phase studies. *J. Org. Chem.* **2000**, *65*, 1022-1030.10.1021/jo9914364
  9. Wang, H.; Ganesan, A. Total synthesis of the quinazoline alkaloids (-)-fumiquinazoline g and (-)-fiscalin b. *J. Org. Chem.* **1998**, *63*, 2432-2433.10.1021/jo980360t



10. Rodrigues, B.S.F.; Sahm, B.D.B.; Jimenez, P.C.; Pinto, F.C.L.; Mafezoli, J.; Mattos, M.C.; Rodrigues-Filho, E.; Pfenning, L.H.; Abreu, L.M.; Costa-Lotufu, L.V., *et al.* Bioprospection of cytotoxic compounds in fungal strains recovered from sediments of the brazilian coast. *Chem. Biodivers.* **2015**, *12*, 432-442.10.1002/cbdv.201400193
11. Fujimoto, H.; Negishi, E.; Yamaguchi, K.; Nishi, N.; Yamazaki, M. Isolation of new tremorgenic metabolites from an ascomycete, *corynascus setosus*. *Chem. Phar. Bull.* **1996**, *40*, 1843-1848
12. Wong, S.-M.; Musza, L.L.; Kydd, G.C.; Kullnig, R.; Gillum, A.M.; Cooper, R. Fiscalins: New substance p inhibitors produced by the fungus *neosartorya fisheri* taxonomy, fermentation, structure, and biological properties. *J. Antibiot.* **1993**, *46*, 545-553
13. Wu, B.; Chen, G.; Liu, Z.-g.; Pei, Y. Two new alkaloids from a marine-derived fungus *neosartorya fischeri*. *Rec. Nat. Prod.* **2015**, *9*, 271-275
14. Wong, S.M.; Musza, L.L.; Kydd, G.C.; Kullnig, R.; Gillum, A.M.; Cooper, R. Fiscalins: New sibstamnce p inhibitors produced by the fungus *neosartorya fischeri*. Taxonomy, fermentation, structures, and biological properties. *J. Antibiot.* **1993**, *46*, 545-553
15. Long, S.; Resende, D.I.S.P.; Kijjoa, A.; Silva, A.M.S.; Fernandes, R.; Xavier, C.P.R.; Vasconcelos, M.H.; Sousa, E.; Pinto, M.M.M. Synthesis of new proteomimetic quinazolinone alkaloids and evaluation of their neuroprotective and antitumor effects. *Molecules* **2019**, *24*, 534
16. Long, S.; Resende, D.I.S.P.; Kijjoa, A.; Silva, A.M.S.; Pina, A.; Fernández-Marcelo, T.; Vasconcelos, M.H.; Sousa, E.; Pinto, M.M.M. Antitumor activity of quinazolinone alkaloids inspired by marine natural products. *Mar. Drugs* **2018**, *16*.10.3390/md16080261

17. Gawande, M.B.; Shelke, S.N.; Zboril, R.; Varma, R.S. Microwave-assisted chemistry: Synthetic applications for rapid assembly of nanomaterials and organics. *Acc. Chem. Res.* **2014**, *47*, 1338-1348.10.1021/ar400309b
18. Gedye, R.; Smith, F.; Westaway, K.; Ali, H.; Baldisera, L.; Laberge, L.; Rousell, J. The use of microwave ovens for rapid organic synthesis. *Tetrahedron Lett.* **1986**, *27*, 279-282.[https://doi.org/10.1016/S0040-4039\(00\)83996-9](https://doi.org/10.1016/S0040-4039(00)83996-9)
19. Polshettiwar, V.; Varma, R.S. Aqueous microwave chemistry: A clean and green synthetic tool for rapid drug discovery. *Chem. Soc. Rev.* **2008**, *37*, 1546-1557.10.1039/B716534J
20. Cledera, P.; Sánchez, J.D.; Caballero, E.; Yates, T.; Ramírez, E.G.; Avendaño, C.; Ramos, M.T.; Menéndez, J.C. Microwave-assisted, solvent-free synthesis of several quinazoline alkaloid frameworks. *Synthesis* **2007**, 3390-3398.10.1055/s-2007-990818
21. De La Hoz, A.; Díaz-Ortiz, Á.; Moreno, A. Microwaves in organic synthesis. Thermal and non-thermal microwave effects. *Chem. Soc. Rev.* **2005**, *34*, 164-178.10.1039/b411438h
22. Thierry, B.; Elizabeth, C. Microwave-assisted synthesis of bioactive quinazolines and quinazolinones. *Com. Chem. High throu. Scr.* **2007**, *10*, 903-917.<http://dx.doi.org/10.2174/138620707783220356>
23. C. Oliver Kappe, A.S., Doris Dallinger. *Microwave in organic and medicinal chemistry*. Second ed.; Wiley-VCH Verlag & Co. KGaA: Weinheim, Germany, 2012; p 678.
24. Liu, J.-F.; Wilson, C.J.; Ye, P.; Sprague, K.; Sargent, K.; Si, Y.; Beletsky, G.; Yohannes, D.; Ng, S.-C. Privileged structure-based quinazolinone natural product-

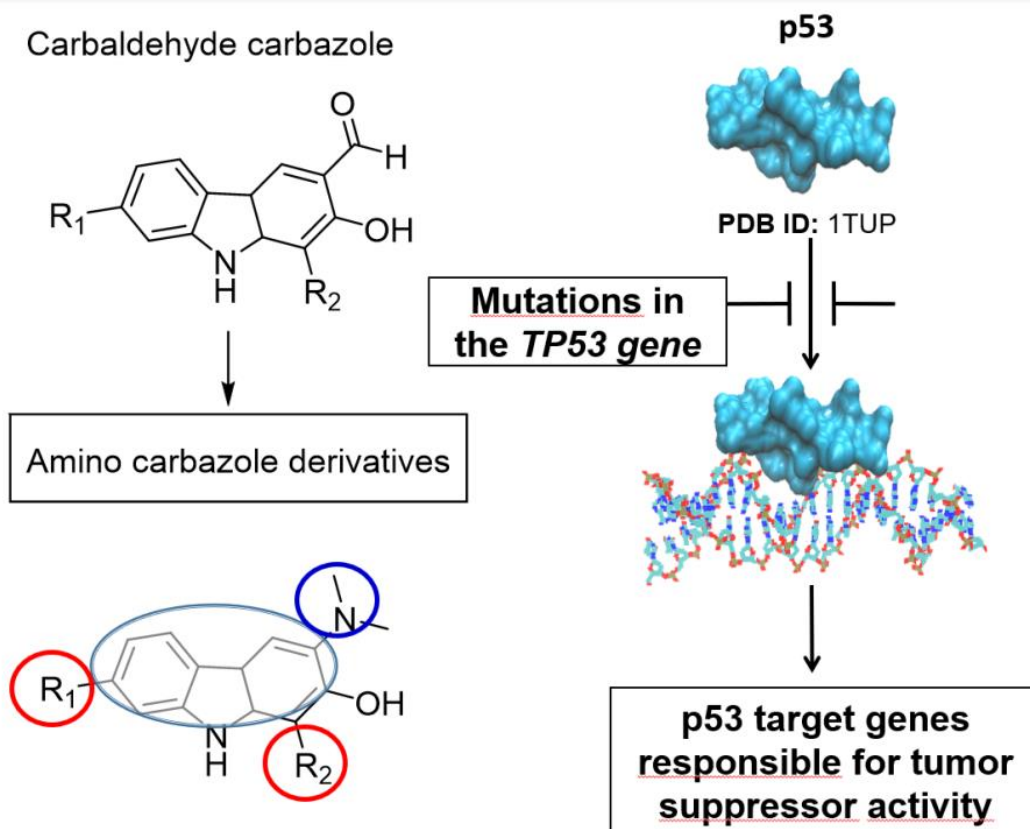
- templated libraries: Identification of novel tubulin polymerization inhibitors. *Bioorg. Med. Chem. Lett.* **2006**, *16*, 686-690. <https://doi.org/10.1016/j.bmcl.2005.10.022>
25. Liu, J.-F.; Kaselj, M.; Isome, Y.; Chapnick, J.; Zhang, B.; Bi, G.; Yohannes, D.; Yu, L.; Baldino, C.M. Microwave-assisted concise total syntheses of quinazolinobenzodiazepine alkaloids. *J. Org. Chem.* **2005**, *70*, 10488-10493. [10.1021/jo051876x](https://doi.org/10.1021/jo051876x)
26. Liu, J.-F.; Ye, P.; Sprague, K.; Sargent, K.; Yohannes, D.; Baldino, C.M.; Wilson, C.J.; Ng, S.-C. Novel one-pot total syntheses of deoxyvasicinone, mackinazolinone, isaindigotone, and their derivatives promoted by microwave irradiation. *Org. Lett.* **2005**, *7*, 3363-3366. [10.1021/ol0513084](https://doi.org/10.1021/ol0513084)
27. Liu, J.-F.; Lee, J.; Dalton, A.M.; Bi, G.; Yu, L.; Baldino, C.M.; McElory, E.; Brown, M. Microwave-assisted one-pot synthesis of 2,3-disubstituted 3h-quinazolin-4-ones. *Tetrahedron Lett.* **2005**, *46*, 1241-1244. <https://doi.org/10.1016/j.tetlet.2005.01.008>
28. Siro, J.G.; Martín, J.; García-Navío, J.; Remuñan, M.J.; Vaquero, J.J. Easy microwave assisted deprotection of n-boc derivatives. *Synlett* **1998**, *1998*, 147-148. [10.1055/s-1998-1604](https://doi.org/10.1055/s-1998-1604)
29. Vanier, G.S. Microwave-assisted solid-phase peptide synthesis based on the fmoc protecting group strategy (cem). *Meth. Mol. Bio.*, 2013; Vol. 1047, pp 235-249.
30. Buenadicha, F.L.; Avendaño, C.; Söllhuber, M. Reactivity as glycine templates of 1,2-dialkyl-2,4-dihydro-1h-pyrazino[2,1-b]quinazoline-3,6-diones. *Tetrahedron Asymm.* **2001**, *12*, 3019-3028. [https://doi.org/10.1016/S0957-4166\(01\)00515-8](https://doi.org/10.1016/S0957-4166(01)00515-8)
31. E., B. Ueber eine einfache methode der darstellung von benzoësäureäthern. *Berichte deutsch chem Gesellschaft* **1886**, *19*, 3218-3222. [doi:10.1002/cber.188601902348](https://doi.org/10.1002/cber.188601902348)
32. C., S. Ueber die oxydation des piperidins. *Berichte der deutschen chemischen Gesellschaft* **1884**, *17*, 2544-2547. [doi:10.1002/cber.188401702178](https://doi.org/10.1002/cber.188401702178)

33. Kantharaju; Patil, B.S.; Suresh Babu, V.V. Synthesis of fmoc-amino acid chlorides assisted by ultrasonication, a rapid approach. *Int. J. Peptid. Res. Therap.* **2002**, *9*, 227-229
34. Phakhodee, W.; Wangngae, S.; Pattarawarapan, M. Approach to the synthesis of 2,3-disubstituted-3h-quinazolin-4-ones mediated by  $\text{Ph}_3\text{P/I}_2$ . *J. Org. Chem.* **2017**, *82*, 8058-8066.10.1021/acs.joc.7b01322
35. Sheldrick, G.M. A short history of shelx. *Acta Crystallographica Section A: Found. Crystallo.* **2008**, *64*, 112-122.10.1107/S0108767307043930

# Chapter 8

## Synthesis of small molecules of amino carbazoles and their effect on restoration of p53 activity

Graphical abstract





# Synthesis of small molecules of amino carbazoles and their effect on restoration of p53 activity

Solida Long<sup>1</sup>, Joana B. Loureiro<sup>2</sup>, Joana Soares<sup>2</sup>, Ploenthip Puthongking<sup>3</sup>, Luis Gales<sup>4,5</sup>, Lucilia Saraiva<sup>2</sup>, Madalena M. M. Pinto<sup>1</sup>, and Emília Sousa<sup>1\*</sup>

<sup>1</sup> Laboratory of Organic and Pharmaceutical Chemistry, Department of Chemical Sciences, Faculty of Pharmacy, University of Porto, Rua de Jorge Viterbo Ferreira, 228, 4050-313 Porto, Portugal & Interdisciplinary Centre of Marine and Environmental Research (CIIMAR), 4450-208 Matosinhos, Portugal

<sup>2</sup> Laboratory of Microbiology (UCIBIO/REQUIMTE), Department of Biological Sciences, Faculty of Pharmacy, University of Porto, Porto, Portugal

<sup>3</sup> Faculty of Pharmaceutical Sciences, Khon Kean University, 40002, Thailand

<sup>4</sup> Institute for the Biomedical Science Abel Salazar (ICBAS), University of Porto, Rua de Jorge Viterbo Ferreira, 228, 4050-313 Porto, Portugal

<sup>5</sup> Instituto de Biologia Molecular e Celular (i3S-IBMC), University of Porto, Porto, Portugal

\*Corresponding author: [esousa@ff.up.pt](mailto:esousa@ff.up.pt)

**Abstract:** The tumor suppressor p53 is mutationally inactivated in approximately 50% of human cancers. Small molecules that bind to p53 mutants and stabilize them could be effective anticancer drugs. Herein, we report the effect of carbazole alkaloids and their amino derivatives on reactivating of p53. Twelve amino carbazole alkaloids were synthesized from heptaphylline (**1**), 7-methoxyheptaphylline (**2**), and 7-methoxymukonal (**3**), isolated from *Clausena harmandiana*, using a reductive amination protocol. Naturally-occurring

carbazoles **1-3** and their amino derivatives were evaluated for their potential effect on p53 using a yeast screening assay and their ability to restore p53 function and inhibit cell growth on human cancer cell lines. Naturally-occurring carbazoles **1-3** showed the most potent inhibitory effects on induced-growth in wtp53, being heptaphylline (**1**) the most promising in all the investigated cell lines. Semi-synthetic amino carbazole **1d** showed to be selective against the induced-growth of mutp53 MDA-MB-648-R273H and **2b** selective on A375 cell lines with GI<sub>50</sub> values of 4.50 and 5.83  $\mu$ M, respectively. The results obtained indicate that carbazole alkaloids may represent a promising start point to research for new mutp53-reactivating agents with promising application in cancer therapy.

**Keywords:** amino carbazoles, heptaphylline, alkaloids, tumor, p53, mutant

## 1. Introduction

Natural products of carbazole, the alkaloids are mostly isolated from the higher plant of Rutaceae family and are major components of the *Clausena* genus [1,2]. These alkaloids have been of interested since the isolation of carbazole core from coal tar in 1872 [3] and the evaluation on antimicrobial of murrayanine in 1965 [4]. Natural-occurring carbazole alkaloids (Figure 1) have been reported to exhibit a broad pharmacological profile, including antitumor (*i.e.* heptaphylline (**1**) [5], 7-methoxyheptaphylline (**2**) [6], 2-hydroxy-7-methoxy-9*H*-carbazole-3-carbaldehyde or 7-methoxydymukonal (**3**) [7]), antiplasmodial (*i.e.* compounds **1** [8] and **3** [7]), antiplatelet aggregation and vasorelaxing (*i.e.* clausine E (**4**) [9]), antibacterial (*i.e.* clausamine B (**5**), clausine F (**6**) [10] , and clausenal (**7**) [11]), antifungal (*i.e.* compound **7** [11]), and antidiabetic (*i.e.* koenidine (**8**) [12]). Recently, heptaphylline (**1**) was reported to induce apoptosis in human colon adenocarcinoma cell [13] and was considered a promising model for anticancer drugs. In addition, the carbazole



nucleus can be easily functionalized mainly at positions 3, 6, and 9 to construct interesting analogues [2,6]. Examples are compound **9** (Figure 1) reported as anti-Alzheimer's [14], and compound **10** as anti-HIV-1 [15]; derivatives **11** and **12** of carbazoles **1** and **2** exhibited strong cytotoxicity against NCI-H187 and KB cells 138 fold stronger than ellipticine standard [6,16-19] while *N*-substituted derivatives, compounds **13** and **14**, were reported as antiproliferative agents against leukemia cell ECM, Jurkat, and Raji with IC<sub>50</sub> values around 12 μM [17].

The tumor suppressor protein p53 is a transcription factor that plays a key role in the prevention of cancer development because it provides a key difference between normal and cancer cells [20,21]. Over 50% of p53 protein is missense mutation, generating a defective protein in high level in cells due to the impairment of MDM2 mediated negative feedback. p53 is known as a guardian of the genome because one of the most important p53 functions is its ability to activate apoptosis; the disruption of this process can promote tumor progression and chemoresistance [22]. In cancer cells, *in vivo* studies have shown the restoration of p53 function to be highly therapeutic, thus reactivating mutant p53 has been a goal in anticancer drug development [23]. Some small molecules in the group of carbazole alkaloids have been reported to reactivate mutant p53 by restoration of wild-type structure/function [24,25]. For example, PhiKan083 (**15**), an amino derivative of a carbazole alkaloid obtained from an *in silico* screening [26], was reported as a small molecule for restoring wild-type p53 function by targeting Y220 p53 mutation [26,27]. It provided electrostatic and hydrogen bonding interaction among residues of Y220 which give additional stability to Y220 mutant p53. This mutation creates a druggable surface crevice destabilizing the protein and stabilizing the structure of this mutant of p53 and increasing the level of p53 with the wild-type conformation and activity [27,28]. Up to date, none of the natural isolated carbazole alkaloids or their chemical modified compounds were reported to have effect on mutants of p53. Herein, a series of semisynthetic amino carbazoles from

naturally-occurring heptaphylline (**1**) and its derivatives **2** and **3** was discovered with effects in restoring p53 activity.

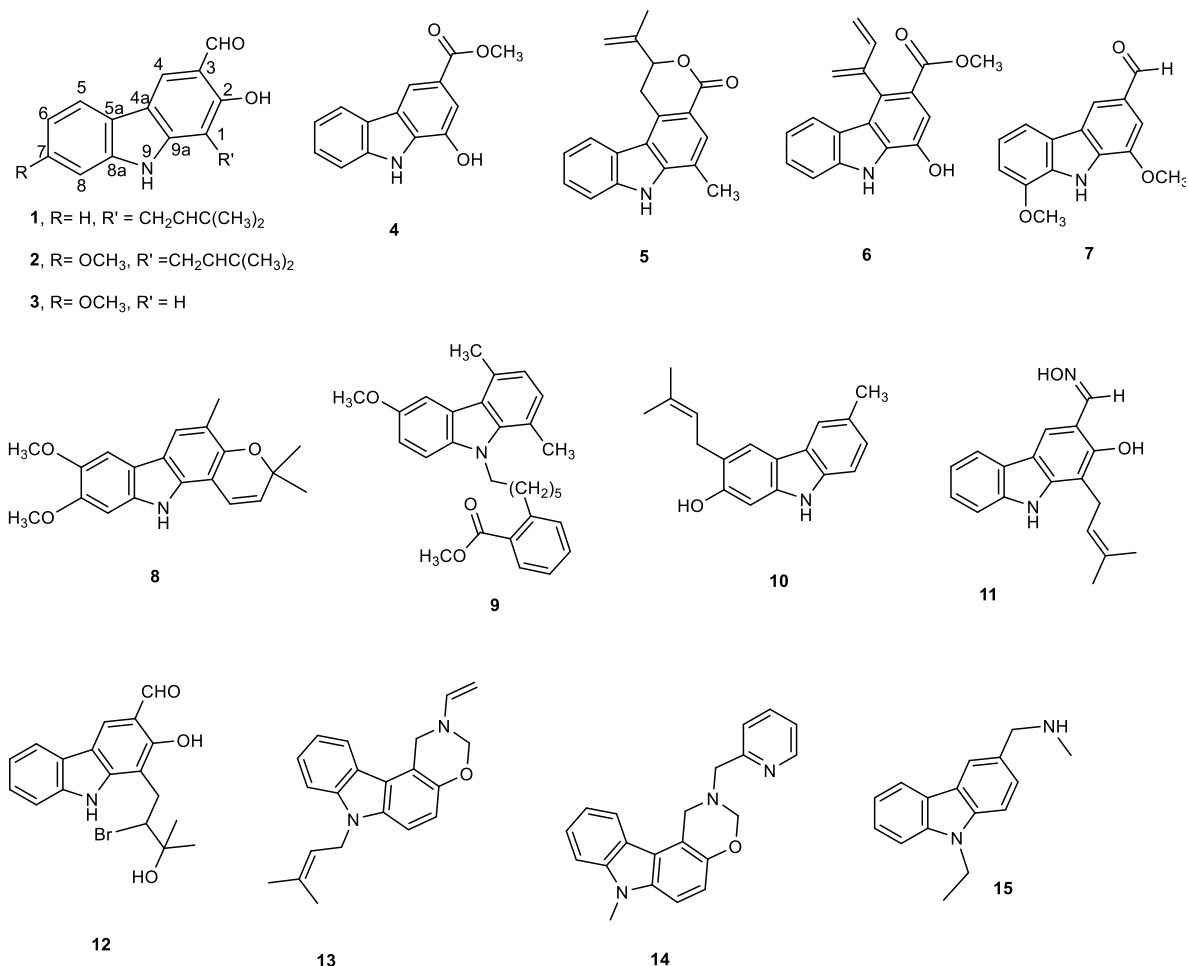


**Fig. 1:** Some examples of carbazole alkaloids: Natural isolated carbazoles (**1-8**) and synthetic analogues (**9-15**).

## 2. Results and discussion

### 2.5. Synthesis of amino carbazole alkaloids by direct reductive amination

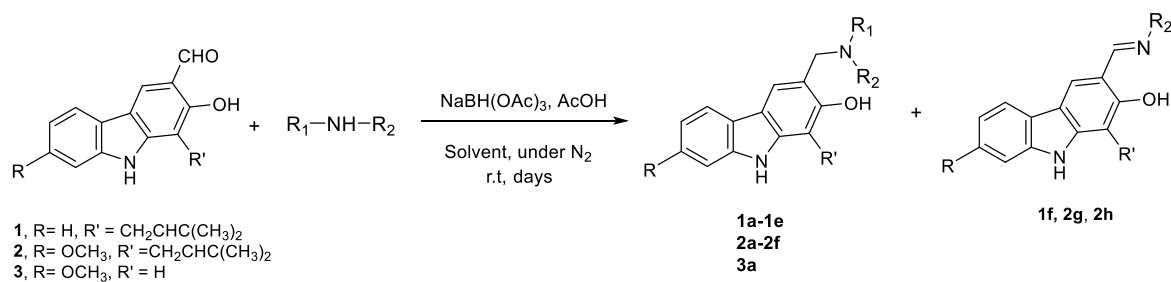
The reaction of carbonyl groups, aldehydes or ketones, with amines in the presence of reducing agents to give corresponding amines, known as reductive amination (of carbonyl compounds) or reductive alkylation (of amine compounds) is one of the most useful and important methods in the synthesis of different kind of amines and also a powerful reaction

to obtain drug candidates [29]. The choice and understanding of the reducing agent are essential for the selection of the type of reaction. Sodium triacetoxyborohydride [NaBH(OAc)<sub>3</sub>, STAB] was reported as one of the most powerful reducing agent in direct reductive amination due to its stability and safety.

Reductive aminations of **1**, **2**, and **3** were performed in an one-pot conversion of their carbonyl group in the present of STAB as reducing agent in two different solvents – dried tetrahydrofuran (THF) or dried 1,2-dichloroethane (DCE) with selected amines precursors present in inhibitors of p53:MDM2 interaction. The reaction mixtures were stirred under nitrogen until no further development to yield amino carbazole alkaloids derivatives **1a-1e**, **2a-2f**, and **3a**. Products were treated with different work-up procedures, described in the experimental section, before purification.

Generally, in the present of STAB, the reactions of **1**, **2**, and **3** with primary amines yielded secondary amines (entry 3-5 and 8-10), via imine intermediates, and the reaction with secondary amines yielded tertiary amines (entry 1-2, 6-7, and 11-12), via enamine intermediates. The final products were categorized into 3 groups, alkylated linear amino carbazoles, compounds **1a**, **2a**, and **3a**, heterocyclic amino carbazoles, compounds **1b**, **2b**, and **2f**, and halogenated amino carbazoles, compounds **1c-1e** and **2c-2e**. The reactions mostly showed no further development between 3-10 days. All the reactions require long reaction times due to the substituent's hydroxyl at position 2 and/or prenyl group at position 1. Amino carbazoles modified from **2**, compounds **2a-2f**, and from **3**, compound **3a**, required longer reaction time than those derived from **1**, compounds **1a-1e**, in both conditions. This result should be because of the donating group methoxy at position 7. The reductive aminations with primary amines were faster than with secondary amines (entry 4-6 and 8-10).

**Table 1:** Synthesis of aminocarbazoles compounds **1a-1e**, **2a-2f**, and **3a** from natural-occurring carbazoles **1**, **2** and **3**.



Entry	R	R'	R <sub>1</sub>	R <sub>2</sub>	Products	Solvent	Time (day)	Yield (%)
1	H	Prenyl	-		<b>1a</b>	THF	5	39
						DCE	3	49
2	H	Prenyl	-		<b>1b</b>	THF	4	44
						DCE	3	90
3	H	Prenyl	H		<b>1c</b>	THF	3	31
						DCE	-	-
4	H	Prenyl	H		<b>1d</b>	THF	3	15
						DCE	3	42
5	H	Prenyl	H		<b>1e/1f</b>	THF	5	47
						DCE	3	64/17
6	OCH <sub>3</sub>	Prenyl	-		<b>2a</b>	THF	5	16
						DCE	4	51
7	OCH <sub>3</sub>	Prenyl	-		<b>2b</b>	THF	8	21
						DCE	5	39
8	OCH <sub>3</sub>	Prenyl	H		<b>2c/2g</b>	THF	4	15
						DCE	4	34/9
9	OCH <sub>3</sub>	Prenyl	H		<b>2d/2h</b>	THF	4	13
						DCE	4	30/15
10	OCH <sub>3</sub>	Prenyl	H		<b>2e</b>	THF	5	35
						DCE	3	86
11	OCH <sub>3</sub>	Prenyl	-		<b>2f</b>	THF	10	25
						DCE	-	-
12	OCH <sub>3</sub>	H	-		<b>3a</b>	THF	7	51
						DCE	-	-

Dashes represent as Not applicable, THF = Dried-tetrahydrofuran, DCE = Dried-dichloroethane

Reactions performed in DCE required shorter times and produced higher yields (3-5 days, 34-90%) compared to those performed in THF (3-10 day, 13-51%), and these were in agreement with previous reports [30]. It was also observed that in the reactions in DCE with primary amines the imine intermediates could be isolated as compounds **1f**, **2g**, and **2h** in 17, 9, and 15 % yields, respectively (entry 5, 8, and 9).

All the compounds structures were confirmed by one- and two-dimensional NMR and high-resolution mass spectrometry. The chemical shift of protons and carbons of **1**, **2**, and **3** were in accordance to literature [31-33]. The analysis of (+) HRMS-ESI,  $^1\text{H}$ ,  $^{13}\text{C}$  NMR, HSQC, HMBC, and X-ray crystallographic data (in case of compound **1b**) revealed the successful of the reductive amination to produce amine derivatives. Compounds **1a-1f** and **2e-2h** derived from **1** and **2**, showed the signals of protons H-1' as doubles (d) with  $\delta$  values *c.a* 3.50 - 3.68 ppm while the signals of protons H-3' appeared as singlets with  $\delta$  values *c.a* 3.74 – 3.83 ppm (compounds **1a-1e** and **2e-2e**) or *c.a* 8.47 – 8.55 ppm (compounds **1f**, **2g**, and **2h**). The proton H-4 signals always appeared as singlets with  $\delta$  values *c.a* 7.38 - 7.53 ppm while the chemical shifts of protons of one of the methyl group of prenyl showed as singlets *c.a* 1.90 ppm while another methyl signals appeared as a narrow doubles *c.a* 1.76 ppm due to the correlation to H-1'. Amino carbazoles derived from **1**, compound **1c**, **1d**, **1e**, and compounds derived from **2**, compound **2c**, **2d**, and **2e**, presenting secondary amine moieties showed signals of protons H-5' as singlets with  $\delta$  values *c.a* 4.14 and 4.05 ppm, respectively (see in experimental section). The key protons of amine derivatives **1a-1f** and **2e-2h** obtained from substrate **1** and **2** are summarized in Fig. 2. For compounds derived from **1**, the signals of protons H-5, appeared as doublets with  $\delta$  values *c.a* 7.89-7.90 ppm, H-6 were doublet-doublet-doublets with  $\delta$  values *c.a* 7.15-7.16 ppm, protons H-7 were doublet-doublets with  $\delta$  values *c.a* 7.28-7.31 ppm, and proton H-8 signals were doublets with  $\delta$  values *c.a* 7.36-7.38 ppm, respectively. For compounds of series **2** and **3**, having a methoxy group at position 7, the signal of protons H-6 appeared as doublet-doublets with  $\delta$

values *c.a* 6.71-6.78 ppm, and proton H-8 signals appeared as doublets with  $\delta$  values *c.a* 6.82-6.88 ppm, respectively.

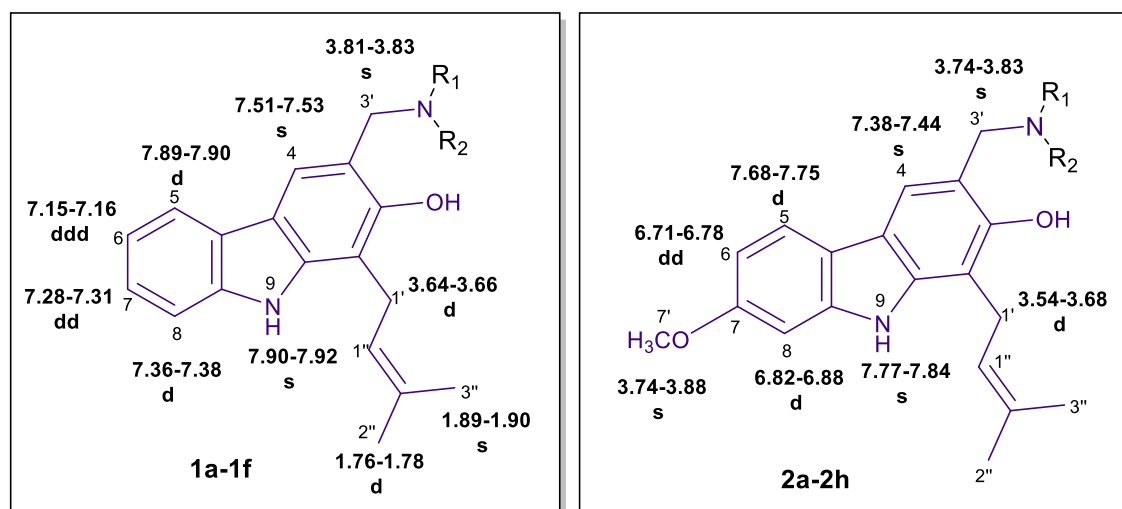


**Fig. 2:** Key protons for compounds **1a-1f** and **2a-2h**.

Compound **1b** was obtained as a crystal from the mixture of methanol and ethyl acetate. The X-ray crystallographic data of compound **1b** and the analyses of HSQC and HMBC for correlation of compound **1b** are presented in Fig. 3. The Ortep diagram confirmed the structure of **1b**. The key proton H-4 showed correlations with C-3', C-2, and C-9a while the H-5 showed correlations with C-7 and C-8a. The proton of the indole group H-9 showed correlations with C-8 and C-9a while proton H-3' showed correlations with C-4', C-2, and C-4, respectively.

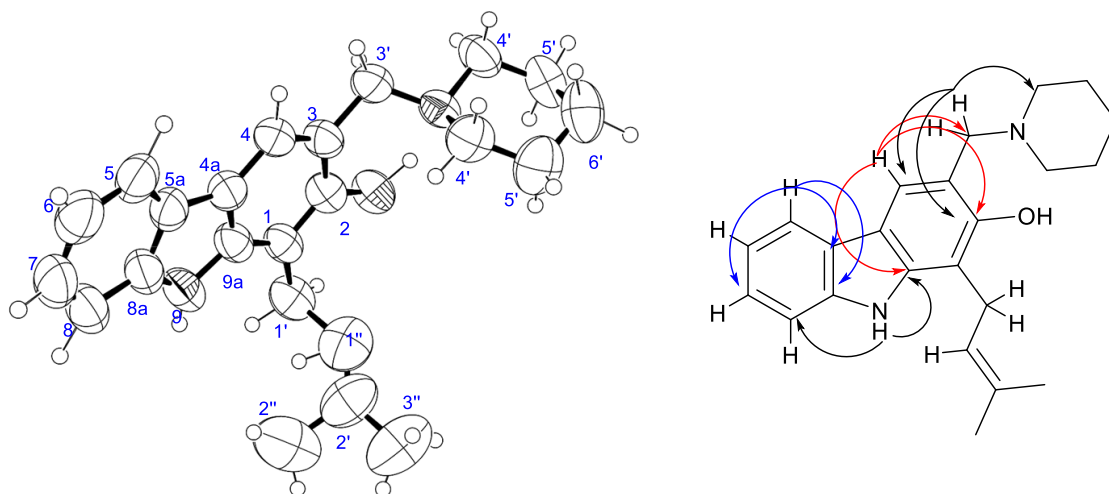


**Fig. 3:** Ortep view of compound **1b** and its key HMBC correlations.

### 3.2. Identification of amino carbazoles as potential p53 activators using a yeast-based screening assay

Compounds containing carbazole core have been identified and tested against a certain mutation of p53 and showed to stabilize T-p53c-Y220C [26]. In this work, to identify small molecules of amino carbazoles that could restore the p53 pathway signalling, four amino carbazoles derived from heptaphylline (**1**) were preliminary tested for their ability to reactivate mutant p53, using a previously developed yeast-based screening assay [34]. In the yeast assay used in this work, the human expressing mutant p53 as R2080K, Y220C, G245D, and R273H are investigated with fixed concentration of 10  $\mu$ M of the tested compounds **1a-1d**. Only compound **1d** showed no effect on the induced-growth of yeast expressing all tested mutant p53 while others could inhibit the induced-growth of some yeast expressing mutant p53 (Table 2). These preliminary results indicated that amino carbazoles could be considered to study their restoring capacity of the protein p53.

**Table 2:** Effect of heptaphylline derivatives **1a-1d** (10  $\mu$ M) on the growth of yeast expressing hotspot mutant p53 forms.

Mutant p53	1a	1b	1c	1d
<b>R280K</b>	-	21.1 $\pm$ 5.4	-	-
<b>Y220C</b>	33.3 $\pm$ 6.2	-	21.3 $\pm$ 3.2	-
<b>G245D</b>	-	55.4 $\pm$ 9.5	-	-
<b>R273H</b>	33.2 $\pm$ 6.6	-	-	-

Results correspond to the percentage of wild-type p53-induced growth inhibition restored by compounds in yeast expressing mutant p53. Data are mean  $\pm$  SEM of 4 independent experiments. Dashes represent no significant effect observed.

### 3.3. *Indolocarbazoles exhibit a p53-dependent tumor growth-inhibitory effect*

The tumor cell growth-inhibitory potential of amino carbazoles and contribution of the p53 pathway to their activity were thereafter ascertained using human colon adenocarcinoma HCT116 cell lines with wild p53 (HCT116wt) and its p53-null isogenic derivative (HCT116 p53<sup>-/-</sup>), p53-null lung (NCI-H1299null), wild p53 fibroblast (HFFwt), and mutant p53 types like HT-29-R273H, Huh-7-Y220, SW837-R248W, MDA-MB-468-R273R, and A375 cell lines. All naturally-occurring carbazoles **1-3** showed good inhibitory effect while their amino carbazoles **1a-1e**, **2b-2e** and **3a** showed moderate inhibitory effects (IC<sub>50</sub> range between 4.5 to > 50  $\mu$ M) in all tested cell lines (Table 3) in which heptaphylline (**1**) is the most promising with IC<sub>50</sub> values range from 3.3 to 7.20  $\mu$ M. Moreover, the IC<sub>50</sub> values obtained for naturally-occurring carbazoles, compounds **1**, **2**, **3**, and their amino carbazoles **1a-1e**, **2a**, **2c-2e** and **3a** on HCT116wt and mutant type Hub-7-Y220C and SW837-R248W revealed that natural-occurring carbazoles showed better inhibitory effects compared to their indolocarbazoles derivatives.



**Table 3:** The IC<sub>50</sub> concentrations of **1**, **2**, **3**, and amino carbazoles **1a-1e** and **2a-2e** on human cancer cell lines.

Cell line	HCT116 (wt)	HCT116 -/-	H1299 (null)	HFF (wt)	HT-29 (R273H)	Huh-7 (Y220C)	SW837 (R248W)	MDA-MB-468 (R273H)	A375
<b>1</b>	4.33 ± 0.48	-	8.9	16	14	6.10 ± 0.30	7.20 ± 0.40	<3.13	-
<b>2</b>	8.76 ± 0.72	-	-	-	-	21.50 ± 0.5	30.50 ± 2.50	-	-
<b>3</b>	5.74 ± 0.95	-	-	-	-	6.30 ± 2.20	6.10 ± 1.20	-	-
<b>1a</b>	> 50	-	-	-	>50	-	-	>50	-
<b>1b</b>	18.09 ± 0.88	-	21	-	18	> 50	23.00 ± 3.00	16	-
<b>1c</b>	22.58 ± 4.46	-	-	-	-	30.50 ± 0.50	29.00 ± 2.00	-	-
<b>1d</b>	11.51 ± 0.31	-	41	-	18	28.50 ± 0.50	26.00 ± 2.00	4.5	-
<b>1e</b>	30.57 ± 2.81	27.00 ± 3.00	-	-	-	>50	23.00 ± 1.00	-	38.23 ± 1.89
<b>1f</b>	-	-	-	-	-	-	-	-	-
<b>2a</b>	-	-	-	-	-	-	-	-	-
<b>2b</b>	9.44 ± 0.72	12.43 ± 1.73	-	-	-	>50	>50	-	5.83 ± 0.34
<b>2c</b>	25.00 ± 1.78	29.00 ± 2.65	-	-	-	45.00 ± 3.00	>50	-	30.67 ± 3.67
<b>2d</b>	27.00 ± 4.36	41.00 ± 1.00	-	-	-	33.5 ± 5.50	37.5 ± 0.50	-	38.33 ± 3.18
<b>2e</b>	16.11 ± 3.54	22.27 ± 2.96	-	-	-	23.00 ± 3.00	10.75 ± 1.25	-	27.77 ± 3.03
<b>2f</b>	-	-	-	-	-	-	-	-	-
<b>2g</b>	-	-	-	-	-	-	-	-	-
<b>2h</b>	-	-	-	-	-	-	-	-	-
<b>3a</b>	22.25 ± 0.95	24.00 ± 1.15	-	-	-	15.50 ± 3.50	18.00 ± 0.00	-	29.67 ± 1.76

Data are mean ± SEM of 3 independent experiments. Dashes represent no significant effect observed or undetected.

however, compounds **1d** showed selective inhibitory effects in breast cancer expressing mutant p53 (MDA-MB-648-R273H) and, while compound and **2b** showed inhibitory on melanoma expressing wild type p53 (A375) cell lines with IC<sub>50</sub> values of 4.5 and 5.83 μM, respectively. In addition, compound **2e** inhibited rectum cancer cell line expressing mutant p53 (SW837-R248W) three time stronger than the parent compound **2** with IC<sub>50</sub> value of 10.75 μM.

### 3. Conclusions

Amino carbazoles derived from carbazoles natural **1-3** products were successfully synthesized and evaluated on reactivated p53 models. The natural derivatives **1-3** were active in the investigated cell lines while the amino-derivatives showed activity only in some mutant p53 cell lines. This result revealed a modest antitumor activity and no selectivity to the p53 pathway, in human tumor cells for the natural products **1-3**. Despite this, the results obtained indicate that the amino carbazole semisynthetic derivatives may represent a promising starting point to search for new mutant p53-reactivating agents with promising application in cancer therapy.

### 4. Materials and methods

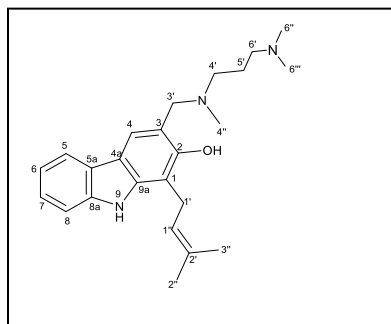
#### 4.1. Isolation

The root bark of *Clausena harmandiana* was collected in Roi Et Province, Thailand, in June 2016. The plant was identified voucher specimen (KKU No. 21145; Teerapat Bootchan 67) and deposited at Faculty of Sciences, Khon Kaen University, Khon Kaen, Thailand. The root barks (2.29 kg) were air-dried, ground and sequentially extracted at room temperature for overnight with dichloromethane (4 times). The extracts were evaporated *in vacuo* to obtain crude dichloromethane (140 g). The crude CH<sub>2</sub>Cl<sub>2</sub> was isolated by open column chromatography on silica gel 60 and subsequently eluted with a gradient of *n*-hexane and ethyl acetate (EtOAc) to give **1** (310 mg;  $1.4 \times 10^{-2}$  of dry weight), **2** (340 mg;  $1.5 \times 10^{-2}$  of dry weight), and **3** (170 mg;  $0.7 \times 10^{-2}$  of dry weight). All isolated compounds were structurally elucidated by comparison with the authentic samples, which were identical in all respects.

#### 4.2 General synthesis of the amino carbazole derivatives of heptaphylline (**1**), 7-methoxyheptaphylline (**2**), and 7-methoxymukonal (**3**)

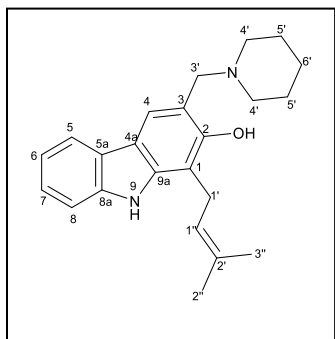
Naturally carbazole alkaloid heptaphylline (**1**, 40 mg, 0.132 mmol) or 7-methoxyheptaphylline (**2**, 41 mg, 0.132 mmol) or 7-methoxymukonal (**3**, 32 mg, 0.132 mmol) and the amine precursors *N,N,N*-trimethyl-1,3-propanediamine (0.52 mL, 3.5 mmol, 27 equiv.) for compounds **1a**, **2a**, and **3a**, or piperidine (0.1 mL, 3.5 mmol, 27 equiv.) for compounds **1b** and **2b**, or 4-chlorobenzylamine (0.081 mL, 0.66 mmol, 5 equiv.) for compounds **1c** and **2c**, or 4-fluorobenzylamine (0.075 mL, 0.66 mmol, 5 equiv.) for compounds **1d** and **2d**, or 4-bromobenzylamine (0.083 mL, 0.66 mmol, 5 equiv.) for compounds **1e** and **2e**, or 1,2,3,4-tetrahydroisoquinoline (28 mg, 0.184 mmol, 1.4 equiv.) for compound **2f**, were dissolved in dried THF or DCE and added to the reaction mixture the STAB (84.8 mg, 0.36 mmol, 3 equiv.). After adding the acetic acid (8.2  $\mu$ L, 0.132 mmol, 1 equiv.), the mixture was stirred at r.t under N<sub>2</sub> no longer than 14 days. For monitoring the synthesis of amino carbazole derivatives by TLC, two chromatographic systems were used: *n*-hexane:EtOAc 7:3 and CHCl<sub>3</sub>:Acetone: TEA 100:0.1 for amine. The crude product obtained from the reactions was subjected to different work-up strategies. After reaction of compounds **1a-1b**, **2a-2b**, **2f**, and **3a** the crudes were extracted with CHCl<sub>3</sub> (3 x 50 mL), then solid phase extraction (SPE) through cation exchange cartridge Discovery® DSC-SCX using 1% NH<sub>3</sub> in CH<sub>3</sub>OH. The basic fractions were purified on flash column using *n*-hexane:EtOAc 7:3. For compounds **1c-1e** and **2c-2e**, after reaction, the crudes extracts were treated with 5% of NaOH in CHCl<sub>3</sub> (3 x 50 mL) to remove excess STAB, the organic phases were treated with 5M HCl in CHCl<sub>3</sub> to remove excess amines. Then, the aqueous phases

were treated with 20% of NaOH in CHCl<sub>3</sub>. The combination of organic phases was subjected to SPE through cation exchange cartridge Discovery® DSC-SCX using 1% NH<sub>3</sub> in CH<sub>3</sub>OH. The basic fractions were purified on flash column using *n*-hexane:EtOAc 7:3.



**3-(((3-(Dimethylamino)propyl)(methyl)amino)methyl)-1-(3-methylbut-2-en-1-yl)-9H-carbazol-2-ol (1a).** 25.2 mg; 49%; greenish yellow solid; mp:100-101.3 IR (KBr)  $\nu_{max}$  cm<sup>-1</sup>: 3319, 2924, 1632, 1439, 1374, 1205, 740; <sup>1</sup>H NMR (CDCl<sub>3</sub>, 300 MHz)  $\delta$ : 7.92 (1H, br, NH), 7.89 (1H, d, *J* = 7.8

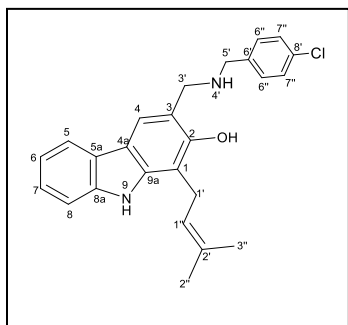
Hz, H-5), 7.53 (1H, s, H-4), 7.37 (1H, d, *J* = 7.9 Hz, H-8), 7.28 (1H, ddd, *J* = 8.5, 7.0, 1.7 Hz, H-7), 7.15 (1H, dt, *J* = 7.5, 1.1 Hz, H-6), 5.36 (1H, ddd, *J* = 6.8, 5.4 and 1.4 Hz, H-1''), 3.84 (2H, s, H-3'), 3.64 (2H, d, *J* = 6.7 Hz, H-1'), 2.56 (2H, t, *J* = 7.5 Hz, H-4'), 2.33 (3H, s, H-4''), 2.36 (2H, t, *J* = 7.5 Hz, H-6'), 2.23 (6H, s, H-6''), 1.90 (3H, s, H-2''), 1.79 (2H, q, *J* = 7.3 Hz, H-5'), 1.76 (3H, d, *J* = 1.2 Hz, H-3''); <sup>13</sup>C NMR (CDCl<sub>3</sub>, 75 MHz): 154.1 (C-2), 140.0 (C-8a), 139.4 (C-9a), 132.9 (C-2'), 124.0 (C-7), 123.8 (C-5a), 122.7 (C-1''), 119.3 (C-6), 119.1 (C-5), 117.6 (C-4), 115.4 (C-4a), 115.3 (C-3), 110.4 (C-8), 109.3 (C-1), 62.3 (C-3'), 57.4 (C-6'), 54.8 (C-4'), 45.3 (C-6''), 41.1 (C-4''), 25.8 (C-3''), 25.0 (C-5'), 18.1 (C-2'').



**1-(3-Methylbut-2-en-1-yl)-3-(piperidin-1-ylmethyl)-9H-carbazol-2-ol (1b).** 39.2 mg; 90%; greenish yellow oil;

mp:155.0-155.7°C; IR (KBr)  $\nu_{max}$   $\text{cm}^{-1}$ :3425, 2923, 1633, 1438, 1374, 1222, 741;  $^1\text{H}$  NMR ( $\text{CDCl}_3$ , 300 MHz)  $\delta$ : 7.90 (1H, br, NH), 7.89 (1H, d,  $J = 7.7$  Hz, H-5), 7.51 (1H, s, H-4), 7.36 (1H,

d,  $J = 7.9$  Hz, H-8), 7.29 (1H, ddd,  $J = 8.0, 6.8, 1.1$  Hz, H-7), 7.15 (1H, dd,  $J = 7.1, 1.1$  Hz, H-6), 5.37 (1H, ddd,  $J = 6.8, 5.1$  and  $1.3$  Hz, H-1''), 3.81 (2H, s, H-3'), 3.65 (2H, d,  $J = 6.8$  Hz, H-1'), 2.55 (4H, m, H-4'), 1.90 (3H, s, H-2''), 1.76 (3H, d,  $J = 1.2$  Hz, H-3''), 1.65 (4H, m, H-5'), 1.51 (2H, m, H-6');  $^{13}\text{C}$  NMR ( $\text{CDCl}_3$ , 75 MHz): 154.3 (C-2), 140.0 (C-8a), 139.3 (C-9a), 132.9 (C-2'), 124.0 (C-7), 123.9 (C-5a), 122.7 (C-1''), 119.2 (C-6), 119.0 (C-5), 117.6 (C-4), 117.6 (C-3), 115.3 (C-4a), 115.0 (C-1), 110.3 (C-8), 62.8 (C-3'), 53.7 (C-4'), 25.8 (C-5'), 25.7 (C-2''), 24.1 (C-6'), 23.8 (C-1'), 18.1 (C-3''); HRMS-ESI  $m/z$  349.2270 ( $\text{M} + \text{H}$ )<sup>+</sup> (calculated for  $\text{C}_{23}\text{H}_{28}\text{N}_2\text{O}$ , 349.2280).

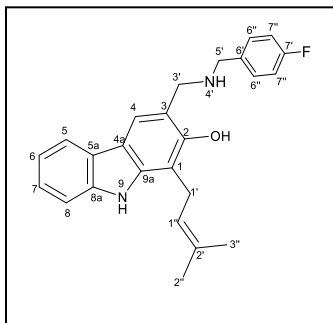


**3-(((4-Chlorobenzyl)amino)methyl)-1-(3-methylbut-2-en-1-yl)-9H-carbazol-2-ol (1c).** 21.1 mg; 49 %; greenish yellow

solid; mp:98.3-99.6°C; IR (KBr)  $\nu_{max}$   $\text{cm}^{-1}$ : 3420, 2917, 1635, 1463, 1378, 729, 668;  $^1\text{H}$  NMR ( $\text{CDCl}_3$ , 300 MHz)  $\delta$ : 7.93 (1H, br, NH), 7.89 (1H, d,  $J = 7.8$  Hz, H-5), 7.55 (1H, s, H-4), 7.38

(1H, d,  $J = 7.8$  Hz, H-8), 7.34-7.29 (2H, m, H-6''), 7.28 (1H, ddd,  $J = 7.6, 5.1,$  and  $3.4$  Hz, H-7), 7.16 (1H, ddd,  $J = 9.1, 6.8$  and  $1.2$  Hz, H-6), 7.10-6.99 (2H, m, H-7''), 5.36 (1H, ddd,  $J = 6.8, 4.1$  and  $1.4$  Hz, H-1''), 4.14 (2H, s, H-3'), 3.84 (2H, s, H-5'), 3.66 (2H, d,  $J = 6.7$  Hz, H-1'), 1.91 (3H, s H-2''), 1.76 (3H, d,  $J = 1.2$  Hz, H-3'');  $^{13}\text{C}$  NMR ( $\text{CDCl}_3$ , 75 MHz): 154.1 (C-2), 140.1 (C-9a), 139.4 (C-8a), 134.1 (C-6'), 133.0 (C-2'), 130.1 (C-6''), 130.0 (C-

8'), 124.1 (C-7), 124.0 (C-5a), 123.9 (C-2''), 122.5 (C-1''), 119.3 (C-6), 119.1 (C-5), 117.7 (C-4), 115.6 (C-4a), 115.4 (C-7''), 115.2 (C-3), 110.4 (C-8), 109.8 (C-1), 52.5 (C-3'), 51.8 (C-5'), 23.9 (C-1'), 25.8 (C-2''), 18.1 (C-3''); HRMS-ESI  $m/z$  405.1782 ( $M + H$ )<sup>+</sup> (calculated for C<sub>25</sub>H<sub>25</sub>N<sub>2</sub>ClO, 405.1733).



**3-(((4-Fluorobenzyl)amino)methyl)-1-(3-methylbut-2-en-1-**

**yl)-9H-carbazol-2-ol (1d).** 38.5 mg; 42 %; greenish yellow

solid; mp:96.1-96.5 °C; IR (KBr)  $\nu_{max}$  cm<sup>-1</sup>: 3421, 2923, 1633,

1438, 1375, 1222, 741; <sup>1</sup>H NMR (CDCl<sub>3</sub>, 300 MHz)  $\delta$ : 7.92 (1H,

br, NH), 7.89 (1H, d,  $J = 7.5$  Hz, H-5), 7.55 (1H, s, H-4), 7.36 (

1H, d,  $J = 7.5$  Hz, H-8), 7.31 (2H, m, H-6''), 7.30 (1H, ddd,  $J = 8.5, 7.0, 1.7$  Hz, H-7), 7.18

(2H, dt,  $J = 8.5, 2.5$  Hz, H-7''), 7.14 (1H, ddd,  $J = 8.5, 7.0, 1.1$  Hz, H-6), 5.36 (1H, ddd,  $J =$

6.9, 4.6, and 1.5 Hz, H-1''), 4.14 (2H, s, H-3'), 3.84 (2H, s, H-5'), 3.66 (2H, d,  $J = 6.7$  Hz, H-1'),

1.91 (3H, d,  $J = 0.6$  Hz, H-2''), 1.77 (3H, d,  $J = 1.2$  Hz, H-3''); <sup>13</sup>C NMR (CDCl<sub>3</sub>, 75 MHz)

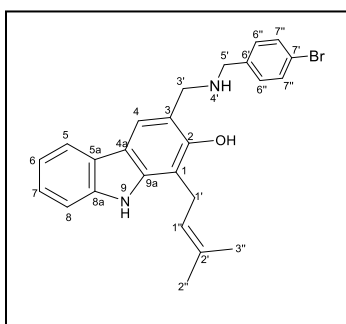
160.5 (C-7'), 154.3 (C-2), 140.2 (C-9a), 139.4 (C-8a), 136.9 (C-6'), 133.1 (C-2'), 130.1 (C-

6''), 124.1 (C-7), 122.6 (C-1''), 119.7 (C-6), 119.6 (C-5), 117.8 (C-4), 115.9 (C-3), 115.8 (C-

4a), 115.7 (C-5a), 115.5 (C-7''), 109.6 (C-1), 110.3 (C-8), 52.4 (C-3'), 51.8 (C-5'), 23.7 (C-

1'), 25.8 (C-2''), 18.1 (C-3''); HRMS-ESI  $m/z$  389.2023 ( $M + H$ )<sup>+</sup> (calculated for

C<sub>25</sub>H<sub>25</sub>N<sub>2</sub>FO, 389.2062).



**3-(((4-Bromobenzyl)amino)methyl)-1-(3-methylbut-2-en-1-**

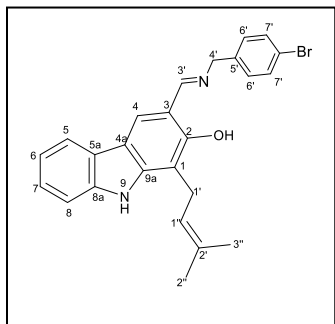
**yl)-9H-carbazol-2-ol (1e).** 41.33 mg; 64 %; greenish yellow

solid; mp:145.6-146.4 °C; IR (KBr)  $\nu_{max}$  cm<sup>-1</sup>: 3319, 2924, 1632,

1439, 1374, 1205, 740, ; <sup>1</sup>H NMR (CDCl<sub>3</sub>, 300 MHz)  $\delta$ : 7.92

(1H, br, NH), 7.90 (1H, d,  $J = 7.9$  Hz, H-5), 7.55 (1H, s, H-4),

7.49 (2H, m, H-7''), 7.38 (1H, d,  $J = 8.0$  Hz, H-8), 7.31 (1H, ddd,  $J = 8.3, 7.5, 1.2$ , H-7), 7.21 (2H, dt,  $J = 8.5, 2.5$  Hz, H-6''), 7.16 (1H, ddd,  $J = 8.5, 7.0, 1.1$  Hz, H-6), 5.36 (1H, m, H-1''), 4.14 (2H, s, H-3'), 3.83 (2H, s, H-5'), 3.66 (2H, d,  $J = 6.8$  Hz, H-1'), 1.91 (3H, s, H-2''), 1.77 (3H, d,  $J = 1.1$  Hz, H-3'');  $^{13}\text{C}$  NMR ( $\text{CDCl}_3$ , 75 MHz) 153.7 (C-2), 140.2 (C-9a), 139.4 (C-8a), 138.9 (C-6'), 133.1 (C-2'), 131.8 (C-7''), 130.4 (C-6''), 124.5 (C-7), 123.6 (C-5a), 122.5 (C-1''), 121.5 (C-7'), 119.5 (C-6), 119.3 (C-5), 117.9 (C-4), 115.7 (C-3), 115.3 (C-4a), 109.8 (C-1), 110.6 (C-8), 52.5 (C-3'), 51.7 (C-5'), 23.6 (C-1'), 25.8 (C-2''), 18.1 (C-3'').



**(E)-3-(((4-bromobenzyl)imino)methyl)-1-(3-methylbut-2-en-1-**

**yl)-9H-carbazol-2-ol (1f)** 11.2 mg; 17.48 %; orange solid; mp:

168.6-170.0; IR (KBr)  $\nu_{\text{max}}$   $\text{cm}^{-1}$ : 3422, 2962, 2916, 2848, 1624,

1486, 1328, 1235, 1100, and 798;  $^1\text{H}$  NMR ( $\text{CDCl}_3$ , 300 MHz)

$\delta$ : 8.49 (s, 1H, H-3'), 7.98 (1H, br, NH), 7.88 (dd, 1H,  $J = 13.3$

and 7.8 Hz, H-5), 7.74 (s, 1H, H-4), 7.45-7.37 (2H, m, C-6'), 7.31 (ddd, 2H,  $J$  10.2, 6.4 and

1.0 Hz, H-6 and H-7), 7.23 (d, 1H,  $J$  9.7 Hz, H-8), 7.18-6.13 (m, 2H, H-6''), 5.27 (1H, m, H-

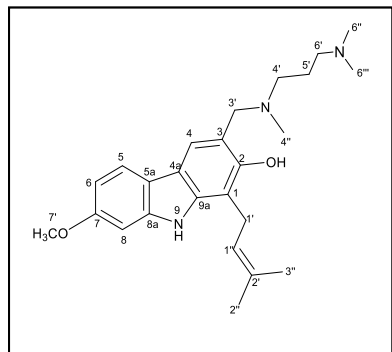
1''), 4.69 (2H, s, H-4'), 3.59 (2H, d,  $J = 6.7$  Hz, H-1'), 1.83 (3H, s, H-2''), 1.70 (d, 3H,  $J$  0.6

Hz, H-3'');  $^{13}\text{C}$  NMR ( $\text{CDCl}_3$ , 75 MHz): 166.5 (C-3'), 157.5 (C-2), 140.2 (C-9a), 139.9 (C-

8a), 133.6 (C-2'), 131.7 (C-2'), 129.5 (C-6''), 125.9 (C-4a), 125.3 (C-7), 125.0 (C-5a), 122.2

(C-4), 122.0 (C-1''), 121.3 (C-7'), 120.1 (C-6) 119.5 (C-5), 110.6 (C-8), 109.1 (C-1), 62.30

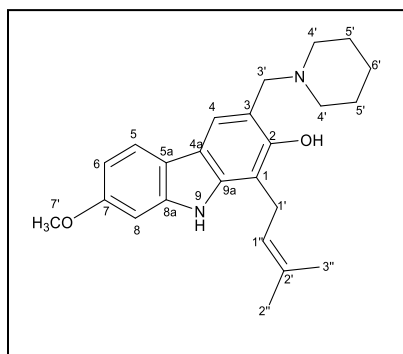
(C-4'), 25.8 (C-2''), 23.4 (C-1'), 18.16 (C-3'').



**3-(((3-(Dimethylamino)propyl)(methyl)amino)methyl)-7-methoxy-1-(3-methylbut-2-en-1-yl)-9H-carbazol-2-ol (2a)**

27.1 mg; 51.17 %; greenish yellow solid; mp: 162.7-163.8 °C; IR (KBr)  $\nu_{max}$   $\text{cm}^{-1}$ : 3319, 2924, 1632, 1439, 1374, 1205, 740;  $^1\text{H}$  NMR ( $\text{CDCl}_3$ , 300 MHz)  $\delta$ : 7.84 (1H, br, NH), 7.74 (1H, d,  $J = 8.5$  Hz, H-5), 7.42 (1H, s, H-4), 6.88

(1H, d,  $J = 2.1$  Hz, H-8), 6.78 (1H, dd,  $J = 8.5, 2.3$  Hz, H-6), 5.35 (1H, m, H-1''), 3.88 (3H, s, H-7'), 3.82 (2H, s, H-3'), 3.62 (2H, d,  $J = 6.7$  Hz, H-1'), 2.56 (2H, t,  $J = 7.3$  Hz, H-4'), 2.42 (2H, t,  $J = 7.5$  Hz, H-6'), 2.32 (9H, s, H-4'' and 6''), 1.89 (3H, s, H-2''), 1.82 (2H, t,  $J = 7.5$  Hz, H-5'), 1.76 (3H, d,  $J = 1.1$  Hz, H-3'');  $^{13}\text{C}$  NMR ( $\text{CDCl}_3$ , 75 MHz) 157.9 (C-7), 153.1 (C-2), 140.6 (C-8a), 139.9 (C-9a), 132.9 (C-2'), 122.7 (C-1''), 119.7 (C-5), 117.9 (C-5a), 116.9 (C-4), 115.6 (C-4a), 115.1 (C-3), 109.4 (C-1), 107.7 (C-6), 95.0 (C-8), 62.3 (C-3'), 57.1 (C-6'), 55.7 (C-4'), 44.8 (C-6''), 41.1 (C-4''), 25.9 (C-3''), 24.2 (C-5'), 18.1 (C-2'').



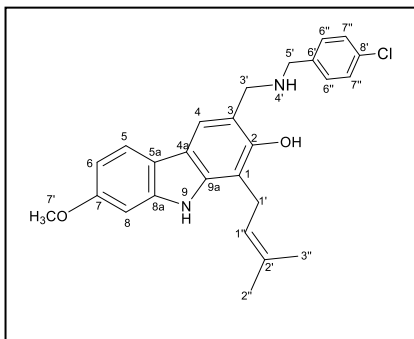
**7-Methoxy-1-(3-methylbut-2-en-1-yl)-3-(piperidin-1-ylmethyl)-9H-carbazol-2-ol (2b)**

31.2 mg; 39.1 %; greenish yellow oil; mp: 157.8-159.4 °C; IR (KBr)  $\nu_{max}$   $\text{cm}^{-1}$ : 3397, 2919, 1652, 1449, 1361, 1035, 817, 784;  $^1\text{H}$  NMR ( $\text{CDCl}_3$ , 300 MHz)  $\delta$ : 7.84 (1H, br, NH), 7.74 (1H, d,  $J = 8.5$  Hz, H-5), 7.41 (1H, s, H-4), 7.88 (1H, d,  $J = 2.2$  Hz, H-8), 6.77 (1H, dd,  $J = 8.5, 2.2$  Hz, H-6), 5.56 (1H, m, H-1''), 3.88 (3H, s, H-7'), 3.79 (2H, s, H-3'), 3.63 (2H, d,  $J = 6.7$  Hz, H-1'), 2.63 (4H, m, H-4'), 1.90 (3H, s, H-2''), 1.76 (3H, d,  $J = 1.2$  Hz, H-3''), 1.65 (4H, m, H-5'), 1.48 (2H, m, H-6');

$^{13}\text{C}$  NMR ( $\text{CDCl}_3$ , 75 MHz): 157.8



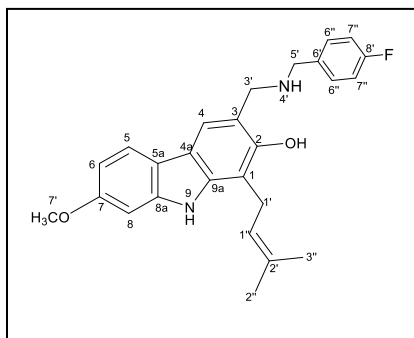
(C-7), 153.4 (C-2), 140.5 (C-8a), 139.9 (C-9a), 132.9 (C-2'), 122.8 (C-1''), 119.7 (C-5), 117.9 (C-5), 116.9 (C-4), 115.5 (C-4a), 114.8 (C-1), 107.6 (C-6), 94.9 (C-8), 62.8 (C-3'), 53.7 (C-4'), 25.8 (C-5'), 25.7 (C-2''), 24.1 (C-6'), 23.8 (C-1'), 18.1 (C-3'').



**3-(((4-Chlorobenzyl)amino)methyl)-7-methoxy-1-(3-methylbut-2-en-1-yl)-9H-carbazol-2-ol (2c).** 19.3 mg; 34

%; greenish yellow oil; mp: 109.8-110.2 °C; IR (KBr)  $\nu_{max}$   $cm^{-1}$ : 3318, 2917, 1617, 1492, 1361, 1016, 801, 669;  $^1H$  NMR (CDCl<sub>3</sub>, 300 MHz)  $\delta$ : 7.78 (1H, br, NH), 7.75 (1H,

d,  $J = 8.5$  Hz, H-5), 7.44 (1H, s, H-4), 7.32 (dt, 2H,  $J = 9.4, 3.0$  Hz, H-6''), 7.26 (m, 2H, H-7''), 6.89 (1H, d,  $J = 2.1$  Hz, H-8), 6.78 (1H, dd,  $J = 8.5, 2.2$  Hz, H-6), 5.35 (1H, m, H-1'), 4.12 (2H, s, H-3'), 3.88 (3H, s, H-7'), 3.82 (2H, s, H-5'), 3.64 (2H, d,  $J = 6.7$  Hz, H-1'), 1.90 (3H, s, H-2''), 1.76 (3H, d,  $J = 1.1$  Hz, H-3'');  $^{13}C$  NMR (CDCl<sub>3</sub>, 75 MHz): 157.9 (C-7), 153.2 (C-2), 140.5 (C-8a), 140.0 (C-9a), 137.1 (C-6'), 133.3 (C-8'), 133.0 (C-2'), 129.8 (C-6''), 128.8 (C-7''), 122.6 (C-1''), 119.8 (C-5), 117.9 (C-5a), 116.9 (C-4), 115.7 (C-3), 115.5 (C-4a), 109.8 (C-1), 107.6 (C-6), 95.0 (C-8), 52.7 (C-3'), 51.8 (C-5'), 23.9 (C-1'), 25.8 (C-2''), 18.1 (C-3'').

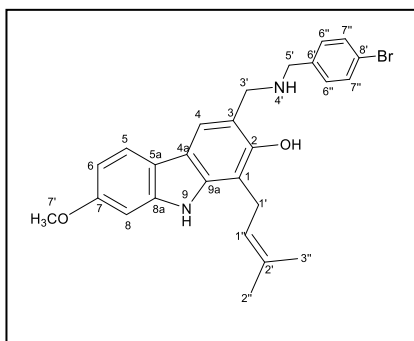


**3-(((4-Fluorobenzyl)amino)methyl)-7-methoxy-1-(3-methylbut-2-en-1-yl)-9H-carbazol-2-ol (2d)** 16.1 mg; 30

%; greenish yellow oil; mp: 94.2-95.1 °C; IR (KBr)  $\nu_{max}$   $cm^{-1}$ : 3418, 2923, 1620, 1456, 1377, 1077, 1225, 803;  $^1H$  NMR (CDCl<sub>3</sub>, 300 MHz)  $\delta$ : 7.84 (1H, br, NH), 7.75 (1H,

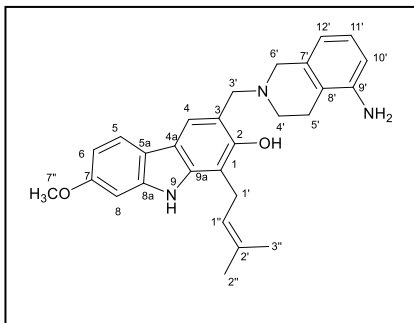
d,  $J = 8.5$  Hz, H-5), 7.45 (1H, s, H-4), 7.30 (dt, 2H,  $J = 9.4, 3.0$  Hz, H-6''), 7.03 (2H, m, H-7''), 6.89 (1H, d,  $J = 2.2$  Hz, H-8), 6.78 (1H, dd,  $J = 8.5, 2.2$  Hz, H-6), 5.29 (1H, m, H-1'),

4.12 (2H, s, H-3'), 3.88 (3H, s, H-7'), 3.83 (2H, s, H-5'), 3.75 (s, 1H, NH), 3.64 (2H, d,  $J = 6.7$  Hz, H-1'), 1.90 (3H, s, H-2''), 1.76 (3H, d,  $J = 1.1$  Hz, H-3'');  $^{13}\text{C}$  NMR ( $\text{CDCl}_3$ , 75 MHz): 160.7 (C-8'), 157.9 (C-7), 153.2 (C-2), 140.6 (C-8a), 140.0 (C-9a), 134.4 (C-6'), 132.9 (C-2'), 130.0 (C-6''), 122.5 (C-1''), 119.7 (C-5), 117.9 (C-5a), 116.9 (C-4), 115.7 (C-4a), 115.4 (C-7''), 115.1 (C-3), 109.8 (C-1), 107.7 (C-6), 95.0 (C-8), 55.7 (C-7'), 52.6 (C-3'), 51.8 (C-5'), 25.8 (C-2''), 23.8 (C-1'), 18.1 (C-3'').



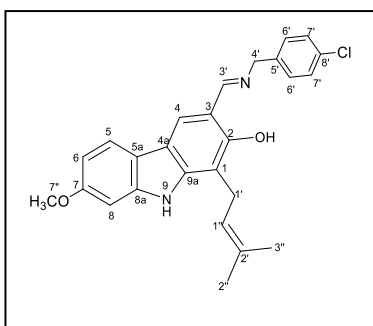
**3-(((4-Bromobenzyl)amino)methyl)-7-methoxy-1-(3-methylbut-2-en-1-yl)-9H-carbazol-2-ol (2e)** 53.7 mg; 86.47 %; greenish yellow oil; mp: 117.1-118.4; IR (KBr)  $\nu_{\text{max}}$   $\text{cm}^{-1}$ : 3445, 2919, 1652, 1449, 1361, 801, 669;  $^1\text{H}$  NMR ( $\text{CDCl}_3$ , 300 MHz)  $\delta$ : 7.85 (1H, br, NH), 7.75 (1H, d,  $J = 8.5$  Hz, H-5), 7.48 (2H, m C-6''), 7.44 (1H, s, H-4), 7.21 (dd, 2H,  $J = 8.5, 2.5$  Hz, H-6''), 6.89 (1H, d,  $J = 2.2$  Hz, H-8), 6.78 (1H, dd,  $J = 8.5, 2.3$  Hz, H-6), 5.35 (1H, m, H-1''), 4.11 (2H, s, H-3'), 3.88 (3H, s, H-7'), 3.81 (2H, s, H-5'), 3.65 (2H, d,  $J = 6.7$  Hz, H-1'), 1.90 (3H, s, H-2''), 1.76 (3H, d,  $J = 1.1$  Hz, H-3'');  $^{13}\text{C}$  NMR ( $\text{CDCl}_3$ , 75 MHz): 157.9 (C-7), 153.2 (C-2), 140.6 (C-8a), 140.0 (C-9a), 137.5 (C-6'), 132.9 (C-2'), 131.8 (C-6''), 130.1 (C-7''), 122.6 (C-1''), 121.4 (C-8'), 119.7 (C-5), 117.8 (C-5a), 116.9 (C-4), 115.7 (C-4a), 115.3 (C-3), 109.8 (C-1), 107.8 (C-6), 95.0 (C-8), 55.7 (C-7'), 52.6 (C-3'), 51.8 (C-5'), 25.8 (C-2''), 23.8 (C-1'), 18.1 (C-3'').

d,  $J = 8.5$  Hz, H-5), 7.48 (2H, m C-6''), 7.44 (1H, s, H-4), 7.21 (dd, 2H,  $J = 8.5, 2.5$  Hz, H-6''), 6.89 (1H, d,  $J = 2.2$  Hz, H-8), 6.78 (1H, dd,  $J = 8.5, 2.3$  Hz, H-6), 5.35 (1H, m, H-1''), 4.11 (2H, s, H-3'), 3.88 (3H, s, H-7'), 3.81 (2H, s, H-5'), 3.65 (2H, d,  $J = 6.7$  Hz, H-1'), 1.90 (3H, s, H-2''), 1.76 (3H, d,  $J = 1.1$  Hz, H-3'');  $^{13}\text{C}$  NMR ( $\text{CDCl}_3$ , 75 MHz): 157.9 (C-7), 153.2 (C-2), 140.6 (C-8a), 140.0 (C-9a), 137.5 (C-6'), 132.9 (C-2'), 131.8 (C-6''), 130.1 (C-7''), 122.6 (C-1''), 121.4 (C-8'), 119.7 (C-5), 117.8 (C-5a), 116.9 (C-4), 115.7 (C-4a), 115.3 (C-3), 109.8 (C-1), 107.8 (C-6), 95.0 (C-8), 55.7 (C-7'), 52.6 (C-3'), 51.8 (C-5'), 25.8 (C-2''), 23.8 (C-1'), 18.1 (C-3'').



**3-((5-Amino-3,4-dihydroisoquinolin-2(1H)-yl)methyl)-7-methoxy-1-(3-methylbut-2-en-1-yl)-9H-carbazol-2-ol (2f).** 18.8 mg 25.22%; orange solid; mp: 220-221 °C; IR (KBr)  $\nu_{max}$   $\text{cm}^{-1}$ : 3378, 2927, 1617, 1257, 1466, and 1344;  $^1\text{H}$  NMR ( $\text{CDCl}_3$ , 300 MHz)  $\delta$ : 7.86 (1H, br, NH), 7.76

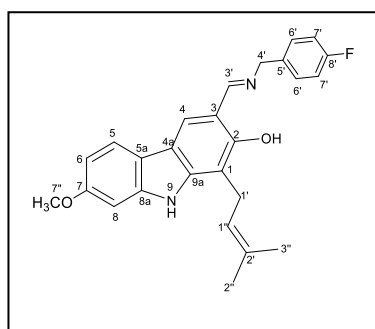
(1H, d,  $J = 8.5$  Hz, H-5), 7.49 (1H, s, H-4), 7.69 (1H, dd,  $J = 8.9$  and 6.6 Hz, H-11'), 6.89 (1H, d,  $J = 2.2$  Hz, H-8), 6.79 (1H, dd,  $J = 8.5$  and 2.2 Hz, H-6), 6.57 (1H, d,  $J = 7.5$  Hz, H-12'), 6.47 (1H, d,  $J = 7.5$  Hz, H-10'), 5.35 (1H, ddd,  $J = 6.8, 5.4$  and 1.4 Hz, H-1''), 4.00 (2H, s, H-3'), 3.89 (3H, s, H-7'), 3.57 (2H, s, H-6'), 3.60 (2H, d,  $J = 6.8$  Hz, H-1'), 2.89 (2H, t,  $J = 6.0$  Hz, H-5''), 2.61 (2H, t,  $J = 7.7$  Hz, H-4'), 1.88 (3H, s, H-2''), 1.75 (2H, d,  $J = 1.1$  Hz, H-3'');  $^{13}\text{C}$  NMR ( $\text{CDCl}_3$ , 75 MHz): 157.8 (C-7), 154.1 (C-2), 144.1 (C-9'), 140.7 (C-8a), 139.8 (C-9a), 136.3 (C-7'), 133.0 (C-2'), 126.4 (C-11'), 122.5 (C-1'), 119.8 (C-5), 119.5 (C-8'), 117.8 (C-5a), 117.5 (C-4), 117.1 (C-12'), 115.7 (C-4a), 115.4 (C-3), 112.7 (C-10'), 109.6 (C-1), 107.6 (C-6), 95.1 (C-8), 56.7 (C-6'), 55.4 (C-7'), 52.8 (C-3'), 51.0 (C-4'), 25.7 (C-2''), 24.9 (C-5'), 23.9 (C-1'), 18.1 (C-3'').



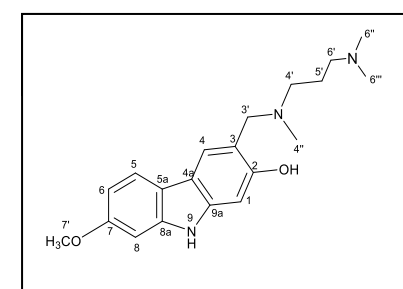
**(E)-3-(((4-chlorobenzyl)imino)methyl)-1-(3-methylbut-2-en-1-yl)-9H-carbazol-2-ol (2g).** 5.2 mg; 9.29 %; orange solid; mp: 124.8-126.1; IR (KBr)  $\nu_{max}$   $\text{cm}^{-1}$ : 3423, 2962, 2919, 2850, 1617, 1435, 1319, 1090, and 800;  $^1\text{H}$  NMR ( $\text{CDCl}_3$ , 300 MHz)  $\delta$ : 8.55 (s, 1H, H-3'), 7.94 (1H, br, NH), 7.79 (1H,

d,  $J = 8.5$  Hz, H-5), 7.70 (s, 1H, H-4), 7.37-7.23 (2H, m, C-6'), 7.10-6.98 (m, 2H, H-6''), 6.90 (1H, d,  $J = 2.1$  Hz, H-8), 6.82 (dd, 1H,  $J = 8.5, 2.3$  Hz, H-6), 5.33 (1H, m, H-1''), 4.78

(2H, s, H-2'), 3.90 (3H, s, H-7''), 3.65 (2H, d,  $J = 6.7$  Hz, H-1'), 1.90 (3H, s, H-2''), 1.76 (s, 3H, H-3'');  $^{13}\text{C}$  NMR ( $\text{CDCl}_3$ , 75 MHz): 166.5 (C-3'), 158.5 (C-7), 156.8 (C-2), 142.5 (C-9a), 141.1 (C-8a), 137.2 (C-5'), 133.5 (C-8'), 133.0 (C-2'), 129.1 (C-7'), 128.8 (C-6'), 122.1 (C-1''), 121.1 (C-4), 120.6 (C-5), 117.6 (C-5a), 116.2 (C-4a), 112.9 (C-3), 109.2 (C-1), 108.2 (C-6), 95.3 (C-8), 62.2 (C-4'), 55.7 (C-7''), 25.8 (C-2''), 23.4 (C-1'), 18.1 (C-3'').



**(E)-3-(((4-fluorobenzyl)imino)methyl)-1-(3-methylbut-2-en-1-yl)-9H-carbazol-2-ol (2h).** 8.0 mg; 14.86 %; orange solid; mp:136.3-136.5; IR (KBr)  $\nu_{\text{max}}$   $\text{cm}^{-1}$ : 3426, 2961, 2921, 2831, 1627, 1437, 1318, 1110, and 826;  $^1\text{H}$  NMR ( $\text{CDCl}_3$ , 300 MHz)  $\delta$ : 8.47 (s, 1H, H-3'), 7.89 (1H, br, NH), 7.71 (1H, d,  $J = 8.5$  Hz, H-5), 7.62 (s, 1H, H-4), 7.27-7.23 (2H, m, C-6'), 7.23-7.18 (m, 2H, H-6''), 6.82 (1H, d,  $J = 2.3$  Hz, H-8), 6.75 (dd, 1H,  $J = 8.5, 2.2$  Hz, H-6), 5.35 (1H, m, H-1''), 4.69 (2H, s, H-2'), 3.82 (3H, s, H-7''), 3.57 (2H, d,  $J = 6.8$  Hz, H-1'), 1.82 (s, 3H, H-2''), 1.69 (3H, d,  $J = 1.1$  Hz, H-3'');  $^{13}\text{C}$  NMR ( $\text{CDCl}_3$ , 75 MHz): 166.3 (C-3'), 160.2 (C-8'), 158.4 (C-7), 156.8 (C-2), 142.6 (C-9a), 141.1 (C-8a), 134.4 (C-6'), 133.5 (C-2'), 129.5 (C-7'), 122.1 (C-1''), 121.1 (C-4), 120.1 (C-5), 117.6 (C-5a), 115.6 (C-6''), 115.3 (C-4a), 112.9 (C-3), 109.2 (C-1), 108.2 (C-6), 95.3 (C-8), 62.1 (C-3'), 55.7 (C-7''), 25.8 (C-2''), 23.4 (C-1'), 18.1 (C-3'').



**3-(((3-(Dimethylamino)propyl)(methyl)amino)methyl)-7-methoxy-9H-carbazol-2-ol (3a)** 15 mg; 51.38 %; greenish yellow solid; mp: 99-100 °C, IR (KBr)  $\nu_{\text{max}}$   $\text{cm}^{-1}$ : 3319, 2924, 1632, 1439, 1374, 1205, 740;  $^1\text{H}$  NMR ( $\text{CDCl}_3$ , 300 MHz)  $\delta$ : 7.99 (1H, br, H-9), 7.75 (1H, d,  $J = 8.5$  Hz, H-5),

7.53 (1H, s, H-4), 6.99 (1H, s, H-2'), 6.87 (1H, d,  $J = 2.1$  Hz, H-8), 6.83 (1H, s, H-1), 6.79 (1H, dd,  $J = 8.5, 2.3$  Hz, H-6), 3.88 (3H, s, H-7'), 3.83 (2H, s, H-3'), 2.58 (2H, dd,  $J = 14.7$  and  $7.4$  Hz, H-4'), 2.32 (3H, s, H-4''), 2.22 (6H, s, H-6''), 2.02 (2H, dd,  $J = 14.3$  and  $6.8$  Hz, H-6'), 1.76 (2H, dt  $J = 14.7$  and  $7.4$ , H-6');  $^{13}\text{C}$  NMR (  $\text{CDCl}_3$ , 75 MHz) 159.1 (C-2), 157.5 (C-7), 142.6 (C-8a), 140.9 (C-9a), 120.5 (C-5), 117.9 (C-5a), 116.9 (C-4), 115.6 (C-4a), 115.1 (C-3), 107.7 (C-6), 96.9 (C-1), 95.2 (C-8), 62.3 (C-3'), 56.7 (C-6'), 55.7 (C-4'), 44.6 (C-6''), 41.5 (C-4''), 24.2 (C-5').

### 4.3. Crystallography

A single crystal was mounted on a cryoloop using paratone. X-ray diffraction data were collected at room temperature with a Gemini PX Ultra equipped with  $\text{CuK}_\alpha$  radiation ( $\lambda = 1.54184 \text{ \AA}$ ). The structure was solved by direct methods using SHELXS-97 and refined with SHELXL-97 [35]. Crystal was monoclinic, space group  $\text{P2}_1/\text{c}$ , cell volume  $2047.89(15) \text{ \AA}^3$  and unit cell dimensions  $a = 18.0056(9) \text{ \AA}$ ,  $b = 9.3592(3) \text{ \AA}$  and  $c = 12.7126(6) \text{ \AA}$  and  $\beta = 107.074(5)^\circ$  (uncertainties in parentheses). Non-hydrogen atoms were refined anisotropically. Hydrogen atoms were either placed at their idealized positions using appropriate HFIX instructions in SHELXL and included in subsequent refinement cycles or were directly found from difference Fourier maps and were refined freely with isotropic displacement parameters. The refinement converged to  $R(\text{all data}) = 12.46\%$  and  $wR2(\text{all data}) = 29.12\%$ .

### 4.4 Yeast screening assay

*Saccharomyces cerevisiae* cells expressing human mutp53 R280K, Y220C, G245D or R273H (or empty vector as control) were obtained in previous works [36]. Yeast cells expressing human wtp53 were obtained in previous work [36] and were used as positive controls. For expression of human wtp53 or mutp53, cells (routinely grown in minimal selective medium) were incubated in galactose selective medium with all the amino acids required for yeast growth (50 µg/mL) except leucine as described [36], in the presence of 10 µM of amino carbazole derivatives, compounds **1a-1d**, or 0.1% DMSO, for approximately 42 h (time required by control yeast incubated with DMSO to achieve 0.4 OD<sub>600</sub>). Yeast growth was analyzed by colony-forming unit counts as described. Percentage of growth inhibition was calculated considering the wtp53-induced yeast growth inhibition as 100%.

#### *4.5 Human tumor cell lines and growths conditions*

Human colon adenocarcinoma HCT116 cell lines expressing wt p53 (HCT116 p53<sup>+/+</sup>) and its p53-null isogenic derivative (HCT116 p53<sup>-/-</sup>) were provided by B. Vogelstein (The Johns Hopkins Kimmel Cancer Center, Baltimore, MD, USA); human colon adenocarcinoma HT-29, non-small cell lung cancer NCI-H1299, breast adenocarcinoma MDA-MB-468, melanoma A375, and non-tumorigenic foreskin fibroblasts HFF-1 cell lines were purchase from ATCC. Human hepatocarcinoma HuH-7 cell lines were purchase from JCRB cell bank. Cancer cells were routinely cultured in RPMI-1640 medium with UltraGlutamine (Lonza, VWR, Carnaxide, Portugal) supplemented with 10% fetal bovine serum (FBS; Gibco, Alfacene, Lisboa, Portugal). HFF-1 cells were cultured in DMEM/F-12 supplemented with 10% FBS. All cells were maintained at 37°C in a humidified atmosphere of 5% CO<sub>2</sub>. Cells were routinely tested for mycoplasma infection using the MycoAlert™ PLUS mycoplasma detection kit (Lonza, VWR, Carnaxide, Portugal).

#### *4.6 Sulforhodamine B (SRB) assay*

Human cell lines were seeded in 96-well plates at a density of  $5.0 \times 10^3$  (HCT116, HeLa, SJSA-1, A375, HT-29, NCI-1299, MDA-MB-468, HuH-7), and  $1.0 \times 10^4$  (HFF-1) cells/well, for 24 h. Cells were treated with serial dilutions of compounds (ranging from 3-150  $\mu\text{M}$ ), for additional 48 h. Effect on cell proliferation was measured by SRB assay, as described [37], and  $\text{IC}_{50}$  (concentration that causes 50% growth inhibition) values were determined for each cell line using the GraphPad Prism software (version 6.0).

#### **Acknowledgments**

S.L. thanks Erasmus Mundus Action 2 (LOTUS+, LP15DF0205) for full PhD scholarship, to Nanthicha Thongdee, Susanya peerasiri and Pang phattarapon for laboratory assistant, and to Dr. Sara Cravo for technical supports.

#### **Funding**

This research was partially supported by the Strategic Funding UID/Multi/04423/2013 through national funds provided by FCT—Foundation for Science and Technology and European Regional Development Fund (ERDF), in the framework of the program PT2020. The authors thank to national funds provided by FCT—Foundation for Science and Technology and European Regional Development Fund (ERDF) and COMPETE under the Strategic Funding UID/Multi/04423/2013, and the projects POCI-01-0145-FEDER-028736.

**Conflict of interest:** Authors reports no conflict of interests.

## References

1. Xin, Z.Q.; Lu, J.J.; Ke, C.Q.; Hu, C.X.; Lin, L.P.; Ye, Y. Constituents from clausena excavata. *Chemical and Pharmaceutical Bulletin* **2008**, *56*, 827-830. 10.1248/cpb.56.827
2. Knölker, H.-J.; Reddy, K.R. Isolation and synthesis of biologically active carbazole alkaloids. *Chemical Reviews* **2002**, *102*, 4303-4428. 10.1021/cr020059j
3. Wu, T.S.; Huang, S.C.; Wu, P.L.; Kuoh, C.S. Alkaloidal and other constituents from the root bark of clausena excavata. *Phytochemistry* **1999**, *52*, 523-527. 10.1016/S0031-9422(99)00220-4
4. Das, K.C.; Chakraborty, D.P.; Bose, P.K. Antifungal activity of some constituents of murraya koenigii spreng. *Experientia* **1965**, *21*, 340-340. 10.1007/BF02144703
5. Chakthong, S.; Bindulem, N.; Raknai, S.; Yodwaree, S.; Kaewsanee, S.; Kanjana-Opas, A. Carbazole-pyranocoumarin conjugate and two carbazole alkaloids from the stems of clausena excavata. *Natural Product Research* **2016**, *30*, 1690-1697. 10.1080/14786419.2015.1135143
6. Thongthoom, T.; Promsuwan, P.; Yenjai, C. Synthesis and cytotoxic activity of the heptaphylline and 7-methoxyheptaphylline series. *European Journal of Medicinal Chemistry* **2011**, *46*, 3755-3761. <https://doi.org/10.1016/j.ejmech.2011.05.041>
7. Thongthoom, T.; Songsiang, U.; Phaosiri, C.; Yenjai, C. Biological activity of chemical constituents from clausena harmandiana. *Archives of Pharmacal Research* **2010**, *33*, 675-680. 10.1007/s12272-010-0505-x



8. Yenjai, C.; Sripontan, S.; Sriprajun, P.; Kittakooop, P.; Jintasirikul, A.; Tanticharoen, M.; Thebtaranonth, Y. Coumarins and carbazoles with antiplasmodial activity from *clausena harmandiana*. *Planta Medica* **2000**, *66*, 277-279. 10.1055/s-2000-8558
9. Tian-Shung, W.; Shiow-Chyn, H.; Pei-Lin, W.; Che-Ming, T. Carbazole alkaloids from *clausena excavata* and their biological activity. *Phytochemistry* **1996**, *43*, 133-140. [https://doi.org/10.1016/0031-9422\(96\)00212-9](https://doi.org/10.1016/0031-9422(96)00212-9)
10. Maneerat, W.; Phakhodee, W.; Ritthiwigrom, T.; Cheenpracha, S.; Promgool, T.; Yossathera, K.; Deachathai, S.; Laphookhieo, S. Antibacterial carbazole alkaloids from *clausena harmandiana* twigs. *Fitoterapia* **2012**, *83*, 1110-1114. <https://doi.org/10.1016/j.fitote.2012.04.026>
11. Chakraborty, A.; Saha, C.; Podder, G.; Chowdhury, B.K.; Bhattacharyya, P. Carbazole alkaloid with antimicrobial activity from *clausena heptaphylla*. *Phytochemistry* **1995**, *38*, 787-789. [https://doi.org/10.1016/0031-9422\(94\)00666-H](https://doi.org/10.1016/0031-9422(94)00666-H)
12. Patel, O.P.S.; Mishra, A.; Maurya, R.; Saini, D.; Pandey, J.; Taneja, I.; Raju, K.S.R.; Kanojiya, S.; Shukla, S.K.; Srivastava, M.N., *et al.* Naturally occurring carbazole alkaloids from *murraya koenigii* as potential antidiabetic agents. *Journal of Natural Products* **2016**, *79*, 1276-1284. 10.1021/acs.jnatprod.5b00883
13. Boonyarat, C.; Yenjai, C.; Vajragupta, O.; Waiwut, P. Heptaphylline induces apoptosis in human colon adenocarcinoma cells through bid and akt/nf-kb (p65) pathways. *Asian Pacific Journal of Cancer Prevention* **2014**, *15*, 10483-10487. 10.7314/APJCP.2014.15.23.10483

14. Saturnino, C.; Iacopetta, D.; Sinicropi, M.; Rosano, C.; Caruso, A.; Caporale, A.; Marra, N.; Marengo, B.; Pronzato, M.; Parisi, O., *et al.* N-alkyl carbazole derivatives as new tools for alzheimer's disease: Preliminary studies. *Molecules* **2014**, *19*, 9307.
15. Krahl, M.P.; Jäger, A.; Krause, T.; Knölker, H.J. First total synthesis of the 7-oxygenated carbazole alkaloids clauszoline-k, 3-formyl-7-hydroxycarbazole, clausine m, clausine n and the anti-hiv active siamenol using a highly efficient palladium-catalyzed approach. *Organic and Biomolecular Chemistry* **2006**, *4*, 3215-3219. 10.1039/b607792g
16. Wangboonskul, J.D.; Pummangura, S.; Chaichantipyuth, C. Five coumarins and a carbazole alkaloid from the root bark of clausena a harmandiana. *Journal of Natural Products* **1984**, *47*, 1058-1059. 10.1021/np50036a038
17. Issa, S.; Walchshofer, N.; Kassab, I.; Termoss, H.; Chamat, S.; Geahchan, A.; Bouaziz, Z. Synthesis and antiproliferative activity of oxazinocarbazole and n,n-bis(carbazolylmethyl)amine derivatives. *European Journal of Medicinal Chemistry* **2010**, *45*, 2567-2577. 10.1016/j.ejmech.2010.02.045
18. Chen, Y.L.; Hung, H.M.; Lu, C.M.; Li, K.C.; Tzeng, C.C. Synthesis and anticancer evaluation of certain indolo[2,3-b]quinoline derivatives. *Bioorganic and Medicinal Chemistry* **2004**, *12*, 6539-6546. 10.1016/j.bmc.2004.09.025
19. Compain-Batissou, M.; Latreche, D.; Gentili, J.; Walchshofer, N.; Bouaziz, Z. Synthesis and diels-alder reactivity of ortho-carbazolequinones. *Chemical and Pharmaceutical Bulletin* **2004**, *52*, 1114-1116. 10.1248/cpb.52.1114

20. Joerger, A.C.; Fersht, A.R. Structural biology of the tumor suppressor p53 and cancer-associated mutants. In *Advances in cancer research*, Academic Press: 2007; Vol. 97, pp 1-23.
21. Vousden, K.H.; Lane, D.P. P53 in health and disease. *Nature Reviews Molecular Cell Biology* **2007**, *8*, 275. 10.1038/nrm2147
22. Fridman, J.S.; Lowe, S.W. Control of apoptosis by p53. *Oncogene* **2003**, *22*, 9030. 10.1038/sj.onc.1207116
23. Muller, P.A.J.; Vousden, K.H. Mutant p53 in cancer: New functions and therapeutic opportunities. *Cancer cell* **2014**, *25*, 304-317. 10.1016/j.ccr.2014.01.021
24. Yu, X.; Blanden, A.R.; Narayanan, S.; Jayakumar, L.; Lubin, D.; Augeri, D.; David Kimball, S.; Loh, S.N.; Carpizo, D.R. Small molecule restoration of wildtype structure and function of mutant p53 using a novel zinc-metallochaperone based mechanism. *Oncotarget* **2014**, *5*, 8879-8892. 10.18632/oncotarget.2432
25. Liu, X.; Wilcken, R.; Joerger, A.C.; Chuckowree, I.S.; Amin, J.; Spencer, J.; Fersht, A.R. Small molecule induced reactivation of mutant p53 in cancer cells. *Nucleic acids research* **2013**, *41*, 6034-6044. 10.1093/nar/gkt305
26. Boeckler, F.M.; Joerger, A.C.; Jaggi, G.; Rutherford, T.J.; Veprintsev, D.B.; Fersht, A.R. Targeted rescue of a destabilized mutant of p53 by an in silico screened drug. *Proceedings of the National Academy of Sciences of the United States of America* **2008**, *105*, 10360-10365. 10.1073/pnas.0805326105

27. Bauer, M.R.; Jones, R.N.; Baud, M.G.J.; Wilcken, R.; Boeckler, F.M.; Fersht, A.R.; Joerger, A.C.; Spencer, J. Harnessing fluorine-sulfur contacts and multipolar interactions for the design of p53 mutant y220c rescue drugs. *ACS chemical biology* **2016**, *11*, 2265-2274. 10.1021/acscchembio.6b00315
28. Rauf, S.M.A.; Endou, A.; Takaba, H.; Miyamoto, A. Effect of y220c mutation on p53 and its rescue mechanism: A computer chemistry approach. *The Protein Journal* **2013**, *32*, 68-74. 10.1007/s10930-012-9458-x
29. Roughley, S.D.; Jordan, A.M. The medicinal chemist's toolbox: An analysis of reactions used in the pursuit of drug candidates. *Journal of Medicinal Chemistry* **2011**, *54*, 3451-3479. 10.1021/jm200187y
30. Abdel-Magid, A.F.; Carson, K.G.; Harris, B.D.; Maryanoff, C.A.; Shah, R.D. Reductive amination of aldehydes and ketones with sodium triacetoxyborohydride. Studies on direct and indirect reductive amination procedures<sup>1</sup>. *The Journal of Organic Chemistry* **1996**, *61*, 3849-3862. 10.1021/jo960057x
31. Joshi, B.S.; Kamat, V.N.; Gawad, D.H.; Govindachari, T.R. Structure and synthesis of heptaphylline. *Phytochemistry* **1972**, *11*, 2065-2071. 10.1016/S0031-9422(00)90173-0
32. Joshi, B.S.; Rane, D.F. Synthesis of heptaphylline. *Chemistry and Industry (London)* **1968**, *21*, 685.
33. Joshi, B.S.; Kamat, V.N.; Saksena, A.K.; Govindachari, T.R. Structure of heptaphylline, a carbazole alkaloid from *clausena heptaphylla* wt. & arn. *Tetrahedron Letters* **1967**, *8*, 4019-4022. [https://doi.org/10.1016/S0040-4039\(01\)89728-8](https://doi.org/10.1016/S0040-4039(01)89728-8)

34. Leão, M.; Gomes, S.; Soares, J.; Bessa, C.; MacIel, C.; Ciribilli, Y.; Pereira, C.; Inga, A.; Saraiva, L. Novel simplified yeast-based assays of regulators of p53-mdmx interaction and p53 transcriptional activity. *FEBS Journal* **2013**, *280*, 6498-6507. 10.1111/febs.12552
35. Sheldrick, G.M. A short history of shelx. *Acta Crystallographica Section A: Foundations of Crystallography* **2008**, *64*, 112-122. 10.1107/S0108767307043930
36. Soares, J.; Raimundo, L.; Pereira, N.A.L.; Monteiro, Â.; Gomes, S.; Bessa, C.; Pereira, C.; Queiroz, G.; Bisio, A.; Fernandes, J., *et al.* Reactivation of wild-type and mutant p53 by tryptophan-derived oxazoloisindolinone slmp53-1, a novel anticancer small-molecule. *Oncotarget* **2015**, *7*, 4326-4343. 10.18632/oncotarget.6775
37. Soares, J.; Raimundo, L.; Pereira, N.A.L.; dos Santos, D.J.V.A.; Pérez, M.; Queiroz, G.; Leão, M.; Santos, M.M.M.; Saraiva, L. A tryptophan-derived oxazolopiperidone lactam is cytotoxic against tumors via inhibition of p53 interaction with murine double minute proteins. *Pharmacological Research* **2015**, *95-96*, 42-52. <https://doi.org/10.1016/j.phrs.2015.03.006>



# Chapter 9

## General Discussion and Conclusions





Alkaloids are a remarkable source of scaffolds for the discovery of multidrug resistance (MDR) modulators. The first review article (chapter 2), highlights the family of alkaloids along with others MNPs like terpenoids, sterols, polyketides, diketopiperazines, peptides, and miscellaneous. This work was helpful in the guidance of the scope of this thesis towards MDR and chemotherapeutics based on alkaloids containing indole group – the quinazolinone-containing indole alkaloids and the carbazole alkaloids.

From chapter 3, it could be concluded that fiscalin B (**26**) and derivatives can be synthesized regioselectively and are moderate cell growth inhibitors without P-glycoprotein (P-gp) inhibitory effects. In chapter 3, a library of fiscalin B (**26**) and their homologues was obtained to evaluate antitumor activity and P-gp inhibitory effect (Table 1, chapter 3) namely, quinazolinone **76-83** which were synthesized by a multi-step Mazurkiewicz-Ganesan approach (compounds **76**, **79**, **80**, and **83**) and by an one-pot three components microwave assisted approach (compounds **77**, **78**, **81**, and **82**). These syntheses also revealed that the bulky groups of *i*-Pr and *i*-Bu presented at C-1 failed to form *syn*-isomers via the microwave method which allowed to construct only *anti*-isomers<sup>96</sup> and described the partial epimerization occurring at C1 and/or C1/C4 of piperazine ring during microwave irradiation. The stereochemistry of those enantiomers was confirmed NMR (Figure 2, Table 2 and 3, chapter 3) and their purity was evaluated by enantioselective liquid chromatography. The compounds displayed no effect on P-gp modulation and moderate cell growth inhibitory effect with GI<sub>50</sub> ranging from 31 to 81 μM (Table 4, chapter 3). We found that the increase of one methylene at position C-1 was associated to the rise of the antitumor activity. Isomers having *4R* configurations showed better activity compared to *4S* isomers.

Based on these results, we decided to further explore this scaffold for antitumor activity with derivatives containing different groups at C-1 such as -CH<sub>3</sub>, -CH(CH<sub>3</sub>)C<sub>2</sub>H<sub>5</sub>, -(CH<sub>2</sub>)<sub>2</sub>SCH<sub>3</sub>, -indoyl, -CH<sub>2</sub>C<sub>6</sub>H<sub>4</sub>OCH<sub>2</sub>C<sub>6</sub>H<sub>5</sub>, and -CH<sub>2</sub>C<sub>6</sub>H<sub>4</sub>OH (chapter 4). Quinazolinones **84-94** were synthesized via two different methods previously described (Scheme 1, chapter 3 and 4). By the synthesis via microwave, the epimerization and/or isomerization occurred, producing two pairs of diastereoisomers and four enantiomers, in case of compounds in which at C-1 were present aromatic groups, i.e. compound **90**, and **91**. Structure-activity relationship (SAR) studies for antitumor activity revealed that, the configuration *R* at C-4 is important for this activity and increasing the molecular weight at C-1 improved the activity. Among tested compounds, **84-94**, a hit compound for antitumor activity was disclosed,

compound **84**, with GI<sub>50</sub> values lower than 20 μM (Table 1, chapter 4) for lung cancer NCI-H460 and pancreatic adenocarcinoma cancer BxPC3 and PANC1 cell lines.

Some quinazolinone alkaloids displayed a moderate neuroprotective effect (chapter 4). Inspired in fiscalin B (**26**) which was reported as a substance P inhibitor to NK-1 receptor ( $K_i = 174 \mu\text{M}$ )<sup>67, 76-78</sup> and other derivatives such as fiscalin A (**27**)<sup>67, 69, 71-73</sup>, fiscalin C<sup>67, 69, 71-73</sup>, and (-)-spiroquinazoline<sup>202</sup> which were also reported as substance P inhibitors, the neuroprotection potential for compounds **78**, **84-94** library was accessed by a rotenone-damage human neuroblastoma cell model (Figure 2, chapter 4). Four compounds revealed more than 25% of protection (**78**, **84**, **87**, and **89**), considered as neuroprotectant agents. Compound **89**, having a sulfur atom, showing the best protection (about 40%). The 4*R* configuration was also found to be crucial for activity with the 4*S* enantiomers being inactive. Increasing the size of the C-1 substituent decreased the neuroprotective activity (Figure 4, chapter 4).

The main conclusion from chapter 5 was that the halogenated quinazolinone alkaloids are potent antimicrobials also in MDR strains. Inspired in neofiscalin A (**28**), which exhibited a potent antibacterial activity against *Staphylococcus aureus* and *Enterococcus faecalis* (MIC = 8 μM), and cotoquinazolin D which showed moderate antifungal activity against *Candida albicans* (MIC = 22.6 μM), we initially performed the screening on sixteen non-halogenated compounds, **76-83**, **86-93** for antimicrobial and antifungal activities. None of these derivatives inhibited the growth of microorganisms. Many studies indicated that other 2,3-disubstituted quinazolinones have valuable antimicrobial properties, and the structure activity relationship of quinazolinone derivatives in various studies on literature have revealed that substitutions at positions 5 and 14, existence of halogen atom at positions 9 and 11, and substitution (mainly amine or substituted amine) at position 6 of the quinazolinone ring can improve the antimicrobial activity. Based on these considerations, *anti*-isomers of the indolymethyl pyrazinoquinazoline ring system with different groups at positions 9 and 11 as well as in the anthranilic acid moiety were synthesized using the one-pot three component polycondensation microwave-assisted method. Compounds **95-109**, from 3,5-disubstituted anthranilic acids (Table 1, chapter 5) were synthesized. The screening for antibacterial activity of compound **95-109** against different strains of two Gram-positive (*S. aureus* ATCC 29213 and *E. faecalis* ATCC29212), two Gram-negative (*E. coli* ATCC25922 and *P. aeruginosa* ATCC27853), five environmental multidrug-resistant strains (*S. aureus* 66/1(MRSA), *S. aureus* 40/61/24, *E. faecalis* B3/101 (VRE), *E. coli* SA/2, *E. faecalis* A5/102 (VRE)), behaved similarly to neofiscalin A (**28**), none of the compounds was active against Gram-negative

bacteria, but some compounds such as **95-100**, **103-104** revealed inhibitory effects against Gram-positive bacteria (Table 2, chapter 5). Regarding multidrug-resistant strains, compounds **99** and **100** could also inhibit the growth of *S. aureus* resistant strains with MIC = 8  $\mu$ M. We found a hit compound, ((1*S*,4*R*)-4-((1*H*-indol-3-yl)methyl)-8,10-dichloro-1-isobutyl-1,2-dihydro-6*H*-pyrazino[2,1-*b*]quinazoline-3,6(4*H*)-dione) (**99**), for antibacterial on Gram positive and MDR strains (Table 2, chapter 5). The antifungal activity of compounds **94-113** against yeast and filamentous fungi such as *C. albicans*, *A. fumigatus*, *T. rubrum*, *M. canis*, and *E. floccosum* revealed compounds **99**, **101**, and **102** with inhibitory effects on a dermatophyte strain (*T. rubrum* FF55) with MIC values of 128  $\mu$ M and MFC >128  $\mu$ M (Table 3, chapter 5). To better understand the influence of the stereochemistry in the antimicrobial activity, the enantiomers of quinazolinone compounds **95**, **96** and **99**, which showed better antibacterial and/or antifungal activities, were selected for semipreparative liquid chromatography employing a *tris*-3,5-dimethylphenylcarbamate amylose phase, using polar organic solvent conditions and multi injections to obtain enantiopure compounds for further evaluation. The results revealed that no enantiomeric differences were observed for compound **95**; however, the pure enantiomer compound **99a** (1*S*, 4*R*) exhibited antibacterial activity with MIC = 4  $\mu$ M while its enantiomer **99b** (1*R*, 4*S*) showed no activity (Table 2, chapter 5). Comparing with the marine natural product neofiscalin A (**28**), a two-fold reduction in the MIC was observed<sup>74</sup>. These excellent and inspiring results obtained in the present study show that simpler molecules can retain antimicrobial activity.

Fiscalin B (**26**) and derivatives were characterized as antimalarial agents in chapter 6. The quinazolinone is the basic nucleus of febrifugine (**17**), a secondary metabolite of the Chinese medicinal plant Chang Shan (*Dichroa febrifuga*) that has been used in traditional medicine as antimalarial. This compound inhibits the formation of hemozoin (crystal resulting from the biomineralization of heme groups resulting from the digestion of hemoglobin in the digestive tract of the parasite during its erythrocyte development) necessary for the maturation of the parasite in the trophozoite stage. Febrifugine has an appreciable antimalarial effect and is easy to obtain<sup>203</sup>; however, the adverse side effects such as liver toxicity, preventing its clinical use<sup>204</sup>. In chapter 6, twenty-nine synthetic derivatives, namely **76-84**, **87**, **89**, **91**, **93-97**, **99-100**, **103-113** were evaluated for their antimalarial activity using an *in vitro* susceptibility assay with *P. falciparum* 3D7 strain. Compounds **78**, **79**, **82**, and **99** showed dose-response curves with IC<sub>50</sub> values of 0.1, 0.15, 0.05, and 0.2  $\mu$ M, respectively (Table 2, chapter 6). The results revealed that 4*R* is the preferable stereochemistry for this activity while

increasing the substituent size at C-1 decreased the inhibitory effect on *P. falciparum*. Introducing substituents on Ant moiety showed also a decrease in antimalarial activity. Compounds **78**, **82**, and **99** showed relatively low DL<sub>50</sub> values of 1.91, 1.78, and 14.00 μM when investigating on a non-tumor cell line, and all compounds showed SI values > 19 (Table 3, chapter 6), indicating an acceptable therapeutic window for the development of antimalarial agents. The hemotoxicity was tested to investigate the direct toxicity of the three hit compounds (**78**, **82**, and **99**). The percentages of hemolysis of the three compounds were < 10 % (Figure 2, chapter 6) which considered these compounds as nonhemolytics. However, these three compounds did not significantly inhibit the polymerization of β-hemetic *in vitro*. In this study, the three candidates, **78**, **82**, and **99**, were hypothesized by docking studies to bind to prolyl t-RNA synthetase, which could be useful for guiding the development of new antimalarial agents with this scaffold.

Feasible gram-scale syntheses of a synthetic fiscalin B (**78**) and its derivative **99** by the one-pot microwave-assisted irradiation were reported in chapter 7. In 2005, Lui *et al.* developed a microwave-assisted domino method using a three-component one-pot reaction to synthesize naturally-occurring fiscalin B (**26**) via a *N*-protected benzoxazine-4-one as intermediate <sup>111</sup>. This approach allowed, in this thesis, an easy access to the quinazolinone scaffold. The same authors also reported a gram-scale synthesis of (1*S*)-1-methyl-2,4-dihydro-1*H*-pyrazino[2,1-*b*]quinazoline-3,6-dione in a moderate yield of 53% starting from 10 mmol of anthranilic acid (Ant), *N*-Boc-L-alanine, and glycine methyl ester hydrochloride <sup>111</sup>. Herein, we were able to synthesize a synthetic fiscalin B (**78**) and derivative **99** in a single step by using parallel synthesis of 5 mL reaction vials volume for 2 minutes under microwave irradiation. As a result, we obtained 0.75 g of compound **99** (16.6%) and 1.79g (22.7%) of synthetic fiscalin B (**78**). The crystalline structure of *ent*-fiscalin B (+)-**78** was also reported in this chapter.

The main achievements of the work developed with quinazolinone derivatives in the framework of this thesis were:

- thirty-eight quinazolinone derivatives of fiscalin B (**26**) and fumiquinazoline G (**20**) were synthesized for the first time;
- synthetic fumiquinazoline G (**84**) ((1*R*,4*R*)-4-((1*H*-indol-3-yl)methyl)-1-methyl-1,2-dihydro-6*H*-pyrazino[2,1-*b*]quinazoline-3,6(4*H*)-dione) was a potent inhibitor of the tumor cell growth with GI<sub>50</sub> values between 7.6 to 17.3 μM;

- one quinazolinone derivative, compound **89** ((1*S*,4*R*)-4-((1*H*-indol-3-yl)methyl)-1-(2-(methylthio)ethyl)-1,2-dihydro-6*H*-pyrazino[2,1-*b*]quinazolin-3,6(4*H*)-dione), showed about 40% protection in rotenone-damage human neuroblastoma cell model;
- two chlorinated quinazolinone compounds, **99** ((1*S*,4*R*)-4-((1*H*-indol-3-yl)methyl)-8,10-dichloro-1-isobutyl-1,2-dihydro-6*H*-pyrazino[2,1-*b*]quinazolin-3,6(4*H*)-dione) and **100** ((1*S*,4*R*)-4-((1*H*-indol-3-yl)methyl)-1-((*S*)-*sec*-butyl)-8,10-dichloro-1,2-dihydro-6*H*-pyrazino[2,1-*b*]quinazolin-3,6(4*H*)-dione) presented effective activity against *Staphylococcus aureus* ATCC 29213 strain with MIC values of 4 µg/mL, and against two multidrug resistant strains of *S. aureus* 66/1 (MRSA) and *S. aureus* 40/61/24 strains with MIC values of 8 µg/mL;
- three halogenated quinazolinone compounds, **99**, **101** ((1*S*,4*R*)-4-((1*H*-indol-3-yl)methyl)-8-iodo-1-isopropyl-1,2-dihydro-6*H*-pyrazino[2,1-*b*]quinazolin-3,6(4*H*)-dione), and **102** ((1*S*,4*R*)-4-((1*H*-indol-3-yl)methyl)-8-bromo-1-isopropyl-1,2-dihydro-6*H*-pyrazino[2,1-*b*]quinazolin-3,6(4*H*)-dione), presented antifungal effect against *T. rubrum* FF5 with MIC values of 128 µg/mL;
- four quinazolinone alkaloids, compounds **78** ((1*S*,4*R*)-4-((1*H*-indol-3-yl)methyl)-1-isopropyl-1,2-dihydro-6*H*-pyrazino[2,1-*b*]quinazolin-3,6(4*H*)-dione), **79** ((1*R*,4*R*)-4-((1*H*-indol-3-yl)methyl)-1-isopropyl-1,2-dihydro-6*H*-pyrazino[2,1-*b*]quinazolin-3,6(4*H*)-dione), **82** ((1*S*,4*R*)-4-((1*H*-indol-3-yl)methyl)-1-isobutyl-1,2-dihydro-6*H*-pyrazino[2,1-*b*]quinazolin-3,6(4*H*)-dione), and **99**, presented to be effective against growth *P. falciparum* 3D7 strain with IC<sub>50</sub> values of 0.15, 0.1, 0.05, and 0.2 µM, respectively;
- five quinazolinone alkaloids, compounds **78**, **82**, **95**, **96**, and **99**, were successfully purified using semipreparative enantioselective liquid chromatography;
- gram-scale syntheses of synthetic fiscalin B (**78**) and compound **99** in a single step were accomplished;
- overall SAR could be established for the library of compounds synthesized (Figure 8A) and the most important synthetic challenges could be highlighted (Figure 8B)

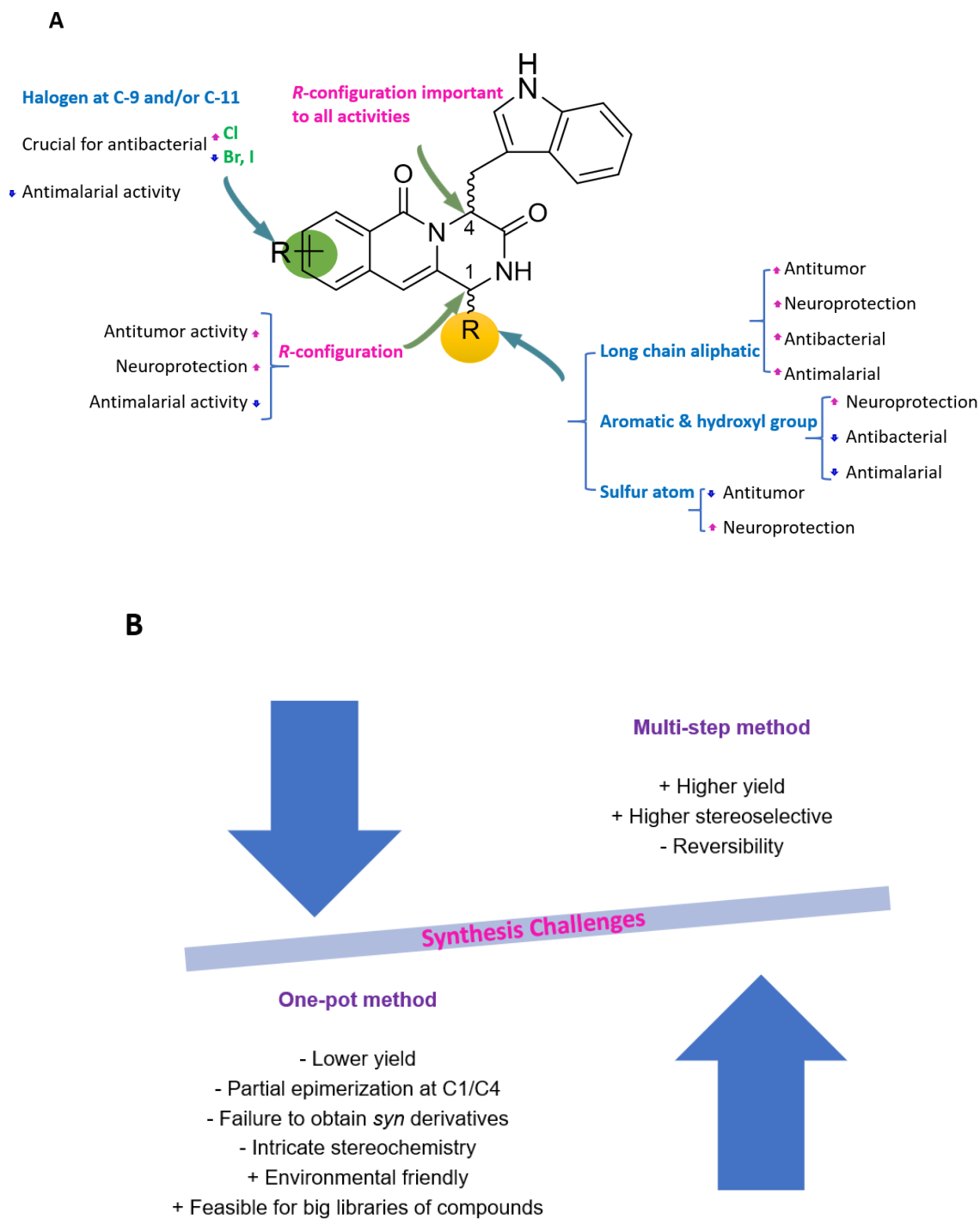


**Figure 8:** (A) Overall SAR of quinazolinone alkaloids for antitumor, neuroprotection, antimicrobial, and antimalarial activities. (B) Synthetic challenges in the synthesis of this library of compounds.

The global picture of this quinazoline scaffold SAR (Figure 8) shows that compounds that exhibited moderate to excellent effects in biological activities were the *anti*-isomers in which the *4R* configuration was found to be very important for all the activities; this library had no effect on P-glycoprotein modulation (Figure 8). The SAR study for antitumor shows that substituents and stereochemistry at C-1 strongly influence the activity. The *1R* configuration was associated to a stronger antitumor activity, and the bulky group at C-1 was found to improve the activity. However, the study of enantiomeric pure quinazolinones on their inhibitory effect on the growth of tumor cells is needed. This opens a window towards the antitumor activity investigation of the compounds having *1R*, *4R* configuration. The SAR for antimicrobial activity was quite robust revealing that only halogenated derivatives were active in both sensitive and MDR strains. This could draw the attention towards the study of halogenated derivatives also on antitumor activity models. The antimicrobial activity of halogenated compounds puts forward the *1S,4R* configuration as crucial. Future studies are needed to help understanding their antimicrobial mechanism of action and on resistance. From the SAR for neuroprotection, it is necessary to enlarge molecular modification of the compounds containing-sulfur. For the first time, this work explores this scaffold for antimalarial activity and insights in their mechanism of action are needed. Herein, we produced feasible quinazolinone alkaloid compounds, some of which targeting multiple activities. This result draws attention towards the putative toxicity profile for this scaffold that deserves to be explored beyond their biological properties. Therefore, further studies will consider their mechanisms of action for each activity and their toxicity profile earning to maximize potency and eliminate putative toxicity.

The main conclusion of chapter 8 was that amino carbazole alkaloids showed potential for p53 restoration. Three natural-isolated carbazole alkaloids – heptaphylline (**57**), 7-methoxyheptaphylline (**62**), and 7-methoxymukonal (**63**) were obtained from the group of Professor Phloentip Puthongking, isolated from a plant growth in Thailand, *Clausena harmandiana*. A different amino carbazole alkaloid has been reported to bind to p53, Phikan083 (**76**), by stabilizing the structure of mutant p53, and increasing the level of p53 with a wild-type conformation and activity<sup>205-206</sup>. In this work, a similar mechanism was hypothesized for heptaphylline (**57**) and its derivatives **62** and **63** for their cell growth inhibitory action. We developed a small library of twelve aminated derivatives, **114-125**, obtained by semi-synthesis to establish the role of the aldehyde in the activity and also the role of other amines. The natural carbazole alkaloids **57**, **62**, and **63** exhibited better activity, inhibiting all the investigated tumor cell lines both with wild-type and mutant isoforms of p53 when compared to the semi-synthetic

amino derivatives, compounds **114-125**. In contrast, compounds **117** and **120** showed some selectivity inhibiting the growth of cell lines expressing mutant p53 isoforms (Table 3, chapter 8).

The main achievements of chapter 8 were:

- twelve amino carbazole alkaloids, **114-125**, were obtained with moderate to good yields;
- derivatives of heptaphylline **114-125** showed a selective effect against cell lines expressing p-53 and some showed to activate several p53 mutants in a yeast model.

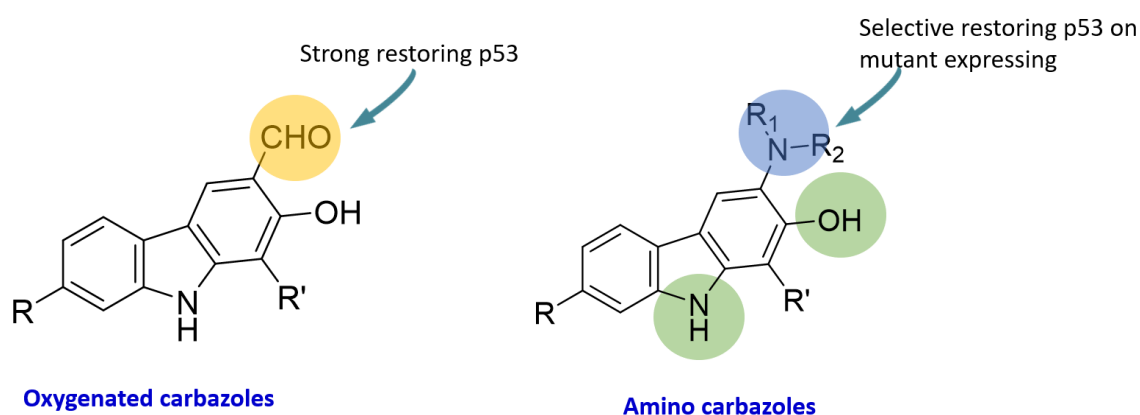


**Figure 9:** SAR of carbazole alkaloids for restoring p53 activity. The right side represents the structure naturally-occurring carbazole and the left side represents amino carbazole alkaloids.

Future work with this library of amino carbazoles will include the investigation of the full library in the yeast model to help understanding their effect on restoring p53 activity. The study of molecular modifications on positions 2 or 9 for this biological activity should be considered to increase the SAR of this carbazole scaffold for p53 modulation.



## Final Remarks

Until now, the design and synthesis of NPs analogues relied largely on trial and error, supplemented with hunches and experience of scientists. Attempts to synthesize the complex NPs is a big challenging in term of yield or/and time consuming. In this work, a library of NP quinazolinones was developed in a one-pot reaction. Through molecular modifications, we were able to produce compounds exhibiting moderate to excellent biological activities. Although several modifications did not improve the activity, these were important to stablish robust SAR. This thesis bares several pathways for the hit-to-lead optimization of the most promising hits, particularly in the quinazolinone library of compounds. Overall, we can say that this thesis contributes to the enlargement of the chemical/biological space of these families of alkaloids.



# Chapter 10

## References



The search for references used in the present thesis was made using following browsers  
(last access in January 2019)

<http://atoz.ebsco.com/titles.asp?id=uniporto&sid=122887192&TabID=2>

<http://apps.isiknowledge.com/>

<http://www.ncbi.nlm.nih.gov/pubmed/>

<http://pubs.rsc.org/en/search/advancedsearch>

<http://www.scirus.com/>

<http://www.scopus.com/scopus/home.url>

<http://onlinelibrary.wiley.com/advanced/search>

<http://www.google.pt/>

<http://www.sciencedirect.com/>

<http://pubs.acs.org/search/advanced>

<http://www.cas.org/>

1. Cobb, R. R. a. M., L. J., Drug Discovery: Design and Development. In *Principles and Practice of Pharmaceutical Medicine*, **2010**.
2. Cragg, G. M.; Newman, D. J., Natural products: A continuing source of novel drug leads. *Biochimica et Biophysica Acta (BBA) - General Subjects* **2013**, *1830* (6), 3670-3695.
3. Jiménez, C., Marine Natural Products in Medicinal Chemistry. *ACS Medicinal Chemistry Letters* **2018**, *9* (10), 959-961.
4. Romano, G.; Costantini, M.; Sansone, C.; Lauritano, C.; Ruocco, N.; Ianora, A., Marine microorganisms as a promising and sustainable source of bioactive molecules. *Marine Environmental Research* **2017**, *128*, 58-69.
5. Newman, D. J.; Cragg, G. M., Natural Products as Sources of New Drugs from 1981 to 2014. *Journal of Natural Products* **2016**, *79* (3), 629-661.
6. Jampilek, J.; Musiol, R.; Finster, J.; Pesko, M.; Carroll, J.; Kralova, K.; Vejsova, M.; O'Mahony, J.; Coffey, A.; Dohnal, J.; Polanski, J., Investigating biological activity spectrum for novel styrylquinazoline analogues. *Molecules* **2009**, *14* (10), 4246-4265.
7. Bérdy, J., Thoughts and facts about antibiotics: Where we are now and where we are heading. *The Journal Of Antibiotics* **2012**, *65*, 441.

8. Rateb, M. E.; Ebel, R., Secondary metabolites of fungi from marine habitats. *Natural Product Reports* **2011**, *28* (2), 290-344.
9. Blunt, J. W.; Copp, B. R.; Keyzers, R. A.; Munro, M. H. G.; Prinsep, M. R., Marine natural products. *Natural Product Reports* **2017**, *34* (3), 235-294.
10. Gribble, G. W., Biological Activity of Recently Discovered Halogenated Marine Natural Products. *Marine Drugs* **2015**, *13* (7), 4044-4136.
11. Choudhary, A.; Naughton, M. L.; Montánchez, I.; Dobson, D. A.; Rai, K. D., Current Status and Future Prospects of Marine Natural Products (MNPs) as Antimicrobials. *Marine Drugs* **2017**, *15* (9).
12. Ruiz-Torres, V.; Encinar, J. A.; Herranz-López, M.; Pérez-Sánchez, A.; Galiano, V.; Barrajón-Catalán, E.; Micol, V., An Updated Review on Marine Anticancer Compounds: The Use of Virtual Screening for the Discovery of Small-Molecule Cancer Drugs. *Molecules* **2017**, *22* (7), 1037.
13. Zhang, G.; Li, J.; Zhu, T.; Gu, Q.; Li, D., Advanced tools in marine natural drug discovery. *Current Opinion in Biotechnology* **2016**, *42*, 13-23.
14. Kong, D.-X.; Jiang, Y.-Y.; Zhang, H.-Y., Marine natural products as sources of novel scaffolds: achievement and concern. *Drug Discovery Today* **2010**, *15* (21), 884-886.
15. Montaser, R.; Luesch, H., Marine natural products: A new wave of drugs? *Future Medicinal Chemistry* **2011**, *3* (12), 1475-1489.
16. Guo, Z., The modification of natural products for medical use. *Acta Pharmaceutica Sinica B* **2017**, *7* (2), 119-136.
17. Hopkins, A. L.; Groom, C. R.; Alex, A., Ligand efficiency: A useful metric for lead selection. *Drug Discovery Today* **2004**, *9* (10), 430-431.
18. Aicher, T. D.; Buszek, K. R.; Fang, F. G.; Forsyth, C. J.; Jung, S. H.; Kishi, Y.; Matelich, M. C.; Scola, P. M.; Spero, D. M.; Yoon, S. K., Total Synthesis of Halichondrin B and Norhalichondrin B. *Journal of the American Chemical Society* **1992**, *114* (8), 3162-3164.
19. Liu, G. T., From the study of Fructus schizandrae to the discovery of biphenyl dimethyl-dicarboxylate. *Acta Pharmaceutica Sinica* **1983**, *18* (9), 714-720.
20. Istvan, E. S.; Deisenhofer, J., Structural mechanism for statin inhibition of HMG-CoA reductase. *Science* **2001**, *292* (5519), 1160-1164.

21. Finnin, M. S.; Donigian, J. R.; Cohen, A.; Richon, V. M.; Rifkind, R. A.; Marks, P. A.; Breslow, R.; Pavletich, N. P., Structures of a histone deacetylase homologue bound to the TSA and SAHA inhibitors. *Nature* **1999**, *401* (6749), 188-193.
22. Higgins, D. L.; Chang, R.; Debabov, D. V.; Leung, J.; Wu, T.; Krause, K. M.; Sandvik, E.; Hubbard, J. M.; Kaniga, K.; Schmidt Jr, D. E.; Gao, Q.; Cass, R. T.; Karr, D. E.; Benton, B. M.; Humphrey, P. P., Telavancin, a multifunctional lipoglycopeptide, disrupts both cell wall synthesis and cell membrane integrity in methicillin-resistant *Staphylococcus aureus*. *Antimicrobial Agents and Chemotherapy* **2005**, *49* (3), 1127-1134.
23. Liu, X.; Bai, K., Reconnaissance of ancient kiln sites at Hutian in Jingdezhen. *Wen Wu (Cultural Relics)* **1980**, *11*, 39-49.
24. Nomura, S.; Sakamaki, S.; Hongu, M.; Kawanishi, E.; Koga, Y.; Sakamoto, T.; Yamamoto, Y.; Ueta, K.; Kimata, H.; Nakayama, K.; Tsuda-Tsukimoto, M., Discovery of canagliflozin, a novel C-glucoside with thiophene ring, as sodium-dependent glucose cotransporter 2 inhibitor for the treatment of type 2 diabetes mellitus (1). *Journal of Medicinal Chemistry* **2010**, *53* (17), 6355-6360.
25. Lee, F. Y. F.; Borzilleri, R.; Fairchild, C. R.; Kamath, A.; Smykla, R.; Kramer, R.; Vite, G., Preclinical discovery of ixabepilone, a highly active antineoplastic agent. *Cancer Chemotherapy and Pharmacology* **2008**, *63* (1), 157-166.
26. Amirkia, V.; Heinrich, M., Alkaloids as drug leads – A predictive structural and biodiversity-based analysis. *Phytochemistry Letters* **2014**, *10*, xlviii-lviii.
27. Gul, W.; Hamann, M. T., Indole alkaloid marine natural products: An established source of cancer drug leads with considerable promise for the control of parasitic, neurological and other diseases. *Life Sciences* **2005**, *78* (5), 442-453.
28. Sravanthi, T. V.; Manju, S. L., Indoles — A promising scaffold for drug development. *European Journal of Pharmaceutical Sciences* **2016**, *91*, 1-10.
29. Chadha, N.; Silakari, O., Indoles as therapeutics of interest in medicinal chemistry: Bird's eye view. *European Journal of Medicinal Chemistry* **2017**, *134*, 159-184.
30. Lal, S.; Snape, T. J., 2-Arylindoles: A Privileged Molecular Scaffold with Potent, Broad-Ranging Pharmacological Activity. *Current Medicinal Chemistry* **2012**, *19* (28), 4828-4837.
31. Hui, X.; Min, L., Developments of Indoles as Anti-HIV-1 Inhibitors. *Current Pharmaceutical Design* **2009**, *15* (18), 2120-2148.

32. Yohimbine: The Effects on Body Composition and Exercise Performance in Soccer Players AU - Ostojic, Sergej M. *Research in Sports Medicine* **2006**, 14 (4), 289-299.
33. Isaac, M. T., Review: Combining pindolol with an SSRI improves early outcomes in people with depression - Commentary. *Evidence-Based Mental Health* **2004**, 7 (4), 107.
34. Lednicer, D., *The Organic Chemistry of Drug Synthesis-A* **2007**, 7, 141-154.
35. Kolli, P. S., Apaziquone for non-muscle invasive bladder cancer: a critical review AU - Witjes, J Alfred. *Expert Opinion on Investigational Drugs* **2008**, 17 (7), 1085-1096.
36. Leneva, I. A.; Russell, R. J.; Boriskin, Y. S.; Hay, A. J., Characteristics of arbidol-resistant mutants of influenza virus: Implications for the mechanism of anti-influenza action of arbidol. *Antiviral Research* **2009**, 81 (2), 132-140.
37. Prince, H. M.; Bishton, M., Panobinostat (LBH589): A novel pan-deacetylase inhibitor with activity in T cell lymphoma. *Haematologica Meeting Reports* **2009**, 3 (1), 33-38.
38. Khan, I.; Ibrar, A.; Abbas, N.; Saeed, A., Recent advances in the structural library of functionalized quinazoline and quinazolinone scaffolds: Synthetic approaches and multifarious applications. *European Journal of Medicinal Chemistry* **2014**, 76, 193-244.
39. Resende, D. I. S. P.; Boonpothong, P.; Sousa, E.; Kijjoa, A.; Pinto, M. M. M., Chemistry of the fumiquinazolines and structurally related alkaloids. *Natural Product Reports* **2018**.
40. Zhang, J.; Liu, J.; Ma, Y.; Ren, D.; Cheng, P.; Zhao, J.; Zhang, F.; Yao, Y., One-pot synthesis and antifungal activity against plant pathogens of quinazolinone derivatives containing an amide moiety. *Bioorganic and Medicinal Chemistry Letters* **2016**, 26 (9), 2273-2277.
41. Kikuchi, H.; Yamamoto, K.; Horoiwa, S.; Hirai, S.; Kasahara, R.; Hariguchi, N.; Matsumoto, M.; Oshima, Y., Exploration of a New Type of Antimalarial Compounds Based on Febrifugine. *Journal of Medicinal Chemistry* **2006**, 49 (15), 4698-4706.
42. Kraemer, T.; Maurer, H. H., Chapter 6 Sedatives and hypnotics. In *Handbook of Analytical Separations*, Bogusz, M. J., Ed. Elsevier Science B.V.: 2008; Vol. 6, pp 243-286.
43. Demeunynck, M.; Baussanne, I., Survey of recent literature related to the biologically active 4(3H)-quinazolinones containing fused heterocycles. *Current Medicinal Chemistry* **2013**, 20 (6), 794-814.
44. Penn, J.; Mantle, P. G.; Bilton, J. N.; Sheppard, R. N., Gyantrypine, a novel anthranilic acid-containing metabolite of *Aspergillus clavatus*. *Journal of Chemical Society Perkin Transactions 1* **1992**, 1495-1496.



45. Fan, Y.-Q.; Li, P.-H.; Chao, Y.-X.; Chen, H.; Du, N.; He, Q.-X.; Liu, K.-C., Alkaloids with cardiovascular effects from the marine-derived fungus *Penicillium expansum* Y32. *Marine Drugs* **2015**, *13* (10), 6489-6504.
46. Liu, Y.; Li, X.-M.; Meng, L.-H.; Wang, B.-G., N-Formyllapatin A, a new N-formylspiroquinazoline derivative from the marine-derived fungus *Penicillium adametzioides* AS-53. *Phytochemistry Letters* **2014**, *10*, 145-148.
47. Peng, J.; Lin, T.; Wang, W.; Xin, Z.; Zhu, T.; Gu, Q.; Li, D., Antiviral alkaloids produced by the mangrove-derived fungus *Cladosporium* sp. PJX-41. *Journal of Natural Products* **2013**, *76* (6), 1133-1140.
48. Zhuang, Y.; Teng, X.; Wang, Y.; Liu, P.; Wang, H.; Li, J.; Li, G.; Zhu, W., Cyclopeptides and polyketides from coral-associated fungus, *Aspergillus versicolor* LCJ-5-4. *Tetrahedron* **2011**, *67* (37), 7085-7089.
49. Zhou, Y.; Debbab, A.; Mándi, A.; Wray, V.; Schulz, B.; Müller, W. E. G.; Kassack, M.; Lin, W.; Kurtán, T.; Proksch, P.; Aly, A. H., Alkaloids from the sponge-associated fungus *Aspergillus* sp. *European Journal of Organic Chemistry* **2013**, *5* (5), 894-906.
50. Belofsky, G. N.; Anguera, M.; Jensen, P. R.; Fenical, W.; Köck, M., Oxepinamides A-C and Fumiquinazolines H-I: Bioactive Metabolites from a Marine Isolate of a Fungus of the Genus *Acremonium*. *Chemistry European Journal* **2000**, *6* (8), 1355-1360.
51. Numata, A.; Takahashi, C.; Matsushita, T.; Miyamoto, T.; Kawai, K.; Usami, Y.; Matsumura, E.; Inoue, M.; Ohishi, H.; Shingu, T., Fumiquinazolines, novel metabolites of a fungus isolated from a saltfish. *Tetrahedron Letters* **1992**, *33* (12), 1621-1624.
52. Takahashi, C.; Matsushita, T.; Doi, M.; Minoura, K.; Shingu, T.; Kumeda, Y.; Numata, A., Fumiquinazolines A–G, novel metabolites of a fungus separated from a *Pseudolabrus* marine fish. *Journal of Chemical Society Perkin Transaction 1* **1995**, 2345-2353.
53. Shao, C.-L.; Xu, R.-F.; Wei, M.-Y.; She, Z.-G.; Wang, C.-Y., Structure and absolute configuration of fumiquinazoline L, an alkaloid from a gorgonian-derived *Scopulariopsis* sp. fungus. *Journal of Natural Products* **2013**, *76* (4), 779-782.
54. Liao, L.; You, M.; Chung, B. K.; Oh, D.-C.; Oh, K.-B.; Shin, J., Alkaloidal metabolites from a marine-derived *Aspergillus* sp. fungus. *Journal of Natural Products* **2015**, *78* (3), 349-354.
55. Tamiya, H.; Ochiai, E.; Kikuchi, K.; Yahiro, M.; Toyotome, T.; Watanabe, A.; Yaguchi, T.; Kamei, K., Secondary metabolite profiles and antifungal drug susceptibility of *Aspergillus fumigatus* and

- closely related species, *Aspergillus lentulus*, *Aspergillus udagawae*, and *Aspergillus viridinutans*. *Journal of Infection and Chemotherapy* **2015**, 21 (5), 385-391.
56. He, F.; Sun, Y.-L.; Liu, K.-S.; Zhang, X.-Y.; Qian, P.-Y.; Wang, Y.-F.; Qi, S.-H., Indole alkaloids from marine-derived fungus *Aspergillus sydowii* SCSIO 00305. *Journal of Antibiotics* **2012**, 65 (2), 109-111.
  57. Han, X.-x.; Xu, X.-y.; Cui, C.-b.; Gu, Q.-q., Alkaloidal compounds produced by a marine-derived fungus, *Aspergillus fumigatus* H1-04, and their antitumor activities. *Chinese Journal of Organic Chemistry* **2007**, 17 (4), 232-237.
  58. Hwang, I. H.; Che, Y.; Swenson, D. C.; Gloer, J. B.; Wicklow, D. T.; Peterson, S. W.; Dowd, P. F., Haenamindole and fumiquinazoline analogs from a fungicolous isolate of *Penicillium lanosum*. *Journal of Antibiotic* **2016**, 69 (8), 631-636.
  59. Gauthier, T.; Wang, X.; Dos Santos, J.; Fysikopoulos, A.; Tadrist, S.; Canlet, C.; Artigot, M. P.; Loiseau, N.; Oswald, I. P.; Puel, O., Trypacidin, a spore-borne toxin from *Aspergillus fumigatus*, is cytotoxic to lung cells. *PLoS ONE* **2012**, 7 (2), e29906.
  60. Kang, D.; Son, G. H.; Park, H. M.; Kim, J.; Choi, J. N.; Kim, H. Y.; Lee, S.; Hong, S.-B.; Lee, C. H., Culture condition-dependent metabolite profiling of *Aspergillus fumigatus* with antifungal activity. *Fungal Biology* **2013**, 117 (3), 211-219.
  61. Li, X.-J.; Zhang, Q.; Zhang, A.-L.; Gao, J.-M., Metabolites from *Aspergillus fumigatus*, an Endophytic Fungus Associated with *Melia azedarach*, and Their Antifungal, Antifeedant, and Toxic Activities. *Journal of Agricultural and Food Chemistry* **2012**, 60 (13), 3424-3431.
  62. Silva, M. G.; Furtado, N. A. J. C.; Pupo, M. T.; Fonseca, M. J. V.; Said, S.; Filho, A. A. d. S.; Bastos, J. K., Antibacterial activity from *Penicillium corylophilum* Dierckx. *Microbiology Research* **2004**, 159 (4), 317-322.
  63. Ates, E.; Godula, M.; Stroka, J.; Senyuva, H., Screening of plant and fungal metabolites in wheat, maize and animal feed using automated on-line clean-up coupled to high resolution mass spectrometry. *Food Chemistry* **2014**, 142, 276-284.
  64. Larsen, T. O.; Frydenvang, K.; Frisvad, J. C.; Christophersen, C., UV-guided isolation of alantrypinone, a novel *Penicillium* alkaloid. *Journal of Natural Products* **1998**, 61 (9), 1154-1157.
  65. Lan, W.-J.; Fu, S.-J.; Xu, M.-Y.; Liang, W.-L.; Lam, C.-K.; Zhong, G.-H.; Xu, J.; Yang, D.-P.; Li, H.-J., Five New Cytotoxic Metabolites from the Marine Fungus *Neosartorya pseudofischeri*. *Marine Drugs* **2016**, 14 (1), 18-30.

66. Afiyatullof, S. S.; Zhuravleva, O. I.; Antonov, A. S.; Kalinovsky, A. I.; Pivkin, M. V.; Menchinskaya, E. S.; Aminin, D. L., New metabolites from the marine-derived fungus *Aspergillus fumigatus*. *Natural Product Communications* **2012**, 7 (4), 497-500.
67. Wong, S.-M.; Musza, L. L.; Kydd, G. C.; Kullnig, R.; Gillum, A. M.; Cooper, R., Fiscalins: new substance P inhibitors produced by the fungus *Neosartorya fisheri* taxonomy, fermentation, structure, and biological properties. *Journal of Antibiotic* **1993**, 46 (4), 545-553.
68. Snider, B. B.; Zeng, H., Total synthesis of (-)-fumiquinazolines A, B, C, E, H, and I. Approaches to the synthesis of fiscalin A. *Journal of Organic Chemistry* **2003**, 68 (2), 545-563.
69. Buttachon, S.; Chandrapatya, A.; Manoch, L.; Silva, A.; Gales, L.; Bruyère, C.; Kiss, R.; Kijjoa, A., Sartorymensin, a new indole alkaloid, and new analogues of tryptoquivaline and fiscalins produced by *Neosartorya siamensis* (KUFC 6349). *Tetrahedron* **2012**, 68 (15), 3253-3262.
70. Sodngam, S.; Sawadsitang, S.; Suwannasai, N.; Mongkolthamaruk, W., Chemical constituents, and their cytotoxicity, of the rare wood decaying fungus *Xylaria humosa*. *Natural Product Communications* **2014**, 9 (2), 157-158.
71. Sodngam, S.; Sawadsitang, S.; Suwannasai, N.; Mongkolthamaruk, W., Chemical constituents, and their cytotoxicity, of the rare wood decaying fungus *Xylaria humosa*. *Natural Product Communications* **2014**, 9 (2), 157-158.
72. Prata-Sena, M.; Ramos, A. A.; Buttachon, S.; Castro-Carvalho, B.; Marques, P.; Dethoup, T.; Kijjoa, A.; Rocha, E., Cytotoxic activity of Secondary Metabolites from Marine-derived Fungus *Neosartorya siamensis* in Human Cancer Cells. *Phytotherapy Research* **2016**, 30 (11), 1862–1871.
73. War May Zin, W.; Prompanya, C.; Buttachon, S.; Kijjoa, A., Bioactive Secondary Metabolites from a Thai Collection of Soil and Marine-Derived Fungi of the Genera *Neosartorya* and *Aspergillus*. *Current Drug Delivery* **2016**, 13 (3), 378-388.
74. Bessa, L. J.; Buttachon, S.; Dethoup, T.; Martins, R.; Vasconcelos, V.; Kijjoa, A.; da Costa, P. M., Neofiscalin A and fiscalin C are potential novel indole alkaloid alternatives for the treatment of multidrugresistant Gram-positive bacterial infections. *FEMS Microbiology Letters* **2016**, 363 (15).
75. Zin, W. W. M.; Prompanya, C.; Buttachon, S.; Kijjoa, A., Bioactive secondary metabolites from a thai collection of soil and marine-derived fungi of the genera *neosartorya* and *aspergillus*. *Current Drug Delivery* **2016**, 13 (3), 378-388.

76. Rodrigues, B. S. F.; Sahm, B. D. B.; Jimenez, P. C.; Pinto, F. C. L.; Mafezoli, J.; Mattos, M. C.; Rodrigues-Filho, E.; Pfenning, L. H.; Abreu, L. M.; Costa-Lotufo, L. V.; Oliveira, M. C. F., Bioprospection of cytotoxic compounds in fungal strains recovered from sediments of the Brazilian coast. *Chemistry and Biodiversity* **2015**, *12* (3), 432-442.
77. Fujimoto, H.; Negishi, E.; Yamaguchi, K.; Nishi, N.; Yamazaki, M., Isolation of new tremorgenic metabolites from an Ascomycete, *Corynascus setosus*. *Chemical and Pharmaceutical Bulletin* **1996**, *40* (11), 1843-1848.
78. Wu, B.; Chen, G.; Liu, Z.-g.; Pei, Y., Two new alkaloids from a marine-derived fungus *Neosartorya fischeri*. *Record of Natural Products* **2015**, *9* (3), 271-275.
79. Sawadsitang, S.; Mongkolthanaruk, W.; Suwannasai, N.; Sodngam, S., Antimalarial and cytotoxic constituents of *Xylaria* cf. *cubensis* PK108. *Natural Product Research* **2015**, *29* (21), 2033-6.
80. Yu, G.; Zhou, G.; Zhu, M.; Wang, W.; Zhu, T.; Gu, Q.; Li, D., Neosartoryadins A and B, fumiquinazoline alkaloids from a mangrove-derived fungus *Neosartorya udagawae* HDN13-313. *Organic Letters* **2016**, *18* (2), 244-7.
81. Kshirsagar, U. A., Recent developments in the chemistry of quinazolinone alkaloids. *Organic and Biomolecular Chemistry* **2015**, *13* (36), 9336-9352.
82. Rajput, R.; Mishra, A. P., A review on biological activity of quinazolinones. *International Journal of Pharmacy and Pharmaceutical Sciences* **2012**, *4* (2), 66-70.
83. Eguchi, S., Quinazoline Alkaloids and Related Chemistry. *Topics in Heterocyclic Chemistry* **2006**, *6*, 113-156.
84. Eguchi, S., Recent progress in the synthesis of heterocyclic natural products by the Staudinger/intramolecular aza-Wittig reaction. *Arkivoc* **2005**, *2005* (2), 98-99.
85. Mhaske, S. B.; Argade, N. P., The chemistry of recently isolated naturally occurring quinazolinone alkaloids. *Tetrahedron* **2006**, *62* (42), 9787-9826.
86. Kshirsagar, U. A., Recent developments in the chemistry of quinazolinone alkaloids. *Organic and Biomolecular Chemistry* **2015**, *13* (36), 9336-52.
87. Tseng, M.-C.; Chu, Y.-H., Zinc triflate-catalyzed synthesis of pyrazino 2,1-b quinazoline-3,6-diones. *Tetrahedron* **2008**, *64* (40), 9515-9520.
88. Kshirsagar, U. A.; Rohokale, R. S., Advanced Synthetic Strategies for Constructing Quinazolinone Scaffolds. *Synthesis* **2016**, *48* (09), 1253-1268.

89. Avendano, C.; Menéndez, J. C., Chemistry of Pyrazino[2,1-b]quinazoline-3,6-diones. *Current Organic Chemistry* **2003**, 7 (2), 149-173.
90. Takeuchi, H.; Eguchi, S., A new route to quinazolinones via intramolecular aza-Wittig reaction. *Tetrahedron Letters* **1989**, 30 (25), 3313-3314.
91. Takeuchi, H.; Hagiwara, S.; Eguchi, S., A new efficient synthesis of imidazolinones and quinazolinone by intramolecular aza-Wittig reaction. *Tetrahedron* **1989**, 45 (20), 6375-6386.
92. Sugimori, T.; Okawa, T.; Eguchi, S.; Kakehi, A.; Yashima, E.; Okamoto, Y., The first total synthesis of (-)-benzomalvin A and benzomalvin B via the intramolecular aza-Wittig reactions. *Tetrahedron* **1998**, 54 (28), 7997-8008.
93. Mazurkiewicz, R., Synthesis and rearrangement of 4-imino-4H-3,1-benzoxazines. *Monatshefte für Chemie* **1989**, 120 (11), 973-980.
94. Wang, H.; Ganesan, A., Total Synthesis of the Quinazoline Alkaloids (-)-Fumiquinazoline G and (-)-Fiscalin B. *Journal of Organic Chemistry* **1998**, 63 (8), 2432-2433.
95. Wang, H.; Ganesan, A., Total Synthesis of the Fumiquinazoline Alkaloids: Solution-Phase Studies1. *Journal of Organic Chemistry* **2000**, 65 (4), 1022-1030.
96. Liu, J.-F.; Lee, J.; Dalton, A. M.; Bi, G.; Yu, L.; Baldino, C. M.; McElory, E.; Brown, M., Microwave-assisted one-pot synthesis of 2,3-disubstituted 3H-quinazolin-4-ones. *Tetrahedron Letters* **2005**, 46 (8), 1241-1244.
97. He, F.; Snider, B. B., Total synthesis of (+)-fumiquinazoline G and (+)-dehydrofumiquinazoline G. *Synlett* **1997**, (5), 483-484.
98. Snider, B. B.; Busuyek, M. V., Synthesis of circumdatin F and sclerotigenin. Use of the 2-nitrobenzyl group for protection of a diketopiperazine amide; synthesis of ent-fumiquinazoline G. *Tetrahedron* **2001**, 57 (16), 3301-3307.
99. He, F.; Foxman, B. M.; Snider, B. B., Total Syntheses of (-)-Asperlicin and (-)-Asperlicin C. *J. Am. Chem. Soc.* **1998**, 120 (25), 6417-6418.
100. Hernández, F.; Buenadicha, F. L.; Avendaño, C.; Söllhuber, M., 1-Alkyl-2,4-dihydro-1H-pyrazino[2,1-b]quinazoline-3,6-diones as glycine templates. Synthesis of Fiscalin B. *Tetrahedron Asymmetry* **2001**, 12 (24), 3387-3398.
101. Wipf, P.; Miller, C. P., A new synthesis of highly functionalized oxazoles. *J. Org. Chem.* **1993**, 58 (14), 3604-3606.

102. He, F.; Snider, B. B., Rearrangement of 4-Imino-4H-3,1-benzoxazines to 4-Quinazolinones via Amidine Carboxamides. *Journal of Organic Chemistry* **1999**, *64* (4), 1397–1399.
103. Hart, D. J.; Magomedov, N. A., Synthesis of (-)-alantrypinone. *Tetrahedron Letters* **1999**, *40* (30), 5429–5432.
104. Hart, D. J.; Magomedov, N. A., Synthesis of ent-Alantrypinone. *Journal of American Chemical Society* **2001**, *123* (25), 5892-5899.
105. Wang, H.; Sim, M. M., Total Solid Phase Syntheses of the Quinazoline Alkaloids: Verrucines A and B and Anacine. *Journal of Natural Products* **2001**, *64* (12), 1497-1501.
106. Witt, A.; Bergman, J., Total Syntheses of the Benzodiazepine Alkaloids Circumdatin F and Circumdatin C. *Journal of Organic Chemistry* **2001**, *66* (8), 2784-2788.
107. Snider, B. B.; Zeng, H., Total Syntheses of (-)-Fumiquinazolines A, B, and I. *Organic Letters* **2000**, *2* (25), 4103-4106.
108. Wang, H.; Ganesan, A., Total Synthesis of the Fumiquinazoline Alkaloids: Solid-Phase Studies. *Journal of Combinatorial Chemistry* **2000**, *2* (2), 186-194.
109. Snider, B. B.; Zeng, H., Total Syntheses of (-)-Fumiquinazolines C, E, and H. *Organic Letters* **2002**, *4* (7), 1087-1090.
110. Cledera, P.; Sánchez, J. D.; Caballero, E.; Yates, T.; Ramírez, E. G.; Avendaño, C.; Ramos, M. T.; Menéndez, J. C., Microwave-assisted, solvent-free synthesis of several quinazoline alkaloid frameworks. *Synthesis* **2007**, (21), 3390-3398.
111. Liu, J. F.; Ye, P.; Zhang, B.; Bi, G.; Sargent, K.; Yu, L.; Yohannes, D.; Baldino, C. M., Three-component one-pot total syntheses of glyantrypine, fumiquinazoline F, and fiscalin B promoted by microwave irradiation. *Journal of Organic Chemistry* **2005**, *70* (16), 6339-6345.
112. Knölker, H.-J.; Reddy, K. R., Chapter 5 - Chemistry of Carbazole Alkaloids. In *The Alkaloids: Chemistry and Biology*, Cordell, G. A., Ed. Academic Press: 2008; Vol. 65, pp 195-383.
113. Knölker, H.-J.; Reddy, K. R., Isolation and Synthesis of Biologically Active Carbazole Alkaloids. *Chemical Reviews* **2002**, *102* (11), 4303-4428.
114. Tsutsumi, L. S.; Gündisch, D.; Sun, D., Carbazole scaffold in medicinal chemistry and natural products: A review from 2010-2015. *Current Topics in Medicinal Chemistry* **2016**, *16* (11), 1290-1313.
115. Tian-Shung, W.; Shiow-Chyn, H.; Pei-Lin, W.; Che-Ming, T., Carbazole alkaloids from *Clausena excavata* and their biological activity. *Phytochemistry* **1996**, *43* (1), 133-140.

116. Maneerat, W.; Phakhodee, W.; Ritthiwigrom, T.; Cheenpracha, S.; Promgool, T.; Yossathera, K.; Deachathai, S.; Laphookhieo, S., Antibacterial carbazole alkaloids from *Clausena harmandiana* twigs. *Fitoterapia* **2012**, 83 (6), 1110-1114.
117. Chakraborty, A.; Saha, C.; Podder, G.; Chowdhury, B. K.; Bhattacharyya, P., Carbazole alkaloid with antimicrobial activity from *clausena heptaphylla*. *Phytochemistry* **1995**, 38 (3), 787-789.
118. Yenjai, C.; Sripontan, S.; Sriprajun, P.; Kittakoo, P.; Jintasirikul, A.; Tanticharoen, M.; Thebtaranonth, Y., Coumarins and carbazoles with antiplasmodial activity from *Clausena harmandiana*. *Planta Medica* **2000**, 66 (3), 277-279.
119. Saturnino, C.; Iacopetta, D.; Sinicropi, M.; Rosano, C.; Caruso, A.; Caporale, A.; Marra, N.; Marengo, B.; Pronzato, M.; Parisi, O.; Longo, P.; Ricciarelli, R., N-Alkyl Carbazole Derivatives as New Tools for Alzheimer's Disease: Preliminary Studies. *Molecules* **2014**, 19 (7), 9307.
120. Krahl, M. P.; Jäger, A.; Krause, T.; Knölker, H. J., First total synthesis of the 7-oxygenated carbazole alkaloids clauszoline-K, 3-formyl-7-hydroxycarbazole, clausine M, clausine N and the anti-HIV active siamenol using a highly efficient palladium-catalyzed approach. *Organic and Biomolecular Chemistry* **2006**, 4 (17), 3215-3219.
121. Wangboonskul, J. D.; Pummangura, S.; Chaichantipyuth, C., Five Coumarins and A Carbazole Alkaloid from the Root Bark of *Clausena Harmandiana*. *Journal of Natural Products* **1984**, 47 (6), 1058-1059.
122. Issa, S.; Walchshofer, N.; Kassab, I.; Termoss, H.; Chamat, S.; Geahchan, A.; Bouaziz, Z., Synthesis and antiproliferative activity of oxazinocarbazole and N,N-bis(carbazolylmethyl)amine derivatives. *European Journal of Medicinal Chemistry* **2010**, 45 (6), 2567-2577.
123. Chen, Y. L.; Hung, H. M.; Lu, C. M.; Li, K. C.; Tzeng, C. C., Synthesis and anticancer evaluation of certain indolo[2,3-b]quinoline derivatives. *Bioorganic and Medicinal Chemistry* **2004**, 12 (24), 6539-6546.
124. Compain-Batissou, M.; Latreche, D.; Gentili, J.; Walchshofer, N.; Bouaziz, Z., Synthesis and Diels-Alder reactivity of ortho-carbazolequinones. *Chemical and Pharmaceutical Bulletin* **2004**, 52 (9), 1114-1116.
125. Thongthoom, T.; Promsuwan, P.; Yenjai, C., Synthesis and cytotoxic activity of the heptaphylline and 7-methoxyheptaphylline series. *European Journal of Medicinal Chemistry* **2011**, 46 (9), 3755-3761.

126. Schmidt, A. W.; Reddy, K. R.; Knölker, H.-J., Occurrence, Biogenesis, and Synthesis of Biologically Active Carbazole Alkaloids. *Chemical Reviews* **2012**, *112* (6), 3193-3328.
127. Bhattacharyya, P.; Chowdhury, B. K.; Mustapha, A.; Garba, M., Carbazole and 3-methylcarbazole from *Glycosmis pentaphylla*. *Phytochemistry* **1987**, *26* (7), 2138-2139.
128. Roy, S.; Bhattacharyya, P.; Chakraborty, D. P., 3-methylcarbazole from *Clausena heptaphylla*. *Phytochemistry* **1974**, *13* (6), 1017.
129. Chakrabarty, M.; Nath, A. C.; Khasnobis, S.; Chakrabarty, M.; Konda, Y.; Harigaya, Y.; Komiyama, K., Carbazole alkaloids from *Murraya koenigii*. *Phytochemistry* **1997**, *46* (4), 751-755.
130. Ito, C.; Wu, T.-S.; Furukawa, H., New Carbazole Alkaloids from *Murraya euchrestifolia*. *Chemical and pharmaceutical bulletin* **1988**, *36* (7), 2377-2380.
131. Pieper, A. A.; Xie, S.; Capota, E.; Estill, S. J.; Zhong, J.; Long, J. M.; Becker, G. L.; Huntington, P.; Goldman, S. E.; Shen, C. H.; Capota, M.; Britt, J. K.; Kotti, T.; Ure, K.; Brat, D. J.; Williams, N. S.; MacMillan, K. S.; Naidoo, J.; Melito, L.; Hsieh, J.; De Brabander, J.; Ready, J. M.; McKnight, S. L., Discovery of a Proneurogenic, Neuroprotective Chemical. *Cell* **2010**, *142* (1), 39-51.
132. Zhu, L.; Hites, R. A., Identification of Brominated Carbazoles in Sediment Cores from Lake Michigan. *Environmental Science & Technology* **2005**, *39* (24), 9446-9451.
133. Furukawa, H.; Ohta, T.; Wu, T. S.; Kuoh, C. S., Chemical Constituents of *Murraya Euchrestifolia* Hayata. Structures of Novel Carbazolequinones and Other New Carbazole Alkaloids. *Chemical and Pharmaceutical Bulletin* **1985**, *33* (10), 4132-4138.
134. Cuong, N. M.; Hung, T. Q.; Sung, T. V.; Taylor, W. C., A New Dimeric Carbazole Alkaloid from *Glycosmis stenocarpa* Roots. *Chemical and Pharmaceutical Bulletin* **2004**, *52* (10), 1175-1178.
135. Fiebig, M.; Pezzuto, J. M.; Soejarto, D. D.; Kinghorn, A. D., Koenoline, a further cytotoxic carbazole alkaloid from *Murraya koenigii*. *Phytochemistry* **1985**, *24* (12), 3041-3043.
136. Chakraborty, D. P.; Barman, B. K.; Bose, P. K., On the constitution of murrayanine, a carbazole derivative isolated from *Murraya koenigii* Spreng. *Tetrahedron* **1965**, *21* (2), 681-685.
137. Bhattacharyya, P.; Chakraborty, D. P., Murrayanine and dentatin from *Clausena heptaphylla*. *Phytochemistry* **1973**, *12* (7), 1831-1832.



138. Sripisut, T.; Cheenpracha, S.; Ritthiwigrom, T.; Prawat, U.; Laphookhieo, S., Chemical Constituents from the Roots of *Clausena excavata* and Their Cytotoxicity. *Records of Natural Products* **2012**, 6 (4), 386-389.
139. Ito, C.; Katsuno, S.; Itoigawa, M.; Ruangrunsi, N.; Mukainaka, T.; Okuda, M.; Kitagawa, Y.; Tokuda, H.; Nishino, H.; Furukawa, H., New Carbazole Alkaloids from *Clausena anisata* with Antitumor Promoting Activity. *Journal of Natural Products* **2000**, 63 (1), 125-128.
140. Bhattacharyya, P.; Maiti, A. K.; Basu, K.; Chowdhury, B. K., Carbazole alkaloids from *Murraya koenigii*. *Phytochemistry* **1994**, 35 (4), 1085-1086.
141. Jiang, H.-Y.; Zhang, W.-J.; You, C.-X.; Yang, K.; Fan, L.; Feng, J.-B.; Chen, J.; Yang, Y.-J.; Wang, C.-F.; Deng, Z.-W.; Yin, H.-B.; Du, S.-S., Two new cytotoxic constituents from the *Clausena lansium* (Lour.) Skeels. *Phytochemistry Letters* **2014**, 9, 92-95.
142. Ito, C.; Katsuno, S.; Ohta, H.; Omura, M.; Kajijura, I.; Furukawa, H., Constituents of *Clausena excavata*. Isolation and Structural Elucidation of New Carbazole Alkaloids. *Chemical and pharmaceutical bulletin* **1997**, 45 (1), 48-52.
143. Xin, Z. Q.; Lu, J. J.; Ke, C. Q.; Hu, C. X.; Lin, L. P.; Ye, Y., Constituents from *Clausena excavata*. *Chemical and Pharmaceutical Bulletin* **2008**, 56 (6), 827-830.
144. Lin, W.; Wang, Y.; Lin, S.; Li, C.; Zhou, C.; Wang, S.; Huang, H.; Liu, P.; Ye, G.; Shen, X., Induction of cell cycle arrest by the carbazole alkaloid Clauszoline-I from *Clausena vestita* D. D. Tao via inhibition of the PKC $\delta$  phosphorylation. *European Journal of Medicinal Chemistry* **2012**, 47, 214-220.
145. Wu, T.-S.; Huang, S.-C., CLAUSINE-D AND -F, TWO NEW 4-PRENYLCARBAZOLE ALKALOIDS FROM *CLAUSENA EXCAVATA*. *Chemical and pharmaceutical bulletin* **1992**, 40 (4), 1069-1071.
146. Ruangrunsi, N.; Ariyaprayoon, J.; Lange, G. L.; Organ, M. G., Three New Carbazole Alkaloids Isolated from *Murraya siamensis*. *Journal of Natural Products* **1990**, 53 (4), 946-952.
147. Chakraborty, A.; Chowdhury, B. K.; Jash, S. S.; Biswas, G. K.; Bhattacharyya, S. K.; Bhattacharyya, P., Carbazole alkaloids from *Glycosmis pentaphylla*. *Phytochemistry* **1992**, 31 (7), 2503-2505.
148. Kongkathip, B.; Kongkathip, N.; Sunthitikawinsakul, A.; Napaswat, C.; Yoosook, C., Anti-HIV-1 constituents from *Clausena excavata*: Part II. carbazoles and a pyranocoumarin. *Phytotherapy Research* **2005**, 19 (8), 728-731.

149. Uvarani, C.; Jaivel, N.; Sankaran, M.; Chandraprakash, K.; Ata, A.; Mohan, P. S., Axially chiral biscarbazoles and biological evaluation of the constituents from *Murraya koenigii*. *Fitoterapia* **2014**, *94*, 10-20.
150. Tian-Shung, W.; Shio-Chyn, H.; Jeng-Shio, L.; Che-Ming, T.; Feng-Nien, K.; Chang-Sheng, K., Chemical and antiplatelet aggregative investigation of the leaves of *Clausena excavata*. *Phytochemistry* **1993**, *32* (2), 449-451.
151. Joshi, B. S.; Kamat, V. N.; Saksena, A. K.; Govindachari, T. R., Structure of heptaphylline, a carbazole alkaloid from *clausena heptaphylla* wt. & arn. *Tetrahedron Letters* **1967**, *8* (41), 4019-4022.
152. Chaichantipyuth, C.; Pummangura, S.; Naowsaran, K.; Thanyavuthi, D.; Anderson, J. E.; McLaughlin, J. L., Two New Bioactive Carbazole Alkaloids from the Root Bark of *Clausena Harmandiana*. *Journal of Natural Products* **1988**, *51* (6), 1285-1288.
153. Kumatia, E. K.; Annan, K.; Dickson, R. A.; Mensah, A. Y.; Amponsah, I. K.; Appiah, A. A.; Tung, N. H.; Edoh, D. A.; Habtemariam, S., Antiinflammatory and analgesic effects in rodent models of ethanol extract of *Clausena anisata* roots and their chemical Constituents. *Natural Product Communications* **2017**, *12* (1), 67-72.
154. Boonyarat, C.; Yenjai, C.; Vajragupta, O.; Waiwut, P., Heptaphylline induces apoptosis in human colon adenocarcinoma cells through Bid and Akt/NF- $\kappa$ B (p65) pathways. *Asian Pacific Journal of Cancer Prevention* **2014**, *15* (23), 10483-10487.
155. Chakthong, S.; Bindulem, N.; Raknai, S.; Yodwaree, S.; Kaewsanee, S.; Kanjana-Opas, A., Carbazole-pyranocoumarin conjugate and two carbazole alkaloids from the stems of *Clausena excavata*. *Natural Product Research* **2016**, *30* (15), 1690-1697.
156. Kanokmedhakul, K.; Kanokmedhakul, S., A new coruleoellagic acid derivative from stems of *Rhodamnia dumetorum* AU - Lakornwong, Waranya. *Natural Product Research* **2018**, *32* (14), 1653-1659.
157. Songsiang, U.; Thongthoom, T.; Boonyarat, C.; Yenjai, C., Claurailas A-D, cytotoxic carbazole alkaloids from the roots of *Clausena harmandiana*. *Journal of Natural Products* **2011**, *74* (2), 208-212.
158. Kato, S.; Kawai, H.; Kawasaki, T.; Toda, Y.; Urata, T.; Hayakawa, Y., Studies on Free Radical Scavenging Substances from Microorganisms I. Carazostatin, a New Free Radical Scavenger

- Produced by *Streptomyces Chromofuscus* DC 118. *Journal of Antibiotics* **1989**, 42 (12), 1879-1881.
159. Misato, I.; Etsuo, N.; Shinichiro, K.; Koji, N., Antioxidant Activities of  $\alpha$ -Tocopherol and Hydroxycarbazole against Lipid Peroxidation in Homogeneous Solution and in Liposomal Membranes. *Chemistry Letters* **1992**, 21 (9), 1735-1738.
  160. Mo, C. J.; Ya, K.; Furihata, K.; Furihata, K.; Shimazu, A.; Hayakawa, Y.; Seto, H., Isolation and structural elucidation of antioxidative agents, antiostatins a1-4 and b2-5. *Journal of Antibiotics* **1990**, 43 (10), 1337-1340.
  161. Schneider, K.; Nachtigall, J.; Hänchen, A.; Nicholson, G.; Goodfellow, M.; Süßmuth, R. D.; Fiedler, H.-P., Lipocarbazoles, Secondary Metabolites from *Tsukamurella pseudospumae* Acta 1857 with Antioxidative Activity. *Journal of Natural Products* **2009**, 72 (10), 1768-1772.
  162. Wen-Shyong, L.; McChesney, J. D.; El-Ferally, F. S., Carbazole alkaloids from *Clausena lansium*. *Phytochemistry* **1991**, 30 (1), 343-346.
  163. Ma, C.; Case, R. J.; Wang, Y.; Zhang, H.-J.; Tan, G. T.; Van Hung, N.; Cuong, N. M.; Franzblau, S. G.; Soejarto, D. D.; Fong, H. H. S.; Pauli, G. F., Anti-Tuberculosis Constituents from the Stem Bark of *Micromelum hirsutum*. *Planta Medecine* **2005**, 71 (03), 261-267.
  164. Chowdhury, B. K.; Jha, S.; Bhattacharyya, P.; Mukherjee, J., Two new carbazole alkaloids from *Murraya koenigii*. *Indian Journal of Chemistry - Section B Organic and Medicinal Chemistry* **2001**, 40 (6), 490-494.
  165. Meragelman, K. M.; McKee, T. C.; Boyd, M. R., Siamenol, a New Carbazole Alkaloid from *Murraya siamensis*. *Journal of Natural Products* **2000**, 63 (3), 427-428.
  166. Chakraborty, A.; Chowdhury, B. K.; Bhattacharyya, P., Clausenol and clausenine—two carbazole alkaloids from *Clausena anisata*. *Phytochemistry* **1995**, 40 (1), 295-298.
  167. Porterat, O.; Puder, C.; Bolek, W.; Wagner, K.; Ke, C.; Ye, Y.; Gillardon, F., Clausine Z, a new carbazole alkaloid from *Clausena excavata* with inhibitory activity on CDK5. *Pharmazie* **2005**, 60 (8), 637-639.
  168. Pacher, T.; Bacher, M.; Hofer, O.; Greger, H., Stress induced carbazole phytoalexins in *Glycosmis* species. *Phytochemistry* **2001**, 58 (1), 129-135.
  169. Bhattacharyya, P.; Chakraborty, P. K.; Chowdhury, B. K., Glycozolidol, an antibacterial carbazole alkaloid from *Glycosmis pentaphylla*. *Phytochemistry* **1985**, 24 (4), 882-883.

170. Ito, C.; Itoigawa, M.; Sato, A.; Hasan, C. M.; Rashid, M. A.; Tokuda, H.; Mukainaka, T.; Nishino, H.; Furukawa, H., Chemical constituents of *Glycosmis arborea*: Three new carbazole alkaloids and their biological activity. *Journal of Natural Products* **2004**, *67* (9), 1488-1491.
171. Thongthoom, T.; Songsiang, U.; Phaosiri, C.; Yenjai, C., Biological activity of chemical constituents from *Clausena harmandiana*. *Archives of Pharmacal Research* **2010**, *33* (5), 675-680.
172. Ito, C.; Katsuno, S.; Ohta, H.; Omura, M.; Kajijura, I.; Furukawa, H., Constituents of *Clausena excavata*. Isolation and structural elucidation of new carbazole alkaloids. *Chemical and Pharmaceutical Bulletin* **1997**, *45* (1), 48-52.
173. Peng, W. W.; Zeng, G. Z.; Song, W. W.; Tan, N. H., A new cytotoxic carbazole alkaloid and two new other alkaloids from *Clausena excavata*. *Chemistry and Biodiversity* **2013**, *10* (7), 1317-1321.
174. Hibino, S.; Tonari, A.; Choshi, T.; Sugino, E., The new approach to antibiotic carbazomycins. The formal total synthesis of carbazomycins A and B. *Heterocycles* **1993**, *35* (1), 441-444.
175. Hook, D. J.; Yacobucci, J. J.; O'Connor, S.; Lee, M.; Kerns, E.; Krishnan, B.; Matson, J.; Hesler, G., Identification of the inhibitory activity of carbazomycins b and c against 5-lipoxygenase, a new activity for these compounds. *Journal of Antibiotics* **1990**, *43* (10), 1347-1348.
176. Kato, S.; Kawasaki, T.; Urata, T.; Mochizuki, J., In vitro and ex vivo free radical scavenging activities of carazostatin, carbazomycin b and their derivatives. *Journal of Antibiotics* **1993**, *46* (12), 1859-1865.
177. Feng, N.; Ye, W.; Wu, P.; Huang, Y.; Xie, H.; Wei, X., Two new antifungal alkaloids produced by *Streptoverticillium morookaense*. *Journal of Antibiotics* **2007**, *60* (3), 179-183.
178. Czerwonka, R.; Reddy, K. R.; Baum, E.; Knölker, H. J., First enantioselective total synthesis of neocarazostatin B, determination of its absolute configuration and transformation into carquinostatin A. *Chemical Communications* **2006**, (7), 711-713.
179. Kotoda, N.; Shin-Ya, K.; Furihata, K.; Hayakawa, Y.; Seto, H., Isolation and structure elucidation of novel neuronal cell protecting substances, carbazomadurins A and B produced by *Actinomadura madurae*. *Journal of Antibiotics* **1997**, *50* (9), 770-772.
180. Yoshimi, N.; Haruaki, Y.; Masami, H.; Minoru, H.; Yasuo, F.; Toshikazu, O., Epocarbazolins A And B, Novel 5-Lipoxygenase Inhibitors Taxonomy, Fermentation, Isolation, Structures And Biological Activities. *the journal of antibiotics* **1992**, *46* (1), 25-33.

181. Naid, T.; Kaneda, M.; Nakamura, S., Carbazomycins C, D, E and F, Minor Components of the Carbazomycin Complex. *The Journal of Antibiotics* **1987**, *40* (2), 157-164.
182. Xin, Z.-Q.; Lu, J.-J.; Ke, C.-Q.; Hu, C.-X.; Lin, L.-P.; Ye, Y., Constituents from *Clausena excavata*. *Chemical and Pharmaceutical Bulletin* **2008**, *56* (6), 827-830.
183. Eijkman, J. F., Sur les principes constituants de l'*Illicium religiosum* (Sieb.) (Shikimi-no-ki en japonais). *Recueil des Travaux Chimiques des Pays-Bas* **1885**, *4* (2), 32-54.
184. Dewick, P. M., *Medicinal Natural Products: A Biosynthetic Approach: Third Edition*. 2009; p 1-539.
185. Iron–Diene Complexes. In *Transition Metals for Organic Synthesis*.
186. Akermark, B.; Ebersson, L.; Jonsson, E.; Pettersson, E., Palladium-promoted cyclization of diphenyl ether, diphenylamine, and related compounds. *The Journal of Organic Chemistry* **1975**, *40* (9), 1365-1367.
187. Cadogan, J. I. G.; Cameron-Wood, M.; Mackie, R. K.; Searle, R. J. G., 896. The reactivity of organophosphorus compounds. Part XIX. Reduction of nitro-compounds by triethyl phosphite: a convenient new route to carbazoles, indoles, indazoles, triazoles, and related compounds. *Journal of the Chemical Society (Resumed)* **1965**, (0), 4831-4837.
188. Kano, S.; Sugino, E.; Shibuya, S.; Hibino, S., Synthesis of carbazole alkaloids hyellazole and 6-chlorohyellazole. *The Journal of Organic Chemistry* **1981**, *46* (19), 3856-3859.
189. Chakraborty, D. P.; Roy, S., Carbazole Alkaloids IV. In *Fortschritte der Chemie organischer Naturstoffe / Progress in the Chemistry of Organic Natural Products*, Chakraborty, D. P.; Krohn, K.; Messner, P.; Roy, S.; Schäffer, C., Eds. Springer Vienna: Vienna, 2003; pp 125-230.
190. Sharma, R. B.; Kapil, R. S., Synthesis of lansine and 6-methoxyheptaphylline. *Chemistry and Industry (London)* **1980**, No 4, 158.
191. Joshi, B. S.; Kamat, V. N.; Gawad, D. H.; Govindachari, T. R., Structure and synthesis of heptaphylline. *Phytochemistry* **1972**, *11* (6), 2065-2071.
192. Noji, T.; Fujiwara, H.; Okano, K.; Tokuyama, H., Synthesis of substituted indoline and carbazole by benzyne-mediated cyclization-functionalization. *Organic Letters* **2013**, *15* (8), 1946-1949.
193. Okano, K., Synthetic studies on natural products with aromatic nitrogen heterocycles based on development of the methods for the formation of aryl carbon-nitrogen bond. *Yakugaku Zasshi* **2013**, *133* (10), 1065-1078.

194. Hesse, R.; Kataeva, O.; Schmidt, A. W.; Knölker, H.-J., Synthesis of Prenyl- and Geranyl-Substituted Carbazole Alkaloids by DIBAL-H Promoted Reductive Pyran Ring Opening of Dialkylpyrano[3,2-a]carbazoles. *Chemistry – A European Journal* **2014**, *20* (31), 9504-9509.
195. Dhara, K.; Mandal, T.; Das, J.; Dash, J., Synthesis of Carbazole Alkaloids by Ring-Closing Metathesis and Ring Rearrangement–Aromatization. *Angewandte Chemie International Edition* **2015**, *54* (52), 15831-15835.
196. Ma, D.; Dai, J.; Qiu, Y.; Fu, C.; Ma, S., Gram scale synthesis of 7-methoxy-O-methylmukonal, clausine-O, clausine-K, clausine-H, 7-methoxymukonal, and methyl 2-hydroxy-7-methoxy-9H-carbazole-3-carboxylate. *Organic Chemistry Frontiers* **2014**, *1* (7), 782-791.
197. Bessa, L. J.; Buttachon, S.; Dethoup, T.; Martins, R.; Vasconcelos, V.; Kijjoa, A.; da Costa, P. M., Neofiscalin A and fiscalin C are potential novel indole alkaloid alternatives for the treatment of multidrug-resistant Gram-positive bacterial infections. *FEMS Microbiology Letters* **2016**, *363* (15), 1-5.
198. Leão, M.; Gomes, S.; Soares, J.; Bessa, C.; Maclel, C.; Ciribilli, Y.; Pereira, C.; Inga, A.; Saraiva, L., Novel simplified yeast-based assays of regulators of p53-MDMX interaction and p53 transcriptional activity. *FEBS Journal* **2013**, *280* (24), 6498-6507.
199. Long, S.; Sousa, E.; Kijjoa, A.; Pinto, M. M. M., Marine natural products as models to circumvent multidrug resistance. *Molecules* **2016**, *21* (7).
200. Long, S.; Resende, D. I. S. P.; Kijjoa, A.; Silva, A. M. S.; Pina, A.; Fernández-Marcelo, T.; Vasconcelos, M. H.; Sousa, E.; Pinto, M. M. M., Antitumor Activity of Quinazolinone Alkaloids Inspired by Marine Natural Products. *Marine Drugs* **2018**, *16* (8).
201. Long, S.; Resende, D. I. S. P.; Kijjoa, A.; Silva, A. M. S.; Fernandes, R.; Xavier, C. P. R.; Vasconcelos, M. H.; Sousa, E.; Pinto, M. M. M., Synthesis of New Proteomimetic Quinazolinone Alkaloids and Evaluation of Their Neuroprotective and Antitumor Effects. *Molecules* **2019**, *24* (3), 534.
202. Barrow, C. J.; Sun, H. H., Spiroquinazoline, a novel substance P inhibitor with a new carbon skeleton, isolated from *Aspergillus flavipes*. *J. Nat. Prod.* **1994**, *57* (4), 471-476.
203. Zhu, S.; Zhang, Q.; Gudise, C.; Wei, L.; Smith, E.; Zeng, Y., Synthesis and biological evaluation of febrifugine analogues as potential antimalarial agents. *Bioorganic and Medicinal Chemistry* **2009**, *17* (13), 4496-4502.

204. Kato, M.; Inaba, M.; Itahana, H.; Ohara, E.; Nakamura, K.; Uesato, S.; Inouye, H.; Fujita, T., Studies on anticoccidial constituents of crude drugs and related plants (I). Isolation and biological activities of cis- and trans-febrifugine from *Hydrangea macrophylla*. *Japanese Journal of Pharmacognosy* **1990**, *44* (4), 288-292.
205. Boeckler, F. M.; Joerger, A. C.; Jaggi, G.; Rutherford, T. J.; Veprintsev, D. B.; Fersht, A. R., Targeted rescue of a destabilized mutant of p53 by an in silico screened drug. *Proceedings of the National Academy of Sciences of the United States of America* **2008**, *105* (30), 10360-10365.
206. Bauer, M. R.; Jones, R. N.; Baud, M. G. J.; Wilcken, R.; Boeckler, F. M.; Fersht, A. R.; Joerger, A. C.; Spencer, J., Harnessing Fluorine-Sulfur Contacts and Multipolar Interactions for the Design of p53 Mutant Y220C Rescue Drugs. *ACS chemical biology* **2016**, *11* (8), 2265-2274.

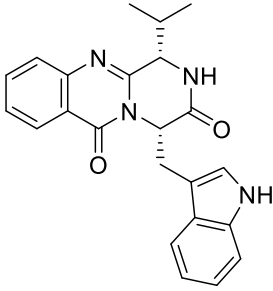
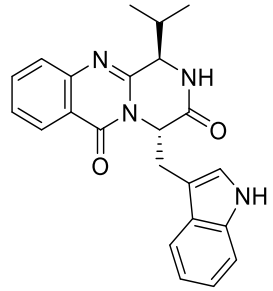
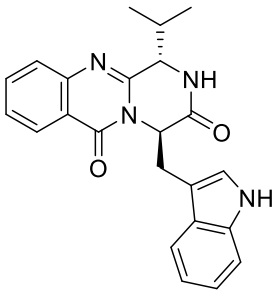


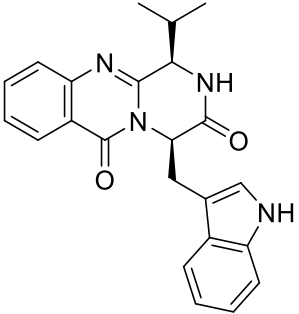
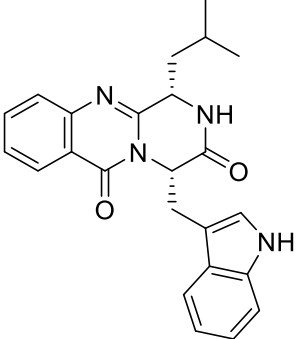
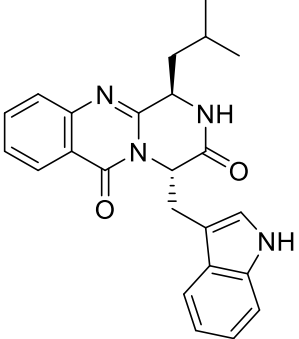


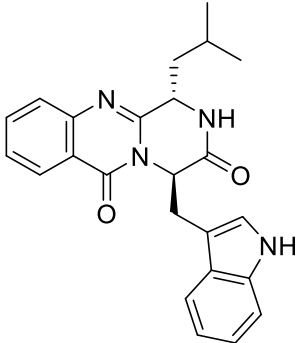
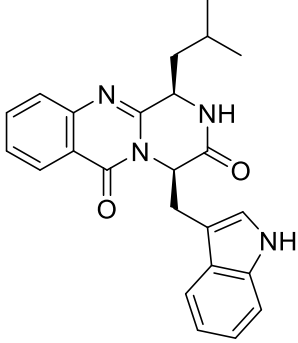
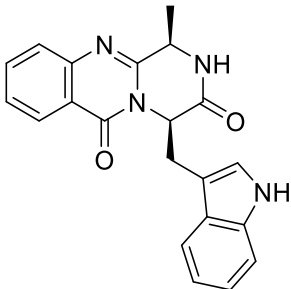
# Annexes

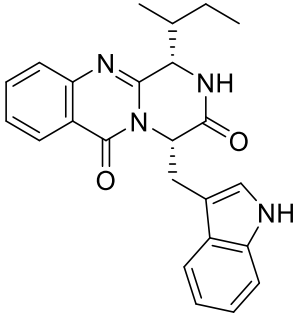
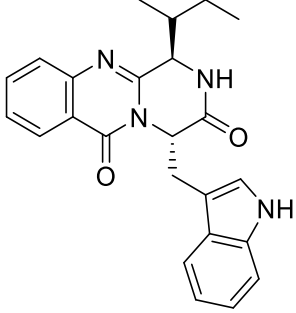
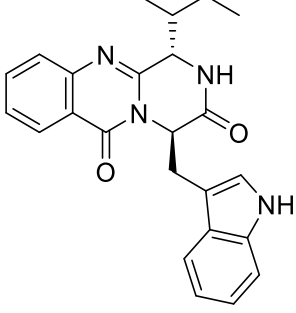


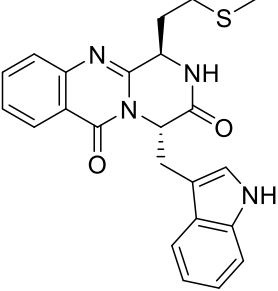
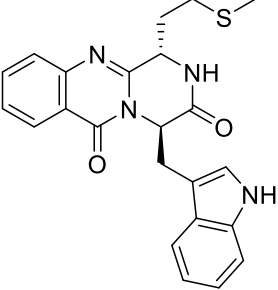
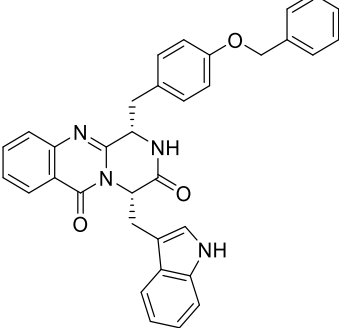
The structures of compounds investigated in this thesis and their IUPAC names are presented in the following table. The table is also highlighting the number of compounds using in each chapter.

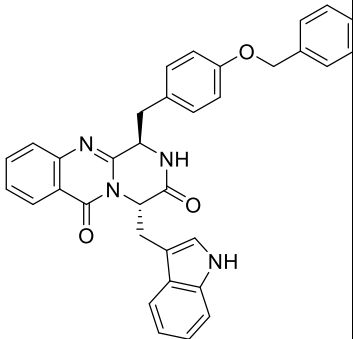
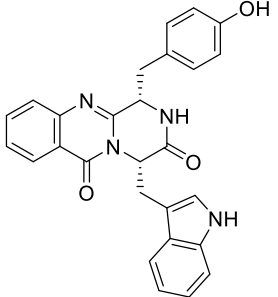
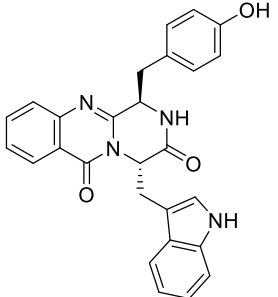
Nr. (Thesis)	Structure	Chapter3	Chapter 4	Chapter 5	Chapter 6	Chaper7	Chapter 8
76	 <p>(1S,4S)-4-((1H-indol-3-yl)methyl)-1-isopropyl-1,2-dihydro-6H-pyrazino[2,1-b]quinazoline-3,6(4H)-dione</p>	4a		5	6		
77	 <p>(1R,4S)-4-((1H-indol-3-yl)methyl)-1-isopropyl-1,2-dihydro-6H-pyrazino[2,1-b]quinazoline-3,6(4H)-dione</p>	4b		6	7		
26 /78*	 <p>(1S,4R)-4-((1H-indol-3-yl)methyl)-1-isopropyl-1,2-dihydro-6H-pyrazino[2,1-b]quinazoline-3,6(4H)-dione</p>	4c	3	7	8	1	
		* 26 refers to the natural product fiscalin B and 78 refers to the synthetic product obtained in this thesis (with a e.r. of 69:31 )					

Nr. (Thesis)	Structure	Chapter3	Chapter 4	Chapter 5	Chapter 6	Chaper7	Chapter 8
79	 <p data-bbox="354 638 683 758">(1<i>R</i>,4<i>R</i>)-4-((1<i>H</i>-indol-3-yl)methyl)-1-isopropyl-1,2-dihydro-6<i>H</i>-pyrazino[2,1-<i>b</i>]quinazoline-3,6(4<i>H</i>)-dione</p>	4d		8	9		
80	 <p data-bbox="354 1150 683 1270">(1<i>S</i>,4<i>S</i>)-4-((1<i>H</i>-indol-3-yl)methyl)-1-isobutyl-1,2-dihydro-6<i>H</i>-pyrazino[2,1-<i>b</i>]quinazoline-3,6(4<i>H</i>)-dione</p>	5a		9	10		
81	 <p data-bbox="354 1661 683 1780">(1<i>R</i>,4<i>S</i>)-4-((1<i>H</i>-indol-3-yl)methyl)-1-isobutyl-1,2-dihydro-6<i>H</i>-pyrazino[2,1-<i>b</i>]quinazoline-3,6(4<i>H</i>)-dione</p>	5b		10	11		

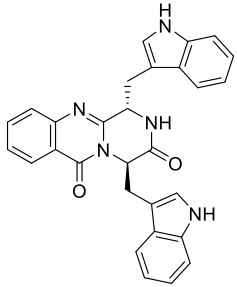
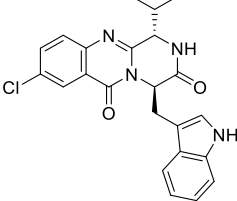
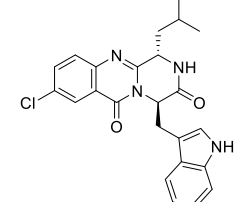
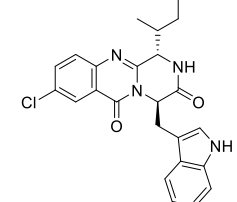
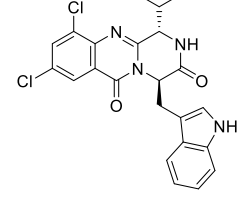
Nr. (Thesis)	Structure	Chapter3	Chapter 4	Chapter 5	Chapter 6	Chaper7	Chapter 8
82	 <p data-bbox="472 667 802 785">(1<i>S</i>,4<i>R</i>)-4-((1<i>H</i>-indol-3-yl)methyl)-1-isobutyl-1,2-dihydro-6<i>H</i>-pyrazino[2,1-<i>b</i>]quinazoline-3,6(4<i>H</i>)-dione</p>	5c		11	12		
83	 <p data-bbox="472 1182 802 1299">(1<i>R</i>,4<i>R</i>)-4-((1<i>H</i>-indol-3-yl)methyl)-1-isobutyl-1,2-dihydro-6<i>H</i>-pyrazino[2,1-<i>b</i>]quinazoline-3,6(4<i>H</i>)-dione</p>	5d		12	13		
20/84	 <p data-bbox="456 1675 829 1793">(1<i>R</i>,4<i>R</i>)-4-((1<i>H</i>-indol-3-yl)methyl)-1-methyl-1,2-dihydro-6<i>H</i>-pyrazino[2,1-<i>b</i>]quinazoline-3,6(4<i>H</i>)-dione</p>	1	14				
		<p data-bbox="850 1650 1533 1793">* <b>20</b> refers to the natural product fumiquinazoline G and <b>84</b> refers to the synthetic product obtained in this thesis (with a <i>e.r.</i> of 93:7)</p>					

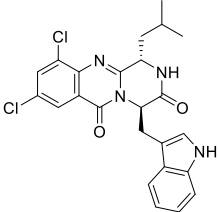
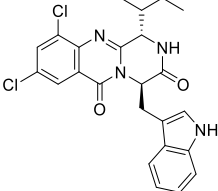
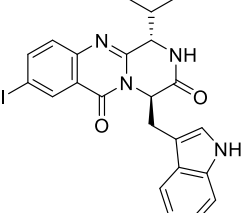
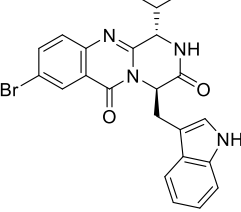
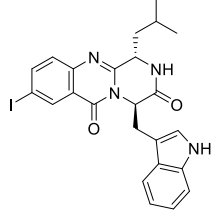
Nr. (Thesis)	Structure	Chapter3	Chapter 4	Chapter 5	Chapter 6	Chaper7	Chapter 8
85	 <p data-bbox="337 638 711 762">(1<i>S</i>,4<i>S</i>)-4-((1<i>H</i>-indol-3-yl)methyl)-1-((<i>S</i>)-sec-butyl)-1,2-dihydro-6<i>H</i>-pyrazino[2,1-<i>b</i>]quinazoline-3,6(4<i>H</i>)-dione</p>		2				
86	 <p data-bbox="337 1125 711 1249">(1<i>R</i>,4<i>S</i>)-4-((1<i>H</i>-indol-3-yl)methyl)-1-((<i>R</i>)-sec-butyl)-1,2-dihydro-6<i>H</i>-pyrazino[2,1-<i>b</i>]quinazoline-3,6(4<i>H</i>)-dione</p>		4	13			
87	 <p data-bbox="337 1612 711 1736">(1<i>S</i>,4<i>R</i>)-4-((1<i>H</i>-indol-3-yl)methyl)-1-((<i>S</i>)-sec-butyl)-1,2-dihydro-6<i>H</i>-pyrazino[2,1-<i>b</i>]quinazoline-3,6(4<i>H</i>)-dione</p>		5	14	15		

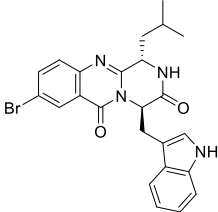
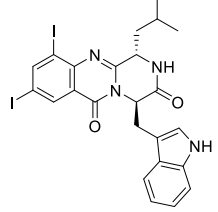
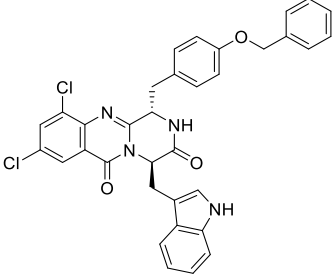
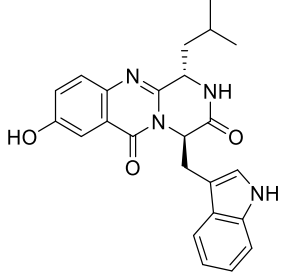
Nr. (Thesis)	Structure	Chapter3	Chapter 4	Chapter 5	Chapter 6	Chaper7	Chapter 8
88	 <p data-bbox="467 617 813 758">(1R,4S)-4-((1H-indol-3-yl)methyl)-1-(2-(methylthio)ethyl)-1,2-dihydro-6H-pyrazino[2,1-b]quinazoline-3,6(4H)-dione</p>		6	15			
89	 <p data-bbox="467 1100 813 1241">(1S,4R)-4-((1H-indol-3-yl)methyl)-1-(2-(methylthio)ethyl)-1,2-dihydro-6H-pyrazino[2,1-b]quinazoline-3,6(4H)-dione</p>		7	16	16		
90	 <p data-bbox="459 1625 834 1703">(1S,4S)-4-((1H-indol-3-yl)methyl)-1-(4-(benzyloxy)benzyl)-1,2-dihydro-6H-pyrazino[2,1-b]quinazoline-3,6(4H)-dione</p>		8	17			

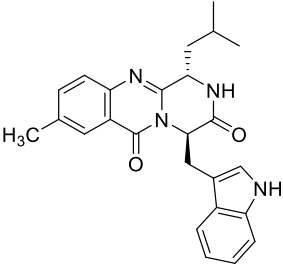
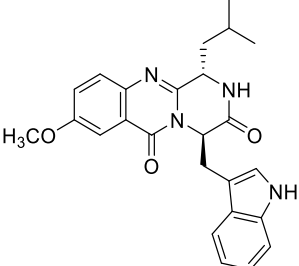
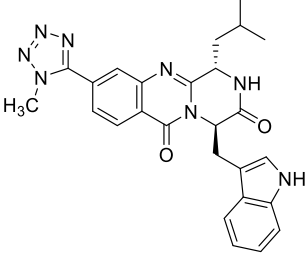
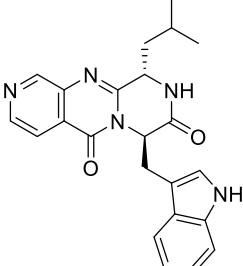
Nr. (Thesis)	Structure	Chapter3	Chapter 4	Chapter 5	Chapter 6	Chaper7	Chapter 8
91	 <p data-bbox="337 661 716 737">(1<i>R</i>,4<i>S</i>)-4-((1<i>H</i>-indol-3-yl)methyl)-1-(4-(benzyloxy)benzyl)-1,2-dihydro-6<i>H</i>-pyrazino[2,1-<i>b</i>]quinazoline-3,6(4<i>H</i>)-dione</p>		9	18	17		
92	 <p data-bbox="337 1081 716 1157">(1<i>S</i>,4<i>S</i>)-4-((1<i>H</i>-indol-3-yl)methyl)-1-(4-hydroxybenzyl)-1,2-dihydro-6<i>H</i>-pyrazino[2,1-<i>b</i>]quinazoline-3,6(4<i>H</i>)-dione</p>		10	19			
93	 <p data-bbox="337 1495 716 1570">(1<i>R</i>,4<i>S</i>)-4-((1<i>H</i>-indol-3-yl)methyl)-1-(4-hydroxybenzyl)-1,2-dihydro-6<i>H</i>-pyrazino[2,1-<i>b</i>]quinazoline-3,6(4<i>H</i>)-dione</p>		11	20	18		

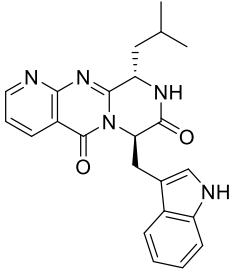
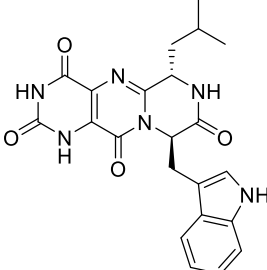
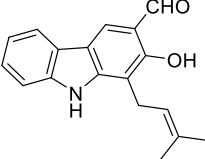
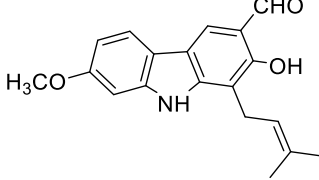
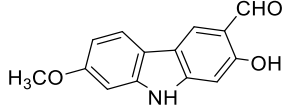


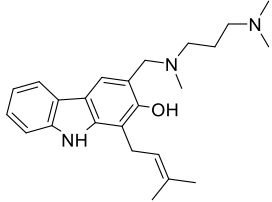
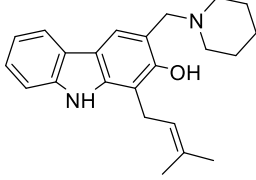
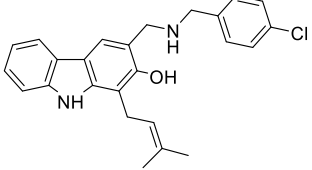
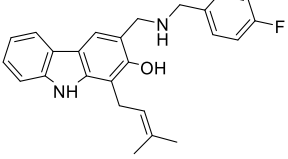
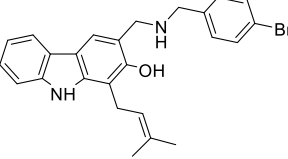
Nr. (Thesis)	Structure	Chapter3	Chapter 4	Chapter 5	Chapter 6	Chaper7	Chapter 8
94	 <p data-bbox="456 600 821 678">(1S,4R)-1,4-bis((1H-indol-3-yl)methyl)-1,2-dihydro-6H-pyrazino[2,1-b]quinazoline-3,6(4H)-dione</p>				34		
95	 <p data-bbox="456 909 821 978">(1S,4R)-4-((1H-indol-3-yl)methyl)-8-chloro-1-isopropyl-1,2-dihydro-6H-pyrazino[2,1-b]quinazoline-3,6(4H)-dione</p>			22			
96	 <p data-bbox="456 1215 821 1285">(1S,4R)-4-((1H-indol-3-yl)methyl)-8-chloro-1-isobutyl-1,2-dihydro-6H-pyrazino[2,1-b]quinazoline-3,6(4H)-dione</p>			23	19		
97	 <p data-bbox="456 1522 821 1591">(1S,4R)-4-((1H-indol-3-yl)methyl)-1-((S)-sec-butyl)-8-chloro-1,2-dihydro-6H-pyrazino[2,1-b]quinazoline-3,6(4H)-dione</p>			24	20		
98	 <p data-bbox="456 1818 821 1887">(1S,4R)-4-((1H-indol-3-yl)methyl)-8,10-dichloro-1-isopropyl-1,2-dihydro-6H-pyrazino[2,1-b]quinazoline-3,6(4H)-dione</p>			25			

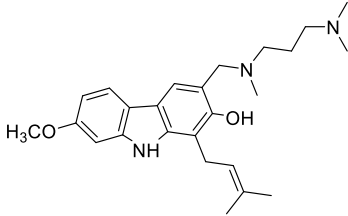
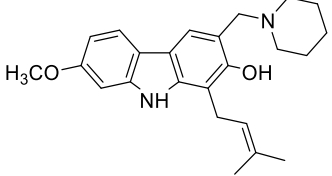
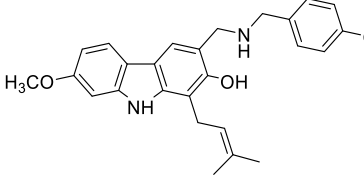
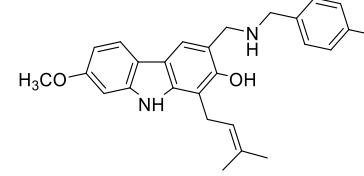
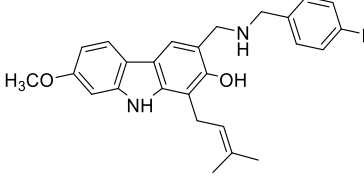
Nr. (Thesis)	Structure	Chapter3	Chapter 4	Chapter 5	Chapter 6	Chaper7	Chapter 8
99	 <p data-bbox="337 527 708 583">(1S,4R)-4-((1H-indol-3-yl)methyl)-8,10-dichloro-1-isobutyl-1,2-dihydro-6H-pyrazino[2,1-b]quinazoline-3,6(4H)-dione</p>			26	21	2	
100	 <p data-bbox="337 814 708 871">(1S,4R)-4-((1H-indol-3-yl)methyl)-1-((S)-sec-butyl)-8,10-dichloro-1,2-dihydro-6H-pyrazino[2,1-b]quinazoline-3,6(4H)-dione</p>			27	22		
101	 <p data-bbox="337 1140 708 1197">(1S,4R)-4-((1H-indol-3-yl)methyl)-8-iodo-1-isopropyl-1,2-dihydro-6H-pyrazino[2,1-b]quinazoline-3,6(4H)-dione</p>			28			
102	 <p data-bbox="337 1476 708 1533">(1S,4R)-4-((1H-indol-3-yl)methyl)-8-bromo-1-isopropyl-1,2-dihydro-6H-pyrazino[2,1-b]quinazoline-3,6(4H)-dione</p>			29			
103	 <p data-bbox="337 1791 708 1848">(1S,4R)-4-((1H-indol-3-yl)methyl)-8-iodo-1-isobutyl-1,2-dihydro-6H-pyrazino[2,1-b]quinazoline-3,6(4H)-dione</p>			30	23		

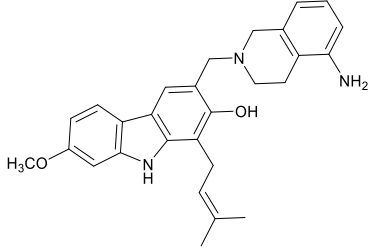
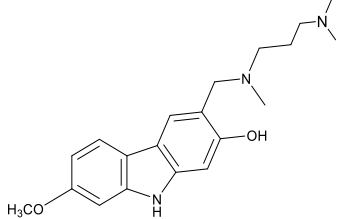
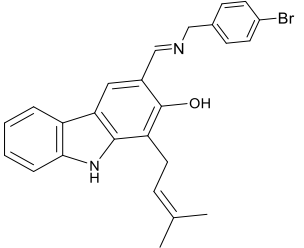
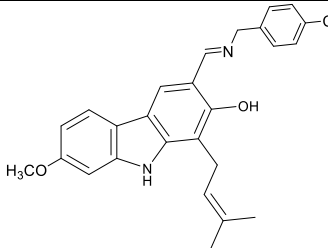
Nr. (Thesis)	Structure	Chapter3	Chapter 4	Chapter 5	Chapter 6	Chaper7	Chapter 8
104	 <p data-bbox="456 527 834 583">(1<i>S</i>,4<i>R</i>)-4-((1<i>H</i>-indol-3-yl)methyl)-8-bromo-1-isobutyl-1,2-dihydro-6<i>H</i>-pyrazino[2,1-<i>b</i>]quinazoline-3,6(4<i>H</i>)-dione</p>			31	24		
105	 <p data-bbox="456 837 834 894">(1<i>S</i>,4<i>R</i>)-4-((1<i>H</i>-indol-3-yl)methyl)-8,10-diiodo-1-isobutyl-1,2-dihydro-6<i>H</i>-pyrazino[2,1-<i>b</i>]quinazoline-3,6(4<i>H</i>)-dione</p>			32	25		
106	 <p data-bbox="456 1205 834 1262">(1<i>S</i>,4<i>R</i>)-4-((1<i>H</i>-indol-3-yl)methyl)-1-(4-(benzyloxy)benzyl)-8,10-dichloro-1,2-dihydro-6<i>H</i>-pyrazino[2,1-<i>b</i>]quinazoline-3,6(4<i>H</i>)-dione</p>		12		26		
107	 <p data-bbox="456 1579 834 1635">(1<i>S</i>,4<i>R</i>)-4-((1<i>H</i>-indol-3-yl)methyl)-8-hydroxy-1-isobutyl-1,2-dihydro-6<i>H</i>-pyrazino[2,1-<i>b</i>]quinazoline-3,6(4<i>H</i>)-dione</p>				27		

Nr. (Thesis)	Structure	Chapter3	Chapter 4	Chapter 5	Chapter 6	Chaper7	Chapter 8
108	 <p data-bbox="337 583 711 653">(1<i>S</i>,4<i>R</i>)-4-((1<i>H</i>-indol-3-yl)methyl)-1-isobutyl-8-methyl-1,2-dihydro-6<i>H</i>-pyrazino[2,1-<i>b</i>]quinazoline-3,6(4<i>H</i>)-dione</p>				28		
109	 <p data-bbox="337 961 711 1031">(1<i>S</i>,4<i>R</i>)-4-((1<i>H</i>-indol-3-yl)methyl)-1-isobutyl-8-methoxy-1,2-dihydro-6<i>H</i>-pyrazino[2,1-<i>b</i>]quinazoline-3,6(4<i>H</i>)-dione</p>				29		
110	 <p data-bbox="337 1329 711 1430">(1<i>S</i>,4<i>R</i>)-4-((1<i>H</i>-indol-3-yl)methyl)-1-isobutyl-9-(1-methyl-1<i>H</i>-tetrazol-5-yl)-1,2-dihydro-6<i>H</i>-pyrazino[2,1-<i>b</i>]quinazoline-3,6(4<i>H</i>)-dione</p>				32		
111	 <p data-bbox="337 1738 711 1808">(1<i>S</i>,4<i>R</i>)-4-((1<i>H</i>-indol-3-yl)methyl)-1-isobutyl-1,2-dihydro-6<i>H</i>-pyrazino[1,2-<i>a</i>]pyrido[3,4-<i>d</i>]pyrimidine-3,6(4<i>H</i>)-dione</p>				30		

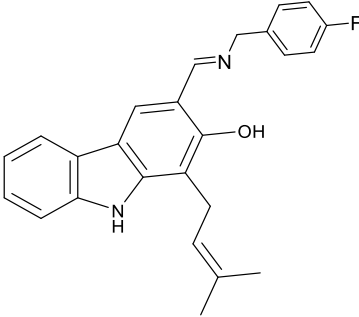
Nr. (Thesis)	Structure	Chapter3	Chapter 4	Chapter 5	Chapter 6	Chaper7	Chapter 8
112	 <p data-bbox="456 579 821 653">(7<i>R</i>,10<i>S</i>)-7-((1<i>H</i>-indol-3-yl)methyl)-10-isobutyl-9,10-dihydro-5<i>H</i>-pyrazino[1,2-<i>a</i>]pyrido[2,3-<i>d</i>]pyrimidine-5,8(7<i>H</i>)-dione</p>				31		
113	 <p data-bbox="456 957 821 1031">(6<i>S</i>,9<i>R</i>)-9-((1<i>H</i>-indol-3-yl)methyl)-6-isobutyl-6,7-dihydro-1<i>H</i>-pyrimido[5,4-<i>d</i>]pyrimidine-2,4,8,11(3<i>H</i>,9<i>H</i>)-tetraone</p>				33		
57	 <p data-bbox="456 1241 821 1293">2-hydroxy-1-(3-methylbut-2-en-1-yl)-9<i>H</i>-carbazole-3-carbaldehyde</p>						1
62	 <p data-bbox="456 1524 821 1608">2-hydroxy-7-methoxy-1-(3-methylbut-2-en-1-yl)-9<i>H</i>-carbazole-3-carbaldehyde</p>						2
63	 <p data-bbox="456 1755 821 1797">2-hydroxy-7-methoxy-9<i>H</i>-carbazole-3-carbaldehyde</p>						3

Nr. (Thesis)	Structure	Chapter3	Chapter 4	Chapter 5	Chapter 6	Chaper7	Chapter 8
114	 <p data-bbox="337 520 711 583">3-(((3-(dimethylamino)propyl)(methyl)amino)methyl)-1-(3-methylbut-2-en-1-yl)-9H-carbazol-2-ol</p>						1a
115	 <p data-bbox="337 814 711 867">1-(3-methylbut-2-en-1-yl)-3-(piperidin-1-ylmethyl)-9H-carbazol-2-ol</p>						1b
116	 <p data-bbox="337 1083 711 1125">3-(((4-chlorobenzyl)amino)methyl)-1-(3-methylbut-2-en-1-yl)-9H-carbazol-2-ol</p>						1c
117	 <p data-bbox="337 1339 711 1381">3-(((4-fluorobenzyl)amino)methyl)-1-(3-methylbut-2-en-1-yl)-9H-carbazol-2-ol</p>						1d
118	 <p data-bbox="337 1587 711 1629">3-(((4-bromobenzyl)amino)methyl)-1-(3-methylbut-2-en-1-yl)-9H-carbazol-2-ol</p>						1e

Nr. (Thesis)	Structure	Chapter3	Chapter 4	Chapter 5	Chapter 6	Chaper7	Chapter 8
119	 <p data-bbox="456 537 850 625">3-(((3-(dimethylamino)propyl)(methyl)amino)methyl)-7-methoxy-1-(3-methylbut-2-en-1-yl)-9H-carbazol-2-ol</p>						2a
120	 <p data-bbox="472 852 834 905">7-methoxy-1-(3-methylbut-2-en-1-yl)-3-(piperidin-1-ylmethyl)-9H-carbazol-2-ol</p>						2b
121	 <p data-bbox="472 1127 802 1192">3-(((4-chlorobenzyl)amino)methyl)-7-methoxy-1-(3-methylbut-2-en-1-yl)-9H-carbazol-2-ol</p>						2c
122	 <p data-bbox="456 1419 834 1461">3-(((4-fluorobenzyl)amino)methyl)-7-methoxy-1-(3-methylbut-2-en-1-yl)-9H-carbazol-2-ol</p>						2d
123	 <p data-bbox="472 1684 802 1749">3-(((4-bromobenzyl)amino)methyl)-7-methoxy-1-(3-methylbut-2-en-1-yl)-9H-carbazol-2-ol</p>						2e

Nr. (Thesis)	Structure	Chapter3	Chapter 4	Chapter 5	Chapter 6	Chaper7	Chapter 8
124	 <p data-bbox="342 562 711 604">3-((5-amino-3,4-dihydroisoquinolin-2(1H)-yl)methyl)-7-methoxy-1-(3-methylbut-2-en-1-yl)-9H-carbazol-2-ol</p>						2f
125	 <p data-bbox="342 852 711 894">3-(((3-(dimethylamino)propyl)(methyl)amino)methyl)-7-methoxy-9H-carbazol-2-ol</p>						3a
126	 <p data-bbox="342 1171 711 1213">(E)-3-(((4-bromobenzyl)imino)methyl)-1-(3-methylbut-2-en-1-yl)-9H-carbazol-2-ol</p>						1f
127	 <p data-bbox="342 1486 711 1528">(E)-3-(((4-chlorobenzyl)imino)methyl)-7-methoxy-1-(3-methylbut-2-en-1-yl)-9H-carbazol-2-ol</p>						2f



Nr. (Thesis)	Structure	Chapter3	Chapter 4	Chapter 5	Chapter 6	Chaper7	Chapter 8
128	 <p data-bbox="456 632 846 684">(E)-3-(((4-fluorobenzyl)imino)methyl)-1-(3-methylbut-2-en-1-yl)-9H-carbazol-2-ol</p>						2h